



UNIVERSITAT^{DE}
BARCELONA

Testing the hypothesis of adaptive radiation and its eco-phenotypic implications

Adrià Bellvert Bantí



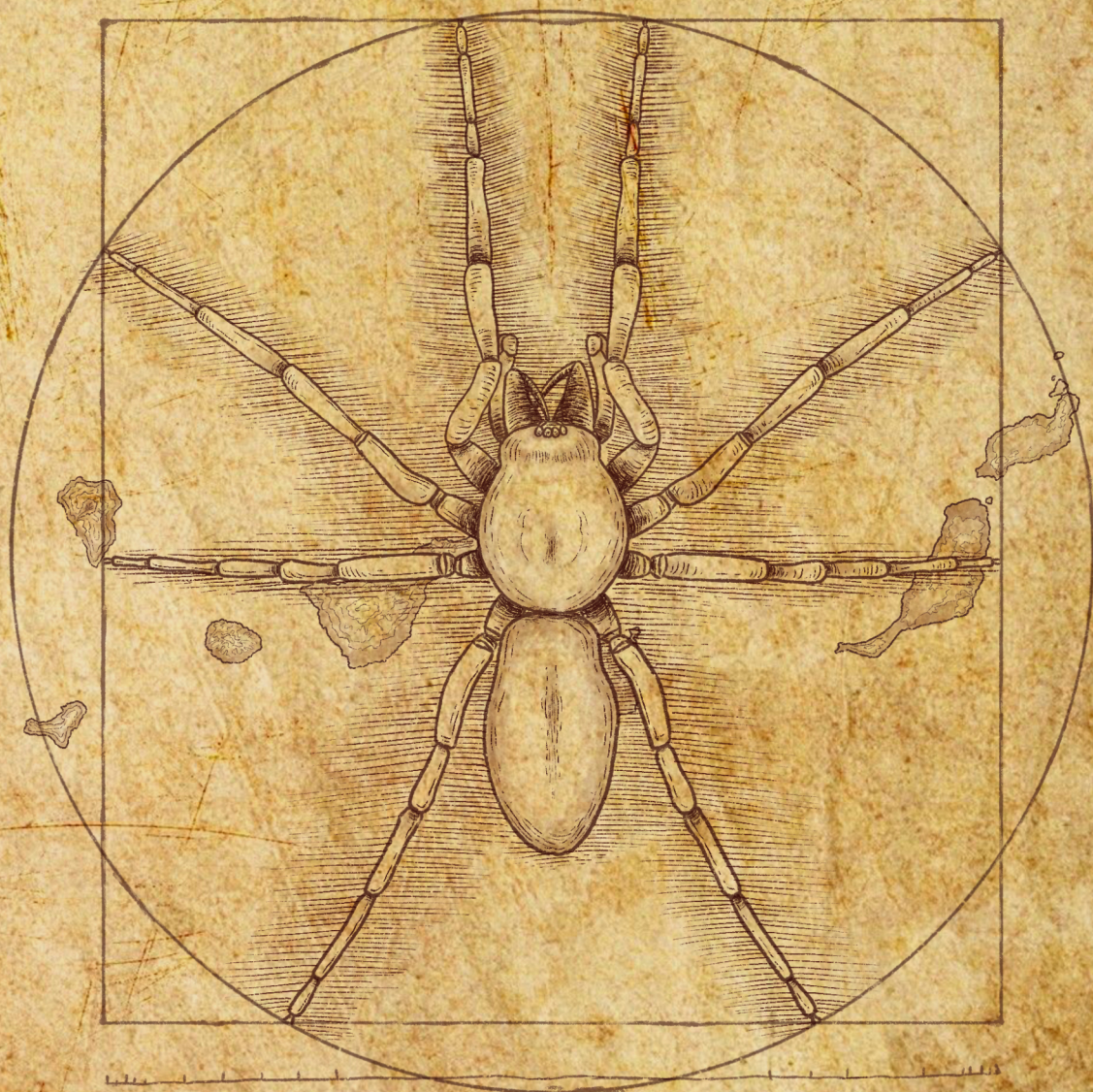
Aquesta tesi doctoral està subjecta a la llicència **Reconeixement 4.0. Espanya de Creative Commons.**

Esta tesis doctoral está sujeta a la licencia **Reconocimiento 4.0. España de Creative Commons.**

This doctoral thesis is licensed under the **Creative Commons Attribution 4.0. Spain License.**

TESTING THE HYPOTHESIS OF
ADAPTIVE RADIATION AND ITS
ECO-PHENOTYPIC IMPLICATIONS

ADRIÀ BELVERT





UNIVERSITAT DE
BARCELONA

Programa de Doctorat en Biodiversitat

Facultat de Biologia

Dept. de Biologia Evolutiva, Ecologia i Ciències Ambientals

Testing the hypothesis of adaptive radiation and its eco-phenotypic implications

Memòria presentada per

Adrià Bellvert Banti

per optar al grau de

Doctor per la Universitat de Barcelona

Doctorand:

Adrià Bellvert Banti

Director i tutor de la Tesi:

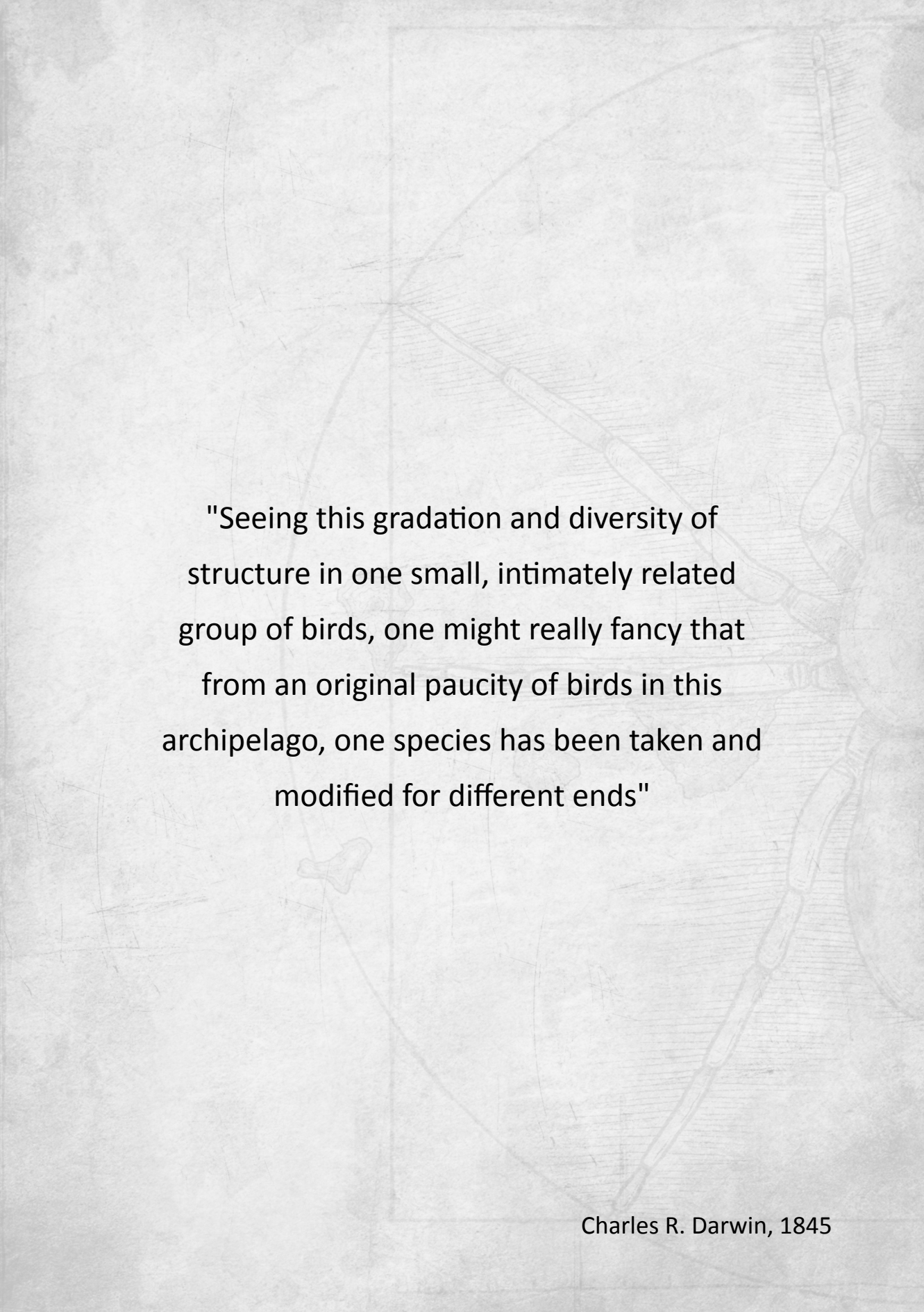
**Prof. Miquel Àngel Arnedo
Lombarte**

Professor catedràtic de la UB
Facultat de Biologia

Directora de la Tesi:

**Dra. Antigoni
Kaliontzopoulou**

Investigadora Ramon y
Cajal de la UB
Facultat de Biologia



"Seeing this gradation and diversity of structure in one small, intimately related group of birds, one might really fancy that from an original paucity of birds in this archipelago, one species has been taken and modified for different ends"

Charles R. Darwin, 1845

Agraïments

Tot i que els coneixements que aconseguies fent un doctorat indubtablement van en augment al llarg dels anys, el camí pel qual et porta és una muntanya russa d'emocions. Durant el temps que dura una tesi, experimentes molts moments de gran felicitat, però a vegades també et trobes amb moments d'estrès, frustracions i manca de son. Els moments alegres són els que et compensen tots els moments complicats, però és la gent que està al teu costat qui t'ajuda a superar-los. I és que amb l'experiència viscuda que he tingut durant aquests anys, he descobert que un doctorat va molt més enllà de la part acadèmica, que és més evident per a un observador extern.

És per això que els presents agraïments engloben un divers mosaic de persones que han contribuït tant des de la part més purament científica com a la meua capacitat d'afrontar emocionalment les parts més complicades. Tot i que considero que tant uns com altres han estat igual d'importants i que molts podrien entrar en ambdues categories, la llista ha de començar per alguna banda. No obstant això, si de mi depengués, tothom ocuparia el primer lloc.

Per començar, m'agradaria agrair als meus dos directors de tesi, en Miquel A. Arnedo i l'Antigoni Kaliontzopoulou, tot l'ajuda, suport i aprenentatge que he rebut per part seva. No hi ha dubte que sense ells ara no tindria el nivell científic que està a anys llum de l'estudiant inexpert que va arribar a Barcelona fa 8 anys. Tot i això, seria injust centrar-me únicament en la part acadèmica, ja que les cerveses, xerrades i fins i tot algunes "francesinhas" han proporcionat moments molt agradables.

A tota la gent que està o ha estat en el grup, agraeixo tots els bons moments que hem compartit. Des del Marc i les competicions internacionals (deixaré la frase aquí), a l'Alba pels consells, suport i sobretot les cerveses, i a la Silvia amb qui he descobert que un 10x és una cobertura força baixa. A Luís Carlos da Fonseca Crespo, a qui en la seva llengua materna m'agradaria dir-li "arriar u callao". Al Manu per la seva alegria i entusiasme. A la Martina i en Tin, a en Jesús, la Vanina i en Marcos pel seu ajut i consells. A en Carles i en Víctor, que sempre estan disposats a passar les tardes al Dakana. Sense oblidar-me del Jagoba, també pels seus consells i per l'elaboració de la meravellosa portada que encapçala aquesta tesi.

També m'agradaria donar les gràcies a la gent que m'ha acollit durant les estades de la meua tesi i als seus grups, com en Peter Michalik i la Laura Pollock, amb els quals he pogut veure més enllà de la meua universitat.

A tota la gent de la universitat que m'ha ajudat o simplement, i no és poc, m'ha alegrat la meua estada en aquesta institució, com la Jessica, la Maria José, en Carles, l'Humbert, en Cesc, en Juli i l'Eduardo, que també han sigut membres de la meua comissió de seguiment, la Marta, la Marina... Crec que aquesta llista podria ser molt llarga i ja demano disculpes a tots aquells que m'hagin deixat fora. En definitiva, vull expressar el

meu agraïment a tota la gent meravellosa que he tingut l'oportunitat de conèixer durant aquests anys.

També un agraïment a tota la gent de les Canàries, coautors i/o persones amb les quals he pogut compartir moments de camp tant en aquestes encantadores illes com en altres llocs on he tingut l'oportunitat de mostrejar, com la Nuria, en Pere, en Salva, en Jairo i tota la gent de La Laguna per la seva hospitalitat. I un calorós record al Mestro Pedro i en Valico.

També m'agradaria donar les gràcies als meus pares per tot el seu suport i sobretot per no perdre el cap quan el seu fill els hi va dir que es volia dedicar a les aranyes.

I finalment, però ni de bon tros menys important, a la meva parella, la Naouel, per haver estat al meu costat tant en els moments bons com en els més difícils.

Moltes gràcies i sabeu que aquest treball no hauria estat possible sense vosaltres.

Abstract

Without a shadow of a doubt, adaptive radiation processes have played a major role in our current understanding of how species evolved on our planet. Since the original proposal of the theory of evolution by natural selection was published by Charles Darwin and Alfred Wallace more than 150 years ago, examples of adaptive radiations have been extensively studied, particularly in oceanic islands. Because of their well-known geochronology, well defined boundaries, and simpler ecosystems when compared with continental regions, volcanic archipelagos had been referred as natural laboratories to study evolutionary or ecological process. The focus of this thesis is the spider genus *Dysdera*, which has undergone a remarkable diversification in the Canary Islands—a volcanic archipelago situated off the northwestern coast of Africa. The primary objective of this thesis is to test the hypothesis that the great diversification of the group was the result of an adaptive radiation process and gain insights into the drivers of their eco-phenotypic differentiation.

First, we conducted an integrative taxonomic revision of the group, employing a combination of molecular and morphological data. Our specific objectives were to determine whether DNA barcodes reveal the presence of previously overlooked lineages and help resolve any conflicts that may arise between different datasets. Additionally, we aimed to investigate whether species that are morphologically distinguishable can potentially be identified using DNA barcodes.

Second, using geometric morphometrics, we analysed various morphological structures of the spider body. Our goal was to establish a comprehensive guide for studying variation in the body plan of a non-model system. By integrating different views of similar phenotypic structures, we revealed that the different body parts analysed are interconnected, providing insights into various ecological factors. This research sheds light on the importance of considering multiple morphological characters when studying organismal variation.

Third, we have integrated geometric morphometric tools and experimental approaches with a fully resolved phylogeny. With that we have characterized the different cheliceral morphologies present in the archipelago and unveiled their dietary function. Additionally, we tested if they evolved multiple times independently during the diversification of the group and unveil if trophic specialization could be a case of irreversibility in the *Dysdera* spiders from the Canary Islands. We identified nine different cheliceral morphologies. We confirmed that some of these morphologies were indeed related to either “generalist” or “woodlice-specialized” diets. We provided significant support for the evolutionary convergence of cheliceral morphs in the context of an adaptive radiation. Finally, our results pointed towards the irreversibility of trophic specialization in these spiders.

Four, we investigated the diversification patterns and the role that trophic specialization played in this

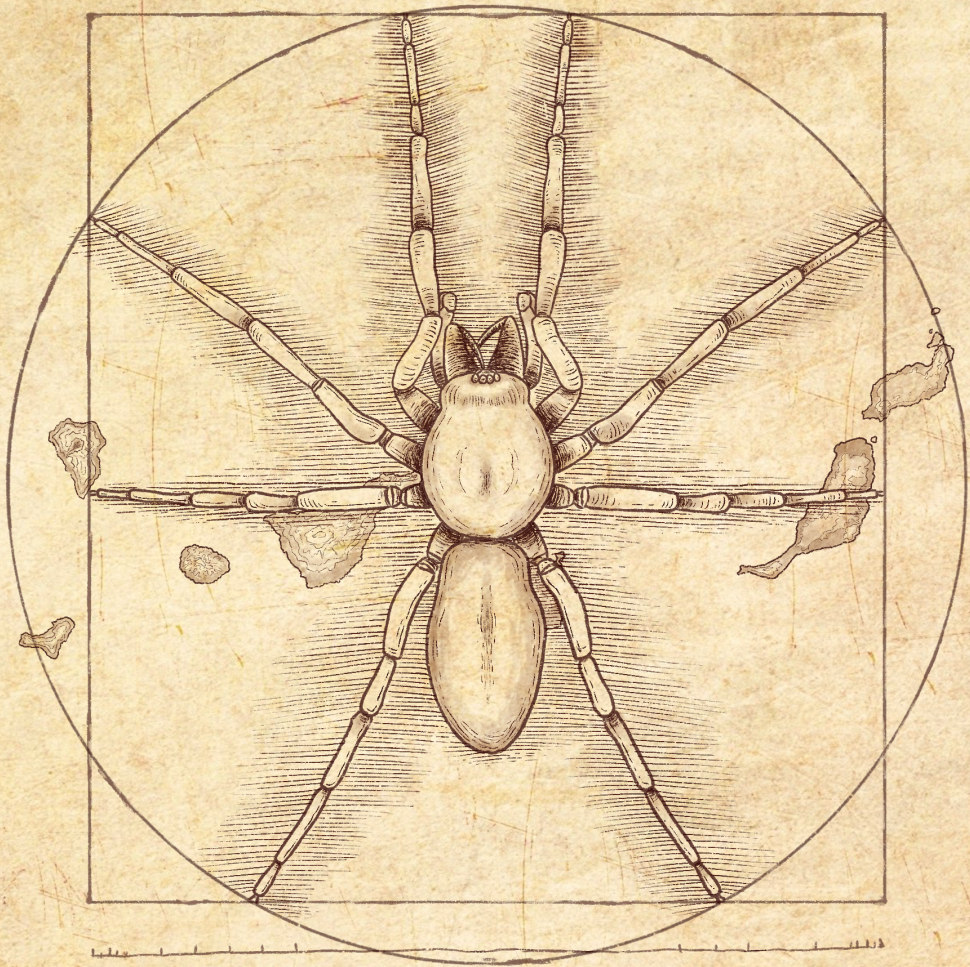
diversification. Additionally, with the use of climatic variables and occurrence data, we unveiled the underlying mode of speciation in the islands. Our results provide support for the hypothesis of adaptive radiation, showing an initial burst of diversification followed by a deceleration in diversification rates. We also found that trophic specialization played a significant role in shaping the diversification patterns within the group. Furthermore, our analysis suggests that speciation primarily occurred in allopatry, followed by secondary contact events.

Five, we tested whether species underwent an ecological release process following colonization of low competition environments. With that aim, we employed a multidimensional approach to evaluate various aspects of the species' ecological niche. Specifically, we considered trophic breadth, morphological disparity, and climatic and distributional range. Our findings demonstrate that the potential for experiencing an ecological niche release in Canarian *Dysdera* is strongly influenced by their trophic specialization. Specialist species exhibit the ability to expand their spatial range and trophic breadth to a greater extent compared to generalist species.

The present work provides compelling evidence supporting the *Dysdera* genus diversification as a case of adaptive radiation in the Canary Islands, and the ecological and evolutionary effects associated with their cheliceral morphology.

Index

INTRODUCTION	17
OBJECTIVES	47
SUPERVISOR'S REPORT	49
CHAPTER 1	53
CHAPTER 2	147
CHAPTER 2.1	149
CHAPTER 2.2	167
CHAPTER 3	205
CHAPTER 3.1	207
CHAPTER 3.2	241
GENERAL DISCUSSION	281
CONCLUSIONS	297
REFERENCES	301
APPENDICES	319
APPENDIX 1	321
APPENDIX 2.1	345
APPENDIX 2.2	349



INTRODUCTION

Introduction

1. Evolution, adaptive radiations, and oceanic islands

Species evolve. The idea that species are independent units not related to each other, which was historically promoted by religious beliefs and/or ignorance, gave way to more rational and scientific approaches that seek to explain the extant biodiversity that surrounds us, a science known as evolutionary biology. While some of the current ideas in evolutionary biology can be traced back to ancient Greece, such as Anaximander's proposal that humans descended from fishes, these types of myths cannot be viewed as precursors to scientific evolutionary theories (Futuyma 1998). It was not until the beginning of the seventeenth century that some of the first views close to the modern understanding of how species evolve started to flourish. One of the earliest and most prominent modern approaches to the concept of evolving species was best exemplified by the French naturalist Jean-Baptiste Pierre Antoine de Monet chevalier de Lamarck, who more than 200 years ago proposed that species were not immutable (Lamarck 1809), but rather changed towards more perfected beings through the individual improvement of specific organs that would then be inherited by their descendants. This concept is known as the inheritance of acquired characters (Koonin & Wolf 2009). However, Lamarck's conclusions have since been thoroughly disproven. It was only 50 years after the publication of this theory that two scientists, Charles R. Darwin and Alfred R. Wallace, parallely laid the foundations of the theory of evolution by natural selection that we know today.

Although over 150 years have passed since the modern foundations of our current understanding of evolution were established, comprehending the influence of species ecology on evolutionary and historical processes remains a major challenge (Lessard *et al.* 2012). A large amount of the underlying general patterns of how species evolve are still beyond our comprehension. Evolution is complex, multifactorial, and has

unfolded over hundreds of millions of years, forming a continuum of large temporal and spatial scale processes, which greatly complicates our understanding of the origins of biodiversity (Gillespie 2016). However, after the publication of the theory of island biogeography (MacArthur & Wilson 1967), islands and other isolated biotas began to be viewed as useful natural experiments for understanding evolutionary, ecological, and biogeographical patterns, which contrast with the more complex and deeper in time processes that shape the patterns found in continental regions. These isolated systems have well-defined boundaries, relatively simple ecosystems, and well-known geo-chronologies, which help to simplify the inherent complexity of the species' eco-evolutionary history. It should be noted that islands in a broad ecological sense encompass all environments suitable for a given species that are surrounded by unfavorable conditions which limits their dispersal abilities (Brown 1978), such as mountain tops or glacial lakes. Additionally, oceanic islands, such as hot-spot archipelagos (i.e., island chains that are the combined result of a volcanic hot-spot on the oceanic crust and tectonic movement), provide independent snapshots of the evolutionary process (Gillespie & Roderick 2002). Not surprisingly, both Darwin in the

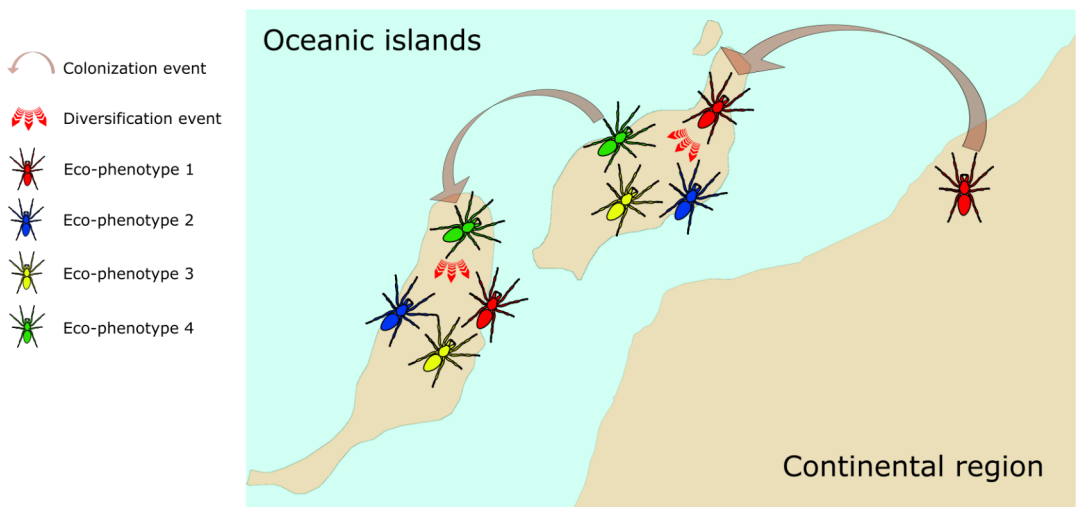


Figure 1. Graphical representation of a hypothetical species under a process of adaptive radiation in an oceanic archipelago. Different colors represent the species' different phenotypes related to ecological pressures. The colonization of a different island which have similar habitats than the first colonized island, leads species to adapt similarly independently.

Galapagos (1859) and Wallace in Indonesia (1881), extracted their conclusions from observations of the fauna and flora found in these insular environments.

Evolutionary radiations, or periods of accelerated species diversification, have been a prominent feature of life's history on Earth (Linder & Bouchenak-Khelladi 2017). Among these, adaptive radiations have garnered significant attention due to their importance in shaping the planet's biodiversity (Harmon *et al.* 2010) and shed light on the link between evolution and ecology (Givnish & Sytsma 1997). Typically, adaptive radiations are characterized by the evolution of eco-phenotypically distinct species from a single common ancestor (Futuyma 1998; Schluter 2000; Losos 2010), and the fast synchronous diversification of lineages after the colonization of a new environment, which slows down as ecological niches are filled (Glor 2010). The study of adaptive radiations has greatly contributed to understanding the mechanisms that drive speciation and promote eco-phenotypic diversification, along with many other related ecological and evolutionary processes (Gillespie *et al.* 2020). Although this process has been observed in various environments, young and isolated regions such as volcanic archipelagos offer ideal conditions for studying these phenomena (Schluter 2000) (Fig. 1). For this reason, the most prominent cases of adaptive radiation have been studied in such environments (Harmon *et al.* 2010; Patton *et al.* 2021; Cerca *et al.* 2023) such as the Hawaiian silverswords (Purugganan & Robichaux 2005), the Darwin's finches from the Galapagos (Lack 1947) or the anoles lizards in the Caribbean (Losos 2009).

However, while many species diversifications on islands can be defined as adaptive radiations, not all of them can be classified as such. In the past, some island species proliferations have been mistakenly referred to as adaptive radiations without investigating whether they were truly adaptive or not. These nonadaptive radiations involve lineages of species that show little or no ecological divergence (Czekanski-Moir & Rundell 2019). One example is the Hawaiian spider genus *Orsonwelles* Hormiga,

2002, whose diversification occurred due to geographical isolation from the sequential colonization of islands in the archipelago. As natural selection does not play a significant role in their evolution, sister species in this group are ecologically similar and differ only in their phenotypic characters due to the random accumulation of changes after differentiation, which is evidenced by a strong phylogenetic signal in their character data (Hormiga *et al.* 2003).

Additionally, although the definition of adaptive radiation may seem well established, different interpretations of patterns that sustain a species' diversification under this process can be problematic, as some distinctive features may be absent, while others that are not essential may be included (Givnish 2015). For instance, some authors have claimed that under adaptive radiation species emerge in a short period of time (Soulebeau *et al.* 2015), but evidence shows that some adaptive radiations evolve over extended time periods (Nilsson *et al.* 2010), which has been recognized as a possible scenario since the original definition of adaptive radiations (Simpson 1953). Moreover, our understanding of the underlying mechanisms of these phenomena remains incomplete. While the evolution of ecologically and phenotypically distinct species from a common ancestor is a hallmark of adaptive radiations (Futuyma 1986), few other common patterns have emerged from studies of these processes. For instance, the link between lineage and phenotypic diversification has not been found in some adaptive radiation cases (see Pincheira-Donoso *et al.* 2015). The typical signature in adaptive radiations of an early-burst followed by a slowdown in lineage diversification (Phillimore & Price 2008; Rabosky & Lovette 2008; Harmon *et al.* 2010) has failed to find support in some cases (Slater *et al.* 2010), indicating that the dynamics of adaptive radiations may be more complex than previously thought. Furthermore, the triggers of the diversifications remain unclear. While theory predicts that ecological opportunities promote species' lineage diversification (Losos 2010; Pincheira-Donoso *et al.* 2015), and the historically widespread belief was that

speciation was mainly accomplished by geographical isolation (Mayr 1963), no general consensus exists regarding the early stages of adaptive radiations. Consequently, an increasing amount of efforts have been put on characterizing the temporal, spatial, and genetic/morphological patterns in adaptive radiations (see Gavrillets & Losos 2009). In this context, additional model systems including different ecological pressures are needed to test the species' response to one of the most influential processes of species evolution on our planet.

After considering the aforementioned points, the question that arises is how to demonstrate that a presumed species lineage diversification is indeed an adaptive radiation. Moreover, one should consider which phenotypic characters should be examined as relevant in this radiation and what ecological and diversification patterns are associated with it. The focus of the present thesis is to address these questions using the species of the highly diverse spider genus *Dysdera* endemic to the Canary Islands as a model system.

2. Species' boundaries and their phylogenetic relationships

To ensure accurate results in any evolutionary study, it is crucial to have a proper and unbiased delimitation of the target species, as under- or biased species sampling may lead to erroneous outcomes in various analyses, such as estimation of time divergence (Beaulieu *et al.* 2015), ancestral character reconstruction (Li *et al.* 2010) or the inference of diversification dynamics (Fitzjohn *et al.* 2009). The definition of a species has long been a challenging issue in biology, with different proposals put forward (Mallet 1995). Nonetheless, the concept of metapopulations that evolve independently from each other seems to have gathered all the aspects of what we can consider that define two separate species. However, how can we identify these independent evolved lineages? Historically, species delimitation was based solely on morphological differences. However, this approach was often hampered by biological

factors such as polymorphic or cryptic characters, leading to either over-splitting or overlooked species. The advent of molecular techniques introduced new tools for delimiting animal species that provide more objective and reliable criteria for distinguishing two distinct species compared to previous approaches, which relied solely on the expertise of the taxonomist describing the group.

A popular technique for delimiting species has been the use of short-standardized mitochondrial DNA sequence fragments, the DNA barcoding, which has been extremely useful for species delimitation (Hubert & Hanner 2016) or discovery (Matz & Nielsen 2005). However, due to the inherent limitations of relying solely on a single marker of maternal inheritance, several alternative methods have been developed to address the issue of taxonomic uncertainty. These include the Barcode Index Number (BIN) assignment (Ratnasingham & Hebert 2013), the distance-based ASAP model (Puillandre *et al.* 2021), the character-based mPTP model (Kapli *et al.* 2017) or the GMYC, which use a species ultrametric tree to perform the delimitation. Nevertheless, these methods are not immune to bias and may produce varying results depending on the assumptions made. To minimize the potential for bias, it is common practice to use multiple methods in taxonomic revisions. However, these methods have not been exempt of drawbacks (Rubinoff 2006), as the results of a single marker of maternal inheritance can be compromised by all the multitude of processes involved in the species speciation, and the use of nuclear markers is advised. In addition, incomplete lineage sorting as a result of recent speciation times, and short coalescent times and large effective population sizes (Maddison 1997), can result in scenarios under which the gene tree is not expected to accurately reflect the species tree. For this reason, when using mitochondrial genes only for species delimitation, as usually done with the Cytochrome c Oxidase subunit 1 (COI), the combined use of molecular and morphological criteria to perform a species group revision, could provide more reliable outcomes compared when these two techniques are applied separately.

Another important aspect in evolutionary studies is to understand how these species are related to each other. Early phylogenies based on Sanger sequencing of single or a few markers outperformed those based solely on morphological characters (Aguinaldo *et al.* 1997). With the more modern nucleotide sequencing technologies, longer genetic data was able to be incorporated into phylogenies recovering more robust species relationships. However, although the cost of obtaining these genetic data has been reduced considerably, obtaining the whole genomic information of all the species in a studied group is not always feasible. In addition, the information provided in Sanger sequencing could be relevant for ecological and evolutionary processes (Fernández *et al.* 2018; Macías-Hernández *et al.* 2020) and some studies has proven that the combination of Sanger information with genomic data have improved the systematics and evolutionary knowledge of certain studied groups (Azevedo *et al.* 2022). For this reason, including different sources of genetic information, even if some of them are incomplete, could contribute to more accurate hypothesis of the species relationships.

3. Eco-phenotypical properties of species

After characterizing how many species exist in the studied group, the next step is to investigate whether their diversification was driven by natural selection and which ecological pressures influenced their divergence. Specifically, researchers may ask whether the diversification represents an example of adaptive radiation and what anatomical features have been influenced by ecological pressures, a hallmark of such radiations. To answer these questions, various methods can be used, such as comparative analyses of morphological and ecological traits, statistical modeling of trait evolution, and tests of convergence and divergence among species. However, the first step would be to select the phenotype(s) which we hypothesize are influenced by specific ecological pressures throughout the history of the group, something that in non-model organisms is not always straightforward.

3.1 The choice of ecologically relevant characters and the use of geometric morphometric tools

The impact of natural selection on phenotypic traits has been extensively studied in the scientific literature (Andersson 2009). Morphological features that improve an organism's performance in its environment, through adaption to specific ecological requirements, are known as functional traits (McGill *et al.* 2006). However, species are not subject to a single ecological pressure, but rather to a n dimensional hypervolume that define their fundamental niche (Hutchinson 1957). Despite the progress made in understanding the effects of selection on individual traits, there is still much to learn about how selection operates on the multivariate phenotype (Blankers *et al.* 2017). Therefore, to understand the morphological differentiation among different species, a multidimensional phenotypic approach is needed (Guillerme 2018), and to infer the evolutionary pressures that have driven such differentiation we need to know how phenotypes and their function relate with their ecological environment.

In addition, ecological traits that are shaped by different evolutionary pressures are not completely independent of each other, as organisms function as a whole system (Klingenberg 2009). However, the degree of covariation between traits can vary depending on the relationships between different body parts (Olson & Miller 1958). Traits with higher levels of covariation (i.e., integration) form composite units, or modules, that are affected by more similar evolutionary pressures compared to other body parts. These modules are interconnected and form the whole body of an organism, which needs to function in a coordinated manner, where changes in one trait can inevitably lead to changes in others (Adams 2016). The integration of different modules can arise due to various reasons, including genetic, developmental, functional or evolutionary factors (Klingenberg 2008a). A consequence of trait integration is that determining whether certain phenotypes have been shaped by specific evolutionary pressures or whether trait variation emerges as a result of co-

evolution with other interconnected modules is not always straightforward. Thus, understanding which sets of traits show high covariation is crucial to discern the different biological factors that may explain their evolution.

Characterizing certain phenotypes and retaining this information for downstream analyses can be challenging. Morphometrics is the research field that aims to characterize shape variation and its relation with other variables (Bookstein 1991). Traditionally, this was achieved by means of multivariate analyses of linear measurements of the structures of interest (Fig. 2A), although sometimes ratios or angles were also used (Rohlf & Marcus 1993). Those were the so called “traditional” morphometrics. However, differences in linear measurements of a specific structure

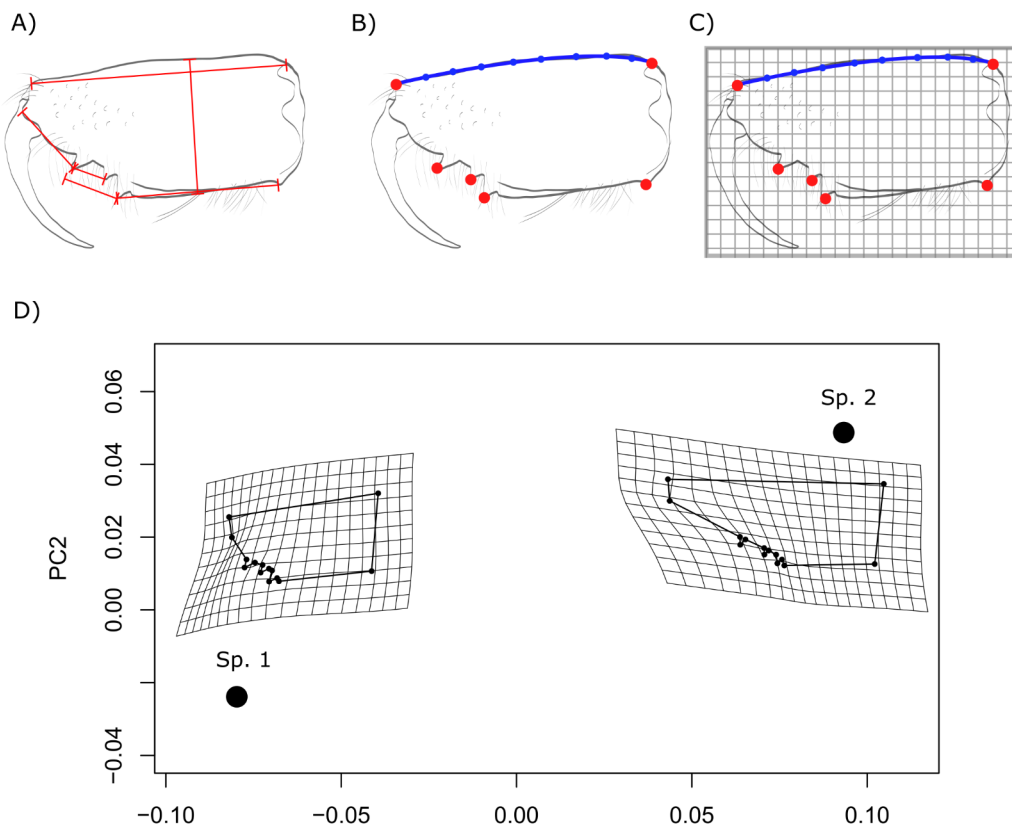


Figure 2. A) Example of traditional morphometrics with multiple linear measurements to capture variation in shape of a structure of interest. B) Same previous structure but with the landmarks (red dots) and semi-landmarks (blue line) used for the study of shape variation with geometric morphometrics. This method uses a system of cartesian coordinates system (C) to calculate shape differences between the specimens or species analyzed (D).

or organism, had been seen to be highly correlated with size in linear morphometrics (Humphries *et al.* 1981), and although many efforts were made for size correction (Sundberg 1989; Jungers *et al.* 1995), no standardized agreements have been reached (Adams *et al.* 2004).

One solution to the aforementioned problems is the use of geometric morphometrics, which differs from traditional morphometrics by using two- (or three-) dimensional landmark and semi-landmark coordinates instead of linear measurements (Fig. 2B). This method quantifies shape variation based on the relative position of these landmarks in a cartesian coordinate system (Fig. 2C-D). To remove all variation between landmarks related to orientation, position and scale, superimposition methods are applied, aligning the landmark coordinates according to some optimization criterion, among them the known as Generalized Procrustes Analysis (GPA, Rohlf & Slice 1990). The result is the mathematical removal of all non-shape information, including size (Adams *et al.* 2004). Several software packages can be used to apply this methodology, such as MorphoJ (Klingenberg 2008b) or the TPS series packages (Rohlf 2015). However, the package “geomorph” (Collyer & Adams 2018; Adams *et al.* 2021; Baken *et al.* 2021), implemented in the R statistical environment (R Core Team 2022), allows for a better integration of morphometric data with other non-morphological information and implements most cutting-edge techniques in the field of morphometrics. In addition, this package allows the combination of different structures’ landmark configurations (Collyer *et al.* 2020) and tests the integration between them (Adams & Collyer 2016, 2019). By using this method, in combination with knowledge on the ecology of different species and after selecting the phenotypic structures that compose the relevant body parts of an organism, we can unravel the relationship between ecology and morphology and the level of integration and co-evolution between these different structures.

3.2 Testing the hypothesis of adaptive radiation and the phylogenetic comparative method.

A common underlying pattern of adaptive radiation processes is the rapid synchronous diversification of lineages and phenotypes (Glor 2010). Moreover, similar phenotypic outcomes are frequently during the evolutionary history of the group (Fig. 1). The explanation for such patterns lay in the similar ecological regimes of newly colonized environments by not closely related species which triggers similar adaptive responses in their traits (Rundle *et al.* 2000; Schluter 2000; Brakefield 2006; Losos 2011), producing remarkably similar phenotypes (Losos *et al.* 1998). This can result in species clades with homoplasy in their phenotypic characteristics, a phenomenon known as repeated evolution, which englobes the two previous concepts (see Cerca 2022 for a review in the topic). This is the main point that distinguishes between adaptive and non-adaptive radiations: in the later, ecological pressures are not the main driver in the diversification, which leads sister species to be more similar between them. However, how the ecological influence can be tested in a specific study group? The study of species evolution has traditionally relied on the comparative method, which involves analysing the co-variation of phenotypic traits and ecological characteristics of interest, across a selected group of species (the comparison of phenotypes with other phenotypes, environmental variables, chromosome numbers, etc.). However, because species share a common evolutionary history and thus are not independent from one another, assuming independence in statistical methods can lead to misleading results (Felsenstein 1985). Solving this problem resulted in the development of phylogenetic comparative methods, which utilize the species' phylogenetic relationships to infer evolutionary patterns in their traits (Harvey & Pagel 1991; Pennell & Harmon 2013). These methods allow us to investigate the tempo and mode of the species evolution (Simpson 1944), and to test hypotheses about the relationship between ecology and morphology in the context of an evolutionary radiation.

Species are constantly evolving, but they are not always exposed to the same ecological pressures or evolve at the same rate. Some species, as seen in non-adaptive radiations, may diversify due to geographical isolation yet maintain the same ecological requirements. In such a scenario, and due to the stochastic accumulation of random changes, closely related species are expected to be more similar between them than with distantly related ones. This is known as a Brownian motion model of evolution (Hansen & Orzack 2005). Conversely, if species are subject to different ecological pressures, this is expected to be reflected in their phenotypes. In such a case, ecologically similar species will be more similar to other species that have faced similar selective pressures, even if they are less closely related. These patterns can be detected using statistical methods that account for the evolutionary history of species, such as the quantification of phylogenetic signal, which measures the degree to which a trait's value depends on phylogenetic relationships (Revell *et al.* 2008). When species differences are due to the stochastic accumulation of random mutations and closely related species are more similar than the distant related ones, high phylogenetic signal will be observed, meaning that the species differences are correlated with their phylogenetic relationships. This is expected under a Brownian

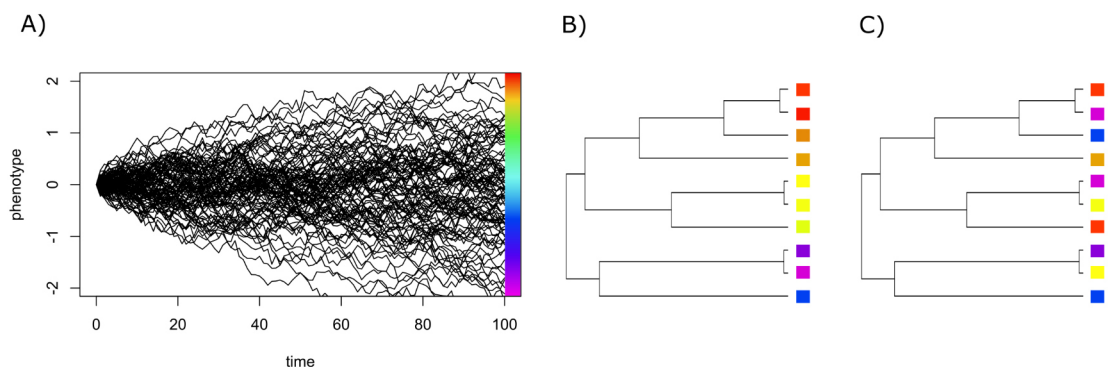


Figure 3. A) Example of the possible variation of a phenotype through time under a Brownian motion stochastic model, with a mean value of 0 and an increasing variance depending on time. A species diversification under this model will show closely related species to be more phenotypically similar than distantly related ones B). This is due to the fact that no selective pressures are affecting this phenotype, and its variation depends on time since divergence between species pairs. C) Alternatively, if distantly related species are under similar ecological pressures that affects the selected species trait, distantly related species will be more similar compared with the closely related ones.

model of evolutionary change through time (Revell & Harmon 2022) (Fig. 3A-B). However, in adaptive radiations, where the repeated independent evolution of similar adaptive phenotypes is a common pattern (Losos *et al.* 1998), phenotypic differences or similarities among species may not be correlated with phylogenetic relationships (Fig. 3C), which translates into a weak phylogenetic signal.

Two main approaches are available to statistically test for phylogenetic signal, Pagel's λ and Blomberg's K (Blomberg *et al.* 2003), although there are alternative methods (see Münkemüller *et al.* 2012 for a review). The main difference between Pagel's λ and Blomberg's K is that the first transforms the phylogeny to ensure the best fit of trait data to a Brownian motion model, while the second is based on comparing the mean and mean squared error between the expected data under a Brownian motion model of evolution, and the observed data given their phylogenetic relationships (Münkemüller *et al.* 2012). Several R packages provide functions to perform these tests, such as "picante" (Kembel *et al.* 2010) or "phytools" (Revell 2012). However, Pagel's λ is not implemented for multivariate geometric morphometric data and currently only the Blomberg's K can be tested with the "geomorph" package ; Adams *et al.* 2021; Baken *et al.* 2021). However, despite the low phylogenetic signal that is typically found in a trait of a species clade that has undergone an adaptive radiation, this does not necessarily suggest a convergent evolution of characters. The importance of identifying the repeated evolution of a trait in a given species clade, is capital to differentiate a group with ecomorphological differences among species, from an adaptive radiation (Stayton 2015a). To date, few softwares provide significance values to test for convergence, e.g. SURFACE (Ingram & Mahler 2013), the Wheatsheaf index (Arbuckle *et al.* 2014) or the R package "convevol" (Stayton 2015b, 2018). The last software provides different metrics which show complementary views on how exceptional the similarity between two taxa is. This is done by considering the ratio between the phenotypic distance between the

two potentially convergent taxa and the maximum distance observed between any pair of taxa (either ancestral or extant) across the evolutionary history of these lineages. In addition, phylogenetic comparative methods can also shed light on other patterns related to adaptive radiations. As explained previously, one typical diversification pattern observed in adaptive radiations, although not always a prerequisite (Givnish 2015), is an early burst in species lineages, followed by a slowdown in their speciation rates (Phillimore & Price 2008; Losos & Mahler 2010). This has been interpreted as the early occupation of niches in the early stages of colonization, followed by a decrease in the rate of speciation once those niches are filled (Schluter 2000; Gavrillets & Vose 2005). Phylogenetic comparative methods can provide valuable information not only about the speciation patterns but also the extinction rates in a species group. Two simple methods that rely only on the information provided by a time-calibrated phylogeny are the lineage-through-time (LTT) plots and the γ statistic (Pybus & Harvey 2000). The LTT plot represents the accumulation of lineages through time. Under a constant-rate process of stochastic speciation without extinction (i.e. a *pure birth* model, REF), species lineage accumulation will be constant from the early ages of the phylogeny to the more recent distal tips. However, if the species group has undergone an early burst of higher diversification rates in the first stages of their speciation, the LTT plot will show an initial increase with a posterior stabilization. Conversely, if speciation rate has increased in the more recent part of the phylogeny, an exponential pattern known as the "pull of the present" will be observed. This pattern is linked to past extinction events and subsequent recovery of species richness. Complementary to these plots, the γ method provides significance values by converting observed patterns to a summary statistic that can be compared to *pure birth* (Nee *et al.* 1994). The R package "phytools" (Revell 2012) offers easy-to-use functions to perform these analyses.

Another relevant point is that species diversification dynamics can be influenced by

specific traits known as "diversifying traits" that can increase diversification in specific lineages (Miller *et al.* 2023). Although not necessary, the evolution of these traits, along with key innovations that allow species to occupy new ecological niches, has been traditionally considered a core component of adaptive radiations (Simpson 1953). Phylogenetic comparative methods can also provide valuable information about whether speciation or extinction in a specific clade has been influenced by specific traits. There are numerous statistical methods available to test the influence of traits on species evolution, such as the State Speciation and Extinction (SSE) models. In its simpler version, the Binary State Speciation and Extinction (BiSSE) model (Maddison *et al.* 2007), phylogenetic relationships are used to test if the diversification of a group of species is dependent on a specific binary trait. This method compares a null model where the phylogenetic tree evolves under a birth-death process without influence from the trait to an alternative model where diversification depends on the value of the binary trait (Maddison *et al.* 2007; Revell & Harmon 2022). Additionally, the BiSSE model can provide information about what state of the character influences the diversification of the species. The R package "diversitree" (Fitzjohn 2012) includes several versions of the SSE models, including quantitative, multistate, or geographic characters. However, as mentioned earlier, evolution is complex and multifactorial, and speciation can be influenced by unaccounted traits, either as the main diversification drivers or complementing the effects of the target trait (Beaulieu & O'Meara 2016). When testing against a null model that assumes constant speciation and extinction rates, a state-dependent model may perform better, but the challenge lies in identifying whether the variation in rates is due to the target character or other unaccounted factors (Rabosky & Goldberg 2015). One proposed solution is the use of hidden-state speciation and extinction models (HiSSE, Beaulieu & O'Meara 2016), which fit models that take into account state-dependency of diversification rates based on one or several unaccounted factors, or even more complex models that consider the combined effect of unaccounted factors and the target characters. The R

package "hisse" (Beaulieu & O'Meara 2016) provides functions to fit these model combinations.

4. Speciation patterns and their ecological outcomes

As mentioned earlier, adaptive radiation refers to the diversification of ecophenotypically diverse species from a single common ancestor. So far, we have discussed how to test if the evolution of a given lineage follow the expected early burst pattern expected from an adaptive radiation model and identify the drivers promoting this diversification. However, a crucial question arises: how do these cladogenetic events, where a single species gives rise to two distinct populations or metapopulations that eventually become separate species, initiate? What processes lead to the divergence of populations? Historically, allopatric speciation, which typically involves the geographical isolation of a population either by the rising of barriers or colonization of new areas and time to diverge, was considered the primary mode of speciation (Mayr 1963). This mechanism contrasts with ecological speciation models, which occurs by the direct involvement of natural selection without the need for geographical separation of populations. (Bolnick & Fitzpatrick 2007). So how can we test the main mode of speciation in a given group of organisms? How can we capture the complex speciation events that may have been influenced by various factors? And finally, what are the species ecological consequences of colonizing a new habitats?

4.1 Testing diversification patterns: Age-range correlations and joint species distribution modelling

There is currently no consensus regarding the role of geography in adaptive radiation (Matsubayashi & Yamaguchi 2022). As a result, there is a need for statistical tests that can help disentangle the types of biogeographic distributions that precede cladogenetic events. Furthermore, the interaction and complex combination of

different mechanisms in an adaptive radiation can often impede our understanding of how species have diversified. For example, a common pattern observed in adaptive radiation is allopatric speciation followed by ecological divergence in sympatry (Stroud & Losos 2016), which results in extant species with a sympatric distribution despite having originated allopatrically.

The age-range correlation (ARC) method has been employed to address these issues. This method hypothesizes that the range overlap between two species will initially depend on the geography of speciation, but will become randomized over time due to distributional shifts, resulting in a statistical relationship between time since divergence and range overlap (Lynch 1989; Barraclough 1998; Barraclough & Vogler 2000; Berlocher & Feder 2002; Fitzpatrick & Turelli 2006). It also sustains that the overlap between ranges of two different species will eventually become unrelated to their original geographic context of speciation, and rather reflect the independent biogeographic movements they have experienced throughout their evolutionary history after divergence. A commonly used R package for performing these analyses is "phyloclim" (Heibl & Calange 2018), which integrates phylogenetics and climatic niche modeling. However, estimating species ranges is not always straightforward. Species distribution modeling (SDMs) provides an efficient method for estimating species ranges that can be used to calculate the overlap between species pairs. SDMs combine species occurrence data with environmental characteristics of the sampled localities as predictors to characterize the natural distributions of species (see Elith & Leathwick 2009 for a review). However, these methods only consider abiotic interactions and do not account for biotic ones, which are equally important (Ospovat 1981). An alternative method that can capture all the species interactions, including those unrelated to climatic predictors, is joint species distribution modeling (jSDM). This approach decomposes the patterns of occurrence explained by abiotic factors and residual patterns of co-occurrence, which represent species interactions that

cannot be explained by the climatic environment (Pollock *et al.* 2014). In cases where the distributional range of species cannot be solely explained by climatic conditions, the residual correlations may provide better predictions of species interactions, and subsequent evolutionary questions should be addressed using these data rather than relying solely on environmental responses. R packages such as "jSDM" (Clément & Vieilledent 2022) and "Hmsc" (Tikhonov *et al.* 2020, 2022) provide functions for performing these analyses.

4.2 The colonization of new environments and ecological release

Allopatric speciation is a common pattern in adaptive radiations, particularly in oceanic archipelagos where speciation may occur on different islands (Stroud & Losos 2016). When a population of a species, either through its dispersal ability or by random geographic events, colonizes a different island with lower competition or predatory levels compared to its original distribution, it may encounter new ecological resources that can be exploited, which is known as ecological opportunity. This can lead to a relaxation of selective pressures that the species was previously subjected to (Losos & De Queiroz 1997; Yoder *et al.* 2010; Des Roches *et al.* 2015), resulting in an expansion of the species' niche. This phenomenon is referred to as ecological release. As a result of the relaxed selection, the colonizing population may exhibit changes in habitat, population density, phenotypic disparity, and/or resource usage (MacArthur *et al.* 1972; Bolnick *et al.* 2007; Parent & Crespi 2009; Gillespie 2020). However, while a species' niche involves multiple ecological axes (Hutchinson 1957), most studies usually focus only on one of them (e.g. Buckley & Jetz 2007; Parent & Crespi 2009; Andrades *et al.* 2019; Battey 2019), and the response of different aspects of species ecology during an ecological release event remains poorly explored.

An increase in phenotypic disparity, or directional change in species morphology, both possible consequences of ecological release, can be easily quantified using morphometric data (Foote 1993; Collyer & Adams 2013), even in high-dimensional

datasets produced by geometric morphometric methods (Collyer *et al.* 2015). The R package "geomorph" (Adams *et al.* 2021; Baken *et al.* 2021), as mentioned earlier, provides useful and easy-to-implement functions for performing statistical tests to assess changes in morphology between selected groups. However, addressing changes in other niche axes that may be affected by ecological release can pose more challenges.

Inferring the complete distribution of a species is often hampered by undersampling, particularly in the case of small mobile organisms like arthropods, as compared to immobile organisms like plants or large mammals, which have better-known distributions due to their traceability. Predictions made by SDMs can then be used to assess changes in spatial range between species or groups occurring in situations like colonization events, which facilitates testing hypothesis of ecological release. In R, there are several packages that can perform SDMs, such as "dismo" (Hijmans *et al.* 2022), which implements various models and provides functions that can be used in conjunction with other packages, such as "gam" (Hastie 2022), which offers tools for fitting and working with generalized additive models.

Another important aspect of a species' niche easily affected by ecological release is that of trophic preferences. However, quantifying the trophic niche of species has not always been straightforward. In the past, direct observations or gut content analyses have been used to determine species' diets. However, these methods may not be feasible in some organisms such as spiders that feed on liquified preys (Pompanon *et al.* 2012). Molecular methods, such as metabarcoding, have improved diet analyses for species that pose challenges in data gathering due to their size or feeding behavior (e.g. Macías-Hernández *et al.* 2018; Kennedy *et al.* 2019; Novotny *et al.* 2021; Ortiz *et al.* 2021). However, issues such as the presence of endosymbionts, degraded DNA, or the prevalence of predator DNA rather than prey DNA in samples have hampered the use of this technique. Stable isotope analyses have been

recognized as a useful approach to address questions about species' trophic niche space (Newsome *et al.* 2007). Ratios of different isotopes, such as Carbon C13 and Nitrogen N15, have been shown to provide information about the type of diet and trophic level of species in terrestrial fauna (Bearhop *et al.* 2004). Incorporating metrics such as standard ellipse area (SEA) has simplified the assessment of changes in trophic niche breadth (Jackson *et al.* 2011). The R package "SIBER" (Jackson *et al.* 2011) enables the calculation and comparison of ellipse areas using Bayesian inference based on isotopic data.

5. The study system

5.1 The Canary Islands

The Canary Islands are an archipelago of volcanic origin located in the northeast of the Atlantic Ocean, between 27° and 29° N, and 13° and 18°W, approximately 100 kilometres off the northwest coast of Africa (Fig. 4A). Together with the Azores, Cabo Verde, Madeira, and Selvagens, they form the biogeographic region known as "Macaronesia," although this definition is currently under discussion (Freitas *et al.* 2019). The archipelago is composed of seven major islands, which are geochronologically arranged due to the movement of the tectonic plate above a volcanic hotspot. The oldest islands, Lanzarote and Fuerteventura (15 million years and 23 million years, respectively), are located at the easternmost side, while the islands become progressively younger towards the western side (Fig. 4A), from east to west: Gran Canaria (subaerial age 15 million years), Tenerife (12 million years), La Gomera (11 million years), La Palma (1.7 million years), and El Hierro (1.1 million years) (Van Den Bogaard 2013).

The smaller islands are located in the westernmost part of the archipelago, with El Hierro covering an area of 278 km² and reaching an altitude of 1500m, La Gomera covering 378 km² and reaching an altitude of 1487m, and La Palma covering 700 km²

and reaching an altitude of 2426m. The larger islands in the archipelago are Lanzarote, covering 795 km² with an altitude of 607m, Gran Canaria, covering 1532 km² with an altitude of 1949m, Fuerteventura, covering 1732 km² with an altitude of 807m, and Tenerife, covering 2052 km² with an altitude of 3718m (Troll & Carracedo 2016). The Canary Islands exhibit a pattern in both area and altitudinal range that is commonly observed in hotspot archipelagos, showing an increase in both factors with time, reaching a peak of maximum topographic complexity in the middle-aged island of Tenerife, followed by a decrease in area and altitude in the older and younger islands. This pattern is consistent with the hump-shaped pattern of islands' ontogeny, as described by Whittaker *et al.* (2009).

Despite their relatively small size, the Canary Islands exhibit a great climatological complexity, with six main ecological regions and distinct bioclimatic and vegetation

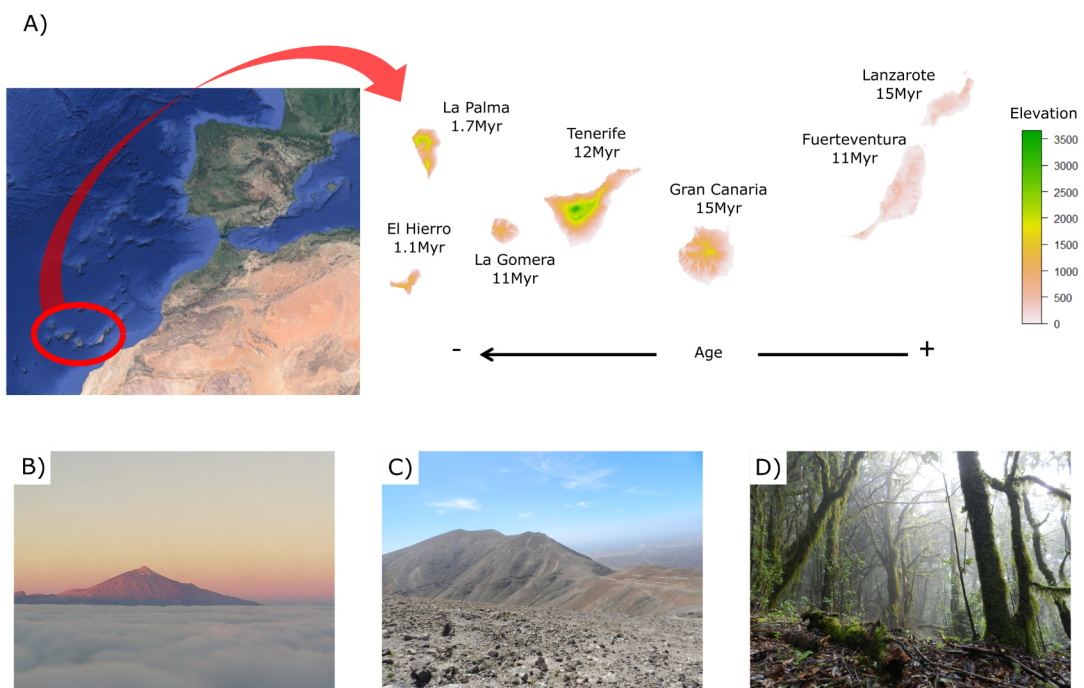


Figure 4. A) Map of the Canary Islands with the altitudinal gradient for each island. B) Teide mountain emerging from the cloud bell in Tenerife. C) Arid environment from Lanzarote. D) Humid laurel forest from the National parc of Garajonay (La Gomera).

differences between the northern and southern slopes of the islands. The local communities encompass a wide range of habitats, including xerophytic shrub communities, thermo-sclerophyllous woodlands, subtropical mesic to humid laurel forests influenced by the cloud belt (Fig. 4B), native pine forests, mesic to dry endemic *Pinus canariensis* forests, dry subalpine scrubs, and scarce vegetation in the mountaintops (Macías-Hernández *et al.* 2016). Furthermore, due to erosion in the older islands, Lanzarote and Fuerteventura have reduced habitat diversity compared to the younger islands, exhibiting a more general arid environment in contrast to the humid forests found in other islands (Fig. 4C-D). This habitat complexity has provided an ideal scenario for colonizing species to adapt to new and diverse environments, leading to diversification processes that may have been more restricted in their original continental regions.

The Canary Islands are known for their high levels of endemism in their biota, with approximately 27% of vascular plants and around 50% of invertebrates found only in these islands (Arechavaleta *et al.* 2010). Remarkably, more than half (64%) of the spider species in the Canary Islands are endemic to the archipelago (Juan *et al.* 2000). Throughout the geological history of the islands, colonization and neo-endemism have led to adaptive radiation events in some species' clades, particularly in plants (Gillespie & Roderick 2002; Meimberg *et al.* 2006).

5.2 The red devil spider genus *Dysdera*

Spiders, classified under the order Araneae, are a highly diverse group with approximately 51,000 known extant species (World Spider Catalog 2023). However, new species discoveries are common in this group, with tens or hundreds of publications every year. The spider body consists of two main sections: the anterior part known as the prosoma, also known as cephalothorax, and the posterior part known as the opisthosoma or abdomen. The prosoma bears the eyes, the locomotory appendages, the palps and the chelicerae, which constitute the spider's mouthparts,

while the opisthosoma is characterized by the presence of the spinnerets, the organs used by spiders to produce silk and the genital opening (Fig. 5A). The general differences between males and females are the sexual organs in the adult stage, with males possessing secondary copulatory structures at the distal part of their palps, the copulatory bulbs, and females having a vulva located at the ventral anterior part of the opisthosoma.

Spiders are globally distributed and can be found on every continent, except for Antarctica. Their species richness generally shows an increasing pattern towards equatorial zones, although there are exceptions, such as the Linyphiidae family, which peaks at temperate zones. Spiders exhibit ecological diversity and are known to prey on a wide variety of organisms. Due to their high species richness and worldwide distribution, spiders have been widely studied as models for understanding evolution,

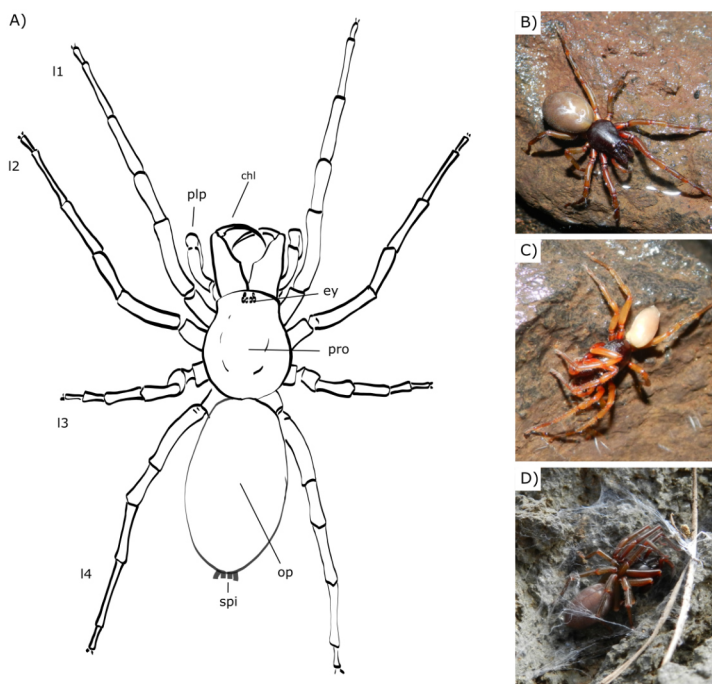


Figure 5. A) Anatomy of a spider, l1-4: legs 1 to 4; plp: pedipalp; chl: chelicera; ey: eyes; pro: prosoma; op: opisthosoma; spi: spinnerets. B) *Dysdera insulana* from Tenerife. C) *Dysdera brevisetae* from Tenerife. D) *Dysdera* sp. in its typical cocoon under a rock (Photo credit: A. Bellvert).

predicting species extinction patterns, and working as indicators of ecosystem health or pest control agents (Marc *et al.* 1999; McGregor *et al.* 2008; Cardoso *et al.* 2010). However, in some cases, spiders are still underrepresented as model organisms compared to other animal groups (Mammola & Isaia 2017).

The family Dysderidae C. L. Koch, 1837 is a group of small to mid-sized spiders with six eyes, distributed from Eurasia to the northern part of Africa. This family belongs to the Synespermiata clade, which includes cribellate spiders, meaning they lack cribellum or calamistrum, which are special web-spinning organs, and haplogyne spiders, referring to the simplified male copulatory organs and lack of external female genital structures (Michalik & Ram 2014). The Dysderidae family comprises 25 different genera, with the genus *Harpactea* Bristowe, 1939 and *Dysdera* Latreille, 1804 contributing to over half of the total species richness. The genus *Dysdera*, commonly known as red devil spiders, is the most species-rich genus within the family, with approximately 300 described species (World Spider Catalog 2023). These spiders are typically nocturnal and are commonly found in warm and wet environments, where they construct silk nests under rocks, barks, or dead logs (Macías-Hernández *et al.* 2008). The genus shows a western Palearctic distribution, mostly circumscribed to the Mediterranean basin (Deeleman-Reinhold & Deeleman 1988), with the exception of the synanthropic species *D. crocata* C.L. Koch 1839 (Deeleman-Reinhold & Deeleman 1988). The north-western Atlantic Macaronesian archipelagos represent the westernmost limit of its range (Arnedo & Ribera 1999a; Arnedo *et al.* 2001). Although *Dysdera* has colonized all Macaronesian archipelagos (Crespo *et al.* 2021), it has been in the Canary Islands, and in a lesser degree in Madeira (Crespo *et al.* 2021), where it has undergone major diversification. In the Canary archipelago alone, 47 valid species of *Dysdera* have been described (Arnedo & Ribera 1999a, 1999b, 1999c; Arnedo *et al.* 2000; Macías-Hernández *et al.* 2010, 2016) (Fig. 5B-D), most of which are single island endemics, accounting for one-fifth of the total diversity of the genus

(World Spider Catalog 2023). Although the actual number of colonization events that account for such a remarkable diversity has been contentious (Arnedo *et al.* 2001, Macías-Hernández *et al.* 2008) recent mitogenomic data supports the single origin of all Canarian endemics except for one (Adrián-Serrano *et al.* 2020). The ancestor of the species *Dysdera lancerotensis* Simon, 1907 colonised the archipelago (Lanzarote and Fuerteventura), independently and at a later time than the ancestor of all remaining species.

Species within the genus *Dysdera* have been consistently reported to feed on woodlice (Bristowe 1958; Sunderland & Sutton 1980; Hopkin & Martin 1985; Raupach 2005), a prey that is typically avoided by generalist predators due to the woodlice's defensive mechanisms and their accumulation of heavy metals (Pekár *et al.* 2016), which makes them difficult to digest. *Dysdera* also exhibits unusual variability in mouthpart morphology, which has been suggested to be related to different levels of dietary specialization and prey capture strategies, specifically driven by feeding on woodlice (Řezáč & Pekár 2007). Similarly, *Dysdera* species from the Canary Islands, like their mainland counterparts, display high variability in cheliceral morphology, including morphotypes similar to continental species, and some of these morphotypes have been associated with different metabolic adaptations for feeding on isopods (Toft & Macías-Hernández 2021), suggestive of the role of trophic specialization in driving phenotypic diversification in the group. Recent transcriptomic analyses have also revealed potential instances of convergent evolution of trophic specialization in Canarian *Dysdera* species (Vizueta *et al.* 2019). Moreover, in addition to the variability in cheliceral mouthparts and trophic adaptations, *Dysdera* species from the Canary Islands also exhibit other remarkable adaptations that are not found in continental counterparts. For instance, the Canary Islands are home to several obligate cave-dwelling species of *Dysdera* that exhibit somatic modifications such as the loss of eyes and pigmentation, or extreme elongation of extremities, as seen in

Dysdera unguimanis Ribera *et al.*, 1985, and some epigeal species exhibit unusual modifications in the shape of the carapace (Arnedo & Ribera, 1999).

Because of the remarkable diversification that *Dysdera* spiders have undergone, the high variability of their phenotypic characters, the different levels of trophic specialization and their ability to adapt to different climatic environments in the archipelago, this genus represents a perfect test case to investigate the link between morphological traits to either habitat or diet requirements, examine the evolutionary consequences of trophic specialization and test whether the diversification of these spiders in the Canary Islands constitute a case of adaptive radiation.

OBJECTIVES

The main aim of this thesis is to investigate whether the diversification of the *Dysdera* spider genus in the Canary Islands can be classified as a case of adaptive radiation, and identify the ecological and evolutionary drivers of the diversification of these spiders within the archipelago. To achieve these goals, we have established the following specific objectives:

1. To conduct an integrative taxonomic revision of the spider genus *Dysdera* in the Canary Islands and reveal putative cases of overlooked species (Chapter 1).
2. To test the link between different spider's body parts and different ecological pressures, and build a framework for future eco-phenotypic studies in non-model systems (Chapter 2).
3. To statistically characterize the different cheliceral morphotypes present in the islands and assess its relationship with different levels of trophic specialization (Chapter 2).
4. To detect cases of parallel divergent selection in the macroevolutionary landscape of *Canarian Dysdera* (Chapter 2).
5. To test evolutionary irreversibility following trophic specialization of these spiders (Chapter 2)
6. To test whether diversification in this group followed an early burst model of evolution (Chapter 3).
7. To assess if the trophic specialization, or the different cheliceral morphologies, influenced diversification rates during their evolutionary history of these species (Chapter 3).
8. To test whether the diversification of species on the islands was driven by geographic isolation, and species co-occurrence is the result of secondary contact (Chapter 3).
9. To test whether species colonizing islands with lower levels of interspecific competition experienced ecological release (Chapter 3).

SUPERVISOR'S REPORT

As a supervisor of the doctoral thesis entitled "Testing the hypothesis of adaptive radiation and their ecological consequence", carried out by Adrià Bellvert Bantí, I present this report detailing the contribution of the doctoral student on the following publications and their IF.

Chapter 1:

Bellvert, C. Arenas, A. Enguídanos, N. Macías-Hernández, M. Roca-Cusachs, M. A. Arnedo. **Endless species most beautiful: Using DNA barcodes to inform species delimitation in the red devil *Dysdera* spiders of the Canary Islands, with description of ten new species.** [In prep.]

- Contribution of the doctoral student: Description of the 10 new species, discussion of results and writing of the manuscript.

Chapter 2:

Bellvert A., Roca-Cusachs M., Tonzo V., Arnedo M.A. & Kaliontzopoulou A. 2022. **The Vitruvian spider: segmenting and integrating over different body parts to describe eco-phenotypic variation.** *Journal of Morphology* **283**: 1425–1438.

- Contribution of the doctoral student: Digitalizing morphological data, analyzing, elaboration and discussion of results and writing of the manuscript.
- About the journal: **Impact factor: Impact factor: 0.504, Q1, Category: Animal Science and Zoology.**

Adrià Bellvert, Silvia Adrián-Serrano, Nuria Macías-Hernández, Søren Toft, Antigoni Kaliontzopoulou, Miquel A. Arnedo. [2023]. **The non-dereliction in evolution: Trophic specialisation drives convergence in the radiation of red devil spiders (Araneae: Dysderidae) in the Canary Islands.** *Systematic Biology*.

- Contribution of the doctoral student: Digitalizing morphological data, analyzing, elaboration and discussion of results and writing of the manuscript.
- About the journal: **Impact factor: Impact factor: 9.16, Q1, Category: Ecology, Evolution, Behavior and Systematics.**

Chapter 3:

Adrià Bellvert, Jairo Patiño, Laura Pollock, Antigoni Kaliontzopoulou & Miquel A. Arnedo. **Tempo and mode in the diversification of the red devil spiders (Araneae: Dysderidae) radiation from the Canary Islands.** [In prep.]

- Contribution of the doctoral student: Analyzing, elaboration and discussion of results and writing of the manuscript.

Adrià Bellvert, Alba Enguídanos, Laura Pollock, Antigoni Kaliontzopoulou & Miquel A. Arnedo. **How the turntables: Species traits modulate ecological release in red devil spiders (Araneae: Dysderidae)?** [In prep.]

- Contribution of the doctoral student: Analyzing, elaboration and discussion of results and writing of the manuscript.



Prof. Miquel A. Arnedo Lombarte

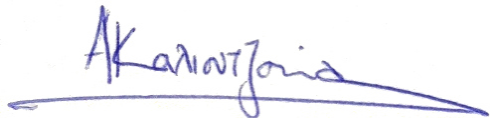
Dept. Biologia Evolutiva, Ecologia i

Ciències Ambientals

Facultat de Biologia

Institut de Recerca de la Biodiversitat -UB

Universitat de Barcelona (UB)



Dr. Antigoni Kaliontzopoulou

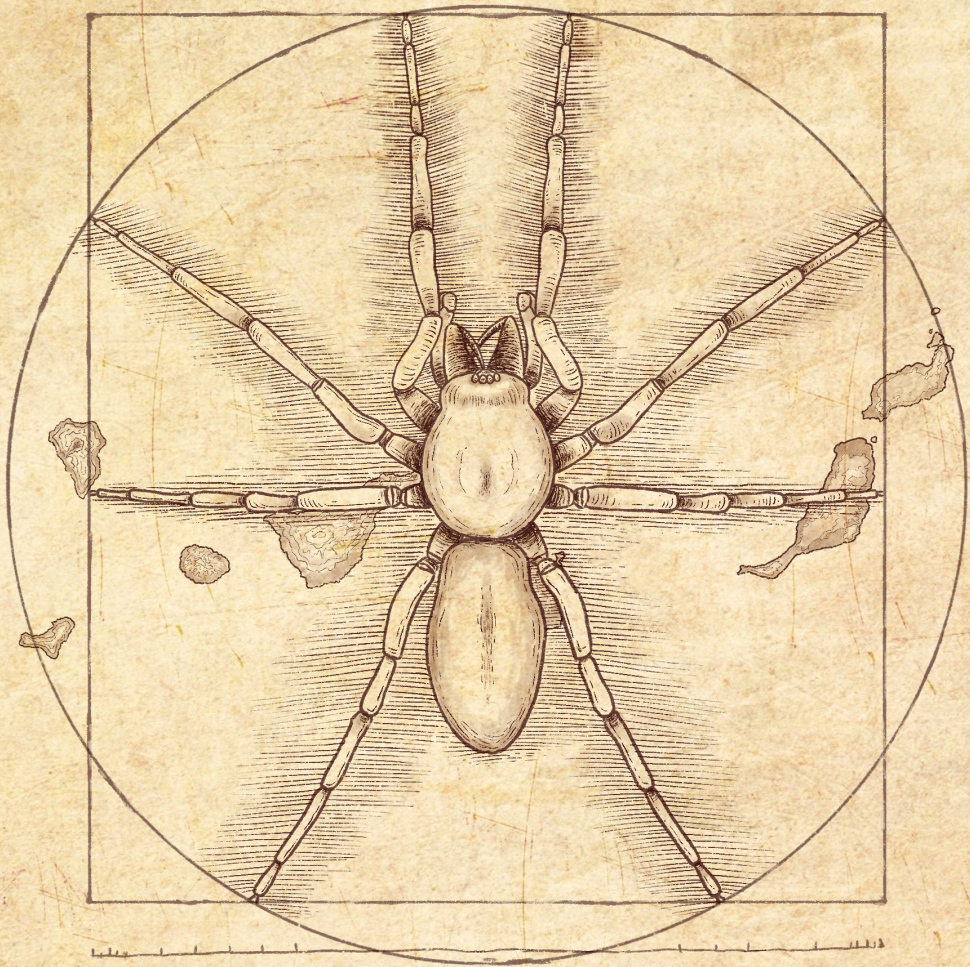
Dept. Biologia Evolutiva, Ecologia i

Ciències Ambientals

Facultat de Biologia

Institut de Recerca de la Biodiversitat -UB

Universitat de Barcelona (UB)



CHAPTER 1

Endless species most beautiful: Using DNA barcodes to inform species delimitation in the red devil spiders (Araneae: Dysderidae) of the Canary Islands, with description of ten new species

Endless species most beautiful: Using DNA barcodes to inform species delimitation in the red devil spiders (Araneae: Dysderidae) of the Canary Islands, with description of ten new species

A. Bellvert^{1,2}, C. Arenas^{1,2}, A. Enguádanos^{1,2}, N. Macías-Hernández³, M. Roca-Cusachs^{1,2} & M. A. Arnedo^{1,2}.

1 Departament de Biologia Evolutiva, Ecologia i Ciències Ambientals, Universitat de Barcelona (UB), Av. Diagonal, 643, 08028 Barcelona, Spain.

2 Institut de Recerca de la Biodiversitat (IRBio), Universitat de Barcelona (UB), Barcelona, Spain.

3 Departamento de Biología Animal, Edafología y Ecología, Universidad de la Laguna, Tenerife, Canary Islands, Spain.

Abstract

The use of DNA barcodes has greatly contributed to ease identification and discovery of new candidate species. However, this approach is far from flawless. Single molecular markers on their own may fail to convey the complexity of evolutionary history and multi-faceted nature of species. Potentially overlooked species disclose by DNA barcodes should be further delimited using additional nuclear markers and phenotypic data. The red devil spiders of the genus *Dysdera* has colonized and highly diversified the Canary Islands. This genus has been object of several taxonomic revisions in the last decades, which have raised the number of currently accepted species to approximately 50. We present the results of a large DNA barcode analysis of the Canarian *Dysdera* to specifically address (1) whether morphologically diagnosable species are also well defined and potentially diagnosed using DNA barcodes, (2) whether DNA barcodes uncover the existence of previously overlooked lineages and (3) unravel potential conflicts between data set that may hint to specific evolutionary processes. Results of a phylogenetic analysis of mitochondrial markers and the nuclear ITS-2, revealed few instances of non-monophyly across markers. Character-based species delimitation methods revealed that in two-thirds of the species molecular data matches nominal species, while most of the remaining disagreements involve molecular splits related to intraspecific geographic structure. We also identified two potential instances of introgression between species, and two of incomplete lineage sorting. Despite barcode analyses failed to identify the existence of a barcoding gap among the individuals analysed, the success rate of correct assignment of unknown individuals was well above 90%. With the integration of this molecular data with morphological diagnosable characters we provide description for 10 new species to science namely: *D. aniepa* sp.n., *D. banot* sp.n., *D. gaifa* sp.n., *D. garoei* sp.n., *D. guamet* sp.n., *D. herii* sp.n., *D. marmorata* sp.n., *D. tabona* sp.n., *D. undupe* sp.n. and *D. yballa* sp.n. Additionally, we describe for the first time of the male of *D. hirguan* and the female *D. orahan*.

Keywords: Macaronesia, Taxonomy, Arachnida, *Dysdera*, island radiation, COI, ITS-2

Introduction

“Stat rosa pristina nomine, nomina nuda tenemus”

Umberto Eco, 1980. The Name of the Rose

In recent years, the use of a short, standardized DNA sequence fragment, as a species identifier to overcome some of the former limitations of morphology only identifications, has become extremely popular. DNA barcodes have revealed themselves as extremely useful in taxonomy with a huge variety of different applications. However, from the onset of the proposal of the DNA barcoding technique, the approach has also been extensively used for species discovery and to help to assist in species delimitation. With that aim in mind, a plethora of assignment algorithms and methods have been developed, ranging from fast, yet strictly operational criteria to more computationally consuming methods based on evolutionary optimisation (Fujisawa and Barraclough 2013; Zhang et al. 2013). The use of DNA barcodes for species delimitation however is not exempt of pitfalls and drawbacks. To start with, a single marker, haploid and maternally inherited in the case of the Animal barcode, can hardly resolve all the multitude of processes involved in the speciation process, and hence the use of multi-locus approaches, specially through the inclusion of unlinked nuclear markers, is strongly advised. The use of DNA barcode of either identification or species discovery can be seriously compromised in scenarios under which the gene tree is not expected to accurately reflect the species tree. Such scenarios include incomplete lineage sorting as a result of recent speciation times, and short coalescent times and large effective population sizes (Maddison 1997), or in the presence of postspeciation gene-flow and paralogy. Despite these limitations, DNA barcode screenings provide a starting ground to (1) generate working hypothesis of candidate species and (2) provide additional evidence to identify and assign problematic taxa.

Because the unusual characteristics of isolation, species able to colonize volcanic islands usually undergo to a set of ecological and evolutionary changes, often result in

adaptive radiation (Gillespie 2007). Islands adaptive radiations may provide a challenging system for the use of DNA barcodes, since in many cases the radiation process may have involved either recent or fast speciation events. In addition, the phylogenetic and spatial closeness of island taxa may offer ample opportunities for introgression (Shaw 2002). The volcanic archipelago of the Canary Islands is located 100km in front of the African Nord-west coast and is formed by 7 major islands (Fig. 1). Because of the movement of the tectonic plates above the volcanic hotspot, these islands are chronologically arranged with the oldest islands in the east (Lanzarote and Fuerteventura with 15 and 23 My respectively) and becoming younger to the west (Gran Canaria 15 My, Tenerife 12 My, La Gomera 11 My, La Palma 1.7 My and El Hierro 1.1 My) (Van Den Bogaard 2013).

The red devil spider genus *Dysdera* Latreille, 1804, is one of the most species-rich genera in the western Palearctic. To date, over 300 species have been described (World Spider Catalog 2023). Species in this genus are ground dwellers of nocturnal habits that actively hunt their prey. They are usually found in warm and wet environments under rocks, barks or tree logs (Macías-Hernández et al. 2008), where they spend the daytime under cocoons (Roberts 1995; pers. com). Because of their habits they are frequently found in caves, and some species have evolved cave adaptive traits (Arnedo et al. 2007). The genus has colonized all the Macaronesian archipelago, which represent the westernmost limit of its distribution (Arnedo and

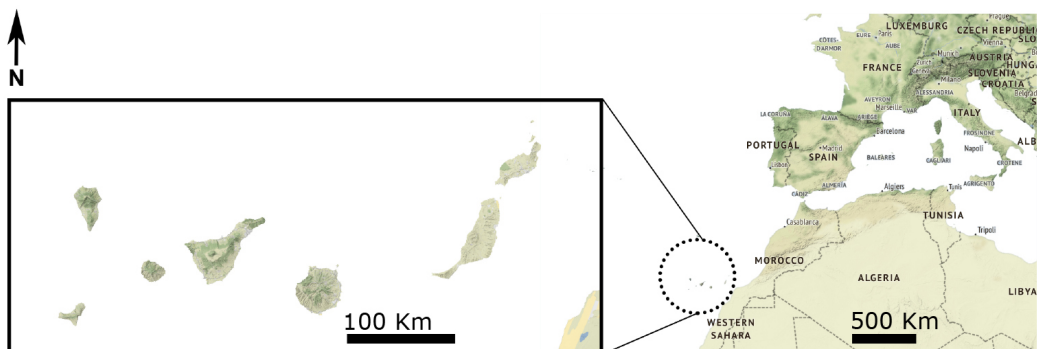


Figure 1. Map of the Canary Islands

Ribera 1999a). In the Canary Islands, the first endemic *Dysdera* species were described by Eugene Simon (1883), namely *D. cribellate*, *D. macra* Simon, 1883, *D. verneui* Simon, 1883 and *D. insulana* Simon, 1883, along with the record of the synanthropic species *D. crocata* C. L. Koch, 1838. Since then, several samplings and studies conducted in the archipelago have raised the species number to 51 (see Simon 1907; Strand 1911; Schmidt 1973; Ribera *et al.* 1985; Wunderlich 1987; Wunderlich 1991; Ribera and Arnedo 1994; Arnedo *et al.* 1997; Arnedo and Ribera 1999a; Arnedo and Ribera 1999b; Arnedo *et al.* 2000; Arnedo *et al.* 2007; Macías-Hernández *et al.* 2010). Most of these studies delineated species only based on morphological traits, and in certain cases, the presence of intraspecific variation that requires additional investigation was emphasized. Furthermore, successive surveys have yielded a substantial amount of new material, some of which may contain new species.

Here we conduct an extensive DNA barcode analyses of the endemic species of the red devil *Dysdera* spiders from the Canary Islands. The aims of the study were twofold. First, we want to assess how well the DNA barcodes recover the current, mostly morphology-based taxonomy of the groups and, second, to reveal putative cases of overlooked specimens more specifically of unaccounted deeply divergent lineages that may deserve species status. Furthermore, the DNA barcode library developed in the study will be a useful tool for non-specialist identification, which may help to preserve this amazing component of the Canarian Biota. In addition, based on morphological evidence with support from the DNA markers analysed, we described 10 new species of endemic Canarian *Dysdera*.

Material and methods

Specimens were collected in the field by the authors, with the help of several field assistants and colleagues, through several collection trips conducted over the last 20 years. Adult specimens were identified to species using available taxonomic revisions

on the group (Arnedo and Ribera 1997, 1999b, 1999a; Arnedo et al. 2000a, 2007; Macías-Hernández et al. 2010). Immatures could not be identified other than to genus level but were included in the molecular analyses to refine the distribution range of some of the species. When possible, specimens collected in the field were fixed in 95% ethanol and stored at -20°C for subsequent molecular analysis. In some cases, we had to rely on suboptimal material, mostly including specimens preserved in 75% ethanol or/and kept at room temperature. Recently collected specimens (<5 years old) in these conditions were successfully amplified, especially when using primers targeting shorter (i.e. ~300 bp) fragments.

Molecular lab protocols

Whole DNA was extracted from one or two legs, or the whole-body following puncturing for small and immature specimens, using the SpeedTools Tissue DNA Extraction Kit (Biotools), following the manufacturer's protocol. DNA extractions were amplified by means of the Polymerase Chain Reaction (PCR). We targeted two regions, the standard animal barcode, the first half of the mitochondrial cytochrome c oxidase subunit I gene (COI), and the nuclear Internal transcribed spacer 2 (ITS-2), the most popular nuclear marker for examining shallow relationships in animals (Agnarsson 2010). In addition, we included a mitochondrial gene fragment spanning the second half of the large subunit of the rRNA (16S, the tRNA leu (L1) and the first half of the NADH dehydrogenase subunit 1 (nad1) to improve resolution in the mitochondrial tree inference. All PCR's were made with a mixture of the following reagents: Taq polymerase (0.2 µL), direct and reverse primers with a 10 µM concentration, MyTaq Red DNA polymerase (Bioline) (5 µL), distilled water (12µL) and 2µL of the DNA extract, for a total volume of 20µL per sample. PCR conditions were as follows: a first step of 94°C for 5', followed by 25 cycles of 94°C for 30'' denaturalization, 42°C to 52°C (depending on the primer pair) for 35'' primer hybridization, and 72°C for 45'' for extension, and a final step of 72°C for 5' for finishing extension of all fragments. The

amplicons were sequenced in both directions in Macrogen Inc.

Sequence editing and manipulation

Editing of the raw sequences, primer removal and manipulation of consensus sequences were conducted with the program Geneious v. 10.2.6 (<https://www.geneious.com>). Newly generated sequences were uploaded to Genbank, and the COI sequences also to BOLD (<https://boldsystems.org/>).

We assembled individual data matrices for the COI and ITS markers, and the concatenated mitochondrial gene fragments, by combining the newly generated sequences with those available in Genbank from previous studies. The sequence alignment of COI and *nad1* fragments was trivial since no evidence of indel mutation was observed. The final COI and *nad1* alignment were translated to aminoacids to ensure that no stop codons were present within the sequences. For the 16S and ITS-2 automatic alignments of the DNA fragments were built with the online version of the program MAFFT v.7.427, using the G-INS-I algorithm with default parameter. For the ITS2, we determined the gametic phases of heterozygous individuals using the algorithms provided by PHASE (Stephens et al. 2001; Stephens and Donnelly 2003), as implemented in the DnaSP v6.11.01 program (Rozas et al. 2017). Identical sequences (i.e. COI haplotypes and ITS sequences types) were detected and removed from downstream analyses under the criterion implemented in RAxML v.8 (Stamatakis 2014).

Molecular phylogenetic analyses

We inferred phylogenetic relationships of the concatenated mitochondrial data matrix and the ITS2 data matrix using a combination of parsimony, maximum likelihood and Bayesian tree inference methods. For parsimony, we first coded ITS2 gaps as absence/presence characters following the simple coding method proposed by Simmons and Ochoterena (2000) with the help of the program FastGap v1.2

(Borchsenius 2009). We inferred the best tree with the computer program TNT v. 1.5 (Goloboff A et al. 2008), following a “new search strategy” (xmult=hits 10 nouupdate nocss replic 10 ratchet 10 fuse 1 drift 5 hold 100 noautoconst keepall; bbreak = tbr). We assessed node support by means of 1,000 jackknife resampled matrices (heuristic search per replicate: mult=replic 10 tbr hold 1000). We implemented maximum likelihood with the help of IQ-TREE v. 2.1.2 (Minh et al. 2020). We selected the best model for the IQ-TREE analysis using ModelFinder (Kalyaanamoorthy et al. 2017), starting with splitting by gene and codon in the case of the protein coding genes, and nodal support was estimated by means of 1,000 replicates of ultrafast bootstrapping (Hoang et al. 2018). We implemented Bayesian inference with MrBayes v.3.2.6 (Ronquist et al. 2012). We selected the best partition scheme and evolutionary model with PartitionFinder v2.1.1 (Lanfear et al. 2017). We collected samples from two independent runs (8 chains each) of 10 million generations each, sampled every 1,000. Support values were calculated as posterior probabilities. We assessed convergence of the chains, correct mixing and the number of burn-in generations with Tracer v. 1.7 (Rambaut et al. 2018). We ran all model-based analyses remotely at the CIPRES Science Gateway v.3.3 (Miller et al. 2010) and trees were visualized using the program FigTree v.1.4.4 (available at <https://github.com/rambaut/figtree/releases>). All trees were rooted using *D. crocata* and *D. lancerotensis* as outgroups.

Species delimitation

We explored delimitation schemes inferred using character based approaches (DeSalle and Goldstein 2019) on the COI data matrix. Specifically, we implement the mPTP (Kapli et al. 2017) and the GMYC (Fujisawa and Barraclough 2013) models. The mPTP delimitation relies on the relative branch length information provided by a gene tree to identify a transition point between inter- and intra-specific divergences, i.e., distinguishing putative speciation from coalescence events. The ML tree inferred with IQ-TREE was used to delimit genetic clusters using the mPTP model as implemented

in the computer programme mPTP v 0.2.4 (Kapli et al. 2017, available at <https://github.com/Pas-Kapli/mptp>). We first identified the minimum branch length (0.0011069466), which was subsequently used to delimit clusters and assess their support by means of three Markov Chain Monte Carlo sampling chains ran for 50 million generations, discarding the first 2 million MCMC steps. Unlike mPTP, the GMYC delimitation method relies on a tree. With that aim, we conducted a time estimation analysis of the data using a Bayesian approach, as implemented in the program BEAST v.10.4 (Drummond et al. 2012). We selected a coalescent tree prior (constant population size), which has been suggested to provide a more rigorous test of delimitation since the model assumes a single species as the null option (Monaghan et al. 2009). We defined the best partition schemes and evolutionary models selected by PartitionFinder, and estimated absolute divergence times by defining a single lognormal relaxed clock with a normal prior on the substitution rate prior (ucl.d.mean) with a starting and mean value of 0.0125 and standard deviation of 0.005, based on spider substitution rate estimates available in the literature for spiders (Bidegaray-Batista and Arnedo 2011). We ran three independent chains of 10 million generations each, sampling every 1000 generations. We monitored the chain convergence, the correct mixing, and the number of generations to discard as burn-in (10%) with Tracer. Three chains of 10 million generations were run for each analysis. The accompanying programs LOGCOMBINER and TREEANNOTATOR were used to remove the burn-in generations, to combine the results of three independent chains, and select the optimal distribution of posterior parameters and tree values. The GMYC cluster was identified with the help of the R package SPLITS (Ezard et al. 2017).

We compared the results of the two molecular delimitation approaches to the morphologically determined species. We categorized molecular clusters as either “match”, “split”, “merge” or “mixture”, depending on whether they assigned specimens to the same morphological species, split specimens of the same species

into more than one cluster, merged specimens from two or more species or merged some specimens of one species with those of another, respectively.

We further explored the ability of COI DNA barcodes to correctly assign Canarian *Dysdera* specimens by using distance-based methods. We first built a neighbour joining tree based on distances computed using the Kimura 2-parameter model (K2P) with the computer program MEGA v11 (Tamura et al. 2021), to ease visualization of genetic divergences. The presence of a ‘barcoding gap’ was checked graphically by plotting the maximum intraspecific K2P genetic distance to the smallest interspecific K2P genetic distance. We used two metrics to assess success in identification using DNA barcode information, namely (1) the nearest neighbour criterion (NN), which assigns the query sequence to the same species as its closest sequence in the reference library, and (2) a threshold-based analysis, which assigns the query sequence to the closest individual unless it is further than a given threshold, which results in no identification. We obtained a graphic representation of identification error rates (i.e. false negative, false positive) by testing 50 thresholds from 0.01 to 0.15. All analyses were conducted in the R environment with the help of the package SPIDER (Brown et al. 2012).

We did not conduct species delimitation analyses on the ITS2 data, as this data was mostly intended to corroborate the results of the better sampled COI data set. It is well known that the haplotypic nature of the maternally inherited mitochondrial genes may identify spurious grouping and failed to identified instances of hybridization (Funk and Omland 2003; Ballard and Whitlock 2004; Rubinoff et al. 2006).

Morphological analyses and species descriptions

Specimens were examined and illustrated using a LEICA MZ16A stereoscopic microscope with a camera lucida. Digital images were taken with a high-resolution

digital camera LEICA DFC 450 attached to the microscope with the help of the software Leica Application Suite v4.4 and mounted with the software Helicon Focus (Helicon Soft, Ltd.) and a FLIR digital camera with a THORLABS C-mount CML15 lens attached to a ZEISS Axio LAB.A1 microscope. Measurements of the specimens were taken from the scaled images with the program LAS v4.4. Female vulva was removed with the help of entomological forceps and hypodermic needles. To remove the membranous tissues and kept the sclerotized parts, the genitalia was enzymatically digested in pancreatin and borax solution following Alvarez-padilla & Hormiga (2007). To visualize the structures of the male copulatory bulb, scanning electron microscope images (SEM) were performed with a Q-200 (FEI Co.). The palp was removed from the body cutting the structure between the tibia and the tarsus and sonicated with a Nahita ZCC001 ultrasonic bath for around 30 seconds and air dried for 24 hours. Before scanning, all the palps were carbon sputter-coated the day before.

All characters of the new species description were recorded in DELTA format (Dallwitz 1980; Dallwitz et al. 1993) from a previous database focused on the description of *Dysdera* species from the Canary Islands (Arnedo and Ribera 1997, 1999b, 1999a; Arnedo et al. 2007). The “additional material examined” has been recorded using the spreadsheet to expedite taxonomic publications (Magalhaes 2019). The nomenclature used for the description of the somatic and genitalic characters were all named after general work at the genus level (Deeleman-Reinhold and Deeleman 1988) and Canarian *Dysdera* specific revision of the genitalic features (Arnedo et al. 2000b).

All maps were performed using the ggmap package (Kahle and Wickham 2013) in R software (R Development Core Team 2021); map tiles where obtained from <http://stamen.com/>, under <http://creativecommons.org/licenses/by/3.0>", and data from <http://openstreetmap.org/>, under ODbL.

Abbreviations

Somatic characters:

AME – Anterior Median Eyes

PLA – Posterior Lateral Eyes

PME – Posterior Median Eyes

B – Basal tooth

D – Distal tooth

M – Median tooth

Fe – Femur

Pa – Patella

Ti – tibia

Me – Metatarsus

Ta – Tarsus

Male genitalia:

AR – Arch-like Ridge

AC – Additional Crest

AL – Additional Lateral Sheet

C - Crest

DD – Distal Division

DH – Distal hematodocha

ES – External Sclerite

IS – Internal Sclerite

MA – Medial Apophysis

L – Lateral sheet

P – Posterior apophysis

Female genitalia:

AD – Anterior Diverticulum

AVD – Additional Ventral Diverticulum

DA – Dorsal Arch

DF – Dorsal Fold

MF – Major Fold

PD – Posterior Diverticulum

S – Spermathecae

TB – Transversal Bar

VA – Ventral Arch

Results

Molecular analysis

The complete list of sequences available for the present study are listed in supplementary Table S1. In total we sampled 542 specimens of Canarian *Dysdera*, representing 45 nominal Canarian species, all except *D. volcania* Ribera, Fernández & Blasco, 1985, and 10 morphologically diagnosable new species (see results for formal description). For those species known from more than one island (10 species), we included samples from all the islands reported—except *D. orahan* Arnedo, Oromí &

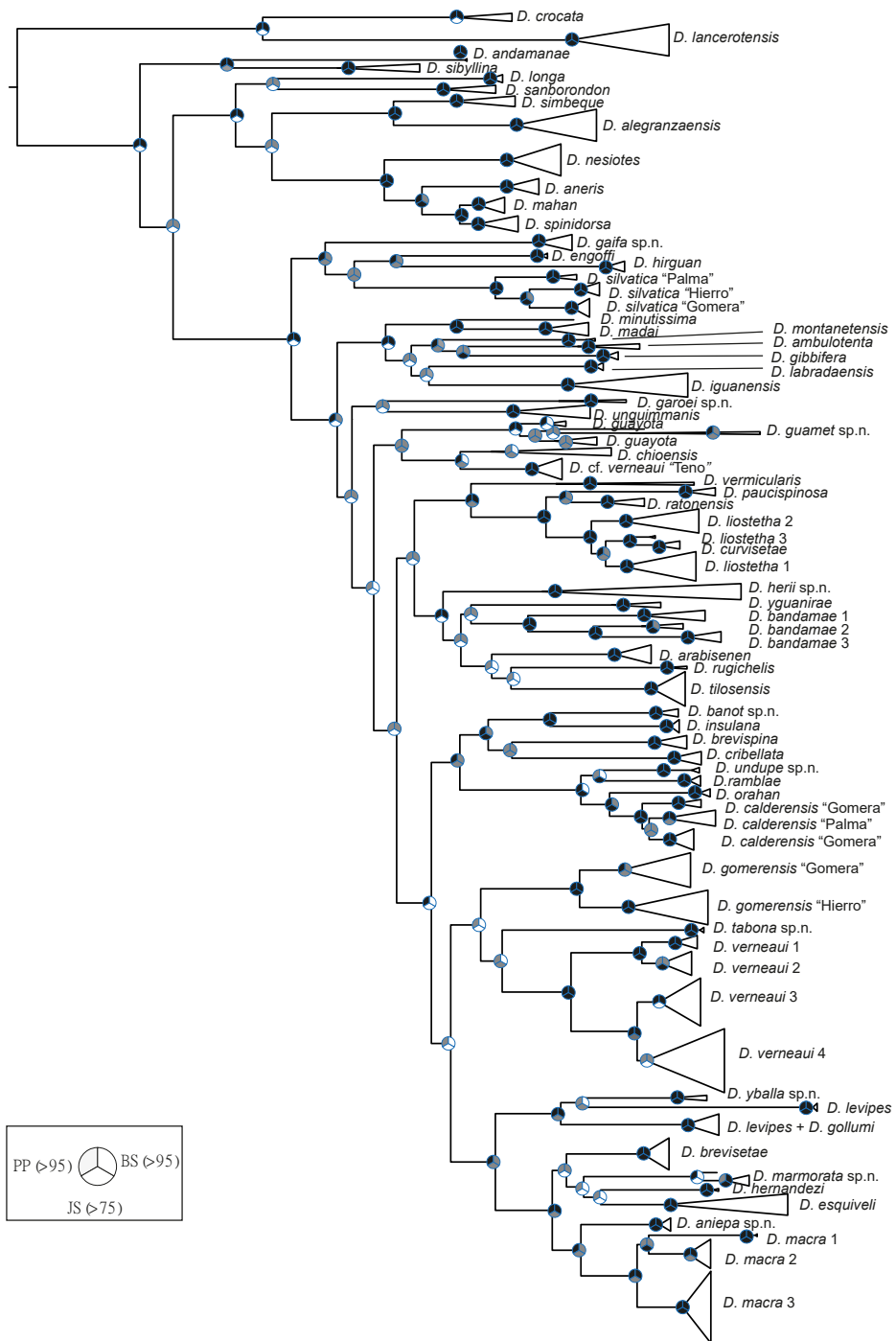


Figure 2. Bayesian inference tree of the mitochondrial concatenated data matrices. Pies on nodes refer to clade supports. Upper left corresponds to Bayesian Inference, upper right to maximum likelihood and lower to parsimony. The colour code corresponds to support level as follows: black corresponds to either Jackknife parsimony > 75%, bootstrap maximum likelihood > 95%, and Bayesian inference posterior probability > 0.95; grey to supports below to any of the thresholds, and white clade was not recovered. Species and main intraspecific clades collapsed to ease visualization.

Ribera, 1997 known from La Gomera and El Hierro but only represented from the last island. All species were represented by most than one individual, except in 3 cases. In addition, we included specimens of the species *D. lancerotensis* Simon, 1907 (15 specimens), a Canarian endemic yet not related to the species treated in the present study, the synanthropic *D. crocata* (3 specimens), closely related to the former species, and the species *D. aneris* Macías-Hernández & Arnedo, 2010 (7) and *D. vermicularis* Berland, 1936 (2) endemic to the Selvagens Islands and Cabo Verde, respectively (Arnedo et al. 2001). We generated 564 sequences of COI of a maximum length of 646 bp, representing 453 unique haplotypes, 205 sequences of the 16S, of 637 aligned positions, 143 of the nad1, spanning 381 bp, and 243 sequences of ITS2, which resolved into 216 different sequence types.

Figures 2 and 3 illustrate the Bayesian inference tree for the mitochondrial and ITS2 data, respectively. These trees also show the support values derived using the three different inference approaches. The trees generated by parsimony were less resolved and supports were lower than those generated by the other two approaches, and the mitochondrial tree was better resolved than the ITS2 tree. Maximum likelihood and Bayesian analyses both confirm the monophyly of the endemic species of the Eastern and those of the Western Canaries, with the exclusion of *D. sibyllina* Arnedo, 2007 and *D. andamanae* Arnedo & Ribera, 1997. These two species were supported as either a sister clade (mitochondrial) or as a grade (ITS2) to the remaining Canarian species. Overall, clade support increased towards the tips. In the mitochondrial tree, all nominal species were shown as monophyletic, except for *D. verneaui*, which was polyphyletic, and *D. liostetha* Simon, 1907 and *D. levipes* Wunderlich, 1987, which were paraphyletic with regards to *D. curvisetae* Wunderlich, 1992 and *D. gollumi* Ribera & Arnedo, 1994, respectively. For the ITS-2, all species were monophyletic except for *D. levipes*, which like the mitochondrial tree was paraphyletic regarding *D. gollumi*, but also *D. nesiotetes* Simon, 1907, which was paraphyletic regarding *D. aneris*,

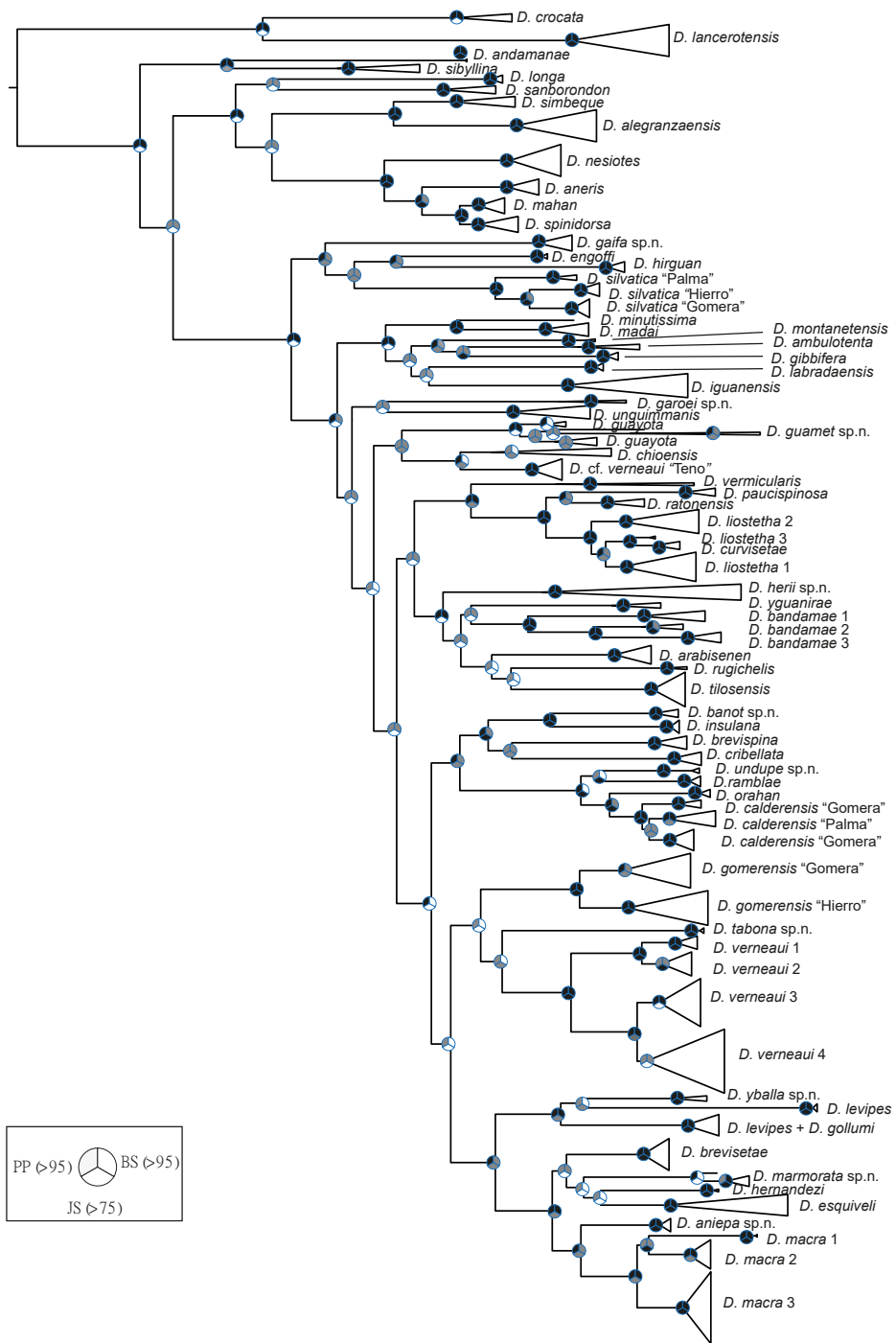


Figure 3. Bayesian inference tree of the ITS data matrix. Upper left corresponds to Bayesian Inference, upper right to maximum likelihood and lower to parsimony. The colour code corresponds to support level as follows: black corresponds to either Jackknife parsimony > 75%, bootstrap maximum likelihood > 95%, and Bayesian inference posterior probability > 0.95; grey to supports below to any of the thresholds, and white clade was not recovered. Species and main intraspecific clades collapsed to ease visualization.

and *D. aniepa* sp.n., which sequences types were intermixed with those of *D. macra*. Interestingly, ITS2 recovered both *D. verneai* and *D. lisotetha* as monophyletic.

Molecular delimitation

The mPTP method delimited a total of 73 clusters, while the GMYC recovered 83 clusters, with a confidence interval from 77 to 91 (Fig. 4). In both cases the number of delimited species were higher than the 57 morphologically diagnosed species—*D. lancerotensis* and *D. crocata* were removed from the delimitation analyses. Approximately 60% of the molecular based delimitations matched the nominal species. The matches were higher for the mPTP delimitation—39 species, 68.4%—than for the GMYC one—34 species, 59.6%. Conversely, the GMYC split more species than mPTP—19 (33.3%) and 12 (21.1%), respectively. Intraspecific clusters mostly fell into three categories, namely island populations of multi-island species (eg. *D. calderensis* Wunderlich, 1987, *D. gomerensis* Strand, 1911 or *D. silvatica* Schmidt, 1981), cave-dwelling species (eg. *D. chioensis* Wunderlich, 1992, *D. esquiveli* Ribera & Blasco, 1986, *D. sibyllina* or *D. unguimanis* Ribera, Ferrández & Blasco, 1986) or species with widespread distributions within the same island (eg. *D. bandamae* Schmidt, 1973, *D. macra* or *D. verneai*). On the other hand, mPTP merged two species pairs, the Eastern Canarian endemics *D. spinidorsa* Wunderlich, 1992 and *D. mahan* Macías-Hernández & Arnedo, 2010, which were also merged by GMYC, and the cave-dwelling species *D. ambulotenta* Ribera, Ferrández & Blasco, 1986 and *D. gibbifera* Wunderlich, 1992. Both methods agreed in identifying mixture in two species pairs, corresponding to the species *D. curvisetae* and *D. gollumi*, which rendered *D. liostetha* and *D. levipes* haplotypes, paraphyletic, as indicated above.

Barcode analysis

The neighbour joining tree build from K2P distances is included as supplementary Fig. S1. We failed to identify a ‘barcoding gap’ among Canarian *Dysdera* COI sequences, since maximum intraspecific (mean= 0.07, maximum=0.18) and the

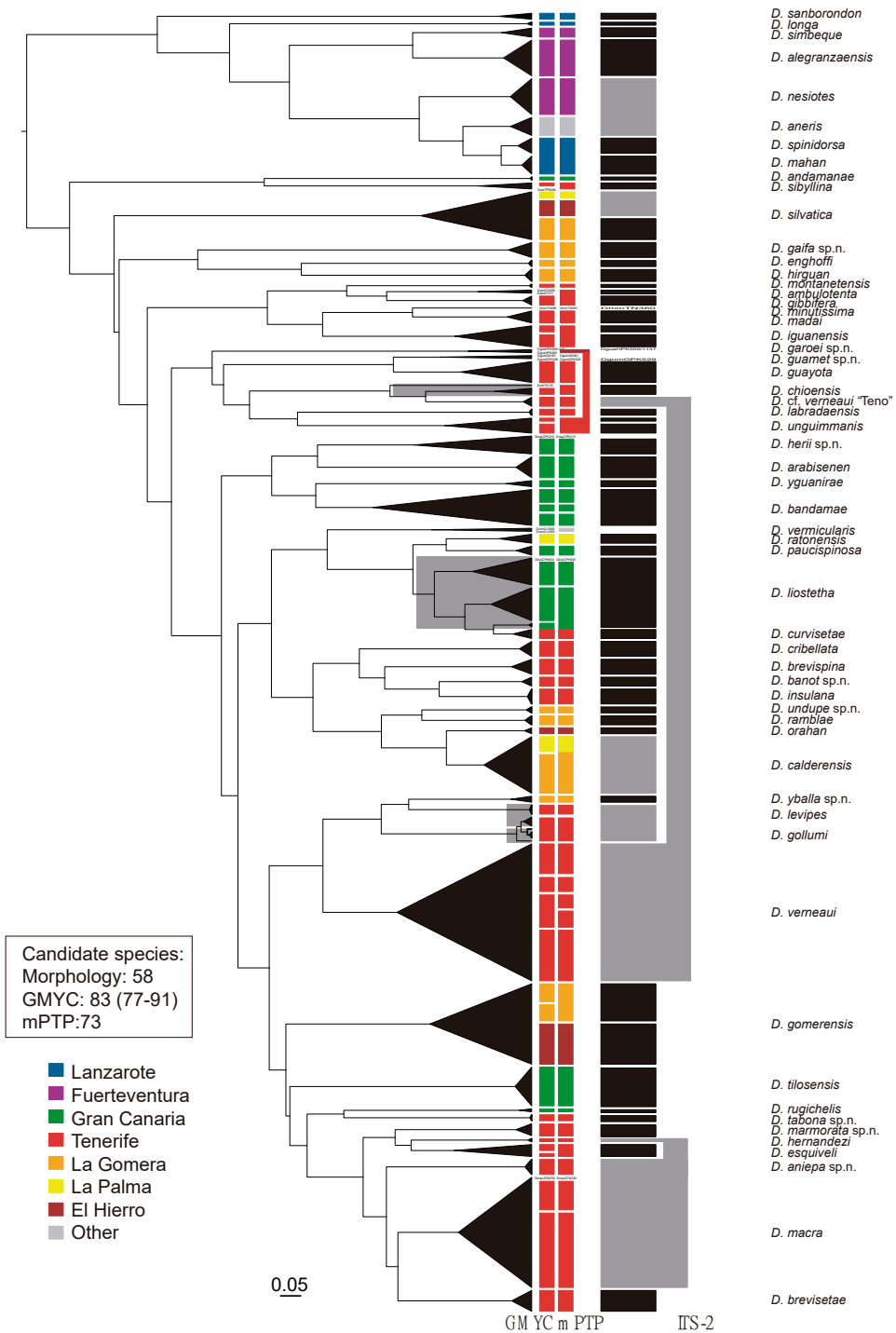


Figure 4. Ultrametric tree of the COI data set inferred with BEAST. Columns on the right indicate clusters recovered with the GMYC (left) and mPTP (middle) models. Each square is a delimited cluster, and the colour indicate the source islands. The rightmost column corresponds to clusters the clades recovered in the analysis of the ITS. The black squares denote congruence between the COI and the ITS2 circumscription, and the grey squares mismatches.

nearest interspecific genetic distance (mean= 0.1, minimum=0,004) overlapped. Several pairwise comparison fell below the 1:1 line, indicating that the maximum intraspecific genetic distance was lower than the distance to the nearest neighbour (Fig. 5). However, the NN resulted in 99% identification success in species represented by more than one sequence in the reference library. The only false identifications corresponded to one specimen of *D. chioensis* (X116), which was assigned to the *D. verneui*, once specimen of *D. gollumi* (K36) which was assigned to *D. levipes*, and one of the *D. levipes* (PK539) that was assigned to *D. gollumi*, and the two specimens of *D. gaifa* sp.n. which were assigned to *D. guayota* Arnedo & Ribera, 1999. By contrast, the threshold criterion performed worse, due to the overlapping of false negatives and positives (supplementary Fig. S2). The *localMinima* function of the Spider R package determined 0.028 as the optimum threshold for minimizing the cumulative identification error, which resulted in 92.5% of correct identifications.

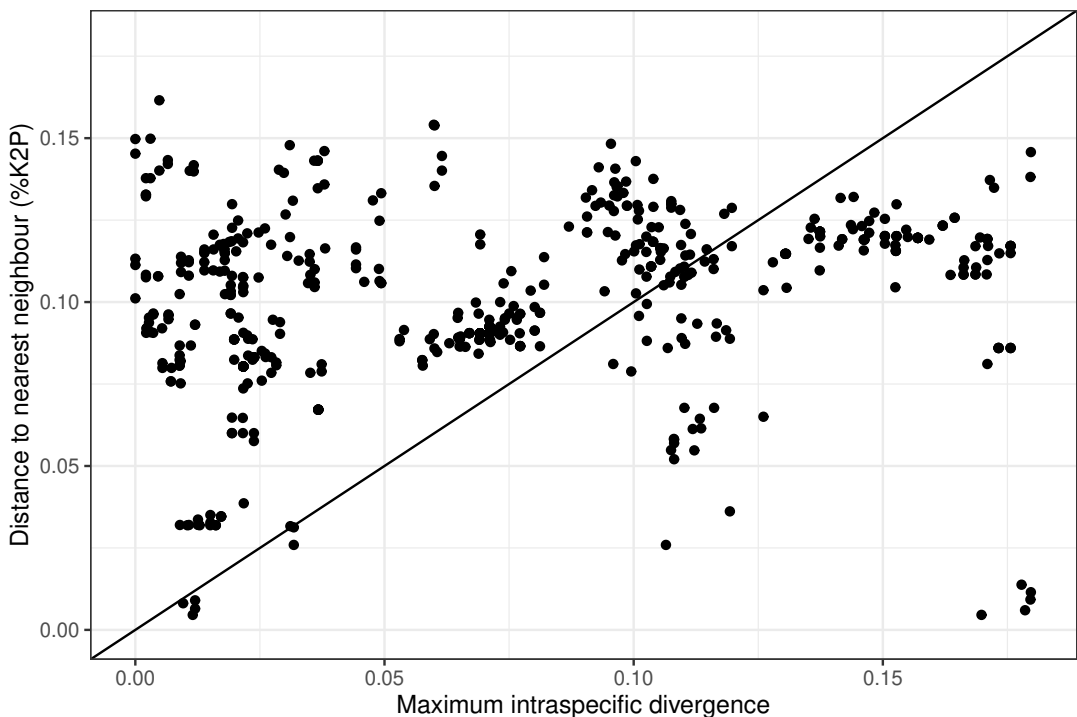


Figure 5. Plot comparing the minimum interspecific Kimura two-parameter (K2P) distance to the maximum intraspecific K2P distance. Values below the 1:1 line indicate the absence of a ‘barcode gap’.

Misidentifications included 1 wrong identification, 11 false negatives (lumping) and 29 false positives (splitting).

Based on the integration of the morphological and molecular analyses, we propose the existence of 10 new species for science. Furthermore, we provide the first description of the male of the *D. hirguan* Arnedo, Oromí & Ribera, 1997 and the female of *D. orahan*.

Taxonomy

Family **Dysderidae C. L. Koch, 1837**

Subfamily **Dysderini Deeleman-Reinhold, 1988**

Genus ***Dysdera* Latreille, 1804**

Type species. *Dysdera erythrina* (Walckenaer, 1802)

***Dysdera aniepa* sp.n. Bellvert & Arnedo**

(Figs. 6A, 7A, 8A, 9A-E, 10A-C)

Type material

Holotype: Spain. Canary Islands: Tenerife, Buenavista del Norte, El Aderno. Altos de Buenavista, 28.358258, -16.864456, N. Macías & H. López coll., 12/15/2006, 1 ♂ (NMH000850)

Paratypes: Spain. Canary Islands: Tenerife, Buenavista del Norte, El Aderno. Altos de Buenavista, 28.358258, -16.864456, N. Macías & H. López coll., 12/15/2006, 1 ♀ (NMH000860), 1 ♀ (NMH000856), 1 ♂ (NMH000849).

Additional Material examined. Spain. Canary Islands: Tenerife, Santiago del Teide, Las Arenas, 28.299588, -16.795435, S. de la Cruz coll., 13/IV/2005, 1 ♂ ; El Rosario, Morada del Viento (Pista Siete Fuentes). Las Lagunetas, 28.411180, -16.424427, N.

Macías coll., 22/XII/2006, 1 ♂; Santiago del Teide, Cumbre Bolico, 28.314186, -16.826940, N. Macías, S. de la Cruz, H. López & H. Morales coll., 06/VI/2009, 1 ♂ 2 ♀; Buenavista, Teno Alto, 28.335996, -16.865760, 1 ♀; Teno Alto 2, D. Suarez coll., 17/III/

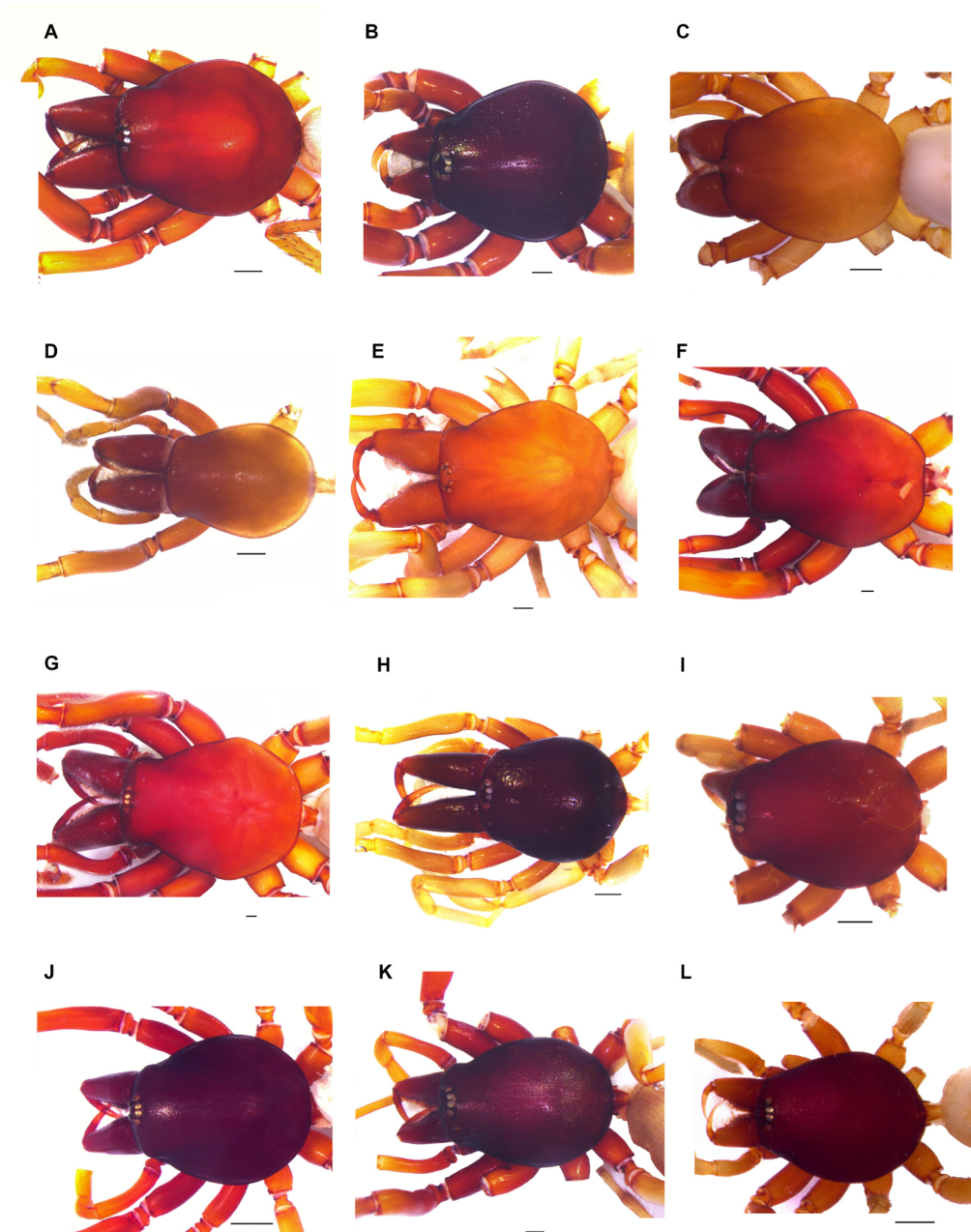


Figure 6. Prosoma dorsal view (A) *D. aniepa* sp.n.; (B) *D. banot* sp.n.; (C) *D. gaifa* sp.n.; (D) *D. garoei* sp.n.; (E) *D. guamet* sp.n.; (F) *D. herii* sp.n.; (G) *D. hirguan*; (H) *D. marmorata* sp.n.; (I) *D. orahan*; (J) *D. tabona* sp.n.; (K) *D. undupe* sp.n.; (L) *D. yballa* sp.n. Scalebar = 1mm.

2017, 1 ♂; Camino el Fraile, 26/III/2017, 1 ♀; Buenavista del Norte, El Aderno. Altos de Buenavista, 28.358258, -16.864456, N. Macías & H. López coll., 15/XII/2006, 2 ♂
8 ♀ 3 imm.

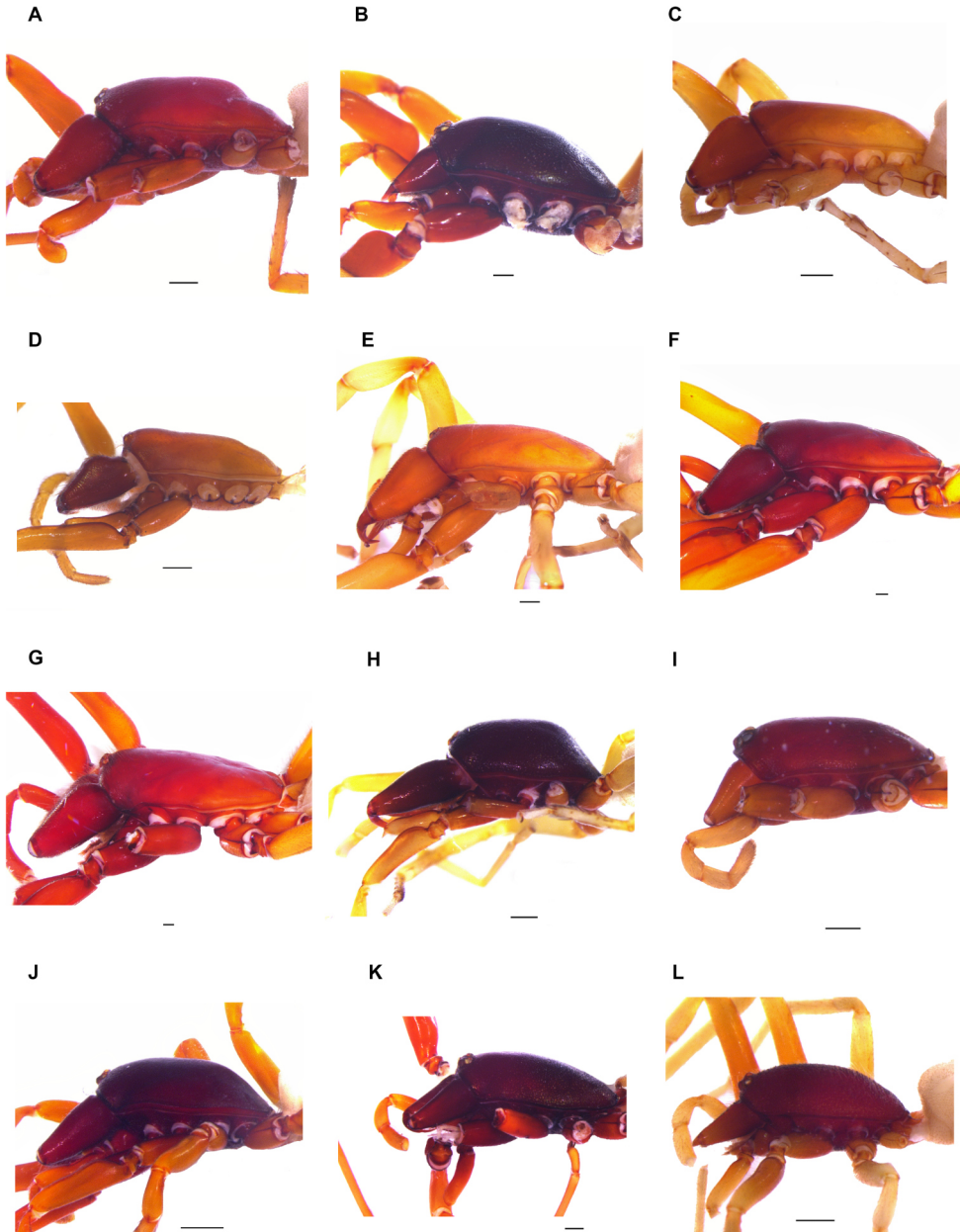


Figure 7. Prosoma lateral view (A) *D. aniepa* sp.n.; (B) *D. banot* sp.n.; (C) *D. gaifa* sp.n.; (D) *D. garoei* sp.n.; (E) *D. guamet* sp.n.; (F) *D. herii* sp.n.; (G) *D. hirguan*; (H) *D. marmorata* sp.n.; (I) *D. orahan*; (J) *D. tabona* sp.n.; (K) *D. undupe* sp.n.; (L) *D. yballa*

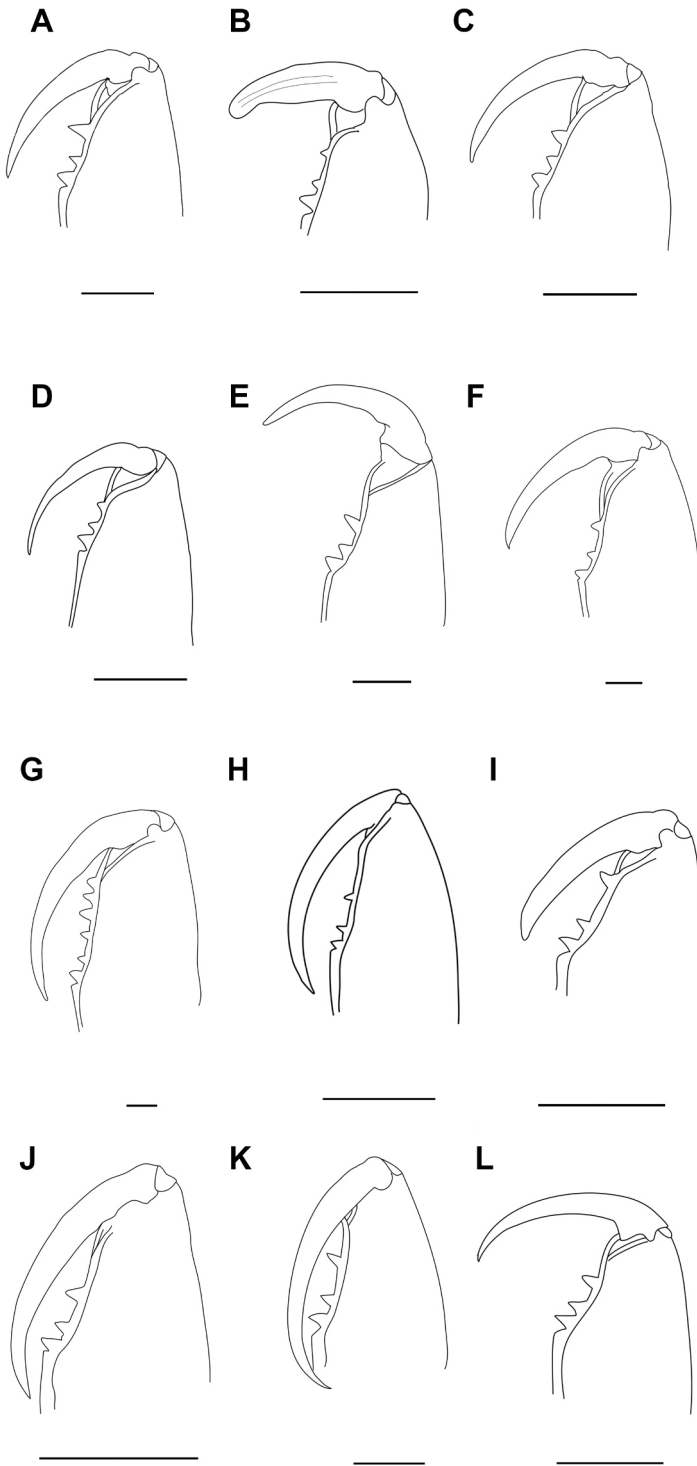


Figure 8. Chelicera dorsal view (A) *D. aniepa* sp.n.; (B) *D. banot* sp.n.; (C) *D. gaifa* sp.n.; (D) *D. garoei* sp.n.; (E) *D. guamet* sp.n.; (F) *D. herii* sp.n.; (G) *D. hirguan*; (H) *D. marmorata* sp.n.; (I) *D. orahan*; (J) *D. tabona* sp.n.; (K) *D. undupe* sp.n.; (L) *D. yballa* sp.n. Scalebar = 1mm.

Etymology

The specific name in apposition refers to a very elaborate spear (*añepa* in the original Spanish translation) that preceded the king from the aboriginal culture from the Canary Islands. As all the other names of the newly described species in this paper, comes from the original language of the Guanches, aborigines of the Canary Islands.

Diagnosis

Dysdera aniepa sp.n. is distinguished from the morphologically similar *D. breviseta* Wunderlich, 1992 by the M teeth close to B instead of D (Fig. 8A), and from the also closely similar *D. macra* by the light red coloration in *D. aniepa* (Fig. 6A, 7A) instead of dark red. Males are distinguished from the closely similar *D. macra* by the lack of distal teeth in P (Fig. 9E). Clearly distinguished from *D. breviseta* by the L distal border parallel instead of 45° (Fig. 9D). C proximal border concave decreasing instead of convex (Fig. 9C-D). Vulva very similar to the *D. macra* and *D. breviseta* but can be distinguished by a shorter S attachment to AD (Fig. 10A).

Description - Male Holotype (NMH000850): (Figs 6A, 7A, 8A, 9A-E). Carapace 3.60 long; maximum width 3.00; minimum width 2.05. Red, frontally darker, becoming lighter towards back; smooth with some small black grains mainly at front. Anterior border roughly straight, from 1/2 to 3/5 carapace length; anterior lateral borders divergent; rounded at maximum dorsal width, posterior lateral borders rounded; posterior margin narrow, straight (Fig. 6A); stepped in lateral view (Fig. 7A). AME diameter 0.18; PLE 0.14; PME 0.12; AME on edge of anterior border, separated from one another by about 1 diameter or more, close to PLE; PME touching to each other, about 1/2 PME diameter from PLE. Labium trapezoid-shaped, base wider than distal part; longer than wide at base; semicircular groove at tip. Sternum orange, darkened on borders; very slightly wrinkled, mainly between legs and anterior border; uniformly covered in slender black hairs.

Chelicerae 1.65 long, about 1/2 of carapace length in dorsal view; fang medium-sized, 1.26; basal segment, proximal dorsal and ventral side, scantily covered with piligerous granulations. Chelicera inner groove medium-size, about 2/5 cheliceral length; armed with three teeth and lamina at base; $D > B > M$; D triangular, located near segment tip; B close to basal lamina; M close to B (Fig. 8A). Anterior legs dark orange, posterior legs yellow. Lengths of male described above: fe1 2.70; pa1 1.70; ti1 2.30; me1 2.15; ta1 0.55; total 9.40; fe2 2.05; pa2 1.55; ti2 2.00; me2 1.95; ta2 0.55; total 8.10; fe3 1.85; pa3 1.10; ti3 1.25; me3 1.70; ta3 0.50; total 6.40; fe4 2.05; pa4 1.25; ti4 1.70; me4 2.15; total 7.15; relative length: $1 > 2 > 4 > 3$. Leg1 and leg2 spineless; leg3 spineless; leg4 spineless. Dorsal side of Anterior legs smooth; ventral side of pedipalp covered with small piligerous grains; long, spine-like hairs on ventral posterior tb, fe. Claws with 8 teeth or less; hardly larger than claw width.

Abdomen 3.50 long; grey; cylindrical. Abdominal dorsal hairs 0.02 long; thick, roughly straight, compressed, blunt, lateral knob at the tip; uniformly, thickly distributed.

Male copulatory bulbus T as long as DD (Fig. 9A-B); external distal border sloped backwards; internal sloped backwards. DD not bent, same T axis in lateral view; internal distal border not expanded. IS, ES proximally fused, similarly developed; IS truncated at DD middle part; ES bend markedly sclerotized. DD tip straight in lateral view. C present, short (Fig. 9C-D); distal end beside DD internal tip; well developed; located close to DD distal tip; proximal border sharply decreasing; distal border stepped, upper tip not projected, rounded, external side hollowed. AC present. LF present; distally not projected. L well developed. LF poorly developed. L external border not sclerotized, distally markedly folded; distal border approximately parallel, continuous. LA absent. F absent. AL present, very poorly developed; proximal border in posterior view fused with DH. P fused to T; perpendicular to T in lateral view (Fig. 9E); lateral length from 1/3 to 2/5 of T width; ridge present, perpendicular to T; not

expanded, upper margin smooth; not distally projected; posterior margin slightly folded towards internal side.

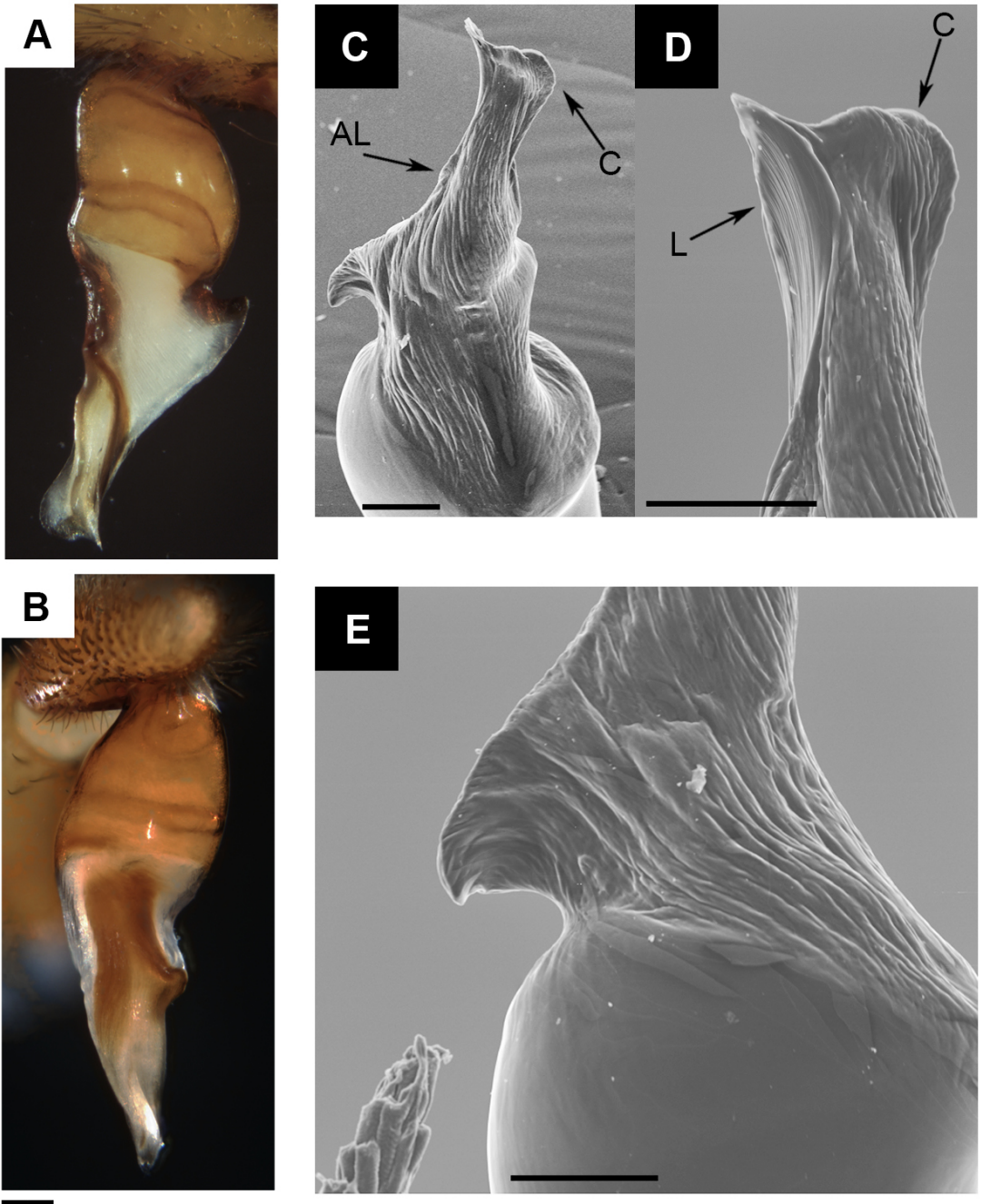


Figure 9. *D. aniepa* sp.n. (A) left palp retrolateral view; (B) left palp frontal view; (C) DD right palp frontal-prolateral view; (D) DD right palp prolateral view; (E) P right palp prolateral view. Scalebar = 0.1mm

Female paratype (NMH000856): (Fig. 10A-C). All characters as in male except: carapace 3.60 long; maximum width 2.97; minimum width 2.02. AME diameter 0.17; PLE 0.15; PME 0.14; AME on edge of Anterior border, separated from one another by about 2/3 diameter, close to PLE; PME touching to each other, about 1/3 PME diameter from PLE. Sternum orange, frontally darker, becoming lighter towards back.

Chelicerae 1.70 long, about 1/2 of carapace length in dorsal view; fang long, 1.42 mm. Lengths of female described above: fe1 2.48; pa1 1.73; ti1 2.10; me1 1.89; ta1 0.51; total 8.71; fe2 2.15; pa2 1.55; ti2 1.83; me2 1.72; ta2 0.47; total 7.72; fe3 1.79; pa3 1.11; ti3 1.15; me3 1.58; ta3 0.46; total 6.09; fe4 2.23; pa4 1.29; ti4 1.61; me4 2.05; ta4 0.51; total 7.69; fe Pdp 1.58; pa Pdp 0.85; ti Pdp 0.63; ta Pdp 0.83; total 3.89; relative length 1>2>4>3.

Abdomen 3.67 long; grey; cylindrical. Abdominal dorsal hairs 0.05 long.

Vulva DA clearly distinguishable from VA; DA slightly wider than long (Fig. 10A); DF wide in dorsal view. MF margins fused (Fig. 10B), sheet-like, well developed, completely sclerotized. VA rectangle-like; Anterior region completely sclerotized; posterior region sclerotized in most anterior area; AVD absent. S attachment not projected under VA (Fig. 10C); arms as long as DA, slightly curved; tips not projected; neck as wide as arms. TB usual shape.

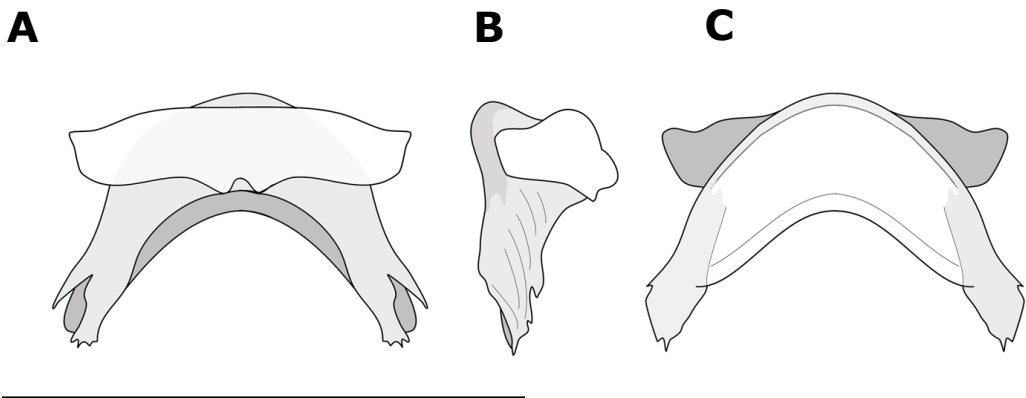


Figure 10. *D. aniepa* sp.n. vulva (A) ventral; (B) lateral; (C) dorsal view. Scalebar = 0.65mm

Table 1. Intraspecific leg measurements variability of *D. aniepa* sp.n (males/females).

	I	II	III	IV
Fe	2.5-2.7/2.25-2.75	2.05-2.35/1.9-2.3	1.65-2/1.6-1.8	2.05-2.35/1.95-2.45
Pa	1.6-1.8/1.45-1.8	1.45-1.65/1.3-1.65	1.05-1.15/0.95-1.2	1.05-1.3/1.1-1.4
Ti	2.15-2.45/1.85-2.3	1.8-2.1/1.55-2.05	1.2-1.35/1.05-1.3	1.7-1.85/1.55-1.8
Mt	1.9-2.15/1.65-2.05	1.8-1.95/1.55-1.85	1.55-1.75/1.4-1.65	1.85-2.25/1.8-2.15
Ta	0.45-0.55/0.4-0.55	0.45-0.55/0.45-0.5	0.45-0.5/0.4-0.5	0.45-0.5/0.45-0.5
Total	8.65-9.4/7.65-9.45	7.7-8.5/6.8-8.25	5.9-6.75/5.45-6.3	7.4-8.25/6.95-8.25

Intraspecific variation

Male cephalothorax ranges in length from 3.40-3.85 (N=4), females from 3.10-3.85 (N=5). Distal teeth could be closer to medial, almost at the same distance that goes from medial to basal. Leg measurements variability is listed in table 1.

Distribution

This species is known from the island of Tenerife, mainly found in Teno, in the north-west of the island and from one locality from Las Lagunetas (Fig. 11).

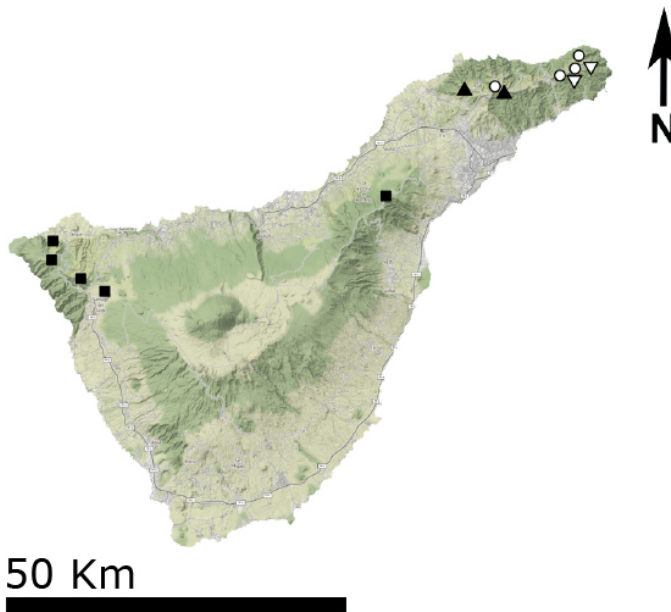


Figure 11. Map of Tenerife with the new species localities. *D. aniepa* sp.n. = black squares; *D. banot* sp.n. = white circles; *D. marmorata* sp.n. = black triangles; *D. tabona* sp.n. = inverted white triangles.

***Dysdera banot* sp.n.**

(Figs 6B, 7B, 8B, 12A-C)

Type material

Holotype: Spain. Canary Islands: Tenerife, Santa Cruz de Tenerife, Las Carboneras, 28.539290, -16.275800, N. Macías & S. Febles coll., 02/X/2015, 1 ♀ (NMH002929).

Paratypes: Spain. Canary Islands: Tenerife, Santa Cruz de Tenerife, Cabeza del Tejo, 28.565090, -16.165982, Netbiome coll., 23/I/2013, 1 ♀ (NMH002943).

Additional material examined: Spain. Canary Islands: Tenerife, Santa Cruz de Tenerife, Pista de Ijuana, 28.560191, -16.169190, N. Macías coll., 22/V/2006, 1 ♀; El Pijaral. Anaga, 28.551966, -16.189225, Netbiome coll., 11/I/2013, 1 ♀; Cabeza del Tejo, 28.565090, -16.165982, 23/I/2013, 1 ♀; P. Oromí coll., 23/I/2013, 1 imm.

Etymology

The specific name in apposition refers to a rod or spear fire-hardened used by the Guanches, characterized by the bulge in the upper third to be grasped.

Diagnosis

Can be clearly distinguished from all the other *Dysdera* species from Tenerife by the short chelicera (Fig. 6B) and the flat and enlarged fang (Fig. 8B). *D. banot* sp.n. is distinguished from the morphologically similar *D. hernandezi* Arnedo & Ribera, 1999 by the lack of eyes reduction in the former and the two-time bigger size. Males distinguished from *D. hernandezi* by the presence of AVD (Fig. 12A).

Description - Female holotype (NMH002929): (Figs 6B, 7B, 8B, 12A-C). Carapace 4.05 long; maximum width 3.50; minimum width 2.00. Dark red, uniformly distributed; heavily foveate, covered with circular depressions, some small black grains mainly at front (Fig. 6B, 7B). Anterior border roughly round, markedly smaller than 1/2 carapace length; anterior lateral borders convergent; rounded at maximum

dorsal width, posterior lateral borders rounded; posterior margin narrow, straight. AME diameter 0.22; PLE 0.22; PME 0.16; AME slightly back from anterior border, separated from one another by about 1/2 diameter, touching PLE; PME very close to each other, less than 1/4 PME diameter from PLE. Labium trapezoid-shaped, base wider than distal part; as long as wide at base; semicircular groove at tip. Sternum brownish orange, darkened on borders; very slightly wrinkled, mainly between legs and anterior border; covered in hairs mainly on margin.

Chelicerae 1.05 long, about 1/4 of carapace length in dorsal view; fang short, 0.85; enlarged on middle part; basal segment smooth, with no granulations. Chelicera inner groove short, about 1/3 cheliceral length; armed with three teeth and lamina at base; B>M>D; D triangular, located near segment tip; B close to basal lamina; M close to B (Fig. 8B). Legs dark orange-coloured. Lengths of female described above: fe1 2.45; pa1 1.85; ti1 1.85; me1 1.65; ta1 0.50; total 8.30; fe2 2.25; pa2 1.75; ti2 1.75; me2 1.75; ta2 0.50; total 8.00; fe3 2.05; pa3 1.25; ti3 1.40; me3 1.75; ta3 0.55; total 7; fe4 2.85; pa4 1.60; ti4 2.15; me4 2.70; ta4 0.65; total 9.95; fe Pdp 1.28; pa Pdp 0.83; ti Pdp 0.63; ta Pdp 0.97; total 3.71; relative length 4>1>2>3. Leg1 and leg2 spineless. Fe3d spineless; pa3 3 anterodorsal; tb3d spines arranged in four bands; proximal 2.2.0; medial-proximal 2.2.1; medial-distal 1.0.0; distal 2.0.0; tb3v spines arranged in two bands; proximal 1.2.0; medial-proximal 0; medial-distal 0; distal 1.0.0; with two terminal spines. Fe4d spineless; pa4 spineless; tb4d spines arranged in four bands; proximal 1.0.0; medial-proximal 1.3.1; medial-distal 0.1.0; distal 1.0.1; tb4v spines arranged in two bands; proximal 1.2.0; medial-proximal 0; medial-distal 0; distal 1.1.0; with two terminal spines. Dorsal side of anterior legs covered with hairs, lacking small grains; ventral side of pedipalp covered with small piligerous grains; Distal part of the metatarsus III and IV densely covered with short hair. Claws with 8 teeth or less; hardly larger than claw width.

Abdomen 4.45 long; cream-coloured; cylindrical. Abdominal dorsal hairs 0.08 long;

medium-sized, curved, not compressed, pointed; uniformly, thickly distributed.

Vulva DA clearly distinguishable from VA (Fig. 12B); DA as wide as long; DF wide in dorsal view (Fig. 12C). MF margins not fused, well developed, completely sclerotized, projected backwards, as long as DA lateral length. VA rectangle-like; anterior region completely sclerotized; posterior region sclerotized except for most internal area; sclerotized ridge at ventral VA external margin, as long as VA, bent to internal side; AVD present (Fig. 12A). S attachment not projected under VA; arms as long as DA, clearly curved; tips not projected; neck wider than arms. TB usual shape.

Intraspecific variation

Female cephalothorax ranges in length from 4.05-4.5 (N=5). Anterior part of prosoma could be slightly wider in proportion to middle part. Opisthosoma grey colored or whitish. Spination and leg measurements variability is listed in tables 2-3 respectively.

Distribution

This species is known from Anaga, in the Northern-east of the island of Tenerife (Fig. 11).

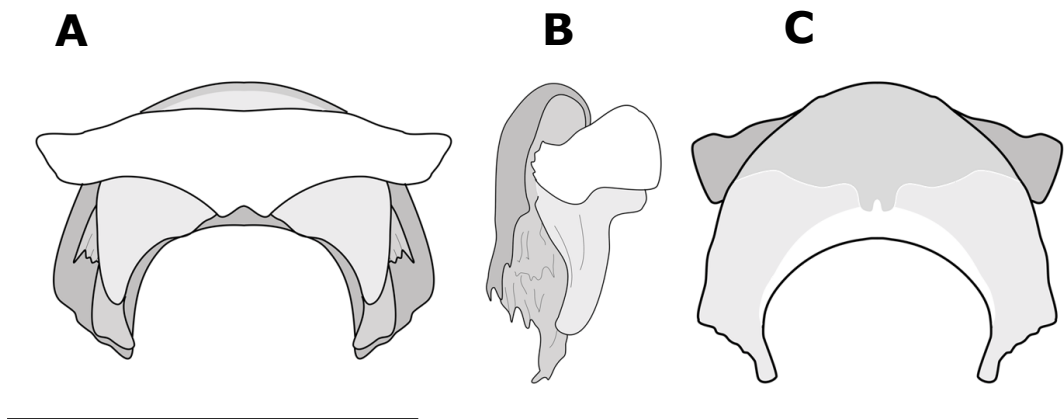


Figure 12. *D. banot* sp.n. vulva (A) ventral; (B) lateral; (C) dorsal view. Scalebar = 0.65mm

Table 2. Intraspecific spination variability of *D. banot* sp.n.

	Proximal	Medial-Proximal	Medial-Distal	Distal
Tibia 3 dorsal	0-2.1-3.0-1	0-3.2.0-1	0-2.0-1.0	1.0.0
Tibia 4 dorsal	1.0-2.0-1	0-1.0-3.0-1	0-1.0-2.0-1	0-1.0.0-1
Tibia 3 ventral	0-1.0-2.0	0-1.1-2.0-1	1-0.0.0	1-2.1-2.0-1
Tibia 4 ventral	0-2.1-2.1	0-1.0-1.0-1	0-1.0-1.0	2-1.1.0-1
	Number of rows		Number of spines	
Femur 3 dorsal	0	0	0	0
Femur 4 dorsal	0	0	0	0

Table 3. Intraspecific leg measurements variability of *D. banot* sp.n.

	I	II	III	IV
Fe	2.45-2.8	2.25-2.45	2.05-2.35	2.85-3.1
Pa	1.85-2.1	1.75-1.9	1.15-1.4	1.6-1.8
Ti	1.85-2.1	1.75-1.95	1.35-1.5	2.05-2.25
Mt	1.55-1.75	1.65-1.75	1.75-1.95	2.7-2.85
Ta	0.5-0.6	0.5-0.6	0.55-0.65	0.65-0.7
Total	8.3-9.25	8-8.5	7-7.8	9.95-10.65

***Dysdera gaifa* sp.n.**

(Figs 6C, 7C, 8C, 13A-C)

Type material

Holotype: Spain. Canary Islands: La Gomera, San Sebastián, Playa de Avalo, 28.114684, -17.113168, Planas E. & Espluga R. coll., 17/II/2011, 1 ♀ (NMH002927).

Paratypes: Spain. Canary Islands: La Gomera, Valle Gran Rey, Montaña de Las Pilas. La Mérica, 28.960000, -17.335703, S. de la Cruz & N. Macías coll., 04/II/2008, 1 ♀ (NMH001440).

Etymology

The specific name in apposition refers to spirited Canary. Also was a noble who joined Doràmas in the uprising against Guanarteme de Gáldar during XV century.

Diagnosis

D. gaifa sp.n. is distinguished from the morphologically similar *D. guamet* sp.n. by its small size, twice times shorter in carapace length, short and thick cheliceral basal segment shorter than half the size of the carapace length in the former, instead of slightly elongated with the same size than half of the carapace length. Can be clearly distinguished from all the other sympatric *Dysdera* species from La Gomera by the bulgy chelicera in lateral view (Fig. 7C).

Description – Female holotype (NMH002927): (Figs 6C, 7C, 8C, 13A-C). Carapace 3.03 long; maximum width 2.53; minimum width 1.72. Red orange, frontally darker, becoming lighter towards back (Fig. 6C); smooth with some small black grains mainly at front. Anterior border roughly round, from 1/2 to 3/5 carapace length; anterior lateral borders divergent; rounded at maximum dorsal width, posterior lateral borders straight; posterior margin narrow, straight. AME diameter 0.09; PLE 0.09; PME 0.11; AME on edge of anterior border, separated from one another by about 2 diameters, touching PLE; PME about one quarter of diameter apart, about 3/5 PME diameter from PLE. Labium trapezoid-shaped, base wider than distal part; longer than wide at base; semicircular groove at tip. Sternum orange, frontally darker, becoming lighter towards back or darkened on borders; smooth; uniformly covered in slender black hairs.

Chelicerae 1.58 long, about 1/2 of carapace length in dorsal view; fang long, 1.06; basal segment, proximal dorsal and ventral side, scantily covered with piligerous granulations. Chelicera inner groove short, about 1/3 cheliceral length; armed with three teeth and lamina at base; D=B>M; D triangular, located near segment tip; B close to basal lamina; M close to B (Fig. 8C). Anterior legs dark orange, posterior legs yellow. Lengths of female described above: fe1 1.99; pa1 1.39; ti1 1.65; me1 1.33; ta1 0.43; total 6.79; fe2 1.85; pa2 1.33; ti2 1.63; me2 1.36; ta2 0.45; total 6.62; fe3 1.49; pa3 0.99; ti3 1.04; me3 1.39; ta3 0.58; total 5.49; fe4 1.84; pa4 1.21; ti4 1.47; me4 1.72;

ta4 0.56; total 6.8; fe Pdp 1.34; pa Pdp 0.68; ti Pdp 0.51; ta Pdp 0.77; total 3.30; relative length 4=1>2>3. Leg1 and leg2 spineless. Fe3d spines in one row; 1; pa3 spineless; tb3d spines arranged in two bands; proximal 1.1.1; medial-proximal 0; medial-distal 0; distal 1.0.1.; tb3v spines arranged in two bands; proximal 1.2.0; medial-proximal 0; medial-distal 0; distal 1.0.1; with two terminal spines. Fe4d spines in two rows; forward 1; backward 3; pa4 spineless; tb4d spines arranged in three bands; proximal 0.0.1; medial-proximal 0; medial-distal 1.1.1; distal 1.0.1; tb4v spines arranged in three bands; proximal 0.0-1.0; medial-proximal 0.2.1; medial-distal 0; distal 1.0.1; with two terminal spines. Dorsal side of anterior legs smooth; ventral side of pedipalp covered with small piligerous grains. Claws with 8 teeth or less; hardly larger than claw width.

Abdomen 3.79 long; cream-coloured; cylindrical. Abdominal dorsal hairs 0.12 long; thin, curved, not compressed, pointed; uniformly, thickly distributed.

Vulva DA clearly distinguishable from VA (Fig. 13B); DA as wide as long (Fig. 13C); DF wide in dorsal view. MF margins fused, sheet-like, well developed, completely sclerotized. VA rectangle-like; anterior region completely sclerotized; posterior region sclerotized except for most internal area; AVD absent (Fig. 13A). S attachment projected under VA; arms are shorter than DA, straight; tips not projected; neck wider than arms. TB usual shape.

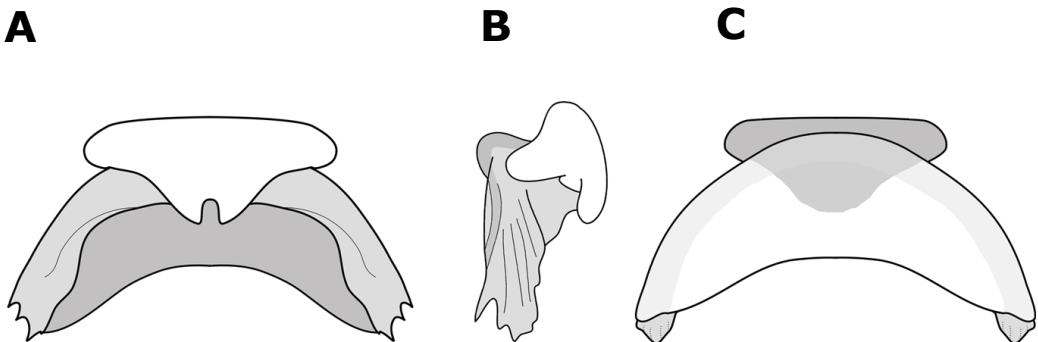


Figure 13. *D. gajifa* sp.n. vulva (A) ventral; (B) lateral; (C) dorsal view. Scalebar = 0.65mm

Table 4. Intraspecific spination variability of *D. gaifa* sp.n.

	Proximal	Medial-Proximal	Medial-Distal	Distal
Tibia 3 dorsal	1.1.0-1	0.0.0	0.0.0	1.0.1
Tibia 4 dorsal	0-1.0.1	0-1.1.0-1	0.0.0	1.0.1
Tibia 3 ventral	1.1.1	0.0.0	0.0.0	1.0.1
Tibia 4 ventral	0.2-0.0	0-1.1-2.1	0.0.0	1.0.1
	Number of rows		Number of spines	
Femur 3 dorsal	0	▼	0	
Femur 4 dorsal	2	▼	1/3-4	

Table 5. Intraspecific leg measurements variability of *D. gaifa* sp.n.

	I	II	III	IV
Fe	1.988-1.998	1.816-1.852	1.491-1.495	1.839-1.885
Pa	1.253-1.386	1.317-1.335	0.993-1.048	1.08-1.207
Ti	1.627-1.655	1.633-1.647	1.044-1.098	1.473-1.495
Mt	1.326-1.352	1.356-1.407	1.39	1.723-1.813
Ta	0.432-0.484	0.449-0.479	0.584	0.509-0.559
Total	6.704-6.797	6.625-6.666	5.502	6.782-6.801

Intraspecific variation

Female cephalothorax ranges in length from 2.99-3.09 (N=2). Carapace color frontally red. PME could be closer to PLE. Distal teeth could almost double the size of basal. Spination and leg measurements variability is listed in tables 4-5 respectively.

Distribution

This species is known from two localities of la Gomera (Fig. 14)

***Dysdera garoei* sp.n.**

(Figs 6D, 7D, 8D, 15A-C)

Type material

Holotype: Spain. Canary Islands: El Hierro, El Pinar, Pista del Mercader, 27.71294436, -18.02217517, GIET coll., 15/1/2011, 1 ♀ (CRBA002063).

Paratypes: Spain. Canary Islands: El Hierro, Frontera, Supra Casa Forestal Frontera, 27.735116, -18.0243833, H. López coll., 30/XI/2017, 1 ♀ (NMH003416).

Additional material examined: Spain. Canary Islands: El Hierro, Frontera, Cueva de la Curva, 27.69234819, -17.972877, GIET coll., 15/2/2004, 1 imm.; Supra Casa Forestal Frontera, 27.735116, -18.0243833, H. López coll., 30/XI/2017, 1 ♀.

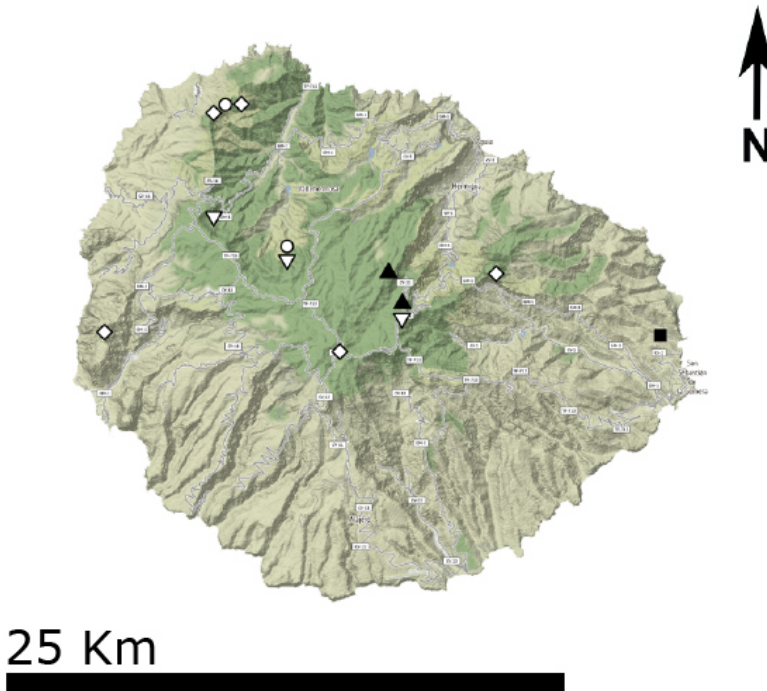


Figure 14. Map of La Gomera with the new species localities. *D. gaifa* sp.n. = black squares; *D. guamet* sp.n. = white circles; *D. hirguan* = black triangles; *D. undupe* sp.n. = inverted white triangles; *D. yballa* sp.n. = white diamond.

Etymology

The name is given after Garoé de la Cruz Macías-Hernandez, name of the son of Nuria Macías-Hernandez, one of the authors of this paper.

Diagnosis

D. garoei sp.n. clearly distinguished from all the other *Dysdera* species from El Hierro by the bulgy chelicera in lateral view (Fig. 7D), eye reduction and 3 terminal prolatral spines in fe1. Female of *D. garoei* sp.n. distinguished from the sympatric species *D. gomerensis* and *D. silvatica* by the wide S curved backwards in ventral view.

Description – Female holotype (CRBA002063): (Figs 6D, 7D, 8D, 15A-C). Carapace 2.70 long; maximum width 2.02; minimum width 1.41. Red orange, frontally darker, becoming lighter towards back; smooth with some small black grains mainly at front; hairy, covered with black hairs mainly at lateral and posterior borders. Anterior border roughly round, from 1/2 to 3/5 carapace length; anterior lateral borders divergent; rounded at maximum dorsal width, posterior lateral borders rounded; posterior margin narrow, straight (Fig. 6D). Eyes markedly reduced but all present; AME diameter 0.05; PLE 0.045; PME 0.05; AME separation 0.24; AME-PLE separation 0.04; PLE-PME separation 0.08. Labium trapezoid-shaped, base wider than distal part; longer than wide at base; semicircular groove at tip. Sternum orange, uniformly distributed; smooth; uniformly covered in slender black hairs.

Chelicerae 1.31 long, about 1/2 of carapace length in dorsal view; fang medium-sized, 0.78; basal segment dorsal, ventral side completely covered with piligerous granulations. Chelicera inner groove short, about 1/3 cheliceral length; armed with three teeth and lamina at base; $B > D = M$; D triangular, located near segment tip; B close to basal lamina; M close to B (Fig. 8D). Anterior legs dark orange, posterior legs yellow. Lengths of female described above: fe1 2.2; pa1 1.34; ti1 1.76; me1 1.66; ta1 0.45; total 7.41; fe2 2.01; pa2 1.22; ti2 1.59; me2 1.55; ta2 0.43; total 6.8; fe3 1.8; pa3 0.93;

ti3 1.17; me3 1.58; ta3 0.47; total 5.95; fe4 2.05; pa4 1.11; ti4 1.66; me4 2.01; ta4 0.59; total 7.42; fe Pdp 1.13; pa Pdp 0.65; ti Pdp 0.52; ta Pdp 0.73; total 3.03; relative length 4=1>2>3. Leg 1 3-2 terminal spines on forward margin; leg2 spineless. Fe3d spines in one row; 3; pa3 spineless; tb3d spines arranged in three bands; proximal 1-0.0.0; medial-proximal 1.1.1; medial-distal 0; distal 1.0.1.; tb3v spines arranged in three bands; proximal 1.0.1; medial-proximal 0.1.1; medial-distal 0; distal 1.0.0; with two terminal spines. Fe4d spines in two rows; forward 1; backward 5; pa4 spineless; tb4d spines arranged in two bands; proximal 1.1.1; medial-proximal 0; medial-distal 0; distal 1.0.1; tb4v spines arranged in three bands; proximal 0.1.0; medial-proximal 1.1.1; medial-distal 0; distal 1.1.1; with two terminal spines. Dorsal side of anterior legs covered with small piligerous grains; ventral side of pedipalp covered with small piligerous grains. Claws with 8 teeth or less; hardly larger than claw width.

Abdomen 3.59 mm long; cream-coloured; cylindrical. Abdominal dorsal hairs 0.11 mm long; thin, roughly straight, not compressed, pointed; uniformly, thickly distributed.

Vulva DA clearly distinguishable from VA (Fig. 15B); DA slightly wider than long (Fig. 15C); DF wide in dorsal view. MF margins not fused, well developed, completely

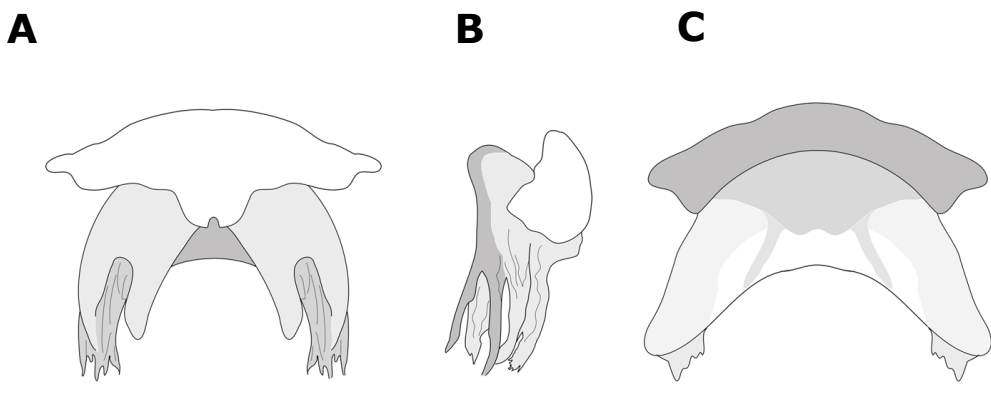


Figure 15. *D. garoei* sp.n. vulva (A) ventral; (B) lateral; (C) dorsal view. Scalebar = 0.65mm

Table 6. Intraspecific spination variability of *D. garoei* sp.n.

	Proximal	Medial-Proximal	Medial-Distal	Distal
Tibia 3 dorsal	1.1-2.1	0.0.0	0.0.0	1.0.1
Tibia 4 dorsal	1.1.1	0.0.0	0.0.0	1.0.1
Tibia 3 ventral	1.0-1.1	0.1.1-2	0.0.0	1.0.1
Tibia 4 ventral	0.1.0	1.1.1	0.0-1.0-1	0-1.1.1
	Number of rows		Number of spines	
Femur 3 dorsal	1	3		
Femur 4 dorsal	2	1/5		

Table 7. Intraspecific leg measurements variability of *D. garoei* sp.n.

	I	II	III	IV
Fe	2.066-2.75	2.01-2.6	1.547-2.05	1.905-2.05
Pa	0.994-1.6	1.22-1.5	0.768-1.1	1.07-1.11
Ti	1.661-2.2	1.59-2	1.084-1.55	1.546-1.66
Mt	1.468-1.9	1.55-1.9	1.447-1.85	1.877-2.01
Ta	0.45-0.481	0.43-0.5	0.466-0.5	0.406-0.59
Total	6.67-8.9	6.8-8.5	5.312-7.05	6.804-7.42

sclerotized, projected backwards, shorter than DA lateral length. VA rectangle-like; anterior region completely sclerotized; posterior region sclerotized except for most internal area (Fig. 15A); tooth-shaped expansion from internal posterior border; joined to lateral sclerotization, except for its back ends, slightly shorter than DF lateral margins; AVD absent. S attachment not projected under VA; arms as long as DA, slightly curved; tips not projected; neck as wide as arms. TB usual shape.

Intraspecific variation

Female cephalothorax ranges in length from 2.69-3.11 (N=3). Leg colors vary from pale darkish orange in the anterior legs to bright orange. Sternum could have a brighter coloration. In the tibia from leg 2 could present a ventral spine. Spination and leg measurements variability is listed in tables 6-7 respectively.

Distribution

This species is known from the south of the island of El Hierro (Fig. 16)

***Dysdera guamet* sp.n.**

(Figs 6E, 7E, 8E, 17A-E, 18A-C)

Type material

Holotype: Spain. Canary Islands: La Gomera, Vallehermoso, Teselinde. Ermita de Santa Clara, 28.1963, -17.28754, N. Macías & S. Toft coll., 08/IV/2011, 1 ♂ (CRBA002058).

Paratypes: Spain. Canary Islands: La Gomera, Vallehermoso, Teselinde. Ermita de Santa Clara, 28.1963, -17.28754, GIET coll., 06/VIII/2002, 1 ♀ (NMH002996); N. Macías & S. de la Cruz coll., 10/III/2012, 1 ♀ (CRBA002056, NMH001883); M. Rezac coll., 16/X/2010, 1 ♂ (CRBA002495).

Additional material examined: Spain. Canary Islands: La Gomera, Vallehermoso, Teselinde. Ermita de Santa Clara, 28.1963, -17.28754, N. Macías & S. de la Cruz coll., 10/III/2012, 2 imm.; M. Rezac coll., 15/X/2010, 1 imm.; Arnedo, Bellvert & Oromí coll., 17/3/2017, 1 ♂, 2 imm.; Ctra. Cumbre, altura Mora Gaspar, 28.14614, -17.262784,



Figure 16. Map of El Hierro (left) and La Gomera (right) with the new species localities. *D. garoei* sp.n. = black squares; *D. orahan* sp.n. = white circles.

Arnedo, Bellvert, Domènech & Oromí coll., 21/III/2019, 2 imm.; Vallehermoso, Teselinde. Ermita de Santa Clara, 28.1963, -17.28754, 1 imm.

Etymology

The specific name in apposition refers to a Guamet, king of La Gomera, which later was Christianised as Sebastian.

Diagnosis

Dysdera guamet sp.n. is distinguished from the morphologically similar *D. silvatica* by the bulgy chelicera in the former and flattened carapace (Fig. 7E), a light red colored prosoma and light orange or yellow legs instead of dark red. Males are distinguished from *D. silvatica* by the P upper margin ridge expansion and C tip projected distally (Fig. 17A, C, E). Females are distinguished from *D. silvatica* by the S lateral tips directed backwards instead of markedly projected forward in ventral view (Fig. 18A).

Description – Male holotype (CRBA002058): (Figs 6E, 7E, 8E, 17A-E). Carapace 4.66 long; maximum width 3.58; minimum width 2.41. Orange, frontally darker, becoming lighter towards back; smooth with some small black grains mainly at front; hairy, uniformly covered with white hairs (Fig. 6E). Anterior border roughly straight, from 1/2 to 3/5 carapace length; anterior lateral borders divergent; pointed at maximum dorsal width, posterior lateral borders straight; posterior margin narrow, straight. AME diameter 0.16; PLE 0.10; PME 0.12; AME on edge of anterior border, separated from one another by about 2 diameters, touching PLE; PME about one diameter apart, about 1/3 PME diameter from PLE. Labium trapezoid-shaped, base wider than distal part; longer than wide at base; semicircular groove at tip. Sternum orange, darkened on borders; very slightly wrinkled, mainly between legs and anterior border; uniformly covered in slender black hairs.

Chelicerae 2.02 mm long, about 2/5 of carapace length in dorsal view; fang

medium-sized, 1.66 mm; basal segment dorsal, ventral side completely covered with piligerous granulations. Chelicera inner groove medium-size, about $2/5$ cheliceral length; armed with three teeth and lamina at base; $D > B > M$; D triangular, located roughly at centre of groove; B close to basal lamina; M close to B (Fig. 8E). Legs orange. Lengths of male described above: fe1 3.39; pa1 2.23; ti1 2.97; me1 2.6; ta1 0.69; total 11.88; fe2 3.04; pa2 2.12; ti2 2.84; me2 2.57; ta2 0.62; total 11.194; fe3 2.51; pa3 1.5; ti3 1.97; me3 2.31; ta3 0.72; total 9.01; fe4 3.07; pa4 1.58; ti4 2.43; me4 2.29; ta4 0.72; total 11.96; fe Pdp 2.19; pa Pdp 1.14; ti Pdp 1.14; ta Pdp 0.97; total 5.44; relative length: $4 > 1 > 2 > 3$. Leg1 and leg2 spineless. Fe3d spines in one row; 3; pa3 spineless; tb3d spines arranged in three bands; proximal 0.0.0-1; medial-proximal 1.0.1; medial-distal 0; distal 1-0.0.0; tb3v spines arranged in three bands; proximal 1.2.0; medial-proximal 0.0-1.0; medial-distal 0; distal 1.0.0; with two terminal spines. Fe4d spines in two rows; forward 1; backward 5; pa4 spineless; tb4d spines arranged in three bands; proximal 0-1.0.1; medial-proximal 1.0.1; medial-distal 0; distal 1.0.1; tb4v spines arranged in three bands; proximal 1.1-2.1; medial-proximal 0.1-2.0; medial-distal 0; distal 0-1.0.1; with two terminal spines. Dorsal side of anterior legs smooth; ventral side of pedipalp covered with small piligerous grains. Claws with 8 teeth or less; hardly larger than claw width.

Abdomen 6.41 long; grey; cylindrical. Abdominal dorsal hairs 0.10 long; thin, roughly straight, compressed, pointed; uniformly, thickly distributed.

Male copulatory bulbus T slightly longer than DD (Fig. 17A); external distal border sloped backwards; internal sloped backwards. DD slightly bent in lateral view, clearly less than 45° ; internal distal border not expanded. IS, ES equally developed; IS truncated at DD middle part (Fig. 17B). DD tip sloped towards back in lateral view; anterior (upper) sheet internal part markedly projected above posterior (lower) sheet. C present, short; distal end beside DD internal tip; well developed; located close to DD distal tip; proximal border sharply decreasing; distal border markedly sloped, upper

tip not projected, pointed, external side hollowed (Fig. 17C). AC present (Fig. 17D). LF absent. L well developed; external border not sclerotized, laterally slightly folded, distally projected; distal border divergent, continuous. LA absent. F absent. AL present, well developed (Fig. 17E); proximal border in posterior view toothed on its internal half-part. P fused to T; perpendicular to T in lateral view; lateral length from

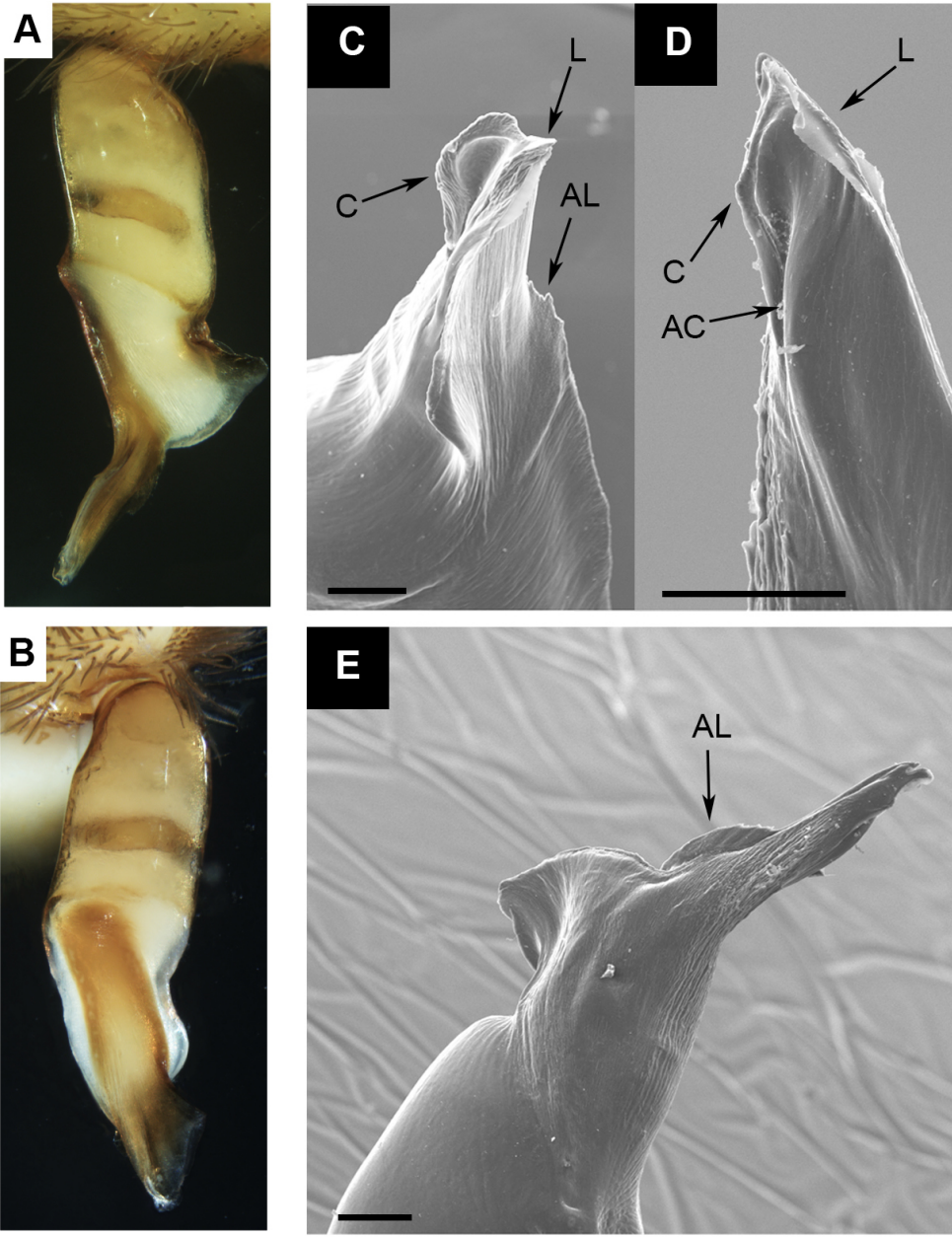


Figure 17. *D. guamet* sp.n. (A) left palp retrolateral view; (B) left palp frontal view; (C) DD right palp frontal-retrolateral view; (D) DD right palp retrolateral view; (E) DD right palp frontal-prolateral view. Scalebar = 0.1mm

2/5 to 1/2 of T width; ridge present, perpendicular to T; distinctly expanded, rounded, upper margin smooth; not distally projected; posterior margin slightly folded towards internal side.

Female paratype (CRBA002056): (Fig. 18A-C). All characters as in male except: carapace 5.39 mm long; maximum width 4.27; minimum width 2.97. Dark red, frontally darker, becoming lighter towards back. Anterior border roughly round. AME diameter 0.23; PLE 0.15; PME 0.12; PME about one diameter apart, about 3/5 PME diameter from PLE. Sternum brown red, darkened on borders.

Chelicerae 2.52 long, about 1/2 of carapace length in dorsal view; fang medium-sized, 2.02. Chelicera inner groove short, about 1/3 cheliceral length; armed with three teeth and lamina at base; $D > B > M$; D triangular, located near segment tip; B close to basal lamina; M at middle of B and D. Lengths of female described above: fe1 3.98; pa1 2.63; ti1 3.4; me1 2.82; ta1 0.66; total 13.49; fe2 3.75; pa2 2.48; ti2 3.15; me2 2.73; ta2 0.69; total 12.8; fe3 3.02; pa3 1.82; ti3 2.22; me3 2.76; ta3 0.62; total 10.44; fe4 3.67; pa4 2.14; ti4 2.48; me4 3.69; ta4 0.69; total 12.67; fe Pdp 2.61; pa Pdp 1.31; ti Pdp 1.1; ta Pdp 1.32; total 6.34; relative length $1 > 2 > 4 > 3$. Fe3d spineless; tb3d spines arranged in two bands; proximal 1.0.1; medial-proximal 0; medial-distal 0; distal 1.0.1. ; tb3v spines arranged in two bands; proximal 1.2.0; medial-proximal 0; medial-distal

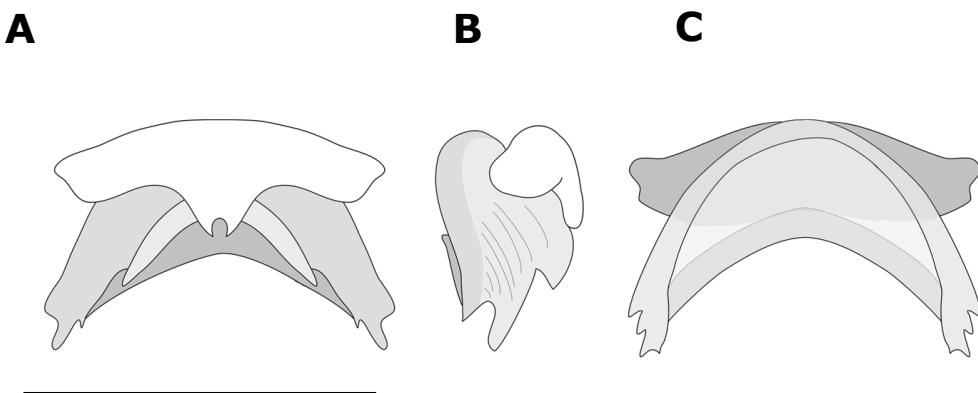


Figure 18. *D. guamet* sp.n. vulva (A) ventral; (B) lateral; (C) dorsal view. Scalebar = 0.65mm

Table 8. Intraspecific spination variability of *D. guamet* sp.n.

	Proximal	Medial-Proximal	Medial-Distal	Distal
Tibia 3 dorsal	1.0.1-0	0-1.0.0-1	0.0.0	1.0.0-1
Tibia 4 dorsal	1.0.1	0-1.0-1.0-1	0-1.0.0	1.0.1
Tibia 3 ventral	1.2.0-1	0.0.0	0.0.0	1.0.0-1
Tibia 4 ventral	1-2.2.0-1	1.0-1.1	0.0.0	1-0.0.1-0
	Number of rows	Number of spines		
Femur 3 dorsal	1	0-3		
Femur 4 dorsal	2	1/5		

Table 9. Intraspecific leg measurements variability of *D. guamet* sp.n (males/females).

	I	II	III	IV
Fe	3.39-4.116/2.264-3.98	3.04-3.913/2.058-3.75	2.51-3.088/1.613-3.02	3.07-3.837/2.132-3.67
Pa	2.23-2.696/1.45-2.63	2.12-2.528/1.37-2.48	1.5-1.819/0.911-1.82	2.07-2.16/1.204-2.14
Ti	2.97-3.828/1.801-3.4	2.84-3.596/1.57-3.15	1.97-2.179/1.045-2.22	2.43-2.842/1.609-2.48
Mt	2.6-3.374/1.574-2.82	2.57-3.37/1.552-2.73	2.31-3.045/1.45-2.76	2.29-3.751/2.073-3.69
Ta	0.69-0.76/0.473-0.66	0.62-0.773/0.466-0.69	0.71-0.72/0.4-0.62	0.72-0.77/0.53-0.69
Total	11.88-14.755/7.562-13.49	11.19-13.945/7.016-12.8	9.01-10.841/5.419-10.44	10.58-13.215/7.548-12.67

0; distal 1.0.0; with two terminal spines. Fe4d spines in two rows; forward 1; backward 5; pa4 spineless; tb4d spines arranged in three bands; proximal 1.0.1; medial-proximal 0-1.0-1.0; medial-distal 0; distal 1.0.1; tb4v spines arranged in two bands; proximal 1.2.1; medial-proximal 0; medial-distal 0; distal 1.0-1.1; with two terminal spines.

Abdomen 6.57 long; grey. Abdominal dorsal hairs 0.18 long.

Vulva DA clearly distinguishable from VA (Fig. 18A); DA twice as wide as long; DF wide in dorsal view. MF margins fused (Fig. 18B), sheet-like, well developed, completely sclerotized. VA rectangle-like; anterior region completely sclerotized; posterior region sclerotized except for most internal area; tooth-shaped expansion from internal posterior border (Fig. 18C); joined to lateral sclerotization, along its lateral border or except for its back ends, markedly reduced in size; AVD absent. S attachment projected under VA; arms are shorter than DA, slightly curved; tips not projected; neck as wide as arms. TB usual shape.

Intraspecific variation

Male cephalothorax ranges in length from 4.66-5.50 (N=3), females from 2.87-5.39 (N=2). Some specimens could be significantly smaller. Teeth could be equidistant between each other. Carapace color could range from light orange to dark red. Spination and leg measurements variability is listed in tables 8-9 respectively.

Distribution

This species is known from the north-west of the island of La Gomera (Fig. 14)

Dysdera herii sp.n.

(Figs 6F, 7F, 8F, 19A-E, 20A-C)

Type material

Holotype: Spain. Canary Islands: Gran Canaria, Ingenio, Barranco del Draguillo, 27.9415683310482, -15.4299929537, H. López coll., 08/VIII/2015, 1 ♂ (NMH003345).

Paratypes: Spain. Canary Islands: Gran Canaria, Agaete, El Sao, 28.068764, -15.65699, H. López coll., 01/IV/2013, 1 ♀ (NMH002745); Telde, Caldera de los Marteles, 27.9522425, -15.527475, 26/3/2016, 1 ♂ (NMH003361); Ingenio, Barranco del Draguillo, 27.9415683, -15.429992, 28/XII/2008, 1 ♀ (NMH001486).

Additional material examined: Spain. Canary Islands: Gran Canaria, Telde, Ojos de Garza (litoral), 27.95386594, -15.37676092, H. López coll., 02/I/2002, 1 imm.; Vecindario, Cueva La Luna, 27.91031944, -15.5300565, 02/I/2005, 1 imm.; Valsequillo, Mina La Federica, M. Naranjo & D. Suárez coll., 03/III/2018, 1 imm.; Ingenio, Los Majaletes, 27.94016127, -15.4991995, H. López coll., 03/V/2006, 1 imm.; Barranco del Draguillo, 27.9415683, -15.429992, 26/III/2016, 8 imm.; Valsequillo, Mina de los

Llanetes, 27.98840205, -15.4789812, M. Naranjo coll., 06/XII/2013, 1 imm.; Ingenio, Barranco del Draguillo, 27.941568331, -15.42999295, H. López coll., 08/VIII/2015, 1 imm., 1 imm., 1 imm.; 27.9415683, -15.429992, 13/VIII/2018, 1 imm.; 12/VIII/2017, 1 imm., 1 imm.; Telde, Caldera de los Marteles, 27.9522425, -15.527475, 1 ♀; Ingenio, Los Majaletes, 27.94016127, -15.499199578, 12/IX/2005, 1 imm.; Barranco del Draguillo, 27.9415683, -15.429992, 23/XII/2007, 1 imm.; Mogán, Barranco de Tasarte, Mina del Pino Cortado, 27.90405, -15.77354, M. Naranjo coll., 15/VI/2013, 1 imm.; Ingenio, Barranco del Draguillo, 27.9415683, -15.429992, H. López coll., 16/VIII/2007, 1 imm., 1 imm.; Los Majaletes, 27.94016127, -15.499199578, 2 imm.; Barranco del Draguillo, 27.9415683, -15.429992, 19/IV/2019, 1 imm.; 26/XII/2006, 3 imm.; Telde, Caldera de los Marteles, 27.9522425, -15.527475, 26/III/2016, 1 imm.; Ingenio, Barranco del Draguillo, 27.9415683, -15.429992, H. Lopez coll., 28/XII/2008, 1 imm.; H. López coll., 28/XII/2008, 1 imm.; 30/XII/2011, 1 imm.; Telde, Caldera de los Marteles, 27.952243, -15.527475, 30/XII/2019, 1 ♀ .

Etymology

The name is given after Heriberto “Heri” Lopez, friend and collage who has sampled extensively the Canary Islands and found for the first-time specimens of this species.

Diagnosis

D. herii sp.n. is distinguished from the morphologically similar *D. arabisenen* Arnedo & Ribera, 1997 by the presence of spines in femurs 3 and 4 and the lack of pilosity in the carapace in the former. *D. herii* sp.n. is clearly distinguished from the other sympatric species from Gran Canaria by its huge size, twice bigger than *D. arabisenen*, de second bigger *Dysdera* spider from Gran Canaria.

Description – Male holotype (NMH003345): (Figs 6F, 7F, 8F, 19A-E). Carapace 7.87 long; maximum width 6.13; minimum width 3.75. Red orange, frontally darker,

becoming lighter towards back; smooth with some small black grains mainly at front (Fig. 6F). Anterior border roughly round, markedly smaller than 1/2 carapace length; anterior lateral borders divergent; pointed at maximum dorsal width, posterior lateral borders straight; posterior margin wide, straight. AME diameter 0.23; PLE 0.23; PME 0.20; AME on edge of anterior border, separated from one another by about 2 diameters, close to PLE; PME about one quarter of diameter apart, about 1 PME diameter from PLE. Labium trapezoid-shaped, base wider than distal part; longer than wide at base; semicircular groove at tip. Sternum orange, frontally darker, becoming lighter towards back; very slightly wrinkled, mainly between legs and anterior border; uniformly covered in slender black hairs.

Chelicerae 3.92 long, about 1/2 of carapace length in dorsal view; fang medium-sized, 2.35; basal segment dorsal, ventral side completely covered with piligerous granulations. Chelicera inner groove short, about 1/3 cheliceral length; armed with three teeth and lamina at base; $D=B>M$; D triangular, located roughly at centre of groove; B close to basal lamina; M close to B (Fig. 8F). Legs orange. Lengths of male described above: fe1 7.36; pa1 4.56; ti1 6.88; me1 6.64; ta1 1.20; total 26.64; fe2 6.72; pa2 4.32; ti2 5.84; me2 6.08; ta2 1.20; total 24.16; fe3 5.20; pa3 2.96; ti3 4.16; me3 5.04; ta3 1.12; total 18.48; fe4 6.88; pa4 3.76; ti4 5.28; me4 6.64; ta4 1.20; total 23.76; fe Pdp 3.93; pa Pdp 2.05; ti Pdp 1.86; ta Pdp 1.631; total 9.48; relative length: $1>2>4>3$. Leg2 one terminal spine on the forward margin. Fe3d spines in two rows; forward 4-3; backward 1; pa3 spineless; tb3d spines arranged in four bands; proximal 1.0.1; medial-proximal 1.1.1; medial-distal 1.0.0; distal 1.0.1; tb3v spines arranged in three bands; proximal 1.1.0; medial-proximal 0.1.1; medial-distal 0; distal 1.1.0; with two terminal spines. Fe4d spines in two rows; forward 4-3; backward 7-8; pa4 spineless; tb4d spines arranged in four bands; proximal 0-1.0-1.1; medial-proximal 1.0-1.1; medial-distal 1.1.0-1; distal 1.0.1; tb4v spines arranged in four bands; proximal 0.1-2.0; medial-proximal 1.1-2.1; medial-distal 1.1.1; distal 1.1-2.1; with two terminal spines. Dorsal

side of anterior legs smooth; ventral side of pedipalp smooth. Claws with 8 teeth or less; hardly larger than claw width.

Abdomen 10 long; cream-coloured; cylindrical. Abdominal dorsal hairs 0.125 long; thick, roughly straight, compressed, blunt, tip not enlarged; uniformly, thickly distributed.

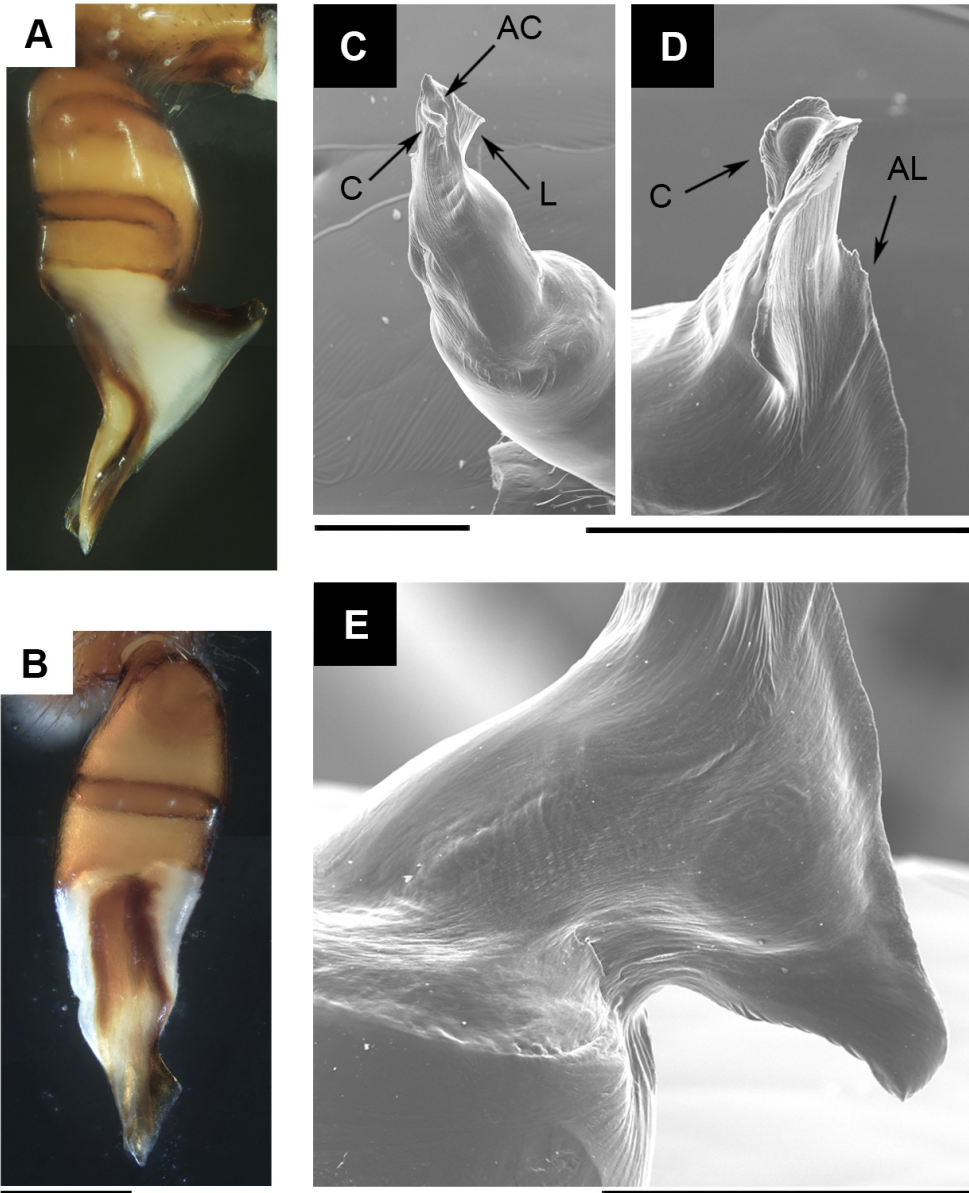


Figure 19. *D. herii* sp.n. (A) left palp retrolateral view; (B) left palp frontal view; (C) DD right palp frontal view; (D) DD right palp retrolateral view; (E) P right palp retrolateral view. Scalebar = 0.5mm

Male copulatory bulbus T slightly shorter than DD (Fig. 19A); external distal border sloped backwards; internal sloped backwards. DD slightly bent in lateral view, clearly less than 45° ; internal distal border not expanded. IS, ES proximally fused, similarly developed (Fig. 19B); IS truncated at DD middle part. DD tip straight in lateral view. C present, short; distal end on DD internal tip; well developed; located close to DD distal tip; proximal border sharply decreasing; distal border sloping in its base, upper tip not projected, pointed, external side hollowed (Fig. 19D). AC present (Fig. 19C). LF absent. L well developed; external border not sclerotized, not folded; distal border divergent, continuous. LA absent. F absent. AL present, very poorly developed or reduced to a small tooth; proximal border in posterior view fused with DH. P fused to T; perpendicular to T in lateral view (Fig. 19E); lateral length from $1/2$ to $2/3$ of T width; ridge present, perpendicular to T; not expanded, upper margin slightly toothed, mainly on external side, along its extent; few teeth (4-6); distally slightly projected; posterior margin slightly folded towards internal side.

Female paratype (NMH001486): (Fig. 20A-C). All characters as in male except: carapace 8.70 long; maximum width 6.90; minimum width 4.20. AME diameter 0.24; PLE 0.20; PME 0.24; PME very close to each other, about 1 PME diameter from PLE. Sternum dark orange, frontally darker, becoming lighter towards back.

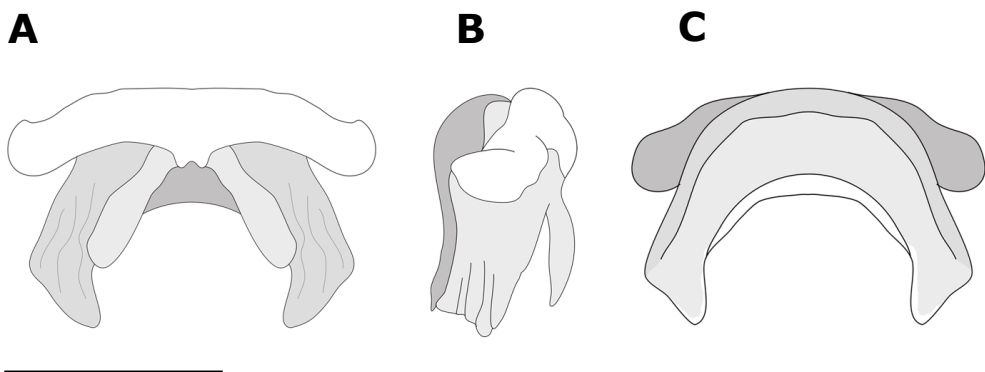


Figure 20. *D. herii* sp.n. vulva (A) ventral; (B) lateral; (C) dorsal view. Scalebar = 0.65mm

Table 10. Intraspecific spination variability of *D. herii* sp.n.

	Proximal	Medial-Proximal	Medial-Distal	Distal
Tibia 3 dorsal	1.0-1.0-1	1.1.1	0-1.0-1.0-1	0-1.0.0-1
Tibia 4 dorsal	1.0-1.0-1	1.0-1.0-1	0-1.0-1.0-1	1.0.1
Tibia 3 ventral	0-1.0-1.0	0-1.1.1	0-1.0-1.0-1	1.0-1.0
Tibia 4 ventral	0-2.1-2.0	1.1.1	1.0-2.0-1	1.1.0-1
	Number of rows		Number of spines	
Femur 3 dorsal	2	4/1-2		
Femur 4 dorsal	2	3-4/8-9		

Table 11. Intraspecific leg measurements variability of *D. herii* sp.n (males/females).

	I	II	III	IV
Fe	7.36-7.44/7.055-7.9	6.64-6.72/6.64-6.72	5.2-5.44/5.19-5.9	6.88/6.926-7.2
Pa	4.56-4.88/4.67-5.1	4.32-4.48/3.71-4.6	2.96-3.04/2.813-3.5	3.76-3.84/3.651-4
Ti	6.88-7.04/6.4-7	5.84-6.32/5.782-6.2	4.16/3.66-4.1	5.28-5.68/5.35-5.9
Mt	6.4-6.64/6.34-6.7	6.08/5.828-6.1	4.88-5.04/4.77-5.3	6.64/6.34-6.7
Ta	1.2/1.17-1.369	1.2/1.17-1.276	1.04-1.12/1.081-1.13	1.12-1.2/1.1-1.22
Total	26.64-26.96/25.924-27.9	24.16-24.72/23.1-25.3	18.48-18.56/17.704-19.9	23.76-24.16/23.68-24.9

Chelicerae 3.80 long, about 2/5 of carapace length in dorsal view; fang long, 3.25. Chelicera inner groove medium-size, about 2/5 cheliceral length; D triangular, located near segment tip. Lengths of female described above: fe1 7.90; pa1 5.10; ti1 7.00; me1 6.70; ta1 1.20; total 27.90; fe2 7.20; pa2 4.60; ti2 6.20; me2 6.10; ta2 1.20; total 25.30; fe3 5.90; pa3 3.50; ti3 4.10; me3 5.30; ta3 1.10; total 19.90; fe4 7.20; pa4 4.00; ti4 5.90; me4 6.70; ta4 1.10; total 24.90; fe Pdp 4.14; pa Pdp 2.27; ti Pdp 1.84; ta Pdp 2.38; total 10.63; relative length 1>2>4>3. Leg2 one terminal spine on the forward margin. Fe3d spines in two rows; forward 4-3; backward 2; pa3 spineless; tb3d spines arranged in four bands; proximal 1.0.1; medial-proximal 1.1.1; medial-distal 1.0.0; distal 1.0.1.; tb3v spines arranged in three bands; proximal 1.1.0; medial-proximal 0.1.1; medial-distal 0; distal 1.2.0-1; with two terminal spines. Fe4d spines in two rows; forward 3; backward 7-8; pa4 spineless; tb4d spines arranged in four bands; proximal 2-1.0.1; medial-proximal 1.1.1; medial-distal 1.2.1; distal 1.0.1; tb4v spines arranged in four bands; proximal 1.1.1; medial-proximal 1.1-2.1; medial-distal 1.1-2.1; distal 1.1-3.1;

with two terminal spines. Dorsal side of anterior legs smooth; ventral side of pedipalp covered with small piligerous grains.

Abdomen 9.00 long. Abdominal dorsal hairs 0.16 long.

Vulva DA clearly distinguishable from VA (Fig. 20B); DA as wide as long; DF wide in dorsal view (Fig. 20C). MF margins not fused, well developed, completely sclerotized. VA rectangle-like; anterior region completely sclerotized; posterior region sclerotized except for most internal area; sclerotized ridge at ventral VA external margin, as long as VA, bent to internal side; tooth-shaped expansion from internal posterior border; not joined to lateral sclerotization (Fig. 20A), about half of DF lateral margins; AVD absent. S attachment not projected under VA; arms as long as DA, clearly curved; tips not projected; neck wider than arms. TB usual shape.

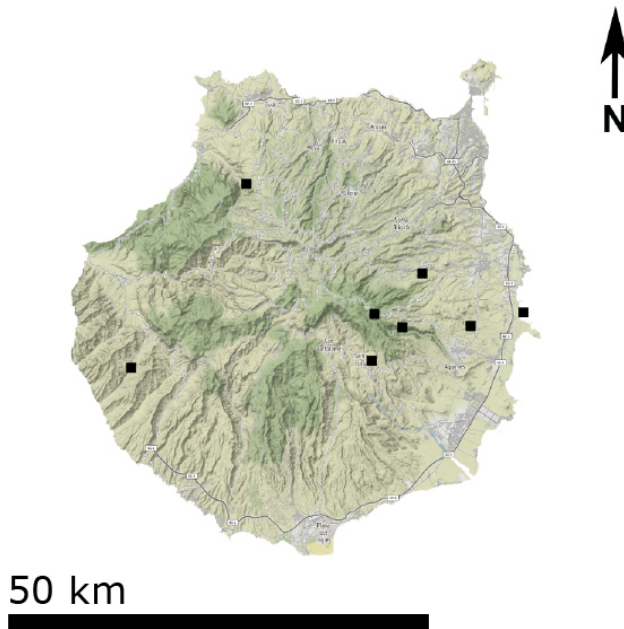


Figure 21. Map of Gran Canaria with the new species localities. *D. herii* sp.n. = black squares.

Intraspecific variation

Male cephalothorax ranges in length from 7.875-7.92 mm (N=2), females from 8.109-8.7 mm (N=3). Spination and leg measurements variability is listed in tables 10-11 respectively.

Distribution

This species is known from several localities spread across the island of Gran Canaria (Fig. 21)

Dysdera hircuan Arnedo et al. 1997

Dysdera hircuan Arnedo et al. 1997, fig: 12A-E, 13A-B #f. Reventón Oscuro, Bosque del Cedro, La Gomera.

(Figs 6G, 7G, 8G, 22A-B)

Material examined: Spain. Canary Islands: La Gomera, Hermigua, Reventón Oscuro, Bosque del Cedro, 28.137044, -17.222569, J.M. Fernandez, 12/IV/1975, 1 ♀; P. Oromí, 12/X/2004, 1 imm.; P. Oromí & D. Hernandez, 26/VII/2008, 1 imm.; H. López & P. Oromí, 5/II/2009, 1 ♂, 2 imm.; P. Oromí, 30/VI/2009, 1 imm.; P. Oromí, 4/I/2010, 1 imm.; Vallehermoso, Pista Mora Gaspar, 28.588937, -17.717572, M. Arnedo, A. Bellvert, M. Domènech & P. Oromí, 20/III/2019, carapace remains.

Diagnosis

This species can be easily distinguished from the other species from La Gomera by his huge size, more than twice the size of these species. Distinguished from the similar *D. enghoffi* Arnedo, Oromí & Ribera, 1997 and *D. silvatica* by the presence of five cheliceral teeth (Fig. 8G). Male can be distinguished by the extremely elongated TT, almost double the size of DD (Fig. 22A).

Description male (NMH1453): (Figs 6G, 7G, 8G, 22A-B). Carapace 9.36 long; maximum width 7.44; minimum width 4.48. Dark orange, frontally darker, becoming lighter towards back; smooth with some small black grains mainly at front (Fig. 6G, 7G). Anterior border roughly round, markedly smaller than $1/2$ carapace length; anterior lateral borders divergent; pointed at maximum dorsal width, posterior lateral borders straight; posterior margin wide, straight. AME diameter 0.32; PLE 0.34; PME 0.30; AME on edge of anterior border, separated from one another by about 1 diameter or more, close to PLE; PME touching to each other, about $2/5$ PME diameter from PLE. Labium trapezoid-shaped, base wider than distal part; longer than wide at base; semicircular groove at tip. Sternum orange, frontally darker, becoming lighter towards back; smooth; uniformly covered in slender black hairs.

Chelicerae 4.32 long, about $2/5$ of carapace length in dorsal view; fang medium-sized, 3.40; basal segment, proximal dorsal and ventral side, scantily covered with piligerous granulations. Chelicera inner groove long, about $1/2$ cheliceral length; armed with six teeth and lamina at base; $D1=B>D2>D3>M1=M2$; D triangular, located near segment tip; B close to basal lamina; M at middle of B and D (Fig. 8G). Anterior legs dark orange, posterior legs yellow. Lengths of male described above: fe1 8.90; pa1 6.10; ti1 8.40; me1 8.00; ta1 1.30; total 32.70; fe2 8.00; pa2 5.40; ti2 7.50; me2 7.10; ta2 1.30; total 29.30; fe3 6.60; pa3 3.80; ti3 5.40; me3 6.40; ta3 1.20; total 23.40; fe4 8.30; pa4 4.40; ti4 6.60; me4 7.90; ta4 1.30; total 28.50; fe Pdp 5.01; pa Pdp 2.70; ti Pdp 2.63; ta Pdp 2.13; total 12.47; relative length: $1>2>4>3$. Leg1 and leg2 spineless. Fe3d spineless; pa3 spineless; tb3d spines arranged in four bands; proximal 1.0.1; medial-proximal 0.1-2.0-1; medial-distal 1.1.1; distal 1.0.1.; tb3v spines arranged in three bands; proximal 1.1.0; medial-proximal 0; medial-distal 0.0.0-1; distal 1.0.0; with two terminal spines. Fe4d spines in one row; 2; pa4 spineless; tb4d spines arranged in four bands; proximal 1.0.1; medial-proximal 1.2.1; medial-distal 0.0-1.0; distal 1.0.1; tb4v spines arranged in three bands; proximal 1.1.1; medial-proximal 0;

medial-distal 1.0.1; distal 1.0.1; with two terminal spines. Dorsal side of anterior legs covered with small piligerous grains; ventral side of pedipalp covered with small piligerous grains. Claws with 10-14 teeth; hardly larger than claw width.

Abdomen 8.65 long; cream-coloured; cylindrical. Abdominal dorsal hairs 0.04 long; thick, roughly straight, compressed, blunt, tip not enlarged; uniformly, thickly distributed.

Male copulatory bulbus T slightly longer than DD (Fig. 22A); external distal border straight; internal sloped backwards. DD bent about 45° in lateral view; internal distal border not expanded. IS, ES equally developed (Fig. 22B); IS truncated at DD middle

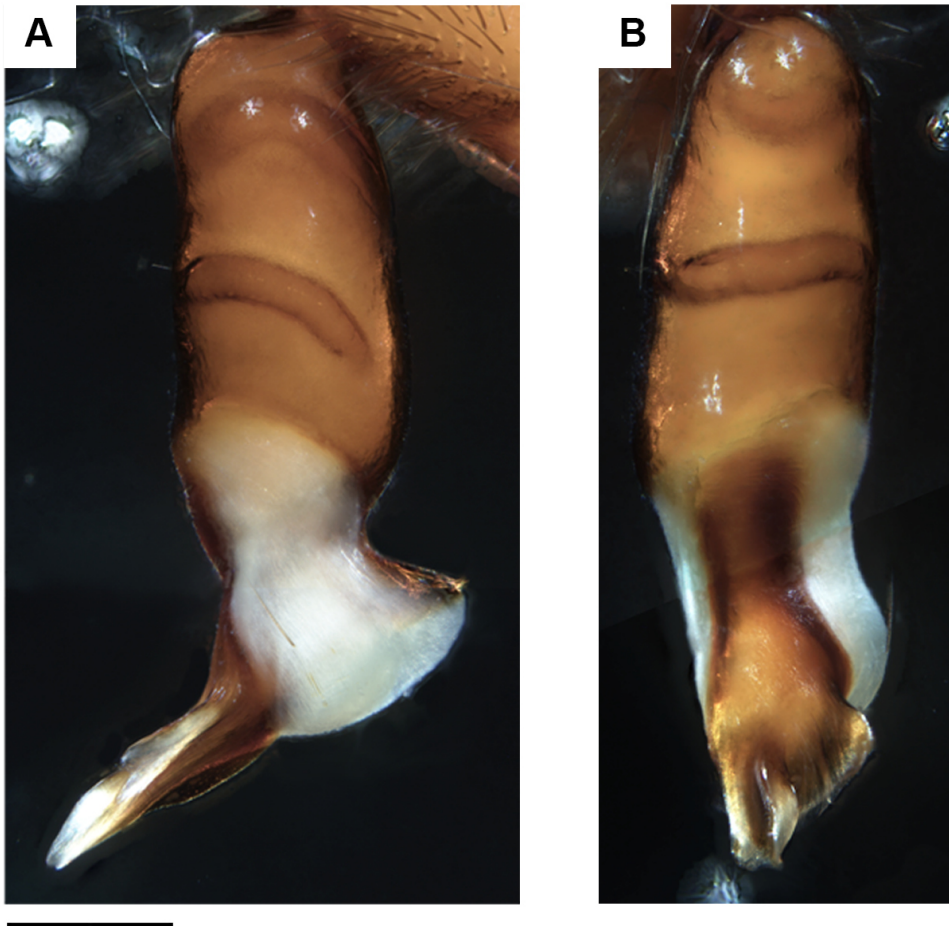


Figure 22. *D. hirguan* (A) left palp retrolateral view; (B) left palp frontal view. Scalebar = 0.5mm

Table 12. Intraspecific spination variability of *D. hirguan*.

	Proximal	Medial-Proximal	Medial-Distal	Distal
Tibia 3 dorsal	1.0-2.1	1.0-2.1	0.0-1.0-1	1.0.1
Tibia 4 dorsal	1.0.1	1.0-2.1	0.0-1.0	1.0.1
Tibia 3 ventral	0-1.1.0	0.0.1	0.0.0	1.0.0
Tibia 4 ventral				
	Number of rows	Number of spines		
Femur 3 dorsal	0	0		
Femur 4 dorsal	1-0	0/0-2		

part. DD tip straight in lateral view. P not fused to T; perpendicular to T in lateral view; lateral length from 2/5 to 1/2 of T width; not distally projected; posterior margin not folded.

Intraspecific variation

Spination variability is listed in table 12.

Distribution

This species is known from laurel forest of La Gomera (Fig. 14)

Dysdera marmorata sp.n.

(Figs 6H, 7H, 8H, 23A-E, 24A-C)

Type material

Holotype: Spain. Canary Islands: Tenerife, Santa Cruz de Tenerife, Monte Aguirre. Anaga, 28.529534, -16.268309, P. Oromí coll., 02/I/2013, 1 ♂ (NMH003018).

Paratypes: Spain. Canary Islands: Tenerife, Santa Cruz de Tenerife, Barranco de Nieto, 28.534069, -16.316254, NetBiome coll., 04/I/2013, 1 ♀ (NMH002947), 1 ♂ (NMH002949); 21/XII/2012, 1 ♀ (NMH002946).

Additional material examined: Spain. Canary Islands: Tenerife, San Cristóbal de La Laguna, Monte Aguirre. Anaga, 28.529534, -16.268309, NetBiome coll., 01/II/2013, 3 ♂; Santa Cruz de Tenerife, S.de la Cruz coll., 01/II/2013,; P. Oromí coll., 02/I/2013, 1 ♀, 1 ♂; Barranco de Nieto, 28.534069, -16.316254, Perez coll., 04/I/2013, 1 ♀, 1 ♂, 1 imm.; NetBiome coll., 04/I/2013, 2 ♀, 4 ♂, 2 imm.

Etymology

The epithet is an adjective meaning “marbled” in Latin, and refers to the colour pattern of the opisthosoma, which resemble that of marble.

Diagnosis

D. marmorata sp.n. is distinguished from the other sympatric species by his elongated and slender chelicera, 3/5 of the length of the carapace (Fig. 6H), small cheliceral tooth and D teeth slightly under the centre of the groove. *D. marmorata* sp.n. is similar in size as the sympatric *D. levipes*, but clearly distinguished by straight shape of the carapace in lateral view of the former instead of semi-circular (Fig. 7H).

Description – Male holotype (NMH003018): (Figs 6H, 7H, 8H, 23A-E). Carapace 2.08 long; maximum width 1.72; minimum width 1.28. Dark red, uniformly distributed; heavily foveate, covered with circular depressions, some small black grains mainly at front (Fig. 6H). Anterior border roughly round, about 3/5 carapace length; anterior lateral borders divergent; rounded at maximum dorsal width, posterior lateral borders rounded; posterior margin narrow, straight. AME diameter 0.11; PLE 0.10; PME 0.09; AME on edge of anterior border, separated from one another by about 1 diameter or more, close to PLE; PME touching to each other, about 1/3 PME diameter from PLE. Labium trapezoid-shaped, base wider than distal part; as long as wide at base; triangular groove at tip. Sternum dark red, darkened on borders; heavily wrinkled; uniformly covered in slender black hairs.

Chelicerae 1.23 long, about 3/5 of carapace length in dorsal view; fang long, 0.95;

basal segment, proximal dorsal and ventral side, scantily covered with piligerous granulations. Chelicera inner groove medium-size, about 2/5 cheliceral length; armed with three teeth and lamina at base; $B > D = M$; D triangular, slightly under centre of groove; B close to basal lamina; M close to B (Fig. 8H). Legs yellow. Lengths of male described above: fe1 1.36; pa1 0.92; ti1 1.08; me1 1.00; ta1 0.36; total 4.72; fe2 1.24; pa2 0.88; ti2 0.96; me2 0.92; ta2 0.36; total 4.36; fe3 0.96; pa3 0.56; ti3 0.64; me3 0.80; ta3 0.32; total 3.28; fe4 1.32; pa4 0.76; ti4 0.96; me4 1.16; ta4 0.40; total 4.60; fe Pdp 0.85; pa Pdp 0.48; ti Pdp 0.43; ta Pdp 0.49; total 2.25; relative length: $1 > 4 > 2 > 3$. Leg1 and leg2 spineless. Fe3d spineless; pa3 spineless; tb3d spines arranged in three bands; proximal 0.2.0; medial-proximal 1.0.1; medial-distal 0; distal 1.0.0; tb3v spines arranged in one band; proximal 0.1.0; medial-proximal 0; medial-distal 0; distal 0; with two terminal spines. Fe4d spineless; pa4 spineless; tb4d spines arranged in two bands; proximal 0.1.0, or 0.0-1.0; medial-proximal 0; medial-distal 0; distal 1.2.1; tb4v spines arranged in two bands; proximal 0.1.0; medial-proximal 0; medial-distal 0; distal 0.1.0; with two terminal spines. Dorsal side of anterior legs covered with hairs, lacking small grains; ventral side of pedipalp covered with hairs, lacking grains. Claws with 8 teeth or less; hardly larger than claw width.

Abdomen 2.08 long; cream-coloured; cylindrical. Abdominal dorsal hairs 0.02 long; thick, curved, compressed, blunt, tip not enlarged; uniformly, thickly distributed.

Male copulatory bulbus T slightly shorter than DD (Fig. 23A); external distal border straight; internal sloped backwards. DD not bent, same T axis in lateral view; internal distal border not expanded. IS, ES equally developed (Fig. 23B); IS truncated at DD middle part. DD tip straight in lateral view. C present, short; distal end beside DD internal tip (Fig. 23D); well developed; located close to DD distal tip; proximal border sharply decreasing; distal border sloping in its base, upper tip not projected, rounded, external side hollowed (Fig. 23C). AC absent. LF absent. L well developed; external border not sclerotized, laterally slightly folded; distal border approximately parallel,

continuous. LA absent. F absent. AL present (Fig. 23E), reduced to a small tooth; proximal border in posterior view fused with DH. P fused to T; perpendicular to T in lateral view; lateral length from 1/3 to 2/5 of T width; ridge present, perpendicular to T; not expanded, upper margin smooth; not distally projected; posterior margin slightly folded towards internal side.

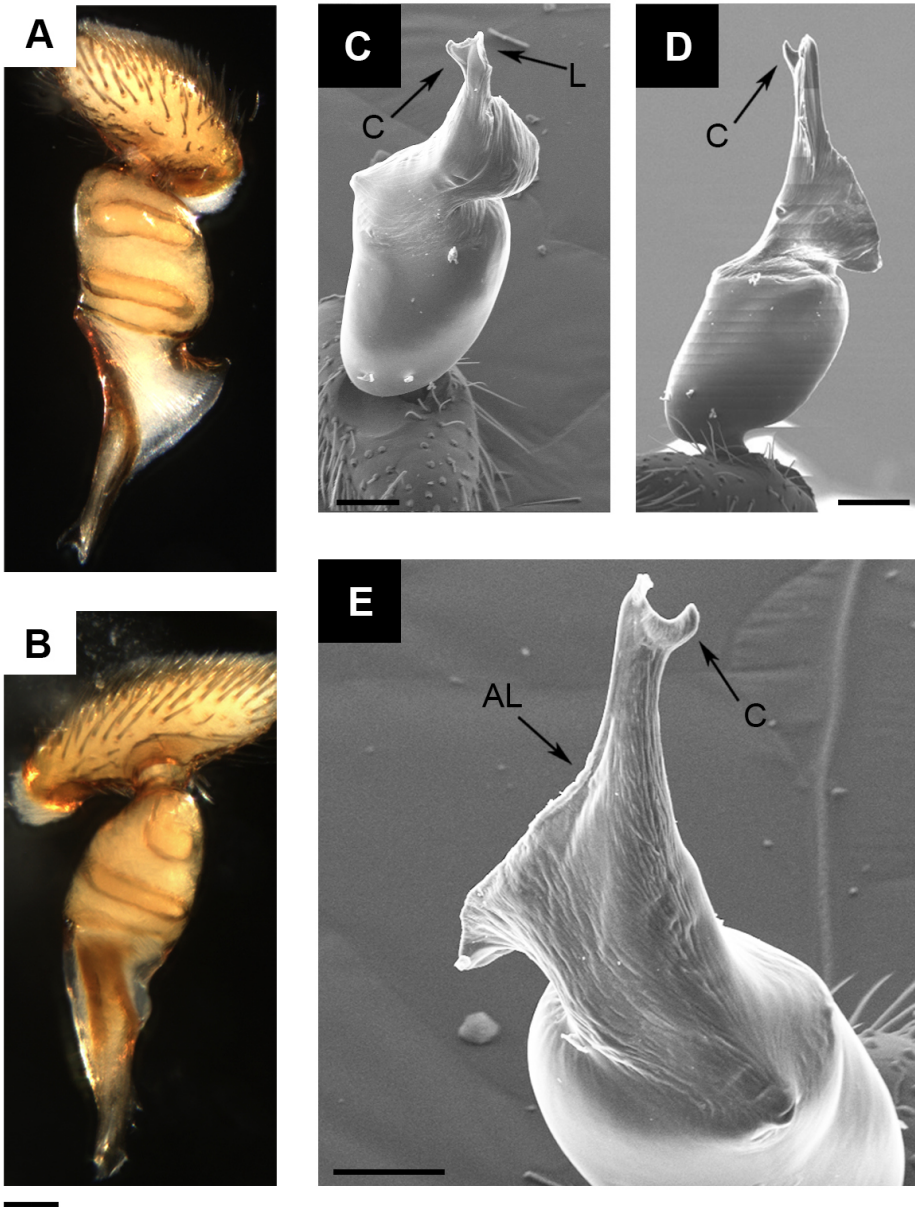


Figure 23. *D. marmorata* sp.n. (A) left palp retrolateral view; (B) left palp frontal view; (C) right palp frontal-retrolateral view; (D) right palp retrolateral view; (E) DD right palp frontal-prolateral view. Scalebar = 0.1mm

Female paratype (NMH002947): (Fig. 24A-B). All characters as in male except: carapace 2.04 long; maximum width 1.68; minimum width 1.28. AME diameter 0.12; PLE 0.12; PME 0.09; AME on edge of anterior border, separated from one another by about 2/3 diameter, close to PLE.

Chelicerae 1.28 long, about 3/5 of carapace length in dorsal view; fang long, 1.04; basal segment, proximal dorsal and ventral side, scantily covered with piligerous granulations. Lengths of female described above: fe1 1.20; pa1 0.88; ti1 0.96; me1 0.88; ta1 0.32; total 4.24; fe2 1.12; pa2 0.80; ti2 0.92; me2 0.84; ta2 0.32; total 4.00; fe3 0.96; pa3 0.56; ti3 0.56; me3 0.80; ta3 0.28; total 3.16; fe4 1.28; pa4 0.76; ti4 0.92; me4 1.16; ta4 0.36; total 4.48; fe Pdp 0.82; pa Pdp 0.47; ti Pdp 0.29; ta Pdp 0.48; total 2.06; relative length $4 > 1 > 2 > 3$. Leg1 and leg2 spineless. Fe3d spineless; pa3 spineless; tb3d spines arranged in three bands; proximal 1.2.0; medial-proximal 1.2.1; medial-distal 0; distal 1.0.0; tb3v spines arranged in one band; proximal 0.1.0; medial-proximal 0; medial-distal 0; distal 0; with two terminal spines. Fe4d spineless; pa4 spineless; tb4d spines arranged in one band; proximal 1.2.1; medial-proximal 0; medial-distal 0; distal 0; tb4v spines arranged in two bands; proximal 0.0-1.0; medial-proximal 0; medial-distal 0; distal 0.1.0; with two terminal spines. Dorsal side of anterior legs covered with small piligerous grains; ventral side of pedipalp covered

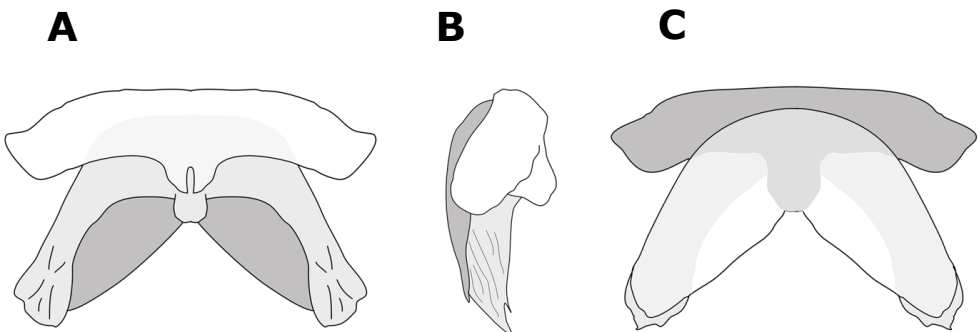


Figure 24. *D. marmorata* sp.n. vulva (A) ventral; (B) lateral; (C) dorsal view. Scalebar = 0.65mm

Table 13. Intraspecific spination variability of *D. marmorata* sp.n.

	Proximal	Medial-Proximal	Medial-Distal	Distal
Tibia 3 dorsal	0-2.1-2.0	0-1.0-2.1	0-1.0.0	0-1.0.0-2
Tibia 4 dorsal	0.0-1.0	0-1.1-2.0-1	0-1.0.0	0-1.0.0-1
Tibia 3 ventral	0.0.0	0.0-1.0	1-0.0.0	0.0.0
Tibia 4 ventral	0.0-1.0-1	0-1.1.0	1.0.1	0.0.0
	Number of rows		Number of spines	
Femur 3 dorsal	0	0	0	0
Femur 4 dorsal	0	0	0	0

Table 14. Intraspecific leg measurements variability of *D. marmorata* sp.n (males/females).

	I	II	III	IV
Fe	0.88-1.44/1.2-1.36	0.88-1.24/1.12-1.2	0.72-1.08/0.96-1.08	1-1.44/1.28-1.4
Pa	0.68-0.96/0.88-0.96	0.64-0.92/0.8-0.88	0.44-0.64/0.52-0.64	0.56-0.8/0.72-0.8
Ti	0.8-1.08/0.96-1.04	0.72-0.96/0.84-0.96	0.52-0.72/0.56-0.64	0.72-1.04/0.88-0.96
Mt	0.72-1/0.84-1	0.68-0.96/0.84-0.92	0.64-0.88/0.8-0.88	0.84-1.36/1.16-1.24
Ta	0.24-0.4/0.32-0.36	0.28-0.36/0.32-0.4	0.28-0.48/0.28-0.36	0.32-0.4/0.36-0.4
Total	3.44-4.88/4.24-4.64	3.24-4.44/4-4.28	2.6-3.68/3.16-3.48	3.48-5.04/4.48-4.72

with small piligerous grains.

Abdomen 2.68 long; cream-coloured; cylindrical. Abdominal dorsal hairs 0.04 long; thick, roughly straight, compressed, blunt, tip not enlarged; uniformly, thickly distributed.

Vulva DA clearly distinguishable from VA (Fig. 24B); DA slightly wider than long (Fig. 24C); DF wide in dorsal view. MF margins fused, sheet-like, well developed, completely sclerotized. VA rectangle-like; anterior region completely sclerotized; posterior region sclerotized except for most internal area; AVD absent (Fig. 24A). S attachment projected under VA; arms are shorter than DA, slightly curved; tips not projected; neck as wide as arms. TB usual shape.

Intraspecific variation

Male cephalothorax ranges in length from 1.64-2.28 (N=6), females from 2.04-2.24

(N=5). Legs color could range from dark orange to pale yellow. Cheliceral teeth could be extremely reduced. Spination and leg measurements variability is listed in tables 13-14 respectively.

Distribution

This species is known from two localities of Anaga, in the North-eastern part of the island of Tenerife (Fig. 11).

Dysdera orahan Arnedo et al. 1997

D. orahan Arnedo et al. 1997: fig. 17A-D, 18A-D, 19A-D ♂ . Puntallana, La Gomera.

(Figs 6I, 7I, 8I, 25A-C)

Material examined: Spain. Canary Islands: La Gomera, San Sebastian, Puntallana, 28.127989, -17.106446, P. Oromí, 12/II/1993, ♂ ; El Hierro, Frontera, Mirador de Bascos, 27.754861, -18.118217, P. Oromí, 2/III/1997, 2 ♂ ; Las Cancelitas, 27.809530, -17.927239, GIET, 11/II/2001, 2 ♂ ; Valverde, Ventejís, Tiñor, 27.785991, -17.937508, N. Macías, 22/IV/2013, 1 ♀ , 2 ♂ ; M. Arnedo, A. Bellvert & J. Rozas, 23/III/2017, 2 ♀ .

Diagnosis

D. orahan is distinguished from the similar sympatric *D. ramblae* Arnedo, Oromí & Ribera, 1997 by the spineless dorsal tibia IV. Female distinguished from the other sympatric species from la gomera by the short S distally slightly directed backwards and absence of AVD (Fig.25A).

Description – Female (CRBA2891): (Figs 6I, 7I, 8I, 25A-C). Carapace 2.84 long; maximum width 2.20; minimum width 1.46. Red, darkened at borders; slightly foveate at borders, slightly wrinkled with small black grains mainly at front (Fig. 6I, 7I). Anterior border roughly round, markedly smaller than 1/2 carapace length; anterior

lateral borders divergent; rounded at maximum dorsal width, posterior lateral borders rounded; posterior margin narrow, straight. AME diameter 0.21; PLE 0.17; PME 0.19; AME on edge of anterior border, separated from one another by about 1/2 diameter, touching PLE; PME touching to each other, less than 1/4 PME diameter from PLE. Labium trapezoid-shaped, base wider than distal part; as long as wide at base; semicircular groove at tip. Sternum orange red, darkened on borders; very slightly wrinkled, mainly between legs and anterior border; uniformly covered in slender black hairs.

Chelicerae 1.00 long, about 1/3 of carapace length in dorsal view; fang short, 0.83; basal segment proximal dorsal side scantily covered with piligerous granulations. Chelicera inner groove long, about 1/2 cheliceral length; armed with three teeth and lamina at base; $D=B>M$; D triangular, located near segment tip; B close to basal lamina; M close to B. Legs orange (Fig. 8I). Lengths of female described above: fe1 2.03; pa1 1.34; ti1 1.69; me1 1.65; ta1 0.47; total 7.17; fe2 1.93; pa2 1.34; ti2 1.55; me2 1.50; ta2 0.44; total 6.77; fe3 1.60; pa3 0.91; ti3 1.08; me3 1.43; ta3 0.44; total 5.46; fe4 2.21; pa4 1.24; ti4 1.72; me4 2.06; ta4 0.51; total 7.74; fe Pdp 1.05; pa Pdp 0.64; ti Pdp 0.49; ta Pdp 0.74; total 2.92; relative length $4>1>2>3$. Leg1 and leg2 spineless. Fe3d spineless; pa3 spineless; tb3d spines arranged in two bands; proximal 1.0.0; medial-proximal 0; medial-distal 0; distal 1.0.0; tb3v spines spineless; with two terminal spines. Fe4d spineless; pa4 spineless; tb4d spines spineless; tb4v spines arranged in one band; proximal 0.1.0; medial-proximal 0; medial-distal 0; distal 0; with two terminal spines. Dorsal side of anterior legs covered with hairs, lacking small grains; ventral side of pedipalp covered with small piligerous grains; Distal part of the metatarsus III and IV densely covered with short hair. Claws with 10-14 teeth; hardly larger than claw width.

Abdomen 4.22 long; grey; cylindrical. Abdominal dorsal hairs 0.07 long; thick, curved, compressed, blunt, tip not enlarged; uniformly, thickly distributed.

Vulva DA clearly distinguishable from VA (Fig. 25B); DA slightly wider than long; DF wide in dorsal view (Fig. 25C). MF margins fused, sheet-like, well developed, completely sclerotized, projected backwards, shorter than DA lateral length. VA rectangle-like; projected under DA; anterior region completely sclerotized; posterior region sclerotized except for most internal area; AVD absent. S attachment projected under VA (Fig. 25A); arms are shorter than DA, slightly curved; tips dorsally projected; neck as wide as arms. TB usual shape.

Distribution

This rare species is known from the islands of El Hierro and from one locality in the east coast of La Gomera (Fig. 16).

Dysdera tabona sp.n.

(Figs 6J, 7J, 8J, 26A-E, 27A-C)

Type material

Holotype: Spain. Canary Islands: Tenerife, Santa Cruz de Tenerife, La Ensilada (Aparcamiento). Anaga, 28.556190, -16.179817, N. Macías coll., 13/IV/2007, 1 ♂ (NMH001213).

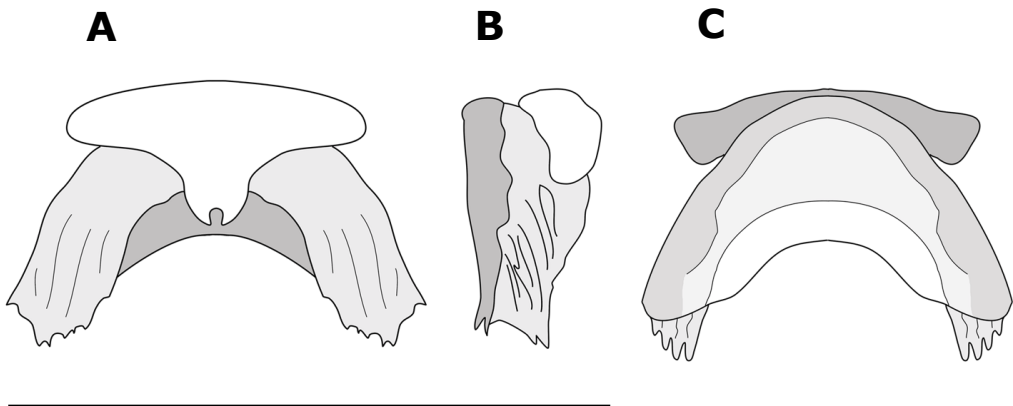


Figure 25. *D. orahan* sp.n. vulva (A) ventral; (B) lateral; (C) dorsal view. Scalebar = 0.65mm

Paratypes: Spain. Canary Islands: Tenerife, San Cristóbal de La Laguna, Camino La Ensellada-Chamorga, Anaga, 28.556208, -16.179827, M. Rezac coll., 04/III/2006, 1 ♀ (NMH000701), 1 ♀ (NMH000702); Santa Cruz de Tenerife, Cabezo del Tejo 2, 28.565090, -16.165982, N. Macías coll., 16/V/2006, 1 ♀ (NMH000661). Tenerife, Santa Cruz de Tenerife, La Ensellada (Aparcamiento). Anaga, 28.556190, -16.179817, N. Macías coll., 13/IV/2007, 1 ♂ (NMH001214)

Additional material examined: Spain. Canary Islands: Tenerife, Santa Cruz de Tenerife, La Ensellada (Aparcamiento). Anaga, 28.556190, -16.179817, N. Macías coll., 13/IV/2007, 1 ♀; San Cristóbal de La Laguna, Camino La Ensellada-Chamorga, Anaga, 28.556208, -16.179827, 14/V/2006, 1 imm.

Etymology

The specific name in apposition refers to the sharpened stones used by the Guanches as a cutting instrument or weapon.

Diagnosis

Dysdera tabona sp.n. is distinguished from the morphologically similar *D. insulana* by the smaller size, the orange legs in the former instead of dark red, and the cream-colored opisthosoma instead of brownish. Males distinguished from *D. insulana* by the P slightly curved upper margin ridge expansion instead of straight (Fig. 26A, 26E), stepped C (Fig. 26C) instead of curved spoon shaped. Clearly distinguished from the other sympatric species of Anaga by the concave chelicera in lateral view (Fig. 7J).

Description – Male holotype (NMH001213): (Figs 6J, 7J, 8J, 26A-E). Carapace 4.45 long; maximum width 3.75; minimum width 2.40. Dark red, uniformly distributed; smooth with some small black grains mainly at front (Fig. 6J). Anterior border roughly round, from 1/2 to 3/5 carapace length; anterior lateral borders parallel; rounded at maximum dorsal width, posterior lateral borders rounded; posterior margin narrow, straight. AME diameter 0.23; PLE 0.10; PME 0.18; AME on edge of anterior border,

separated from one another by about $2/3$ diameter, touching PLE; PME touching to each other, less than $1/4$ PME diameter from PLE. Labium trapezoid-shaped, base wider than distal part; as long as wide at base; semicircular groove at tip. Sternum dark red, frontally darker, becoming lighter towards back or darkened on borders; very slightly wrinkled, mainly between legs and anterior border; uniformly covered in slender black hairs.

Chelicerae 2.00 long, about $2/5$ of carapace length in dorsal view; fang long, 1.72; basal segment, proximal dorsal and ventral side, scantily covered with piligerous granulations. Chelicera inner groove medium-size, about $2/5$ cheliceral length; armed with three teeth and lamina at base; $B > D > M$; D triangular, located roughly at centre of groove; B close to basal lamina; M close to B (Fig. 8J). Legs orange. Lengths of male described above: fe1 2.85; pa1 2.00; ti1 2.50; me1 2.30; ta1 0.55; total 10.20; fe2 2.70; pa2 1.85; ti2 2.20; me2 2.20; ta2 0.55; total 9.50; fe3 2.20; pa3 1.35; ti3 1.45; me3 1.95; ta3 0.55; total 7.50; fe4 2.75; pa4 1.55; ti4 2.10; me4 2.70; ta4 0.60; total 9.70; relative length: $1 > 4 > 2 > 3$. Leg1 and leg2 spineless. Fe3d spineless; pa3 spineless; tb3d spines arranged in three bands; proximal 0.0.1; medial-proximal 1.2.1; medial-distal 0; distal 1.0.1-0; tb3v spines arranged in four bands; proximal 1.1.1, or 0-1.3.0; medial-proximal 1.2.0; medial-distal 1.0.0; distal 0; with two terminal spines. Fe4d spines in two rows; forward 0-1; backward 2; pa4 spineless; tb4d spines arranged in four bands; proximal 0-1.0.0; medial-proximal 1.3-1.1; medial-distal 0; distal 1.0.1; tb4v spines arranged in four bands; proximal 0.3-2.0; medial-proximal 1.2.1; medial-distal 1.0.0; distal 0; with two terminal spines. Dorsal side of anterior legs smooth; ventral side of pedipalp covered with hairs, lacking grains. Claws with 8 teeth or less; hardly larger than claw width.

Abdomen 5.50 long; cream-coloured; cylindrical. Abdominal dorsal hairs 0.12 long; thick, curved, not compressed, pointed, tip enlarged; uniformly, thickly distributed.

Male copulatory bulbus T slightly shorter than DD (Fig. 26A); external distal border

sloped backwards; internal sloped backwards. DD slightly bent in lateral view, clearly less than 45° ; internal distal border not expanded. IS, ES proximally fused, similarly developed (Fig. 26B); IS truncated at DD middle part. DD tip straight in lateral view. C present, short; distal end beside DD internal tip; well developed; located close to DD distal tip; proximal border stepwise decreasing (Fig. 26C); distal border rounded,

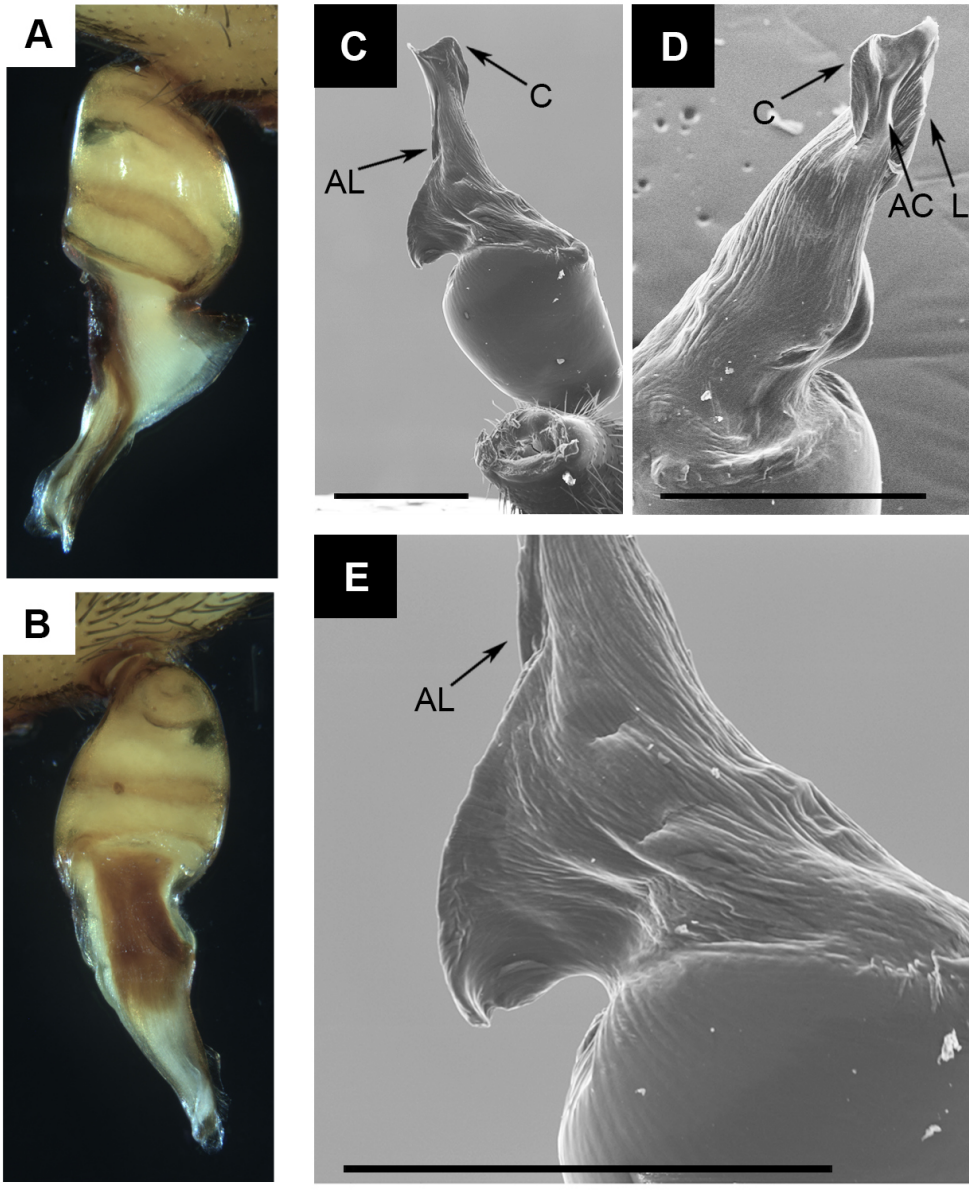


Figure 26. *D. tabona* sp.n. (A) left palp retrolateral view; (B) left palp frontal view; (C) right palp prolateral view; (D) DD right palp frontal-retrolateral view; (E) P right palp prolateral view. Scalebar = 0.5mm

hardly stepped, upper tip not projected, rounded, external side hollowed (Fig. 26D). AC present. LF present; distally projected. L well developed. LF poorly developed. L external border not sclerotized, laterally markedly folded; distal border approximately parallel, continuous. LA absent. F absent. AL present, very poorly developed (Fig. 26E). P fused to T; perpendicular to T in lateral view; lateral length from 1/3 to 2/5 of T width; ridge present, perpendicular to T; not expanded, upper margin smooth; not distally projected; posterior margin slightly folded towards internal side.

Female paratype (NMH000661): (Fig. 27A-B). All characters as in male except: carapace 4.45 long; maximum width 3.70; minimum width 2.40. AME diameter 0.19; PLE 0.19; PME 0.17; AME on edge of anterior border, separated from one another by about 1 diameter or more, touching PLE; PME touching to each other, about 1/3 PME diameter from PLE.

Chelicerae 2.35 long, about 1/2 of carapace length in dorsal view; fang long, 1.69. Lengths of female described above: fe1 3.05; pa1 2.05; ti1 2.30; me1 2.20; ta1 0.60; total 10.20; fe2 2.70; pa2 1.90; ti2 2.20; me2 2.05; ta2 0.55; total 9.40; fe3 2.45; pa3 1.40; ti3 1.45; me3 2.00; ta3 0.55; total 7.85; fe4 2.90; pa4 1.65; ti4 2.00; me4 2.55; ta4 0.60; total 9.70; relative length $1 > 4 > 2 > 3$. Leg1 and leg2 spineless. Fe3d spineless; pa3 spineless; tb3d spines arranged in four bands; proximal 1.0.1; medial-proximal

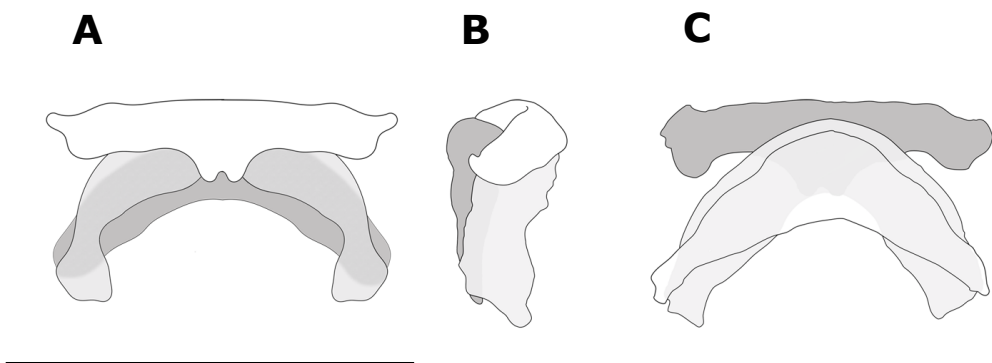


Figure 27. *D. tabona* sp.n. vulva (A) ventral; (B) lateral; (C) dorsal view. Scalebar = 0.65mm

Table 15. Intraspecific spination variability of *D. tabona* sp.n.

	Proximal	Medial-Proximal	Medial-Distal	Distal
Tibia 3 dorsal	0-1.0.0-1	1.1.1	0.0-2.0	0-1.0.0-1
Tibia 4 dorsal	0-1.0.0-1	1.1.1	0.0.0	1.0.1
Tibia 3 ventral	1-0.3.0	1.2-1.1-0	0.0.0	1.0.0
Tibia 4 ventral	1.2.0-1	0-1.1-2.0-1	0.0.0	1.1.0-1
	Number of rows	Number of spines		
Femur 3 dorsal	0	0		
Femur 4 dorsal	2	1/2		

Table 16. Intraspecific leg measurements variability of *D. tabona* sp.n.

	I	II	III	IV
Fe	2.75-3.15/2.95-3.05	2.55-2.85/2.7-2.8	2.2-2.45/2.35-2.45	2.65-3.05/2.9-2.9
Pa	1.85-2.05/2.05-2.05	1.75-1.85/1.7-1.9	1.25-1.4/1.4-1.4	1.55-1.65/1.65-1.75
Ti	2.45-2.55/2.3-2.6	2.2-2.2/2.1-2.3	1.4-1.6/1.45-1.55	1.85-2.25/2-2.2
Mt	2.25-2.5/2.2-2.35	2.15-2.2/2.05-2.1	1.7-2.15/2-2.15	2.45-2.8/2.55-2.8
Ta	0.55-0.6/0.6-0.6	0.55-0.55/0.5-0.55	0.55-0.55/0.5-0.55	0.6-0.65/0.6-0.65
Total	9.9-10.85/10.2-10.6	9.2-9.6/9.1-9.65	7.15-8.15/7.7-8.1	9.1-10.4/9.7-10.25

1.2.1; medial-distal 0; distal 0; tb3v spines arranged in four bands; proximal 0.3.0; medial-proximal 1.2-3.0; medial-distal 0; distal 1.1.0; with two terminal spines. Fe4d spines in two rows; forward 2; backward 1; pa4 spineless; tb4d spines arranged in four bands; proximal 0.0.1; medial-proximal 1.1.1; medial-distal 0; distal 1.0.1; tb4v spines arranged in four bands; proximal 1.6-3.1; medial-proximal 1.1-0.0; medial-distal 0; distal 0.0.1; with two terminal spines. Dorsal side of anterior legs smooth; ventral side of pedipalp smooth. Claws with 8 teeth or less; hardly larger than claw width.

Abdomen 4.19 long; cream-coloured; cylindrical. Abdominal dorsal hairs 0.12 long; thin, roughly straight, compressed, pointed; uniformly, thickly distributed.

Vulva DA clearly distinguishable from VA (Fig. 27B); DA longer than wide; DF wide in dorsal view. MF margins not fused, well developed, completely sclerotized. VA rectangle-like; anterior region completely sclerotized; posterior region sclerotized except for most internal area; AVD absent. S attachment projected under VA (Fig.

27A); arms slightly longer than DA (Fig. 27C), straight; tips not projected; neck as wide as arms. TB usual shape.

Intraspecific variation

Male cephalothorax ranges in length from 4.20-4.65 (N=3), females from 4.45-4.70 (N=3). Distal teeth could be closer to medial, almost at the same distance that goes from medial to basal. Carapace coloration range from darker red, almost black to slightly lighter than the holotype description. Spination and leg measurements variability is listed in tables 15-16 respectively.

Distribution

This species is known from the most Eastern part of Anaga, in the island of Tenerife (Fig. 11).

***Dysdera undupe* sp.n.**

(Figs 6K, 7K, 8K, 28A-E, 29A-C)

Type material

Holotype: Spain. Canary Islands: La Gomera, Monte de la Zarza, 28.156704, -17.292207, H. Contreras coll., 11/V/2003, 1 ♂ (CRBA001454).

Paratypes: Spain. Canary Islands: La Gomera, Ctra. Cumbre, altura Mora Gaspar, 28.146139, -17.262783, D. Hernández coll., 02/VII/2008, 1 ♂ (NMH001448); Vallehermoso, Pista Mora Gaspar, 28.588937, -17.717572, Arnedo, Bellvert, Domènech & Oromí coll., 20/III/2019, 1 ♀ (CRBA003624); Hermigua, Reventón Oscuro. Bosque del Cedro, 28.125809, -17.216615, N. Macías & S. Toft coll., 08/IV/2011, 1 ♀ (CRBA002057).

Etymology

The specific name in apposition refers to Undupe, king of La Gomera, husband of Gara, one of the main protagonists in the legend of Gara and Jonay.

Diagnosis

Dysdera undupe sp.n. is distinguished from the morphologically similar *D. calderensis* by the M tooth markedly closer to B in the former instead of equidistantly distributed (Fig. 8K) and carapace more markedly cribellate (Fig. 6K). Male distinguished from *D. calderensis* by the L border markedly curved 45° (Fig. 28C) instead of slightly curved 20°. Female of *D. undupe* sp.n. distinguished from *D. calderensis* by S laterally pointed projected forward in the former instead of rounded and backwards directed (Fig. 29A).

Description – Male holotype (CRBA001454): (Figs 6K, 7K, 8K, 28A-E). Carapace 4.78 long; maximum width 3.59; minimum width 2.24. Dark red, darkened at borders; heavily foveate, covered with circular depressions, some small black grains mainly at front (Figs 6K, 7K). Anterior border roughly round, from 1/2 to 3/5 carapace length; anterior lateral borders divergent; rounded at maximum dorsal width, posterior lateral borders rounded; posterior margin narrow, straight. AME diameter 0.26; PLE 0.16; PME 0.17; AME on edge of anterior border, separated from one another by about 1 diameter or more, touching PLE; PME touching to each other, about 1/3 PME diameter from PLE. Labium trapezoid-shaped, base wider than distal part; as long as wide at base; semicircular groove at tip. Sternum dark red, frontally darker, becoming lighter towards back; heavily wrinkled; covered in hairs mainly on margin.

Chelicerae 1.81 long, about 1/3 of carapace length in dorsal view; fang medium-sized, 1.64; basal segment proximal dorsal side scantily covered with piligerous granulations. Chelicera inner groove long, about 1/2 cheliceral length; armed with three teeth and lamina at base; D=B>M; D triangular, located roughly at centre of

groove; B close to basal lamina; M close to B (Fig. 8K). Anterior legs dark orange, posterior legs yellow. Lengths of male described above: fe1 4.06; pa1 2.67; ti1 3.56; me1 3.43; ta1 0.77; total 13.96; fe4 3.69; pa4 2.05; ti4 3.03; me4 3.04; ta4 0.72; total 12.52; fe Pdp 2.08; pa Pdp 1.16; ti Pdp 0.98; ta Pdp 1.02; total 5.24. Leg4 spineless. Dorsal side of anterior legs covered with hairs, lacking small grains; ventral side of pedipalp covered with hairs, lacking grains. Claws with 8 teeth or less; hardly larger than claw width.

Abdomen 6.25 long; grey; cylindrical. Abdominal dorsal hairs 0.06 long; thin, roughly straight, compressed, blunt, tip not enlarged; uniformly, thickly distributed.

Male copulatory bulbus T slightly shorter than DD (Fig. 28A); external distal border sloped backwards; internal sloped backwards. DD slightly bent in lateral view, clearly less than 45°; internal distal border not expanded. IS, ES equally developed (Fig. 28B); IS truncated at DD middle part. DD tip sloped towards back in lateral view. C present, short; distal end beside DD internal tip; well developed; located close to DD distal tip; proximal border sharply decreasing; distal border markedly sloped, upper tip not projected, pointed, external side hollowed (Fig. 28D). AC absent. LF absent. L well developed (Fig. 28C); external border not sclerotized, laterally slightly folded; distal border divergent, continuous. LA absent. F absent. AL present, very poorly developed (Fig. 28E); proximal border in posterior view fused with DH. P fused to T; perpendicular to T in lateral view; lateral length from 2/5 to 1/2 of T width; ridge present, perpendicular to T; not expanded, upper margin smooth; distally slightly projected; posterior margin slightly folded towards internal side.

Female paratype (CRBA002057): (Fig. 29A-C). All characters as in male except: carapace 4.43 long; maximum width 3.53; minimum width 2.17. AME diameter 0.24; PLE 0.26; PME 0.23; AME on edge of anterior border, separated from one another by about 2/3 diameter, close to PLE; PME touching to each other, about 1/3 PME diameter from PLE.

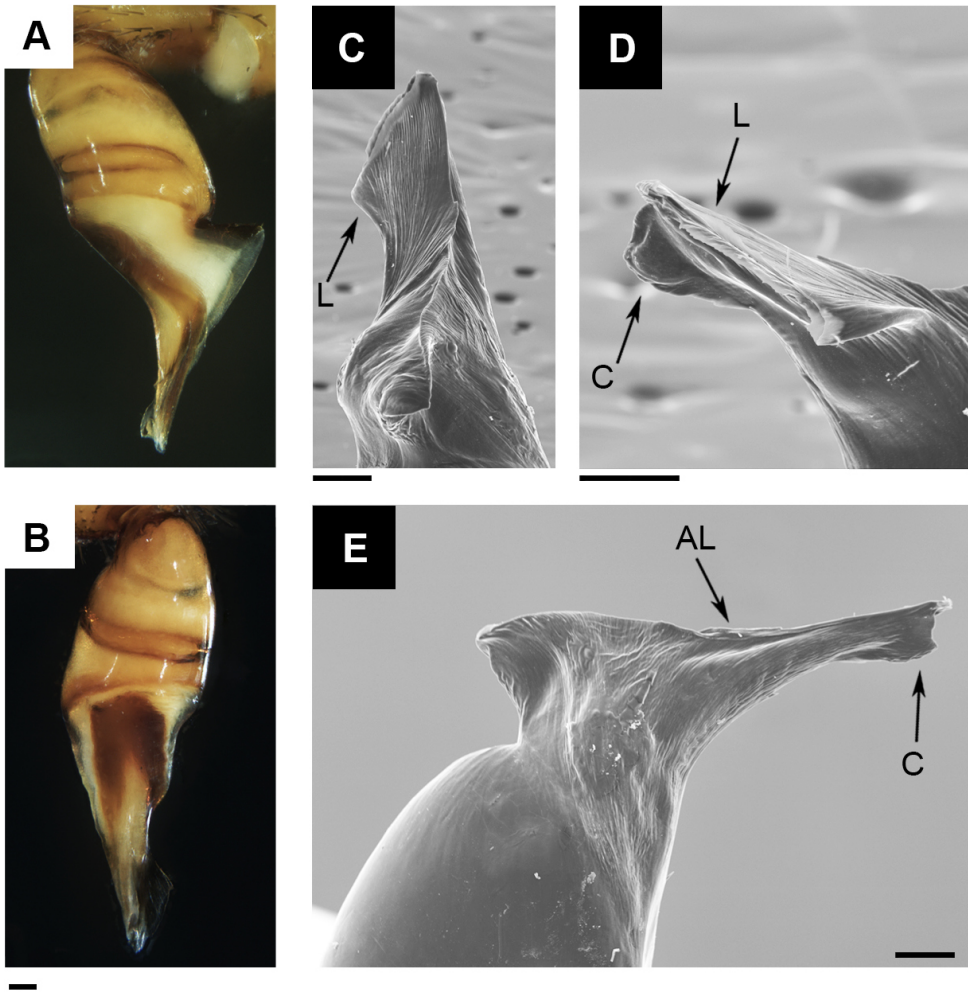


Figure 28. *D. undupe* sp.n. (A) left palp retrolateral view; (B) left palp frontal view; (C) DD right palp dorsal view; (D) DD right palp retrolateral view; (E) P right palp prolateral view. Scalebar = 0.1mm

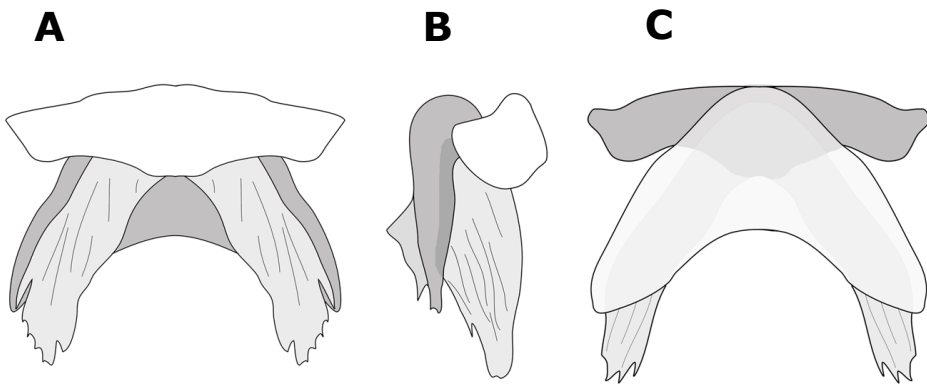


Figure 29. *D. undupe* sp.n. vulva (A) ventral; (B) lateral; (C) dorsal view. Scalebar = 0.65mm

Table 17. Intraspecific leg measurements variability of *D. undupe* sp.n.

	I	II	III	IV
Fe	4.06-4.542/3.72-3.8	4.012/3.32-3.534	3.12/2.6-2.772	3.69-4.181/3.56-3.84
Pa	2.67-2.958/2.37-2.57	2.657/2.3-2.337	1.789/1.5-1.596	2.05-2.398/1.957-1.98
Ti	3.56-4.027/3.16-3.477	3.431/2.8-2.949	2.053/1.799-1.85	3.03-3.16/2.797-2.87
Mt	3.43-3.913/3.06-3.304	3.591/2.84-3.075	2.855/2.2-2.467	3.04-4/3.26-3.516
Ta	0.77-0.864/0.64-0.75	0.736/0.69-0.701	0.653/0.665-0.67	0.72-0.844/0.72-0.791
Total	14.49-16.304/13.14-13.711	14.427/11.95-12.596	10.47/8.82-12.621	12.53-14.583/12.621-12.67

Chelicerae 1.93 long, about 2/5 of carapace length in dorsal view; fang medium-sized, 1.57. Chelicera inner groove medium-size, about 2/5 cheliceral length. Lengths of female described above: fe1 3.80; pa1 2.37; ti1 3.16; me1 3.06; ta1 0.75; total 13.14; fe2 3.32; pa2 2.30; ti2 2.80; me2 2.84; ta2 0.69; total 11.95; fe3 2.60; pa3 1.50; ti3 1.85; me3 2.20; ta3 0.67; total 8.82; fe4 3.84; pa4 1.98; ti4 2.87; me4 3.26; ta4 0.72; total 12.67; fe Pdp 1.65; pa Pdp 1.01; ti Pdp 0.82; ta Pdp 1.24; total 4.72; relative length 1>4>2>3. Leg1 and leg2 spineless; leg3 spineless; leg4 spineless. Dorsal side of anterior legs smooth; ventral side of pedipalp covered with hairs, lacking grains.

Abdomen 7.18 long; grey; cylindrical. Abdominal dorsal hairs 0.15 long; thin, roughly straight, not compressed, pointed; uniformly, thickly distributed.

Vulva DA clearly distinguishable from VA (Fig. 29B); DA slightly wider than long (Fig. 29C); DF wide in dorsal view. MF margins fused, sheet-like, well developed, completely sclerotized. VA rectangle-like; projected under DA (Fig. 29A); anterior region completely sclerotized; posterior region sclerotized except for most internal area; AVD absent. Ventral narrow dark bands developed from S attachment. S attachment not projected under VA; arms as long as DA, slightly curved; tips not projected; neck as wide as arms. TB usual shape.

Intraspecific variation

Male cephalothorax ranges in length from 4.78-5.52 (N=2), females from 4.43-4.75 (N=2). Carapace color could be dark red almost black. Leg measurements variability is

listed in table 17.

Distribution

This species is known from the laurel forest of La Gomera (Fig. 14).

Dysdera yballa sp.n.

(Figs 6L, 7L, 8L, 30A-D, 31A-C)

Type material

Holotype: Spain. Canary Islands: La Gomera, Hermigua, Pajarito, 28.108856, -17.241604, P. Oromí & Arnedo coll., 29/4/1995, 1 ♂ (UB2909).

Paratypes: Spain. Canary Islands: La Gomera, Vallehermoso, Teselinde. Ermita de Santa Clara, 28.1963, -17.28754, N. Macías & S. de la Cruz coll., 27/3/2013, 1 ♂ (NMH002301); Hermigua, Pajarito, 28.10885609, -17.24160433, P. Oromí & Arnedo coll., 29/4/1995, 1 ♀ (UB2908), 1 ♀ (UB2915).

Additional material examined: Spain. Canary Islands: La Gomera, Enchereda, 28.13665, -17.179063, S. de la Cruz coll., 02/V/2008, 1 ♀, 1 ♀; Vallehermoso, Teselinde. Ermita de Santa Clara, 28.1963, -17.28754, N. Macías & S. Toft coll., 08/IV/2011, 1 ♀; Valle Gran Rey, La Mérica, 28.11577, -17.33604, Arnedo, Bellvert & Oromí coll., 17/III/2017, 1 ♂; Vallehermoso, Teselinde. Ermita de Santa Clara, 28.1963, -17.28754, 1 ♀; N. Macías & S. de la Cruz coll., 27/III/2013, 1 ♀, 1 ♀; Plain Land between Barranco Higuera and Barranco San Juan., 28.193319, -17.292939, P. Oromí & Arnedo coll., 30/IV/1995, 1 ♀.

Etymology

The specific name in apposition refers to Yballa, an aboriginal from the isle of La Gomera with which Fernán Peraza had a furtive relationship which led to an uprising

by the natives of the isle.

Diagnosis

Dysdera yballa sp.n. is distinguished from the closely related *D. levipes* by the bigger size and the less obvious pilosity in the prosoma in the former. Clearly distinguished from the other sympatric species from la Gomera by the semi-circular shape of the prosoma in lateral view and the abundant pilosity of the carapace (Fig. 7L).

Description – Male holotype (UB2909): (Figs 6L, 7L, 8L, 30A-D). Carapace 2.27 long. Dark red, darkened at borders; slightly foveate at borders, wrinkled at middle, covered with small black grains; hairy, uniformly covered with white hairs (Fig. 6L). Anterior border roughly round, markedly smaller than $1/2$ carapace length; anterior lateral borders convergent; rounded at maximum dorsal width, posterior lateral borders rounded; posterior margin narrow, straight. AME diameter 0.12; PLE 0.13; PME 0.10; AME on edge of anterior border, separated from one another by about $2/3$ diameter, close to PLE; PME touching to each other, about $1/3$ PME diameter from PLE. Labium trapezoid-shaped, base wider than distal part; as long as wide at base; semicircular groove at tip. Sternum dark red, uniformly distributed; heavily wrinkled; uniformly covered in slender black hairs.

Chelicerae 0.77 long, about $1/3$ of carapace length in dorsal view; fang short, 0.55; basal segment proximal border of dorsal side strongly covered with piligerous granulations. Chelicera inner groove long, about $1/2$ cheliceral length; armed with three teeth and lamina at base; $D=M=B$; D triangular, located roughly at centre of groove; B close to basal lamina; M close to B (Fig. 8L). Legs yellow. Lengths of male described above: fe1 1.90; pa1 1.07; ti1 1.53; me1 1.51; ta1 0.42; total 6.43; fe2 1.73; pa2 0.95; ti2 1.42; me2 1.40; ta2 0.43; total 5.93; fe3 1.34; pa3 0.70; ti3 0.93; me3 1.22; ta3 0.40; total 4.59; fe4 1.66; pa4 0.89; ti4 1.33; me4 1.66; ta4 0.44; total 5.98;

relative length: 1>4>2>3. Leg1 and leg2 spineless; leg3 spineless; leg4 spineless. Dorsal side of anterior legs smooth; ventral side of pedipalp smooth. Claws with 8 teeth or less; hardly larger than claw width.

Abdomen 2.30 long; cream-coloured; cylindrical. Abdominal dorsal hairs 0.06 long; thin, roughly straight, compressed, pointed; uniformly, thickly distributed.

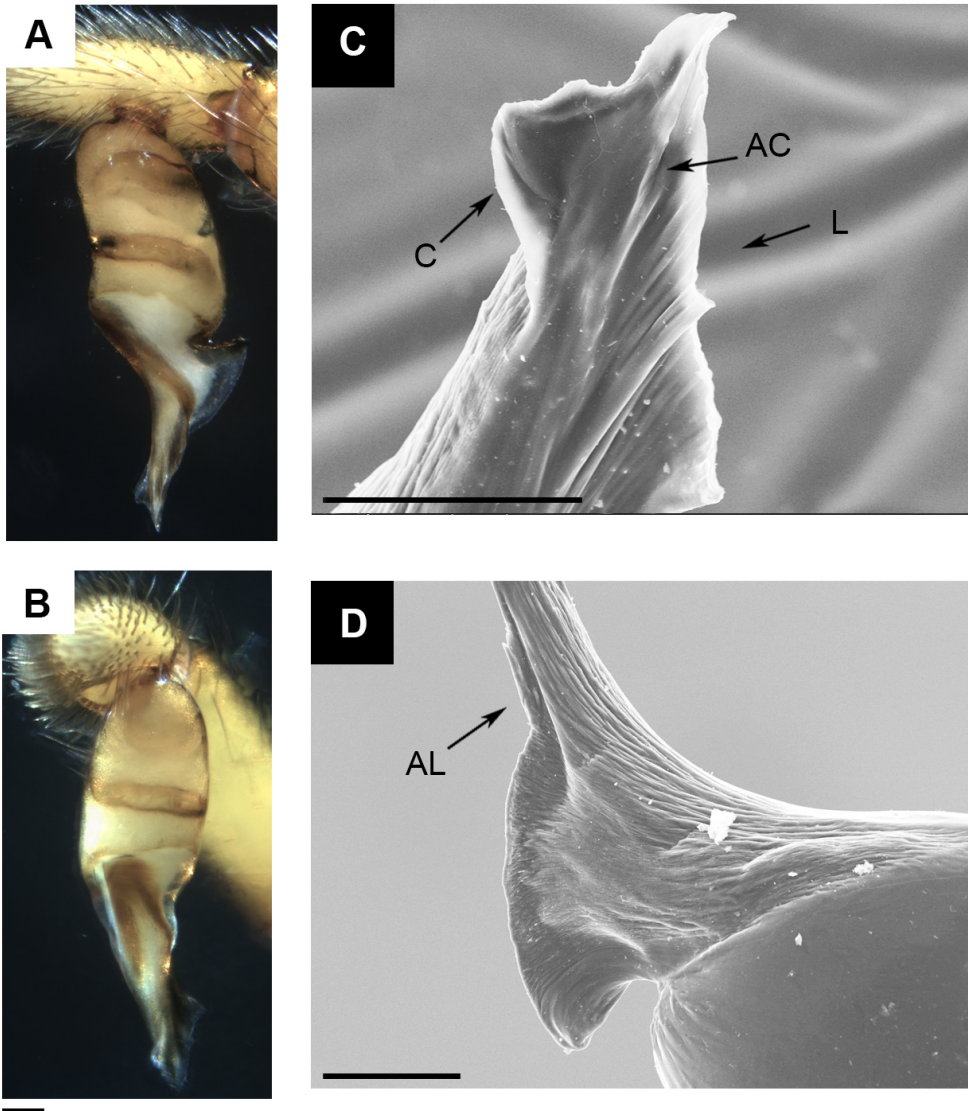


Figure 30. *D. yballa* sp.n. (A) left palp retrolateral view; (B) left palp frontal view; (C) DD right palp retrolateral view; (D) P right palp prolateral view. Scalebar = 0.1mm

Male copulatory bulbus T as long as DD (Fig. 30A); external distal border sloped backwards; internal sloped backwards. DD bent about 45° in lateral view; internal distal border not expanded. IS wider, more sclerotized than ES (Fig. 30B); IS truncated at DD middle part. DD tip straight in lateral view. C present, short; distal end beside DD internal tip; well developed; located close to DD distal tip; proximal border stepwise decreasing; distal border sloping in its base, upper tip projected, pointed, external side hollowed (Fig. 30C). AC present. LF absent. L well developed; external border not sclerotized, laterally slightly folded; distal border divergent, continuous. LA absent. F absent. AL present, poorly developed (Fig. 30D); proximal border in posterior view smooth, not fused with distal haematodoca. P fused to T; perpendicular to T in lateral view; lateral length from 1/3 to 2/5 of T width; ridge present, perpendicular to T; not expanded, upper margin smooth; not distally projected; posterior margin slightly folded towards internal side.

Female paratype (UB2915): (Fig. 31A-C). All characters as in male except: carapace 3.24 long. AME diameter 0.15; PLE 0.14; PME 0.12; AME on edge of anterior border, separated from one another by about 2/3 diameter, close to PLE; PME touching to each other, about 1/3 PME diameter from PLE. Sternum dark red, darkened on borders; wrinkled; uniformly covered in slender black hairs.

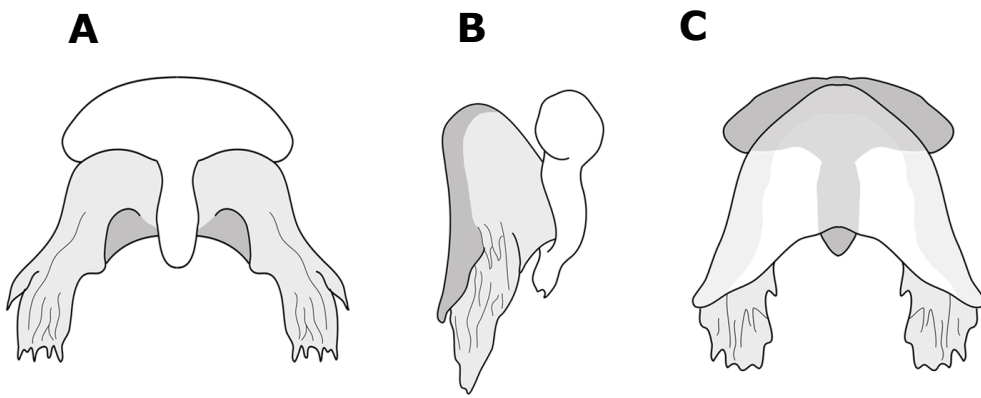


Figure 31. *D. yballa* sp.n. vulva (A) ventral; (B) lateral; (C) dorsal view. Scalebar = 0.65mm

Table 18. Intraspecific leg measurements variability of *D. yballa* sp.n.

	I	II	III	IV
Fe	1.9-2.531/1.955-2.357	1.73-2.312/1.734-2.063	1.34-1.891/1.396-1.72	1.66-2.44/1.792-2.141
Pa	1.07-1.433/1.172-1.391	0.95-1.156/1.016-1.275	0.7-0.976/0.783-0.944	0.89-1.163/0.984-1.134
Ti	1.53-2.261/1.72-2.067	1.42-1.826/1.45-1.811	0.93-1.34/0.988-1.209	1.33-1.91/1.451-1.702
Mt	1.51-2.189/1.584-1.943	1.4-2.334/1.466-1.844	1.22-1.752/1.358-1.49	1.66-2.333/1.798-2.149
Ta	0.42-0.486/0.404-0.513	0.43-0.524/0.435-0.442	0.4-0.48/0.397-0.485	0.44-0.51/0.449-0.504
Total	6.43-8.9/6.835-8.271	5.93-8.152/6.108-7.431	4.59-6.439/4.922-5.848	5.98-8.356/6.474-7.622

Chelicerae 0.97 long, about 1/3 of carapace length in dorsal view; fang short, 0.76; basal segment proximal border of dorsal side strongly covered with piligerous granulations. Chelicera inner groove medium-size, about 2/5 cheliceral length. Legs bicoloured, darker on proximal border, becoming lighter distally. Lengths of female described above: fe1 2.35; pa1 1.39; ti1 2.07; me1 1.94; ta1 0.51; total 8.27; fe2 2.06; pa2 1.39; ti2 1.81; me2 1.84; ta2 0.44; total 7.43; fe3 1.72; pa3 0.94; ti3 1.21; me3 1.49; ta3 0.48; total 5.85; fe4 2.14; pa4 1.13; ti4 1.70; me4 2.15; ta4 0.50; total 7.62; relative length 1>4>2>3. Dorsal side of anterior legs smooth; ventral side of pedipalp covered with hairs, lacking grains.

Abdomen 4.26 long; cream-coloured; cylindrical. Abdominal dorsal hairs 0.09 long.

Vulva DA clearly distinguishable from VA (Fig. 31B); DA longer than wide (Fig. 31C); DF wide in dorsal view. MF margins not fused, well developed, completely sclerotized. VA rectangle-like; anterior region completely sclerotized; posterior region sclerotized except for most internal area; AVD absent. S attachment projected under VA (Fig. 31A); small sclerite between S and VA anterior part present; arms are shorter than DA, slightly curved; tips not projected; neck as wide as arms. TB usual shape.

Intraspecific variation

Male cephalothorax ranges in length from 2.27-3.17 (N=2), females from 2.49-3.24 (N=3). Tibia, metatarsus and tarsus color from bright yellow to orange. Leg measurements variability is listed in table 18.

Distribution

This species is known from different localities spread across the island of La Gomera (Fig. 14).

Discussion

The foundation of any evolutionary, systematic or conservation study is a well-defined set of the species belonging to the target group. Here we provided a solid baseline of the taxonomy of *Dysdera* spiders in the Canary Islands, which are essential for subsequent investigations focusing on the understanding of the evolution.

In the present study, we have raised the number of endemic *Dysdera* species in the Canary Islands to 57. This represents 20% of the worldwide diversity of the genus confined to less than 0.1% of their distribution area (Arnedo et al. 2001). Recently, Crespo *et al.* (2020) also documented a diversification of *Dysdera* in the Madeiran archipelago. Volcanic archipelagos are home to well-known examples of adaptive radiations, which are characterized by the dramatic diversification of species with distinct ecomorphs from a single ancestor (Gillespie 2004; Soulebeau et al. 2015). All of the 57 described species from the Canary Islands but one share a common ancestor (Adrián-Serrano et al. 2020). Furthermore, the Canarian endemics also present a high variability in their cheliceral morphology, also reported in continental species, which seems to be linked to different levels of trophic specialization (Řezáč and Pekár 2007). A recent study has demonstrated that Canarian *Dysdera* species most likely constitute a case of adaptive radiation (Řezáč et al. 2021), although the sparse data used and the lack of an updated phylogeny of the group cast some doubts on the robustness of its conclusions. More studies encompassing a larger sample of individuals, a better resolved complete phylogeny and sound statistical comparative methods will be needed to sustain the claims for the adaptive nature of the diversification process of *Dysdera* in the Canary Islands.

The genetic divergence is not strictly linked to the morphological differentiation (Orr and Smith 1998), being one clear example the cryptic species complex (Hedin and Wood 2002; Sinclair et al. 2004; Boyer et al. 2007). Morphology represented the principal source of evidence in the species delimitation until mid-20th century (Coyne 1994), but nevertheless depending on morphological characters tend to simplify and underestimate the extant diversity (Bond et al. 2001; Bickford et al. 2007). Morphological data present limitations as the almost undifferentiated continuous diversity, low population variability and high sexual dimorphism differentiation could baulk the species identification. For this reason, molecular data are commonly used to check traditional taxonomies (Tautz et al. 2003), as they can help to overcome the limitations of the only morphological based data. Furthermore, species could arise through numerous different processes, which makes the work of species delimitation and identification very complex if they are only based in one single subset of data. Our comparative analyses revealed a high level of correspondence between the nominal species and their underlying genetic structure as revealed by mitochondrial and the nuclear marker ITS2. It should be acknowledged that some of the new species were first identified as separate genetic clusters in preliminary analyses, and were subsequent corroborated using the morphological data, in a reciprocal illumination framework.

Most of the mismatches found between the nominal species and the genetic clustering involved cases of deep geographic structure within species. This was especially obvious in those species with populations in more than one island. In the case of the new species *D. yballa* sp.n., which was formerly considered an island population of *D. levipes*, morphological evidence was clear enough to rise it to species status. Similarly, *D. silvatica*, *D. gomerensis* and *D. calderensis* all shown island populations that were recovered as monophyletic groups and delimited as distinct cluster by some of the delimitation methods implemented. Although we observed

some minor yet consistent morphological differences in some of these island populations, we considered that a wider sampling and more thorough morphological and ecological analyses were required to formally proposed them as new species. A similar pattern of deep geographic structure was also observed in cave-dwelling species. Volcanic lava tubes may constitute an extensive network of continuous habitats also connected through the void and cracks that constitute the volcanic MSS, facilitating the dispersal and maintenance of gene flow between cave populations. However, in some cases the existence of dykes or even massive landslides, may isolated formerly continuous cave populations. This may explain the deep structure revealed in the species *D. ambulotenta*, *D. chioensis*, both of which have divergent populations in lava tubes at both sides of the Orotava valley, which was the result of a major landslide dating back to 0.5 to 0.8 million years ago (García-Olivares et al. 2017). Surprisingly, in other cave-dwelling species, specimens showing high intraspecific divergences were collected in the same caves (eg. *D. esquiveli*, *D. sibyllina*, *D. unguimmanis*). In these cases, additionally sequencing and sampling may help to discard the possibility of mishandling or mislabelling of specimens. The last set of species showing deep intraspecific genetic structure corresponds to species with wide distribution within islands. Several studies have already revealed the existence of deep phylogeographic structure in endemic Canarian *Dysdera* species—*D. alegranzaensis* Wunderlich, 1992, *D. lancerotensis* and *D. nesiotetes* in the Eastern canaries (Macías-Hernández et al. 2013b), and *D. verneui* in Tenerife (Macías-Hernández et al. 2013a)—which has been most likely linked to the highly dynamic geology of the islands, including recurrent eruptive cycles, connection of formerly isolated island and eustatic sea level changes. In this study we have collected additional evidence of phylogeographic structure in other species, for instance *D. macra* in Tenerife, which shows geographic patterns resembling those of *D. verneui*. Of special interest is the discovery of previously overlooked phylogeographic patterns shared among several species in Gran Canaria. Specifically, *D. bandamae*, *D. herii* sp.n.

and *D. liostetha*, show genetically distinct populations in the north-western and the south-eastern sides of the island. Interestingly, similar pattern has been found in curculionid beetles, which have been explain as the result of an explosive eruptive cycle of the Roque Nublo, dated between 3 to 5 million years ago (Emerson et al. 2000). Overall, the evidence of deep phylogeographic structure within endemic species with widespread distribution within islands, could suggest that speciation in the islands is mostly the results of allopatric process acting at the island level because of volcanic activity. Under this scenario, the geographically structured populations constitute the initial stages of speciation that eventually, if isolation persists, will become independent evolutionary lineages, i.e. species. This is of major importance in the context of understanding the driving forces acting during adaptive radiation, since the speciation process could be effectively uncoupled from the ecological diversification, which could be mostly driven by postpositional competitive processes (Kennedy et al. 2022).

We have found very few cases, in which the molecular and morphological data have revealed potential instances of mixing or merging. In some cases, the incongruences are better explained by the haplotypic nature of the mitochondrial markers. This could be the case of the mitochondrial markers of the species *D. curviseta*, which rendered the species *D. liostetha* as paraphyletic. However, the ITS2 supported the monophyly of *D. liostetha*. Since both species inhabit different islands, the most plausible scenario is that following split of the ancestor of *D. curviseta* because of the colonization of Tenerife, gene flow homogenized the genome of the *D. liostetha*. Of special interest is the lack of sorting in molecular markers in the species pairs *D. levipes*-*D. gollumi* and *D. mahan*-*D. spinidorsum*. In this case the most plausible scenario is a rapid speciation because of an ecological shift. Indeed, in the two cases, one of the species shows a clear departure from the ancestral ecological preferences, i.e. forest ground dweller, in one case to adapt to the underground

environment (*D. gollumi*) and in the other to the intertidal habitat (*D. mahan*).

Recent studies have suggested that hybridization may promote adaptive radiations by creating novel phenotypes (Kagawa and Takimoto 2018). Our data, however, show little evidence of hybridization among Canarian *Dysdera* endemics. In fact, only one well-contrasted case and a potential second one could be identified. The existence of introgression in *D. vernaui* had been already unravel in a previous study (Macías-Hernández et al. 2013a). However, here, using a more thorough sampling of specimens, we have disclosed that the introgression was probably the result of the capture of a mitochondrial lineage belonging to a ghost lineage more closely related to *D. chioensis* by *D. verneui*. A second case of hybridization could have account for the unsorting of ITS2 sequence types between *D. aniepa* sp.n. and *D. macra*. It could be argued instead that *D. aniepa* sp.n. is not a good species and should be better considered as a population of the geographically well-structured *D. macra*. Indeed, other Tenerife endemics, e.g. *D. iguanensis* Wunderlich 1987, show a phylogeographic break between the populations in the Teno area, which originated as an independent volcanic edifice that was subsequently connected to the rest of the island following volcanic activity in the central edifice, dated between 0.2 to 3.5 million years ago (Ancochea et al. 1999; Cantagrel et al. 1999). However, unlike *D. iguanensis*, the mitochondrial lineages of *D. aniepa* sp.n. are not exclusive to Teno, and thus are not simply the results of geographical structure. Future studies will have to incorporate along with more specimens and a more thorough representation of genomic information, maybe using ddRADseq or other reduce representation techniques for genome scanning, to untangle the evolutionary processes underlying differentiation between *D. aniepa* sp.n. and *D. macra*.

With our combined results of molecular data and morphological differences observed in the candidate species we support the existence of 10 new species which had been unnoticed in previous morphological based studies. Furthermore,

population cluster has been identified that match with the geography of the islands, this is the case of *D. calderensis*, *D. gomerensis* or *D. silvatica* in different islands or *D. verneaui* which presents a marked population structure inside the same island that has been already observed in a previous study (Macías-Hernández et al. 2013a).

Despite of the large number of specimens collected and examined, some Canarian *Dysdera* species remain only known by one of the sexes. This is the case of the newly described *D. banot* sp.n., *D. gaifa* sp.n., and *D. garoe* sp.n., which are only known by females. In contrast, with the help of the support provided by the molecular data, we were able to complete the descriptions of *D. orahan* and *D. hirguan*. After more than 20 years of sampling and revisionary work (see Arnedo and Ribera 1999a; Arnedo and Ribera 1999b; Arnedo and Ribera 1999c; Arnedo et al. 2001; Arnedo et al. 2007; Macías-Hernández et al. 2010; Macías-Hernández et al. 2016), the distributions ranges and ecological preferences of several species known by both sexes remain poorly unknown due to the small number of known specimens. The causes for the large differences in the abundances across the different species are unclear. In some cases, it may simply be due to the limited effort exerted on habitats, such as the MSS or coastal (including intertidal) habitats. Another potential reason could be the existence of long-term cycles (larger than stational) in the abundance of some species. Although the data at hand is too sparse to test this possibility, based on personal experience it looks like some specie that were abundant 30 years ago are now rare and the other way around, species hardly collected some decades ago are now more easy to spot. We will have to await to further collecting efforts to test these scenarios.

Conclusions

With the present study, we have greatly contributed to improve our current knowledge of the Canarian *Dysdera* spider fauna. We have increased the species richness in the islands by 20% by describing 10 new species. The new described

species include both species diagnosed using morphological characters traditionally used in the group, but also species which morphological differences went unnoticed in previous studies as they were either difficult to differentiate from similar species or the diagnostic had not been considered. The last species were first red-flagged using molecular single-marker delimitation methods. In a good number of cases, molecular information also revealed the existence of deep geographic structure within species, mostly accounting for multi-island species, cave dwelling species and spiders with wide distribution ranges within islands. Despite the potential of islands diversification processes to include recently diverged species or instances of hybridization, we identified only two potential cases of incomplete lineage sorting and two of introgression. Although not perfect, DNA barcoding data has the potential to correctly assign query specimens to most of the *Canarian Dysdera* species.

Acknowledgments

Enric Planas and Vanina Tonzo help with the coding of the R script for barcode analysis.

Bibliography

- Adrián-Serrano S., Lozano-Fernandez J., Pons J., Rozas J., Arnedo M.A. 2020. On the shoulder of giants: Mitogenome recovery from non-targeted genome projects for phylogenetic inference and molecular evolution studies. *J. Zool. Syst. Evol. Res.*:1–26.
- Agnarsson I. 2010. The utility of ITS2 in spider phylogenetics: Notes on prior work and an example from *Anelosimus*. *J. Arachnol.* 38:377–382.
- Alvarez-padilla F., Hormiga G. 2007. A Protocol For Digesting Internal Soft Tissues And Mounting Spiders For Scanning Electron Microscopy. *J. Arachnol.* 35:538–542.
- Ancochea E., Huertas M.J., Cantagrel J.M., Coello J., Fuster J.M., Arnaud N., Ibarrola E. 1999. Evolution of the Cañadas edifice and its implications for the origin of the Cañadas Caldera Tenerife, Canary Islands. *J. Volcanol. Geotherm. Res.* 88:177–199.
- Arnedo M.A. 2003. Lost and Found : Rediscovery of type material of some endemic species of the spider genus *Dysdera* (araneae , Dysderidae) from the Canary Islands, and its nomenclatural and

- taxonomic implications. *Rev. Ibérica Aracnol.* 7:141–148.
- Arnedo M.A., Oromí P., Múrria C., Macías-Hernández N., Ribera C. 2007. The dark side of an island radiation: systematics and evolution of troglobitic spiders of the genus *Dysdera* Latreille (Araneae: Dysderidae) in the Canary Islands. *Invertebr. Syst.* 21:623–660.
- Arnedo M.A., Oromí P., Ribera C. 2000a. Systematics of the Genus *Dysdera* (Araneae, Dysderidae) in the Eastern Canary Islands. *Am. Arachnol. Soc.* 28:261–292.
- Arnedo M.A., Oromí P., Ribera C. 2001. Radiation of the spider genus *Dysdera* (Araneae, Dysderidae) in the Canary Islands: Cladistic assessment based on multiple data sets. *Cladistics.* 17:313–353.
- Arnedo M.A., Oromí P., Ribera C. 2000b. Systematics of the Genus *Dysdera* (Araneae, Dysderidae) in the Eastern Islands. *J. Arachnol.*:261–292.
- Arnedo M.A., Ribera C. 1997. Radiation in the genus *Dysdera* (Araneae, Dysderidae) in the Canary Islands: The island of Gran Canaria. *J. Arachnol.* 27:604–662.
- Arnedo M.A., Ribera C. 1999a. Radiation in the genus *Dysdera* (Araneae, Dysderidae) in the Canary Islands: The island of Tenerife. *J. Arachnol.* 27:604–662.
- Arnedo M.A., Ribera C. 1999b. Radiation in the genus *Dysdera* (Araneae, Dysderidae) in the Canary Islands: The western islands. *J. Arachnol.* 27:604–662.
- Ballard J.W.O., Whitlock M.C. 2004. The incomplete natural history of mitochondria. *Mol. Ecol.* 13:729–744.
- Bickford D., Lohman D.J., Sodhi N.S., Ng P.K.L., Meier R., Winker K., Ingram K.K., Das I. 2007. Cryptic species as a window on diversity and conservation. *Trends Ecol. Evol.* 22:148–155.
- Bidegaray-Batista L., Arnedo M.A. 2011. Gone with the plate: The opening of the Western Mediterranean basin drove the diversification of ground-dweller spiders. *BMC Evol. Biol.* 11.
- Van Den Bogaard P. 2013. The origin of the Canary Island Seamount Province-New ages of old seamounts. *Sci. Rep.* 3:1–7.
- Bond J.E., Hedin M.C., Ramirez M.G., Opell B.D. 2001. Deep molecular divergence in the absence of morphological and ecological change in the californian coastal dune endemic trapdoor spider *Aptostichus simus*. *Mol. Ecol.* 10:899–910.
- Borchsenius F. 2009. FastGap 1.2. Dep. Biosci. Aarhus Univ. Denmark.:Published online at http://www.aubot.dk/FastGap_ho.
- Boyer S.L., Baker J.M., Giribet G. 2007. Deep genetic divergences in *Aoraki denticulata* (Arachnida, Opiliones, Cyphophthalmi): A widespread “mite harvestman” defies DNA taxonomy. *Mol. Ecol.* 16:4999–5016.
- Brown S.D.J., Collins R.A., Boyer S., Lefort M.C., Malumbres-Olarte J., Vink C.J., Cruickshank R.H. 2012.

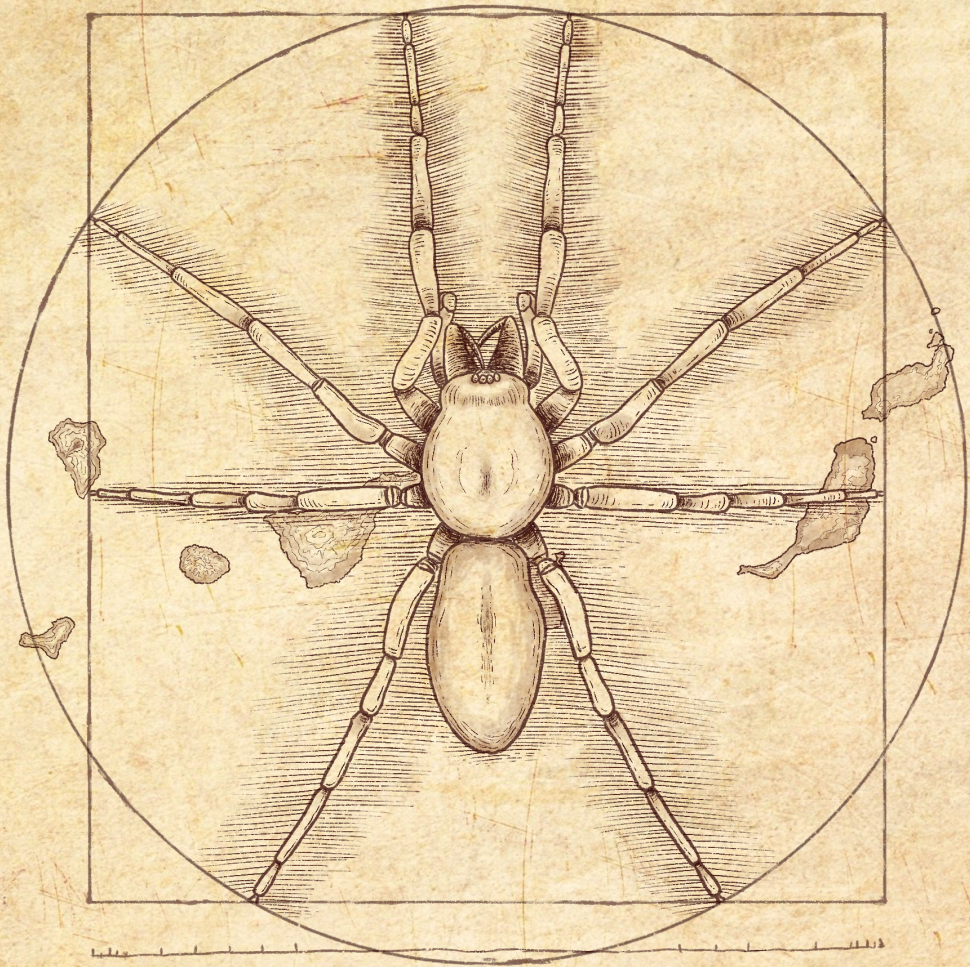
- Spider: An R package for the analysis of species identity and evolution, with particular reference to DNA barcoding. *Mol. Ecol. Resour.* 12:562–565.
- Cantagrel J.M., Arnaud N.O., Ancochea E., Fúster J.M., Huertas M.J. 1999. Repeated debris avalanches on Tenerife and genesis of Las Canadas caldera wall (Canary Islands). *Geology.* 27:739–742.
- Coyne J.A. 1994. Ernst Mayr and the Origin of Species. *Evolution (N. Y.)* 48:19.
- Crespo L.C., Silva I., Enguíanos A., Cardoso P., Arnedo M.A. 2021. Integrative taxonomic revision of the woodlouse-hunter spider genus *Dysdera* (Araneae: Dysderidae) in the Madeira archipelago with notes on its conservation status. *Zool. J. Linn. Soc.* 192:356–415.
- Deeleman-Reinhold C.L., Deeleman P.R. 1988. Revision des Dysderinae (Araneae, Dysderidae), les espèces méditerranéennes occidentales exceptées. *Tijdschr. voor Entomol.* 131:141–269.
- DeSalle R., Goldstein P. 2019. Review and Interpretation of Trends in DNA Barcoding. *Front. Ecol. Evol.* 7:1–11.
- Drummond A.J., Suchard M.A., Xie D., Rambaut A. 2012. Bayesian phylogenetics with BEAUti and the BEAST 1.7. *Mol. Biol. Evol.* 29:1969–1973.
- Emerson B.C., Oromí P., Hewitt G.M. 2000. Colonization and diversification of the species *Brachyderes rugatus* (Coleoptera) on the Canary Islands: Evidence from mitochondrial DNA COII gene sequences. *Evolution (N. Y.)* 54:911–923.
- Ezard T., Fujisawa T., Barraclough T.G. 2017. splits: SPecies' Limits by Threshold Statistics. Version 1.0-20.
- Fujisawa T., Barraclough T.G. 2013. Delimiting species using single-locus data and the generalized mixed yule coalescent approach: A revised method and evaluation on simulated data sets. *Syst. Biol.* 62:707–724.
- Funk D.J., Omland K.E. 2003. Species-Level Paraphyly and Polyphyly: Frequency, Causes, and Consequences, with Insights from Animal Mitochondrial DNA. *Annu. Rev. Ecol. Evol. Syst.* 34:397–423.
- García-Olivares V., López H., Patiño J., Alvarez N., Machado A., Carracedo J.C., Soler V., Emerson B.C. 2017. Evidence for mega-landslides as drivers of island colonization. *J. Biogeogr.* 44:1053–1064.
- Gillespie R. 2004. Community Assembly Through Adaptive Radiation in Hawaiian Spiders. *Science (80-)* 303:356–359.
- Gillespie R.G. 2007. Oceanic Islands: Models of Diversity. *Encycl. Biodivers.* Second Ed.:590–599.
- Goloboff A P., Farris S J., Nixon C K. 2008. TNT, a free program for phylogenetic analysis. *Cladistics.* 24:774–786.
- Hedin M., Wood D.A. 2002. Genealogical exclusivity in geographically proximate populations of

- Hypochilus thorelli Marx (Araneae, Hypochilidae) on the Cumberland Plateau of North America. *Mol. Ecol.* 11:1975–1988.
- Hoang D.T., Chernomor O., Von Haeseler A., Minh B.Q., Vinh L.S. 2018. UFBoot2: Improving the ultrafast bootstrap approximation. *Mol. Biol. Evol.* 35:518–522.
- Kagawa K., Takimoto G. 2018. Hybridization can promote adaptive radiation by means of transgressive segregation. *Ecol. Lett.* 21:264–274.
- Kahle D., Wickham H. 2013. ggmap: spatial visualization with ggplot2. Available from <https://journal.r-project.org/archive/2013-1/kahle-wickham.pdf>.
- Kalyaanamoorthy S., Minh B.Q., Wong T.K.F., Von Haeseler A., Jermini L.S. 2017. ModelFinder: Fast model selection for accurate phylogenetic estimates. *Nat. Methods.* 14:587–589.
- Kapli P., Lutteropp S., Zhang J., Kobert K., Pavlidis P., Stamatakis A., Flouri T. 2017. Multi-rate Poisson tree processes for single-locus species delimitation under maximum likelihood and Markov chain Monte Carlo. *Bioinformatics.* 33:1630–1638.
- Kennedy S., Lim J.Y., Adams S.A., Krehenwinkel H., Gillespie R.G. 2022. What is adaptive radiation? Many manifestations of the phenomenon in an iconic lineage of Hawaiian spiders. *Mol. Phylogenet. Evol.* 175:107564.
- Lanfear R., Frandsen P.B., Wright A.M., Senfeld T., Calcott B. 2017. Partitionfinder 2: New methods for selecting partitioned models of evolution for molecular and morphological phylogenetic analyses. *Mol. Biol. Evol.* 34:772–773.
- Macías-Hernández N., Bidegaray-Batista L., Emerson B.C., Oromí P., Arnedo M. 2013a. The imprint of geologic history on within-island diversification of woodlouse-hunter spiders (Araneae, Dysderidae) in the canary islands. *J. Hered.* 104:341–356.
- Macías-Hernández N., Bidegaray-Batista L., Oromí P., Arnedo M.A. 2013b. The odd couple: Contrasting phylogeographic patterns in two sympatric sibling species of woodlouse-hunter spiders in the Canary Islands. *J. Zool. Syst. Evol. Res.* 51:29–37.
- Macías-Hernández N., López S. de la C., Roca-Cusachs M., Oromí P., Arnedo M.A. 2016. A geographical distribution database of the genus *Dysdera* in the Canary Islands (Araneae, Dysderidae). *Zookeys.* 2016:11–23.
- Macías-Hernández N., Oromí P., Arnedo M.A. 2008. Patterns of diversification on old volcanic islands as revealed by the woodlouse-hunter spider genus *Dysdera* (Araneae, Dysderidae) in the eastern Canary Islands. :589–615.
- Macías-Hernández N., Oromí P., Arnedo M.A. 2010. Integrative taxonomy uncovers hidden species diversity in woodlouse hunter spiders (Araneae, Dysderidae) endemic to the Macaronesian

- archipelagos. *Syst. Biodivers.* 8:531–553.
- Maddison W.P. 1997. Gene trees in species trees. *Syst. Biol.* 46:523–536.
- Magalhaes I.L.F. 2019. Spreadsheets to expedite taxonomic publications by automatic generation of morphological descriptions and specimen lists. *Zootaxa.* 4624:147–150.
- Miller M.A., Pfeiffer W., Schwartz T. 2010. Creating the CIPRES Science Gateway for inference of large phylogenetic trees. 2010 *Gatew. Comput. Environ. Work. GCE 2010.*:1–8.
- Minh B.Q., Schmidt H.A., Chernomor O., Schrempf D., Woodhams M.D., Von Haeseler A., Lanfear R., Teeling E. 2020. IQ-TREE 2: New Models and Efficient Methods for Phylogenetic Inference in the Genomic Era. *Mol. Biol. Evol.* 37:1530–1534.
- Monaghan P., Metcalfe N.B., Torres R. 2009. Oxidative stress as a mediator of life history trade-offs: Mechanisms, measurements and interpretation. *Ecol. Lett.* 12:75–92.
- Orr M.R., Smith T.B. 1998. Ecology and speciation. *Trends Ecol. Evol.* 41:502–506.
- Rambaut A., Drummond A.J., Xie D., Baele G., Suchard M.A. 2018. Posterior summarization in Bayesian phylogenetics using Tracer 1.7. *Syst. Biol.* 67:901–904.
- Řezáč M., Pekár S. 2007. Evidence for woodlice-specialization in *Dysdera* spiders: Behavioural versus developmental approaches. *Physiol. Entomol.* 32:367–371.
- Řezáč M., Pekár S., Arnedo M., Macías-Hernández N., Řezáčová V. 2021. Evolutionary insights into the eco-phenotypic diversification of *Dysdera* spiders in the Canary Islands. *Org. Divers. Evol.*
- Ribera C., Arnedo M.A. 1994. Description of *Dysdera gollumi* (Araneae, Haplogynae), a new troglobitic species from Tenerife, Canary Islands, with some comments on Canarian *Dysdera*. *Mémoires de Biospéologie.* 21:115–119.
- Ribera C., Fernandez M.A., Blasco A. 1985. Araneidos cavernícolas de Canarias II. *Mémoires de Biospéologie.*:51–68.
- Ronquist F., Teslenko M., Van Der Mark P., Ayres D.L., Darling A., Höhna S., Larget B., Liu L., Suchard M.A., Huelsenbeck J.P. 2012. MrBayes 3.2: Efficient bayesian phylogenetic inference and model choice across a large model space. *Syst. Biol.* 61:539–542.
- Rozas J., Ferrer-Mata A., Sanchez-DelBarrio J.C., Guirao-Rico S., Librado P., Ramos-Onsins S.E., Sanchez-Gracia A. 2017. DnaSP 6: DNA sequence polymorphism analysis of large data sets. *Mol. Biol. Evol.* 34:3299–3302.
- Rubinoff D., Cameron S., Will K. 2006. A genomic perspective on the shortcomings of mitochondrial DNA for “barcoding” identification. *J. Hered.* 97:581–594.
- Schmidt G. 1973. Zur Spinnenfauna von Gran Canaria. *Zool. Beiträge.* 19:347–391.
- Shaw K.L. 2002. Conflict between nuclear and mitochondrial DNA phylogenies of a recent species

- radiation: What mtDNA reveals and conceals about modes of speciation in Hawaiian crickets. *Proc. Natl. Acad. Sci. U. S. A.* 99:16122–16127.
- Simmons M.P., Ochoterena H. 2000. Gaps as characters in sequence-based phylogenetic analyses. *Syst. Biol.* 49:369–381.
- Simon E. 1883. Études arachnologiques. 14e Mémoire. XXI. Matériaux pour servir à la faune arachnologique des îles de l’Océan Atlantique (Açores, Madère, Salvages, Canaries, Cap Vert, Sainte-Hélène et Bermudes). *Ann. la Société Entomol. Fr.* 6:259–314.
- Simon E. 1907. Etude sur les araignées de la sous-section des Haplogynes. *Ann. la Société Entomol. Belgique.* 51:246–264.
- Sinclair E.A., Bezy R.L., Bolles K., Camarillo R. J.L., Crandall K.A., Sites J.W. 2004. Testing species boundaries in an ancient species complex with deep phylogeographic history: Genus *Xantusia* (Squamata: Xantusiidae). *Am. Nat.* 164:396–414.
- Soulebeau A., Aubriot X., Gaudeul M., Rouhan G., Hennequin S., Haevermans T., Dubuisson J.Y., Jabbour F. 2015. The hypothesis of adaptive radiation in evolutionary biology: hard facts about a hazy concept. *Org. Divers. Evol.* 15:747–761.
- Stamatakis A. 2014. RAxML version 8: A tool for phylogenetic analysis and post-analysis of large phylogenies. *Bioinformatics.* 30:1312–1313.
- Stephens M., Donnelly P. 2003. A Comparison of Bayesian Methods for Haplotype Reconstruction from Population Genotype Data. *Am. J. Hum. Genet.* 73:1162–1169.
- Stephens M., Smith N.J., Donnelly P. 2001. A new statistical method for haplotype reconstruction from population data. *Am. J. Hum. Genet.* 68:978–989.
- Strand E. 1911. Arachniden von der kanarischen Insel Gomera, gesammelt von Herrn Prof. Dr W. May. *Arch. für Naturgeschichte.* 77:189–201.
- Tamura K., Stecher G., Peterson D., Filipski A., Kumar S. 2021. MEGA6: Molecular evolutionary genetics analysis version 11. *Mol. Biol. Evol.* 38:3022–3027.
- Tautz D., Arctander P., Minelli A., Thomas R.H., Vogler A.P. 2003. A plea for DNA taxonomy. *Trends Ecol. Evol.* 18:70–74.
- World Spider Catalog. 2023. World Spider Catalog. Version 24. Natural History Museum Bern, online at <http://wsc.nmbe.ch>, accessed on {date of access}. doi: 10.24436/2. .
- Wunderlich J. 1987. Die Spinnen der Kanarischen Inseln und Madeiras: Adaptive Radiation, Biogeographie, Revisionen und Neubeschreibungen. .
- Wunderlich J. 1991. Die Spinnen-Fauna der Makaronesischen Inseln: Taxonomie, Ökologie, Biogeographie und Evolution. *Beiträge zur Araneologie.* 1:1–619.

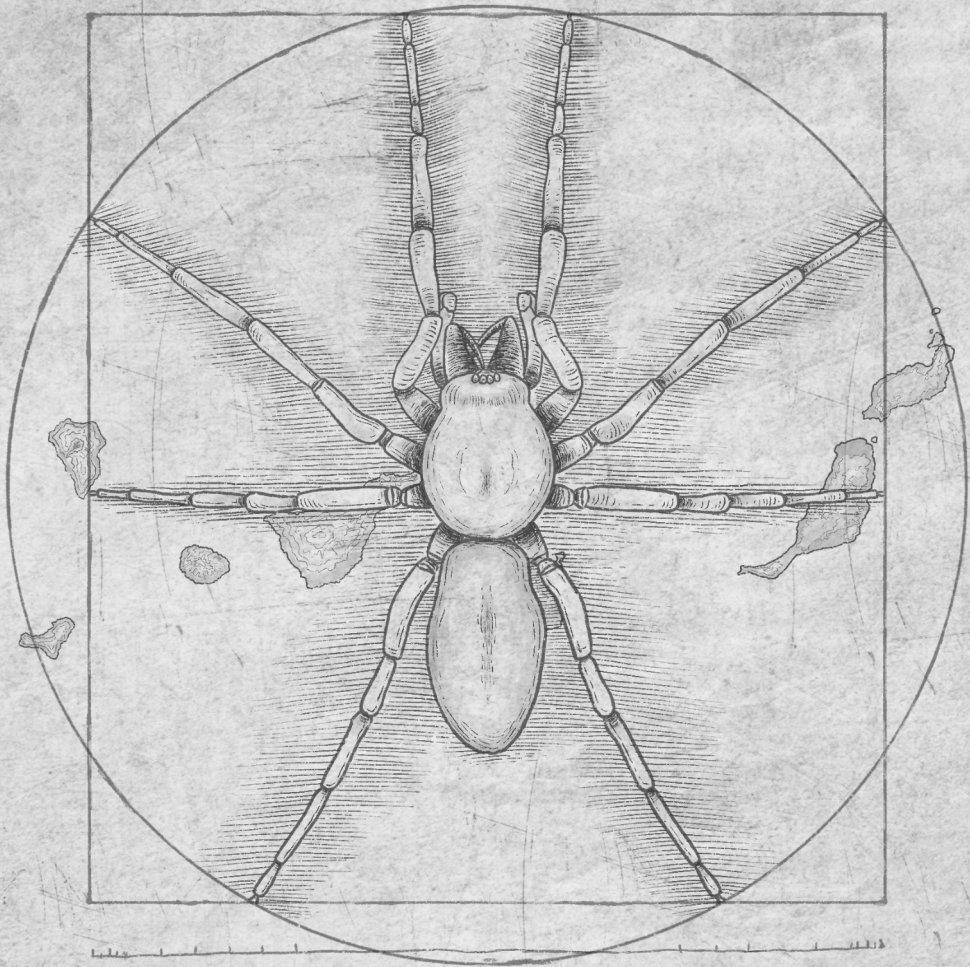
Zhang J., Kapli P., Pavlidis P., Stamatakis A. 2013. A general species delimitation method with applications to phylogenetic placements. *Bioinformatics*. 29:2869–2876.



CHAPTER 2

Test the hypothesis of adaptive radiation in the red devil spiders

(Araneae: Dysderidae) of the Canary Islands



CHAPTER 2.1

The Vitruvian spider: Segmenting and integrating over different body parts to describe ecophenotypic variation



Received: 23 March 2022 | Revised: 2 September 2022 | Accepted: 4 September 2022

DOI: 10.1002/jmor.21516

RESEARCH ARTICLE



The Vitruvian spider: Segmenting and integrating over different body parts to describe ecophenotypic variation

Adrià Bellvert^{1,2} | Marcos Roca-Cusachs^{1,2} | Vanina Tonzo^{1,2} |
Miquel A. Arnedo^{1,2} | Antigoni Kaliontzopoulou^{1,2}

¹Departament de Biologia Evolutiva, Ecologia i Ciències Ambientals, Universitat de Barcelona (UB), Barcelona, Spain

²Institut de Recerca de la Biodiversitat (IRBio), Universitat de Barcelona (UB), Barcelona, Spain

Correspondence

Adrià Bellvert, Departament de Biologia Evolutiva, Ecologia i Ciències Ambientals, Institut de Recerca de la Biodiversitat (IRBio), Universitat de Barcelona (UB), Av. Diagonal, 643, Barcelona 08028, Spain.
Email: abellvertba@gmail.com

Funding information

Systematics Association; European Social Fund, Grant/Award Number: RYC2019-026688-I/AEI/10.13039/501100011033; Agencia Estatal de Investigación, Grant/Award Number: RYC2019-026688-I/AEI/10.13039/501100011033; Ministerio de Asuntos Económicos y Transformación Digital, Gobierno de España, Grant/Award Numbers: BES-2017-080538, CGL2012-36863, CGL2016-80651-P; Generalitat de Catalunya, Grant/Award Number: 2017SGR83

Abstract

Understanding what drives the existing phenotypic variability has been a major topic of interest for biologists for generations. However, the study of the phenotype may not be straightforward. Indeed, organisms may be interpreted as composite objects, comprising different ecophenotypic traits, which are neither necessarily independent from each other nor do they respond to the same evolutionary pressures. For this reason, a deep biological understanding of the focal organism is essential for any morphological analysis. The spider genus *Dysdera* provides a particularly well-suited system for setting up protocols for morphological analyses that encompass a suit of morphological structures in any nonmodel system. This genus has undergone a remarkable diversification in the Canary Islands, where different species perform different ecological roles, exhibiting different levels of trophic specialization or troglomorphic adaptations, which translate into a remarkable interspecific morphological variability. Here, we seek to develop a broad guide, of which morphological characters must be considered, to study the effect of different ecological pressures in spiders and propose a general workflow that will be useful whenever researchers set out to investigate variation in the body plans of different organisms, with data sets comprising a set of morphological traits. We use geometric morphometric methods to quantify variation in different body structures, all of them with diverse phenotypic modifications in their chelicera, prosoma, and legs. We explore the effect of analyzing different combined landmark (LM) configurations of these characters and the degree of morphological integration that they exhibit. Our results suggest that different LM configurations of each of these body parts exhibit a higher degree of integration compared to LM configurations from different structures and that the analysis of each of these body parts captures different aspects of morphological variation, potentially related to different ecological factors.

KEYWORDS

Araneae, Canary Islands, Dysderidae, geometric morphometrics, integration

This is an open access article under the terms of the Creative Commons Attribution-NonCommercial License, which permits use, distribution and reproduction in any medium, provided the original work is properly cited and is not used for commercial purposes.

© 2022 The Authors. *Journal of Morphology* published by Wiley Periodicals LLC.

1 | INTRODUCTION

The study of how the phenotype can be altered by selection goes back to the experiments performed by Darwin before the publication of his book "On the origin of species" in 1859 (Andersson, 2009). However, adaptation is an inherently multivariate process and natural selection often acts upon sets of functionally related traits, rather than on unidimensional phenotypes (Blows, 2007; Lande & Arnold, 1983; Phillips & Arnold, 1989; Schluter & Nychka, 1994). Furthermore, not all evolutionary pressures necessarily drive the different characteristics of organisms toward the same direction. Under the definition of the species' fundamental niche by Hutchinson (1957) as an hypervolume of n dimensions, the existence of a species in a given environment is understood as being determined by its capacity to adapt to different ecological conditions, and its tolerance to these environmental settings is in turn influenced by its phenotypic attributes (Carscadden et al., 2017; Givnish, 1987). The suit of morphological features that improve an organism's performance in its environment is known as functional traits (McGill et al., 2006; Nock et al., 2016). In this context, the multidimensional hutchinsonian niche of n ecological dimensions is also expected to translate into a multidimensional space of different functional morphological traits (Eklöf et al., 2013) that define the phenotypic properties of the species, such as its external shape. Therefore, to understand the morphological differentiation among different species, a multidimensional phenotypic approach is needed (Guillermo, 2018), and to infer the evolutionary pressures that have driven such differentiation, we need to know how phenotypes and their function relate to their ecological environment. The mutual links between these organismal properties and their evolution are summarized in the ecomorphological paradigm (Arnold, 1983). However, understanding the relationship between phenotypic characters, ecological variables, and the effect of phenotypic variation on fitness is not always straightforward. While predictions can be made based on our knowledge of how organisms work, linking patterns of variation in different traits with different ecological pressures in non-model systems may not be clear. Furthermore, depending on the question to be addressed, one may be interested in one particular structure, a set of them, or the entire body, and thus the challenge emerges on how to best choose which traits to investigate and how to combine the information derived from each of them (Guillermo et al., 2020).

Additionally, those ecological-related phenotypes shaped under different evolutionary pressures are not completely independent from each other, because organisms are integrated to function as a whole (Klingenberg, 2009). However, the level of covariation between them could vary depending on the relationships between the different body parts (Olson & Miller, 1958). Traits with higher levels of covariation (i.e., integration), than others, form composite units (modules) affected by more similar evolutionary pressures compared to other body parts. These integrated subunits are interconnected conforming, the whole body of an organism that needs to work in a coordinated manner, where changes in one trait could be inevitably accompanied by changes in others (Adams, 2016).

This integration of different modules has different reasons: genetic, developmental, functional, or evolutionary (Klingenberg, 2008). One of the consequences of trait integration is that determining whether certain phenotypes have been shaped by certain evolutionary pressures or whether, on the contrary, trait variation emerges as a consequence of the coevolution with other interconnected modules is not always straightforward. In this sense, understanding which sets of traits show high covariation is an important aspect to discern the different biological factors that may explain their evolution.

Organisms with a modular body plan, where different structures can be intuitively associated with particular ecological or social functions, and thus predicted to respond to specific evolutionary pressures, provide excellent study cases for establishing how morphological variation can be described quantitatively. In addition, they ease the association of such functional structures to its underlying causes, when previous knowledge is scarce. Spiders, and arachnids in general, are one such case. From the comparative morphology of the chelicera musculature (Wood & Parkinson, 2019) to the use of body size to understand ecophysiology (Canals et al., 2015), most previous studies on spiders have been directed at understanding the function and meaning of a specific character related to a specific adaptation in different sets of species. More recently, however, an increasing number of studies has focused on establishing a standardized framework to investigate different functional traits in spiders (Lowe et al., 2020; Macías-Hernández et al., 2020), highlighting the raised attention to the relation with the ecological and morphological characters in this group of organisms. However, despite the relatively obvious functional implications of some phenotypic characters (e.g., legs for locomotion or social interactions, chelicerae for feeding, etc.), a detailed protocol for obtaining high-resolution morphological data on different body structures and an integrated assessment of such variation with relation to different factors is still not available for spiders.

The inherent complexity of certain body structures is better approached for morphological studies if shape information is considered (Klingenberg, 2010). In technical terms, one major tool for studying the variation in the shape of body parts and the covariation between them (i.e., integration) is landmark (LM)-based geometric morphometrics (GMs). These methods differ from traditional morphometric approaches in how shape information is obtained, as they capture the geometry of the morphological structure of interest, and preserve it throughout the analyses (Adams et al., 2004). These tools have expanded the way we visualize and study shape variation, providing a fine-scale description of morphological structures. However, despite the statistical strength of GM in characterizing the shape of morphological structures, few studies have applied this morphometric technique in spiders. Previously, LM-based analyses have been limited to characterizing genitalic variation across species (Crews, 2009) and intraspecific allometry in sexual dimorphism (Fernández-Montraveta & Marugán-Lobón, 2017; Kallal et al., 2019), and delimiting and identifying species overlooked with traditional methods (Wilson et al., 2021). Thus, although morphological studies on spiders have been extensive, we lack fine-tuned

protocols for shape data acquisition and a detailed knowledge of the variation of different body parts and how these are integrated with each other.

The spider genus *Dysdera* Latreille, 1804, also known as woodlouse-hunter or red devil spiders, has a western Palearctic distribution, with Macaronesia as its westernmost limit (Arnedo & Ribera, 1999), and to date around 300 species have been described (World Spider Catalog, 2022). Of nocturnal habits, these species are usually found under rocks, barks, or dead logs (Macías-Hernández et al., 2008) (Figure 1a). The genus exhibits a high interspecific variability in their cheliceral mouthparts, which has been related with different levels of trophic specialization in feeding on isopods, that is,

oniscophagy (Řezáč & Pekár, 2007), where some more specialized species exhibit varying degrees of preference toward capturing isopods over other arthropod preys, while other species retain a rather generalist diet (Toft & Macías-Hernández, 2021). For this reason, *Dysdera* species have been object of several studies that tried to associate variation in cheliceral shape with their ecological performance (e.g., Řezáč & Pekár, 2007; Řezáč et al., 2021; Toft & Macías-Hernández, 2017, 2021). This genus has diversified extensively in the Canary Islands with numerous endemic species across the seven major islands. In addition to the different levels of oniscophagy, other remarkable adaptations have been recorded. Indeed, the Canary Islands harbor several obligate cave-dwelling

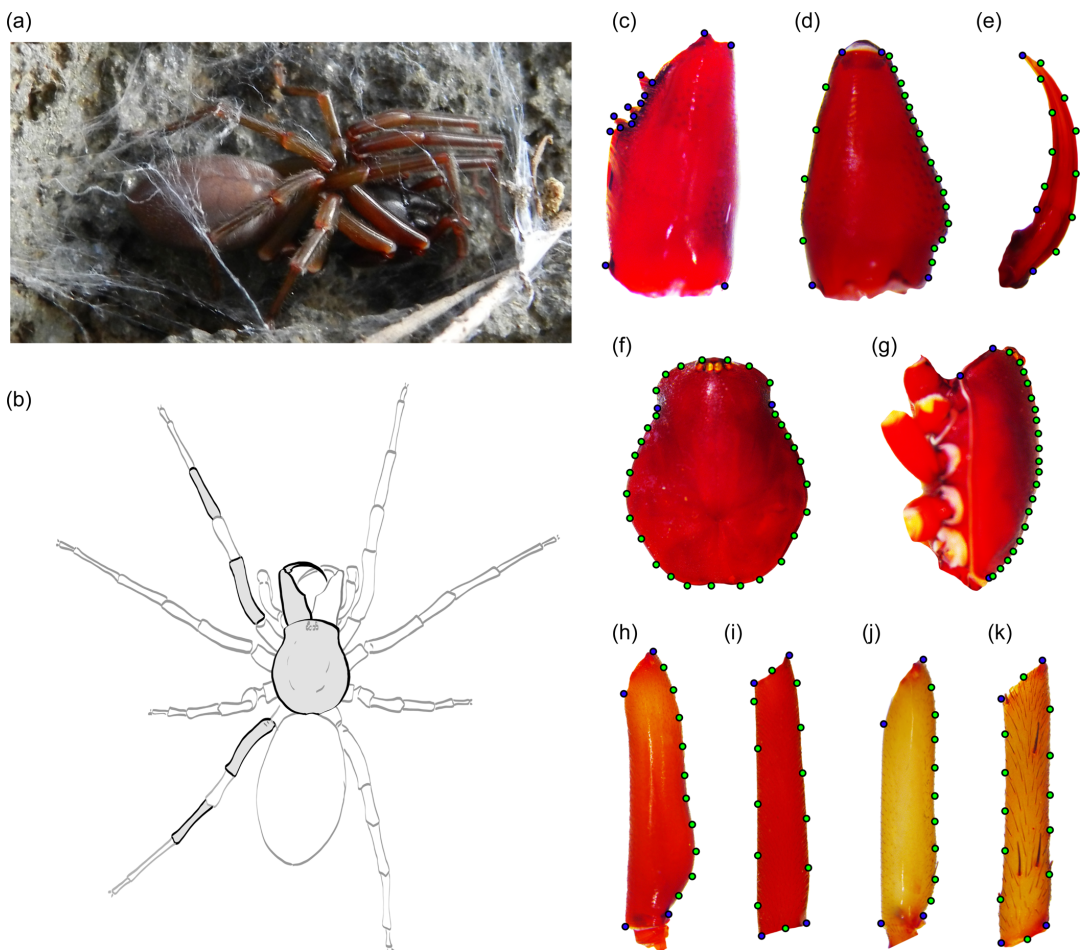


FIGURE 1 Analyzed landmark configurations of the *Dysdera* spider species and digitized landmarks. Blue dots represent fixed landmarks and green dots represent semilandmarks. (a) *Dysdera silvatica* in a typical silk retreat under the rock; (b) different body parts analyzed in the *Dysdera* species of this study (highlighted in gray); (c) ventral view of the chelicera (Q1); (d) lateral view of the chelicera (Q2); (e) ventral view of the fang (Q3); (f) dorsal view of the prosoma (C1); (g) lateral view of the prosoma (C2); (h) lateral view of the leg 1 femur (L11); (i) lateral view of the leg 1 tibia (L14); (j) lateral view of the leg 4 femur (L41); (k) lateral view of the leg 4 tibia (L44).

species that exhibit remarkable somatic modifications (Arnedo et al., 2007), while some epigeal spiders exhibit modifications in the shape of the carapace (Arnedo & Ribera, 1999). Due to these ecological particularities (trophic specialization and cave adaptation), the *Dysdera* species from the Canary Islands constitute a well-suited model for exemplifying high-resolution protocols for quantifying variation in different phenotypic traits and their integration in spiders and other arachnids.

The aims of the present study are to: (1) provide a practical guide for describing shape variation in spiders using GM to integrate information from different body parts; (2) to provide a first assessment on which of these structures may be more informative for exploring phenotypic variation related to particular ecological pressures; (3) to investigate whether morphological variables derived from the same or different body structures tend to covary strongly, or if, by contrast, they may respond independently to different selective pressures; and (4) to provide a practical guide on how information on different body structures may be combined to provide a global or partial view of morphological variation. To this end, we first establish a standardized protocol for obtaining data on the shape variation of different sides and perspectives of the chelicera, legs, and prosoma using two-dimensional LM-based GMs. Due to their function, and if integration mostly occurs across LM configurations of each structure, with different body structures being relatively free to vary independently, we expect that for some body parts (e.g., chelicera, legs) a clear differentiation will occur among species that are also markedly divergent in the dimensions of their niche relevant for that body part (e.g., trophic ecology and cave-dwelling, respectively; see also below). In this case, the distribution of species in global morphospace (i.e., considering all different LM configurations of all studied body structures) may exhibit high levels of "noise," due to the combination of different ecological influences driving different parts of the phenotype in different directions. If, by contrast, different body structures are highly integrated, variation across individuals and species in the global morphospace would rather be dominated by that ecological factor most strongly influencing the phenotype, and it would align quite closely to the partial morphospace that corresponds to the body structure with a direct functional link to such dominant ecological factor. Similarly, to the extent that certain species are morphologically differentiated across several of these ecological axes of interest, a combination of different body structures may better capture this joint differentiation. By contrast, species that are only differentiated in specific axes may become more blurred when considering several body structures together.

2 | MATERIALS AND METHODS

2.1 | Specimens used

All specimens examined were collected during field campaigns conducted by the authors and colleagues during the last 30 years

and are available at the Centre de Recursos de Biodiversitat Animal of the Universitat de Barcelona (CRBA) and the collection of the Departamento de Zoología de la Universidad de La Laguna, Tenerife, Canary Islands (DZUL). Individuals were captured by active searching under rocks, logs, and tree barks. The captured specimens were either preserved in 76% or 95% EtOH and, in some cases, stored at -20°C for subsequent molecular analyses at the Universitat de Barcelona. All specimens were collected following institutional and governmental regulations and the permits for all species captured were granted by the local authorities of each island or by the governing body of each natural reserve (Cabildos of El Hierro, La Gomera, La Palma and Tenerife, Garajonay and Caldera del Taburiente National Parks).

2.2 | Model system

We selected a suit of *Dysdera* species from the Canary Islands that exemplify different ecological habits or that exhibit markedly different phenotypic structures. Note that our objective when selecting these species was not to provide a full assessment of morphological variation in Canarian *Dysdera* and its relation to ecology. Such an endeavor would require a much more comprehensive sampling of species and would also need to take phylogenetic relationships into account and perform formal statistical assessments using phylogenetic comparative methods to assess the relative contribution of adaptation and shared evolutionary history in shaping the evolution of ecomorphological functional traits. However, such an objective lies beyond the scope of this study. Instead, here we aimed at including representatives with obviously different ecological and morphological properties, such as to optimize the technical and analytical protocols for exploring shape variation of different body parts in spiders. For this reason, we selected species representative of extreme morphologies and ecologies, with no consideration whatsoever of their phylogenetic position and relationships, while also including sampling of intraspecific variation (for *D. silvatica*, see below).

We considered three species that occur exclusively in cave environments: *Dysdera unguimmanis* Ribera, Fernandez and Blasco (1986), which exhibits extreme phenotypic cave adaptations (eye loss, depigmentation, and appendage elongation; Figure 2c); *D. ambulotenta* Ribera, Fernandez and Blasco (1986), eyeless and showing appendage elongation, but preserving dark reddish pigmentation in the carapace; and *D. ratonensis* Wunderlich (1992), which shows markedly reduced eye size but no other obvious somatic adaptation to the underground environments. Additionally, we considered species that represent ecomorphs with different trophic adaptations (Toft & Macías-Hernández, 2021). Specifically, we included two species related to a generalist diet with unmodified chelicera, *D. verneui* Simon (1883) (Figure 2a) and *D. silvatica* Schmidt (1981) (Toft & Macías-Hernández, 2021). Recent studies (Řezáč et al., 2021) have defined these two species as oniscophagous, a feeding preference, which could be more related to specialization.

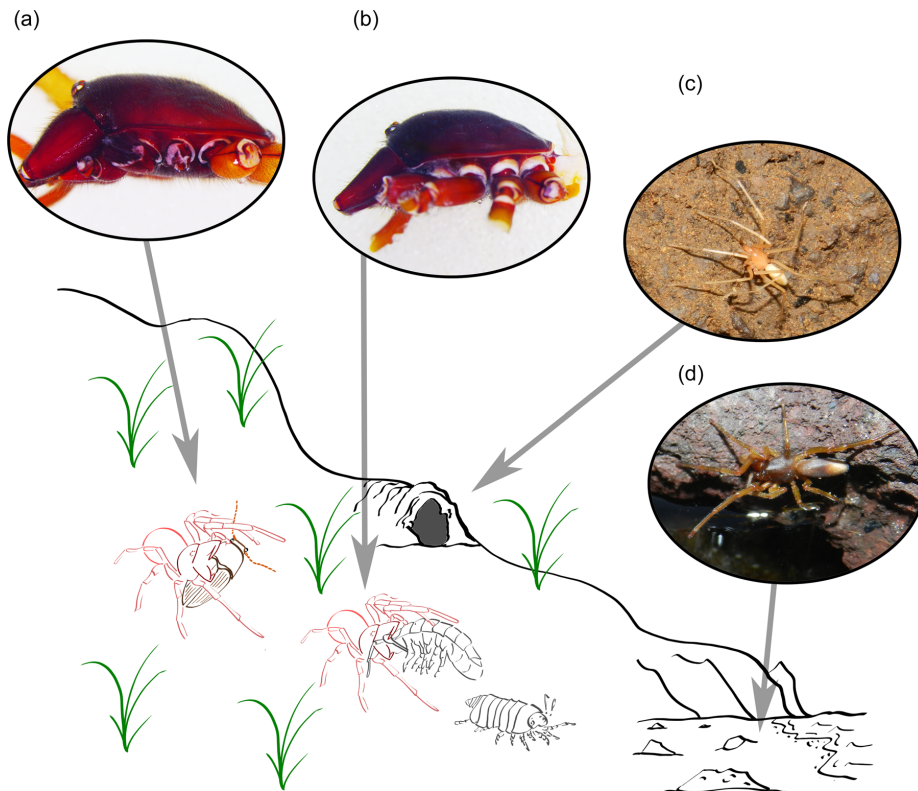


FIGURE 2 Different ecological groups selected for the study. (a) Generalist species; (b) *Onscophagous* species; (c) cave-dwelling species with troglomorphic adaptations; (d) species adapted to intertidal environments.

However, note that the experiments conducted by Řezáč et al. (2021) did not consider the level of trophic adaptation, but rather focused on the tactic used to prey on isopods or on whether these species avoid predated this arthropod. For this reason, we considered it more appropriate to treat them as species with a generalist diet. Additionally, to also include some population-level phenotypic variation in our data set, *D. silvatica* was represented by specimens coming from populations in three different islands (La Gomera, El Hierro, and La Palma). Specimens of each island were analyzed separately. We also included in our data set species that present deviant cheliceral morphologies: *D. insulana* Simon (1883), which carries chelicera with concave-shaped paturon (the basal segment, in lateral view; Figure 2b) and *D. rambrae* Arnedo, Oromí and Ribera (1997), which shows a short and dorsoventrally flattened chelicera fang, both specialized on isopod consumption with different hunting tactics (Řezáč et al., 2008). Similarly, *D. breviseta* Wunderlich (1992) and *D. macra* Simon (1883) carry chelicerae with slightly elongated paturon and have also been associated to a specialist diet, but in addition, these species present a marked bulge in the carapace (in lateral view, referred as step-shaped carapace;

Toft & Macías-Hernández, 2017). Finally, *D. curviseta* Wunderlich (1987) was chosen because it is ecologically quite distinct to the previous species, as it occurs in intertidal environments (Arnedo & Ribera, 1999; Macías-Hernández et al., 2010; Figure 2d). Previous studies have failed to show differences in the somatic morphology between males and females in some *Dysdera* species (Cooke, 1965); for the purpose of the present work, all specimens of the same species had been analyzed indistinctively regarding their gender.

2.3 | GM data acquisition

We took high-resolution photographs of different body parts of all specimens with a digital camera LEICA DFC 450 attached to a LEICA MZ16A stereoscopic microscope using Leica Application Software v.4.4 (Leica Microsystems Ltd.). We photographed nine different perspectives (Figure 1b); three of the chelicera (ventral and lateral side of the paturon, and the ventral side of the fang, Q1, Q2, Q3, respectively; Figure 1c–e), two of the prosoma (dorsal and lateral, C1 and C2; Figure 1f,g) and four perspectives of two different

segments of the first and fourth leg (the retrolateral femur and the retrolateral tibia, L11, L41, L14, and L44, respectively; Figure 1h–k). Whenever possible we used the left chelicera and leg of five females and five males of each species. When this was not possible due to broken parts or bad preservation, we assumed symmetry in the vertical plane and the right side was digitized and reflected. A total of 91 specimens comprising 10 different *Dysdera* species from the Canary Islands were photographed for this study. All photographs of each structure perspective were assembled using the software TpsUtil (Rohlf, 2015) and landmarks and semilandmarks were recorded (Figure 1c–k) using TpsDig2 (Rohlf, 2015). Each landmark configuration was then subjected to a Generalized Procrustes Analysis (Gower, 1975; Rohlf & Slice, 1990) using the function *gpa* to remove nonshape variation related to scaling, position, and rotation from landmark coordinates and obtain shape variables. During superimposition, the position of semilandmarks was optimized by minimizing bending energy. We used the statistical environment R (R Core Team, 2021) and the R package “geomorph” (Adams et al., 2021; Baken et al., 2021) to conduct all data analyses.

2.4 | Integration of different landmark configurations and structures

To examine the covariation of the different LM configurations of each anatomical structure, we grouped them into three subsets according to the morphological structure they represent (i.e., three LM configurations of the chelicera, the dorsal and lateral LM configurations of the carapace, and four LM configurations of distinct leg segments). A pairwise integration test was performed between all pairs of LM configurations belonging to the same subset and across all pairs of LM configurations of different anatomical aggrupation. We used the function *integration.test* to test for morphological integration between the different LM configurations by performing a partial least squares (PLS) analysis. Then, to test whether morphological integration was stronger between LM configurations of the same structure, as compared to across structures, we extracted effect sizes (z-scores) of the aforementioned pairwise PLS analyses as an estimate of the strength of integration of each pair (Adams & Collyer, 2016). Then, we used an analysis of variance (ANOVA) comparison based on 999 random permutations as applied through the function *lm.rpp* of the RRPP R-package (Collyer & Adams, 2018, 2021) to evaluate whether within-structure pairs of LM configurations exhibited higher levels of integration compared to between-structure pairs.

2.5 | Patterns of phenotypic variation across structures

With the function *combine.subsets*, we gathered all different LM configurations belonging to the same morphological structure in combined data sets. We also created a subset combination with all

different LM configurations of all structures together to explore the potential of analyzing all phenotypic information combined. For each subset, we performed a second generalized Procrustes analysis to scale all LM configurations to their unit-centroid size to correct their proportions (Collyer et al., 2020; Stepanova & Womack, 2020). With each of the resulting subset combinations, we conducted two different principal component analyses (PCAs) using the function *gm.prcomp*. The first analysis was performed using the mean coordinates of each species to obtain a clearer view of the relative position of the species' average shape in morphospace. The second analysis used all (previous) analyzed specimens of each species to allow us to inspect intraspecific disparity with each subset combination. We then plotted the first two principal components of the resulting PCAs for each subset to visualize differences in species and individual morphotype occupancy and disparity across LM configuration/structure combinations. To quantify the percentage of total shape variation represented by each separate subset, we first calculated pairwise Euclidean distances between observations (i.e., species means or individual shapes) in each of the considered morphospaces (i.e., global, chelicerae, carapace, limbs). We then performed a Mantel test of matrix association between each of the structures to the subset including all structures. Shape variation across PC axes was visualized through deformation grids produced using the function *plotRefToTarget*. To investigate whether major directions of shape variation as captured by PC axes were concordant at the species and individual levels, we calculated the angle observed between the species-PCA and the individual-PCA vectors and then used a permutation procedure to test whether this angle was significantly different than zero, which would imply a perfect alignment of vector directions (Martinez-Gil et al., 2022).

3 | RESULTS

3.1 | Integration of phenotypic landmark configurations and structures

Integration tests between combinations of different LM configurations and structures indicated significant integration across all pairs (all $p < .01$; Supporting Information: Table S1), which varied extensively in strength depending on the considered pair (Figure 3a). The ANOVA comparison suggested that pairs that encompassed different LM configurations of the same morphological structure exhibited overall higher levels of integration than those that included LM configurations belonging to different structures ($z = 2.4168$, $p = .003$; Figure 3b).

3.2 | Morphospace organization across data subsets

When examining the morphospaces of the different subset combinations derived by the PCA conducted at the species level,

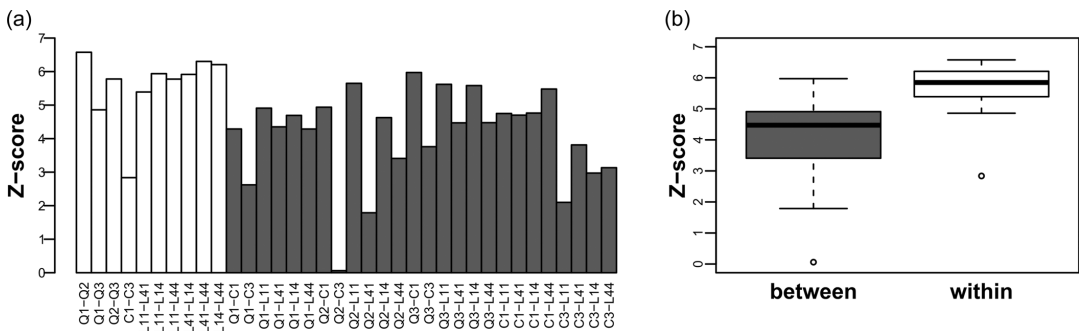


FIGURE 3 Pairwise integration values (a) and overall levels of integration (b) of landmark (LM) configurations related to the same morphological structure (white) versus LM configurations of different morphological structures (gray).

some common patterns could be observed. For instance, the sampled populations of the generalist species *D. silvatica* from different islands and the also generalist *D. verneai* were always close together. Similarly, the cave-adapted species *D. ratonensis* and the intertidal *D. curviseta* also occupy nearby locations in all examined morphospaces. When all phenotypic LM configurations were combined (Figure 4a), PC1 showed the greatest explained variability (78.2%) of all the different subsets. This is most likely due to the marked differentiation of *D. unguimanis*, the species with the most marked cave adaptations, since the remaining species all clustered together in this morphospace. Considering the subset combination of the different LM configurations of the chelicera (Figure 4b), PC1 explained 55.6% of the total variance, while PC2 explained 16.1%. The two extremes of PC1 were occupied by *D. insulana* and *D. ramblae*, both of which exhibit distinct chelicera adaptations in the archipelago, that is, concave chelicera and flat fang, respectively. With the subset combination of the two different carapace LM configurations (Figure 4c), PC1 explained 40.3% and PC2 25.6% of the variance, which translated into a scattered distribution of the analyzed species. Species with a generalist diet (*D. silvatica* and *D. verneai*) occupied the center of the morphospace, while the cavernicolous species were rather scattered across PC1. The two species with the step-shaped carapace (*D. breviseta* and *D. macra*) were differentiated from the rest across PC2. Interestingly, differentiation of other species not related to this carapace shape modification was also observed, as is the case of *D. ramblae*, a species with one of the most extreme modifications in the chelicera (flat fang). The proportion of variance explained by the two first principal components for the subset of all leg LM configurations (Figure 4d) was 55.2% and 25.6% (PC1 and PC2, respectively). Here, all surface species were grouped together; meanwhile, the cave dwellers (*D. ambulotenta*, *D. unguimanis*, and *D. ratonensis*) and the intertidal species (*D. curviseta*) were separated from the rest. Interestingly, the intertidal *D. curviseta* and the cave-dwelling *D. ratonensis* clustered close together, while the other cave dwellers, *D. ambulotenta* and

D. unguimanis, occupied opposite positions in the PC2 of this morphospace. The Mantel test revealed that the distance across species means of the combination of the different LM configurations of the legs were more strongly associated with that observed considering the global morphospace ($r = .68$, $p = .012$ for leg LM configurations combination; $r = .50$, $p = .004$ for the chelicera combination; $r = .48$, $p = .028$ for the carapace combination).

Morphospaces derived from individual-level PCAs (Figure 5), provided additional information on the intraspecific morphological variation as captured by different body structure combinations. Species' morphological properties appeared better defined when using all character subsets together, where individuals of each species were much more tightly packed, occupying a reduced area in the morphospace (Figure 5a). By contrast, when considering each character subset separately, a wider overlap between species was observed. In this case, each of the separate character subsets captured a visibly lower amount of the variation represented by the global combination of all subsets compared to the species-level analysis, although the leg LM configuration subset was again the one most highly correlated to the combination of all structures (Mantel test: for the chelicera, $r = .26$, $p = .001$; for the carapace, $r = .39$, $p = .001$; for the legs, $r = .45$, $p = .001$).

3.3 | Shape variation captured

Shape variation described by PC1 axes aligned between individual and species-level variation only for the limbs ($\theta = 8.85$, $p = 1$), but it expressed slightly different aspects when considering both hierarchical levels for the remaining LM configurations ($\theta = 10.13$, $p = .001$ for all different LM configurations combined; $\theta = 15.86$, $p = .001$ for cheliceral LM configurations; $\theta = 53.22$, $p = .029$ for carapace LM configurations). Focusing on species-level variation, however, deformation grids describing the shape variation observed across the first two principal components when considering all the different LM configurations combined (Figure 6)

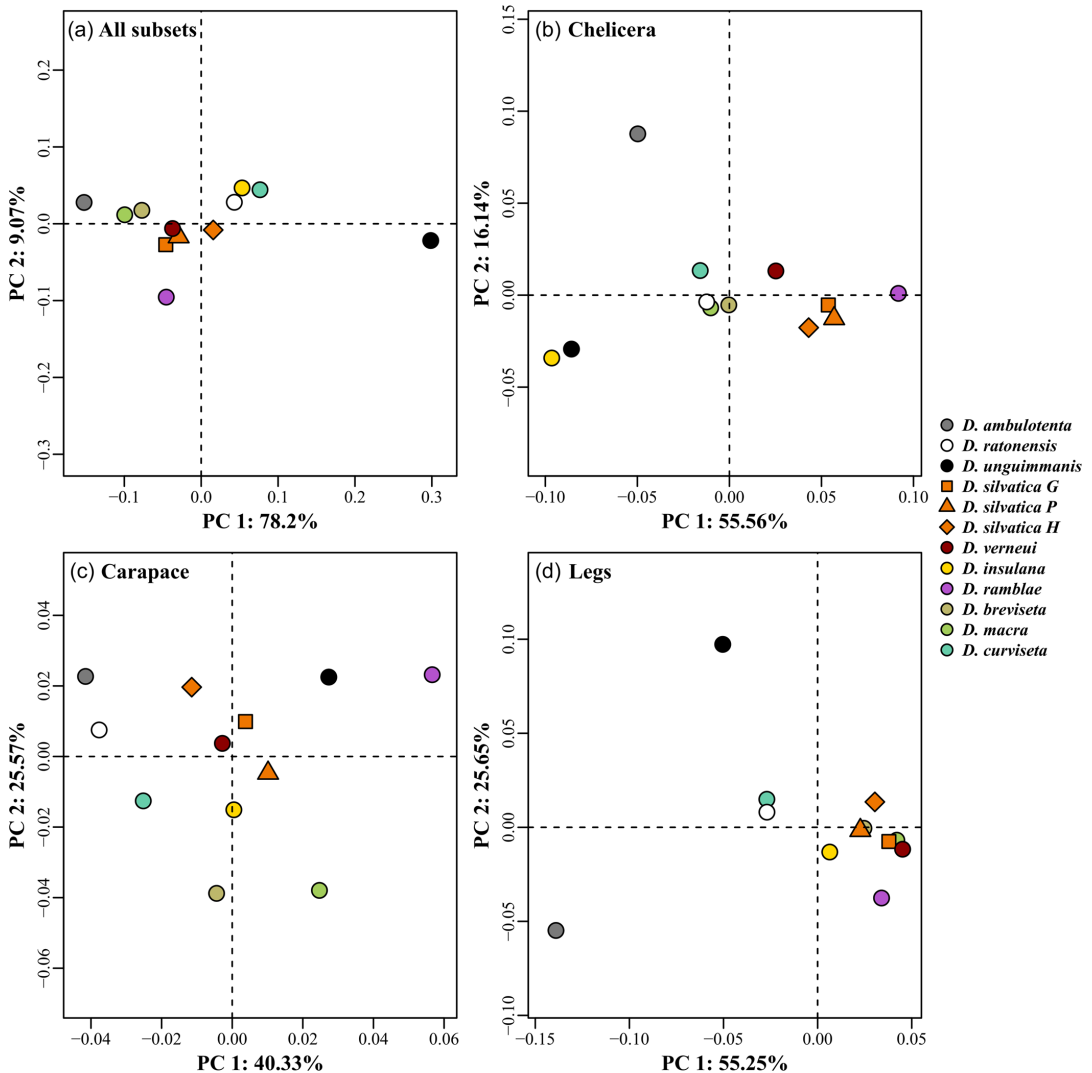


FIGURE 4 Phenotypic space of species means for the different subset combinations. (a) Subset of all landmark (LM) configurations combined. (b) Subset of all chelicera LM configurations (Q1, Q2, and Q3). (c) Subset of all prosoma LM configurations (C1 and C2). (d) Subset of all leg LM configurations (L11, L14, L41, and L44).

seemed to express fairly similar patterns of shape variation as those obtained by analyzing each structure separately, albeit with less intensity.

Focusing on the subset of the chelicera, major directions of shape variation were noticeable in the apical part of the ventral view, which got enlarged or retracted distally, increasing or decreasing the distance between the cheliceral teeth and the distal part of the groove, and in the central part of the fang, making this appendix shorter and wider or more elongated and thinner. Both modifications

were largely driven by the two species on the extremes of the PC1 of these LM configurations, *D. insulana* and *D. ramblae*, both specialist species with distinct cheliceral modifications—elongation of the chelicera and the fang, and a stouter chelicera and flattened fang, respectively. With the subset of the carapace, shape variation was circumscribed to the frontal part in the dorsal LM configuration, making it wider or narrower, and in the central part in the lateral LM configuration. However, shape variation across PC2 was markedly associated with the area of the carapace bulge characteristic of the

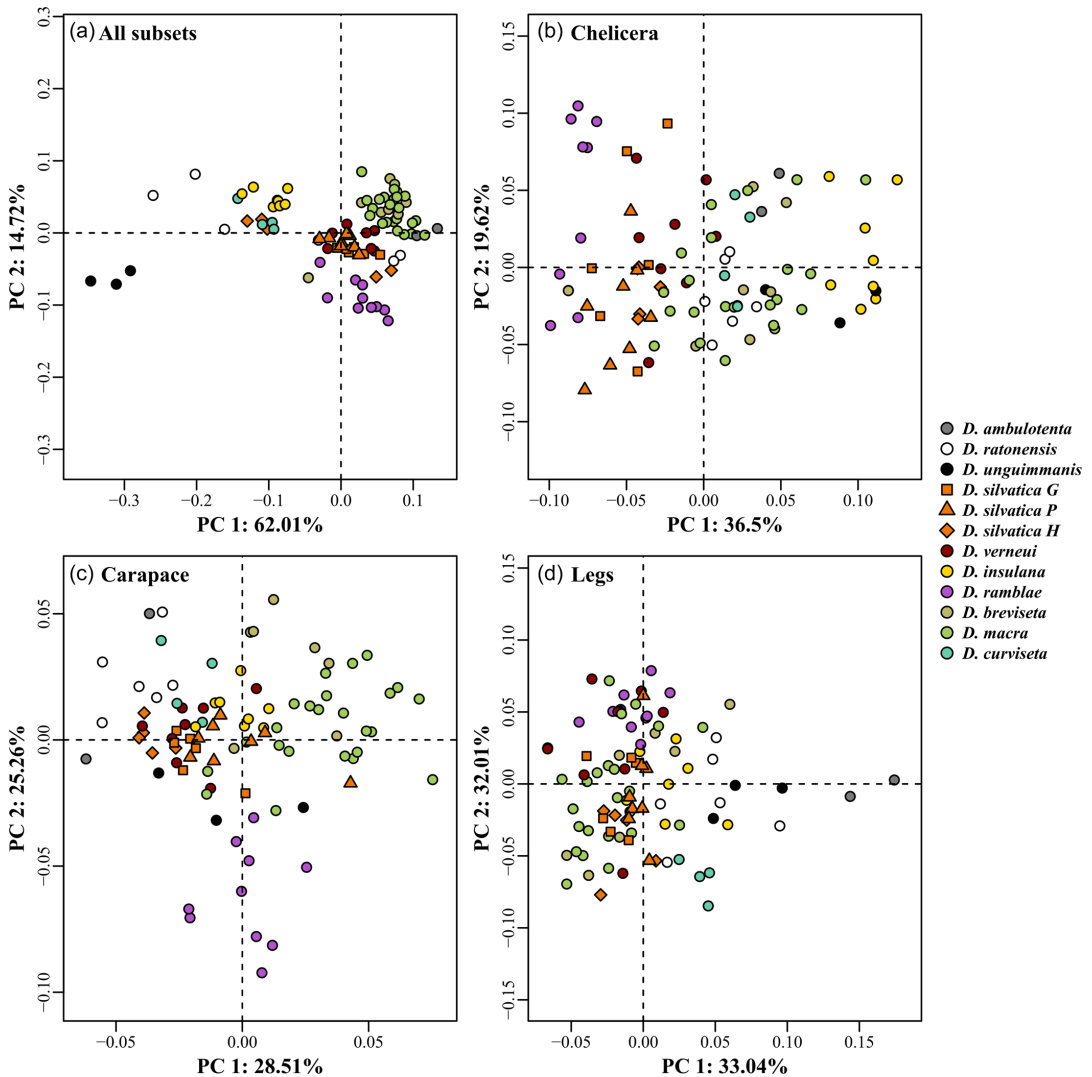


FIGURE 5 Phenotypic space of all specimens analyzed for the different subset combinations. (a) Subset of all landmark (LM) configurations combined. (b) Subset of all chelicera LM configurations (Q1, Q2, and Q3). (c) Subset of all prosoma LM configurations (C1 and C2). (d) Subset of all leg LM configurations (L11, L14, L41, and L44).

two step-shaped carapace species in the Canary Islands (*D. breviseta* and *D. macra*; Figure 6b). Finally, with the subset combination of the different leg LM configurations, the shape variation was visible across all the tibia, with an elongation or shortening of these different LM configurations, and in the basal and apical part of the femur. This elongation in the tibia was associated with the different species that are obligate cave dwellers, *D. unguimmanis* and *D. ambulotenta*. The modification in the femur also conferred to this LM configuration a more slender or stouter shape.

4 | DISCUSSION

Although the study of phenotypes and how morphological variation is related to ecological performance is a field with a long history (e.g., Arnold, 1983), deciding which character is related to which ecological pressure and which traits are then worth investigating is not straightforward in nonmodel organisms. In the present study, we have shown that different LM configurations of the same or closely related structures exhibit

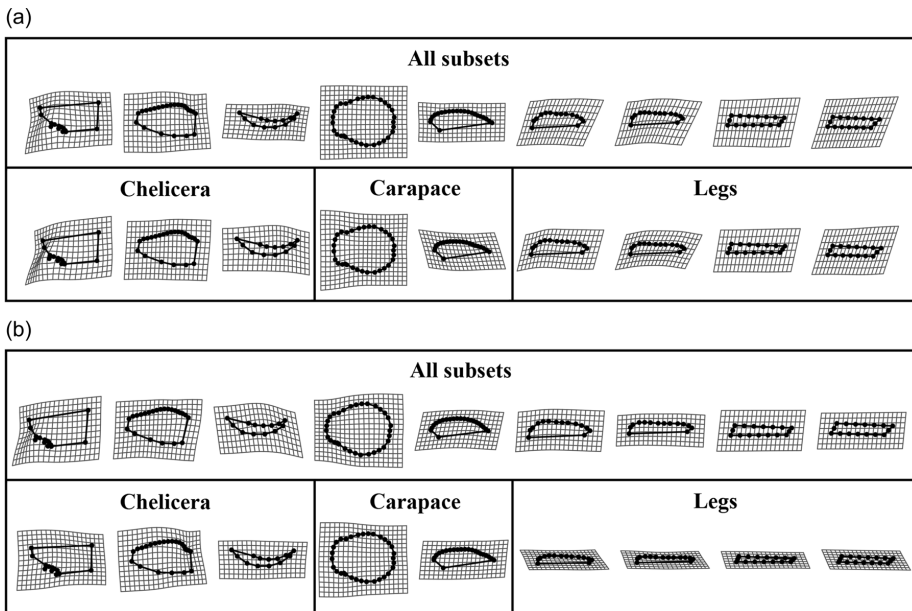


FIGURE 6 Deformation grids depicting shape differences between the minimum and maximum extremes of principal component (PC) axes for all the different LM configurations combined (top), and the subsets of the chelicera, carapace and legs (bottom) in PC1 (a) and PC2 (b).

higher levels of integration, allowing the study of 3D morphologies from the combination of 2D morphometric data acquisition, ensuring in this way the adequate analysis of these traits when technology or time availability are limiting factors. In general, examining each character set separately is more intuitive for linking morphological variation across species to potential underlying ecological pressures: this is the case, for instance, with the putative trophic meaning of the cheliceral morphospace; or with the phenotypic modifications of species adapted to subterranean environments, which are clearly differentiated across the first component of the leg morphospace. However, when all these characters are analyzed together, a greater cohesion of individual variation around species' means is achieved, providing higher resolution to describe the morphospace occupied by each species, without providing relevant information or species aggragations related to any apparent ecological performance. This is concordant with previous studies focusing on characterizing ecological guilds in spiders, based on multivariate analysis of linear morphological traits, where a high overlap of the occupied trait space between different guilds was observed (Wolff et al., 2022). Based on this exploration, we provide a first assessment of the organization of shape variation in the chelicera, legs and prosoma of spiders, and some guidelines on how to choose which structures to analyze based on the biological question at hand.

4.1 | Phenotypic integration of landmark configurations and characters

For the proper function of complex phenotypes, traits must work together in a coordinated manner (Murren, 2012). From a methodological perspective, delimiting which traits can covary, and therefore function as morphological modules, in nonmodel organisms cannot be taken for granted. Here, we explore covariation patterns across different LM configurations representing Canarian *Dysdera* spider's body parts (i.e., the chelicera, carapace and limbs) to provide a simplified protocol that facilitates the choice of trait sets for future studies. Our analyses indicate that, in the empirical system explored here, the different phenotypic LM configurations analyzed exhibit significantly higher values of integration when they represent the same morphological structure. This confirms that the different data, acquired from a single body part, function well as a two-dimensional approximation of three-dimensional structures, thus providing a means of reducing the time and resources required for capturing and analyzing their shape (e.g., data acquired with computed tomography scans). Although some degree of integration is observed in all structures, as expected, our results highlight that different body parts work as more highly integrated modules that may vary independently to a certain extent, thus resolving the constraints imposed by a complete integration of different structures (Goswami et al., 2014). This is mirrored in the different patterns of distribution of species

across the morphospaces corresponding to each structure, where species with different ecological preferences seem to group depending on the character analyzed. In fact, the potential ecological significance of shape variation, which emerges across subset combinations (see below), together with the higher integration values among LM configurations related to the same body part (Figure 3), suggest that integration is constraining the variation of structures in certain directions (Goswami et al., 2014), most likely coordinating the evolution of functional units (Klingenberg, 2010).

4.2 | Trait integration, distribution of species across different morphospaces, and the meaning of shape variation

Differentiation within and across species in the morphospaces, obtained through PCA of different structural subsets (i.e., chelicera, legs, abdomen, total), provides preliminary hints on the potential ecological factors related to patterns of morphological variation. Despite the merely exploratory nature of this study, we have purposefully included species that exemplify extreme ecologies and morphologies to investigate how different morphological subsets may capture the relevant shape variation. Our results match intuitive expectations, based on the functions of different body parts, and add to our knowledge of how body shape variation in spiders may be best described using GMs.

Species distribution across the chelicera morphospace, comprising all different LM configurations of this structure, appears to reflect feeding habits. Species with different levels of oniscophagy are aggregated through the morphospace that represents variation in the chelicera shape (Toft & Macías-Hernández, 2021). This is not surprising as these species were precisely selected because of the high variability in their chelicera morphology that was previously suggested to be related to isopod predation (Řezáč & Pekár, 2007; Řezáč et al., 2021). Similarly, surface species are all phenotypically similar across the leg morphospace (Figures 4c and 5c), while cave-dwelling species are quite distinct phenotypically from all other *Dysdera*, a fact that drives variation across the leg-PC1. The distinctiveness of cave species in this morphospace also fits empirical observations, as one of the main adaptations to subterranean environments is the elongation of the legs (Christiansen, 1992; Deeleman-Reinhold & Deeleman, 1980). However, it is also interesting to note that the cave-dwelling species differ morphologically across PC2 (e.g., *D. ambulotenta* and *D. unguimanis*). These differences may hint at different levels or types of troglomorphic modifications, which could be either due to differences in the time of cave colonization or to the existence of distinct microhabitats within the subterranean environment (Arnedo et al., 2007; Mammola et al., 2020). Interestingly, some intermediate forms between species with marked troglomorphic adaptations and epigeal species can also be observed (e.g., *D. ratonensis* and *D. curviseta*). In this regard, it is worth noting that although one of these species (*D. ratonensis*) has been exclusively collected in caves, it exhibits little evidence of

troglomorphy, except for a reduction of eye size, which varies according to the locality—being slighter in the north and more pronounced in southern caves, suggesting this species has only recently colonized the subterranean environment (Arnedo & Ribera, 1996). A more detailed study specifically quantifying the ecological habits of cave-dwelling species and the extent to which they may have affected their morphological properties and taking phylogenetic relationships into account to test for the differentiation between troglomorphic and epigeal species would definitely add to our knowledge of how the structural habitat used by spiders may have shaped adaptive evolution of the legs in these organisms.

The stronger association observed between the leg shape and the global morphospace, both when examining species means and individual-level variation, could be explained by the marked distinctiveness of the highly adapted cave-dweller species, not only with the surface ones but also between them. Additionally, the leg subset combination is the only one for which we did not find significant differences in the direction of PC1 between individual and species-level patterns of shape variation. This is most likely due to the relative simplicity of these different LM configurations compared to the higher complexity in the chelicera or the carapace: in more complex structures across different data sets (e.g., species means vs. individuals), shape variation caused by different ecological pressures may be concentrated in specific parts of the structure instead of effecting the entire shape of it, as is the case for more simplified body parts as the legs.

In some spider species, where extreme trophic adaptation has translated into a dramatic modification of their chelicera, the musculature related to this structure runs further up to attach to apodemes on the posterior part of the prosoma (see Wood & Parkinson, 2019). Although this is not the general pattern in spiders (e.g., Lin et al., 2021), it would be reasonable to predict that shape variation in the chelicera would also translate into coordinated differences in the carapace. This prediction is partially confirmed by high values of integration of some of the LM configurations of the chelicera and carapace (Figure 3). However, our results show that species that are phenotypically similar across the cheliceral morphospace are not necessarily similar in the carapace morphospace. Interestingly, some of the most extreme morphologies observed in this morphospace corresponded to the step-shaped carapace species (*D. breviseta* and *D. macra*; Arnedo & Ribera, 1999), on the one hand, and to the flat-fang species on the other hand (*D. ramblae*; Figure 4d). The species with this flattened fang is mainly differentiated across PC2, which captures shape variation related to the relative width of the frontal part of the prosoma and the absence or presence of the step-shaped carapace in the lateral view (Figure 6b). Given the particular shape of this extreme modification in the chelicera, the more narrowed frontal part and the absence of a step-shaped carapace observed in this species can be interpreted as a result of a lack of need to accommodate large cheliceral musculature, suggesting that visible coordinated shape variation between the chelicera and the carapace would only be observed in extreme cases. However, a more detailed study of the link between the chelicera musculature

attachments and the carapace shape in the *Dysdera* species will be necessary to confirm or reject such a biomechanical explanation of the integration between both body structures.

The distribution of species across the morphospace corresponding to the subset combination of all the different LM configurations combined does not seem to be associated with any obvious ecological or biomechanical explanation. However, the lower intra-specific dispersion observed and the decrease in the overlap between species indicate that the phenotypic identity of each species is better defined when combining information from all LM configurations across different body structures. This observation is in line with the fact that the use of a greater number of phenotypic variables adds resolution to the description of morphological variation (Collyer et al., 2015). In this sense, then, the phenotypic space that each species occupies can be more properly delimited using whole-body information, rather than focusing on specific traits which, despite capturing the ecological and morphological particularities of each species, they are not as efficient for characterizing interspecific morphological differences.

4.3 | What body structures to study?

Adaptive evolution in response to habitat variation is a major driver of phenotypic variation in arachnids, including spiders (Gonçalves-Souza et al., 2014) and scorpions (Coelho et al., 2021). Our exploratory analysis of species with extreme ecological habits within Canarian *Dysdera* suggests that variation across different dimensions of the ecological niche may be reflected in variation patterns of distinct structures of the spider phenotype. In *Dysdera* species, it seems that the phenotypic variation of the chelicera is associated with trophic adaptations related to the predation on isopods (Řezáč et al., 2021; Toft & Macías-Hernández, 2021) and that adaptation to underground environments is markedly reflected in their leg morphology (Arnedo et al., 2007). However, the evolutionary pressures affecting the shape of different body parts in other spider groups could vary drastically, influencing biological inferences. For instance, some *Tetragnatha* Latreille (1804) spiders exhibit marked sexual dimorphism, where the male phenotype is not related to feeding specialization (Baba et al., 2018; Lesar & Unzicker, 1978; Makoto, 1987). Similarly, in some species of jumping spiders, sexual selection is involved in determining the morphology of the legs in males, as these are involved in courtship behavior (see Lai et al., 2021). Therefore, a good biological knowledge of the species at hand is required before selecting the views and structures to analyze and test the hypotheses to link them to any evolutionary adaptation. Nevertheless, we have shown that variation in trophic habits, in a group without apparent sexual selection pressures in the external phenotype, as is the case of the *Dysdera* spider species (Cooke, 1965), is readily captured by considering different LM configurations of the chelicera. In the same way, some habitat-related questions can be better answered with the analysis of the limbs. Finally, the global phenotypic space occupied by each species would be better

delimited by putting together different, and apparently not related structures to hoard the morphological differences that exist across species. For example, one may be interested in differentiating species regardless of the ecological meaning of phenotypic structures. In such a scenario, analyses of morphological variation become more efficient if considering all the characters that make these species different and examining how they differ across a global morphospace.

5 | CONCLUSIONS

Taken together, the multipart analyses conducted here indicate that a proper definition of the morphospace occupied by different species is optimized by combining information from different unrelated structures. However, our analyses also suggest that different ecological evolutionary pressures influence different parts of the phenotype of the *Dysdera* species from the Canary Islands in different directions. Although a formal, comprehensive analysis of ecomorphological evolution in this model system is still pending, different morphospaces seem associated with distinct ecological features, where species form different groupings and aggregations depending on the body structure analyzed and the ecological function for which it is relevant. We have shown that although all morphological LM configurations show some degree of integration, those related to the same morphological structure (chelicera, prosoma, and legs) exhibit significantly higher integration values, and are thus more strongly interdependent functionally and evolutionarily. The exploration undertaken here provides a guidance for future work focused on the study of morphological structures that seek to link different parts of a phenotype to the potential underlying ecological, biomechanical, social, or other pressures that have shaped them.

AUTHOR CONTRIBUTIONS

Adrià Bellvert: Conceptualization (equal); data curation (lead); formal analysis (equal); methodology (supporting); writing—original draft (lead). **Marcos Roca-Cusachs:** Data curation (supporting); writing—review and editing (supporting). **Vanina Tonzo:** Data curation (supporting); writing—review and editing (supporting). **Miquel A. Arnedo:** Project administration (lead); resources (lead); supervision (equal); writing—review and editing (equal). **Antigoni Kaliontzopoulou:** Conceptualization (lead); formal analysis (equal); methodology (lead); supervision (equal); writing—review and editing (equal).

ACKNOWLEDGMENTS

We thank the Cabildos of El Hierro, La Gomera, La Palma, and Tenerife and the Garajonay and Caldera del Taburiente National Parks for the collection permits. We also acknowledge the two anonymous reviewers who helped in improving the manuscript. This study was supported by project grants CGL2012-36863 and CGL2016-80651-P from the Spanish Ministry of Economy and Competitiveness and 2017SGR83 from the Catalan Government (M. A. A.). A. B. was funded by an individual PhD Grant BES-2017-080538 from the Ministerio de Economía, Industria y Competitividad

of the Spanish government. A. K. is supported by a Ramón y Cajal research grant cofunded by the Spanish State Research Agency and the European Social Fund (RYC2019-026688-I/AEI/10.13039/501100011033). M. R.-C. received a Systematics research fund (2015), granted by the Linnean Society and the Systematics association during his Bsc, which helped in supporting part of this study.

CONFLICT OF INTEREST

The authors declare no conflict of interest.

DATA AVAILABILITY STATEMENT

The data that support the findings of this study are openly available on Github at https://github.com/EvoDysdera/Vitruvian_Dysdera.

ORCID

Adrià Bellvert  <http://orcid.org/0000-0003-1592-3978>

REFERENCES

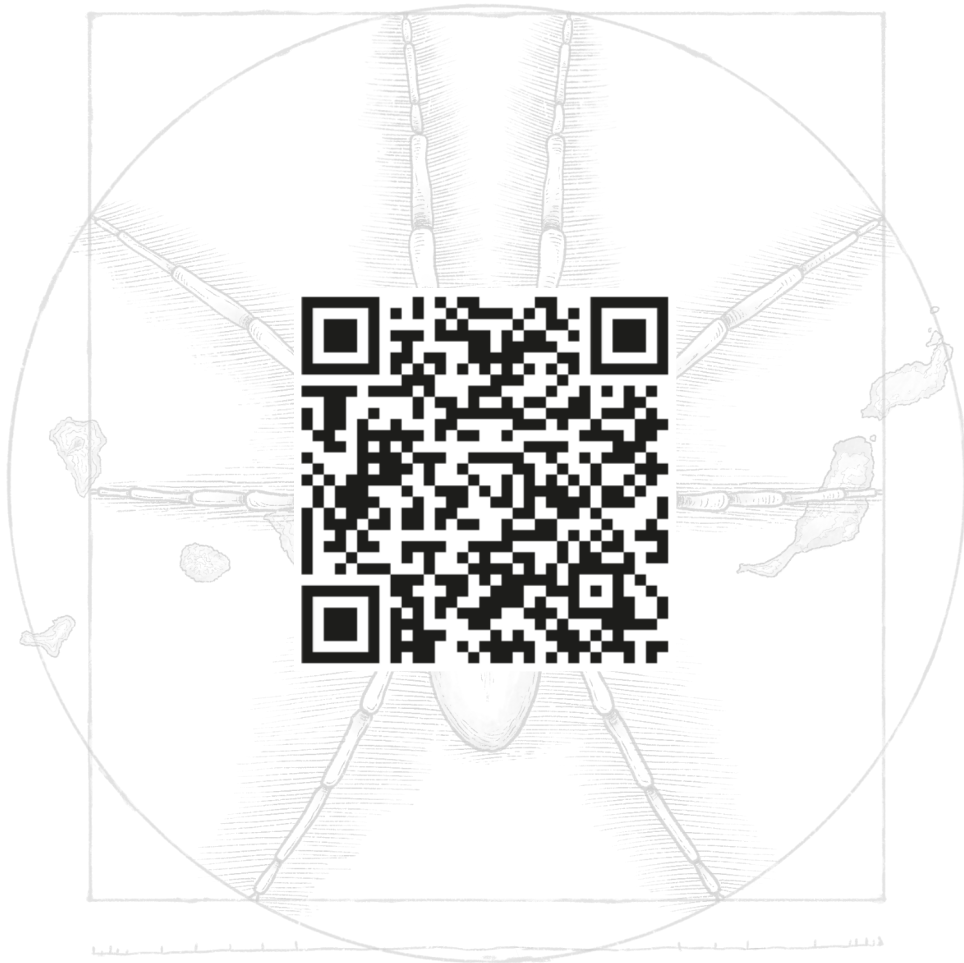
- Adams, D. C. (2016). Evaluating modularity in morphometric data: Challenges with the RV coefficient and a new test measure. *Methods in Ecology and Evolution*, 7, 565–572.
- Adams, D. C., & Collyer, M. L. (2016). On the comparison of the strength of morphological integration across morphometric datasets. *Evolution*, 70, 2623–2631.
- Adams, D. C., Collyer, M. L., Kaliontzopoulou, A., & Baken, E. K. (2021). *Geomorph: Software for geometric morphometric analyses*. R package version 4.0.2. <https://cran-project.org/package=geomorph>
- Adams, D. C., Rohlf, F. J., & Slice, D. E. (2004). Geometric morphometrics: Ten years of progress following the 'revolution'. *Italian Journal of Zoology*, 71, 5–16.
- Andersson, L. (2009). Studying phenotypic evolution in domestic animals: A walk in the footsteps of Charles Darwin. *Cold Spring Harbor Symposia on Quantitative Biology*, 74, 319–325.
- Arnedo, M. A., Oromí, P., Múrria, C., Macías-Hernández, N., & Ribera, C. (2007). The dark side of an island radiation: Systematics and evolution of troglomorphic spiders of the genus *Dysdera* Latreille (Araneae: Dysderidae) in the Canary Islands. *Invertebrate Systematics*, 21, 623–660.
- Arnedo, M. A., & Ribera, C. (1996). *Dysdera ratonensis* Wunderlich, 1991 (Arachnida, Araneae) a troglomorphic species from La Palma, Canary Islands: Description of the male and redescription of the female. *Revue Arachnologique* (Vol. 11, pp. 109–122).
- Arnedo, M. A., & Ribera, C. (1999). Radiation in the genus *Dysdera* (Araneae, Dysderidae) in the Canary Islands: The island of Tenerife. *Journal of Arachnology* 27, 604–662.
- Arnold, S. J. (1983). *Morphology, performance and fitness* (Vol. 23, pp. 347–361). Oxford University Press.
- Baba, Y. G., Tanikawa, A., Takada, M. B., & Futami, K. (2018). Dead or alive? Sexual conflict and lethal copulatory interactions in long-jawed Tetragnatha spiders. *Behavioral Ecology*, 29, 1278–1285.
- Baken, E. K., Collyer, M. L., Kaliontzopoulou, A., & Adams, D. C. (2021). *geomorph v4.0* and *gmShiny*: Enhanced analytics and a new graphical interface for a comprehensive morphometric experience. *Methods in Ecology and Evolution*, 12, 2355–2363.
- Blows, M. W. (2007). A tale of two matrices: Multivariate approaches in evolutionary biology. *Journal of Evolutionary Biology*, 20, 1–8.
- Canals, M., Veloso, C., & Solís, R. (2015). Adaptation of the spiders to the environment: The case of some Chilean species. *Frontiers in Physiology*, 6, 1–9.
- Carscadden, K. A., Cadotte, M. W., & Gilbert, B. (2017). Trait dimensionality and population choice alter estimates of phenotypic dissimilarity. *Ecology and Evolution*, 7, 2273–2285.
- Christiansen, K. (1992). Biological processes in space and time: Cave life in the light of modern evolutionary theory. In A. I. Camacho (Ed.), *The natural history of biospeleology* (pp. 453–480).
- Coelho, P., Kaliontzopoulou, A., Sousa, P., Stockmann, M., & van der Meijden, A. (2022). Reevaluating scorpion Ecomorphs using a naïve approach. *BMC Ecol Evol*, 22, 17.
- Collyer, M. L., & Adams, D. C. (2018). RRPP: An R package for fitting linear models to high-dimensional data using residual randomization. *Methods in Ecology and Evolution*, 9, 1772–1779.
- Collyer, M. L., & Adams, D. C. (2021). *RRPP: Linear model evaluation with randomized residuals in a permutation procedure*. <https://CRAN.R-project.org/package=RRPP>
- Collyer, M. L., Davis, M. A., & Adams, D. C. (2020). Making heads or tails of combined landmark configurations in geometric morphometric data. *Evolutionary Biology*, 47, 193–205.
- Collyer, M. L., Sekora, D. J., & Adams, D. C. (2015). A method for analysis of phenotypic change for phenotypes described by high-dimensional data. *Heredity*, 115, 357–365.
- Cooke, J. A. L. (1965). Systematic aspects of the external morphology of *Dysdera crocata* and *Dysdera erythrina* (Araneae, Dysderidae). *Acta Zoologica*, 46, 41–65.
- Crews, S. C. (2009). Assessment of rampant genitalic variation in the spider genus *Homalonychus* (Araneae, Homalonychidae). *Invertebrate Biology*, 128, 107–125.
- Darwin, C. R. (1859). *On the origin of species by means of natural selection, or the preservation of favoured races in the struggle for life*. John Murray Publishers.
- Deeleman-Reinhold, C. L., & Deeleman, P. R. (1980). Remarks on troglitism in spiders. In H. Egermann (Ed.), *Proceedings of the Eighth International Congress of Arachnology* (pp. 433–438).
- Eklöf, A., Jacob, U., Kopp, J., Bosch, J., Castro-Urgal, R., Chacoff, N. P., Dalsgaard, B., de Sassi, C., Galetti, M., Guimarães, P. R., Lomáscolo, S. B., Martín González, A. M., Pizo, M. A., Rader, R., Rodrigo, A., Tylaniakis, J. M., Vázquez, D. P., & Allesina, S. (2013). The dimensionality of ecological networks. *Ecology Letters*, 16, 577–583.
- Fernández-Montraveta, C., & Marugán-Lobón, J. (2017). Geometric morphometrics reveals sex-differential shape allometry in a spider. *PeerJ*, 5, e3617.
- Givnish, T. J. (1987). Comparative studies of leaf form: Assessing the relative roles of selective pressures and phylogenetic constraints. *New Phytologist*, 106, 131–160.
- Gonçalves-Souza, T., Diniz-Filho, J. A. F., & Romero, G. Q. (2014). Disentangling the phylogenetic and ecological components of spider phenotypic variation. *PLoS ONE*, 9, e89314. <https://doi.org/10.1371/journal.pone.0089314>
- Goswami, A., Smaers, J. B., Soligo, C., & Polly, P. D. (2014). The macroevolutionary consequences of phenotypic integration: From development to deep time. *Philosophical Transactions of the Royal Society B: Biological Sciences*, 369, 20130254. <https://doi.org/10.1098/rstb.2013.0254>
- Gower, J. C. (1975). Generalized procrustes analysis. *Psychometrika*, 40, 33–51.
- Guillaume, T. (2018). *dispRity*: A modular R package for measuring disparity. *Methods in Ecology and Evolution*, 9, 1755–1763.
- Guillaume, T., Cooper, N., Brusatte, S. L., Davis, K. E., Jackson, A. L., Gerber, S., & Donoghue, P. C. J. (2020). Disparities in the analysis of morphological disparity: Analysis of morphological disparity. *Biology Letters*, 16, 20200199. <https://doi.org/10.1098/rsbl.2020.0199rsbl20200199>
- Hutchinson, G. E. (1957). Concluding remarks. *Cold Spring Harbor Symposia on Quantitative Biology*, 22, 415–427.

- Kallal, R. J., Moore, A. J., & Hormiga, G. (2019). The shape of weaver: Investigating shape disparity in Orb-weaving spiders (Araneae, Araneidae) using geometric morphometrics. *Evolutionary Biology*, 46, 317–331.
- Klingenberg, C. P. (2008). Morphological integration and developmental modularity. *Annual Review of Ecology, Evolution, and Systematics*, 39, 115–132.
- Klingenberg, C. P. (2009). Morphometric integration and modularity in configurations of landmarks: Tools for evaluating a priori hypotheses, 421, 405–421.
- Klingenberg, C. P. (2010). Evolution and development of shape: Integrating quantitative approaches. *Nature Reviews Genetics*, 11, 623–635.
- Lai, J., Maddison, W. P., Ma, H., & Zhang, J. (2021). Intra-specific variation of non-genital and genital traits in two euophryine jumping spider species. *Journal of Zoology*, 313, 263–275.
- Lande, R., & Arnold, S. J. (1983). The measurement of selection on correlated characters. *Evolution*, 37, 1210–1226.
- Lesar, C. D., & Unzicker, J. D. (1978). Life history, habits, and prey preferences of *Tetragnatha laboriosa* (Araneae: Tetragnathidae). *Environmental Entomology*, 7, 879–884.
- Lin, S. W., Lopardo, L., & Uhl, G. (2021). Diversification through gustatory courtship: An X-ray micro-computed tomography study on dwarf spiders. *Frontiers in Zoology*, 18, 51.
- Lowe, E. C., Wolff, J. O., Aceves-aparicio, A., Birkhofer, K., Branco, V. V., Cardoso, P., & Mac, N. (2020). Towards establishment of a centralized spider traits database. *Journal of Arachnology*, 48, 103–109.
- Macías-Hernández, N., Oromí, P., & Arnedo, M. A. (2008). Patterns of diversification on old volcanic islands as revealed by the woodlouse-hunter spider genus *Dysdera* (Araneae, Dysderidae) in the eastern Canary Islands. *Biological Journal of the Linnean Society*, 94(3), 589–615.
- Macías-Hernández, N., Oromí, P., & Arnedo, M. A. (2010). Integrative taxonomy uncovers hidden species diversity in woodlouse hunter spiders (Araneae, Dysderidae) endemic to the Macaronesian archipelagos. *Systematics and Biodiversity*, 8, 531–553.
- Macías-Hernández, N., Ramos, C., Domènech, M., Febles, S., Santos, I., Arnedo, M., Borges, P., Emerson, B., & Cardoso, P. (2020). A database of functional traits for spiders from native forests of the Iberian Peninsula and Macaronesia. *Biodiversity Data Journal*, 8, e49159.
- Makoto, Y. (1987). Predatory behavior (Araneae: Of Tetragnatha Tetragnathidae). *Acta Alacnologica*, 35, 57–75.
- Mammola, S., Arnedo, M. A., Fišer, C., Cardoso, P., John Dejanaz, A., & Isaia, M. (2020). Environmental filtering and convergent evolution determine the ecological specialisation of subterranean spiders. *Functional Ecology*, 34(5), 1064–1077.
- Martínez-Gil, H., Martínez-Freiria, F., Perera, A., Enriquez-Urzelai, U., Martínez-Solano, Í., Velo-Antón, G., & Kaliontzopoulou, A. (2022). Morphological diversification of Mediterranean anurans: The roles of evolutionary history and climate. *Biological Journal of the Linnean Society*, 135, 462–477.
- McGill, B., Enquist, B., Weiher, E., & Westoby, M. (2006). Rebuilding community ecology from functional traits. *Trends in Ecology & Evolution*, 21, 178–185.
- Murren, C. J. (2012). The integrated phenotype. *Integrative and Comparative Biology*, 52(1), 64–76.
- Nock, C. A., Vogt, R. J., & Beisner, B. E. (2016). Functional traits. In eLS (pp. 1–8). John Wiley & Sons, Ltd.
- Olson, E. C., & Miller, R. L. (1958). *Morphological integration*. University of Chicago Press.
- Phillips, P. C., & Arnold, S. J. (1989). Visualizing multivariate selection. *Evolution*, 43, 1209–1222.
- R Core Team. (2021). *R: A language and environment for statistical computing*. <https://www.r-project.org/>
- Rohlf, F. J. (2015). The tps series of software. *Hystrix*, 26, 1–4.
- Rohlf, F. J., & Slice, D. (1990). Extensions of the procrustes method for the optimal superimposition of landmarks. *Systematic Zoology*, 39, 40–59.
- Řezáč, M., & Pekár, S. (2007). Evidence for woodlice-specialization in *Dysdera* spiders: Behavioural versus developmental approaches. *Physiological Entomology*, 32, 367–371.
- Řezáč, M., Pekár, S., Arnedo, M., Macías-Hernández, N., & Řezáčová, V. (2021). Evolutionary insights into the eco-phenotypic diversification of *Dysdera* spiders in the Canary Islands. *Organisms Diversity & Evolution*, 21, 79–92.
- Řezáč, M., Pekár, S., & Lubin, Y. (2008). How oniscophagous spiders overcome woodlouse armour. *Journal of Zoology*, 275, 64–71.
- Schluter, D., & Nychka, D. (1994). Exploring fitness surfaces. *The American Naturalist*, 143, 597–616.
- Stepanova, N., & Womack, M. C. (2020). Anuran limbs reflect microhabitat and distal, later-developing bones are more evolutionarily labile. *Evolution*, 74, 2005–2019.
- Toft, S., & Macías-Hernández, N. (2017). Metabolic adaptations for isopod specialization in three species of *Dysdera* spiders from the Canary Islands. *Physiological Entomology*, 42, 191–198.
- Toft, S., & Macías-Hernández, N. (2021). Prey acceptance and metabolic specialisations in some Canarian *Dysdera* spiders. *Journal of Insect Physiology*, 131, 104227.
- Wilson, J. D., Zapata, L. V., Barone, M. L., Cotoras, D. D., Poy, D., & Ramírez, M. J. (2021). Geometric morphometrics reveal sister species in sympatry and a cline in genital morphology in a ghost spider genus. *Zoologica Scripta*, 50, 485–499.
- Wolff, J. O., Wierucka, K., Paterno, G. B., Coddington, J. A., Hormiga, G., Kelly, M. B. J., Herberstein, M. E., & Ramírez, M. J. (2022). Stabilized morphological evolution of spiders despite mosaic changes in foraging ecology. *Systematic Biology*.
- Wood, H. M., & Parkinson, D. Y. (2019). Comparative morphology of cheliceral muscles using high-resolution X-ray microcomputed-tomography in palpimanoid spiders (Araneae, Palpimanoidea). *Journal of Morphology*, 280, 232–243.
- World Spider Catalog. (2022). *World spider catalog*. Version 23.0. Natural History Museum Bern. <https://doi.org/10.24436/2>

SUPPORTING INFORMATION

Additional supporting information can be found online in the Supporting Information section at the end of this article.

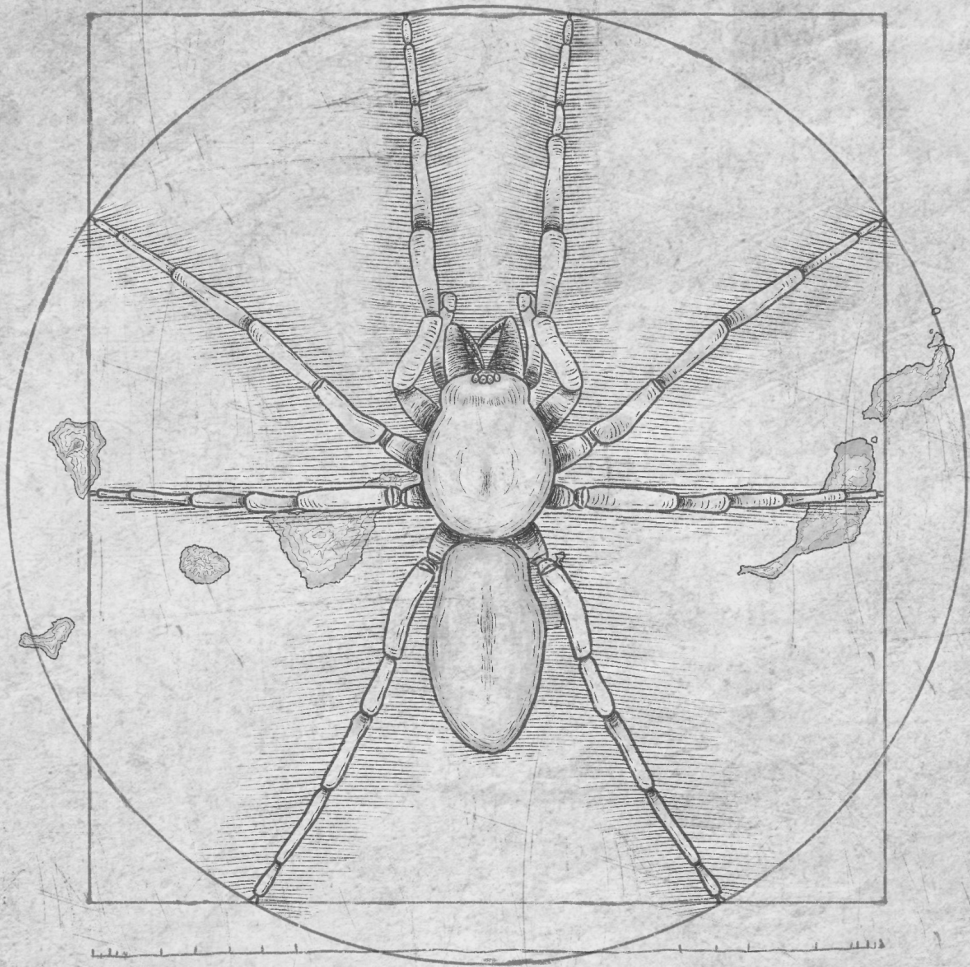
How to cite this article: Bellvert, A., Roca-Cusachs, M., Tonzo, V., Arnedo, M. A., & Kaliontzopoulou, A. (2022). The Vitruvian spider: Segmenting and integrating over different body parts to describe ecophenotypic variation. *Journal of Morphology*, 283, 1425–1438. <https://doi.org/10.1002/jmor.21516>



Adrià Bellvert, Marcos Roca-Cusachs, Vanina Tonzo, Miquel A. Arnedo, Antigoni Kaliontzopoulou.

The Vitruvian spider: Segmenting and integrating over different body parts to describe ecophenotypic variation.

Journal of morphology (2022)



CHAPTER 2.2

The non-dereliction in evolution: Thropic specialisation drives convergence in the radiation of red devil spiders (Araneae:

Dysderidae) in the Canary Islands

The non-dereliction in evolution: Trophic specialisation drives convergence in the radiation of red devil spiders (Araneae:

Dysderidae) in the Canary Islands

Adrià Bellvert^{1,2}, Silvia Adrián-Serrano^{1,2}, Nuria Macías-Hernández^{3,4}, Søren Toft⁵, Antigoni Kaliontzopoulou^{1,2} & Miquel A. Arnedo^{1,2}.

1 Departament de Biologia Evolutiva, Ecologia i Ciències Ambientals, Universitat de Barcelona (UB), Av. Diagonal, 643, 08028 Barcelona, Spain.

2 Institut de Recerca de la Biodiversitat (IRBio), Universitat de Barcelona (UB), Barcelona, Spain.

3 Department of Animal Biology, Edaphology and Geology, Universidad de La Laguna, Tenerife, Canary Islands, Spain.

4 Laboratory for Integrative Biodiversity Research (LIBRe), Finnish Museum of Natural History, University of Helsinki, Finland.

5 Department of Biology, Aarhus University, Ny Munkegade 116, DK-8000 Århus C, Denmark.

Abstract

Natural selection plays a key role in deterministic evolution, as clearly illustrated by the multiple cases of repeated evolution of ecomorphological characters observed in adaptive radiations. Unlike most spiders, *Dysdera* species display a high variability of cheliceral morphologies, which has been suggested to reflect different levels of specialisation to feed on isopods. In this study, we integrate geometric morphometrics and experimental trials with a fully resolved phylogeny of the highly diverse endemic species from the Canary Islands to 1) quantitatively delimit the different cheliceral morphotypes present in the archipelago, 2) test their association with trophic specialisation, as reported for continental species, 3) reconstruct the evolution of these ecomorphs throughout the diversification of the group, 4) test the hypothesis of convergent evolution of the different morphotypes, and 5) examine whether specialisation constitutes a case of evolutionary irreversibility in this group. We show the existence of nine cheliceral morphotypes and uncovered their significance for trophic ecology. Further, we demonstrate that similar ecomorphs evolved multiple times in the archipelago, providing a novel study system to explain how convergent evolution and irreversibility due to specialization may be combined to shape phenotypic diversification in adaptive radiations.

Keywords: Convergent evolution, irreversibility, geometric morphometrics, phylogenetic comparative methods, mitogenomics, adaptive radiation, ecological specializat

Introduction

Understanding the origins of, and identifying the processes that shape, biodiversity are among the major goals of biology ever since Darwin published “On the Origin of Species” (1859). Similarly, the ability to predict organismal response to natural selection lays at the very core of evolutionary biology (Blankers et al. 2017). One well-known process that has helped to shed light on the link between evolution and ecology is that of adaptive radiation (Givnish and Sytsma 1997), which has been defined as the evolution of eco-phenotypically distinct species from a single common ancestor that has occurred in a short period of time (Schluter 2000). Typically, adaptive radiations are characterized by a fast synchronous diversification of lineages and phenotypes after the colonization of a new environment, which slows down as ecological niches are filled (Glor 2010). The study of adaptive radiations has greatly contributed to understanding the mechanisms that drive speciation and promote eco-phenotypic diversification, along with many other related ecological and evolutionary processes (Gillespie et al. 2020).

A common pattern observed in adaptive radiations is the evolution of strikingly similar phenotypic outcomes (Losos et al. 1998) that arise as a result of the adaptation to similar ecological conditions (Rundle et al. 2000; Schluter 2000; Brakefield 2006; Losos 2011). The independent evolution of similarities as a result of common selective regimes, as opposed to those resemblances inherited from common ancestry, is known as convergent evolution (Arbuckle and Speed 2016). Patterns of convergent evolution have been extensively explored in famous cases of adaptive radiation across different taxa, e.g. cichlid fishes (Rüber et al. 1999; Stiassny and Meyer 1999; Hulseay et al. 2019), anole lizards (Kolbe et al. 2011; Mahler et al. 2013; Ord et al. 2013), crickets (Pascoal et al. 2014; Blankers et al. 2017) and spiders (Blackledge and Gillespie 2004). Furthermore, such convergent morphotypes are typically associated with similarities in ecological performance (Irschick and Higham 2015; De Meyer et al.

2019). For instance, the evolution of similar morphotypes in distantly related clades has been shown to be linked to the convergent evolution of specific dietary adaptations in several taxa such as marine tetrapods (Kelley and Motani 2015), rodents (Martinez et al. 2018), cichlid fishes (Muschick et al. 2012) and beetles (Baulechner et al. 2020).

The evolution of trophic adaptations has been frequently investigated as a dichotomy between dietary specialists and generalists, depending on the food resource availability and the fitness benefits gained from each strategy (Levins and MacArthur 1969). However, specialization could represent a wide spectrum of definitions of types of adaptation (Ferry-Graham et al. 2002). Previous studies have defined stenophagy as species occupying a section of the euryphagous species' niche breadth (e.g. herbivore and carnivore as specialist and omnivorous as generalists), in such cases, generalist diets have been seen as macroevolutionary sinks (Burin et al. 2016; Bender and Luiz 2019; Borstein et al. 2019). However, some species are adapted to prey on a resource not (or less) exploited by wider trophic consumers. In such cases, the evolutionary consequences could be completely different, like an evolutionary irreversibility derived of the long term effect of this specialization (Day et al. 2016), compromising the ability of lineages for future evolutionary change (e.g. Cope 1896; Haldane 1951; Kelley and Farrell 1998; Nosil and Mooers 2005; Vamosi *et al.* 2014, Day *et al.* 2016). Stenophagous adaptations often translate into morphological traits that increase the efficiency of feeding on certain specific prey types (Pekar et al. 2011), thus, the irreversibility to a more generalist diet by specialist species could translate into evolutionary irreversibility of their phenotypic characters.

Nevertheless, understanding all these evolutionary processes (adaptive radiation, convergent evolution and irreversibility) is sometimes hampered by species niche conservatism among closely related groups (but see Wiens & Graham 2005 for a review of this topic). Furthermore, patterns of species diversification on continental

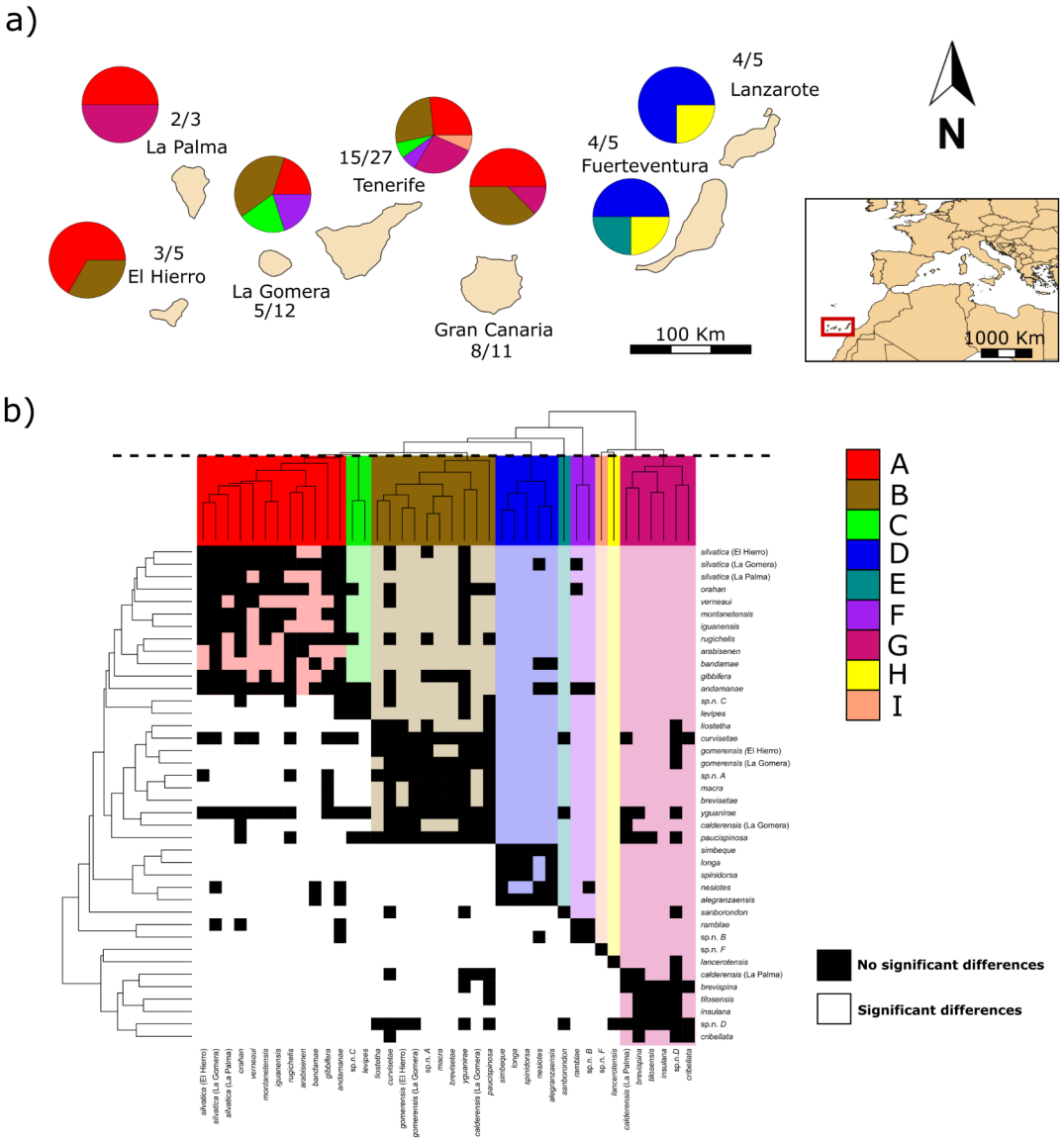


Figure 1 a) Map of the Canary Islands with the proportion of species of each cheliceral morphotype present in each island, as inferred through a clustering of species mean shapes. Numbers indicate the number of species analysed and the total number of species present in each island. b) Combined view of the clustering phenogram performed on pairwise distances among species means of the combined landmark configuration of the three cheliceral perspectives, and the significance of pairwise comparisons of these distances. Black squares indicate no significant differences between pairs of species (p -value > 0.05), white squares indicate significant differences (p -value < 0.05). The horizontal dashed line across the top phenogram delimits the cheliceral morphotypes considered, which are highlighted by different colours (corresponding to letters A-I).

regions are often blurred by the large temporal and spatial scales involved (Gillespie 2016). In contrast, because of their clear boundaries, small size, well dated chronology and multiple replicates, oceanic islands provide natural experiments for studies of species proliferation and ecological adaptation (Losos et al. 1998; Losos and Schluter 2000; Beheregaray et al. 2004; Gillespie 2004; Emerson and Kolm 2005). The Atlantic archipelago of the Canary Islands is formed by 7 major islands and several islets of volcanic origin, located 100 kilometres from the north-western coast of Africa (Fig. 1a). These islands are geo-chronologically arranged with the oldest, Lanzarote and Fuerteventura (15 My and 23 My, respectively), lying at the easternmost side and islands becoming progressively younger towards the western side: Gran Canaria (subaerial age 15 My), Tenerife (12 My), La Gomera (11 My), La Palma (1.7 My) and El Hierro (1.1 My) (Van Den Bogaard 2013). Local communities in the archipelago are highly structured by elevation as a result of the influence of the humid north-east trade winds, which explains the deep differences between the lush and habitat-rich western islands and the arid and highly eroded older islands of Fuerteventura and Lanzarote (Macías-Hernández et al. 2016). Like other isolated oceanic land masses with no former connection to the mainland, the Canary Islands exhibit high levels of endemism, which reaches 66% in the case of spiders (Banco de Datos de Biodiversidad de Canarias, 2022; Cardoso *et al.* 2010).

The red devil spider genus *Dysdera* (Dysderidae) (Fig. 2a), with approximately 300 described species (World Spider Catalog, 2022), has been repeatedly reported to feed on woodlice (Bristowe 1958; Sunderland and Sutton 1980; Hopkin and Martin 1985; Raupach 2005), a prey usually rejected by generalist spiders (Pekár et al. 2016). Concomitantly, *Dysdera* spiders show an unusual variability in their mouthpart morphology, which has been suggested to be related to different levels of dietary specialization for feeding on isopods (i.e. oniscophagy) and prey capture strategies (Řezáč and Pekár 2007; Toft and Macías-Hernández 2017), as well as to metabolic

adaptations (Toft and Macías-Hernández 2021).

With a western Palearctic distribution (Deeleman-Reinhold and Deeleman 1988), *Dysdera* species have colonized all Macaronesian archipelagos (Crespo et al. 2021), which represent the westernmost limit of its range (Arnedo and Ribera 1999; Arnedo et al. 2001). In the Canary Islands, and in a lesser degree in Madeira (Crespo et al. 2020), this genus has undergone major diversification. To date, 47 valid species have been described in the Canarian archipelago (Macías-Hernández et al. 2016), most of which are single-island endemics. The Canarian species assemblage offers an ideal experimental model to study patterns in species radiation as most of their species

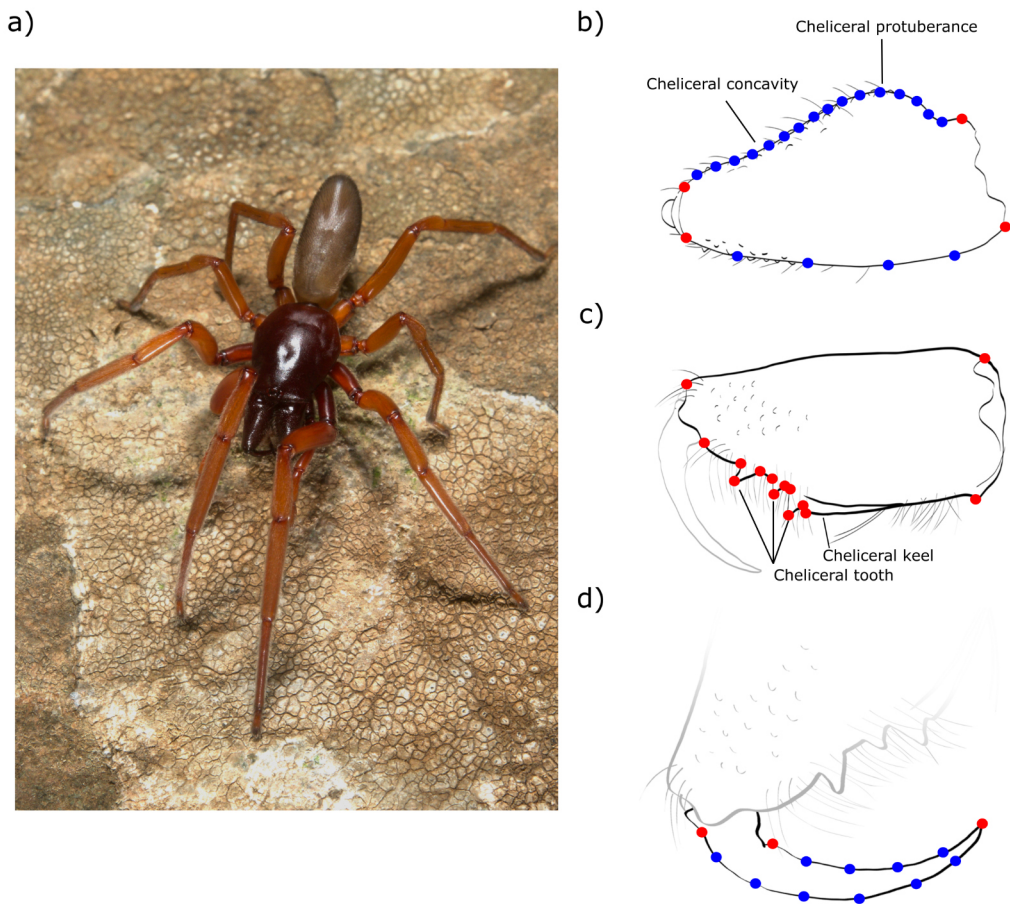


Figure 2 Male individual of *Dysdera simbeque* from Lanzarote (Photo credit M.A.) (a), and position of the landmarks (red) and semilandmarks (blue) considered on the dorsal (b) and ventral (c) view of the chelicera and the fang (d).

have diversified from a single common ancestor in the archipelago (Adrián-Serrano et al. 2020), and show a high variability of phenotypic modifications related to ecological performances (Toft and Macías-Hernández 2017, 2021; Řezáč et al. 2021). A former study based on traditional morphometric analysis suggested the existence of five cheliceral morphotypes in the islands and linked them to different prey-capture strategies (Řezáč et al. 2021). Additionally, oniscophagy was found to be ancestral for *Dysdera* in the Canary Islands and it was suggested that a more generalist diet would have evolved secondarily from specialist ancestors.

In this study we combined Geometric Morphometric (GM) tools with experimental data and phylogenetic comparative methods, incorporating a new fully resolved phylogeny of the group, to investigate the recurrent evolution of cheliceral ecotypes in *Dysdera* spiders from the Canary Islands. Specifically, we aim to 1) quantitatively delimit the different cheliceral morphotypes present in the archipelago, 2) test their association with trophic specialisation, as reported for continental species, 3) reconstruct the evolution of these ecomorphs throughout the diversification of the group, 4) test the hypothesis of convergent evolution of the different morphotypes, and 5) examine whether specialisation constitutes a case of evolutionary irreversibility in this group. By addressing these questions we investigate the interaction between convergence and irreversibility in shaping phenotypic diversification, evolutionary processes that have not been previously explored in combination.

Material & methods

Data collection

All material examined was obtained through field campaigns conducted by the authors and other colleagues during the last 20 years and is deposited at the Centre de Recursos de Biodiversitat Animal of the Universitat de Barcelona (CRBA) and the Departamento de Zoología de la Universidad de La Laguna (DZUL), Tenerife, Canary

Islands collection. The species were mostly captured by active sampling, searching under rocks, logs and tree barks. The captured specimens were either preserved in EtOH at 75% in collections at room temperature at both institutions or at 95% in -20°C freezers at CRBA and DZUL. All specimens were collected following institutional and governmental regulations and permits were granted by the different Cabildos of each island or by the governing body of each natural reserve.

Specimen imaging

Variation in the shape of different cheliceral perspectives was quantified using landmark-based geometric morphometrics (Bookstein 1991; James Rohlf and Marcus 1993; Adams et al. 2004; Zelditch et al. 2004; Mitteroecker and Gunz 2009). For this purpose, we took high-resolution photographs of different perspectives for all the specimens with a digital camera LEICA DFC 450 attached to a LEICA MZ16A stereoscopic microscope using the software Leica Application Software (LAS) v.4.4 (Leica Microsystems Ltd, Switzerland). The chelicera of spiders is formed by two segments. In *Dysdera*, the paturon (the cheliceral segment attached to the prosoma) carries three teeth (distal, medial and basal) on a groove in its internal margin, and the basal tooth develops into a keel that extends proximally (Fig. 2c); and a hinged fang, which folds into the cheliceral groove and shows the opening of the venom conduct at its distal end (Fig. 2d). We followed the protocol of Bellvert et al. (2022) and chose three different perspectives that capture the variations in shape of the chelicera, namely the dorsal and lateral view of the basal segment, and the ventral view of the fang. Whenever possible, we digitized the left chelicera on five females and five males of each species. In case of damaged or missing left structures, we assumed symmetry in the vertical plane and the right side was imaged and inverted. Note that although asymmetry in spider chelicerae has not been previously studied, we are confident that any bias introduced due to this procedure will be minimal at the species level we work here, as studies of other body structures in spiders support the existence of

fluctuating asymmetry (i.e. random in side and magnitude across individuals (e.g. Hendrickx et al. 2003; Uetz et al. 2009; Plăiașu and Băncilă 2018)). Eight Canarian *Dysdera* species are exclusively known from caves and show somatic adaptations to the underground life (e.g. appendage elongation, eye reduction, loss of pigmentation) (Ribera et al. 1985; Ribera and Arnedo 1994; Arnedo and Ribera 1996, 1999; Arnedo et al. 2007). As selective pressures other than prey segregation may be acting differentially on these species compared to their epigeal counterparts, we excluded them from the downstream analyses. A total of 400 specimens comprising 40 of the 57 (including nominal and undescribed) total species of the group were photographed (see Morphometric_sampling of the Supplementary material available on Dryad). Photographs for each view of the chelicera were compiled using the software TpsUtil and landmarks and semilandmarks were digitized using TpsDig2 (Rohlf 2015). Specifically, we considered four fixed landmarks and 20 sliding semilandmarks on the lateral view; 14 landmarks on the dorsal view of the basal chelicera segment; and three fixed landmarks and 10 semilandmarks on the lateral view of the fang (Fig 2b-d).

Geometric Morphometric Analysis

To remove non-shape variation (i.e. related to location, scale and rotation) from individual landmark coordinates, each dataset was subjected to a Generalized Procrustes Analysis (GPA: Gower 1975; Rohlf & Slice 1990) as implemented in the *gpagen* function of the R package “geomorph” (Adams et al. 2021; Baken et al. 2021). During GPA superimposition the position of semilandmarks was optimized by minimizing bending energy. We used the function *combine.subsets* to combine all three perspectives in a single landmark configuration that captured the total shape variation of the chelicerae in our sample. With this combined configuration, we performed a second GPA to scale all perspectives to unit centroid size (Collyer et al. 2020). With the resulting combined superimposed and scaled coordinates, we calculated the mean shape of each species. These mean shapes were subsequently

used to perform a principal component analysis (PCA) using the function *gm.prcomp*. The first two principal components (PC) were used to visualize shape variation across species.

Species clustering

To quantitatively delimit morphotypes present in the *Dysdera* species from the Canary Islands, we applied a hierarchical clustering analysis based on Procrustes distances among species means of cheliceral shape, using the function *hclust* of the *stats* R-package (R core team, 2021). To select the best algorithm for clustering, we calculated the correlation between the original distance matrix and the cophenetic distances on the phenogram derived by each method (ward.D, ward.D2, single, complete, average, mcquitty, median and centroid) and chose the one that maximized this correlation. To delimit clusters that could be interpreted as distinctive morphotypes, we combined the resulting phenogram with pairwise p-values between species obtained using permutation procedures as implemented in the function *pairwise* of RRPP R package (Collyer and Adams 2018, 2021), over an ANOVA comparison of species means performed using the function *procD.lm* of “geomorph” R package (Adams et al. 2021; Baken et al. 2021). Pairwise p-values were plotted as significant or non-significant considering significance at $\alpha = 0.05$. To delimit morphotypes, we selected those clusters that included the highest number of species with non-significant shape differences among them.

Phylogenetic analyses

We inferred relationships of the focal taxa based on mitogenomic information. Mitogenomes were recovered from different sources and forms. We downloaded genomic and transcriptomic information from public repositories (NCBI). In addition, we gathered new Low-Coverage Whole Genome Sequencing data for selected species (see Molecular_Sampling of the Supplementary material available on Dryad). We recovered mitochondrial genes using the pipeline detailed in Adrián-Serrano et

al.(2020). The concatenated data matrix was further completed by adding species represented by at least one of the following genes obtained by Sanger sequencing: cytochrome c oxidase 1 (COI), the NADH dehydrogenase subunit (nad1) and the large (16S) and small (12S) ribosomal subunits, available either from public databases or generated in house.

We included all *Dysdera* species from the Canary Islands represented at least by two individuals and, in the case of multi-island species, individuals from each island, with few exceptions (see Molecular_Sampling of the Supplementary material available on Dryad). Additional *Dysdera* species from the mainland and Madeira were also included to polarize the tree. Finally, representatives of all the families within the Synespermiata clade, including members of the Superfamily Dysderoidea were considered to provide fossil information for calibration. All trees were rooted, assuming a sister group relationship of the families Hypochilidae and Filistatidae with the Synespermiata clade (Garrison et al. 2016; Wheeler et al. 2017; Fernández et al. 2018; Michalik et al. 2019; Kulkarni et al. 2020, 2021; Kallal et al. 2021; Ramírez et al. 2021).

Mitochondrial genes were manipulated and concatenated with Geneious Prime 2020.2.4 (www.geneious.com). Each gene was aligned independently using the software MAFFT (Katoh and Standley 2013) as implemented in Geneious, with the G-INS-I algorithm and default values (0.53 for gap penalty, 0.123 for offset value). We inferred a time-calibrated phylogeny under a Bayesian uncorrelated relaxed molecular clock approach as implemented in BEAST v2.6.3 (Bouckaert et al. 2019). The concatenated data matrix was partitioned by gene, and the best evolutionary model for each gene partition was selected with PartitionFinder 2 (Lanfear et al. 2017). Individual log-normal clocks were defined for each gene, and the tree prior was set to the Birth-Death model.

Calibration information used to constrain nodes for time estimation is summarized

in Online-Appendix, Table S1. In short, we combined 10 fossil calibrations with one biogeographic event. Fossil information was included as lognormal prior distribution on specific nodes, except for the root, which was assigned a uniform prior. The biogeographic information (the Hercynian split of the Iberian plate into present-day major western Mediterranean islands) was defined as a normal prior distribution. We further enforced topological constraints on specific nodes (monophyly of Segestriidae, Oonopidae, Orsolobiidae and Dysderidae, Segestriidae sister to Oonopidae, Orsolobiidae and Dysderidae) following results of recent phylogenomic analyses (Kallal et al. 2021; Kulkarni et al. 2021). A starting tree including time and topological constraints was generated with the program PATHd8 (Britton et al. 2007).

We run three independent chains under selected priors for 100 million generations, sampling every 10,000 generations. Convergence among runs and correct mixing of the chains was monitored with TRACER v.1.7 (<http://tree.bio.ed.ac.uk/software/tracer/>). The burn-in was removed (10%) and the runs were combined with the help of the BEAST accompanying programs LOGCOMBINER and TREEANNOTATOR. Unless specified otherwise, we used the consensus tree for downstream analysis.

Non-Canarian and cave-dwelling *Dysdera* taxa, as well as taxa for which phenotypic data was not available, were pruned from the final posterior distribution of time-stamped trees with the R package 'ape' (Paradis and Schliep 2019).

Phylogenetic signal

To evaluate to what extent the cheliceral morphological resemblance among *Dysdera* species is associated to their shared phylogenetic history, we measured phylogenetic signal using Blomberg's K statistic (Blomberg et al. 2003), as generalized for high-dimensional and multivariate data (Kmult:Adams 2014). In addition, to test if Kmult values were significantly different from one, we developed a simulation

procedure (see R scripts of the Supplementary material available on Dryad) that simulated multivariate phenotypes of the same dimensions as our data, under the empirical evolutionary rate matrix observed in our dataset and using a Brownian Motion model of evolution. This produced a null distribution of expected values of K_{mult} , against which we compared the value observed in our dataset. We calculated the corresponding p-value as the number of times the observed value was more extreme than that expected from the simulated phenotypes. In both analyses, we accounted for phylogenetic uncertainty by estimating K_{mult} and evaluating its significance (for $K_{mult} = 0$) over 1,000 trees subsampled from the posterior distribution of BEAST, using the function *physignal* of the “geomorph” R package.

Prey Preference analysis

For prey preference analyses, we selected 14 phylogenetically spread-out *Dysdera* species of different morphotypes, for which we managed to collect enough specimens for the experiments (Online Appendix, Table S2). Each species was represented by twenty specimens, except for *D. alegranzaensis* (N = 16); *D. tilosensis* (N = 7); *D. insulana* (N = 3) and *D. levipes* (N = 6).

The spiders were maintained at room temperature and starved during the three weeks before experiments. Individuals were placed singly into Petri dishes (30 mm diameter) with a moistened piece of filter paper. The offered prey size was from half to the same body length of the spider. We offered five types of prey: spiders (*Pardosa prativaga*), flies (*Musca domestica*), carabid beetles (*Bembidion lampros*), and two species of woodlice (*Porcellio scaber* and *Armadillidium vulgare*). For the smallest species, *D. levipes* (range of size between 6.5-9 mm.), we tried six types of prey: juvenile spiders (*Pardosa prativaga*), flies (*Drosophila* sp.), staphylinid beetles (Aleocharinae), juveniles of woodlice (*Porcellio scaber* and *Armadillidium vulgare*) and collembola (*Sinella curviseta*). The preys were randomly offered, and if they were not captured within 30 min. we offered another one. We prevented the spider from

consuming the prey to keep it hungry. The proportion of times that each spider preyed on each type of prey were recorded and species average values were calculated.

We first tested for a statistical association between cheliceral morphotype and the prey preference, using a two-block partial least-squares (PLS) analysis implemented in the function *phylo.integration* from the “geomorph” R package (Adams et al. 2021; Baken et al. 2021), with the consensus phylogeny trimmed to match the species analysed. This test evaluates the degree of covariation between two sets of variables, while considering the relationship between species. Then, we used prey preference data to examine whether we could accurately identify species as generalists or specialists. For this purpose, we calculated the proportion of isopod versus non-isopod prey consumed by each individual. With the mean value per species, we then performed a clustering analysis using the function *kmeans* with $k = 2$ to assign species into one of the aforementioned trophic specialization categories.

Ancestral State Reconstruction

To reconstruct the evolutionary history of cheliceral morphotypes, we used stochastic character mapping (Bollback 2006) with the function *make.simmap* of the “phytools” R package (Revell 2012). To take phylogenetic uncertainty into account, we used the same subsample of 1,000 trees as before from the posterior distribution of trees obtained from the BEAST analysis. We simulated 100 stochastic character maps under four different transition-rate scenarios for the nine possible character states (i.e. cheliceral morphotypes), namely: a single-parameter model with equal rates (ER), a model with different rates for each transition (ARD), and a model with equal transition rates except for those from all specialist to all generalist cheliceral groups, which were fixed to 0, to which we referred as “constrained ER”. The last scenario allows to test the irreversibility of trophic specialization, as we constrained the generalist state (cheliceral types A and D, see Results) to potentially being lost but not regained throughout evolution. Goldberg and Igić(2008) have shown that the

hypothesis of irreversibility is better approached through directional models. For this reason, we used a non-stationary root state when reconstructing ancestral state histories as proposed by FitzJohn et al. (2009), a procedure implemented through the parameter $\pi = \text{"fitzjohn"}$ in the function *make.simmap* of "phytools". We evaluated the fit of different models by comparing the AIC values of the alternative scenarios over the 1000 topologies by 100 simmap combinations. Additionally, to take into account the possible acquisition bias (Goldberg and Igić 2008)—due to the fact that only variable states were considered and stochastic mapping simulations were restricted to variable states of the extant tips— we defined a two-state model by grouping all cheliceral types into two states (generalist vs. specialist), and estimated the fraction of trees rejecting irreversibility comparing the two states ARD model with root prior probabilities of 50% for each state (Mk2 model) and a directional two state ARD constrained to $q_{SG}=0$ (constrained Mk2 model), for each of the 1000 distinct topologies. The scripts and datasets used for these analyses can be found in the Supplementary material available on Dryad.

Convergent evolution

We tested evolutionary convergence for cheliceral types B and G, as they represent derived states occurring in multiple terminals (see results). The also derived type F was not tested because it occurred only in two non-related terminals. We quantified the amount of independent evolution of each morphotype using the R package "convevol" (Stayton 2018). For this, we used the morphospace built from the GM data with the first two PCs of cheliceral shape variation (accounting for 62.88% of total variation, see results). We investigated the degree of evolutionary convergence using the distance-based statistics C1 and C3 (Stayton 2015). These two metrics provide a complementary view on how exceptional the similarity between two taxa is, by considering the ratio between the phenotypic distance between the two potentially convergent taxa and the maximum distance observed between any pair of taxa (either

ancestral or extant) across the evolutionary history of these lineages. Each pair comparison was made selecting species belonging to the same cheliceral morphology and calculating if their phenotypical similarities were greater than that expected by chance. While C1 shows if the degree of convergence between two extant taxa exceeds what would be expected by chance (Zelditch et al. 2017), it does not take into account the absolute amount of evolution between lineages. On the contrary, C3 considers phenotypic distance from ancestors to descendants, such that phenotypically similar and closely related species have different values of convergence compared to phenotypically similar but distantly related pairs (Stayton 2015). The significance of departure from the values of C1 and C3 expected under Brownian Motion was assessed using 100 simulations performed through the function `convratsig`, and again we accounted for phylogenetic uncertainty by using a subset of 100 trees from the posterior distribution of BEAST analyses. The scripts and datasets used for this analysis can be found in the Supplementary material available on Dryad.

Results

Characterization of cheliceral morphotypes

The first two components of the PCA of the mean shapes of all species analysed explained 49.85% and 13.02% of chelicera shape variation, respectively. PC1 captured shape variation related to the elongation of the basal segment in dorsal view and the relative distance from the distal cheliceral teeth to the distal part of the basal segment, as well as with the protuberance of the basal segment in lateral view and relative fang length (Online-Appendix, Fig. S1). PC2 was mostly associated with variation in the relative length of the cheliceral groove, the stoutness of the basal segment in lateral view, and the relative width of the fang (Online-Appendix, Fig. S2).

Of all the clustering algorithms used on the pairwise Procrustes distances among species mean shapes, the unweighted pair group method with arithmetic mean (i.e.

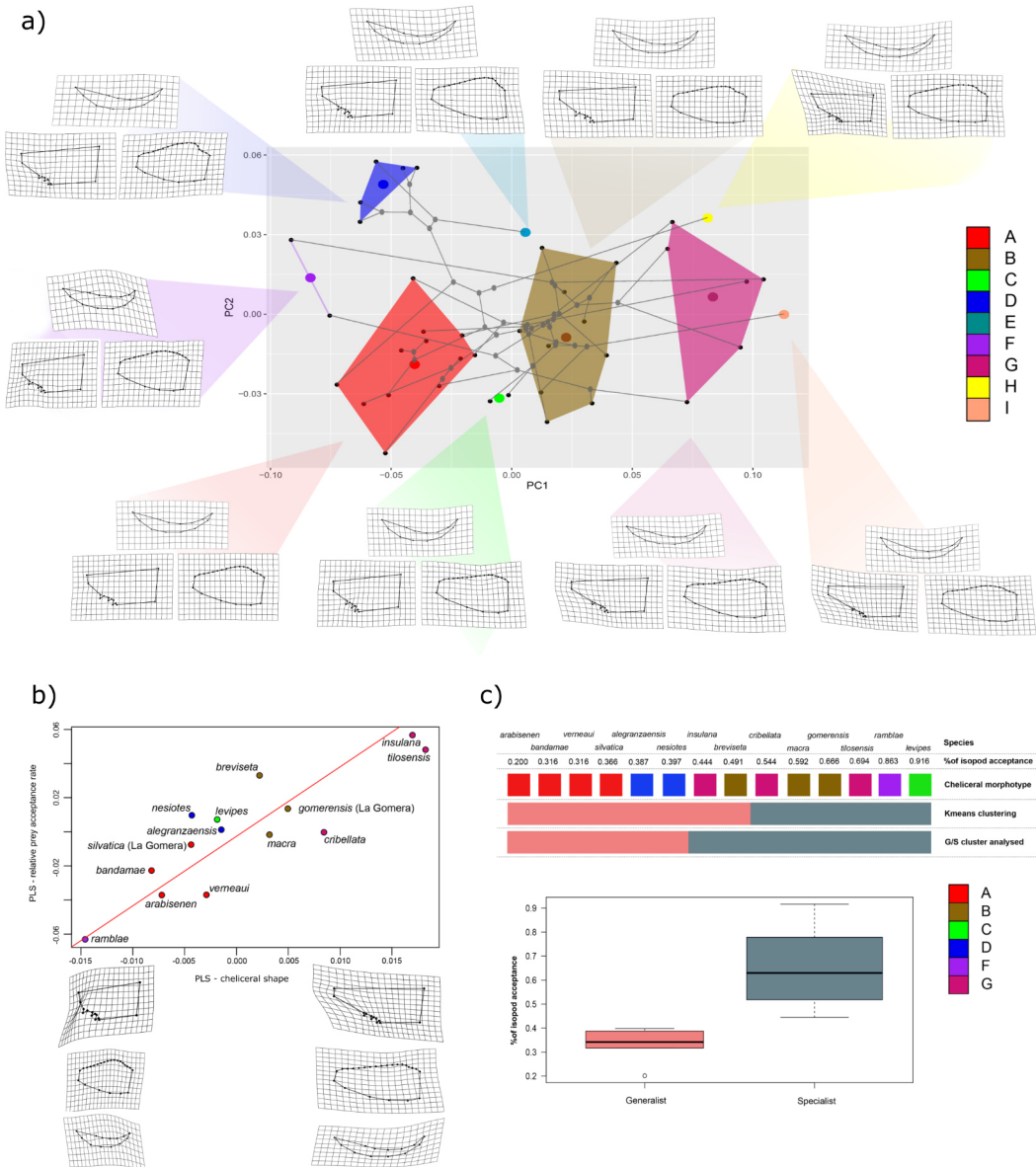


Figure 3 a) Cheliceral phylomorphospace with convex polygons depicting species of the same ecomorph group. Black dots represent the *Dysdera* species analysed, and the coloured dots correspond to the mean shape of each group. Deformation grids represent the mean shape of each group as compared to the global mean of all species. b) PLS analysis between prey preference and cheliceral shape variation. Cheliceral morphotypes are represented with the coloured dots. Deformation grids correspond to the minimum and maximum shape of the PLS axis for each cheliceral view. Shape patterns are magnified x1.3 to enhance visualization. c) Prey acceptance preference between generalist and specialist species. “Kmeans clustering” represents the species cluster delimitation made by the *kmeans* function. The “G/S cluster analysed” showed the clustering analysed without splitting species that belong to the same cheliceral morphotype.

UPGMA) showed the highest correlation between the node distance and the original distance matrix ($r=0.746$). The combined examination of the resulting phenogram with the pairwise p-values between all pairs of species revealed several clusters that maximized non-significant within-group differences in the shape of the chelicera (Fig. 1b). As the best arrangement of the cheliceral variability displayed by *Dysdera* spiders in the Canary Islands, we identified nine morphotypes, hereafter referred to by the letters A to I. Cheliceral morphotypes G, H, and I exhibit an elongation of their structures as described above with the extreme shapes in PC1. Morphotypes C and E have the concavity of the chelicera slightly marked. Morphotype D is characterized by a protruding cheliceral protuberance, and morphotype F represents the stouter chelicera with a short and wide fang (Fig. 3a). The cheliceral morphotypes A, B, C, F, G and I are restricted to the western islands, namely Gran Canaria, Tenerife, La Gomera, La Palma and El Hierro, while morphotypes D, E and H are exclusive to the eastern islands of Lanzarote and Fuerteventura (Fig. 1a). The time-stamped phylogeny inferred from mitogenome data (Online-Appendix Fig. S3), was pruned to include Canarian species with GM information for downstream analyses.

Relationships between morphotypes and dietary preferences

Prey preference behaviour varied extensively across the *Dysdera* species analysed, where the percentage of isopod acceptance ranged between 20% in some species and up to almost 92% in others (Fig. 3c). The phylogenetic PLS analysis showed a significant covariation between prey preference and cheliceral shape ($r\text{-PLS} = 0.863$, $P\text{-value} = 0.002$) (Fig 3b). The composition of the first PLS eigenvector for the prey block indicates that this association is mainly explained by the level of predatory preference for *Armadillidium* isopods (0.788), *Musca* flies (0.463) and *Porcellio* isopods (0.380) (Online-Appendix, Table S3). In terms of shape variation, the preference for *Armadillidium* predation (characteristic of e.g. *D. insulana* and *D. tilosensis*: Online-Appendix, Table S2) is associated with an elongation of all

perspectives analysed, and particularly of the fang and the anterior part of the chelicera (Fig. 3b). By contrast, higher levels of predation on *Porcellio* are associated with more compact chelicera with a relatively flat and short fang, as exemplified in *D. ramblae* (Fig. 3b, Online-Appendix, Table S2). *Dysdera* species with intermediate shapes, occupying the central portion of the PLS space of association between cheliceral shape and dietary preference, exhibit higher levels of acceptance of *Musca* flies. The K-means cluster analysis based on the percentage of acceptance of isopods grouped together species belonging to morphotypes A and D, and all other species were grouped together in the second cluster, with the exception of two species belonging to morphotypes B and G (Fig. 3c). To avoid over-splitting, we assigned these species to the cluster that included the remaining species of their morphotype. Species belonging to the first cluster (species with morphotypes A and D) show lower levels of preference of preying on isopods than the species of the other cluster, hereinafter referred to as generalist and specialist, respectively (Fig. 3c).

Evolution of morphotypes

The best supported model of state transition to describe the evolutionary dynamics of different cheliceral morphotypes was the constrained ER encompassing irreversibility (Akaike Information Criterion, AIC= 137.487 ± 0.998). The second and third most supported models were the ER and SYM models (AIC = 152.284 ± 20.252 and 184.260 ± 6.138 , respectively), and the least supported model was ARD (AIC = 264.266 ± 9.427). All models, except for ARD, identified morphotype A as the most likely ancestral state of all *Dysdera* species from the Canary Islands (Fig. 4, Online-Appendix, Fig. S4-6, Online-Appendix, Table S4-7). The character reconstruction of all nine different cheliceral morphotypes revealed that at least three (B, F and G) out of the six morphotypes represented by more than one species evolved more than once (Fig. 4). Similarly, when a two-state model was defined (generalist vs. specialist), we found little support for reversibility. In all trees, the constrained Mk2 model yielded

lower values than the Mk2 model, with differences in $\Delta AICs$ ranging from 3.7 to 6.3 units (Fig. S7). Cheliceral shape as represented by the combined coordinates of all three examined perspectives exhibited significant phylogenetic signal ($K_{mult} = 0.657 \pm 0.015$, $p\text{-value} = 0.0014 \pm 0.0005$), which suggested a phylogenetic component in the observed phenotypic variation. Furthermore, the observed K value was significantly smaller than one ($p\text{-value} = 0.0144 \pm 0.0023$), as also supported by a lack of phylogenetic structure in phylomorphospace (Fig. 3a).

For the two cheliceral morphotypes analysed (B and G), distance-based measures of convergence revealed significantly higher observed C1 and C3 values than those expected by chance ($p\text{-value} < 0.001$). Specifically, the distance between any two species, was reduced between 50.53 and 63.67%, by subsequent evolution (C1) in morphotype B, and between 41.42 and 63.93% in morphotype G, while convergence was responsible for between 24.86 and 37.67% and between 24.31 and 38.03% of the evolution between those lineages (C3) in morphotypes B and G, respectively.

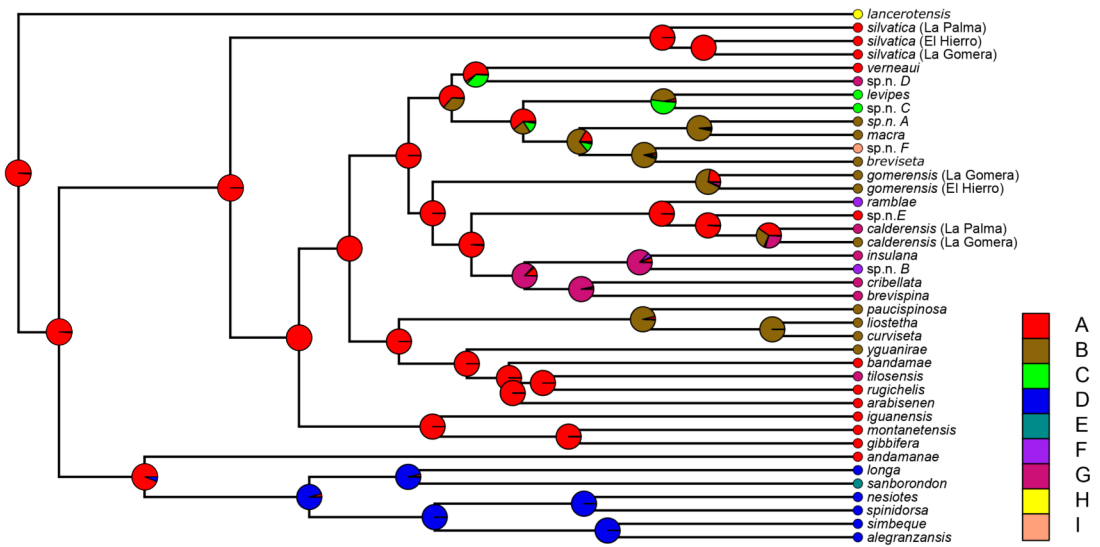


Figure 4 Ancestral state reconstruction obtained under the constrained (irreversible) ER model. Pie-charts at each node represent the state probability obtained through the 100 stochastic character map simulations over 1000 phylogenetic trees sampled from the posterior distribution of BEAST.

Discussion

With the present study we have been able to untangle the effects of ecological pressures that have shaped the phenotypic diversity of a group with a shared evolutionary history. The repeated evolution of characters adapted to different levels of trophic specialization has allowed us to understand the deterministic evolution caused by adaptation to the same ecological needs. Furthermore, our study has shown that to capture complex characters involved in the evolution of the species, fine scale methods able to capture subtle changes are needed to understand the evolutionary pressures that has led the phenotypic disparity in the group.

Although the existence of particular cheliceral morphotypes (Řezáč et al. 2021) and different metabolic abilities to feed on isopods (Toft and Macías-Hernández 2017, 2021) was previously uncovered, here, we statistically characterise for the first time this eco-morphological character using geometric morphometrics and experimentally demonstrate their association to different levels of diet specialisation (here oniscophagy). The finer GM data and more sophisticated statistical analyses used allowed us to delimit nine different cheliceral morphologies, some of which greatly resemble those previously defined (A, D and E to “unmodified”, B and H to “elongated”, C to “dagger”, F to “flattened” and G to “concave”) (Řezáč et al. 2008, 2021).

Cheliceral morphotypes reflect different levels of diet specialisation

Our results demonstrate a close link between morphotype differentiation in *Dysdera* species from the Canary Islands, as reflected in cheliceral modifications and diet specialisation, specifically in the increased frequency of capture and consumption of terrestrial isopods, as already suggested in former studies (Řezáč et al. 2008, 2021; Toft and Macías-Hernández 2017, 2021). This implies an ecological functionality for the different cheliceral morphologies present in the archipelago, which assigns them

a strong evolutionary potential. Interestingly, both generalist and diet specialists are represented by multiple cheliceral morphotypes. Indeed, when analysing dietary preferences in isolation, species with different cheliceral morphotypes could be classified into two main groups, namely, generalists (A and D) and specialists (B, C, F and G). In the case of dietary specialists, the different morphotypes have been related to alternative strategies of woodlice capture and manipulation (Řezáč et al. 2008, 2021). Importantly, our analyses also suggest the existence of two distinct morphotypes with a more generalist diet (A and D). While these two morphotypes are clearly distinct in cheliceral shape (Fig. 3a), lab experiments were not sufficient to fully capture the dietary differences between them.

Island group and specialisation

It is worth noting that the eastern Canaries showed the higher proportion of generalist species. These islands also harbour a lower number of endemic *Dysdera* than other islands of similar size yet of younger age (e.g. Gran Canaria, Tenerife) (Cardoso et al. 2010), which has been suggested to be the result of higher levels of extinction as a result of the mass-wasting processes, and severe climatic degradation endured by these islands (Macías-Hernández et al. 2008). Habitat deterioration and aridification could have posed specific filters on the local ecosystems, which may have hindered the presence of specialist species in the eastern islands. In this regard, it has been reported that specialist predators at high trophic levels are less likely to be present in species-poor island communities (Piechnik et al. 2008). Concomitantly, not all isopod species have evolved proper adaptations to survive in more arid conditions (Cloudsley-Thompson 1975), making them potentially less abundant in the eastern islands, and thus hindering the presence of specialist *Dysdera* in this environment. However, without a deeper knowledge of the isopod abundance between the eastern and western islands this remains highly speculative. Additionally, the different environmental filtering or ecological pressures between the eastern and western

islands could explain the non-overlapping of cheliceral morphotypes between the two islands groups (differentiated across the second PC in Fig. 3a).

A generalist coloniser and convergent evolution of morphotypes

Overall, generalist species are usually considered better colonizers than specialists, as they are able to secure sufficient resources more easily (Ebenhard 1991), and it is assumed that specialist diets commonly evolved from generalist ones (Toft 1995; Stephens and Wiens 2003; Reynolds et al. 2016; Naik et al. 2021). Evidence supporting both statements is found in the present work, contradicting former suggestions (Řezáč et al. 2021). However, the results of this former study were compromised by the fragmentary evidence, including the use of linear measurements to quantify chelicera shape, sparse data ($n=1$ for many species) and the use of an outdated phylogeny. The more updated phylogeny and the use of geometric morphometrics that allows to capture shape variation at a finer scale, has most likely contributed to these dissonant results.

The repeated evolution of convergent ecological and/or morphological traits is a common pattern in adaptive radiations, and is generally interpreted as a response to similar evolutionary pressures (Schluter and Nagel 1995; Losos et al. 1998, 2003; Rundle et al. 2000; Schluter 2000; Nosil et al. 2002; Blackledge and Gillespie 2004; Gillespie 2004; Gavrilets and Losos 2009; Muschick et al. 2012). However, even when ecological pressures have driven the phenotypic evolution of a species group, a total independence of these characters is impossible due to their shared evolutionary history (Felsenstein 1988; Harvey and Pagel 1991; Revell et al. 2008). In this regard, we have shown that the different trophic adaptations presented by *Dysdera* spiders during their diversification in the Canary Islands is, to some extent, related to their shared phylogenetic history, as reflected by significant phylogenetic signal observed for cheliceral shape. However, K_{mult} values were shown to be significantly <1 which, together with the lack of phylogenetic structure that is apparent in the

phylomorphospace plot (Fig. 3a), are suggestive of distantly related species occupying closer phenotypic spaces than expected by chance. Accordingly, the reconstruction of morphotype evolution has showed that some specialized trophic morphotypes—B, G, and F—evolved several times, independently. The multiple evolution of at least three distinct cheliceral types suggests a role of natural selection and convergent evolution in the diversification of the group. Indeed, integrating evidence on convergent evolution with the statistical association between cheliceral shape and levels of trophic specialization (Fig. 3b), we provide evidence that adaptations to increase woodlice consumption played a key role in the evolution and diversification of *Dysdera* in the Canary Islands.

Did the evolution of diet specialisation lead to an evolutionary irreversibility?

Although several studies have shown that transitions from specialist to generalist forms are indeed possible (Lanyon 1992; Muller 1996; Armbruster and Baldwin 1998), the reverse seems to be the common trend (Nosil 2002). Our character reconstruction analysis points towards the second observation, since the model that best fit our data encompassed transitions from generalist to specialist morphotypes but not the opposite, supporting the hypothesis that evolution of specialised chelicerae from generalist ancestors could be the common pattern across *Canarian Dysdera* species. We acknowledge, however, that to convincingly confirm the irreversibility in prey specialisation additional sources of information will be required (e.g. fossil record, developmental data) (Goldberg and Igić 2008). Moreover, the use of methods that explicitly incorporate the effect of character state transformations on diversification rates (e.g. state dependent diversification models) would more accurately reflect the evolutionary effects of prey specialization. Nevertheless, it should be pointed that, as stated by Goldberg and Igić (2008), methods that do not account for character evolution tend to incorrectly reject Dollo's law (i.e. irreversibility), and therefore their implementation would most likely not change our results regarding evolutionary

irreversibility in prey specialisation.

Conclusions

Canarian *Dysdera* evolved a particular set of cheliceral shapes associated with different levels of diet specialisation, specifically to capture and feed on woodlice. Our implementation of geometric morphometrics approaches discerned cheliceral morphologies at finer scales than traditional measurements, as illustrated by the higher number of morphotypes compared to the ones described until now. Furthermore, the use of a newly inferred phylogenetic hypothesis based on mitogenomic data for a complete data set of Canarian endemics revealed a new scenario for the phenotypic and ecological diversification of *Dysdera* in the Canary Islands. The ancestral coloniser of the archipelago was most likely a generalist species, from which specialised forms evolved convergently multiple times. The eastern and western islands harbour different cheliceral morphotypes, which hints at the existence of different ecological and evolutionary filters on each island group, probably related to the dramatic climatic and landscape changes undergone by the older and highly eroded eastern Canaries. Finally, our analysis provide support for specialisation as a derived trait that could potentially lead to evolutionary irreversibility in the diversification of the red devil spiders.

Acknowledgements

To the Cabildos of El Hierro, Fuerteventura, Gran Canaria, Lanzarote, La Gomera, La Palma and Tenerife and to the Garajonay National Park for the collection permits. To Luis Crespo, Salvador de la Cruz, Marc Domènech, Isabel Calderón, Sara Febles, Heriberto López, Pedro Oromí, Martina Pavlek, Tin Rozman and Vanina Tonzo for their help and support in the sampling campaigns and the obtaining of specimens. To Tristan Stayton for his help and information provided about the “convevol” package and their results. To Lauren Esposito, Isabel Sanmartín and two anonymous reviewers

who contributed to increase the quality of the present manuscript.

A.B. was funded by an individual PhD grant BES-2017-080538 from the Ministerio de Economía, Industria y Competitividad of the Spanish government. N.M was funded by an individual postdoctoral grant from the Carlsberg Foundation (Denmark) 2011_01_0066/20 and the Spanish Science Ministry (MINECO). A.K. is supported by a Ramón y Cajal research grant co-funded by the Spanish State Research Agency and the European Social Fund (RYC2019-026688-I/AEI/10.13039/501100011033). This study was supported by project grants CGL2012-36863 and CGL2016-80651-P from the Spanish Ministry of Economy and Competitiveness and 2017SGR83 from the Catalan Government (M.A.).

Author contributions

AB, MA and AK designed the study; AB and AK performed data analyses; SAS and MA conducted the “*de novo*” mitogenomic sequences and reconstructed the phylogeny; NMH and ST performed the prey preference experiments; AB wrote the first version of the manuscript. All authors reviewed and approved the final version of the manuscript.

Supplementary material

Data available from the Dryad Digital Repository: [http://dx.doi.org/10.5061/dryad.\[NNNN\]](http://dx.doi.org/10.5061/dryad.[NNNN])

Conflict of interest

The authors declare no competing interests.

References

- Adams D.C. 2014. A generalized K statistic for estimating phylogenetic signal from shape and other high-dimensional multivariate data. *Syst. Biol.* 63:685–697.
- Adams D.C., Collyer M.L., Kaliontzopoulou A., Baken E.K. 2021. Geomorph: Software for geometric morphometric analyses. R package version 4.0. .
- Adams D.C., Rohlf F.J., Slice D.E. 2004. Geometric morphometrics: Ten years of progress following the ‘revolution.’ *Ital. J. Zool.* 71:5–16.
- Adrián-Serrano S., Lozano-Fernandez J., Pons J., Rozas J., Arnedo M.A. 2020. On the shoulder of giants: Mitogenome recovery from non-targeted genome projects for phylogenetic inference and molecular evolution studies. *J. Zool. Syst. Evol. Res.*:1–26.
- Arbuckle K., Speed M.P. 2016. Analysing Convergent Evolution: A Practical Guide to Methods. In: Pontarotti P., editor. *Evolutionary Biology: Convergent Evolution, Evolution of Complex Traits, Concepts and Methods*. Cham: Springer International Publishing. p. 23–36.
- Armbruster W.S., Baldwin B.G. 1998. Switch from specialized to generalized pollination. *Nature*. 394:632.
- Arnedo M., Ribera C. 1996. *Dysdera ratonensis* Wunderlich, 1991 (Arachnida, Araneae) a troglomorphic species from La Palma, Canary Islands: Description of the male and redescription of the female. *Rev. Arachnol.* 11:109–122.
- Arnedo M.A., Oromí P., Múrria C., Macías-Hernández N., Ribera C. 2007. The dark side of an island radiation: systematics and evolution of troglobitic spiders of the genus *Dysdera* Latreille (Araneae: Dysderidae) in the Canary Islands. *Invertebr. Syst.* 21:623–660.
- Arnedo M.A., Oromí P., Ribera C. 2001. Radiation of the spider genus *Dysdera* (Araneae, Dysderidae) in the Canary Islands: Cladistic assessment based on multiple data sets. *Cladistics*. 17:313–353.
- Arnedo M.A., Ribera C. 1999. Radiation in the genus *Dysdera* (Araneae, Dysderidae) in the Canary Islands: The island of Tenerife. *J. Arachnol.* 27:604–662.
- Baken E.K., Collyer M.L., Kaliontzopoulou A., Adams D.C. 2021. gmShiny and geomorph v4.0: new graphical interface and enhanced analytics for a comprehensive morphometric experience. *Methods Ecol. Evol.*:Submitted.
- Baulechner D., Jauker F., Neubauer T.A., Wolters V. 2020. Convergent evolution of specialized generalists: Implications for phylogenetic and functional diversity of carabid feeding groups. *Ecol. Evol.*:11100–11110.
- Beheregaray L.B., Gibbs J.P., Havill N., Fritts T.H., Powell J.R., Caccone A. 2004. Giant tortoises are not so slow: Rapid diversification and biogeographic consensus in the Galápagos. *Proc. Natl. Acad. Sci.*

U. S. A. 101:6514–6519.

- Bellvert A., Roca-Cusachs M., Tonzo V., Arnedo M.A., Kaliontzopoulou A. 2022. The Vitruvian spider: segmenting and integrating over different body parts to describe eco-phenotypic variation. *J. Morphol.*:1425–1438.
- Bender M.G., Luiz O.J. 2019. Specialization boosts reef fish functional diversity. *Nat. Ecol. Evol.* 3:153–154.
- Blackledge T.A., Gillespie R.G. 2004. Convergent evolution of behavior in an adaptive radiation of Hawaiian web-building spiders. *Proc. Natl. Acad. Sci.* 101:16228–16233.
- Blankers T., Gray D.A., Matthias Hennig R. 2017. Multivariate Phenotypic Evolution: Divergent Acoustic Signals and Sexual Selection in *Gryllus* Field Crickets. *Evol. Biol.* 44:43–55.
- Blomberg S.P., Garland T., Ives A.R. 2003. Testing for phylogenetic signal in comparative data: Behavioral traits are more labile. *Evolution (N. Y.)*. 57:717–745.
- Van Den Bogaard P. 2013. The origin of the Canary Island Seamount Province—New ages of old seamounts. *Sci. Rep.* 3:1–7.
- Bollback J.P. 2006. SIMMAP: Stochastic character mapping of discrete traits on phylogenies. *BMC Bioinformatics.* 7:1–7.
- Bookstein F.L. 1991. *Morphometric tools for landmark data: Geometry and biology*. New York: Cambridge University Press.
- Borstein S.R., Fordyce J.A., O’Meara B.C., Wainwright P.C., McGee M.D. 2019. Reef fish functional traits evolve fastest at trophic extremes. *Nat. Ecol. Evol.* 3:191–199.
- Bouckaert R., Vaughan T.G., Barido-Sottani J., Duchêne S., Fourment M., Gavryushkina A., Heled J., Jones G., Kühnert D., De Maio N., Matschiner M., Mendes F.K., Müller N.F., Ogilvie H.A., Du Plessis L., Poppinga A., Rambaut A., Rasmussen D., Siveroni I., Suchard M.A., Wu C.H., Xie D., Zhang C., Stadler T., Drummond A.J. 2019. BEAST 2.5: An advanced software platform for Bayesian evolutionary analysis. *PLoS Comput. Biol.* 15:1–28.
- Brakefield P.M. 2006. Evo-devo and constraints on selection. *Trends Ecol. Evol.* 21:362–368.
- Bristowe W.S. 1958. *The world of spiders*. London: Collins.
- Britton T., Anderson C.L., Jacquet D., Lundqvist S., Bremer K. 2007. Estimating divergence times in large phylogenetic trees. *Syst. Biol.* 56:741–752.
- Burin G., Kissling W.D., Guimarães P.R., Şekercioglu C.H., Quental T.B. 2016. Omnivory in birds is a macroevolutionary sink. *Nat. Commun.* 7:1–10.
- Cardoso P., Arnedo M.A., Triantis K.A., Borges P.A.V. 2010. Drivers of diversity in Macaronesian spiders and the role of species extinctions. *J. Biogeogr.* 37:1034–1046.

- Cloudsley-Thompson J.L. 1975. Adaptations of Arthropoda to arid environments. *Annu. Rev. Entomol.* 20:261–283.
- Collyer M.L., Adams D.C. 2018. RRPP: An r package for fitting linear models to high-dimensional data using residual randomization. *Methods Ecol. Evol.* 9:1772–1779.
- Collyer M.L., Adams D.C. 2021. RRPP. Linear Model Evaluation with Randomized Residuals in a Permutation Procedure. .
- Collyer M.L., Davis M.A., Adams D.C. 2020. Making Heads or Tails of Combined Landmark Configurations in Geometric Morphometric Data. *Evol. Biol.* 47:193–205.
- Cope E.D. 1896. *The Primary Factors of Organic Evolution*. The Open Court Publishing Company, Chicago.
- Crespo L.C., Silva I., Enguídanos A., Cardoso P., Arnedo M.A. 2020. Integrative taxonomic revision of the woodlouse-hunter spider genus *Dysdera* (Araneae ; Dysderidae) in the Madeira archipelago with notes on its conservation status. *Zool. J. Linn. Soc.* XX:1–60.
- Crespo L.C., Silva I., Enguídanos A., Cardoso P., Arnedo M.A. 2021. The Atlantic connection: coastal habitat favoured long distance dispersal and colonization of Azores and Madeira by *Dysdera* spiders (Araneae: Dysderidae). *Syst. Biodivers.* 19:1–22.
- Darwin C.R. 1859. *On the Origin of Species by Means of Natural Selection, or the Preservation of Favoured Races in the Struggle for Life*. London: John Murray Publishers.
- Day E.H., Hua X., Bromham L. 2016. Is specialization an evolutionary dead end? Testing for differences in speciation, extinction and trait transition rates across diverse phylogenies of specialists and generalists. *J. Evol. Biol.* 29:1257–1267.
- Deeleman-Reinhold C.L., Deeleman P.R. 1988. Revision des Dysderinae (Araneae, Dysderidae), les espèces méditerranéennes occidentales exceptées. *Tijdschr. voor Entomol.* 131:141–269.
- Ebenhard T. 1991. Colonization in metapopulations: a review of theory and observations. *Biol. J. Linn. Soc.* 42:105–121.
- Emerson B.C., Kolm N. 2005. Species diversity can drive speciation. *Nature.* 434:1015–1016.
- Felsenstein J. 1988. Phylogenies And Quantitative Characters. *Annu. Rev. Ecol. Syst.* 19:445–471.
- Fernández R., Kallal R.J., Dimitrov D., Ballesteros J.A., Arnedo M.A., Giribet G., Hormiga G. 2018. Phylogenomics, Diversification Dynamics, and Comparative Transcriptomics across the Spider Tree of Life. *Curr. Biol.* 28:1489-1497.e5.
- Ferry-Graham L.A., Bolnick D.I., Wainwright P.C. 2002. Using functional morphology to examine the ecology and evolution of specialization. *Integr. Comp. Biol.* 42:265–277.
- Fitzjohn R.G., Maddison W.P., Otto S.P. 2009. Estimating trait-dependent speciation and extinction rates

from incompletely resolved phylogenies. *Syst. Biol.* 58:595–611.

Garrison N.L., Rodriguez J., Agnarsson I., Coddington J.A., Griswold C.E., Hamilton C.A., Hedin M., Kocot K.M., Ledford J.M., Bond J.E. 2016. Spider phylogenomics: Untangling the Spider Tree of Life. *PeerJ*. 2016.

Gavrilets S., Losos J.B. 2009. Adaptive Radiation: Contrasting theory with data. *Science* (80-). 323:732–737.

Gillespie R. 2004. Community Assembly Through Adaptive Radiation in Hawaiian Spiders. *Science* (80-). 303:356–359.

Gillespie R.G. 2016. Island time and the interplay between ecology and evolution in species diversification. *Evol. Appl.* 9:53–73.

Gillespie R.G., Bennett G.M., De Meester L., Feder J.L., Fleischer R.C., Harmon L.J., Hendry A.P., Knape M.L., Mallet J., Martin C., Parent C.E., Patton A.H., Pfennig K.S., Rubinoff D., Schluter D., Seehausen O., Shaw K.L., Stacy E., Stervander M., Stroud J.T., Wagner C., Wogan G.O.U. 2020. Comparing Adaptive Radiations Across Space, Time, and Taxa. *J. Hered.* 111:1–20.

Givnish T.J., Sytsma K.J. 1997. *Molecular evolution and adaptive radiation*. Cambridge: Cambridge University Press.

Glor R.E. 2010. Phylogenetic insights on adaptive radiation. *Annu. Rev. Ecol. Evol. Syst.* 41:251–270.

Goldberg E.E., Igić B. 2008. On phylogenetic tests of irreversible evolution. *Evolution* (N. Y). 62:2727–2741.

Gower J.C. 1975. Generalized procrustes Analysis. *Psychometrika*. 40:33–51.

Haldane J.B.S. 1951. *Everything has a History*. Allen & Unwin, London.

Harvey P.H., Pagel M.D. 1991. *The comparative method in evolutionary biology*. Oxford University Press, Oxford, UK.

Hendrickx F., Maelfait J.P., Lens L. 2003. Relationship between fluctuating asymmetry and fitness within and between stressed and unstressed populations of the wolf spider *Pirata piraticus*. *J. Evol. Biol.* 16:1270–1279.

Hopkin S.P., Martin M.H. 1985. Assimilation of zinc, cadmium, lead, copper, and iron by the spider *Dysdera crocata*, a predator of woodlice. *Bull. Environ. Contam. Toxicol.* 34:183–187.

Hulsey C.D., Alfaro M.E., Zheng J., Meyer A., Holzman R. 2019. Pleiotropic jaw morphology links the evolution of mechanical modularity and functional feeding convergence in Lake Malawi cichlids. *Proc. R. Soc. B Biol. Sci.* 286.

Irschick D.J., Higham T.E. 2015. *Animal Athletes: an Ecological and Evolutionary Approach*. Oxford Univ. Press.

- James Rohlf F., Marcus L.F. 1993. A revolution morphometrics. *Trends Ecol. Evol.* 8:129–132.
- Kallal R.J., Kulkarni S.S., Dimitrov D., Benavides L.R., Arnedo M.A., Giribet G., Hormiga G. 2021. Converging on the orb: denser taxon sampling elucidates spider phylogeny and new analytical methods support repeated evolution of the orb web. *Cladistics.* 37:298–316.
- Katoh K., Standley D.M. 2013. MAFFT multiple sequence alignment software version 7: Improvements in performance and usability. *Mol. Biol. Evol.* 30:772–780.
- Kelley N.P., Motani R. 2015. Trophic convergence drives morphological convergence in marine tetrapods. *Biol. Lett.* 11:2–6.
- Kelley S.T., Farrell B.D. 1998. Is specialization a dead end? The phylogeny of host use in *Dendroctonus* bark beetles (scolytidae). *Evolution (N. Y.)*. 52:1731–1743.
- Kolbe J.J., Revell L.J., Szekely B., Brodie E.D., Losos J.B. 2011. Convergent evolution of phenotypic integration and its alignment with morphological diversification in caribbean *Anolis* ecomorphs. *Evolution (N. Y.)*. 65:3608–3624.
- Kulkarni S., Kallal R.J., Wood H., Dimitrov D., Giribet G., Hormiga G. 2021. Interrogating Genomic-Scale Data to Resolve Recalcitrant Nodes in the Spider Tree of Life. *Mol. Biol. Evol.* 38:891–903.
- Kulkarni S., Wood H., Lloyd M., Hormiga G. 2020. Spider-specific probe set for ultraconserved elements offers new perspectives on the evolutionary history of spiders (Arachnida, Araneae). *Mol. Ecol. Resour.* 20:185–203.
- Lanfear R., Frandsen P.B., Wright A.M., Senfeld T., Calcott B. 2017. Partitionfinder 2: New methods for selecting partitioned models of evolution for molecular and morphological phylogenetic analyses. *Mol. Biol. Evol.* 34:772–773.
- Lanyon S.M. 1992. Interspecific brood parasitism in blackbirds (Icterinae): a phylogenetic perspective. *Science (80-)*. 255:77–79.
- Levins R., MacArthur R. 1969. An Hypothesis to Explain the Incidence of Monophagy. *Ecology.* 50:910–911.
- Losos J.B. 2011. Convergence, adaptation, and constraint. *Evolution (N. Y.)*. 65:1827–1840.
- Losos J.B., Jackman T.R., Larson A., De Queiroz K., Rodríguez-Schettino L. 1998. Contingency and determinism in replicated adaptive radiations of island lizards. *Science (80-)*. 279:2115–2118.
- Losos J.B., Leal M., Glor R.E., De Queiroz K., Hertz P.E., Rodríguez Schettino L., Chamizo Lara A., Jackman T.R., Larson A. 2003. Niche lability in the evolution of a Caribbean lizard community. *Nature.* 424:542–545.
- Losos J.B., Schluter D. 2000. Analysis of an evolutionary species-area relationship. 408:847–850.
- Macías-Hernández N., López S. de la C., Roca-Cusachs M., Oromí P., Arnedo M.A. 2016. A geographical

- distribution database of the genus *Dysdera* in the Canary Islands (Araneae, Dysderidae). *Zookeys*. 2016:11–23.
- Macías-Hernández N., Oromí P., Arnedo M.A. 2008. Patterns of diversification on old volcanic islands as revealed by the woodlouse-hunter spider genus *Dysdera* (Araneae, Dysderidae) in the eastern Canary Islands. :589–615.
- Mahler D.L., Ingram T., Revell L.J., Losos J.B. 2013. Exceptional convergence on the macroevolutionary landscape in island lizard radiations. *Science* (80-). 341:292–295.
- Martinez Q., Lebrun R., Achmadi A.S., Esselstyn J.A., Evans A.R., Heaney L.R., Miguez R.P., Rowe K.C., Fabre P.H. 2018. Convergent evolution of an extreme dietary specialisation, the olfactory system of worm-eating rodents. *Sci. Rep.* 8:1–13.
- De Meyer J., Irschick D.J., Vanhooydonck B., Losos J.B., Adriaens D., Herrel A. 2019. The role of bite force in the evolution of head shape and head shape dimorphism in *Anolis* lizards. *Funct. Ecol.* 33:2191–2202.
- Michalik P., Hormiga G., Kallal R., Giribet G. 2019. Phylogenomics and genital morphology of cave raptor spiders (Araneae, Trogloraptoridae) reveal an independent origin of a flow-through female genital system. *J. Zool. Syst. Evol. Res.* 57:737–747.
- Mitteroecker P., Gunz P. 2009. Advances in Geometric morphometrics. *Evol. Biol.* 36:235–247.
- Muller A. 1996. Host-Plant Specialization in Western Palearctic Anthidine Bees (Hymenoptera: Apoidea: Megachilidae). *Ecol. Monogr.* 66:235–257.
- Muschick M., Indermaur A., Salzburger W. 2012. Convergent Evolution within an Adaptive Radiation of Cichlid Fishes. *Curr. Biol.* 22:2362–2368.
- Naik H., Kgaditse M.M., Alexander G.J. 2021. Ancestral Reconstruction of Diet and Fang Condition in the Lamprophiidae: Implications for the Evolution of Venom Systems in Snakes. *J. Herpetol.* 55:1–10.
- Nosil P. 2002. Transition rates between specialization and generalization in phytophagous insects. *Evolution* (N. Y). 56:1701–1706.
- Nosil P., Crespi B.J., Sandoval C.P. 2002. Host-plant adaptation drives the parallel evolution of reproductive isolation. *Nature.* 417:440–443.
- Nosil P., Mooers A.Ø. 2005. Testing hypotheses about eco- logical specialization using phylogenetic trees. *Evolution* (N. Y). 59:2256–2263.
- Ord T.J., Stamps J.A., Losos J.B. 2013. Convergent evolution in the territorial communication of a classic adaptive radiation: Caribbean *Anolis* lizards. *Anim. Behav.* 85:1415–1426.
- Paradis E., Schliep K. 2019. Ape 5.0: An environment for modern phylogenetics and evolutionary analyses in R. *Bioinformatics.* 35:526–528.

- Pascoal S., Cezard T., Eik-Nes A., Gharbi K., Majewska J., Payne E., Ritchie M.G., Zuk M., Bailey N.W. 2014. Rapid convergent evolution in wild crickets. *Curr. Biol.* 24:1369–1374.
- Pekar S., Coddington J., Blackledge T. 2011. Evolution of stenophagy in spiders (Araneae): evidence based on the comparative analysis of spider diets. *Evolution (N. Y.)*. 66:776.
- Pekár S., Líznavá E., Řezáč M. 2016. Suitability of woodlice prey for generalist and specialist spider predators: A comparative study. *Ecol. Entomol.* 41:123–130.
- Piechnik D.A., Lawler S.P., Martinez N.D. 2008. Food-web assembly during a classic biogeographic study: Species' "trophic breadth" corresponds to colonization order. *Oikos*. 117:665–674.
- Plăiașu R., Băncilă R.I. 2018. Fluctuating asymmetry as a bio-marker to account for in conservation and management of cave-dwelling species. *J. Insect Conserv.* 22:221–229.
- Ramírez M.J., Magalhaes I.L.F., Derkarabetian S., Ledford J., Griswold C.E., Wood H.M., Hedin M. 2021. Sequence capture phylogenomics of true spiders reveals convergent evolution of respiratory systems. *Syst. Biol.* 70:14–20.
- Raupach M.J. 2005. Die bedeutung von landasselnalsbeutetiere für insekten un andere arthropoden. *Entomol. heute*. 17:3–12.
- Revell L.J. 2012. phytools: An R package for phylogenetic comparative biology (and other things). *Methods Ecol. Evol.* 3:217–223.
- Revell L.J., Harmon L.J., Collar D.C. 2008. Phylogenetic signal, evolutionary process, and rate. *Syst. Biol.* 57:591–601.
- Reynolds R.G., Collar D.C., Pasachnik S.A., Niemiller M.L., Puente-Rolón A.R., Revell L.J. 2016. Ecological specialization and morphological diversification in Greater Antillean boas. *Evolution*. 70:1882–1895.
- Řezáč M., Pekár S. 2007. Evidence for woodlice-specialization in *Dysdera* spiders: Behavioural versus developmental approaches. *Physiol. Entomol.* 32:367–371.
- Řezáč M., Pekár S., Arnedo M., Macías-Hernández N., Řezáčová V. 2021. Evolutionary insights into the eco-phenotypic diversification of *Dysdera* spiders in the Canary Islands. *Org. Divers. Evol.*
- Řezáč M., Pekár S., Lubin Y. 2008. How oniscophagous spiders overcome woodlouse armour. *J. Zool.* 275:64–71.
- Ribera C., Arnedo M.A. 1994. Description of *Dysdera gollumi* (Araneae, Haplogynae), a new troglobitic species from Tenerife, Canary Islands, with some comments on Canarian *Dysdera*. *Mémoires de Biospéologie*. 21:115–119.
- Ribera C., Fernandez M.A., Blasco A. 1985. Araneidos cavernícolas de Canarias II. *Mémoires de Biospéologie*. 51–68.

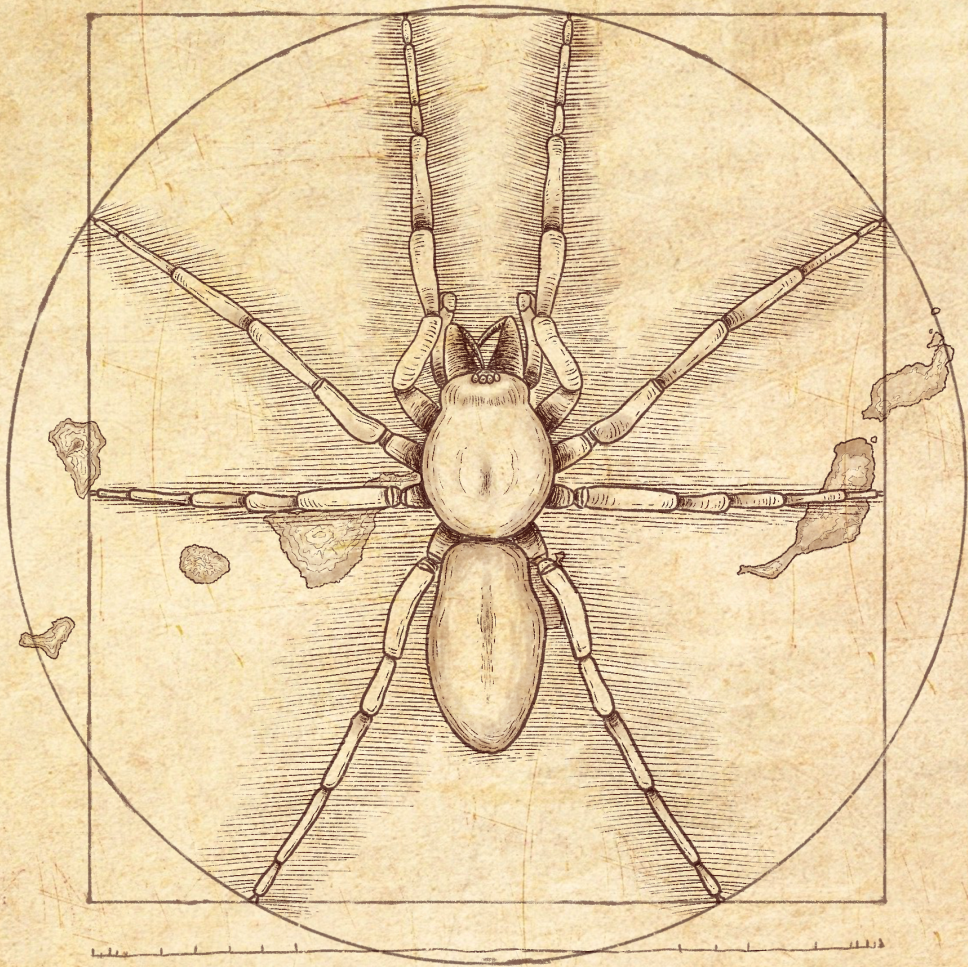
- Rohlf F.J. 2015. The tps series of software. *Hystrix*. 26:9–12.
- Rohlf F.J., Slice D. 1990. Extensions of the procrustes method for the optimal superimposition of landmarks. *Syst. Zool.* 39:40–59.
- Rüber L., Verheyen E., Meyer A. 1999. Replicated evolution of trophic specializations in an endemic cichlid fish lineage from Lake Tanganyika. *Proc. Natl. Acad. Sci. U. S. A.* 96:10230–10235.
- Rundle H.D., Nagel L., Boughman J.W., Schluter D. 2000. Natural selection and parallel speciation in sympatric sticklebacks. *Science* (80-). 287:306–308.
- Schluter D. 2000. *The Ecology of Adaptive Radiation*. Oxford University Press, Oxford.
- Schluter D., Nagel L.M. 1995. Parallel Speciation by Natural Selection. *Am. Nat.* 146:292–301.
- Stayton C.T. 2015. The definition, recognition, and interpretation of convergent evolution, and two new measures for quantifying and assessing the significance of convergence. *Evolution* (N. Y). 69:2140–2153.
- Stayton C.T. 2018. *convevol: Analysis of Convergent Evolution*. R package version 1.3, <<https://CRAN.R-project.org/package=convevol>>. .
- Stephens P.R., Wiens J.J. 2003. Ecological diversification and phylogeny of emydid turtles. *Biol. J. Linn. Soc.* 79:577–610.
- Stiassny M.L.J., Meyer A. 1999. Cichlids of the Rift Lakes. *Sci. Am.* 280:64–69.
- Sunderland K.D., Sutton S.L. 1980. *A Serological Study of Arthropod Predation on Woodlice in a Dune Grassland Ecosystem* Author (s): Keith D . Sunderland and Stephen L . Sutton Published by: British Ecological Society Stable URL: <http://www.jstor.org/stable/4240> Accessed: 22-04-2016 02. *J. Anim. Ecol.* 49:987–1004.
- Toft C. 1995. Evolution of Diet Specialization in Poison-Dart Frogs (*Dendrobatidae*). *Herpetologica*. 51:202–216.
- Toft S., Macías-Hernández N. 2017. Metabolic adaptations for isopod specialization in three species of *Dysdera* spiders from the Canary Islands. *Physiol. Entomol.* 42:191–198.
- Toft S., Macías-Hernández N. 2021. Prey acceptance and metabolic specialisations in some Canary *Dysdera* spiders. *J. Insect Physiol.* 131:104227.
- Uetz G.W., Roberts J.A., Wrinn K.M., Polak M., Cameron G.N. 2009. Impact of a catastrophic natural disturbance on fluctuating asymmetry (fa) in a wolf spider. *Ecoscience*. 16:379–386.
- Vamosi J.C., Scott Armbruster W., Scott Armbruster W., Scott Armbruster W., Renner S.S. 2014. Evolutionary ecology of specialization: Insights from phylogenetic analysis. *Proc. R. Soc. B Biol. Sci.* 281.
- Wheeler W.C., Coddington J.A., Crowley L.M., Dimitrov D., Goloboff P.A., Griswold C.E., Hormiga G.,

Prendini L., Ramírez M.J., Sierwald P., Almeida-Silva L., Alvarez-Padilla F., Arnedo M.A., Benavides Silva L.R., Benjamin S.P., Bond J.E., Grismado C.J., Hasan E., Hedin M., Izquierdo M.A., Labarque F.M., Ledford J., Lopardo L., Maddison W.P., Miller J.A., Piacentini L.N., Platnick N.I., Polotow D., Silva-Dávila D., Scharff N., Szűts T., Ubick D., Vink C.J., Wood H.M., Zhang J. 2017. The spider tree of life: phylogeny of Araneae based on target-gene analyses from an extensive taxon sampling. *Cladistics*. 33:574–616.

Wiens J.J., Graham C.H. 2005. Niche conservatism: Integrating evolution, ecology, and conservation biology. *Annu. Rev. Ecol. Evol. Syst.* 36:519–539.

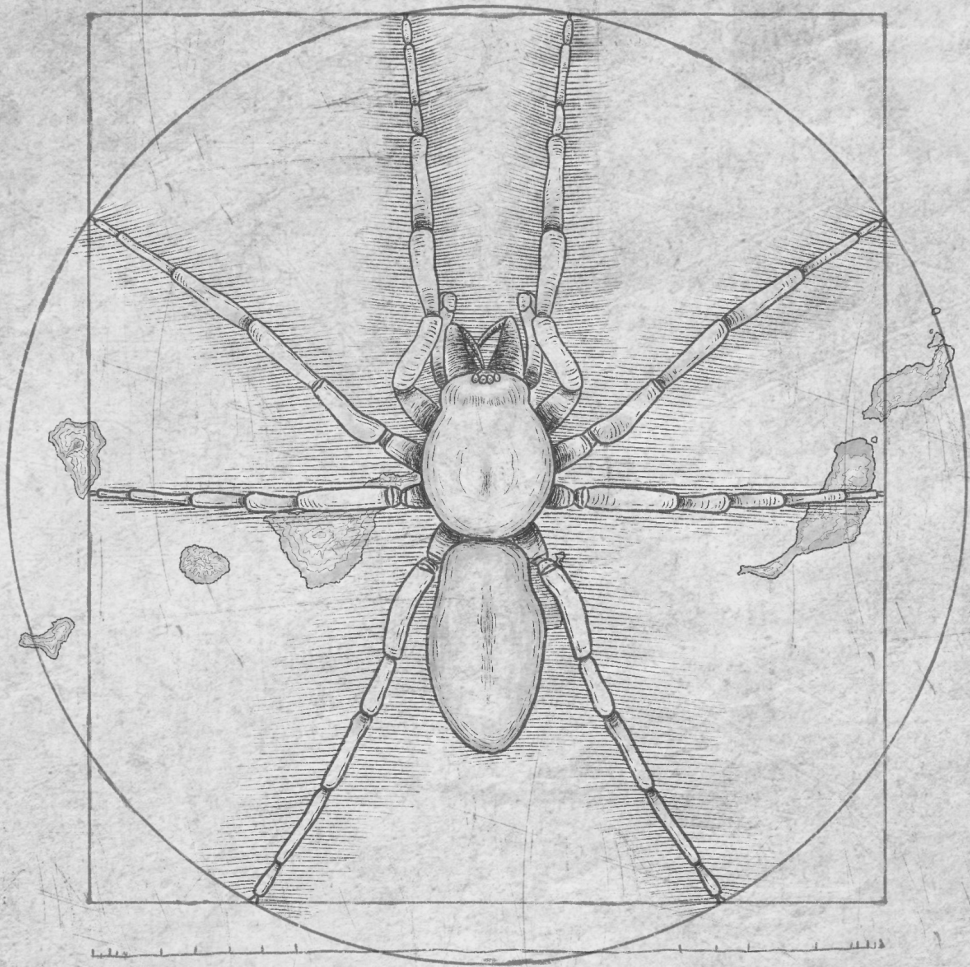
Zelditch M.L., Swiderski D.L., Sheets H.D., Fink W.L. 2004. *Geometric morphometrics for biologists: A primer*. New York: Elsevier Academic Press.

Zelditch M.L., Ye J., Mitchell J.S., Swiderski D.L. 2017. Rare ecomorphological convergence on a complex adaptive landscape: Body size and diet mediate evolution of jaw shape in squirrels (Sciuridae). *Evolution* (N. Y). 71:633–649.



CHAPTER 3

Diversification patterns in the red devil spiders (Araneae:
Dysderidae) of the Canary Islands



CHAPTER 3.1

Tempo and mode of diversification of the red devil spiders

(Araneae: Dysderidae) of the Canary Islands

Tempo and mode of diversification of the red devil spiders (Araneae: Dysderidae) of the Canary Islands

Adrià Bellvert^{1,2}, Jairo Patiño³, Laura Pollock⁴, Antigoni Kaliontzopoulou^{1,2} & Miquel A. Arnedo^{1,2}.

1 Departament de Biologia Evolutiva, Ecologia i Ciències Ambientals, Universitat de Barcelona (UB), Av. Diagonal, 643, 08028 Barcelona, Spain.

2 Institut de Recerca de la Biodiversitat (IRBio), Universitat de Barcelona (UB), Barcelona, Spain.

3 Instituto de Productos Naturales y Agrobiología (IPNA-CSIC), La Laguna, Spain

4 Department of Biology, McGill University, Montreal, Canada

Abstract

The study of adaptive radiations have shed light on our current understanding of evolution. However, few unifying mechanisms have been identified across different taxa and geographic and ecological systems. Previous studies examining the mode in which species diversified, how diversification rates varied, and how ecological specialization affected these processes have reached different conclusion. To gain a more complete picture of how species evolve, additional model systems that encompass alternative ecological requirements are needed. Here, we present the results of a study aimed to unravel the diversification mode and evolutionary drivers of the spider genus *Dysdera*, the red devil spiders, endemic to the Canary Islands. These species exhibit remarkable phenotypic variability in their mouthparts, which has been related to different levels of specialization in the predation of isopods. We explored patterns of lineage diversification and assessed the role of trophic specialization as a driver of species diversification. Additionally, we used climatic variables, occurrence data and morphological information to unravel the underlying mode of speciation by means of joint species distribution models and age-range correlation methods. Our results reveal that red devil spiders underwent an early burst of diversification, followed by a slowdown of diversification rates, which is a hallmark of adaptive radiation. We also found evidence that the trophic morphology shaped diversification, with specialist species exhibiting higher rates of diversification. Finally, our analyses suggest that speciation occurred mostly in allopatry, with subsequent secondary sympatry following range expansion.

Keywords: Adaptive radiation, diversification rates, phylogenetic comparative methods, allopatric speciation

Introduction

Evolutionary radiations, these are periods of accelerated species diversification, have been a prominent feature of life's history on Earth (Linder & Bouchenak-Khelladi 2017). Among these, adaptive radiations – the diversification of ecologically and phenotypically distinct species from a common ancestor (Futuyma 1998; Schluter 2000) – have garnered significant attention due to their importance in shaping the planet's biodiversity (Glor 2010; Harmon *et al.* 2010). Not surprisingly, the study of one of these radiations, the Darwin finches in the Galapagos Islands, was seminal for the development of the theory of evolution by natural selection (Darwin 1859). Indeed, the study of these events offers a unique opportunity to explore the mechanisms of species evolution and the complex relationships among extant species diversity (Givnish & Sytsma 1997; Losos & Mahler 2010). While adaptive radiations are observed in various environments, young and isolated geographic regions such as volcanic islands or glacial lakes offer ideal conditions for studying these phenomena (Schluter 2000) and have been instrumental in advancing our understanding of speciation and other evolutionary processes (Gillespie *et al.* 2020). As a result, many of the most well-known cases of adaptive radiation have occurred in isolated regions (Harmon *et al.* 2010; Patton *et al.* 2021; Cerca *et al.* 2023), including *Tethragnatha* spiders in the Hawaiian Islands (Gillespie 2004), cichlid fishes in the African lakes (Takahashi & Koblmüller 2011), the anoles lizards in the Caribbean (Losos 2009) and the aforementioned Darwin's finches from the Galapagos (Lack 1947), to mention just a few. Hypotheses on what triggers these adaptive radiations have been mainly focused on ecological opportunity, i.e. the availability of new ecological resources not previously accessible (see Stroud & Losos 2016 for a review). Such ecological opportunities may emerge under different circumstances (Simpson 1953), but the colonization of oceanic islands, which are usually more species-depauperate, have provided the clearer examples (Stroud & Losos 2016; Gillespie *et al.* 2020). In this

context, specific traits that allow lineages to enter new “adaptive zones” (Simpson 1944) and promote ecological specialization (Heard & Hauser 1995), the so called “key innovations”, have also been a central element in the discussion of adaptive radiations, as they have been linked to increased species diversification rates (Simpson 1944; Mayr 1963; Losos & Mahler 2010; Wellborn & Langerhans 2015).

Despite the importance of adaptive radiations in shaping Earth’s biodiversity, our understanding of the detailed underlying mechanisms remains incomplete. While the evolution of ecologically and phenotypically distinct species from a common ancestor is the signature of adaptive radiations (Futuyma 1986), few other common processes have emerged from studies of these patterns. For instance, exploring associations between lineage and phenotypic diversification has produced mixed results when studying continental adaptive radiations, with asymmetric diversification between these two patterns (see Pincheira-Donoso *et al.* 2015), and the typical pattern of an early burst followed by a slowdown in lineage diversification (Phillimore & Price 2008; Rabosky & Lovette 2008; Harmon *et al.* 2010), has lacked support in cases where secondary factors could have erased this typical signature (Slater *et al.* 2010). Such inconsistencies suggest that the dynamics of adaptive radiations are more complex than previously thought. Similarly, studies of the macroevolutionary consequences of ecological specialization on species diversification have also yielded disparate results. Historically seen as an evolutionary dead-end, specialist species, or lineages, have been hypothesized to exhibit lower diversification rates than generalists, evolving from them but not in reverse (Schluter 2000; Day *et al.* 2016). However, several studies have shown that both irreversibility and lower diversification rates assumed for specialist species are far from being a general pattern (Nosil 2002; Nosil & Mooers 2005).

The actual drivers of speciation are another potential source of conflict among different adaptive radiation processes. Historically, the widespread view was that

speciation was mainly triggered by geographic isolation (Mayr 1963), that is, obliteration of gene flow coupled with time. However, with the rise of molecular phylogenetics and the use of more sophisticated comparative methods, that allows for quantitative detection of post-speciation range shifts (e.g. age-range correlation methods), it has become evident that the actual mechanisms underlying geographic patterns of species diversification could be more complex. Indeed, several studies have found evidence of sympatric speciation and thus of the potential involvement of natural or sexual selection in the actual speciation process (Bolnick & Fitzpatrick 2007). Comparative methods assessing the relationship between distribution overlapping and phylogenetic relatedness, are based on the assumption that, following the initial speciation stage, the geographical distribution of species becomes randomized due to their dispersal capabilities (Barraclough & Vogler 2000). In cases where a species clade undergoes allopatric diversification, the overlap between their ranges would initially be zero. However, over time, as their ranges randomly change, the overlap increases, resulting in a positive correlation between range overlap and older stages in the species' phylogenetic relationships, relative to more recent cladogenetic events (Fitzpatrick & Turelli 2006). However, it is important to note that these correlations can be misleading when species clades exhibit complex patterns of geographical speciation (Fitzpatrick & Turelli 2006). For example, the randomizations in post-speciation range shifts may be compromised when species experience secondary contact after the original speciation process, as observed in numerous cases of island clade diversification (e.g. Thorpe *et al.* 2010; Macías-Hernández *et al.* 2013).

Given the intricate temporal, ecological and geographic variation in species diversification patterns and processes observed across different species groups, additional model systems that encompass alternative ecological requirements are needed to obtain a more complete understanding of how species emerge and evolve.

The Canary Islands form a volcanic archipelago that includes seven major islands and several islets located 100 kilometres of the north-west of the African coast (Fig. 1A). The islands are geochronologically arranged, with the oldest ones, Lanzarote and Fuerteventura (15 My and 23 My respectively), lying at the easternmost side, and becoming progressively younger towards the western end (from east to west): Gran Canaria (subaerial age 15 My), Tenerife (12 My), La Gomera (11 My), La Palma (1.7 My) and El Hierro (1.1 My) (Van Den Bogaard 2013). These islands have been home to a remarkable diversification in the red devil spiders of the genus *Dysdera* (Fig. 1B), with approximately 60 endemic species recorded in the archipelago (Bellvert *et al.* in prep) out of a total of 300 currently described species (World Spider Catalog 2023). These

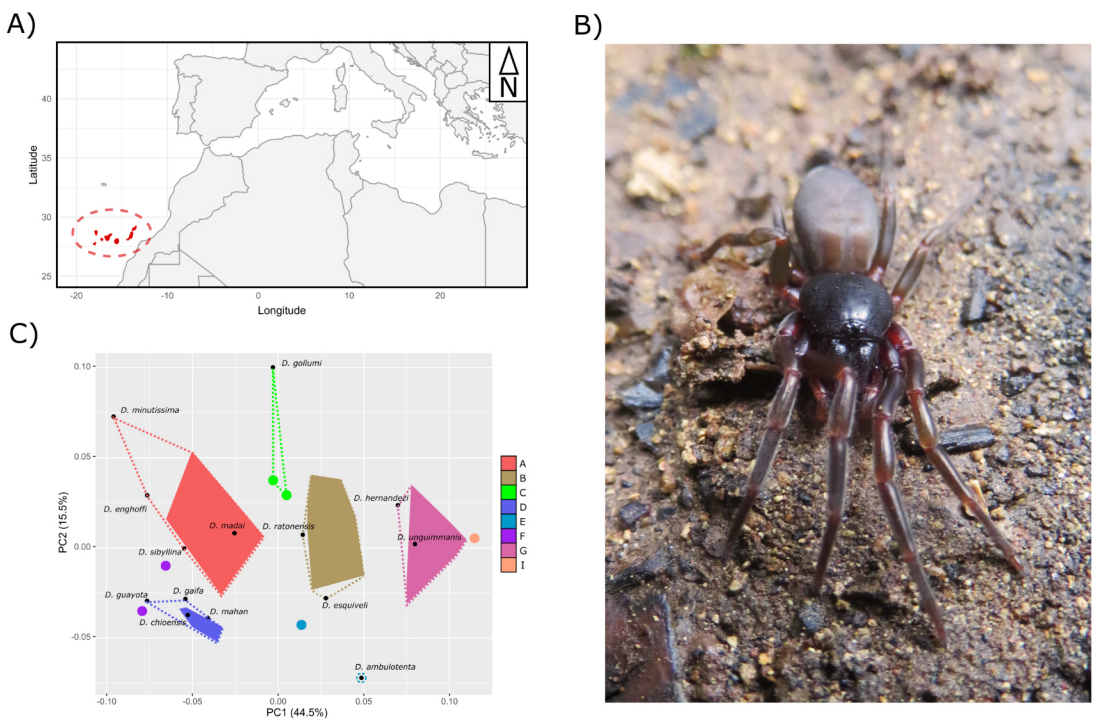


Figure 1. A) Map of the Canary Islands. B) *Dysdera verneauai* from the island of Tenerife (photo credit: Marc Domènech). C) Cheliceral morphospaces obtained with the two first principal components from the morphometric data used for this study from Bellvert *et al.* (2023), with densely-colored convex polygons depicting species of the same ecomorph group. Black dots represent the species not included in the previous study but with morphometric data. Colored dots represent species already previously linked to cheliceral shape but without enough species to build a polygon. Dotted lines represent the change in the cheliceral type polygon space once the species have been assigned to the preexisting cheliceral types by means of the LDA performed in the present study.

species exhibit remarkable phenotypic variation in their cheliceral morphology—the spiders' mouth parts, which has been linked to different levels of trophic specialization (Řezáč *et al.* 2008, 2021; Toft & Macías-Hernández 2017, 2021). Different cheliceral morphologies evolved independently several times during the diversification of the group in the islands (Bellvert *et al.* in press). Because of the single colonization event inferred for these species (but see Adrián-Serrano *et al.* 2020) and the eco-phenotypic differences observed among relatives, this genus has been suggested to be a case of adaptive radiation in the islands (Bellvert *et al.* in press), but this hypothesis has never been formally tested and the exact evolutionary drivers of this diversification remain poorly understood.

In the present study, we used phylogenetic comparative methods and joint species distribution modelling to elucidate the mechanisms underlying the diversification of *Dysdera* spiders in the Canary Islands and examine how it has been influenced by trophic specialization. Our specific objectives were: 1) to test if the temporal pattern of lineage diversification of the group aligns with that expected under a scenario of adaptive radiation, i.e. an early rapid diversification of lineages with a subsequent deceleration (Glor, 2010); 2) to explore whether trophic specialization played a role in this diversification; and 3) to investigate whether allopatry followed by secondary overlapping drove the diversification of these species, similarly to other cases of adaptive radiation in oceanic islands. We conducted a comprehensive study by integrating the fully resolved phylogeny of the group with phenotypic data, occurrence records, and climatic variables. Our investigation aimed to understand the mode and tempo of the genus' evolution in the archipelago, as well as to identify the factors that potentially played a role in its remarkable diversification.

Methods

Specimens and data collection

All specimens used came from field campaigns conducted by the authors and other colleagues and are stored at the Centre de Recursos de Biodiversitat Animal of the Universitat de Barcelona (CRBA) and Departamento de Zoología de la Universidad de La Laguna, Tenerife, Canary Islands collection (DZUL). Individuals were captured by active searching under rocks, logs and tree barks. The captured specimens were preserved in 95% EtOH and stored at -20°C at the former institutions. All specimens were collected following institutional and governmental regulations and the permits for all species captured were granted by the local authorities of each island or by the governing body of each natural reserve. Phenotypic data for the present study came from Bellvert *et al.* (in press). We used the statistical environment R (R Core Team 2022) to conduct all subsequent analyses.

Species lineage diversification

To investigate the diversification mode in the *Dysdera* spiders from the Canary Islands, we used the complete phylogeny of the species from the archipelago from Bellvert *et al.* (in press). However, we removed the species *D. lancerotensis* as it seems to be an independent colonization and is not directly related with the rest of the Canarian species (Adrián-Serrano *et al.* 2020). To obtain a first view on how diversification proceeded across the history of the group, we extracted the branching times with the function *branching.times* from the R package “ape” (Paradis & Schliep 2019) and fitted different variable-rate and constant-rate models to this data using the function *fitdAICrc* from the R package “laser” (Rabosky & Schliep 2013) considering 100 shift points and 6 different models: pure birth, birth-death, an exponential and a logistic variant of density-dependent and speciation rate models, pure birth with a single rate shift and pure birth with two rate shifts. To visualize the number of lineages through time and obtain a summary of diversification rates we used a lineage-through-time plot produced with the function *ltt* from the R package “phytools” (Revell 2012). To consider phylogenetic uncertainty we repeated these analyses over 1000 trees

obtained from the posterior distribution from the study of Bellvert *et al.* (2023). Previous work has delimited, based on geometric morphometric methods, several cheliceral morphotypes that have evolved independently several times during the diversification of these species in the archipelago (Bellvert *et al.* in press), and which are hereby hypothesized to have potentially driven species diversification, specifically through their effect on the species trophic specialization, where certain cheliceral morphologies are associated with generalist predators, while other morphologies exhibit varying degrees of specialization in preying on isopods. However, not all the *Dysdera* diversity from the Canary Islands was represented in the aforementioned study, which only included 40 out of a total of 57 currently recognized species (Bellvert *et al.* in prep). Such undersampling could lead to a bias when analyzing evolutionary rates (Pybus & Harvey 2000) that could compromise the final results of the study. Some of the unrepresented species were due to lack of any specimen to obtain morphometric data; and had to be excluded from the study. However, other specimens were previously ignored because of a lack of intraspecific variation or because they belonged to other ecological regimes (see Bellvert *et al.* in press). To mitigate the effect of the undersampling on the diversification analyses conducted here, we used a Linear Discriminant Analysis (LDA) to classify the species with unknown cheliceral affiliation but with some morphometric data into the already established cheliceral morphotypes. We used the function *prep.lda* from the R package “RRPP” (Collyer & Adams 2018, 2021) to prepare the geometric morphometric data used in Bellvert *et al.* (2023) study and the function *lda* from the R package “MASS” (Venables & Ripley 2002) to run the discriminant analysis. For subsequent analyses, we pruned the complete phylogeny of the *Dysdera* spiders from the Canary Islands with the species with cheliceral type information from Bellvert *et al.* (2023) and the ones that we could recover from the discriminant analyses. We used the function *drop.tip* from the R package “ape” (Paradis & Schliep 2019) to remove all specimens without cheliceral type information from the phylogeny.

State dependent diversification models

To test if trophic specialization as represented by different cheliceral morphotypes increased or decreased the rate at which *Dysdera* species diversified, we fitted a BiSSE model where diversification and extinction rates varied freely between two distinct states of trophic strategy using the function *make.bisse* from the R package “diversitree” (Fitzjohn 2012). Binary states were obtained from Bellvert *et al.* (2023) which link the different cheliceral morphologies to generalist or specialist trophic strategies. We compared this model to a null model with equal diversification and extinction rates by extracting the loglikelihood of each model through the function *find.mle* and comparing both with the function *anova*. Furthermore, to test and visualize differences in diversification rates between trophic strategies, we used Bayesian inference to calculate the posterior distribution of our parameters with the function *mcmc* from the R package “coda” (Plummer *et al.* 2006).

However, it could be the case that cheliceral morphotype by itself, capturing the evolutionary influences of other pressures other than or in addition to trophic strategy, could have affected diversification rates. In order to test if the evolution of different cheliceral morphotypes, rather than their trophic strategy, have an impact on the diversification rates in the *Dysdera* species, an optimal approach would be to use a multi-state speciation and extinction model like MuSSE (Fitzjohn 2012). Unfortunately, in our data some cheliceral morphologies were only represented by one or two species, and the resulting MuSSE model would probably not be trustworthy. Instead, to investigate which cheliceral types, or combination of some of them, could have had a bigger influence on the *Dysdera* diversification, we ran independent BiSSE models for each possible pairwise combination of one specific morphotype vs. the rest within all eight cheliceral morphotypes. From each of these models, we calculated the percentage of times that each cheliceral type appeared in pairwise cheliceral combinations that were inferred to exhibit significantly different

diversification rates when compared to a null model with equal rates between states. We represented the percentage of times that each cheliceral morphotype appeared in significant pairwise combinations with significantly different diversification rates using a spider chart with the function *radarchart* from the R package “fmsb” (Nakazawa 2023). Finally, to examine which cheliceral combination maximized change in diversification rates, we ran a BiSSE model delimiting the binary state with the cheliceral types that showed a higher percentage of occurrence in the previous combinations. We compared a model with different diversification and extinction rates with a null model with equal rates, with the binary state representing each of the two cheliceral types with the highest percentages of occurrence on the one hand and the rest of types on the other. Next, we also examined a model with the binary state defined as the four cheliceral types with the highest percentages and the rest, and finally between the six cheliceral types with the highest percentage and the two cheliceral types that had exhibited significantly different rates at 0% of the previous comparisons (see results).

Note that a trait-state-dependent model with different diversification rates that performs better than a null one, does not necessarily mean that the examined trait is the main driver of the diversification of the group, as an unmeasured factor could have a stronger impact on the species’ diversification (Beaulieu & O’Meara 2016). To account for this possibility, for all previous models with the binary state delimited based on the cheliceral percentages in which the different-rates model performed better than the null, we fit three additional “hidden rate” models (Beaulieu & O’Meara 2016): one in which there is an influence on diversification rates of an unaccounted trait but not of the cheliceral type (CID-2), a four-level hidden rate model (CID-4), which will allow to test for more complex diversification processes (Revell & Harmon 2022), and a full model where both the hidden state and our cheliceral trait have an effect on the Canarian *Dysdera* spider diversification. We used the *hisse* function from

the R package “*hisse*” (Beaulieu & O’Meara 2016) to fit these models. We calculated the AIC of each model with the *AIC* function to test which performed best.

Time dependent diversification models

We tested if diversification rates varied through time in the radiation of the *Dysdera* spiders from the Canary Islands. We used the function *make.bd.t* from the R package “*diversitree*” (Fitzjohn 2012) to fit a model where diversification rates were an arbitrary function of time. We compared the time-dependent model to a null with a constant diversification rate fitting our data with the function *make.bd*. We obtained the maximum likelihood of each model with the function *find.mle* and compared between them with the *anova* function. We also used the *mcmc* function to run a Bayesian MCMC analysis for our time dependent model and plot the posterior distribution through time of speciation (λ) to see the general tendency that this parameter has.

Species overlap and age-range correlation

Finally, to unravel the main speciation pattern of these species in the islands—i.e. allopatric vs sympatric—we analyzed how the overlap between species distribution ranges changed through time. We used Age-range correlation methods (ARC), which seek to establish statistical relationships between species-pairs geographic overlap and the time since their divergence (Fitzpatrick & Turelli 2006). For the pairwise measurements of the niche overlap between species, we used joint species distribution modelling (jSDM) to obtain the residual patterns of occurrence between species, as they capture more complex interactions than other co-occurrence metrics could show (Pollock *et al.* 2014). Those residuals are those features that influence occurrence between species that are not explained by environmental variables. We decided to use these residuals, instead of the species shared environmental responses, because they explain better the difference between allopatric and sympatric species pairs (see results). We used all the species for which we had

sufficient morphometric data from Bellvert *et al.* (in press) (N = 40), and we considered the first two principal components of each species as the trait value for the model to also test for competitive exclusion in the biotic interactions captured by the residual correlations. For the species' occurrence, we built a presence matrix for each species for each locality where *Dysdera* spiders have been collected in the Canary Islands during the last 50 years. Finally, for the model explanatory variables, we selected the 3 different climatic predictors from Patiño (et al. under review) that we hypothesize may have a greater impact on the species' potential distribution, namely the highest temperature of any month, to include the potential effect of aridity; the accumulated precipitation over 1 year, to take into account the effect of the more humid areas; and elevation, which has an influence on temperature but also on the vegetation present in the island. We ran the model with the function *jSDM_binomial_probit* from the "jSDM" R package (Clément & Vieilledent 2022), with 10000 iterations with a burn-in of 5000 and a thinning rate of 20. We extracted the latent variables of the model and the correlation of the response matrix with the *get_residual_cor* and *get_enviro_cor* functions respectively. For the ARC analysis we used with the function *age.range.correlation* from the R package "phyloclim" (Heibl & Calange 2018). An observed negative slope to more distant relationships would point to a sympatric diversification, while a positive one would be indicative of an allopatric diversification (Fitzpatrick & Turelli 2006). We ran the model with 999 iterations to test for the statistical significance.

Results

Best macro-evolutionary candidate model

The gamma statistic exhibited a negative value (-6.18 ± 0.19), being significantly smaller than the expected under a birth death process which would have a normal distribution around 0 (Fig. 2A), which suggests rejection of the hypothesis of constant

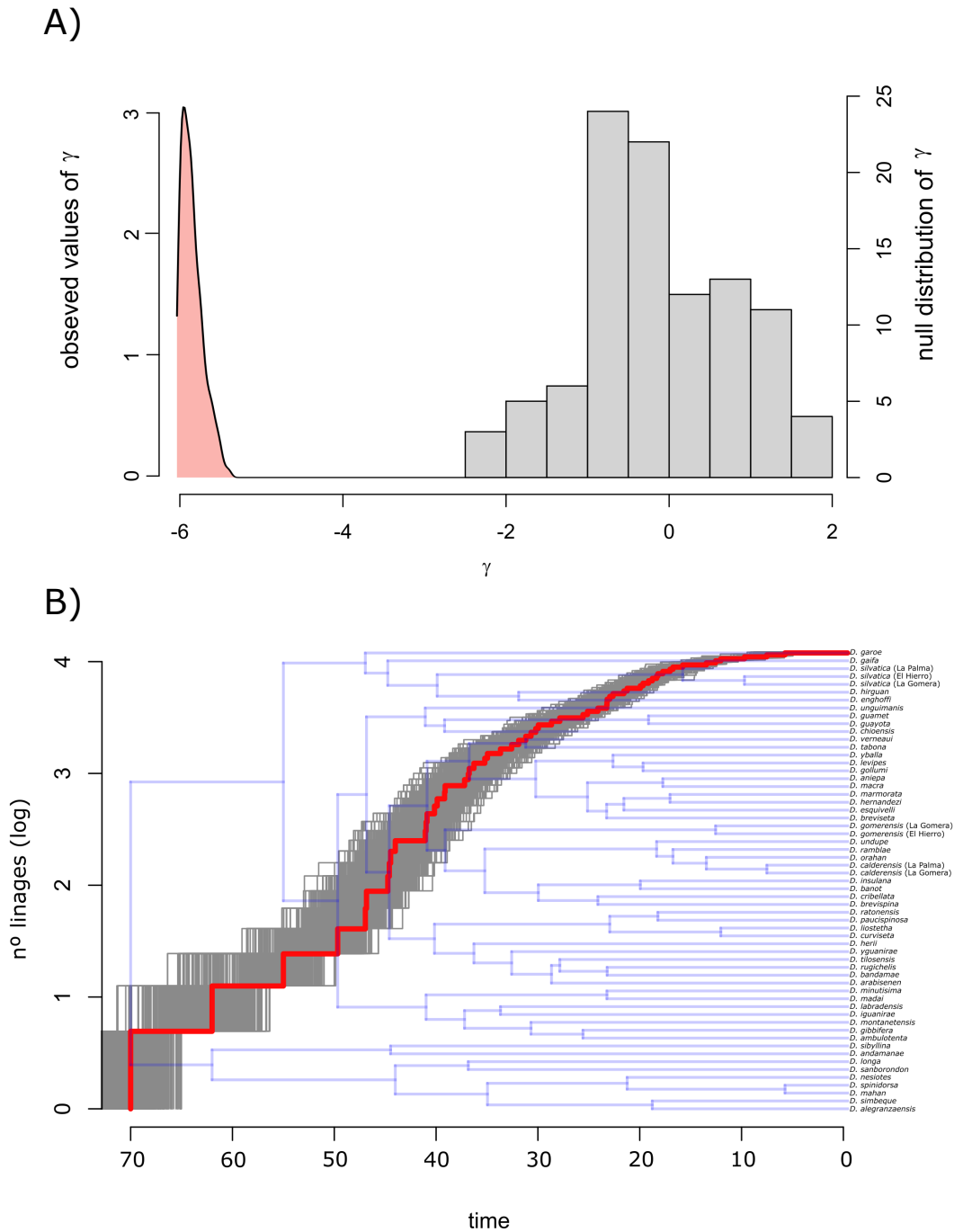


Figure 2. A) observed γ values for 1000 phylogenetic trees obtained from the posterior distribution (red), compared to the γ values from a null distribution under a pure birth model (grey histogram). B) LTT plot for the *Dysdera* species from the Canary Islands. The red line represents the LTT made with the consensus tree, grey lines are the LTTs from the 1000 phylogenetic trees from the posterior distribution used to take phylogenetic uncertainty into account.

rate in the diversification of the group in favor of decreasing diversification through time (Pybus & Harvey 2000). Accordingly, the LTT plot showed a clear hump-shaped increase in the number of lineages with a posterior stabilization (Fig. 2B). Finally, when contrasting different candidate diversification models, the density-dependent speciation model (DDL) showed the best performance with an AIC of 109.02 ± 4.38 , followed by the pure-birth model with two rate shifts (yule 3 rates, AIC = 113.24 ± 4.57), the pure-birth with one shift (yule 2 rates, AIC = 116.45 ± 4.88), the exponential variant of the density-dependent speciation model (DDX, AIC = 133.09 ± 4.38), the pure-birth model (AIC = 151.69 ± 3.31) and the birth-death model (AIC = 153.69 ± 3.31).

BiSSE state-dependent models

The results from the discriminant analysis and the cheliceral type adscription can be found in the supplementary material. The BiSSE model with trophic strategy as the binary state (specialist vs generalist) with free diversification rates (fr), performed poorly compared to the null model with equal rates between states (null), without significant differences between them ($AIC_{fr} = 502.20$, $AIC_{null} = 500.98$, p-value = 0.25). The Bayesian MCMC analysis, on the other hand, showed that the diversification rate of specialist species is higher than that of generalist ones, but not significantly so (p-value = 0.062). When examining all pairwise combinations of binary states among cheliceral types, we found that for 25 out of 254 possible pairwise combinations the model with free diversification rates performed better as compared to the null model with equal rates between states (Table S2 of the supplementary material). From the cheliceral combinations, type G was among the cheliceral morphologies that exhibited a higher diversification rate in 72% of the cases, type B exhibited a higher rate in 68% of the cases, type I in 60% of the cases, type C in a 48%, types F and E in 44% of the cases, while types A and D were never part of the higher diversification rate sets. When creating groups of several cheliceral types to generate the binary state trait for

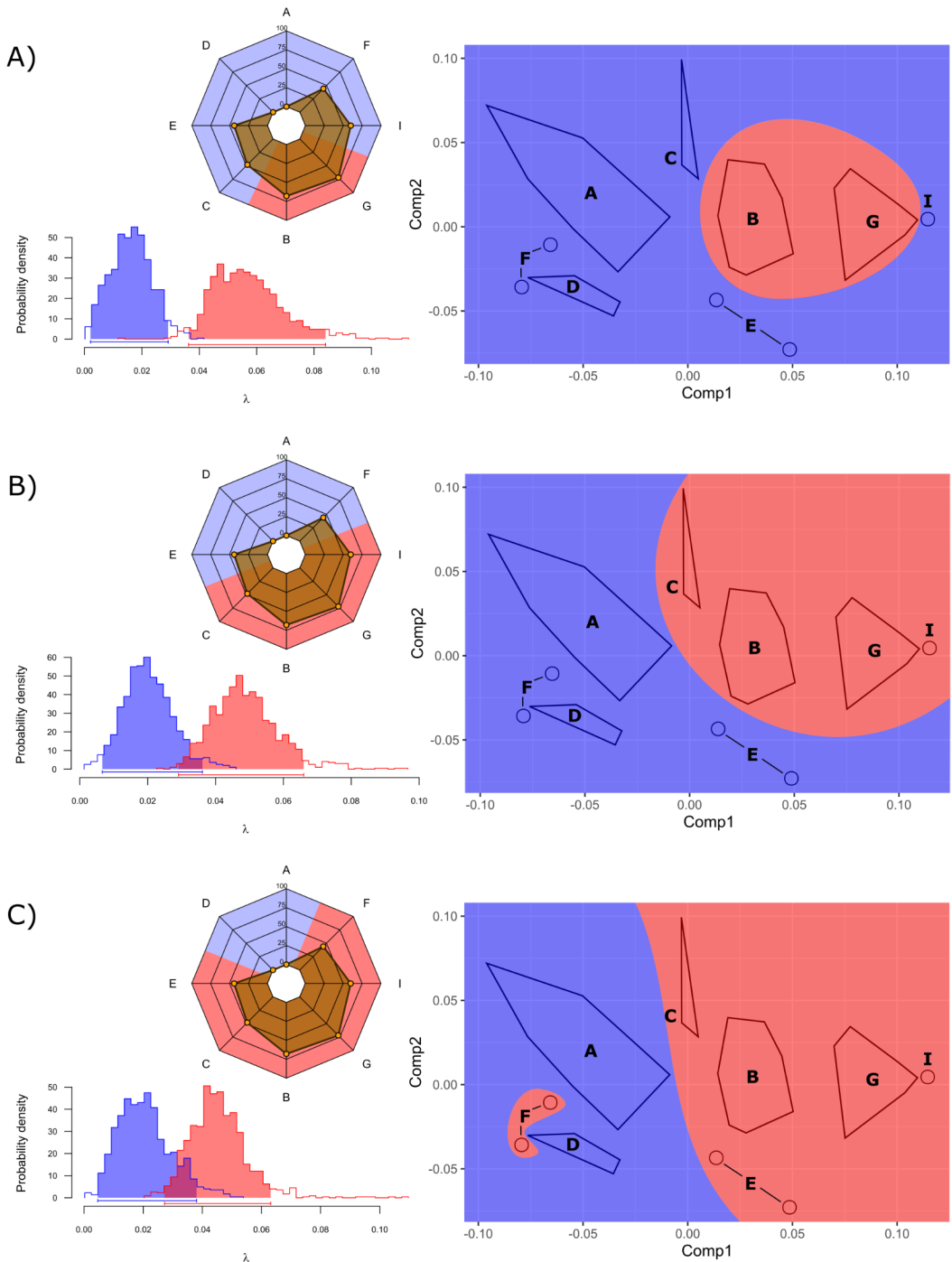


Figure 3. Diversification rates obtained with the BiSSE test for binary states A) $state_{BG}$ (red) and $state_{ICFEAD}$ (blue); B) $state_{BGIC}$ (red) and $state_{FEAD}$ (blue); C) $state_{BGICFE}$ (red) and $state_{AD}$ (blue). The spider chart shows the binary state delimitation with the percentage of occurrence for each state in the binary states combinations (orange). The morphospace (not used for analyses) provides a visual representation of the space occupied by each state combination.

rate comparisons depending on those percentages, we found that when comparing the cheliceral morphotypes B and G grouped versus all other cheliceral types, the BiSSE model with free transition rates exhibited a better performance than the null ($AIC_{fr} = 505.78$ and $AIC_{null} = 510.27$, $p\text{-value} = 0.01$), with stateBG showing higher diversification rate than stateICFEAD (Fig. 3A, $p\text{-value} = 0.006$). When incorporating morphotype I to the free transition rate model the result was close to the previous one ($AIC_{fr} = 504.80$ and $AIC_{null} = 508.52$, $p\text{-value} = 0.02$), as well as when adding morphotype C to this combination ($AIC_{fr} = 504.69$ and $AIC_{null} = 507.56$, $p\text{-value} = 0.03$), also with stateBGIC exhibiting higher diversification rate than stateFEAD (Fig. 3B, $p\text{-value} = 0.015$). However, when further including types F and E to the other rate state, with the binary morphotype delimitation dividing types A and D from the rest, the results changed drastically with the null model performing better than the one with free transition rates ($AIC_{fr} = 511.71$ and $AIC_{null} = 509.15$, $p\text{-value} = 0.48$), with the diversification rate of stateBGICFE not significantly different compared to the stateAD (Fig. 3C, $p\text{-value} = 0.078$).

Hidden state results

When testing for a hidden state character in the different models which supported significant rate differences between groups of cheliceral morphotypes, the results differed depending on the cheliceral type grouping. When modelling with the states that exhibited the largest differences compared to the null model (state_{BG} vs state_{ICFEAD}), the best resulting model was the high complexity model with a four-level hidden-rate (HISSE CID-4 AIC = 378.88, HISSE CID-2 AIC = 383.41, HISSE+BISSE AIC = 383.74, BISSE AIC = 509.26). For the morphotype combination between state_{BGI} vs state_{CFEAD}, the best model was the one-trait hidden-rate (HISSE CID-2 AIC = 355.97, HISSE CID-4 AIC = 402.29, HISSE+BISSE AIC 433.61, BISSE AIC = 523.35), similar to the combination state_{BGIC} vs state_{FEAD} models (HISSE CID-2 AIC = 364.45, HISSE CID-4 AIC = 426.41, HISSE+BISSE AIC 472.78, BISSE AIC = 515.25).

Effect of time on species diversification

When investigating temporal variation in diversification rates, we found that the time-dependent model performed better than the null with no variation in diversification rates (AIC = 125.67 and AIC = 154.04 respectively, p -value $\ll 0.01$). When sampling the posterior distribution using Bayesian inference, we observed a slight decrease in the diversification rate of the group through time (Fig. 4, $\lambda_{\text{a}} = 0.0015 \pm 0.0014$).

Age-range correlation

jSDM showed varying interactions between different species pairs, both in terms of their correlation with the environmental variables and their residual correlations. However, upon examining species pairs that occur on the same island, we found that they generally exhibited positive correlations with both residuals and environmental

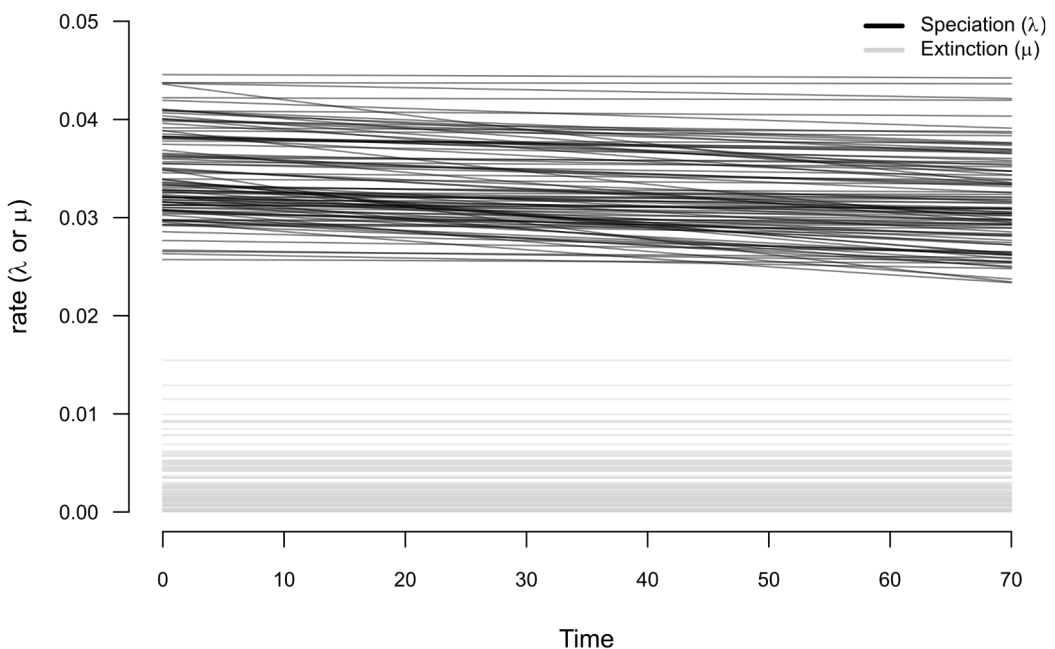
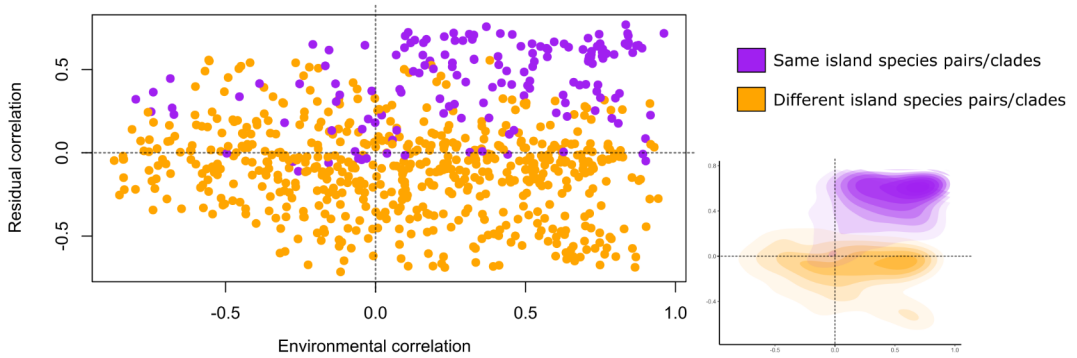


Figure 4. Posterior distribution of the time-dependent speciation and extinction rates obtained with the variable-speciation model..

factors. Conversely, for species pairs that occur on different islands, the correlation with the residuals tends to be neutral but with a bigger disparity in the environmental correlations, with both positive and negative values (Fig. 5A). We opted to utilize residual correlations for conducting the ARC analyses, as they provide better

A)



B)

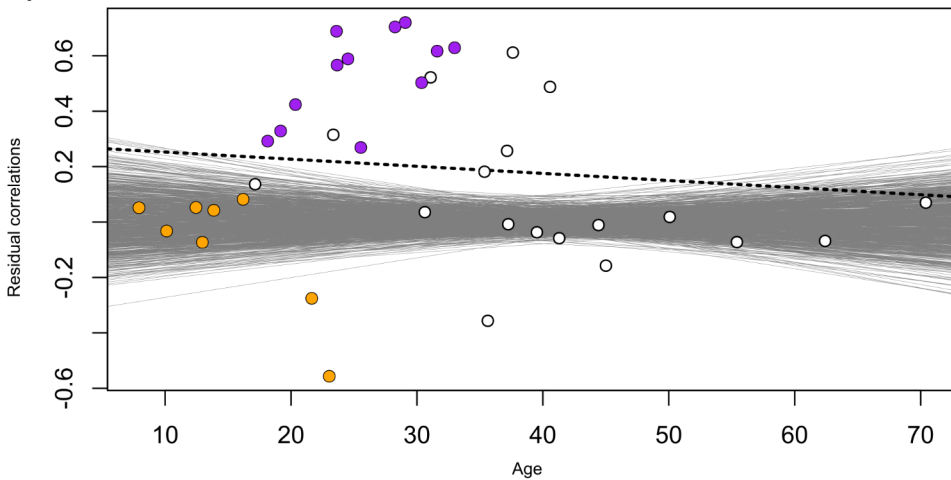


Figure 5. A) Plot with residual correlations and environmental correlations between all *Dysdera* species pairs in the Canary Islands. Purple dots represent species pairs that inhabit the same island, and orange dots species pairs that have a distribution on different islands. Bottom right corner represents the density concentration of sympatric and allopatric species pairs in the residual and the environmental correlations, showing bigger differences between their densities in the residual correlations. B) Age-range correlation of node ages and species residual correlations obtained from the jSDM. Dotted black line is the linear model of mean residual correlation versus node age. Grey lines are the different slopes of the Monte Carlo replicates from the dataset randomizations. Dots represent nodes in the phylogeny: orange dots are sister species pairs that occur on different islands; purple dots are species pairs or clades that occur on the same island; white dots are nodes that cannot be linked because the species relations are too complex to characterize the node as sympatric or allopatric.

discrimination between species pairs with distributions on the same or different islands. It is important to note that having a distribution on the same island does not necessarily imply a sympatric distribution, as the species may occupy different regions within that island. However, the residual correlations offer the clearest representation of what an allopatric distribution could be (i.e., two species on separate islands), and because of that we believe they will contribute more significantly to the ongoing analysis.

The ARC analysis revealed a decrease in the overlap since species divergence (intercept = 0.215; slope = -0.002), indicative of a sympatric speciation with a subsequent loss of contact between species. However, this result was not statistically significant with a p-value of 0.414, showing no significant association between range overlap and time since species divergence. It should be noted, however, that these values were obtained by fitting the results in a linear model, but our ARC plot clearly exhibited a hump-shaped pattern, with low overlap values in the early splits, a subsequent increase in overlapping followed by a decrease toward the present (Fig. 5B).

Discussion

In this study, we have focused in understanding how species diversification varies across time and space, and how it is influenced by ecophenotypic traits and trophic specialization. Moreover, we have provided evidence that the diversification of *Dysdera* spiders in the Canary Islands, where previous studies have highlighted ecophenotypic variation (Bellvert *et al.* in press), constitute a case of adaptive radiation. Evidence derived from modelling speciation and extinction lends support to the hypothesis that trophic specialization and associated morphological evolution shaped the diversification of these species in this archipelago, highlighting the importance of ecological innovation in driving species' diversification. Finally, we have found

evidence that the speciation of the *Dysdera* species in the Canary Islands had been mainly driving by geographic isolation with a posterior secondary contact.

The diversification mode of Canarian *Dysdera* spiders

An early increase in species diversification, followed by a decrease in net speciation rates towards the present is the trademark of an adaptive radiation process (Phillimore & Price 2008; Glor 2010; Losos & Mahler 2010). Declining diversification rates through time are generally interpreted as the results of early occupation of vacant niches until their saturation, which leads to the slowdown of cladogenetic events (Schluter 2000; Gavrillets & Vose 2005). Such a pattern has been usually described by means of lineage-through-time plots (Nee *et al.* 1992; Pybus & Harvey 2000), with density-dependent models describing this asymptotic accumulation of lineages through time (eg. Pincheira-Donoso *et al.* 2015; Linder & Bouchenak-Khelladi 2017). The early increase in number of lineages and the corresponding negative γ values revealed for the *Dysdera* species from the Canary Islands, points towards a rapid filling of ecological niches and a deceleration of speciation rates over time, as also seen with the time-dependent model of diversification. Interestingly, the Canary Islands may have also presented additional episodes of ecological opportunity as new islands emerged over time, which can be reflected in diversification pulses in the LTT plot (Pincheira-Donoso *et al.* 2015). Such pulses can be identified in Fig. 2B. Multi-rate variants of the pure birth model lend further support to this observation, as they exhibited overlapping AIC values when accounting for the phylogenetic uncertainty, however, their mean values had been slightly higher than the density-dependent model. Obviously, undiscovered species could compromise these results, as incompleteness in the taxon sampling could mirror a similar pattern as the density-dependent speciation (Rabosky & Lovette 2008). However, given the solid taxonomic ground established by a series of modern taxonomic treatments of the group (eg. Arnedo & Ribera 1999a, 1999b, 1999c; Arnedo *et al.* 2000; Macías-Hernández *et al.*

2010; Bellvert *et al.* in prep), we doubt that the amount of undiscovered species may actually affect our main conclusions.

Evolutionary consequences of ecological specialization

The ecological and evolutionary consequences of species specialization have been examined repeatedly over the years. Current consensus would claim that the evolution of traits that reduce the breadth of species trophic or ecological niches negatively affect their diversification rates (Vamosi *et al.* 2014), resulting into the so called evolutionary dead-ends (Cope 1896). However, this cannot be taken as a general rule, as many studies have found mixed support for it (Day *et al.* 2016), or directly contradicted the link between specialization and evolutionary dead-ends (Zenil-Ferguson *et al.* 2022). Our results reveal that specialist and generalist *Dysdera* species exhibit similar diversification rates. Nevertheless, pairwise rate comparisons of different cheliceral morphotypes and their combination into coherent groups identified specific sets of ecomorphotypes that exhibit significantly higher diversification rates (Fig. 3A-B). Interestingly, although trophic specialization does not seem to be directly linked to an increase in diversification rates in our studied species, we found a significant increase when combining cheliceral morphologies that have been previously linked to specialist trophic strategies (Bellvert *et al.* in press). The cheliceral type F constitute the single exception, since its inclusion in the set of specialists fail to find significant differences. The cheliceral morphotype F exhibits some particularity regarding the link between ecology and diversification dynamics. Indeed, species bearing this cheliceral morphology, also known as “flat-fang type”, has been experimentally shown to exhibit a very particular capture strategy when preying isopods (Řezáč *et al.* 2008), consisting in piercing the isopod by sliding the flat, widened short fang through its dorsal tergites. In a previous study, we found transitions from generalist cheliceral morphotypes to specialist ones to be irreversible in Canarian *Dysdera* (Bellvert *et al.* in press), supporting that prey specialization is an

evolutionary dead-end (Day *et al.* 2016). However, the high diversification rates found here linked to the majority of specialist cheliceral types, do not support the Idea of an evolutionary dead-end, suggesting instead that trophic specialization in *Dysdera* species may constitute a key innovation rather than a limiting factor in their diversification. On the other hand, the cheliceral morphology with the flat fang (type F), would better fit into the definition of a dead-end, being an irreversible character that has evolved from a generalist state and that is also accompanied by a decrease in species diversification rates (Fig. 3C). Put together, these observations suggest that the evolutionary dead-ends in *Dysdera* spiders would not be so dependent on trophic specialization *per se*, but rather related to specific morphotypes. Indeed, our results show that some specialist states promote an increase in diversification rates, whereas a specific specialist state (cheliceral type F) leads to evolutionary dead-ends. Interestingly, species with F cheliceral type, have evolved multiple times across different species groups and geographic regions in continental *Dysdera*, presumably independently, but they are generally carried by single species with no close relatives exhibiting the same feature, supporting the interpretation of cheliceral type F as an evolutionary dead-end. Overall, our results suggest that the increase or decrease in diversification rates is better explained by morphology rather than by trophic specialization.

On the other hand, although we have found that state-dependent models with the certain cheliceral morphologies performed better than a null model, some other unaccounted factor (or factors) seems to have a stronger influence in the diversification of the *Dysdera* species. HiSSE analyses revealed that the preferred model is highly dependent on the cheliceral type combination used, as the selection of the CID-2 or CID-4 models depended on how the states were characterized. However, the model that accounted for the variation in diversification rates only driven by the focal character, always performed worst. This, of course does not

invalidate the importance of the chelicera in the diversification of *Dysdera* spiders from the Canary Islands, as this is an important ecological character that most likely does not have zero effect on speciation rates (Beaulieu & O'Meara 2016), but apparently it has not acted alone during the evolution of the group. In spiders, similar results have been reported when studying the evolution of silk webs, which seems to have influence diversification dynamics without being its main driver (Fernández *et al.* 2018).

Secondary contact following allopatric speciation

The controversy of how generalized allopatric mode of speciation are compared to sympatric ones, especially in the context of adaptive radiations, is still a hot topic nowadays (see Bolnick & Fitzpatrick 2007). One of the major concerns about deciphering speciation with extant sister taxa has been the range shifts experienced by species that could blur present day patterns (Losos & Glor 2003), which were confronted by methods that account for post-speciation range shifts like ARC methods. The ARC analysis performed with the *Dysdera* spider species from the Canary Islands showed a non-significant negative correlation, related to a sympatric mode of speciation. However, the relation between age and the residual correlations has showed to be non-linear (Fig. 5B). Previous skepticism had already been raised in the past about these methods when analyzing complex patterns of geographical modes of speciation (Fitzpatrick & Turelli 2006). Sympatric patterns are generally explained not as the result of selection driven speciation, but as secondary contact following population expansion once the overlapping lineages fully diverged genetically (Hudson *et al.* 2011). Our results of the ARC analysis would better fit under an allopatric speciation followed by a secondary sympatry, making the correlation presented in this test misleading of a more complex pattern that the *Dysdera* species may have been involved. The posterior decline in the species overlap observed could be a response to the increase of extinction rates expected over time under the general

dynamic model of oceanic island biogeography (Borregaard *et al.* 2017). This allopatric speciation would suit into the expected in an archipelago, where intra-island geographical isolation could be less likely for these species than isolation by colonizing two separate islands (Mittelbach & Schemske 2015). This would match with the observed in our ARC analysis, where cladogenetic events within species pairs in different islands are more recent than the ones with species in the same island (Fig. 5B). For this reason, we argue that the colonization of different islands has been the main, or one of the main, speciation force(s) during the diversification of the *Dysdera* species in the Canary Islands.

Conclusions

The diversification of the *Dysdera* species in the Canary Islands has been previously suggested to be a case of adaptive radiation. Our results unambiguously support this claim by recovering an early burst of species diversification with a posterior slowdown in their speciation, a pattern usually interpreted as the stamp of an adaptive radiation process. The integration of available morphometric data and SSE models, provide evidence that the different cheliceral morphologies exhibited by Canarian *Dysdera* played a role in shaping diversification dynamics in this group, probably by increasing rates as a result of multiple instances of trophic specialization. However, this character does not seem to be the main driving force in the island diversification, with inter-island colonizations most likely having a stronger effect on them. The use of jSDM approaches provided more refine information on species interaction than the use of climatic variables alone, and when used with ARC methods enabled us to propose that inter-island allopatric speciation is the general pattern of diversification among these species with sympatry being the results of secondary contact between them.

Acknowledgments

We would like to thank Dimitar Dimitrov for their help and advice with speciation

and extinction models during the development of the present study.

A.B. was funded by an individual PhD grant BES-2017-080538 from the Ministerio de Economía, Industria y Competitividad of the Spanish government. A.K. is supported by a Ramón y Cajal research grant co-funded by the Spanish State Research Agency and the European Social Fund (RYC2019-026688-I/AEI/10.13039/501100011033). This study was supported by project grants CGL2012-36863 and CGL2016-80651-P from the Spanish Ministry of Economy and Competitiveness and 2017SGR83 from the Catalan Government (M.A.).

References

- Adrián-Serrano S., Lozano-Fernandez J., Pons J., Rozas J. & Arnedo M.A. 2020. On the shoulder of giants: Mitogenome recovery from non-targeted genome projects for phylogenetic inference and molecular evolution studies. *Journal of Zoological Systematics and Evolutionary Research* (January): 1–26. <https://doi.org/10.1111/jzs.12415>
- Arnedo M.A., Oromi P. & Ribera C. 2000. Systematics of the Genus *Dysdera* (Araneae, Dysderidae) in the Eastern Islands. *Journal of Arachnology*: 261–292.
- Arnedo M.A. & Ribera C. 1999a. Radiation in the genus *Dysdera* (Araneae, Dysderidae) in the Canary Islands: The island of Tenerife. *J. Arachnol.* 27: 604–662.
- Arnedo M.A. & Ribera C. 1999b. Radiation in the genus *Dysdera* (Araneae, Dysderidae) in the Canary Islands: The island of Gran Canaria. *J. Arachnol.* 27 (3): 604–662.
- Arnedo M.A. & Ribera C. 1999c. Radiation in the genus *Dysdera* (Araneae, Dysderidae) in the Canary Islands: The western islands. *J. Arachnol.* 27 (3): 604–662.
- Barraclough T.G. & Vogler A.P. 2000. Detecting the geographical pattern of speciation from species-level phylogenies. *American Naturalist* 155 (4): 419–434. <https://doi.org/10.1086/303332>
- Beaulieu J.M. & O’Meara B.C. 2016. Detecting hidden diversification shifts in models of trait-dependent speciation and extinction. *Systematic Biology* 65 (4): 583–601. <https://doi.org/10.1093/sysbio/syw022>
- Bellvert A., Adrián-Serrano S., Macías-Hernández N., Toft S., Kaliontzopoulou A. & Arnedo M.A. (in press). The non-dereliction in evolution: Trophic specialisation drives convergence in the radiation of red devil spiders (Araneae: Dysderidae) in the Canary Islands. *Systematic Biology*.
- Van Den Bogaard P. 2013. The origin of the Canary Island Seamount Province—New ages of old seamounts. *Scientific Reports* 3: 1–7. <https://doi.org/10.1038/srep02107>
- Bolnick D.I. & Fitzpatrick B.M. 2007. Sympatric speciation: Models and empirical evidence. *Annual Review of Ecology, Evolution, and Systematics* 38: 459–487. <https://doi.org/10.1146/annurev.ecolsys.38.091206.095804>
- Borregaard M.K., Amorim I.R., Borges P.A.V., Cabral J.S., Fernández-Palacios J.M., Field R., Heaney L.R., Kreft H., Matthews T.J., Olesen J.M., Price J., Rigal F., Steinbauer M.J., Triantis K.A., Valente L., Weigelt P. & Whittaker R.J. 2017. Oceanic island biogeography through the lens of the general dynamic model: Assessment and prospect. *Biological Reviews* 92 (2): 830–853. <https://doi.org/10.1111/brv.12256>
- Cerca J., Cotoras D.D., Bieker V.C., De-kayne R., Vargas P., Fernández-mazuecos M., López-delgado J., White O., Stervander M., Geneva A.J., Ernesto J., Andino G., Meier J.I., Rooble L., Valdebenito H.,

- Castañeda R., Chaves J.A., Díaz P.J., Valente L., Knope M.L., Price J.P., Rieseberg L.H., Baldwin B.G., Emerson B.C., Rivas-torres G., Gillespie R. & Martin M.D. 2023. Ecology & Evolution Evolutionary genomics of oceanic island radiations. *Trends in Ecology & Evolution*: 1–12. <https://doi.org/10.1016/j.tree.2023.02.003>
- Clément J. & Vieilledent G. 2022. jSDM: Joint Species Distribution Models.
- Collyer M.L. & Adams D.C. 2018. RRPP: An r package for fitting linear models to high-dimensional data using residual randomization. *Methods in Ecology and Evolution* 9 (7): 1772–1779. <https://doi.org/10.1111/2041-210X.13029>
- Collyer M.L. & Adams D.C. 2021. RRPP. Linear Model Evaluation with Randomized Residuals in a Permutation Procedure.
- Cope E.D. 1896. *The Primary Factors of Organic Evolution*. The Open Court Publishing Company, Chicago.
- Darwin C.R. 1859. *On the Origin of Species by Means of Natural Selection, or the Preservation of Favoured Races in the Struggle for Life*. John Murray Publishers, London.
- Day E.H., Hua X. & Bromham L. 2016. Is specialization an evolutionary dead end? Testing for differences in speciation, extinction and trait transition rates across diverse phylogenies of specialists and generalists. *Journal of evolutionary biology* 29 (6): 1257–1267. <https://doi.org/10.1111/jeb.12867>
- Fernández R., Kallal R.J., Dimitrov D., Ballesteros J.A., Arnedo M.A., Giribet G. & Hormiga G. 2018. Phylogenomics, Diversification Dynamics, and Comparative Transcriptomics across the Spider Tree of Life. *Current Biology* 28 (9): 1489-1497.e5. <https://doi.org/10.1016/j.cub.2018.03.064>
- Fitzjohn R.G. 2012. Diversitree: Comparative phylogenetic analyses of diversification in R. *Methods in Ecology and Evolution* 3 (6): 1084–1092. <https://doi.org/10.1111/j.2041-210X.2012.00234.x>
- Fitzpatrick B.M. & Turelli M. 2006. The Geography of Mammalian Speciation: Mixed Signals From Phylogenies and Range Maps. *Evolution* 60 (3): 601–615. <https://doi.org/10.1111/j.0014-3820.2006.tb01140.x>
- Futuyma D.J. 1986. *Evolutionary biology*. Sinauer Associates, Sunderland, Massachusetts, USA.
- Futuyma D.J. 1998. *Evolutionary biology*. Third Edit. Sunderland, MA.
- Gavrilets S. & Vose A. 2005. Dynamic patterns of adaptive radiation. *Proceedings of the National Academy of Sciences of the United States of America* 102 (50): 18040–18045. <https://doi.org/10.1073/pnas.0506330102>
- Gillespie R. 2004. Community Assembly Through Adaptive Radiation in Hawaiian Spiders. *Science* 303 (January): 356–359.

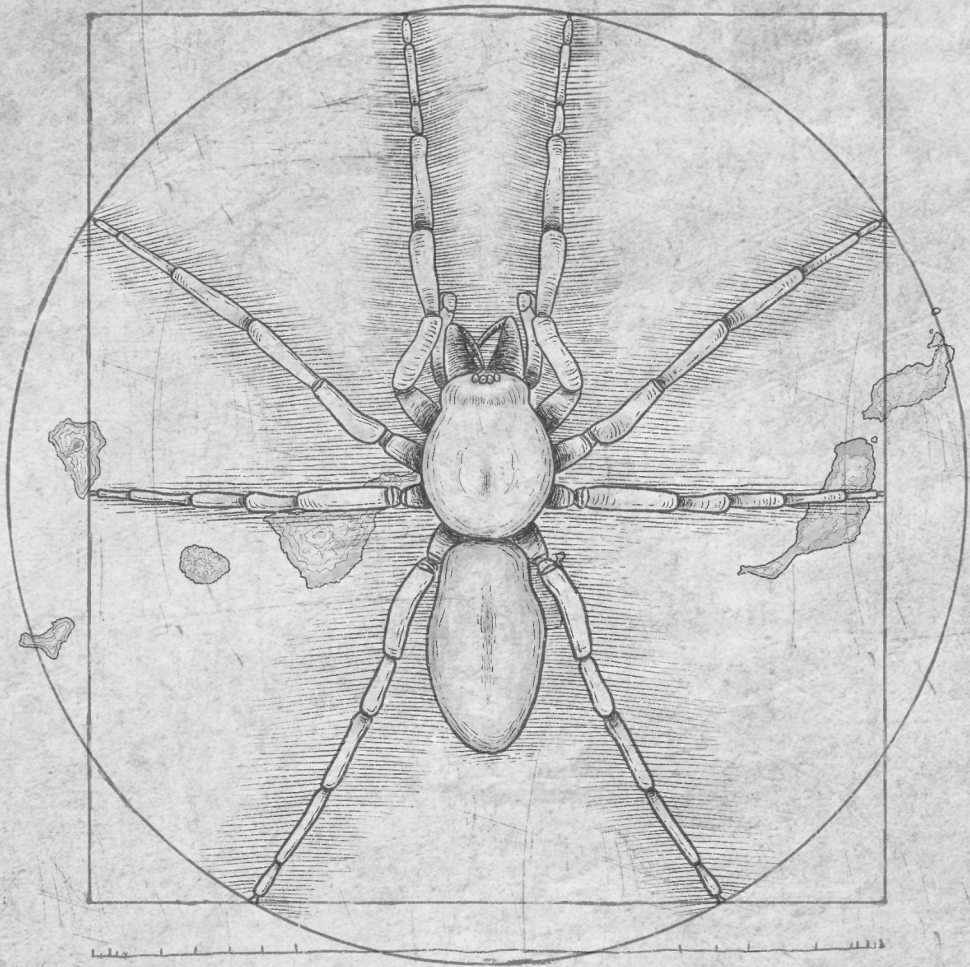
- Gillespie R.G., Bennett G.M., De Meester L., Feder J.L., Fleischer R.C., Harmon L.J., Hendry A.P., Knope M.L., Mallet J., Martin C., Parent C.E., Patton A.H., Pfennig K.S., Rubinoff D., Schluter D., Seehausen O., Shaw K.L., Stacy E., Stervander M., Stroud J.T., Wagner C. & Wogan G.O.U. 2020. Comparing Adaptive Radiations Across Space, Time, and Taxa. *Journal of Heredity* 111 (1): 1–20. <https://doi.org/10.1093/jhered/esz064>
- Givnish T.J. & Sytsma K.J. 1997. *Molecular evolution and adaptive radiation*. Cambridge: Cambridge University Press.
- Glor R.E. 2010. Phylogenetic insights on adaptive radiation. *Annual Review of Ecology, Evolution, and Systematics* 41: 251–270. <https://doi.org/10.1146/annurev.ecolsys.39.110707.173447>
- Harmon L.J., Losos J.B., Jonathan Davies T., Gillespie R.G., Gittleman J.L., Bryan Jennings W., Kozak K.H., McPeck M.A., Moreno-Roark F., Near T.J., Purvis A., Ricklefs R.E., Schluter D., Schulte J.A., Seehausen O., Sidlauskas B.L., Torres-Carvajal O., Weir J.T. & Mooers A.T. 2010. Early bursts of body size and shape evolution are rare in comparative data. *Evolution* 64 (8): 2385–2396. <https://doi.org/10.1111/j.1558-5646.2010.01025.x>
- Heard S.B. & Hauser D.L. 1995. Key evolutionary innovations and their ecological mechanisms. *Historical Biology* 10: 151–173.
- Heibl C. & Calange C. 2018. phyloclim: Integrating Phylogenetics and Climatic Niche Modeling.
- Hudson A.G., Vonlanthen P. & Seehausen O. 2011. Rapid parallel adaptive radiations from a single hybridogenetic ancestral population. *Proceedings of the Royal Society B: Biological Sciences* 278 (1702): 58–66. <https://doi.org/10.1098/rspb.2010.0925>
- Lack D. 1947. *Darwin's Finches*. Cambridge University Press.
- Linder P.H. & Bouchenak-Khelladi Y. 2017. Adaptive radiations should not be simplified: The case of the danthonioid grasses. *Molecular Phylogenetics and Evolution* 117 (June): 179–190. <https://doi.org/10.1016/j.ympev.2017.10.003>
- Losos J.B. 2009. *Lizards in an evolutionary tree: ecology and adaptive radiation of anoles*. University of California Press, Berkeley, CA.
- Losos J.B. & Glor R.E. 2003. Phylogenetic comparative methods and the geography of speciation. *Trends in Ecology and Evolution* 18 (5): 220–227. [https://doi.org/10.1016/S0169-5347\(03\)00037-5](https://doi.org/10.1016/S0169-5347(03)00037-5)
- Losos J.B. & Mahler D.L. 2010. Adaptive Radiation: The Interaction of Ecological Opportunity, Adaptation, and Speciation. In: Bell M., Futuyama D., Eanes W. & Levinton J. (eds) *Evolution since Darwin: The First 150 Years*: 381–420. Sunderland, MA.
- Macías-Hernández N., Bidegaray-Batista L., Emerson B.C., Oromí P. & Arnedo M. 2013. The imprint of geologic history on within-island diversification of woodlouse-hunter spiders (Araneae,

- Dysderidae) in the canary islands. *Journal of Heredity* 104 (3): 341–356. <https://doi.org/10.1093/jhered/est008>
- Macías-Hernández N., Oromí P. & Arnedo M.A. 2010. Integrative taxonomy uncovers hidden species diversity in woodlouse hunter spiders (Araneae, Dysderidae) endemic to the Macaronesian archipelagos. *Systematics and Biodiversity* 8 (4): 531–553. <https://doi.org/10.1080/14772000.2010.535865>
- Mayr E. 1963. *Animal Species and Evolution*. MA: Belknap.
- Mittelbach G.G. & Schemske D.W. 2015. Ecological and evolutionary perspectives on community assembly. *Trends in Ecology and Evolution* 30 (5): 241–247. <https://doi.org/10.1016/j.tree.2015.02.008>
- Nakazawa M. 2023. fmsb: Functions for Medical Statistics Book with some Demographic Data.
- Nee S., Mooers A. & Harvey P.H. 1992. Tempo and mode of evolution revealed from molecular phylogenies. *Proceedings of the National Academy of Sciences of the United States of America* 89 (17): 8322–8326. <https://doi.org/10.1073/pnas.89.17.8322>
- Nosil P. 2002. Transition rates between specialization and generalization in phytophagous insects. *Evolution* 56 (8): 1701–1706. <https://doi.org/10.1111/j.0014-3820.2002.tb01482.x>
- Nosil P. & Mooers A.Ø. 2005. Testing hypotheses about ecological specialization using phylogenetic trees. *Evolution* 59 (10): 2256–2263.
- Paradis E. & Schliep K. 2019. Ape 5.0: An environment for modern phylogenetics and evolutionary analyses in R. *Bioinformatics* 35 (3): 526–528. <https://doi.org/10.1093/bioinformatics/bty633>
- Patton A.H., Harmon L.J., Castañeda R., Frank H.K., Donihue C.M., Herrel A. & Losos J.B. 2021. When adaptive radiations collide: Different evolutionary trajectories between and within island and mainland lizard clades. <https://doi.org/10.1073/pnas.2024451118>
- Phillimore A.B. & Price T.D. 2008. Density-dependent cladogenesis in birds. *PLoS Biology* 6 (3): 0483–0489. <https://doi.org/10.1371/journal.pbio.0060071>
- Pincheira-Donoso D., Harvey L.P. & Ruta M. 2015. What defines an adaptive radiation? Macroevolutionary diversification dynamics of an exceptionally species-rich continental lizard radiation. *BMC Evolutionary Biology* 15 (1): 1–13. <https://doi.org/10.1186/s12862-015-0435-9>
- Plummer M., Best N., Cowles K. & Vines K. 2006. CODA: Convergence Diagnosis and Output Analysis for MCMC. *R News* 6: 7–11. <https://doi.org/10.1515/9783112524282-toc>
- Pollock L.J., Tingley R., Morris W.K., Golding N., O'Hara R.B., Parris K.M., Vesk P.A. & McCarthy M.A. 2014. Understanding co-occurrence by modelling species simultaneously with a Joint Species Distribution Model (JSDM). *Methods in Ecology and Evolution* 5 (5): 397–406. <https://doi.org/>

10.1111/2041-210X.12180

- Pybus O.G. & Harvey P.H. 2000. Testing macro-evolutionary models using incomplete molecular phylogenies. *Proceedings of the Royal Society B: Biological Sciences* 267 (1459): 2267–2272. <https://doi.org/10.1098/rspb.2000.1278>
- R Core Team 2022. R: A Language and Environment for Statistical Computing. Available from <https://www.r-project.org/>.
- Rabosky D.L. & Lovette I.J. 2008. Density-dependent diversification in North American wood warblers. *Proceedings of the Royal Society B: Biological Sciences* 275 (1649): 2363–2371. <https://doi.org/10.1098/rspb.2008.0630>
- Rabosky D.L. & Schliep K. 2013. laser: Likelihood Analysis of Speciation/Extinction Rates from Phylogenies.
- Revell L.J. 2012. phytools: An R package for phylogenetic comparative biology (and other things). *Methods in Ecology and Evolution* 3 (2): 217–223. <https://doi.org/10.1111/j.2041-210X.2011.00169.x>
- Revell L.J. & Harmon L.J. 2022. *Phylogenetic comparative methods in R*. Princeton University Press, New Jersey.
- Řezáč M., Pekár S., Arnedo M., Macías-Hernández N. & Řezáčová V. 2021. Evolutionary insights into the eco-phenotypic diversification of Dysdera spiders in the Canary Islands. *Organisms Diversity and Evolution*. <https://doi.org/10.1007/s13127-020-00473-w>
- Řezáč M., Pekár S. & Lubin Y. 2008. How oniscophagous spiders overcome woodlouse armour. *Journal of Zoology* 275 (1): 64–71. <https://doi.org/10.1111/j.1469-7998.2007.00408.x>
- Schluter D. 2000. *The Ecology of Adaptive Radiation*. Oxford University Press, Oxford.
- Simpson G.G. 1944. *Tempo and mode in evolution*. Columbia University Press, New York.
- Simpson G.G. 1953. *The major features of evolution*. Columbia University Press, New York.
- Slater G.J., Price S.A., Santini F. & Alfaro M.E. 2010. Diversity versus disparity and the radiation of modern cetaceans. *Proceedings of the Royal Society B: Biological Sciences* 277 (1697): 3097–3104. <https://doi.org/10.1098/rspb.2010.0408>
- Stroud J.T. & Losos J.B. 2016. Ecological Opportunity and Adaptive Radiation. *Annual Review of Ecology, Evolution, and Systematics* 47: 507–532. <https://doi.org/10.1146/annurev-ecolsys-121415-032254>
- Takahashi T. & Koblmüller S. 2011. The Adaptive Radiation of Cichlid Fish in Lake Tanganyika: A Morphological Perspective. *International Journal of Evolutionary Biology* 2011: 1–14. <https://doi.org/10.4061/2011/620754>

- Thorpe R.S., Surget-Groba Y. & Johansson H. 2010. Genetic tests for ecological and allopatric speciation in anoles on an Island archipelago. *PLoS Genetics* 6 (4). <https://doi.org/10.1371/journal.pgen.1000929>
- Toft S. & Macías-Hernández N. 2017. Metabolic adaptations for isopod specialization in three species of *Dysdera* spiders from the Canary Islands. *Physiological Entomology* 42 (2): 191–198. <https://doi.org/10.1111/phen.12192>
- Toft S. & Macías-Hernández N. 2021. Prey acceptance and metabolic specialisations in some Canary *Dysdera* spiders. *Journal of Insect Physiology* 131 (June 2020): 104227. <https://doi.org/10.1016/j.jinsphys.2021.104227>
- Vamosi J.C., Scott Armbruster W., Scott Armbruster W., Scott Armbruster W. & Renner S.S. 2014. Evolutionary ecology of specialization: Insights from phylogenetic analysis. *Proceedings of the Royal Society B: Biological Sciences* 281 (1795). <https://doi.org/10.1098/rspb.2014.2004>
- Venables W.N. & Ripley B.D. 2002. *Modern Applied Statistics with S*. Fourth edi. Springer, New York.
- Wellborn G.A. & Langerhans R.B. 2015. Ecological opportunity and the adaptive diversification of lineages. *Ecology and Evolution* 5 (1): 176–195. <https://doi.org/10.1002/ece3.1347>
- World Spider Catalog 2023. World Spider Catalog. Version 24. Natural History Museum Bern, online at <http://wsc.nmbe.ch>, accessed on {date of access}. doi: 10.24436/2.
- Zenil-Ferguson R., McEntee J.P., Burleigh J.G. & Duckworth R.A. 2022. Linking ecological specialization to its macroevolutionary consequences: An example with passerine nest type *Rosana*. *Systematic Biology* c (3): 1–10.



CHAPTER 3.2

How the turtables: Species traits modulate ecological release in red devil spiders (Araneae:Dysderidae)?

How the turtables: Species traits modulate ecological release in red devil spiders (Araneae:Dysderidae)?

Adrià Bellvert^{1,2}, Alba Enguïdanos^{1,2}, Jairo Patiño³, Laura Pollock⁴, Antigoni Kaliontzopoulou^{1,2} & Miquel A. Arnedo^{1,2}.

1 Departament de Biologia Evolutiva, Ecologia i Ciències Ambientals, Universitat de Barcelona (UB), Av. Diagonal, 643, 08028 Barcelona, Spain.

2 Institut de Recerca de la Biodiversitat (IRBio), Universitat de Barcelona (UB), Barcelona, Spain.

3 Instituto de Productos Naturales y Agrobiología (IPNA-CSIC), La Laguna, Spain

4 Department of Biology, McGill University, Montreal, Canada

Abstract

Ecological release, defined as the expansion of range, habitat and/or resource usage by an organism, is a ubiquitous phenomenon in oceanic islands. Species colonising recently formed islands, whose ancestors evolved in highly competitive environments, may experience relaxed selection because of reduced species richness. However, factors other than competition may also be involved in determining the species' ability to expand their niche. Ecological specialization, for instance, has been frequently considered as an evolutionary dead end, preventing the reversal to more generalist states. Here we integrate geometric morphometric methods, stable isotope analyses and species distribution models using the spider genus *Dysdera* as a model to explore the implications of different cheliceral morphotypes, related to different trophic adaptations, on the species' ability to undergo ecological release. Contrary to our expectations, species with morphotypes associated to a more specialist diet, tended to expand their trophic niche, increase their spatial range and modify their phenotype across the same area of morphospace, when compared to generalist species. Our study constitutes one of the first examples of the use of a multidisciplinary approach to better understand the effects of ecological release on colonizing species with contrasting trophic preferences.

Keywords: Ecological opportunity, adaptive radiation, trophic specialization

Introduction

Since the beginning of our understanding of how species evolved by natural selection (Darwin 1859) and how these species exist with respect to their geographical context (Wallace 1881), islands have played a crucial role for evolutionary biologists studying the processes of species diversification. Adaptive radiation, that is, the diversification of eco-phenotypically different species from a single ancestor (Futuyma 1998), has been centrepiece to link ecology and evolution (Givnish and Sytsma 1997) and many hypotheses have been put forward to characterize the sequence of events that drove such a remarkable species diversity on islands (Yoder et al. 2010). Most hypotheses concerning the first steps of adaptive radiations generally assume that ecological opportunity triggers species diversification (Schluter 2000; Stroud and Losos 2016), although it does not always need to be so (Losos 2010). These ecological opportunities could arise under different circumstances (Simpson 1953), among which the colonization of new environments is one of the most reputed examples (Stroud and Losos 2016). The availability of novel habitats with lower pressures from predators or competitors is particularly prevalent in oceanic islands, which offer ample opportunities to occupy vacant niches, unavailable in more complex continental regions (Gillespie et al. 2020). In general, reduced competition and/or the absence of predators are expected to result in a relaxation of selective pressures (Losos and De Queiroz 1997; Yoder et al. 2010; Des Roches et al. 2015) and promote divergence in resource utilization (Parent and Crespi 2009), a phenomenon known as ecological release.

As a result of the newly available resources incorporated into the population's niche (Bolnick et al. 2010), the species' evolutionary responses may translate into a variety of different adaptations, as ecological release has different effects in different colonizer species following the emergence of such ecological opportunities (Des Roches et al. 2011). A widened resource usage (MacArthur and Wilson 1967), and an

increase in both intraspecific morphological disparity (Bolnick et al. 2007) and in species population density (MacArthur et al. 1972) may be the most relevant characteristics observed in species colonizing new habitats. All these effects have already been observed in different organisms experiencing ecological release processes; e.g. increase of population density in lizards (Buckley and Jetz 2007), expansion of trophic niche breadth in intertidal communities (Andrades et al. 2019), range expansion in hummingbirds (Battey 2019) or phenotypic variation in land snails (Parent and Crespi 2009). However, most studies conducted to date looking for evidence on species experiencing an ecological release have focused on a single ecological or eco-phenotypic trait. As such, little is known about how the different axes of the Hutchinsonian species' niche (Hutchinson, 1957) interact in the context of this process.

Additionally, the width of the species ecological niche could be influenced by factors other than competition. Trophic specialization, for instance, could translate into completely different niche widths for two sympatric species, where generalists usually have wider niche tolerance and specialist species show more limited niche breadth (Freeman and Hannan 1983). Species trophic adaptations are not independent of the ecological release process, and it has already been seen that in the presence of vacant niches, or an increase of the resource spectrum, species may experience certain shifts in trophic ecology (Van Valen 1965; Robinson and Wilson 1994). However, specialization may become a one-way evolutionary process (Day et al. 2016) which, although not exempted of exceptions (e.g. Lanyon 1992; Muller 1996; Armbruster and Baldwin 1998), seems to be the common trend (Nosil 2002). The possible irreversibility effects of specialization during the colonization of new environments are poorly understood and little is known about how this may affect the species' ability to undergo ecological release.

To better comprehend the initial stages following the colonization of a new

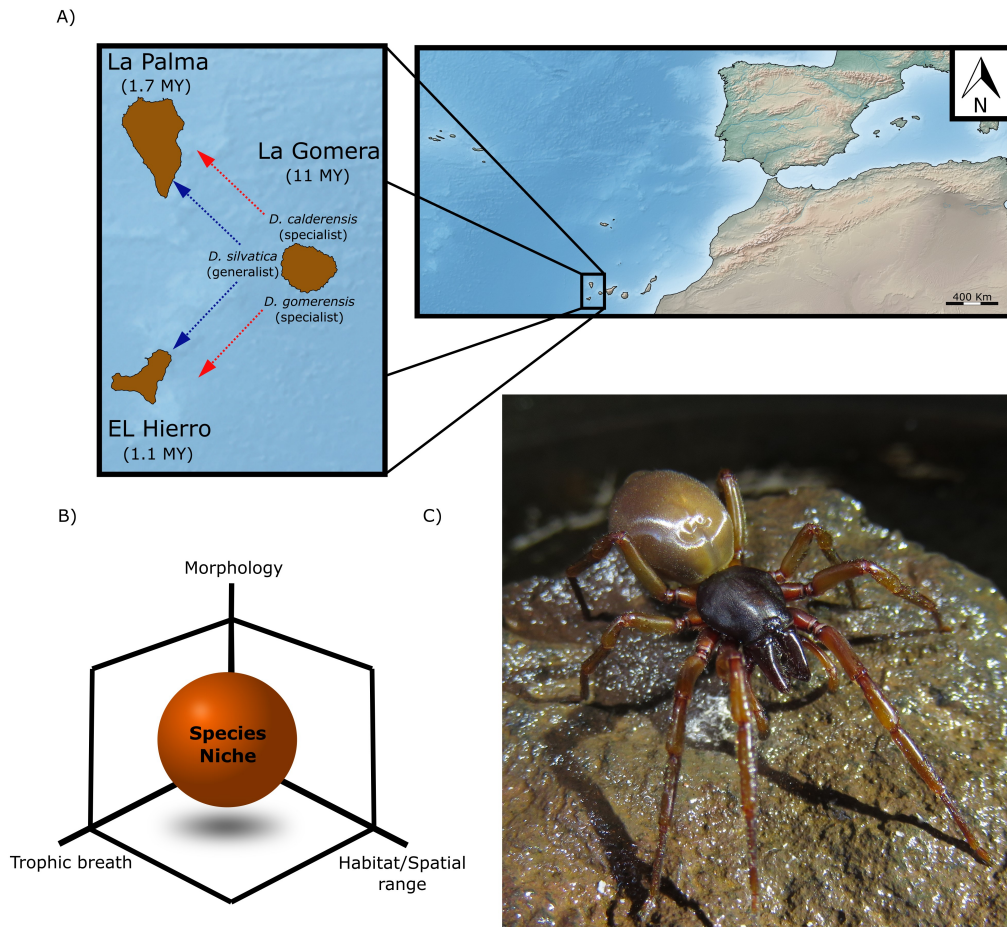


Figure 1. A) Map of the three different islands studied in the present paper, dashed lines show the colonization direction by the three different species, blue: generalist species; red: specialist species. B) Representation of the studied species niche for the present study. C) *Dysdera silvatica* species from the Canary Islands (Photo by Marc Domènech).

environment with novel ecological opportunities, it is essential to employ study models for which we can effectively approach multiple factors influencing the species' ecological niche. This is crucial due to the inherent complexity involved in species evolution. The Canary Islands, located 100 kilometres far from the North-West African coast, is an archipelago formed by 7 major islands and several islets of volcanic origin (Fig. 1A). The islands are geochronological arranged, with the oldest islands, Lanzarote and Fuerteventura (15 My and 23 My respectively), lying at the easternmost side, and

becoming progressively younger towards the west: Gran Canaria (subaerial age 15 My), Tenerife (12 My), La Gomera (11 My), La Palma (1.7 My) and El Hierro (1.1 My) (Van Den Bogaard 2013). These islands show higher levels of endemism (Cardoso et al. 2010) and have been object of several studies focusing on the adaptive radiation of different species groups in the archipelago, especially in plants (e.g. Jorgensen and Olesen 2001; Meimberg et al. 2006). Another species group that has accumulated growing evidence as being a case of adaptive radiation, with approximately 50 endemic species most likely resulting from a single colonization event (Adrián-Serrano et al. 2020) and exhibiting eco-phenotypical differences between species (Bellvert et al. 2022), is the spider genus *Dysdera* (Fig. 1C). This group of ground-dwelling spiders has colonized all Macaronesian archipelagos (Crespo et al. 2021b) and undergone remarkable diversification in the Canary Islands with 47 described species (Macías-Hernández et al. 2016). These species show a high variability of their cheliceral mouthparts and have independently evolved different morphologies several times during the diversification of the group (Bellvert et al. in press). Additionally, the different morphotypes have been linked to different levels of trophic adaptation (Toft and Macías-Hernández 2017, 2021, Bellvert et al. in press), with some cheliceral morphologies linked to generalist species or to species exhibiting different types of specialization in the predation of isopods. The *Dysdera* species richness in the archipelago is unevenly distributed (Macías-Hernández et al. 2016), and seems to be correlated with the area, elevation and habitat diversity present in each island (Arnedo and Ribera 1999; Arnedo et al. 2000; Cardoso et al. 2010). Most of the species are single-island endemics, however some of them have colonized different islands that harbour contrasting numbers of *Dysdera* species (Macías-Hernández et al. 2016). This is the case of the westernmost islands of the archipelago, where several species with different levels of trophic adaptations have colonized younger and species-depauperate islands from more species-rich islands. This scenario offers a perfect framework to test if the colonization of low-competition islands from high-

competition ones leads to ecological release, while simultaneously assessing the impact of trophic specialization in the ability of species to undergo ecological release.

In the present study we combined geometric morphometric methods, stable isotope analysis and species distribution modelling to unravel the ability of *Dysdera* spiders to expand their ecological niche when colonizing low competitive environments and how differences in eco-phenotypic traits may interfere with this ecological process (Fig. 1B). We predict that generalist species will have wider niches as a result of having a higher capacity to take advantage of the new ecological opportunities offered by these new environments. By contrast, because of the restrictions in resource usage that specialization entails, species with more specialized trophic morphotypes would not be able to expand their niche compared to the generalist ones.

Methods

Experimental design and specimen collection

For the present study we targeted three *Dysdera* species endemic to the Canary Islands; *Dysdera calderensis* Wunderlich, 1987, *D. gomerensis* Strand, 1911 and *D. silvatica* Schmidt, 1981. These species provide an ideal testing ground to investigate the response of species with different trophic strategies to reduced levels of interspecific competition. Unlike the remaining *Dysdera* species in the Canaries, which are single-island endemics, these species inhabit at least two of the westernmost islands of the archipelago, namely La Gomera, La Palma and El Hierro (Fig. 1A). The three species are present in La Gomera, along with nine additional species, up to a total of 12 *Dysdera* species, which creates an environment of intense interspecific competition. Conversely, low-competition islands have a lower number of *Dysdera* species. La Palma harbours three species, including *D. calderensis* and *D. silvatica*, while El Hierro has five species, including *D. gomerensis* and *D. silvatica*. It is also

worth mentioning that one of the species in La Palma and one in El Hierro are exclusively known from caves, and hence most likely do not interact with the epigeal species. Interestingly, the three species studied here show different levels of diet specialization. The cheliceral morphology of *D. calderensis* and *D. gomerensis* relates to a feeding preference for isopods, while *D. silvatica* exhibits a cheliceral morphology that denotes a generalist diet (Bellvert et al. in press). Individuals were captured by active searching under rocks, logs and tree barks by the authors and colleagues, and preserved in 95% EtOH in the field and stored at -20°C in the lab. All specimens were collected following institutional and governmental regulations and the permits for all species captured were granted by the local authorities of each island or by the governing body of each natural reserve. Vouchers were deposited at the Centre de Recursos de Biodiversitat Animal of the Universitat de Barcelona (CRBA) and the Departamento de Zoología de la Universidad de La Laguna, Tenerife, Canary Islands collection (DZUL). A total of 115 individuals of the focal species were available for the present study.

Island competitive level and colonization events

We used the number of congeneric species per island as a surrogate for the level of interspecific competition. To control for the impact of different sampling effort across islands on the total number of endemic *Dysdera* species per island, we calculated the effective number of species using rarefaction and extrapolation curves based on sample size (Colwell et al. 2012). We used the *Dysdera* specimen records identified at the species level from the three analysed islands, and calculated the estimated number of species with the function *iNEXT* from the “iNEXT” R package (Hsieh et al. 2016). Similar values in species diversity between the interpolated and extrapolated curves suggest the absence of sampling bias in the island species’ numbers. Specimens used for this analysis are listed in Supplementary Table S1.

Genetic variability and colonization events

We investigated number and timing of colonization events between islands within each species by sequencing the animal DNA barcode (5' half of the cytochrome c oxidase subunit 1, COI). We included a representative sample of individuals from recorded populations of the three species in each island. We performed individual DNA extractions and amplified a 658 bp fragment of the COI by PCR as detailed in Crespo et al. (2021a). Additional sequences were downloaded from GenBank. Sequences were edited and manipulated with Geneious Prime v. 2022.2.2 (<https://www.geneious.com/prime/>).

Sequence alignment was trivial since no indel was inferred. We estimated a gene tree using maximum likelihood as implemented in the with IQ-TREE v. 2.1.1 (Nguyen et al. 2015). We used IQ-TREE to first select the best-fit partitioning scheme and corresponding evolutionary models (Kalyaanamoorthy et al. 2017), and then to infer the best tree and estimate clade support by means of 1000 replicates of non-parametric bootstrapping (Hoang et al. 2018). We rooted trees assuming *D. silvatica* was the earliest offshoot (Crespo et al. 2021b). We used the mPTP method (Kapli et al. 2017) to identify potential evolutionary independent lineages within each species. In short, this is a phylogeny-aware delimitation method that uses a Poisson tree processes (PTP) to distinguish between intra- and interspecific branch lengths allowing different divergence thresholds among lineages. We further implemented the Markov Chain Monte Carlo sampling to assess support of the delimited clusters. Additionally, we identified independent haplotype networks using statistical parsimony following Templeton's et al. (1992) approach, as implemented in software TSC v.1.2.1 (Clement et al. 2000). We estimated uncorrected genetic distances within and between genetic clusters identified by the molecular identification methods with the help of the program MEGA v. 11 (Tamura et al. 2021). Finally, we estimated divergence times between species and island populations, using a Bayesian

framework as implemented in the program BEAST v. 1.10.4 (Suchard et al. 2018). Because the COI sequences included both within and between species samples, we use a multispecies coalescent approach (Heled and Drummond 2012) to infer divergence times. For this, we assigned haplotypes to the independent statistical parsimony networks identified with TCS. We assigned a constant coalescent tree prior to the relationships within each network, while we used a Yule speciation tree prior for the relationships between networks. We defined a single partition and the GTR with invariants and gamma distribution model, as preferred by Partitionfinder v.2.1.1 (Lanfear et al. 2017). We selected a lognormal relaxed clock prior, and obtained absolute divergence times by a normal prior on the ucl.d.mean with mean 0.019 and standard deviation 0.004, based on estimated of substitution rate available in the literature for the family Dysderidae (Bidegaray-Batista and Arnedo 2011). We ran three independent chains of 10 million generations each, sampling every 1,000 generations, remotely on the CIPRES cluster (Miller et al. 2009). We monitored the chain convergence, the correct mixing, and the number of generations to discard as burn-in (10%) with Tracer v. 1.7 (Rambaut et al. 2018). Specimens analysed per species and islands are listed in Supplementary Table S2.

Trophic niche

Trophic niche width was assessed by means of carbon (C) and nitrogen (N) stable isotope analysis. Spiders' legs were removed and dried in an oven P-Selecta "Digitheat-TFT" at 60° for 48 hours. We only used legs, since mixing up different tissues or body parts may create bias in the isotopic values (Kennedy et al. 2019). For larger spiders a single leg was used, while several or all legs were used for smaller specimens. Dried legs were homogenized with a mortar and a pestle. Samples (0.3 mg) were accurately weighed into 3,3 x 5 mm tin cups. All the tin cups were analyzed by combustion at 900°C in an EA-IRMS system. C and N for each sample was calculated with Flash 1112 Elemental analyzer coupled to an isotope ratio mass spectrometer

Delta C (ThermoFinnigan, ThermoFisher Scientific) at the Centres Científics i Tecnològics de la Universitat de Barcelona (www.ccit.ub.edu) in Barcelona, Spain. The abundance of stable isotopes is expressed using the δ notation, where the relative variations of stable isotope ratios are expressed as per mil (‰) deviations from predefined reference scales [atmospheric nitrogen for $\delta^{15}\text{N}$ and Vienna Pee Dee Belemnite (V-PDB) calcium carbonate for $\delta^{13}\text{C}$]. Isotopic reference materials were analyzed with the samples. For nitrogen, several isotopic reference materials of known $^{15}\text{N}/^{14}\text{N}$ ratios were used to a precision of 0.3‰, and these were namely $(\text{NH}_4)_2\text{SO}_4$ (IAEAN1, $\delta^{15}\text{N}=+0.4\text{‰}$, and IAEAN2, $\delta^{15}\text{N}=+20.3\text{‰}$), L-glutamic acid (USGS40, $\delta^{15}\text{N} = -4.5\text{‰}$), and KNO_3 (IAEANO3, $\delta^{15}\text{N} = +4.7\text{‰}$) and caffeine (IAEA 600, $\delta^{15}\text{N} = +1.1\text{‰}$). For carbon, secondary isotopic reference materials of known $^{13}\text{C}/^{12}\text{C}$ ratios were used to a precision of 0.2 ‰, and these were namely polyethylene (IAEACH7, $\delta^{13}\text{C} = -32.15\text{‰}$), sucrose (IAEA CH6, $\delta^{13}\text{C} = -10.4\text{‰}$), L-glutamic acid (USGS40, $\delta^{13}\text{C} = -26.4\text{‰}$), and caffeine (IAEA600, $\delta^{13}\text{C} = -27.77\text{‰}$). These isotopic reference materials were used to recalibrate the system once every 15 samples and were analyzed to compensate any drift over time. The raw data were recalculated, by means a linear regression between theoretical and experimental values of the isotopic reference materials analyzed with the samples.

Whenever possible we selected 5 males and 5 females of each species-island from two different localities for the subsequent analysis. However, due to the scarcity of samples in some of the populations (e.g. *D. calderensis* from La Gomera or *D. silvatica* from El Hierro), some groups were represented by less than 10 specimens or from single localities. Species isotopic niche width was quantified using Bayesian standard ellipses (SEAb) calculated for each species-island. The SEAb area value was calculated with Bayesian inference and account for 95% of variability in posterior distribution with the function *siberEllipses* from the package “SIBER” (Jackson et al. 2011) in the statistical environment R (R Core Team 2022). Bayesian ellipse area's were visualized

using the function *siberDensityPlot*. To estimate if species clades present in low competition islands have significantly different (higher) trophic areas than their counterparts in the high competitive environments, we compared the posterior distribution of the two different groups. The number and codes of the specimens used for the trophic analyses are listed in the Supplementary Table S3.

Morphospace

We have shown in previous studies that different integrated phenotypic structures of the cheliceral morphology of *Dysdera* spiders from the Canary Islands are related with their trophic adaptations (Bellvert et al. 2022). Following Bellvert et al. (2022), we used the dorsal and lateral view of the basal segment, and the lateral view of the fang to explore variation in phenotypic disparity and in the direction of morphological change between the different species-island groups. In brief, we took high-resolution photographs of different views for of all the specimens with a LEICA DFC 450 digital camera attached to a LEICA MZ16A stereoscopic microscope using the software Leica Application Software (LAS) v.4.4 (Leica Microsystems Ltd, Switzerland). We quantified morphological variation using landmark-based geometric morphometrics (Bookstein 1991; James Rohlf and Marcus 1993; Adams et al. 2004; Zelditch et al. 2004; Mitteroecker and Gunz 2009). Whenever possible, we digitized the left chelicera for five females and five males of each species. In case of damaged or missing left structures, we assumed symmetry in the vertical plane and the right side was imaged and mirrored. Photographs for each view of the chelicera were compiled using the software TpsUtil (Rohlf 2015) and landmarks and semilandmarks were digitized using TpsDig2 (Rohlf 2017). Specifically, we considered 14 landmarks on the dorsal view of the basal chelicera segment; four fixed landmarks and 20 sliding semilandmarks on the lateral view; and three fixed landmarks and 10 semilandmarks on the lateral view of the fang (for more information of the landmarks position see Bellvert et al. 2022).

All three landmark configurations were subjected to generalized Procrustes

analysis (GPA) to remove non-shape variation related to location, rotation and scale (Gower 1975; Rohlf and Slice 1990) with the *gpagen* function implemented in the R package “geomorph” (Adams et al. 2021; Baken et al. 2021). Following previous studies focused on the *Dysdera* spider chelicera (Bellvert et al. 2022), we combined all three different datasets in a single landmark configuration that will function as a two-dimensional approximation from a three-dimensional structure (Bellvert et al. 2022) with the function *combine.subsets*. To test the increase or decrease in morphological disparity between populations of the same species inhabiting different islands, we used the function *morphol.disparity* with 999 iterations and the function *dataEllipse* from the “car” package to visualize levels of intraspecific variation. Additionally, to test whether the magnitude and direction of phenotypic change between populations inhabiting different islands differed across species, we used a Phenotypic Trajectory Analysis (Adams and Collyer 2009) as implemented in the function *trajectory.analysis* from the “RRPP” package (Collyer and Adams 2018, 2021) which allows to calculate the magnitude and direction of change in phenotypic space (Adams and Collyer 2009). As this method can only quantify change between two evolutionary levels, we used *D. silvatica* for two different comparison, one involving specimens from La Gomera and La Palma, and a second one involving specimens from La Gomera and El Hierro. The number and codes of the specimens used for the morphological analyses are listed in Supplementary_Table_S4.

Geographic range

Species and environmental data

To investigate sources of environmental variation across species-island distributional ranges, we used a model-based estimation of the potential distribution of each species-island by means of species distribution modelling (SDM). For the species occurrence data, we included all the localities with species presence gathered during field collections, removing repeated or missing coordinates for each species.

We obtained the environmental data from Patiño et al. (in prep). For this study, we selected the 3 predictors that, based on former knowledge, we consider might have a higher impact on the potential species distribution: the highest temperature of any month, to control of the potential effect of aridity; the accumulated precipitation over a year, to take into account humid areas; and elevation, which is known to influence both temperature and vegetation on steep islands. Names and coordinates of each species localities used for the subsequent analyses are listed in Supplementary_Table_S5.

Model based analysis

To perform the SDM we used Generalized Additive Models (GAM) (Hastie and Tibshirani 1986) with presence-background data using 5000 random points for each species-island model. We conducted the analysis with the *gam* function from the “gam” R package (Hastie 2022). Then, we calculated the differences in overlap between the different species-islands pairs, i.e. *D. silvatica* and *D. gomerensis* from La Gomera and El Hierro, and *D. silvatica* and *D. calderensis* from La Gomera and La Palma. We used the “D” similarity statistics (Warren et al. 2008) with the *nicheOverlap* function from the “dismo” package (Hijmans et al. 2022). This statistic ranges from 0 (no overlap) to 1 (identical distribution) computed from the prediction of the species distribution. We designed these comparisons to test for differences in the degree of overlap between pairs of species found in different islands, as indication that species environmental preferences may differ depending on the island where they are present. However, these statistics do not reveal if species increase or decrease their distribution range, but simply the shared space in their potential distribution. To detect the impact on the distribution range of the target species when colonizing a more depauperate island, we applied a threshold of 0.05 in the potential distribution for each species-island and transformed the map generated from this potential distribution to a binary state of presence (values higher than 0.05) or absence (values

lower than 0.05). Then, we calculated the percentage of occupancy of each species in each island to detect the potential increase or decrease in their distributional area. We are well aware that a threshold of 0.05 largely overestimates the actual distribution of the species resulting in a highly unlikely species distribution. However, because the low number of localities and the high number of randomly distributed background points, we are certainly underestimating the potential distribution of the species that, using higher thresholds would translate into an extremely conservative occupancy of the species in the archipelago. Furthermore, as the main point of the analysis was not to understand the distribution of the *Dysdera* species, but to detect variation in their habitat range across islands, a consistent bias applied to all species should not have an impact on the conclusions of our study. As the randomly distributed background points may slightly affect the species potential distribution, we repeated those analysis 1000 times to calculate the deviation present due this randomness. To test for significant difference in the overlaps and the percentage of range occupied by one species in different islands, we performed a Student's t-test with the deviation obtained from the 1000 potential distribution permutations.

Finally, we calculated the percentage of environmental range used by each species compared to the island that they inhabit. The logic behind this was to exclude that the increase in spatial range was being explained by the increase of more suitable conditions in the colonized island. For example, if a specific species adapted to certain residual climatic conditions in the original island, colonize a new island were the conditions that it is adapted represents the majority of the climatic conditions of this new island, the increase in spatial range could be explained because the more suitable conditions for this specific species has also increased, and not because the expansion of its niche. The climatic values were obtained from each locality where the species was present. For the island climatic range, we used 50000 randomly distributed background points to cover all the island surface and took the environmental value for

each predictor from each point. We transformed our data with the *scale* function and build a three-dimensional convex hull using the values of all localities for each specie-island/island with the function *cxhull* from the “*cxhull*” package (Laurent 2022). Then, we calculated the volume for all the different analyzed groups and islands and performed a z-test to compare the proportions of climatic volume used by each species in relation to the island that they inhabit. We used the function *prop.test* to detect differences in the proportion of climatic range used by the species in the different islands.

Results

Island sampling effort and number and timing of colonizations

The sample completeness curves (Fig. 2) obtained from the rarefaction of the species, estimated with a 95% confidence that the extrapolated number of species was 11.486 ± 3.129 , 5 ± 1.084 and 3 for La Gomera, El Hierro and La Palma, respectively. The estimates confirm that the larger number of species in La Gomera

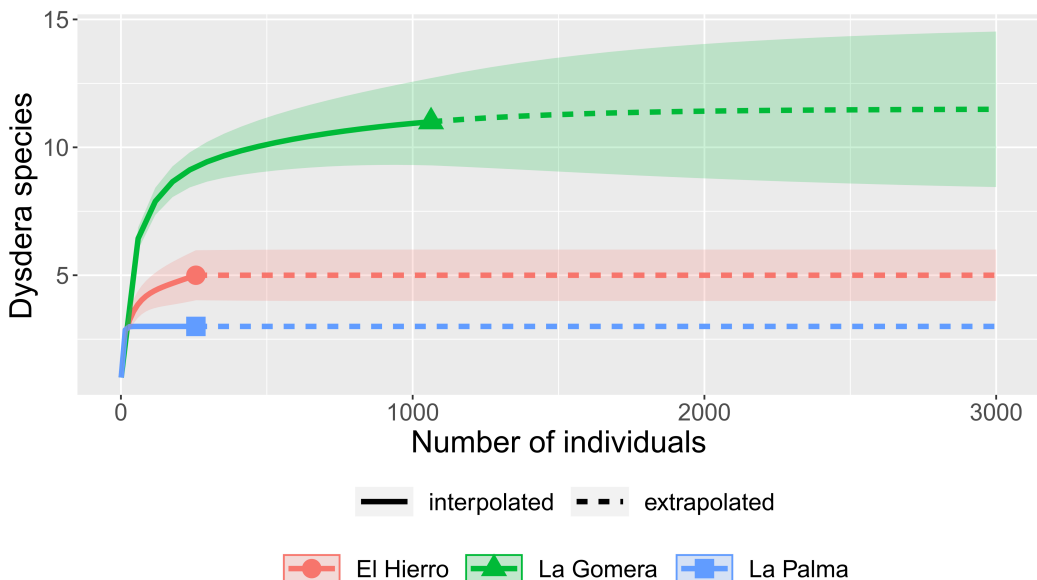


Figure 2. Sample-size-based rarefaction (solid line) and extrapolation (dotted line) sampling curves with 95% confident intervals for the *Dysdera* species richness in the three analysed islands.

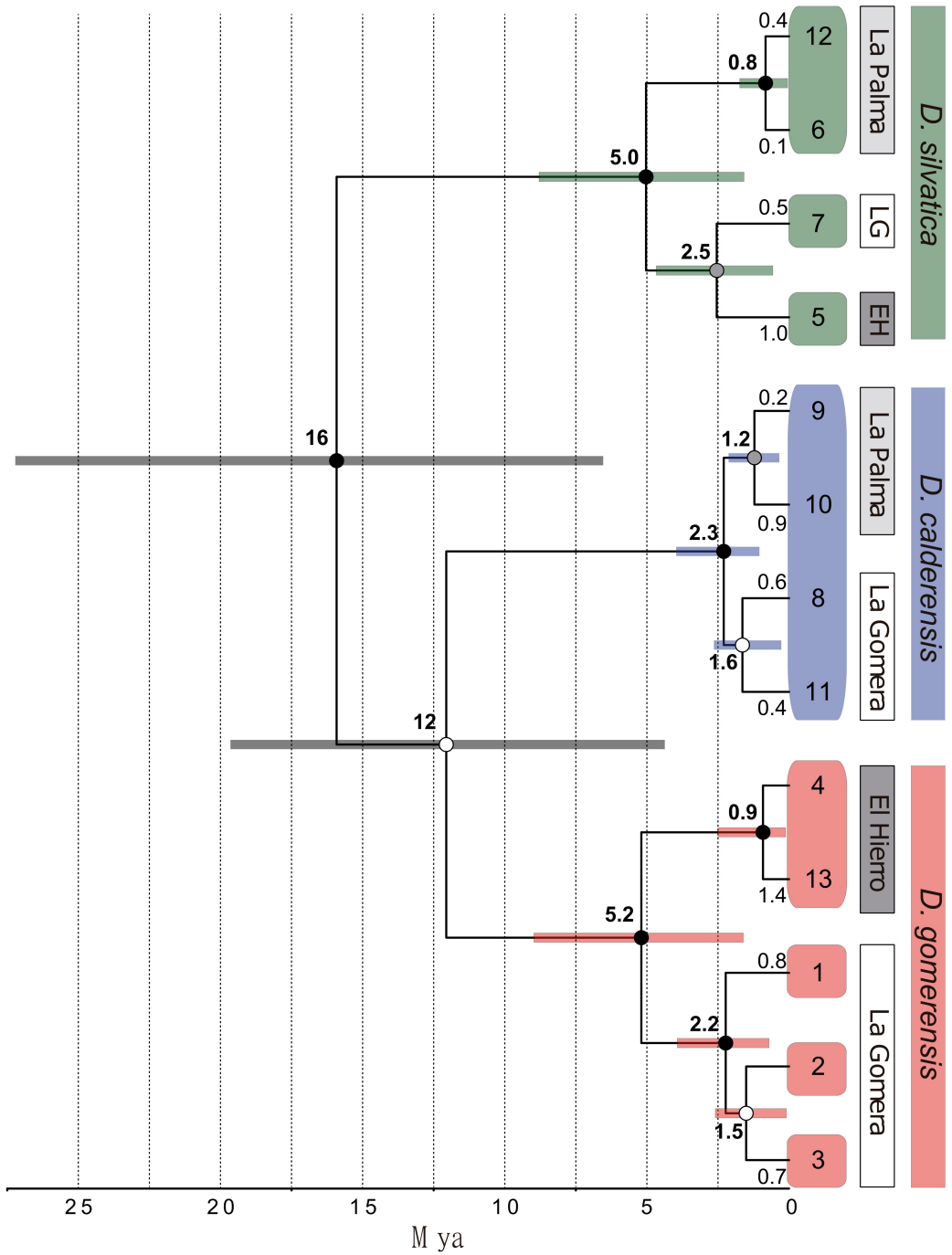


Figure 3. Bayesian multi-coalescent maximum clade credibility species tree. Terminals with numbers correspond to independent holotypes networks identified by statistical parsimony (TCS, see supplementary Fig. S2). Clades are colored according to species and island populations. Bars on nodes denote 95% HPD confidence intervals. Numbers on branches indicate the estimated median age of the corresponding most recent common ancestor (MRCA). Dots on nodes indicate support levels: black=posterior probability (PP) above 0.95, grey= PP above 0.9, white= PP below 0.9. X-axes time millions of years from the present (Mya: million years ago).

compared to the other islands is not an artifact due to differential sampling effort.

We obtained 129679 bp long DNA barcodes, which corresponded to 98 distinct haplotypes. Maximum likelihood analysis supported monophyly of the three species and their respective island populations, except for *D. calderensis* whose internal relationships were unsupported (Fig. S1). Within *D. silvatica*, the haplotypes from La Gomera and El Hierro were recovered as monophyletic. The mPTP and the TCS delimitation methods yielded 8 and 13 clusters, respectively (Table S2, Fig. S1). In all cases clusters were compatible between methods, differences were due to mPTP clusters being further split by TCS. All clusters were formed by populations of single islands and single species. Uncorrected genetic distances of the TCS clusters are summarised in Table S2. The largest within islands intraspecific divergences within islands were found in *D. calderensis* (4% in both La Palma and La Gomera) and *D. gomerensis* (5% and 3.6% on La Gomera and El Hierro, respectively), while the lowest divergence between island populations was found in *D. silvatica* (0.8%, 2.5% and 1.5% in La Gomera, La Palma and El Hierro respectively). A similar pattern was observed in the estimated divergence times (Fig. 3). *D. silvatica* and *D. gomerensis* earlier splits occurred approximately 5 My ago, while *D. calderensis* was estimated at 2.3 My ago. However, the earliest split in *D. silvatica* was between La Palma and the other populations at 5 My (8.8-1.6 My), while La Gomera and El Hierro split as early as 2.5 My ago (4.7-0.6 My), similar to the split of La Gomera and La Palma populations of *D. calderensis* (2.3 My ago, 3.9-1 My), while *D. gomerensis* from La Gomera and El Hierro populations split at 5.2 My (8.9-1.6 My). The time-aware phylogenetic analyses recovered the island populations of *D. calderensis* as reciprocally monophyletic albeit with low support.

Species-island trophic breadth

The stable isotope values revealed that *D. gomerensis* from El Hierro has the higher N value, while *D. silvatica* from La Gomera has the highest C value and *D. silvatica* from

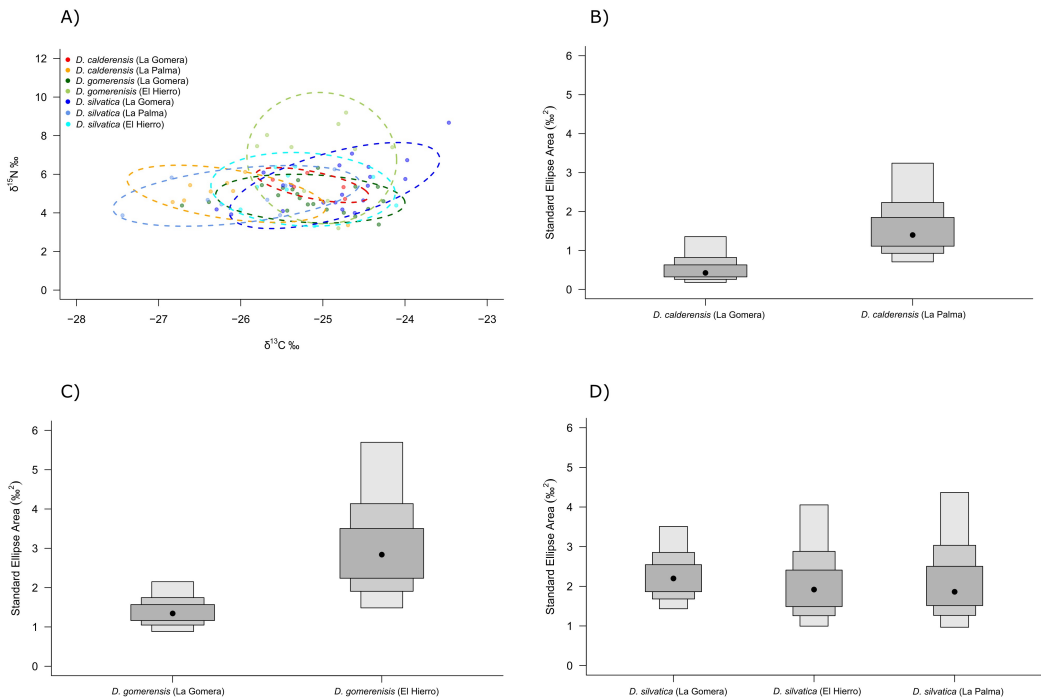


Figure 4. A) Carbon and Nitrogen values for each species-island. Standard ellipses area for each species; B) *D. calderensis*, C) *D. gomerensis* and D) *D. silvatica*.

La Palma the lowest C values (Fig. 4A). The Bayesian standard ellipse areas showed differences in the trophic breadth between species colonizing different islands. *D. calderensis* and *D. gomerensis* from La Gomera had the smallest ellipse area. All the other species-island areas show similar values when compared between them. The posterior distribution of the ellipses indicated that 98.45% of the area of *D. calderensis* from La Gomera was smaller than the one of the same species from La Palma (Fig. 4B). The same pattern was observed when comparing *D. gomerensis* from La Gomera with the populations from El Hierro (98.22%, Fig. 4C). Interestingly, in *D. silvatica*, the posterior distribution of La Gomera population was only 56.95% and 53.34% smaller than the ones from El Hierro and La Palma, respectively (Fig. 4D).

Phenotypic disparity

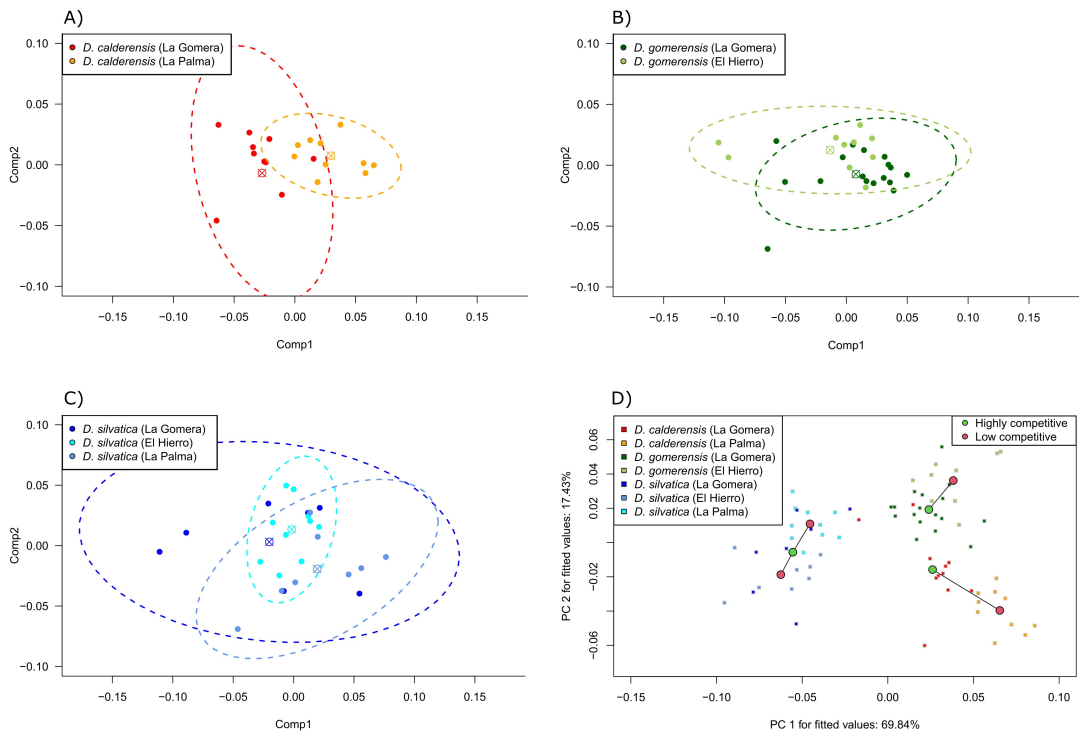


Figure 5. Phenotypic space of all specimens for the cheliceral subset combination. Phenotypic disparity between the high competition islands and low competition islands in A) *D. calderensis*, B) *D. gomerensis* and C) *D. silvatica*. D) Species phenotypic trajectories between high competition islands (green circle) and the low competition islands (red circle).

The geometric morphometric analyses did not reveal significant variation in morphological disparity between low and high competitive environments (Fig. 5A-C), with the single exception of *D. silvatica* from La Gomera, which showed a significant decrease in disparity when compared with representatives from El Hierro (Fig. 5C, Procrustes variance between *D. silvatica* from La Gomera = 0.0049 and from El Hierro = 0.0013, p -value = 0.0035). The other two species did not show any apparent variation in intraspecific disparity when comparing Island populations (Procrustes variance between *D. calderensis* from La Gomera = 0.0043 and from La Palma = 0.0025, p -value = 0.134; and between *D. gomerensis* from La Gomera = 0.0025 and from El Hierro = 0.0028, p -value = 0.714).

The trajectory analysis, however, revealed no significant differences between species colonizing the same islands (Fig. 5D). *D. silvatica* and *D. calderensis* showed the same direction in their phenotypic trajectory when comparing their transition between La Gomera and La Palma (angle = 92.25, p-value = 0.06), and the same pattern was recovered when focusing on the phenotypic transition of *D. silvatica* and *D. gomerensis* from La Gomera to El Hierro (angle = 86.90, p-value = 0.07). It is worth noticing that despite the no significant differences observed in the angles between trajectories, those angles are around 90°, which may seem different trajectories. However, these high values may be related to the sample size used in this study.

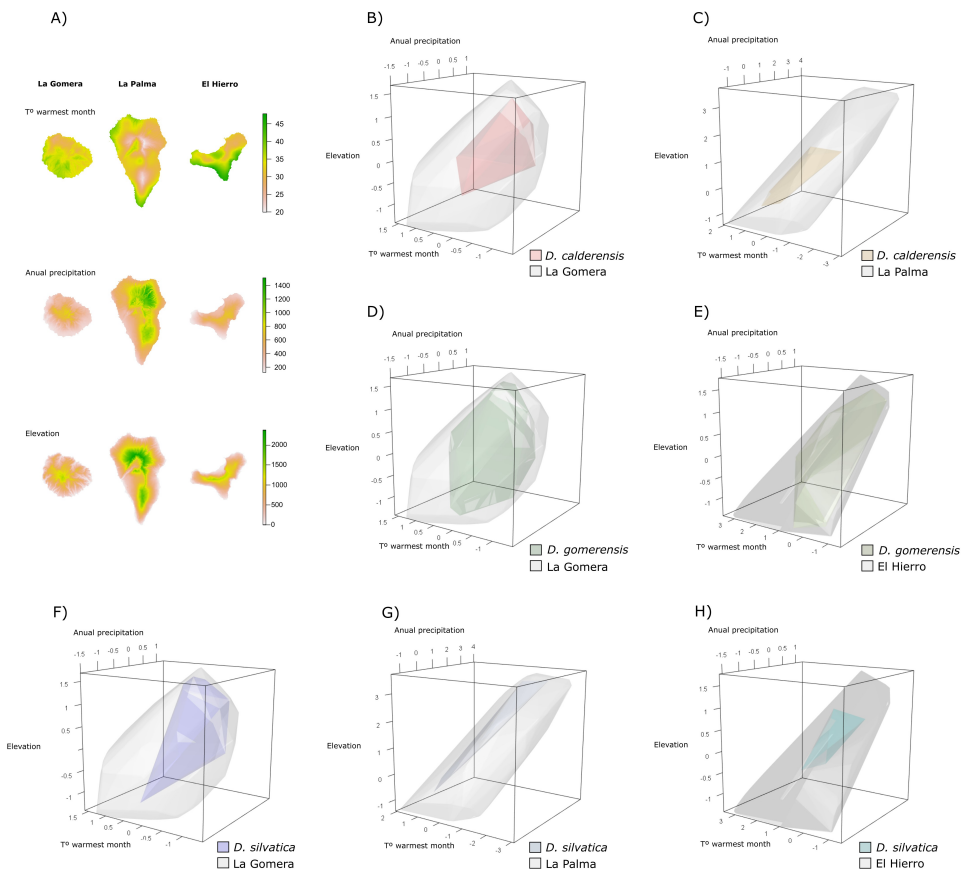


Figure 6. A) Climatic layers used for the climatic and spatial range analyses. B-H) Convex hulls between species-island group and the island that they inhabit.

Geographic range

When testing for differences in the species climatic niche range in relation with the island niche availability based on the selected predictors (Fig. 6A), we observed that none of the species showed significant variation in the proportion of occupied space following colonization of low-competition islands (*D. calderensis* p-value = 0.18, *D. gomerensis* p-value = 0.56, *D. silvatica* in La Palma p-value 0.13, Fig. 6B-G). The only exception was *D. silvatica*, which significantly reduced its occupancy in El Hierro compared to La Gomera (p-value = 0.01862, Fig. 6H).

The niche overlap analysis between the different species pairs that share island distributions revealed a significant overlap reduction in islands with low competition (niche overlap between *D. silvatica*/*D. calderensis* in La Gomera = 0.88 ± 0.02 and in La Palma = 0.75 ± 0.03 , p-value $\ll 0.01$, and *D. silvatica*/*D. gomerensis* in La Gomera = 0.95 ± 0.01 and in El Hierro = 0.87 ± 0.01 , P-value $\ll 0.01$, Fig. 7A). The spatial range for each species-island inferred with the GAM model potential distribution differed

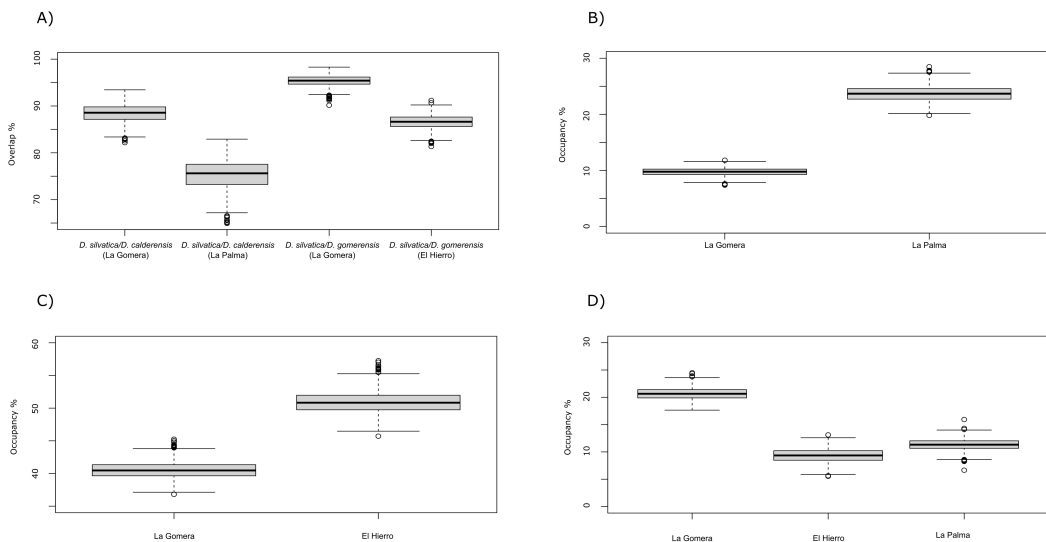


Figure 7. A) Overlap between all the species pairs that share different islands (highly and low competition). Percentage of island occupancy between highly and low competition areas for each species; B) *D. calderensis*, C) *D. gomerensis*, D) *D. silvatica*.

across species. For *D. silvatica*, the percentage of spatial range in La Gomera was significantly larger (p -value $\ll 0.01$) than in the two islands with lower competition (20.6% sd = 1.09%, 11.3% sd = 1.04%, 9.3% sd = 1.24%, for La Gomera, La Palma and El Hierro, respectively (Fig. 7D). Conversely, the other species shown an opposite trend, the percentage of island occupied was larger in the lower competition islands, for both for *D. calderensis* (La Gomera = 9.72% sd = 0.73% and La Palma = 23.7% sd = 1.38%, p -value $\ll 0.01$, Fig. 7B) and for *D. gomerensis* (La Gomera = 40.53% sd = 1.28% and El Hierro = 50.93% sd = 1.73%, p -value $\ll 0.01$, Fig. 7C).

Discussion

In this study, we addressed two key questions for elucidating the interplay between ecological release and specialization. Do species experience ecological release when colonizing new environments with lower competition levels? And, if so, is the response affected by different species-specific eco-morphologies? Here, we have adopted a definition of ecological release as a niche expansion or shift induced by a reduction or removal of interspecific interactions (Herrmann et al. 2021). The classical theory of island biogeography predicts that island populations will have broader niches than their continental counterparts (MacArthur and Wilson 1967), as a result of ecological release. Here we have compared patterns across oceanic islands, where our experimental setting involves older islands with more species and younger islands with less species, which parallels the traditional continent-island comparison. Furthermore, our study involved multiple comparisons across closely related species with contrasting dietary preferences —i.e. generalists versus specialists— which enables us to determine the impact of alternative ecological strategies on the degree and direction of ecological release. While most studies of ecological release are based on the analysis of single ecological or eco-phenotypic traits (e.g. Cox and Ricklefs 2006; Buckley and Jetz 2007; Bolnick et al. 2010; Andrades et al. 2019), here we have integrated different methodologies to analyse different aspects of the species' niche,

namely those captured by the phenotype, diet, habitat and distribution range. This way, we have been able to not only test the effect of ecological opportunity on species with contrasting dietary preferences, but to also provide insights into how and through what mechanisms these species expanded their niches.

The results obtained from genetic analyses indicate that species colonised each island once. Although island populations of each species were reciprocally monophyletic, hampering the inference of the direction of colonization, indirect evidence supports a scenario of colonization from older to younger islands (i.e., from high competition to low competition islands). First, both *D. calderensis* and *D. silvatica* had their sister groups in the older island, La Gomera (Arnedo et al. 2007). Furthermore, although the sister group of *D. gomerensis* remains uncertain, the estimated divergence time between the island clades predates the emergence of the younger island, El Hierro. Moreover, the time of colonization overlaps across species, suggesting that the observed differences in ecological features are neither the result of multiple colonisations nor of the time since colonization.

The use of stable isotope analysis to estimate the trophic niche width of the species has been proven a useful technique compared to other conventional methods (Bearhop et al. 2004; Fink et al. 2012). The comparison of trophic breadth, inferred from the stable isotope data analysed, revealed that, contrary to our expectations, both studied specialist species underwent a significant expansion of their niche after colonizing low competition islands (Fig. 4B-C). By contrast, the generalist species did not exhibit any significant changes in niche breadth, regardless of the island (Fig. 4D). Since an increase in SEAb has been linked to ecological release processes in species facing new ecological opportunities (Andrades et al. 2019), our results suggest that specialist species are more prone to undergo ecological release than generalists, at least in red devil spiders. However, some caution is needed in this interpretation, as our results could have been influenced by sampling biases. It has been shown that

sample sizes below 10 individuals can result in an underestimation of the population niche size (Cucherousset et al. 2020). However, the results obtained with the comparison with species with low sample size (e.g. *D. calderensis*), mirrored those obtained with the ones in which we had a proper representation (e.g. *D. gomerensis*). For this reason, it seems unlikely that the low sampling available for some species has driven the observed patterns.

The cheliceral morphology of *Dysdera* species has been linked to their trophic niche (Řezáč et al. 2008, 2021; Toft and Macías-Hernández 2017, 2021, Bellvert et al. in press). Therefore, following the previous argument regarding the trophic niche, we should expect that species colonizing new environments also undergo an increase in the morphological disparity of their mouthparts. However, our results failed to detect any significant variation, regardless of the species and island. This result do not negate the importance of ecological release for other species' evolutionary processes (Des Roches et al. 2011). Actually, an increase in morphological disparity is poorly documented in ecological release scenarios (Schluter 2000), and it has been pointed out that an increase in resource usage does not necessarily translate into an increase of morphological variability (Bolnick et al. 2007; Costa et al. 2008), although phenotypic traits that grant access to novel resources might be favoured by selection (Bolnick et al. 2003). In all species analysed, when colonizing low competition islands, we have seen that there is no significant difference in the phenotypic trajectory that they show in the morphospace, showing that some selection could have been playing a role in the phenotype change when colonizing these low competition islands. However, the trajectory of change in the generalist species could be deceptive, as the morphospace occupied by the individuals on the low competition island do not exceed the morphospace built by the individuals from La Gomera. Then, more than a real change in the direction of the phenotypic space in *D. silvatica*, what we can see is the occupation of part of the original morphospace by a group with a reduced

morphological disparity.

Interestingly, the two species with the most similar cheliceral morphology (*D. calderensis* and *D. gomerensis*) yielded the lowest differences between all the species-pairs of phenotypic directions (angle = 70.96, p-value = 0.180). These similar morphological trajectories taken by both specialist species may hint the existence of an area in the morphospace that promoted the expansion of other axes of the ecological niche studied here. Following the classification of Bellvert et al. (in press), the morphospace occupied by these two species in the low competitive islands corresponded to a specialist cheliceral morphology. As currently defined, trophic specialisation in red devil spiders mostly refers to a reduction in the different kinds of prey they could feed on, mostly consisting of terrestrial isopods. Such specialisation is generally accompanied by morphological changes in mouthparts and behaviour that facilitate the capture and manipulation of isopods using different hunting strategies to overcome their mechanic defenses (Řezáč et al. 2008). Additionally, specialist red devil spiders show metabolic (Toft and Macías-Hernández 2017) and genetic adaptations (Pekár et al. 2016) to feed on isopods. However, specialist red devil spiders from the Canary Islands have been shown to also consume other types of arthropods, although to a lesser degree (Toft and Macías-Hernández 2017, 2021, Bellvert et al. in press). It should also bear in mind that, because of their defences, terrestrial isopods are prey rejected by most generalist predators (Pekár, Líznavá, & Řezáč, 2016). Therefore, it seems reasonable to conclude that species with specialized chelicerae morphologies are not strict specialists in the sense of having narrowed their potential prey, but quite the opposite, they have developed the ability to include in their diet prey discarded by putative competitors.

Competition plays an important role in species spatial distribution. The absence or reduction of interspecific interactions with other species in the same or similar ecological guild may drive range expansion (Noon 1981). If this is the case, we should

expect larger overlap between the distributions of species pairs in low competition islands, due to an increase of their distribution ranges following colonization of islands with less congeneric species. Conversely, our data indicated a reduction in the overlap of the generalist and specialist species in low competition islands (Fig. 7A). A possible explanation of this pattern lays in the impact of traits related to resource usage on the ability of species to expand their ranges (Betzholtz et al. 2013). In this regard, we did observe that specialist species tend to increase their potential distribution when colonizing low competition islands, while the generalist species reduced its spatial range under the same conditions. Moreover, the reduction of the generalist does not only involve the percentage of occupied area, but also the climatic range used, at least in one of the low competition islands (Fig. 6H). These results are in conflict with the general assumption that a generalist diet would favour range expansion following environmental or habitat shifts (Warren et al. 2001; Pöyry et al. 2009; Betzholtz et al. 2013), by relaxing dietary constraints and facilitating access to more resources. Nevertheless, the former studies that provide evidence for the relationships between generalist strategies and range expansion, focused on the effects of diet breadth in a scenario of climatic change. Situations in which the ecological environment remains similar and the differences only involve the levels of interspecific competition, as the one here studied, may result in different outputs.

Our specialist species underwent a significant increase in their trophic breadth and distribution range following colonization of a low competition island. The expansion of trophic breadth in these two species could be indicative of an evolutionary transition from more specialized strategies to a more generalist prey preference. Shifts in trophic preferences as a result of ecological opportunities are well-documented in the literature (Quevedo et al. 2009; Evangelista et al. 2014). On the other hand, the generalist species, *D. silvatica*, did not seem to experience an increase in neither niche breadth nor geographic range. In fact, at least in one case, the generalist species

decreased its phenotypic variability and climatic range when colonizing a low competition island. This may be indicative that specialization in the *Dysdera* spider genus could be a key innovation that influence the increase of their niches after colonizing new depauperate environments in front of other generalist species which can not take advantage of the new resources present in the island. Increasing the trophic breadth by including prey discarded by other predators would actually benefit so-called specialist red devils to exploit additional resources in novel environments, facilitating ecological release in these species compared to generalist ones. More data on prey availability across islands and habitats and the evaluation of consumed prey in the field, maybe by means of molecular prey detection techniques, will be required to test this possibility.

The short-term effects of ecological release are much better understood than the long-term impact that this process may have on species diversification (Yoder et al. 2010). Here we have demonstrated that for specialized *Dysdera* spiders, new ecological opportunities arising from the colonization of younger islands with lower numbers of congeneric species have translated into an expansion of the ancestral ecological niche. Shifts in the ecological niche have been associated with the early stages of species diversification (Schluter 2000; Stroud and Losos 2016). However, although ecological opportunities can play a key role in speciation (Nosil et al. 2005; Schluter 2009), there is no evidence that ecological release promoted diversification of the red devil *Dysdera* spiders in the Canary Islands. An increase in intraspecific trait variation does not necessarily promote the formation of new species (Bolnick et al. 2007). Some lineages may simply respond to new ecological opportunities by becoming superabundant generalists rather than diversifying (Yoder et al. 2010). The deep phylogeographic structure observed between the island populations of the species analysed in the present study points towards a lineage divergence driven by geographic isolation and time since colonization, which will be framed as a classic

model of allopatric speciation (Mayr 1942; Coyne and Orr 2004; Yoder et al. 2010), rather than a case of ecological speciation. The transition to a broader niche of the colonizing specialist species could be playing an important role in the initial stages of divergence by ensuring higher rates of survival for those new island lineages (Dennis et al. 2011), which would eventually, if genetic isolation persists, become different species from their high competition island ancestral species.

Conclusions

By taking advantage of the experimental conditions provided by the multiple, independent colonisation events of low competition islands by species of red devil *Dysdera* spiders with different dietary preferences, we provide novel insights into the effect of ecological opportunities in species evolution and diversification. We have shown that different morphologies related to trophic specialization, play an important role in predicting the species' ability to increase their ecological niche following the colonization of environments with lower levels of congeneric species. Counterintuitively, ecological release as measured using different aspects of the ecological niche, namely morphology, isotopic signal, and environmental preferences, was evident in specialist but not generalist species. Their ability to feed on isopods, a prey usually rejected by most predators, in addition to other arthropods, may have been instrumental to increase their ecological niche when compared to generalist species. Additionally, our results highlight the need to integrate different approximations to characterize the ecological niche, since the increase of variation associated with ecological release may not be equally evident in different sets of traits. Specifically, we could not detect an increase in morphological variation between populations of the same species inhabiting high and low competition islands, but differences were evident when looking at the isotopic signal and the environmental preferences. Our results offer novel insights into the role of ecological release processes in promoting adaptive radiations in oceanic islands.

Acknowledgements

To the Cabildos of El Hierro, La Gomera and La Palma and to the Garajonay National Park for the collection permits. To Salvador de la Cruz, Marc Domènech, Nuria Macías-Hernández and Pedro Oromí for their help and support in the sampling campaigns and the obtaining of specimens.

A.B. was funded by an individual PhD grant BES-2017-080538 from the Ministerio de Economía, Industria y Competitividad of the Spanish government. A.K. is supported by a Ramón y Cajal research grant co-funded by the Spanish State Research Agency and the European Social Fund (RYC2019-026688-I/AEI/10.13039/501100011033). This study was supported by project grants CGL2012-36863 and CGL2016-80651-P from the Spanish Ministry of Economy and Competitiveness and 2017SGR83 from the Catalan Government to M.A.

References

- Adams, D. C., and M. L. Collyer. 2009. A general framework for the analysis of phenotypic trajectories in evolutionary studies. *Evolution* (N. Y.). 63:1143–1154.
- Adams, D. C., M. L. Collyer, A. Kaliontzopoulou, and E. K. Baken. 2021. Geomorph: Software for geometric morphometric analyses. R package version 4.0.
- Adams, D. C., F. J. Rohlf, and D. E. Slice. 2004. Geometric morphometrics: Ten years of progress following the ‘revolution.’ *Ital. J. Zool.* 71:5–16.
- Adrián-Serrano, S., J. Lozano-Fernandez, J. Pons, J. Rozas, and M. A. Arnedo. 2020. On the shoulder of giants: Mitogenome recovery from non-targeted genome projects for phylogenetic inference and molecular evolution studies. *J. Zool. Syst. Evol. Res.* 1–26.
- Andrades, R., A. L. Jackson, R. M. Macieira, J. A. Reis-Filho, A. F. Bernardino, J.-C. Joyeux, and T. Giarrizzo. 2019. Niche-related processes in island intertidal communities inferred from stable isotopes data. *Ecol. Indic.* 104:648–658. Elsevier.
- Armbruster, W. S., and B. G. Baldwin. 1998. Switch from specialized to generalized pollination. *Nature* 394:632.
- Arnedo, M. A., P. Oromí, C. Múrria, N. Macías-Hernández, and C. Ribera. 2007. The dark side of an island radiation: systematics and evolution of troglobitic spiders of the genus *Dysdera* Latreille (Araneae: Dysderidae) in the Canary Islands. *Invertebr. Syst.* 21:623–660.
- Arnedo, M. A., P. Oromí, and C. Ribera. 2000. Systematics of the Genus *Dysdera* (Araneae, Dysderidae) in the Eastern Islands. *J. Arachnol.* 261–292.
- Arnedo, M. A., and C. Ribera. 1999. Radiation in the genus *Dysdera* (Araneae, Dysderidae) in the Canary Islands: The island of Tenerife. *J. Arachnol.* 27:604–662.
- Baken, E. K., M. L. Collyer, A. Kaliontzopoulou, and D. C. Adams. 2021. gmShiny and geomorph v4.0: new graphical interface and enhanced analytics for a comprehensive morphometric experience. *Methods Ecol. Evol.* Submitted.
- Batthey, C. J. 2019. Ecological release of the anna’s hummingbird during a Northern range expansion. *Am. Nat.* 194:306–315.
- Bearhop, S., C. E. Adams, S. Waldron, R. A. Fuller, and H. Macleod. 2004. Determining trophic niche width: A novel approach using stable isotope analysis. *J. Anim. Ecol.* 73:1007–1012.
- Bellvert, A., M. Roca-Cusachs, V. Tonzo, M. A. Arnedo, and A. Kaliontzopoulou. 2022. The Vitruvian spider: segmenting and integrating over different body parts to describe eco-phenotypic variation. *J. Morphol.* 283:1425–1438.
- Bellvert A., Adrián-Serrano S., Macías-Hernández N., Toft S., Kaliontzopoulou A. & Arnedo M.A. (in

- press). The non-dereliction in evolution: Trophic specialisation drives convergence in the radiation of red devil spiders (Araneae: Dysderidae) in the Canary Islands. *Syst. Biol.*
- Betzholtz, P. E., L. B. Pettersson, N. Ryrholm, and M. Franzén. 2013. With that diet, you will go far: Trait-based analysis reveals a link between rapid range expansion and a nitrogen-favoured diet. *Proc. R. Soc. B Biol. Sci.* 280.
- Bidegaray-Batista, L., and M. A. Arnedo. 2011. Gone with the plate: The opening of the Western Mediterranean basin drove the diversification of ground-dweller spiders. *BMC Evol. Biol.* 11.
- Bolnick, D. I., T. Ingram, W. E. Stutz, L. K. Snowberg, O. L. Lau, and J. S. Pauli. 2010. Ecological release from interspecific competition leads to decoupled changes in population and individual niche width. *Proc. R. Soc. B Biol. Sci.* 277:1789–1797.
- Bolnick, D. I., R. Svanback, M. S. Araujo, and L. Persson. 2007. Comparative support for the niche variation hypothesis that more generalized populations also are more heterogeneous. *Proc. Natl. Acad. Sci.* 104:10075–10079.
- Bolnick, D. I., R. Svanbäck, J. A. Fordyce, L. H. Yang, J. M. Davis, C. D. Hulseley, and M. L. Forister. 2003. The ecology of individuals: Incidence and implications of individual specialization. *Am. Nat.* 161:1–28.
- Bookstein, F. L. 1991. *Morphometric tools for landmark data: Geometry and biology*. Cambridge University Press, New York.
- Buckley, L. B., and W. Jetz. 2007. Insularity and the determinants of lizard population density. *Ecol. Lett.* 10:481–489.
- Cardoso, P., M. A. Arnedo, K. A. Triantis, and P. A. V. Borges. 2010. Drivers of diversity in Macaronesian spiders and the role of species extinctions. *J. Biogeogr.* 37:1034–1046.
- Clement, M., D. Posada, and K. A. Crandall. 2000. TCS: A computer program to estimate gene genealogies. *Mol. Ecol.* 9:1657–1659.
- Collyer, M. L., and D. C. Adams. 2018. RRPP: An r package for fitting linear models to high-dimensional data using residual randomization. *Methods Ecol. Evol.* 9:1772–1779.
- Collyer, M. L., and D. C. Adams. 2021. RRPP. Linear Model Evaluation with Randomized Residuals in a Permutation Procedure.
- Colwell, R. K., A. Chao, N. J. Gotelli, S. Y. Lin, C. X. Mao, R. L. Chazdon, and J. T. Longino. 2012. Models and estimators linking individual-based and sample-based rarefaction, extrapolation and comparison of assemblages. *J. Plant Ecol.* 5:3–21.
- Costa, G. C., D. O. Mesquita, G. R. Colli, and L. J. Vitt. 2008. Niche Expansion and the Niche Variation Hypothesis: Does the Degree of Individual Variation Increase in Depauperate Assemblages? *Am.*

Nat. 172:868–877.

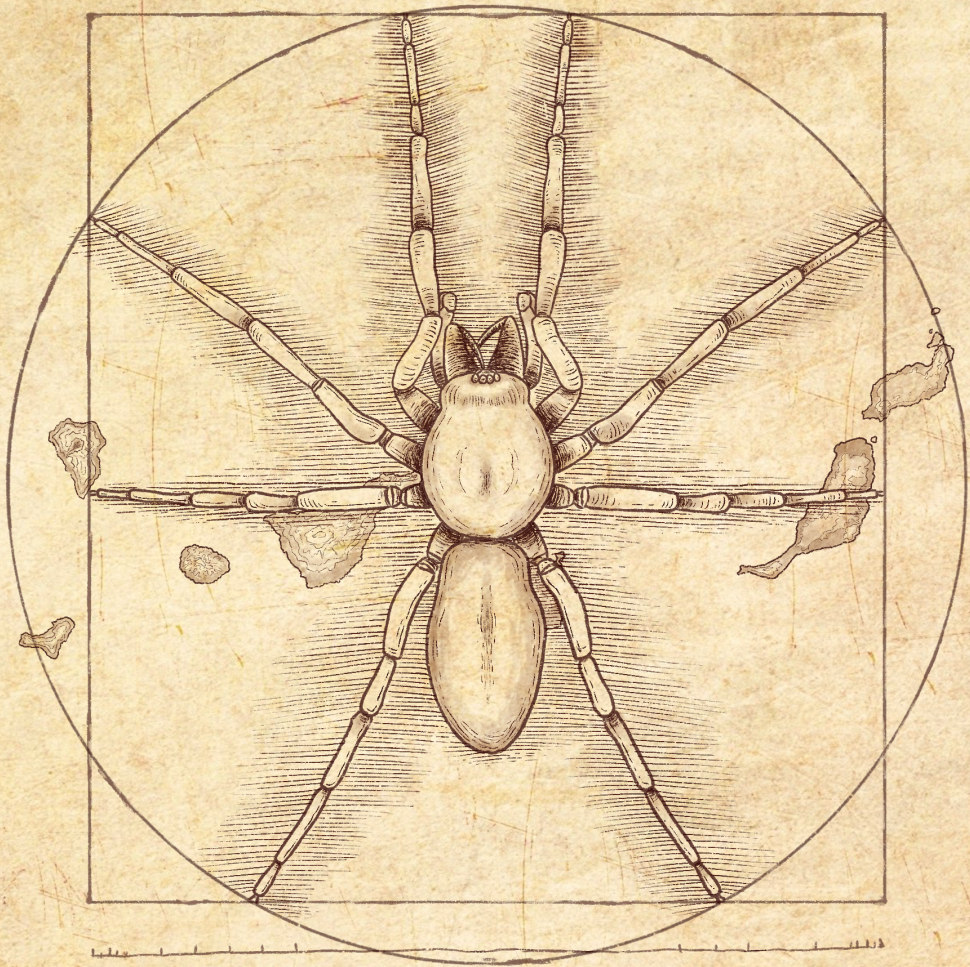
- Cox, G. W., and R. E. Ricklefs. 2006. Species Diversity and Ecological Release in Caribbean Land Bird Faunas. *Oikos* 28:113.
- Coyne, J. A., and H. A. Orr. 2004. *Speciation*. Sinauer Associates, Sunderland, MA.
- Crespo, L. C., I. Silva, A. Enguídanos, P. Cardoso, and M. A. Arnedo. 2021a. Integrative taxonomic revision of the woodlouse-hunter spider genus *Dysdera* (Araneae: Dysderidae) in the Madeira archipelago with notes on its conservation status. *Zool. J. Linn. Soc.* 192:356–415.
- Crespo, L. C., I. Silva, A. Enguídanos, P. Cardoso, and M. A. Arnedo. 2021b. The Atlantic connection: coastal habitat favoured long distance dispersal and colonization of Azores and Madeira by *Dysdera* spiders (Araneae: Dysderidae). *Syst. Biodivers.* 19:1–22. Taylor & Francis.
- Cucherousset, J., L. Závorka, S. Ponsard, R. Céréghino, and F. Santoul. 2020. Stable isotope niche convergence in coexisting native and non-native salmonids across age classes. *Can. J. Fish. Aquat. Sci.* 77:1359–1365.
- Darwin, C. R. 1859. *On the Origin of Species by Means of Natural Selection, or the Preservation of Favoured Races in the Struggle for Life*. John Murray Publishers, London.
- Day, E. H., X. Hua, and L. Bromham. 2016. Is specialization an evolutionary dead end? Testing for differences in speciation, extinction and trait transition rates across diverse phylogenies of specialists and generalists. *J. Evol. Biol.* 29:1257–1267.
- Dennis, R. L. H., L. Dapporto, S. Fattorini, and L. M. Cook. 2011. The generalism-specialism debate: The role of generalists in the life and death of species. *Biol. J. Linn. Soc.* 104:725–737.
- Des Roches, S., M. S. Brinkmeyer, L. J. Harmon, and E. B. Rosenblum. 2015. Ecological release and directional change in White Sands lizard trophic ecomorphology. *Evol. Ecol.* 29.
- Des Roches, S., J. M. Robertson, L. J. Harmon, and E. B. Rosenblum. 2011. Ecological release in white sands lizards. *Ecol. Evol.* 1:571–578.
- Evangelista, C., A. Boiche, A. Lecerf, and J. Cucherousset. 2014. Ecological opportunities and intraspecific competition alter trophic niche specialization in an opportunistic stream predator. *J. Anim. Ecol.* 83:1025–1034.
- Fink, P., E. S. Reichwaldt, C. Harrod, and A. G. Rossberg. 2012. Determining trophic niche width: An experimental test of the stable isotope approach. *Oikos* 121:1985–1994.
- Freeman, J., and M. T. Hannan. 1983. Niche width and the dynamics of organizational populations. *Am. J. Sociol.* 88:1116–1145.
- Futuyma, D. J. 1998. *Evolutionary Biology*. 3rd ed. Sinauer Associates, Sunderland, MA.
- Gillespie, R. G., G. M. Bennett, L. De Meester, J. L. Feder, R. C. Fleischer, L. J. Harmon, A. P. Hendry, M. L.

- Knope, J. Mallet, C. Martin, C. E. Parent, A. H. Patton, K. S. Pfennig, D. Rubinoff, D. Schluter, O. Seehausen, K. L. Shaw, E. Stacy, M. Stervander, J. T. Stroud, C. Wagner, and G. O. U. Wogan. 2020. Comparing Adaptive Radiations Across Space, Time, and Taxa. *J. Hered.* 111:1–20.
- Givnish, T. J., and K. J. Sytsma. 1997. *Molecular evolution and adaptive radiation*. Cambridge: Cambridge University Press.
- Gower, J. C. 1975. Generalized procrustes Analysis. *Psychometrika* 40:33–51.
- Hastie, T. 2022. *gam: Generalized Additive Models*. R package version 1.20.2.
- Hastie, T., and R. Tibshirani. 1986. Generalized additive models. *Stat. Sci.* 1:297–310.
- Heled, J., and A. J. Drummond. 2012. Calibrated tree priors for relaxed phylogenetics and divergence time estimation. *Syst. Biol.* 61:138–149.
- Herrmann, N. C., J. T. Stroud, and J. B. Losos. 2021. The Evolution of ‘Ecological Release’ into the 21st Century. *Trends Ecol. Evol.* 36:206–215. Elsevier Ltd.
- Hijmans, R. J., S. Phillips, J. Leathwick, and J. Elith. 2022. *dismo: Species Distribution Modeling*. R package version 1.3-8.
- Hoang, D. T., O. Chernomor, A. Von Haeseler, B. Q. Minh, and L. S. Vinh. 2018. UFBoot2: Improving the ultrafast bootstrap approximation. *Mol. Biol. Evol.* 35:518–522.
- Hsieh, T. C., K. H. Ma, and A. Chao. 2016. iNEXT: an R package for rarefaction and extrapolation of species diversity (Hill numbers). *Methods Ecol. Evol.* 7:1451–1456.
- Jackson, A. L., R. Inger, A. C. Parnell, and S. Bearhop. 2011. Comparing isotopic niche widths among and within communities: SIBER - Stable Isotope Bayesian Ellipses in R. *J. Anim. Ecol.* 80:595–602.
- James Rohlf, F., and L. F. Marcus. 1993. A revolution morphometrics. *Trends Ecol. Evol.* 8:129–132.
- Jorgensen, T. H., and J. M. Olesen. 2001. Adaptive radiation of island plants: evidence from *Aeonium* (Crassulaceae) of the Canary islands. *Perspect. Plant Ecol. Evol. Syst.* 4:29–42.
- Kalyaanamoorthy, S., B. Q. Minh, T. K. F. Wong, A. Von Haeseler, and L. S. Jermini. 2017. ModelFinder: Fast model selection for accurate phylogenetic estimates. *Nat. Methods* 14:587–589.
- Kapli, P., S. Lutteropp, J. Zhang, K. Kobert, P. Pavlidis, A. Stamatakis, and T. Flouri. 2017. Multi-rate Poisson tree processes for single-locus species delimitation under maximum likelihood and Markov chain Monte Carlo. *Bioinformatics* 33:1630–1638.
- Kennedy, S., J. Y. Lim, J. Clavel, H. Krehenwinkel, and R. G. Gillespie. 2019. Spider webs, stable isotopes and molecular gut content analysis: Multiple lines of evidence support trophic niche differentiation in a community of Hawaiian spiders. *Funct. Ecol.* 33:1722–1733.
- Lanfear, R., P. B. Frandsen, A. M. Wright, T. Senfeld, and B. Calcott. 2017. Partitionfinder 2: New methods for selecting partitioned models of evolution for molecular and morphological

- phylogenetic analyses. *Mol. Biol. Evol.* 34:772–773.
- Lanyon, S. M. 1992. Interspecific brood parasitism in blackbirds (Icterinae): a phylogenetic perspective. *Science* (80-.). 255:77–79.
- Laurent, S. 2022. cxhull: Convex Hull. R package version 0.6.0.
- Losos, J. B. 2010. Adaptive radiation, ecological opportunity, and evolutionary determinism: American society of naturalists E. O. Wilson award address. *Am. Nat.* 175:623–639.
- Losos, J. B., and K. De Queiroz. 1997. Evolutionary consequences of ecological release in Caribbean *Anolis* lizards. *Biol. J. Linn. Soc.* 61:459–483.
- MacArthur, R. H., J. M. Diamond, and J. R. Karr. 1972. Density Compensation in Island Faunas. *Ecology* 53:330–342.
- MacArthur, R. H., and E. O. Wilson. 1967. *The Theory of Island Biogeography*. Princeton University Press, Princeton, NJ. Macieira.
- Macías-hernández, N., S. De, C. López, and M. Roca-cusachs. 2016. A geographical distribution database of the genus *Dysdera* in the Canary Islands (Araneae, Dysderidae). 23:11–23.
- Macías-Hernández, N., S. de la C. López, M. Roca-Cusachs, P. Oromí, and M. A. Arnedo. 2016. A geographical distribution database of the genus *Dysdera* in the Canary Islands (Araneae, Dysderidae). *Zookeys* 2016:11–23.
- Mayr, E. W. 1942. *Systematics and the Origin of Species*. Columbia University Press, New York.
- Meimberg, H., T. Abele, C. Bräuchler, J. K. McKay, P. L. Pérez de Paz, and G. Heubl. 2006. Molecular evidence for adaptive radiation of *Micromeria* Benth. (Lamiaceae) on the Canary Islands as inferred from chloroplast and nuclear DNA sequences and ISSR fingerprint data. *Mol. Phylogenet. Evol.* 41:566–578.
- Miller, M. A., M. T. Holder, R. Vos, P. E. Midford, T. Liebowitz, L. Chan, P. Hoover, and T. Warnow. 2009. The CIPRES Portals.
- Mitteroecker, P., and P. Gunz. 2009. Advances in Geometric morphometrics. *Evol. Biol.* 36:235–247.
- Muller, A. 1996. Host-Plant Specialization in Western Palearctic Anthidine Bees (Hymenoptera : Apoidea : Megachilidae). *Ecol. Monogr.* 66:235–257.
- Nguyen, L. T., H. A. Schmidt, A. Von Haeseler, and B. Q. Minh. 2015. IQ-TREE: A fast and effective stochastic algorithm for estimating maximum-likelihood phylogenies. *Mol. Biol. Evol.* 32:268–274.
- Noon, B. R. 1981. The Distribution of an Avian Guild along a Temperate Elevational Gradient: The Importance and Expression of Competition. *Ecol. Monogr.* 51:105–124.
- Nosil, P. 2002. Transition rates between specialization and generalization in phytophagous insects.

- Evolution (N. Y). 56:1701–1706.
- Nosil, P., T. H. Vines, and D. J. Funk. 2005. Perspective: Reproductive isolation caused by natural selection against immigrants from divergent habitats. *Evolution* (N. Y). 59:705–719.
- Parent, and Crespi. 2009. Ecological Opportunity in Adaptive Radiation of Galápagos Endemic Land Snails. *Am. Nat.* 174.
- Pekár, S., E. Líznarová, and M. Řezáč. 2016. Suitability of woodlice prey for generalist and specialist spider predators: A comparative study. *Ecol. Entomol.* 41:123–130.
- Pöyry, J., M. Luoto, R. K. Heikkinen, M. Kuussaari, and K. Saarinen. 2009. Species traits explain recent range shifts of Finnish butterflies. *Glob. Chang. Biol.* 15:732–743.
- Quevedo, M., R. Svanbäck, and P. Eklöv. 2009. Intrapopulation niche partitioning in a generalist predator limits food web connectivity. *Ecology* 90:2263–2274.
- R Core Team. 2022. R: A Language and Environment for Statistical Computing.
- Rambaut, A., A. J. Drummond, D. Xie, G. Baele, and M. A. Suchard. 2018. Posterior summarization in Bayesian phylogenetics using Tracer 1.7. *Syst. Biol.* 67:901–904.
- Řezáč, M., S. Pekár, M. Arnedo, N. Macías-Hernández, and V. Řezáčová. 2021. Evolutionary insights into the eco-phenotypic diversification of *Dysdera* spiders in the Canary Islands. *Org. Divers. Evol.*, doi: 10.1007/s13127-020-00473-w.
- Řezáč, M., S. Pekár, and Y. Lubin. 2008. How oniscophagous spiders overcome woodlouse armour. *J. Zool.* 275:64–71.
- Robinson, B. W., and D. S. Wilson. 1994. Character Release and Displacement in Fishes: A Neglected Literature. *Am. Nat.* 144:596–627.
- Rohlf, F. J. 2015. The tps series of software. *Hystrix* 26:9–12.
- Rohlf, F. J. 2017. tpsDig2. Stony Brook: Stony Brook University.
- Rohlf, F. J., and D. Slice. 1990. Extensions of the procrustes method for the optimal superimposition of landmarks. *Syst. Zool.* 39:40–59.
- Schluter, D. 2009. Evidence for ecological speciation and its alternative. *Science* (80-.). 323:737–741.
- Schluter, D. 2000. *The Ecology of Adaptive Radiation*. Oxford University Press, Oxford.
- Simpson, G. G. 1953. *The major features of evolution*. Columbia University Press, New York.
- Stroud, J. T., and J. B. Losos. 2016. Ecological Opportunity and Adaptive Radiation. *Annu. Rev. Ecol. Evol. Syst.* 47:507–532.
- Suchard, M. A., P. Lemey, G. Baele, D. L. Ayres, A. J. Drummond, and A. Rambaut. 2018. Bayesian phylogenetic and phylodynamic data integration using BEAST 1.10. *Virus Evol.* 4:1–5.
- Tamura, K., G. Stecher, D. Peterson, A. Filipksi, and S. Kumar. 2021. MEGA6: Molecular evolutionary

- genetics analysis version 11. *Mol. Biol. Evol.* 38:3022–3027.
- Templeton, A. R., K. A. Crandall, and C. F. Sing. 1992. A cladistic analysis of phenotypic associations with haplotypes inferred from restriction endonuclease mapping and DNA sequence data. III. Cladogram estimation. *Genetics* 132:619–633.
- Toft, S., and N. Macías-Hernández. 2017. Metabolic adaptations for isopod specialization in three species of *Dysdera* spiders from the Canary Islands. *Physiol. Entomol.* 42:191–198.
- Toft, S., and N. Macías-Hernández. 2021. Prey acceptance and metabolic specialisations in some Canary *Dysdera* spiders. *J. Insect Physiol.* 131:104227.
- Van Den Bogaard, P. 2013. The origin of the Canary Island Seamount Province—New ages of old seamounts. *Sci. Rep.* 3:1–7.
- Van Valen, L. 1965. Morphological Variation and Width of Ecological Niche. *Am. Nat.* 99:377–390.
- Wallace, A. R. 1881. *Island life: Or, the phenomena and causes of insular faunas and floras, including a revision and attempted solution of the problem of geological climates.* Harper, London.
- Warren, D. L., R. E. Glor, and M. Turelli. 2008. Environmental niche equivalency versus conservatism: Quantitative approaches to niche evolution. *Evolution (N. Y.)* 62:2868–2883.
- Warren, M. S., J. K. Hill, J. A. Thomas, J. Asher, R. Fox, B. Huntley, D. B. Roy, M. G. Telfer, S. Jeffcoate, P. Harding, G. Jeffcoate, S. G. Willis, J. N. Greatorex-Davies, D. Moss, and C. D. Thomas. 2001. Rapid responses of British butterflies to opposing forces of climate and habitat change. *Nature* 414:65–69.
- Yoder, J. B., E. Clancey, S. Des Roches, J. M. Eastman, L. Gentry, W. Godsoe, T. J. Hagey, D. Jochimsen, B. P. Oswald, J. Robertson, B. A. J. Sarver, J. J. Schenk, S. F. Spear, and L. J. Harmon. 2010. Ecological opportunity and the origin of adaptive radiations. *J. Evol. Biol.* 23:1581–1596.
- Zelditch, M. L., D. L. Swiderski, H. D. Sheets, and W. L. Fink. 2004. *Geometric morphometrics for biologists: A primer.* Elsevier Academic Press, New York.



GENERAL DISCUSSION

General discussion

This thesis has mainly focused on answering if the diversification of the *Dysdera* spider species in the Canary Islands constitute a case of adaptive radiation, how these species have diversified, and which ecological responses had derived from these diversification. For this goal, we have employed numerous methods, each targeting distinct aspects of the evolutionary dynamics within this species group. Additionally, we have developed a framework that can guide future evolutionary or ecomorphological investigations in non-model groups. Our research encompasses several key aspects, ranging from determining the number of species present in our study system to identifying the essential characteristics that drive the evolution of our selected species. We also explore the adaptation to diverse ecological regimes and the resulting evolutionary implications. Through this work, we have contributed valuable insights into the intricate nature of studying species evolution, which is often far from straightforward. In the following sections, we discuss the main topics covered and results obtained in each chapter.

How many *Dysdera* species are in the Canary Islands?

A lot of work has been done to describe the Canarian *Dysdera* fauna over the years (see Wunderlich 1987; Arnedo and Ribera 1999a; Arnedo and Ribera 1999b; Arnedo and Ribera 1999c; Arnedo *et al.* 2001; Arnedo *et al.* 2007; Macías-Hernández *et al.* 2010). However, overlooked species is a common phenomenon when using only morphological characters for species delimitation. While *Dysdera* species exhibit distinct phenotypic characteristics that set them apart, such as variations in cheliceral morphologies, leg spination, and unique carapace shapes, it is worth noting that some of these traits are not exclusive to a particular species and are shared with distantly related ones. This

situation could potentially result in misidentifications, leading to an underestimation of the actual diversity of *Dysdera* species in the Canary Islands. The taxonomic revision presented here offers an integrative approach that combines both morphological information and molecular data. This approach aids in determining the distinction between two separate species, thereby reducing the probability of overlooking species due to cryptic morphological differences or misidentifications. A similar integrative taxonomic revision conducted in the Eastern islands of Lanzarote and Fuerteventura has already demonstrated the effectiveness of this method (Macías-Hernández *et al.* 2010), where despite the low species richness compared to other islands in the archipelago (Lanzarote N = 5, Fuerteventura N = 5), with the use of DNA sequence data together with morphological, distributional and ecological information, two new previously overlooked species were described.

With the present work, we have increase up to 57 the number of *Dysdera* spiders in the Canary Islands with 10 newly described species. This reflects once again the dramatic diversification of this group in the islands as it represents a 20% of the total diversity of this genus, although only occupies a 0.1% of its geographic distribution (Arnedo *et al.* 2001). It is true that the efforts put on characterizing the *Dysdera* diversity in the Canary Islands has been much greater than in the continental regions, where a bigger number of species may remain uncovered. However, this difference in species richness between the Canary Islands and other regions had been already noticed, and although every year more species are described outside the archipelago, it seems unlikely that the trend would change in the near future.

Is it possible that in future research new species will be described in the Canary Islands, and the total species richness will be increased. However, after more than 20 years of continuous samplings in the islands and a multitude of works describing the *Dysdera* diversity in the archipelago, these new fundings will rarely affect the possible evolutionary conclusions obtained with the actual species richness.

Which phenotypes are related to which ecological pressures?

Many studies have focused on investigating the adaptive radiation of specific groups by examining the phenotypic characteristics of species, aiming to establish the ecological relationships that drive their diversification. However, when it comes to non-model organisms, establishing a clear link between phenotype and ecology is not straightforward. Furthermore, phenotypes can undergo changes not solely due to direct ecological pressures, but also because organisms are composed of interconnected traits that are not independent of each other. Consequently, the phenotypic variation resulting from natural selection acting on one specific trait can affect other traits that are not directly associated with the same ecological performance. These modifications occur as a consequence of the integration of various characters that constitute the overall body plan of the species. Arthropods, like spiders, offer an ideal study model to confront these problematics, as their segmented body offers more independent integration between distinct phenotypes.

Through our research, we have discovered a significant level of integration among various morphological traits associated with similar structures. With the selection of different species with previous knowledge of being related to different ecological pressures, we have been able to prove that different modules of the spider body parts, have evolved independently from each other adapting to different ecological requirements. Additionally, we have provided valuable guidance for future studies interested in unravelling the spider's adaptation to different aspects of their niche. This guidance can assist researchers in determining the most appropriate approach for analysing the phenotype when investigating environmental, trophic, or evolutionary questions related to these organisms.

Understanding which traits or phenotypic characteristics are influenced by specific ecological pressures is a crucial aspect of evolutionary studies. It has been observed that various components of the ecological niche of species in evolutionary radiations

can be influenced by selection, depending on the stage of diversification. Initially, there is often ecological segregation along macro-habitat axes, followed by subsequent trophic differentiation (Streelman & Danley 2003; Ronco & Salzburger 2021). Understanding these species' evolutionary processes requires identifying the specific phenotypes that should be the focus of study. This knowledge is essential for gaining insight into these intricate evolutionary dynamics.

Is the diversification of *Dysdera* in the Canary Islands a case of adaptive radiation?

We have characterized for the first time cheliceral morphotypes using geometric morphometrics and experimentally demonstrate their association to different levels of diet specialisation (oniscophagy). The existence of different cheliceral morphotypes was first identified in continental *Dysdera* species, using data on the length of the basal segment and the fang relative to carapace length, along with qualitative observations (Řezáč *et al.* 2008). The same morphotypes were subsequently reported in Canarian *Dysdera*, in that case by combining several linear measurements of the chelicera (Řezáč *et al.* 2021). The finer GM data and more sophisticated statistical analyses used here allowed us to delimit nine different cheliceral morphotypes in the Canary Islands, some of which greatly overlapped, but not fully matched, the previously defined morphotypes. Morphotypes A, D and E identified here mostly corresponded with the “unmodified” morphotype of previous studies, morphotype B and H to “elongated”, morphotype F to “flattened” and morphotype G to “concave”. By contrast the morphotypes C and I were identified here for the first time. Interestingly, the different cheliceral morphotypes had been experimentally linked to specific strategies of prey capture (Řezáč *et al.* 2008, 2021). One of these strategies, “dagger” was reported only in one species, *D. levipes*, which our analysis assigned to its own distinct cheliceral morphotype, C. On the other hand, the cheliceral morphotype I, which had not been reported before in the Canaries, closely resembles the “very elongated” morphotype described in continental species (Řezáč *et al.* 2008).

On the other hand, the morphotype D was found to be synapomorphic for the clade of endemic species that inhabits the eastern Canary Islands, which reveals the phylogenetic conservation of this trait in this group. In this case, some kind of environmental filtering may be playing an evolutionary constraint preventing the evolution or surviving of species with a more specialist chelicera.

Contrary to former suggestions (Řezáč *et al.* 2021), our results support that morphotype A was the ancestral state for Canarian *Dysdera*, and hence the ancestral coloniser was most likely a generalist species. The results of the former study, however, were compromised by the fragmentary evidence, including the use of linear measurements to quantify chelicera shape, sparse data ($n=1$ for many species) and the use of an outdated phylogeny. The more updated phylogeny and the use of geometric morphometrics that allows to capture shape variation at a finer scale, has most likely contributed to these dissonant results. The inference of a generalist ancestor in the Canarian *Dysdera*, is well aligned with the observation that specialist diets commonly evolved from generalist ones (Toft 1995; Stephens & Wiens 2003; Reynolds *et al.* 2016; Naik *et al.* 2021). Moreover, generalists are usually considered better colonizers, as they are able to more easily secure sufficient resources (Ebenhard 1991).

We have proven that some of these cheliceral morphotypes have evolved several times independently during the diversification of the *Dysdera* spiders in the Canary Islands. This repeated evolution of similar phenotypes within a species clade, is a common phenomenon among species adaptive radiations (Schluter & Nagel 1995; Losos *et al.* 1998, 2003; Rundle *et al.* 2000; Schluter 2000; Gavrilets & Losos 2009). The relation that this phenotype has with the species trophic specialization as seen here, shows the eco-phenotypic differences present in this group within species, and the role that natural selection has played providing similar outcomes to similar ecological pressures.

As stated above, few common aspects define adaptive radiations. However, the diversification from a common ancestor of eco-phenotypic different species is the hallmark of this process. It was previously shown that the colonization of the *Dysdera* species in the Canary Islands was performed most likely by a single event, with the exception of one species (Adrián-Serrano *et al.* 2020), and with the results presented here, we have seen that the endemic species show eco-phenotypic differences between them, supporting the hypothesis of an adaptive radiation process in the diversification of the *Dysdera* species in the Canary Islands.

The patterns of diversification

A species clade affected under an adaptive radiation process, has been historically seen as a sudden “explosive” diversification of species after the original colonizer reach an area that offers unexploited ecological opportunities. We have seen with the lineage throw time plot (LTT), that the diversification of the *Dysdera* species from the Canary Islands, show a higher diversification rate in their initial stages. This can be seen with the typical hump-shaped pattern in the LTT, which has been supported by the γ statistic pointing to an early increase in lineages with a posterior slowdown and stabilization. This adds support to the adaptive radiation process presented by the eco-phenotypic diversification of these species. This pattern has been explained as a species colonizing new environments with unexploited ecological opportunities, which once they become filled slow down the opportunities to diversify, decreasing the formation of new species in more recent stages (Schluter 2000; Gavrillets & Vose 2005). The occupation of these new niches may carry ecological adaptations to take advantages of those new opportunities, something that could explain how eco-phenotypically divers the *Dysdera* spiders are in the Canary Islands.

The process of diversification

The previous section has shown that species diversify under a pattern expected in an adaptive radiation, however, does not give an explanation about the process that

these species have gone through. The factors that could give rise to an extreme diversification in the early stages of a species radiation and how it is carried out can differ substantially.

We have seen that the diversification rates during the evolution of *Dysdera* in the Canary Islands, are influenced by the cheliceral morphologies presented by these species, with most of the cheliceral types related to a higher trophic specialization increasing these rates. This confronts several cases of evolutionary specialization that leads species to evolutionary dead-ends (Vamosi *et al.* 2014). It is true that specialization in the Canarian *Dysdera* species has shown an irreversibility from more generalist morphotypes, which is one of the characteristics of evolutionary dead-ends. However, the higher diversification rates in specialist species suggest that specialization may actually constitute a key innovation, where new phenotypes allow species in a given group to radiate, rather than to an evolutionary dead end.

The only exception to this trend has been seen with one specific cheliceral morphology. Spider *Dysdera* species has recurrently evolved a flattened fang, that has been reported to overcome isopod's mechanistic defence by introducing one of these fangs between their dorsal sclerites (Řezáč *et al.* 2008). In the Canary Islands, these morphotype has evolved independently two different times, with a third case in the archipelago that has not been analysed due to the lack of specimens (*D. hernandezi* Arnedo & Ribera, 1999). Our analyses indicates that this cheliceral morphology presents lower diversification rates compared to other specialist species. This, together with the irreversibility in trophic specialized morphologies, will suggest that the flattened fang phenotype could be a case of evolutionary dead-end inside *Dysdera* species. In fact, this type of chelicera has evolved several times also in continental species, but usually in single species.

While it has been seen that the cheliceral morphology has an impact on the diversification of the *Dysdera* species, it is important to recognize that evolution is a

multifactorial process, and other factors may also play a role in the diversification of these species. Our analyses have shown that the chelicera morphology is not the main driving force in their diversification. In the *Dysdera* species from the Canary Islands we found two different factors affecting the diversification of the group. On the one hand, we have the cheliceral morphology which increase the diversification of the species that have evolved more specialized trophic strategies. on the other hand, we have a general decreasing diversification rate related with time, which will slow down the speciation most likely as a result of the filling of all available niches in the islands. Is this second factor that may have played a stronger role in the diversification rates of this species group.

Allopatric speciation and the ecological opportunity

While we have discovered convergent evolution in the cheliceral morphology of Canarian *Dysdera* species and have explored the primary driving forces that has led their evolution, the question of how these species initially underwent speciation remains unanswered. In various cases of adaptive radiation processes, it has been documented the independent evolution of similar morphologies originated due to geographic isolation from closely related species (Muschick et al., 2012). However, given conflicting results from previous studies, it is crucial to test this hypothesis in any evolutionary research.

With the use of age-range correlation methods, we have seen that the results statistically point towards a non-significant sympatric speciation. However, these results are biased by the non-linearity of our data. Looking at the correlation between the species overlap and age since divergence, we can clearly see that there is an initial increase in overlap with a posterior decrease in the most distant nodes. This pattern can be explained by an allopatric speciation with a posterior secondary contact, a standard scenario in adaptive radiation processes (Aguilée *et al.* 2013).

The colonization of new islands can have a direct impact on the species ecology. When a colonizer reaches a new environment with reduced competition or predatory pressures compared to the original island, the new populations may expand their niche width to exploit the newly available ecological opportunities. This phenomenon is referred to as ecological release. Through the examination of various *Dysdera* species that have colonized new islands with reduced interspecific competition, we have observed that the ability to undergo ecological release is highly influenced by their cheliceral morphology. Species exhibiting trophic specialization show an expansion of their trophic niche when colonizing low competition islands. Additionally, both analysed specialist species exhibit a similar directional change in morphology, indicating that they are influenced by similar ecological pressures when they colonize new environments. On the other hand, the generalist species does not expand its trophic niche upon colonizing of low competition islands and tends to reduce its spatial range. Once again, this emphasizes the significance of cheliceral morphology throughout the evolutionary history of this group.

Concluding remarks and originality of the contribution

With the present thesis, we have demonstrated that the highly diverse *Dysdera* spider genus in the Canary Islands is a case of adaptive radiation. The eco-phenotypic differences presented by these species, which have independently evolved multiple times during the group's diversification, align with the predictions for a group undergoing this process. Furthermore, the early divergence of lineages followed by subsequent stabilization, though not a prerequisite for adaptive radiations, lends support to this hypothesis. We have statistically proven that the different cheliceral morphologies found in this study are related to different trophic adaptations, and that these have an impact on the group evolution which, although these seem not to be the main driver, they have an effect in the diversification rates of the group. In addition, those different trophic adaptations seem to have a direct effect on the

species ability to experience ecological release once they colonize new depauperate environments with new ecological opportunities.

From a methodological perspective, this thesis has also contributed to facilitate future studies focused on spiders' morphology. We have provided a pipeline describing which phenotypical structures needs to be selected to analyse specific morphologies related with different ecological pressures, which in non-model system species is not always a straightforward link. In addition, with the combination of different views of the same morphological structure, we have been able to analyse 3-dimensional objects from 2-dimensional morphometric data acquisition, avoiding more time and cost consuming methodologies to capture 3D data.

Studies examining species diversification rates can face challenges due to the multistate nature of the character driving the speciation process. Particularly, when there are only a few representatives of certain states within the studied clade, it can undermine the reliability of multistate speciation and extinction models. In this thesis, we employed a binary combinatory approach from a multistate character. This method enabled us to examine the impact of species traits on diversification rates, even when certain states had limited representation within the clade ($N = 1$ or 2). By employing this approach, future studies can avoid oversimplifying the selected traits when investigating species diversification rates.

We have also provided a more integrative view when analysing the species multidimensional niche taking into account different aspects that can play a major role in their ecology (range, habitat, trophic breath and morphology). It has been more than 70 years since Hutchinson defined the species ecological niche as this n multi-dimensional space (Hutchinson 1957). However, most studies focused on the variation of species niche usually only take into account a single axis of this multidimensional space (e.g. Cox and Ricklefs 2006; Buckley and Jetz 2007; Bolnick et al. 2010; Andrades et al. 2019). By assessing how all these different aspects reacts

during an ecological release process, we have been able to provide a better understanding of the effects of colonizing lesser competitive depauperate environments in the species ecology.

Future directions

The *Dysdera* spider fauna of the Canary Islands has been studied for over 20 years. Our findings have now led us to conclude that this group represents an intriguing case of adaptive radiation within the islands, shedding light on the diversification processes that have shaped their evolutionary history. Nonetheless, there is still much work to be done with these species, and further research is needed to fully comprehend their complexities.

In this study, we have paid special attention to the different levels of trophic specialization presented by these species. We have conducted prey experiments and stable isotope analyses to establish connections between this specialization and their cheliceral morphologies. However, further investigations are required to directly analyse the specific diets of each species in their natural habitats. Recent advancements in metabarcoding analyses have shown promise in quantifying gut content in spiders (eg. Ortiz *et al.* 2021; Sierra *et al.* 2021), and ongoing improvements are addressing the challenges posed by arthropod species in such analyses (Krehenwinkel *et al.* 2017; Lafage *et al.* 2020). What distinguishes the dietary preferences between the two types of generalist species found in the archipelago, which exhibit contrasting cheliceral morphologies and inhabit different environments? Do species with similar morphotypes display differences in diet when they coexist in sympatry compared to when they reside in separate areas to mitigate competition? Do the various specialist species exhibit varying degrees of dietary specialization based on their cheliceral morphology? Answering these questions necessitates the application of metabarcoding techniques to analyze the gut content of these species. While an initial study has provided an introductory exploration of

these methods with *Dysdera* species from the Canary Islands (Macías-Hernández *et al.* 2018), further comprehensive research is warranted to unravel the trophic adaptations and preferences that these species have evolved throughout their evolutionary history in the archipelago.

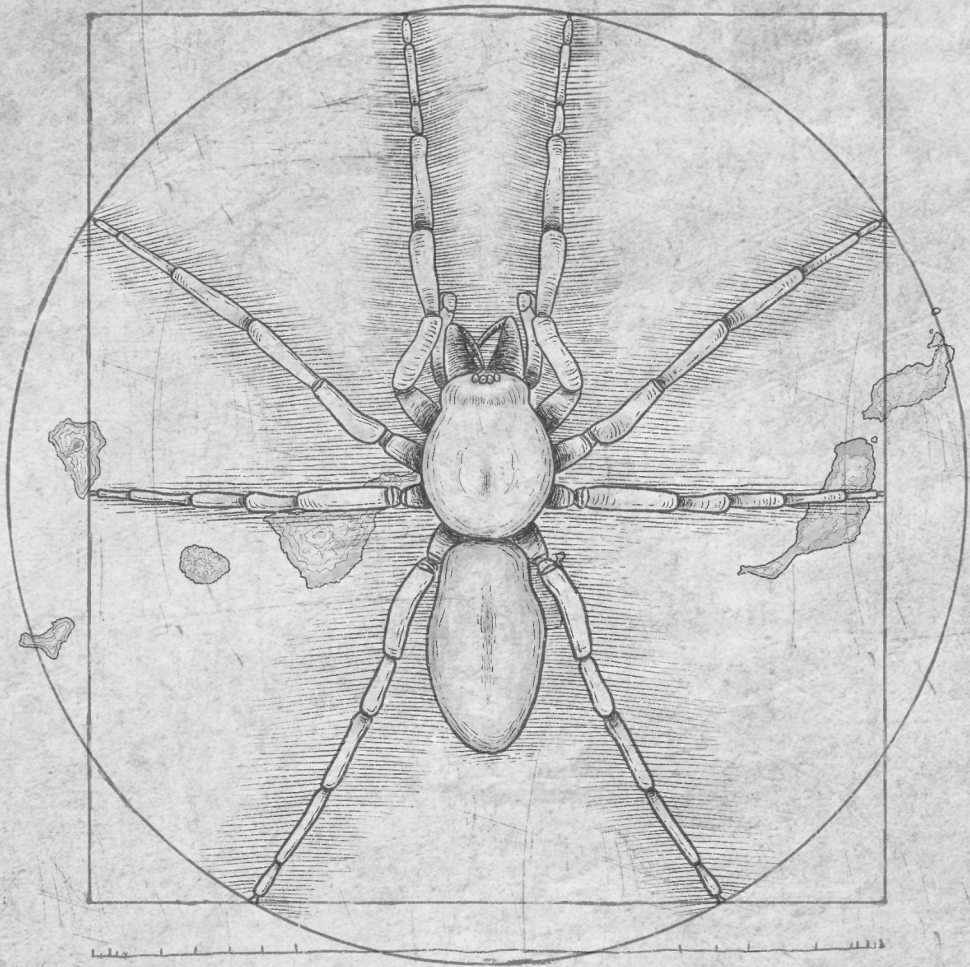
An additional crucial factor influencing species' trophic specialization, which was not discussed in this thesis, is the role of *Dysdera*'s venom composition. As species specialize and narrow their potential range of prey, a distinct set of adaptations evolves to meet their ecological requirements, encompassing behavioral, morphological, and physiological aspects. In spiders, it has been demonstrated that venom composition coevolves with dietary adaptations in closely related taxa (Binford 2001; Pekár *et al.* 2018). *Dysdera* species exhibit a continuum of different degrees of trophic specialization, primarily preying on isopods. This variation in diet may also correlate with differences in their venom composition, raising the question of whether venom or morphology exerts a greater impact on their trophic niche. Further investigation is required to ascertain the relative importance of venom and morphology in shaping their trophic adaptations.

Our research focused on the evolutionary dynamics of *Dysdera* species in the Canary Islands and the various factors that have influenced their adaptation since colonizing the archipelago. However, gaining a comprehensive understanding of their complete evolution necessitates a thorough comprehension of the entire ecosystem in which they are embedded. Currently, our knowledge of arthropod species distribution is generally limited, and the presence and evolution of *Dysdera* spiders may be correlated with the existence of particular prey or predators. Standardized protocols have been proposed to enhance our understanding of species richness in studied areas, encompassing both arthropods in general (Duelli 2010) and spiders specifically (Cardoso 2009). By improving our knowledge of the arthropod community, we can effectively address specific inquiries regarding the role of interspecific

interactions in the evolution of a species clade within an adaptive radiation process.

Finally, our study sheds light on the evolutionary dynamics of *Dysdera* species in the volcanic archipelago of the Canary Islands. However, it is important to note that the colonization of islands extends beyond the Canary Islands alone. These species can also be found in other Macaronesia archipelagos, where they have undergone remarkable diversification processes in some of them (Crespo *et al.* 2020). Do they undergo similar evolutionary processes in a different archipelago? What factors contribute to the extensive diversification observed in some archipelagos compared to others? How do island radiations differ from continental ones? These intriguing questions open avenues for future research with this group of spiders and offer valuable insights into the evolutionary history of species on our planet.

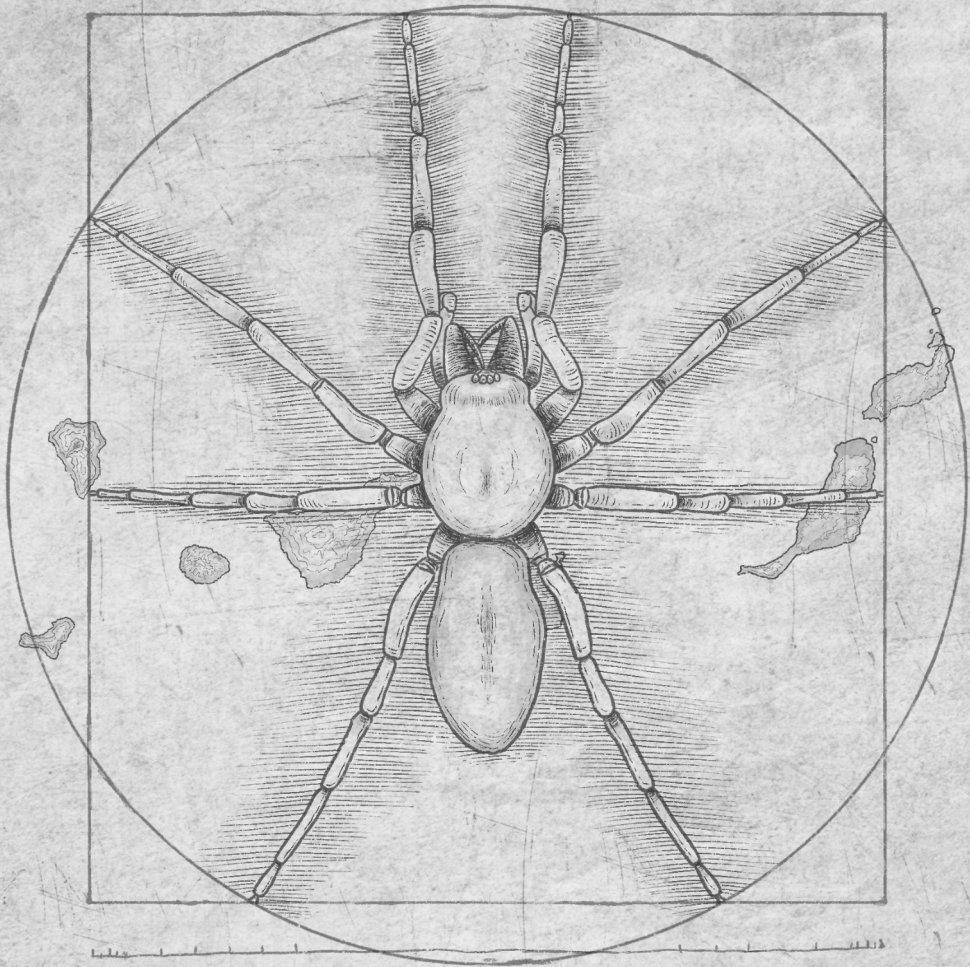
In summary, those are some examples of the future directions that could be taken to fully understand the evolution of a species group under an adaptive radiation process, and there is a lot of work still to be done. Nonetheless, the present work we have provided a stepstone on the insight of how these species evolve and how this evolution can be studied.



CONCLUSIONS

Conclusions

1. Through the implementation of integrative taxonomy in this thesis, we have made significant contributions to our understanding of *Dysdera* species diversity in the Canary Islands. Specifically, we have identified and described 10 previously unknown species, thereby increasing the known species richness by 20%. As a result, the total species count within the genus *Dysdera* now stands at 321.
2. By integrating molecular and morphological delimitations, we have successfully addressed the challenges associated with overlooked species in the genus *Dysdera*. Our approach has enabled us to overcome the limitations posed by subtle or cryptic morphological differences, as well as the tendency for over-splitting often observed with certain molecular methods.
3. The body of *Dysdera* spiders consists of interconnected anatomical modules that are influenced by different ecological pressures. By considering multiple phenotypic traits, we gain a more robust understanding of the morphological diversity and ecological adaptations exhibited by these organisms.
4. We have statistically characterized cheliceral morphologies of *Dysdera* species for the first time and shown their association with trophic specialization in preying on isopods.
5. Once the species evolved a specialist cheliceral morphotype, a transition back to the original state appears unlikely, indicating the process was irreversible within the archipelago.
6. A newly inferred phylogenetic hypothesis, based on mitogenomic data of Canarian endemics, suggests that the initial colonizer of the archipelago was likely a generalist species. Furthermore, multiple independent occurrences of different cheliceral morphotypes during the group's diversification, driven by natural selection pressures, provide compelling evidence that the radiation of *Dysdera* species aligns with an adaptive radiation process.
7. The lineage accumulation across time and the γ -test presented in the present study both support an early burst of species diversification with a posterior slowdown in their speciation, reinforcing the hypothesis of adaptive radiation processes.
8. The diversification rates observed in the *Dysdera* species of the Canary Islands were influenced by specific cheliceral morphologies associated with varying levels of trophic specialization.
9. The speciation in the islands primarily occurred through allopatric isolation followed by secondary sympatric contact, which is a common pattern observed in other adaptive radiation cases.
10. When *Dysdera* species colonize new depauperate environments from more competitive islands, they undergo ecological release of their trophic niche. However, the extent to which they can expand their ecological axes is heavily influenced by the cheliceral morphological type of the species.



REFERENCES

References

- Adams D.C. 2016. Evaluating modularity in morphometric data: challenges with the RV coefficient and a new test measure. *Methods Ecol. Evol.* 7:565–572.
- Adams D.C., Collyer M., Kaliontzopoulou A. 2018. Geomorph: Software for geometric morphometric analysis. R package version 3.0.6. .
- Adams D.C., Collyer M.L. 2016. On the comparison of the strength of morphological integration across morphometric datasets. *Evolution (N. Y.)* 70:2623–2631.
- Adams D.C., Collyer M.L. 2019. Comparing the strength of modular signal, and evaluating alternative modular hypotheses, using covariance ratio effect sizes with morphometric data. *Evolution (N. Y.)* 73:2352–2367.
- Adams D.C., Collyer M.L., Kaliontzopoulou A., Baken E.K. 2021. Geomorph: Software for geometric morphometric analyses. R package version 4.0. .
- Adams D.C., Otárola-Castillo E. 2013. Geomorph: An r package for the collection and analysis of geometric morphometric shape data. *Methods Ecol. Evol.* 4:393–399.
- Adams D.C., Rohlf F.J., Slice D.E. 2004. Geometric morphometrics: Ten years of progress following the ‘revolution.’ *Ital. J. Zool.* 71:5–16.
- Adrián-Serrano S., Lozano-Fernandez J., Pons J., Rozas J., Arnedo M.A. 2020. On the shoulder of giants: Mitogenome recovery from non-targeted genome projects for phylogenetic inference and molecular evolution studies. *J. Zool. Syst. Evol. Res.*:1–26.
- Aguilée R., Claessen D., Lambert A. 2013. Adaptive radiation driven by the interplay of eco-evolutionary and landscape dynamics. *Evolution (N. Y.)* 67:1291–1306.
- Aguinaldo A., Turbeville J.M., Linford L.S., Rivera M.C., Garey T. J.R., Raff R.A., Lake J.A. 1997. Evidence for a clade of nematodes, arthropods and other moulting animals. *Nature.* 387:489–493.
- Andersson L. 2009. Studying phenotypic evolution in domestic animals: A walk in the footsteps of Charles Darwin. *Cold Spring Harb. Symp. Quant. Biol.* 74:319–325.
- Andrades R., Jackson A.L., Macieira R.M., Reis-Filho J.A., Bernardino A.F., Joyeux J.-C., Giarrizzo T. 2019. Niche-related processes in island intertidal communities inferred from stable isotopes data. *Ecol. Indic.* 104:648–658.
- Arbuckle K., Bennett C.M., Speed M.P. 2014. A simple measure of the strength of convergent evolution. *Methods Ecol. Evol.* 5:685–693.
- Arechavaleta M., Rodríguez S., Zurita N., García A. 2010. Lista de especies silvestres de Canarias

(hongos, plantas y animales terrestres).

- Arnedo M.A., Oromí P., Múrria C., Macías-Hernández N., Ribera C. 2007. The dark side of an island radiation: systematics and evolution of troglobitic spiders of the genus *Dysdera* Latreille (Araneae: Dysderidae) in the Canary Islands. *Invertebr. Syst.* 21:623–660.
- Arnedo M.A., Oromí P., Ribera C. 2001. Radiation of the spider genus *Dysdera* (Araneae, Dysderidae) in the Canary Islands: Cladistic assessment based on multiple data sets. *Cladistics.* 17:313–353.
- Arnedo M.A., Oromí P., Ribera C. 2000. Systematics of the Genus *Dysdera* (Araneae, Dysderidae) in the Eastern Islands. *J. Arachnol.*:261–292.
- Arnedo M.A., Ribera C. 1997. Radiation in the genus *Dysdera* (Araneae, Dysderidae) in the Canary Islands: The island of Gran Canaria. *J. Arachnol.* 27:604–662.
- Arnedo M.A., Ribera C. 1999a. Radiation in the genus *Dysdera* (Araneae, Dysderidae) in the Canary Islands: The island of Tenerife. *J. Arachnol.* 27:604–662.
- Arnedo M.A., Ribera C. 1999b. Radiation in the genus *Dysdera* (Araneae, Dysderidae) in the Canary Islands: The western islands. *J. Arachnol.* 27:604–662.
- Azevedo G.H.F., Bougie T., Carboni M., Hedin M., Ramírez M.J. 2022. Combining genomic, phenotypic and Sanger sequencing data to elucidate the phylogeny of the two-clawed spiders (Dionycha). *Mol. Phylogenet. Evol.* 166:107327.
- Baken E.K., Collyer M.L., Kaliontzopoulou A., Adams D.C. 2021. geomorph v4.0 and gmShiny: Enhanced analytics and a new graphical interface for a comprehensive morphometric experience. *Methods Ecol. Evol.* 12:2355–2363.
- Barraclough T.G. 1998. Revealing the factors that promote speciation. *Philos. Trans. R. Soc. B Biol. Sci.* 353:241–249.
- Barraclough T.G., Vogler A.P. 2000. Detecting the geographical pattern of speciation from species-level phylogenies. *Am. Nat.* 155:419–434.
- Batthey C.J. 2019. Ecological release of the anna’s hummingbird during a Northern range expansion. *Am. Nat.* 194:306–315.
- Bearhop S., Adams C.E., Waldron S., Fuller R.A., Macleod H. 2004. Determining trophic niche width: A novel approach using stable isotope analysis. *J. Anim. Ecol.* 73:1007–1012.
- Beaulieu J.M., O’Meara B.C. 2016. Detecting hidden diversification shifts in models of trait-dependent speciation and extinction. *Syst. Biol.* 65:583–601.
- Beaulieu J.M., O’Meara B.C., Crane P., Donoghue M.J. 2015. Heterogeneous Rates of Molecular Evolution and Diversification Could Explain the Triassic Age Estimate for Angiosperms. 64:869–878.

- Berlocher S.H., Feder J.L. 2002. Sympatric speciation in phytophagous insects: moving beyond controversy? *Annu. Rev. Entomol.*:773–815.
- Binford G.J. 2001. Differences in venom composition between orb-weaving and wandering Hawaiian Tetragnatha (Araneae). *Biol. J. Linn. Soc.* 74:581–595.
- Blankers T., Gray D.A., Matthias Hennig R. 2017. Multivariate Phenotypic Evolution: Divergent Acoustic Signals and Sexual Selection in Gryllus Field Crickets. *Evol. Biol.* 44:43–55.
- Blomberg S.P., Garland T., Ives A.R. 2003. Testing for phylogenetic signal in comparative data: Behavioral traits are more labile. *Evolution (N. Y.)*. 57:717–745.
- Van Den Bogaard P. 2013. The origin of the Canary Island Seamount Province-New ages of old seamounts. *Sci. Rep.* 3:1–7.
- Bolnick D.I., Fitzpatrick B.M. 2007. Sympatric speciation: Models and empirical evidence. *Annu. Rev. Ecol. Evol. Syst.* 38:459–487.
- Bolnick D.I., Ingram T., Stutz W.E., Snowberg L.K., Lau O.L., Pauli J.S. 2010. Ecological release from interspecific competition leads to decoupled changes in population and individual niche width. *Proc. R. Soc. B Biol. Sci.* 277:1789–1797.
- Bolnick D.I., Svanback R., Araujo M.S., Persson L. 2007. Comparative support for the niche variation hypothesis that more generalized populations also are more heterogeneous. *Proc. Natl. Acad. Sci.* 104:10075–10079.
- Bookstein F.L. 1991. Morphometric tools for landmark data: Geometry and biology. New York: Cambridge University Press.
- Brakefield P.M. 2006. Evo-devo and constraints on selection. *Trends Ecol. Evol.* 21:362–368.
- Bristowe W.S. 1939. The Comity of Spiders. *Ray Soc. London.* 1:1–228.
- Bristowe W.S. 1958. The world of spiders. London: Collins.
- Brown J.H. 1978. The theory of insular biogeography and the distribution of boreal birds and mammals. *Gt. Basin Nat. Mem.* 2:209–207.
- Buckley L.B., Jetz W. 2007. Insularity and the determinants of lizard population density. *Ecol. Lett.* 10:481–489.
- Cardoso P. 2009. Standardization and optimization of arthropod inventories-the case of Iberian spiders. *Biodivers. Conserv.* 18:3949–3962.
- Cardoso P., Arnedo M.A., Triantis K.A., Borges P.A. V. 2010. Drivers of diversity in Macaronesian spiders and the role of species extinctions. :1034–1046.
- Cerca J. 2022. A simple conceptual framework and nomenclature for studying repeated , parallel and convergent evolution A simple conceptual framework and nomenclature for studying repeated

- , parallel and convergent evolution Abstract. *EcoEvoRxiv*:1–37.
- Cerca J., Cotoras D.D., Bieker V.C., De-kayne R., Vargas P., Fernández-mazuecos M., López-delgado J., White O., Stervander M., Geneva A.J., Ernesto J., Andino G., Meier J.I., Roebler L., Valdebenito H., Castañeda R., Chaves J.A., Díaz P.J., Valente L., Knope M.L., Price J.P., Rieseberg L.H., Baldwin B.G., Emerson B.C., Rivas-torres G., Gillespie R., Martin M.D. 2023. Ecology & Evolution Evolutionary genomics of oceanic island radiations. *Trends Ecol. Evol.*:1–12.
- Clément J., Vieilledent G. 2022. jSDM: Joint Species Distribution Models. .
- Collyer M.L., Adams D.C. 2013. Phenotypic trajectory analysis: Comparison of shape change patterns in evolution and ecology. *Hystrix*. 24:75–83.
- Collyer M.L., Adams D.C. 2018. RRPP: An R package for fitting linear models to high-dimensional data using residual randomization. *Methods Ecol. Evol.* 9:1772–1779.
- Collyer M.L., Davis M.A., Adams D.C. 2020. Making Heads or Tails of Combined Landmark Configurations in Geometric Morphometric Data. *Evol. Biol.* 47:193–205.
- Collyer M.L., Sekora D.J., Adams D.C. 2015. A method for analysis of phenotypic change for phenotypes described by high-dimensional data. *Heredity (Edinb)*. 115:357–365.
- Cox G.W., Ricklefs R.E. 2006. Species Diversity and Ecological Release in Caribbean Land Bird Faunas. *Oikos*. 28:113.
- Crespo L.C., Silva I., Enguídanos A., Cardoso P., Arnedo M.A. 2021a. The Atlantic connection: coastal habitat favoured long distance dispersal and colonization of Azores and Madeira by *Dysdera* spiders (Araneae: Dysderidae). *Syst. Biodivers.* 19:1–22.
- Crespo L.C., Silva I., Enguídanos A., Cardoso P., Arnedo M.A. 2021b. Integrative taxonomic revision of the woodlouse-hunter spider genus *Dysdera* (Araneae: Dysderidae) in the Madeira archipelago with notes on its conservation status. *Zool. J. Linn. Soc.* 192:356–415.
- Czekanski-Moir J.E., Rundell R.J. 2019. The Ecology of Nonecological Speciation and Nonadaptive Radiations. *Trends Ecol. Evol.* 34:400–415.
- Darwin C.R. 1859. *On the Origin of Species by Means of Natural Selection, or the Preservation of Favoured Races in the Struggle for Life*. London: John Murray Publishers.
- Deeleman-Reinhold C.L., Deeleman P.R. 1988. Revision des Dysderinae (Araneae, Dysderidae), les espèces méditerranéennes occidentales exceptées. *Tijdschr. voor Entomol.* 131:141–269.
- Duelli M.K.O.P. 2010. Rapid biodiversity assessment of arthropods for monitoring average local species richness and related ecosystem services. :2201–2220.
- Ebenhard T. 1991. Colonization in metapopulations: a review of theory and observations. *Biol. J. Linn. Soc.* 42:105–121.

- Elith J., Leathwick J.R. 2009. Species distribution models: Ecological explanation and prediction across space and time. *Annu. Rev. Ecol. Evol. Syst.* 40:677–697.
- Felsenstein J. 1985. Phylogenies and the Comparative Method. *Am. Nat.* 125:1–15.
- Fernández R., Kallal R.J., Dimitrov D., Ballesteros J.A., Arnedo M.A., Giribet G., Hormiga G. 2018. Phylogenomics, Diversification Dynamics, and Comparative Transcriptomics across the Spider Tree of Life. *Curr. Biol.* 28:1489-1497.e5.
- Fitzjohn R.G. 2012. Diversitree: Comparative phylogenetic analyses of diversification in R. *Methods Ecol. Evol.* 3:1084–1092.
- Fitzjohn R.G., Maddison W.P., Otto S.P. 2009. Estimating trait-dependent speciation and extinction rates from incompletely resolved phylogenies. *Syst. Biol.* 58:595–611.
- Fitzpatrick B.M., Turelli M. 2006. The Geography of Mammalian Speciation: Mixed Signals From Phylogenies and Range Maps. *Evolution (N. Y.)* 60:601–615.
- Foote M. 1993. Contributions of Individual Taxa to Overall Morphological Disparity. *Paleobiology* 19:403–419.
- Freitas R., Romeiras M., Silva L., Cordeiro R., Madeira P., González J.A., Wirtz P., Falcón J.M., Brito A., Floeter S.R., Afonso P., Porteiro F., Viera-Rodríguez M.A., Neto A.I., Haroun R., Farminhão J.N.M., Rebelo A.C., Baptista L., Melo C.S., Martínez A., Núñez J., Berning B., Johnson M.E., Ávila S.P. 2019. Restructuring of the ‘Macaronesia’ biogeographic unit: A marine multi-taxon biogeographical approach. *Sci. Rep.* 9:1–18.
- Futuyma D.J. 1986. *Evolutionary biology*. Sunderland, Massachusetts, USA: Sinauer Associates.
- Futuyma D.J. 1998. *Evolutionary Biology*. Sunderland, MA: Sinauer Associates.
- Gavrilets S., Losos J.B. 2009. Adaptive Radiation: Contrasting theory with data. *Science* 323:732–737.
- Gavrilets S., Vose A. 2005. Dynamic patterns of adaptive radiation. *Proc. Natl. Acad. Sci. U. S. A.* 102:18040–18045.
- Gillespie R.G. 2016. Island time and the interplay between ecology and evolution in species diversification. *Evol. Appl.* 9:53–73.
- Gillespie R.G. 2020. Ecological Release. *Encycl. Islands*. 251–253.
- Gillespie R.G., Bennett G.M., De Meester L., Feder J.L., Fleischer R.C., Harmon L.J., Hendry A.P., Knope M.L., Mallet J., Martin C., Parent C.E., Patton A.H., Pfennig K.S., Rubinoff D., Schluter D., Seehausen O., Shaw K.L., Stacy E., Stervander M., Stroud J.T., Wagner C., Wogan G.O.U. 2020. Comparing Adaptive Radiations Across Space, Time, and Taxa. *J. Hered.* 111:1–20.
- Gillespie R.G., Roderick G.K. 2002. Arthropods on Islands: Colonization, Speciation, and Conservation. *Annu. Rev. Entomol.* 47:595–632.

- Givnish T.J. 2015. Adaptive radiation versus “radiation” and “explosive diversification”: Why conceptual distinctions are fundamental to understanding evolution. *New Phytol.* 207:297–303.
- Givnish T.J., Sytsma K.J. 1997. *Molecular evolution and adaptive radiation*. Cambridge: Cambridge University Press.
- Glor R.E. 2010. Phylogenetic insights on adaptive radiation. *Annu. Rev. Ecol. Evol. Syst.* 41:251–270.
- Guillerme T. 2018. dispRity: A modular R package for measuring disparity. *Methods Ecol. Evol.* 9:1755–1763.
- Hansen T.F., Orzack S.H. 2005. Assessing Current Adaptation and Phylogenetic Inertia As Explanations of Trait Evolution: the Need for Controlled Comparisons. *Evolution (N. Y.)* 59:2063.
- Harmon L.J., Losos J.B., Jonathan Davies T., Gillespie R.G., Gittleman J.L., Bryan Jennings W., Kozak K.H., McPeck M.A., Moreno-Roark F., Near T.J., Purvis A., Ricklefs R.E., Schluter D., Schulte J.A., Seehausen O., Sidlauskas B.L., Torres-Carvajal O., Weir J.T., Mooers A.T. 2010. Early bursts of body size and shape evolution are rare in comparative data. *Evolution (N. Y.)* 64:2385–2396.
- Harvey P.H., Pagel M.D. 1991. *The comparative method in evolutionary biology*. Oxford University Press, Oxford, UK.
- Hastie T. 2022. gam: Generalized Additive Models. R package version 1.20.2.
- Heibl C., Calange C. 2018. phyloclim: Integrating Phylogenetics and Climatic Niche Modeling.
- Hijmans R.J., Phillips S., Leathwick J., Elith J. 2022. dismo: Species Distribution Modeling. R package version 1.3-8.
- Hopkin S.P., Martin M.H. 1985. Assimilation of zinc, cadmium, lead, copper, and iron by the spider *Dysdera crocata*, a predator of woodlice. *Bull. Environ. Contam. Toxicol.* 34:183–187.
- Hormiga G. 2002. Orsonwelles, a new genus of giant linyphiid spiders (Araneae) from the Hawaiian Islands. *Invertebr. Syst.* 16:369–448.
- Hormiga G., Arnedo M., Gillespie R.G. 2003. Speciation on a conveyor belt: Sequential colonization of the Hawaiian Islands by Orsonwelles spiders (Araneae, Linyphiidae). *Syst. Biol.* 52:70–88.
- Hubert N., Hanner R. 2016. DNA Barcoding, species delineation and taxonomy: a historical perspective. *DNA Barcodes.* 3:44–58.
- Humphries J.M., Bookstein F., Chernoff B., Smith G., Elder R.L., Poss S.G. 1981. MULTIVARIATE DISCRIMINATION BY SHAPE IN RELATION TO SIZE. *Syst. Zool.* 30:291–308.
- Hutchinson G.E. 1957. Concluding Remarks. *Cold Spring Harb. Symp. Quant. Biol.* 22:415–427.
- Ingram T., Mahler D.L. 2013. SURFACE : detecting convergent evolution from comparative data by fitting Ornstein-Uhlenbeck models with stepwise Akaike Information Criterion. :416–425.
- Jackson A.L., Inger R., Parnell A.C., Bearhop S. 2011. Comparing isotopic niche widths among and within

- communities: SIBER - Stable Isotope Bayesian Ellipses in R. *J. Anim. Ecol.* 80:595–602.
- Juan C., Emerson B.C., Oromí P., Hewitt G.M. 2000. Colonization and diversification: towards a phylogeographic synthesis for the Canary Islands. *15:104–109.*
- Jungers W.L., Falsetti A.B., Wall C.E. 1995. Shape , Relative Size , and Size-Adjustments in Morphometrics. *Yearb. Phys. Anthropology.* 38:137–161.
- Kapli P., Lutteropp S., Zhang J., Kobert K., Pavlidis P., Stamatakis A., Flouri T. 2017. Multi-rate Poisson tree processes for single-locus species delimitation under maximum likelihood and Markov chain Monte Carlo. *Bioinformatics.* 33:1630–1638.
- Kembel S.W., Cowan P.D., Helmus M.R., Cornwell W.K., Morlon H., Ackerly D.D., Blomberg S.P., Webb C.O. 2010. Picante: R tools for integrating phylogenies and ecology. *Bioinformatics.* 26:1463–1464.
- Kennedy S., Lim J.Y., Clavel J., Krehenwinkel H., Gillespie R.G. 2019. Spider webs, stable isotopes and molecular gut content analysis: Multiple lines of evidence support trophic niche differentiation in a community of Hawaiian spiders. *Funct. Ecol.* 33:1722–1733.
- Klingenberg C.P. 2008a. Morphological integration and developmental modularity. *Annu. Rev. Ecol. Evol. Syst.* 39:115–132.
- Klingenberg C.P. 2008b. *MorphoJ*. Manchester: UK: Faculty of Life Sciences, University of Manchester.
- Klingenberg C.P. 2009. Morphometric integration and modularity in configurations of landmarks: tools for evaluating a priori hypotheses. *421:405–421.*
- Koonin E. V., Wolf Y.I. 2009. Is evolution Darwinian or/and Lamarckian? *Biol. Direct.* 4:42.
- Krehenwinkel H., Kennedy S., Pekár S., Gillespie R.G. 2017. A cost-efficient and simple protocol to enrich prey DNA from extractions of predatory arthropods for large-scale gut content analysis by Illumina sequencing. *Methods Ecol. Evol.* 8:126–134.
- Lack D. 1947. *Darwin's Finches*. Cambridge University Press.
- Lafage D., Elbrecht V., Cuff J.P., Hambäck P.A., Erlandsson A. 2020. A new primer for metabarcoding of spider gut contents. *:234–243.*
- Lamarck J.-B. 1809. *Philosophie zoologique, ou exposition des considérations relatives à l'histoire naturelle des animaux*. Paris: Dentu: .
- Latreille P.A. 1804. *Tableau methodique des Insectes*. *Nouv. Dict. d'Histoire Nat.* Paris. 24:129–295.
- Lessard J.P., Belmaker J., Myers J.A., Chase J.M., Rahbek C. 2012. Inferring local ecological processes amid species pool influences. *Trends Ecol. Evol.* 27:600–607.
- Li G., Ma J., Zhang L. 2010. Greedy Selection of Species for Ancestral State Reconstruction on Phylogenies: Elimination Is Better than Insertion. *PLOS One.* 5.

- Linder P.H., Bouchenak-Khelladi Y. 2017. Adaptive radiations should not be simplified: The case of the danthonioid grasses. *Mol. Phylogenet. Evol.* 117:179–190.
- Losos J.B. 2009. *Lizards in an evolutionary tree: ecology and adaptive radiation of anoles*. Berkeley, CA: University of California Press.
- Losos J.B. 2010. Adaptive radiation, ecological opportunity, and evolutionary determinism: American society of naturalists E. O. Wilson award address. *Am. Nat.* 175:623–639.
- Losos J.B. 2011. Convergence, adaptation, and constraint. *Evolution (N. Y.)* 65:1827–1840.
- Losos J.B., Jackman T.R., Larson A., De Queiroz K., Rodríguez-Schettino L. 1998. Contingency and determinism in replicated adaptive radiations of island lizards. *Science (80-)* 279:2115–2118.
- Losos J.B., Leal M., Glor R.E., De Queiroz K., Hertz P.E., Rodríguez Schettino L., Chamizo Lara A., Jackman T.R., Larson A. 2003. Niche lability in the evolution of a Caribbean lizard community. *Nature*. 424:542–545.
- Losos J.B., Mahler D.L. 2010. Adaptive Radiation: The Interaction of Ecological Opportunity, Adaptation, and Speciation. In: Bell M., Futuyama D., Eanes W., Levinton J., editors. *Evolution since Darwin: The First 150 Years*. Sunderland, MA. p. 381–420.
- Losos J.B., De Queiroz K. 1997. Evolutionary consequences of ecological release in Caribbean Anolis lizards. *Biol. J. Linn. Soc.* 61:459–483.
- Lynch J.D. 1989. The gauge of speciation: on the frequency of modes of speciation. In: Otte D., Endler J., editors. *Speciation and its consequences*. Sunderland, MA: Sinauer Associates. p. 527–553.
- MacArthur R.H., Diamond J.M., Karr J.R. 1972. Density Compensation in Island Faunas. *Ecology*. 53:330–342.
- MacArthur R.H., Wilson E.O. 1967. *The Theory of Island Biogeography*. Princeton, NJ. Macieira. Princeton University Press.
- Macías-Hernández N., Athey K., Tonzo V., Wangenstein O.S., Arnedo M., Harwood J.D. 2018. Molecular gut content analysis of different spider body parts. *PLoS One*. 13.
- Macías-Hernández N., Domènech M., Cardoso P., Emerson B.C., Borges P.A.V., Lozano-Fernandez J., Paulo O.S., Vieira A., Enguádanos A., Rigal F., Amorim I.R., Arnedo M.A. 2020. Building a Robust, Densely-Sampled Spider Tree of Life for Ecosystem Research. *Diversity*. 12:288.
- Macías-Hernández N., López S. de la C., Roca-Cusachs M., Oromí P., Arnedo M.A. 2016. A geographical distribution database of the genus *Dysdera* in the Canary Islands (Araneae, Dysderidae). *Zookeys*. 2016:11–23.
- Macías-Hernández N., Oromí P., Arnedo M.A. 2008. Patterns of diversification on old volcanic islands as revealed by the woodlouse-hunter spider genus *Dysdera* (Araneae , Dysderidae) in the eastern

- Canary Islands. *Biol. J. Linn. Soc.* 94 (3): 589–615.
- Macías-Hernández N., Oromí P., Arnedo M.A. 2010. Integrative taxonomy uncovers hidden species diversity in woodlouse hunter spiders (Araneae, Dysderidae) endemic to the Macaronesian archipelagos. *Syst. Biodivers.* 8:531–553.
- Maddison W.P. 1997. Gene trees in species trees. *Syst. Biol.* 46:523–536.
- Maddison W.P., Midford P.E., Otto S.P. 2007. Estimating a binary character's effect on speciation and extinction. *Syst. Biol.* 56:701–710.
- Mallet J. 1995. A species definition for the Modern Synthesis. *Trends Ecol. Evol.* 10:294–299.
- Mammola S., Isaia M. 2017. Spiders in caves. *Proc. R. Soc. B Biol. Sci.* 284.
- Marc P., Canard A., Ysnel F. 1999. Spiders (Araneae) useful for pest limitation and bioindication. *Agric. Ecosyst. Environ.* 74:229–273.
- Matsubayashi K.W., Yamaguchi R. 2022. The speciation view: Disentangling multiple causes of adaptive and non-adaptive radiation in terms of speciation. *Popul. Ecol.* 64:95–107.
- Matz M. V., Nielsen R. 2005. A likelihood ratio test for species membership based on DNA sequence data. *Philos. Trans. R. Soc. B Biol. Sci.* 360:1969–1974.
- Mayr E. 1963. *Animal Species and Evolution*. MA. Belknap.
- McGill B.J., Enquist B.J., Weiher E., Westoby M. 2006. Rebuilding community ecology from functional traits. *Trends Ecol. Evol.* 21:178–185.
- Mcgregor A.P., Hilbrant M., Pechmann M., Schwager E.E., Prpic N., Damen W.G.M. 2008. *Cupiennius salei* and *Achaearanea tepidariorum*: spider models for investigating evolution and development. *Bioessays.* 30 (5):487–498.
- Meimberg H., Abele T., Bräuchler C., McKay J.K., Pérez de Paz P.L., Heubl G. 2006. Molecular evidence for adaptive radiation of *Micromeria* Benth. (Lamiaceae) on the Canary Islands as inferred from chloroplast and nuclear DNA sequences and ISSR fingerprint data. *Mol. Phylogenet. Evol.* 41:566–578.
- Michalik P., Ram J. 2014. Evolutionary morphology of the male reproductive system, spermatozoa and seminal fluid of spiders (Araneae, Arachnida) - Current knowledge and future directions. *Arthropod Struct. Dev.* 43:291–322.
- Miller A.H., Stroud J.T., Losos J.B. 2023. The ecology and evolution of key innovations. *Trends Ecol. Evol.* 38:122–131.
- Münkemüller T., Lavergne S., Bzeznik B., Dray S., Jombart T., Schiffrers K., Thuiller W. 2012. How to measure and test phylogenetic signal. *Methods Ecol. Evol.* 3:743–756.
- Naik H., Kgaditse M.M., Alexander G.J. 2021. Ancestral Reconstruction of Diet and Fang Condition in the

- Lamprophiidae: Implications for the Evolution of Venom Systems in Snakes. *J. Herpetol.* 55:1–10.
- Nee S., May R.M., Harvey P.H. 1994. The reconstructed evolutionary process. *Philos. Trans. R. Soc. B Biol. Sci.* 344:305–311.
- Newsome S.D., del Rio C.M., Bearhop S., Phillips D.L. 2007. A niche for isotopic ecology. *Front. Ecol. Environ.* 5:399–452.
- Nilsson M.A., Churakov G., Sommer M., van Tran N., Zemann A., Brosius J., Schmitz J. 2010. Tracking marsupial evolution using archaic genomic retroposon insertions. *PLoS Biol.* 8.
- Novotny A., Zamora-Terol S., Winder M. 2021. DNA metabarcoding reveals trophic niche diversity of micro and mesozooplankton species. *Proc. R. Soc. B Biol. Sci.* 288.
- Olson E.C., Miller R.L. 1958. *Morphological Integration*. Chicago: University of Chicago Press.
- Ortiz D., Petráková Dušátková L., Pekár S. 2021. Gut content metabarcoding of three widespread Iberian ant-eating spiders reveals specialisation on the same abundant harvester ants. *Ecol. Entomol.*:1–9.
- Ospovat D. 1981. *The development of Darwin's theory*. Cambridge, UK: Cambridge: Cambridge University Press.
- Parent, Crespi. 2009. Ecological Opportunity in Adaptive Radiation of Galápagos Endemic Land Snails. *Am. Nat.* 174.
- Patton A.H., Harmon L.J., Castañeda R., Frank H.K., Donihue C.M., Herrel A., Losos J.B. 2021. When adaptive radiations collide: Different evolutionary trajectories between and within island and mainland lizard clades. *PNAS.* 118 (42).
- Pekár S., Líznavá E., Řezáč M. 2016. Suitability of woodlice prey for generalist and specialist spider predators: A comparative study. *Ecol. Entomol.* 41:123–130.
- Pekár S., Petráková L., Šedo O., Korenko S., Zdráhal Z. 2018. Trophic niche, capture efficiency and venom profiles of six sympatric ant-eating spider species (Araneae: Zodariidae). *Mol. Ecol.* 27:1053–1064.
- Pennell M.W., Harmon L.J. 2013. An integrative view of phylogenetic comparative methods: Connections to population genetics, community ecology, and paleobiology. *Ann. N. Y. Acad. Sci.* 1289:90–105.
- Phillimore A.B., Price T.D. 2008. Density-dependent cladogenesis in birds. *PLoS Biol.* 6:0483–0489.
- Pincheira-Donoso D., Harvey L.P., Ruta M. 2015. What defines an adaptive radiation? Macroevolutionary diversification dynamics of an exceptionally species-rich continental lizard radiation. *BMC Evol. Biol.* 15:1–13.
- Pollock L.J., Tingley R., Morris W.K., Golding N., O'Hara R.B., Parris K.M., Vesk P.A., Mccarthy M.A. 2014.

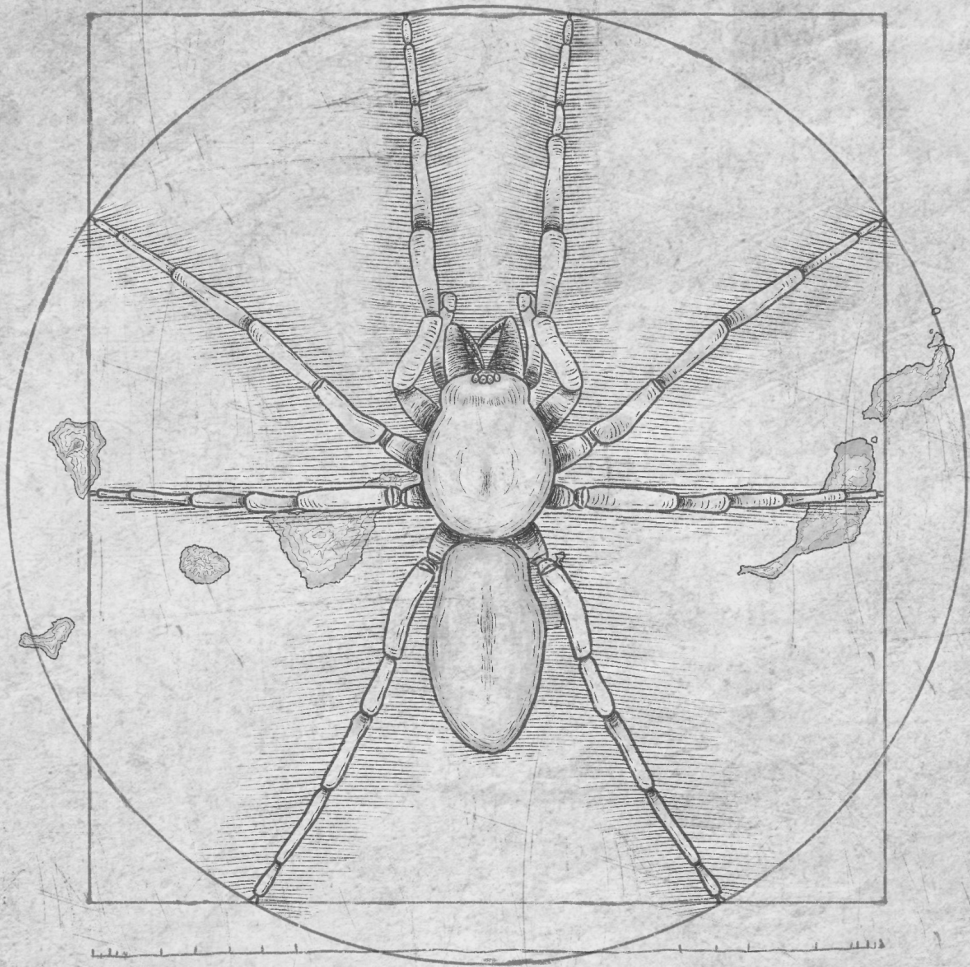
- Understanding co-occurrence by modelling species simultaneously with a Joint Species Distribution Model (JSDM). *Methods Ecol. Evol.* 5:397–406.
- Pompanon F., Deagle B.E., Symondson W.O.C., Brown D.S., Jarman S.N., Taberlet P. 2012. Who is eating what: Diet assessment using next generation sequencing. *Mol. Ecol.* 21:1931–1950.
- Puillandre N., Brouillet S., Achaz G. 2021. ASAP: assemble species by automatic partitioning. *Mol. Ecol. Resour.* 21:609–620.
- Purugganan M.D., Robichaux R.H. 2005. Adaptive Radiation and Regulatory Gene Evolution in the Hawaiian Silversword Alliance (Asteraceae). *Ann. Missouri Bot. Gard.* 92:28–35.
- Pybus O.G., Harvey P.H. 2000. Testing macro-evolutionary models using incomplete molecular phylogenies. *Proc. R. Soc. B Biol. Sci.* 267:2267–2272.
- R Core Team. 2022. R: A Language and Environment for Statistical Computing. Available from <https://www.r-project.org/>.
- Rabosky D.L., Goldberg E.E. 2015. Model inadequacy and mistaken inferences of trait-dependent speciation. *Syst. Biol.* 64:340–355.
- Rabosky D.L., Lovette I.J. 2008. Density-dependent diversification in North American wood warblers. *Proc. R. Soc. B Biol. Sci.* 275:2363–2371.
- Ratnasingham S., Hebert P.D.N. 2013. A DNA-Based Registry for All Animal Species: The Barcode Index Number (BIN) System. *PLoS One.* 8.
- Raupach M.J. 2005. Die bedeutung von landasselnalsbeutetiere für insekten un andere arthropoden. *Entomol. heute.* 17:3–12.
- Revell L.J. 2012. phytools: An R package for phylogenetic comparative biology (and other things). *Methods Ecol. Evol.* 3:217–223.
- Revell L.J., Harmon L.J. 2022. *Phylogenetic comparative methods in R*. New Jersey: Princeton University Press.
- Revell L.J., Harmon L.J., Collar D.C. 2008. Phylogenetic signal, evolutionary process, and rate. *Syst. Biol.* 57:591–601.
- Reynolds R.G., Collar D.C., Pasachnik S.A., Niemiller M.L., Puente-Rolón A.R., Revell L.J. 2016. Ecological specialization and morphological diversification in Greater Antillean boas. *Evolution.* 70:1882–1895.
- Řezáč M., Pekár S., Arnedo M., Macías-Hernández N., Řezáčová V. 2021. Evolutionary insights into the eco-phenotypic diversification of *Dysdera* spiders in the Canary Islands. *Org. Divers. Evol.*
- Řezáč M., Pekár S., Lubin Y. 2008. How oniscophagous spiders overcome woodlouse armour. *J. Zool.* 275:64–71.

- Ribera C., Fernandez M.A., Blasco A. 1985. Araneidos cavernícolas de Canarias II. *Mémoires de Biospéologie*. 51–68.
- Des Roches S., Brinkmeyer M.S., Harmon L.J., Rosenblum E.B. 2015. Ecological release and directional change in White Sands lizard trophic ecomorphology. *Evol. Ecol.* 29.
- Rohlf F.J. 2015. The tps series of software. *Hystrix*. 26:9–12.
- Rohlf F.J., Slice D. 1990. Extensions of the procrustes method for the optimal superimposition of landmarks. *Syst. Zool.* 39:40–59.
- Rohlf J.F., Marcus L.F. 1993. A revolution morphometrics. *Trends Ecol. Evol.* 8:129–132.
- Ronco F., Salzburger W. 2021. The non-gradual nature of adaptive radiation. *Zoology*. 146:125925.
- Rubinoff D. 2006. Utility of mitochondrial DNA barcodes in species conservation. *Conserv. Biol.* 20:1026–1033.
- Rundle H.D., Nagel L., Boughman J.W., Schluter D. 2000. Natural selection and parallel speciation in sympatric sticklebacks. *Science* (80-.). 287:306–308.
- Schluter D. 2000. *The Ecology of Adaptive Radiation*. Oxford University Press, Oxford.
- Schluter D., Nagel L.M. 1995. Parallel Speciation by Natural Selection. *Am. Nat.* 146:292–301.
- Sierra D., Giovany R., Lida G., Franco M., Meijden A. Van Der, González- J.C., Valenzuela- J.C., Fernando C., Quiroga P. 2021. Deciphering the diet of a wandering spider (*Phoneutria boliviensis*; Araneae: Ctenidae) by DNA metabarcoding of gut contents. :5950–5965.
- Simpson G.G. 1944. *Tempo and mode in evolution*. New York: Columbia University Press.
- Simpson G.G. 1953. *The major features of evolution*. New York: Columbia University Press.
- Slater G.J., Price S.A., Santini F., Alfaro M.E. 2010. Diversity versus disparity and the radiation of modern cetaceans. *Proc. R. Soc. B Biol. Sci.* 277:3097–3104.
- Soulebeau A., Aubriot X., Gaudeul M., Rouhan G., Hennequin S., Haevermans T., Dubuisson J.Y., Jabbour F. 2015. The hypothesis of adaptive radiation in evolutionary biology: hard facts about a hazy concept. *Org. Divers. Evol.* 15:747–761.
- Stayton C.T. 2015a. What does convergent evolution mean? The interpretation of convergence and its implications in the search for limits to evolution. *Interface Focus*. 5.
- Stayton C.T. 2015b. The definition, recognition, and interpretation of convergent evolution, and two new measures for quantifying and assessing the significance of convergence. *Evolution* (N. Y). 69:2140–2153.
- Stayton C.T. 2018. *convevol: Analysis of Convergent Evolution*. R package version 1.3, <<https://CRAN.R-project.org/package=convevol>>. .
- Stephens P.R., Wiens J.J. 2003. Ecological diversification and phylogeny of emydid turtles. *Biol. J. Linn.*

- Soc. 79:577–610.
- Streelman J.T., Danley P.D. 2003. The stages of vertebrate evolutionary radiation. *Trends Ecol. Evol.* 18:126–131.
- Stroud J.T., Losos J.B. 2016. Ecological Opportunity and Adaptive Radiation. *Annu. Rev. Ecol. Evol. Syst.* 47:507–532.
- Sundberg P. 1989. Shape and Size-Constrained Principal Components Analysis. *Syst. Zool.* 38:166–168.
- Sunderland K.D., Sutton S.L. 1980. A Serological Study of Arthropod Predation on Woodlice in a Dune Grassland Ecosystem Author (s): Keith D . Sunderland and Stephen L . Sutton Published by: British Ecological Society Stable URL: <http://www.jstor.org/stable/4240> Accessed: 22-04-2016 02. *J. Anim. Ecol.* 49:987–1004.
- Tikhonov G., Opedal Ø.H., Abrego N., Lehikoinen A., de Jonge M.M.J., Oksanen J., Ovaskainen O. 2020. Joint species distribution modelling with the r-package Hmsc. *Methods Ecol. Evol.* 11:442–447.
- Tikhonov G., Ovaskainen O., Oksanen J., Jonge M.M.J. De, Opedal Ø.H., Dallas T. 2022. Hmsc: Hierarchical Model of Species Communities. .
- Toft C. 1995. Evolution of Diet Specialization in Poison-Dart Frogs (Dendrobatidae). *Herpetologica.* 51:202–216.
- Toft S., Macías-Hernández N. 2021. Prey acceptance and metabolic specialisations in some Canary Dysdera spiders. *J. Insect Physiol.* 131:104227.
- Troll V.R., Carracedo J.C. 2016. The Geology of the Canary Islands. .
- Vamosi J.C., Scott Armbruster W., Scott Armbruster W., Scott Armbruster W., Renner S.S. 2014. Evolutionary ecology of specialization: Insights from phylogenetic analysis. *Proc. R. Soc. B Biol. Sci.* 281.
- Vizueta J., Rozas J., Hernández N.M., Gracia A.S. 2019. Chance and predictability in evolution: The genomic basis of convergent dietary specializations in an adaptive radiation. *Mol. Ecol.* 28 (17): 4028–4045.
- Wallace A.R. 1881. *Island life: Or, the phenomena and causes of insular faunas and floras, including a revision and attempted solution of the problem of geological climates.* London: Harper.
- Whittaker R.J., Triantis K.A., Ladle R.J. 2009. A general dynamic theory of oceanic island biogeography: Extending the MacArthur-Wilson theory to accommodate the rise and fall of volcanic islands. *Theory Isl. Biogeogr. Revisit.* 88–115.
- World Spider Catalog. 2023. World Spider Catalog. Version 24. Natural History Museum Bern, online at <http://wsc.nmbe.ch>, accessed on 20/07/2023. doi: 10.24436/2.
- Wunderlich J. 1987. *Die Spinnen der Kanarischen Inseln und Madeiras: Adaptive Radiation,*

Biogeographie, Revisionen und Neubeschreibungen.

Yoder J.B., Clancey E., Des Roches S., Eastman J.M., Gentry L., Godsoe W., Hagey T.J., Jochimsen D., Oswald B.P., Robertson J., Sarver B.A.J., Schenk J.J., Spear S.F., Harmon L.J. 2010. Ecological opportunity and the origin of adaptive radiations. *J. Evol. Biol.* 23:1581–1596.



APPENDICES

APPENDIX 1

Supplementary material for the manuscript:

Endless species most beautiful: Using DNA barcodes to inform species delimitation in the red devil spiders (Araneae: Dysderidae) of the Canary Islands, with description of ten new species

A. Bellvert, C. Arenas, A. Enguídanos, N. Macías-Hernández, M. Roca-Cusachs & M. A. Arnedo

This supplementary material includes 2 figures and 1 table.

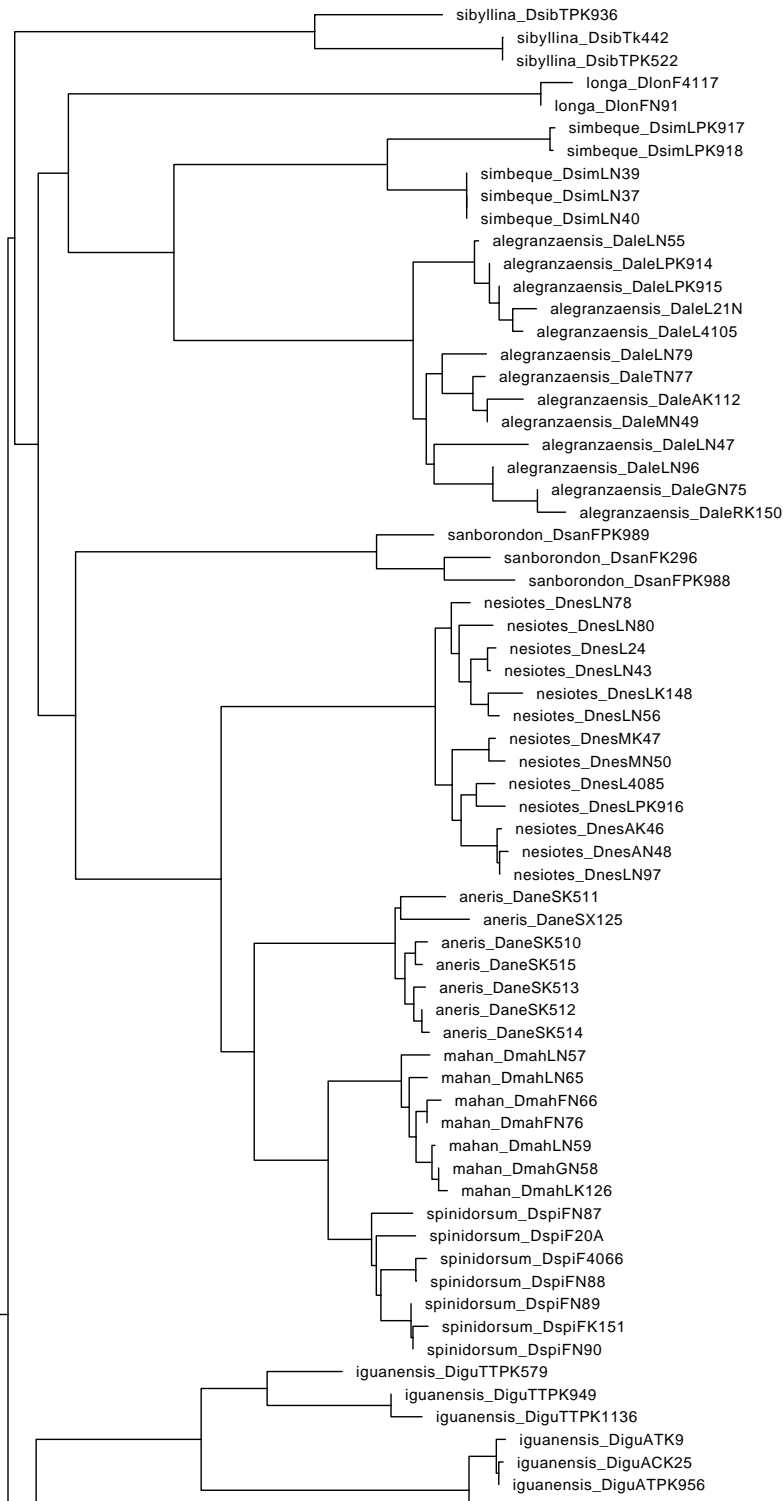
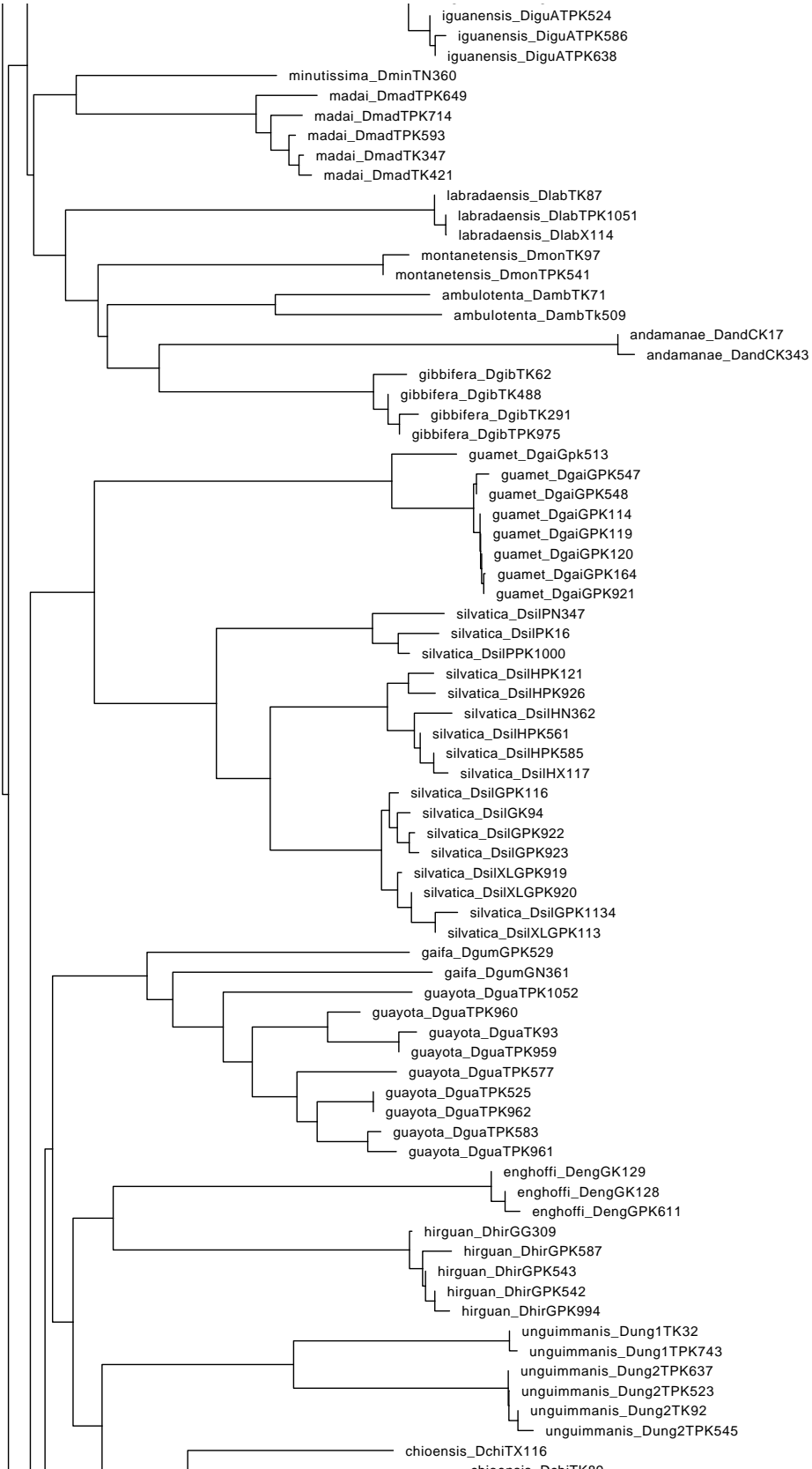
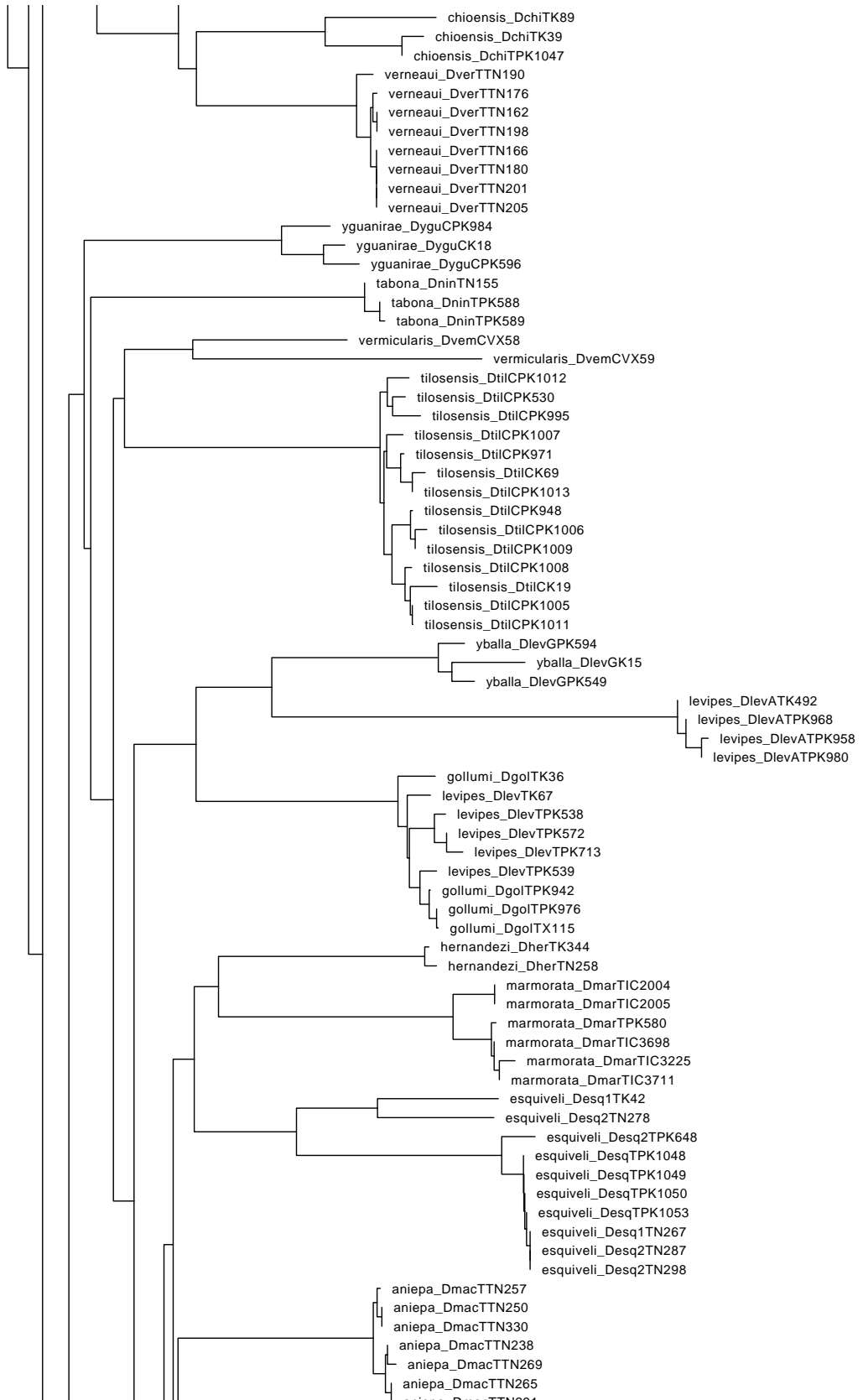
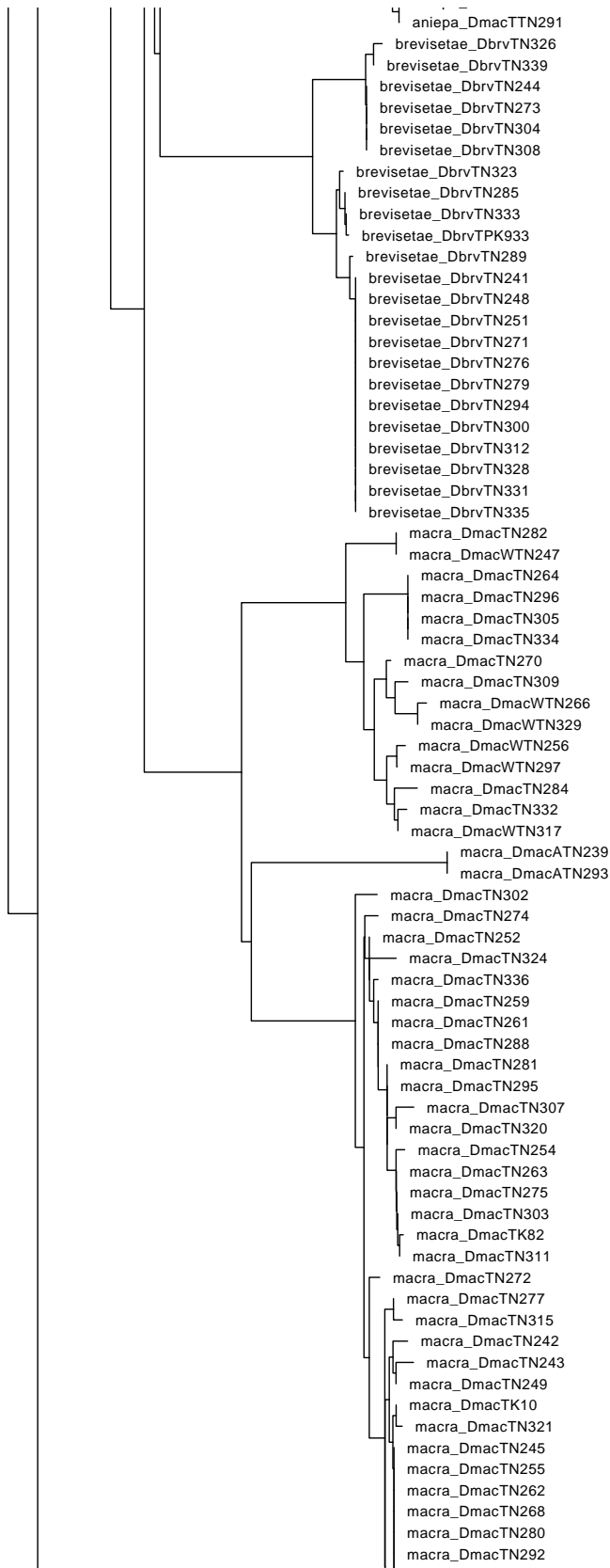
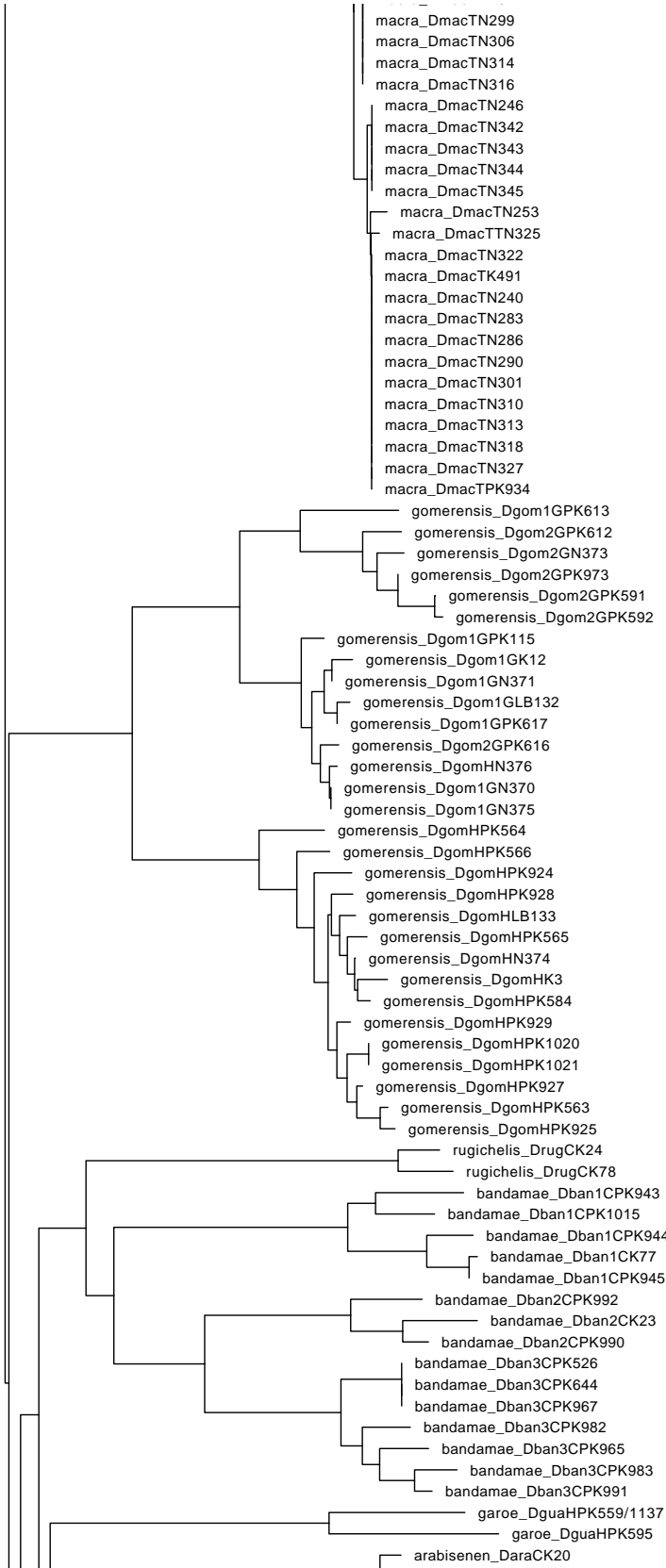


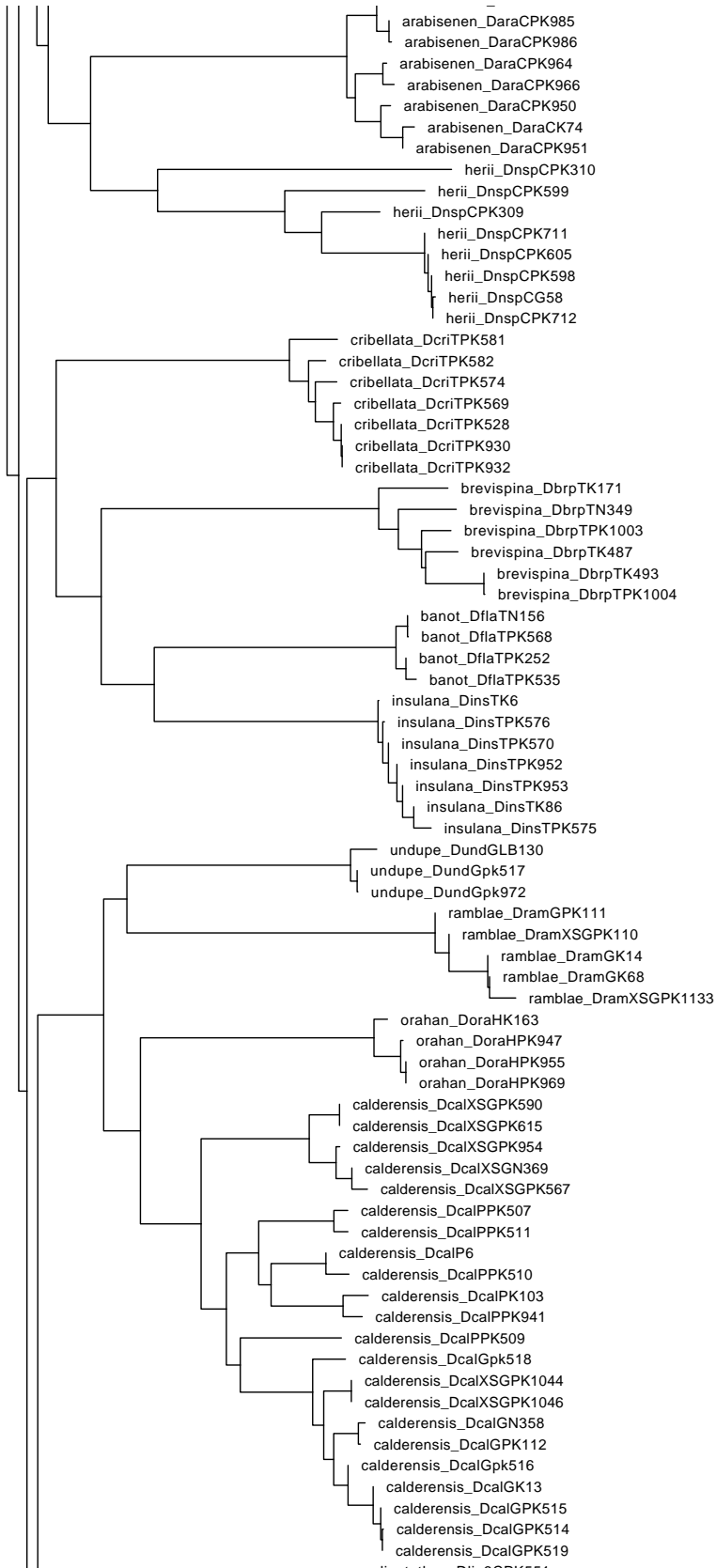
Figure S1 Neighbor-Joining tree build from the COI data matrix. Branch lengths correspond to the evolutionary distances computed using the Kimura 2-parameter model. All ambiguous positions were removed for each sequence pair (pairwise deletion option).

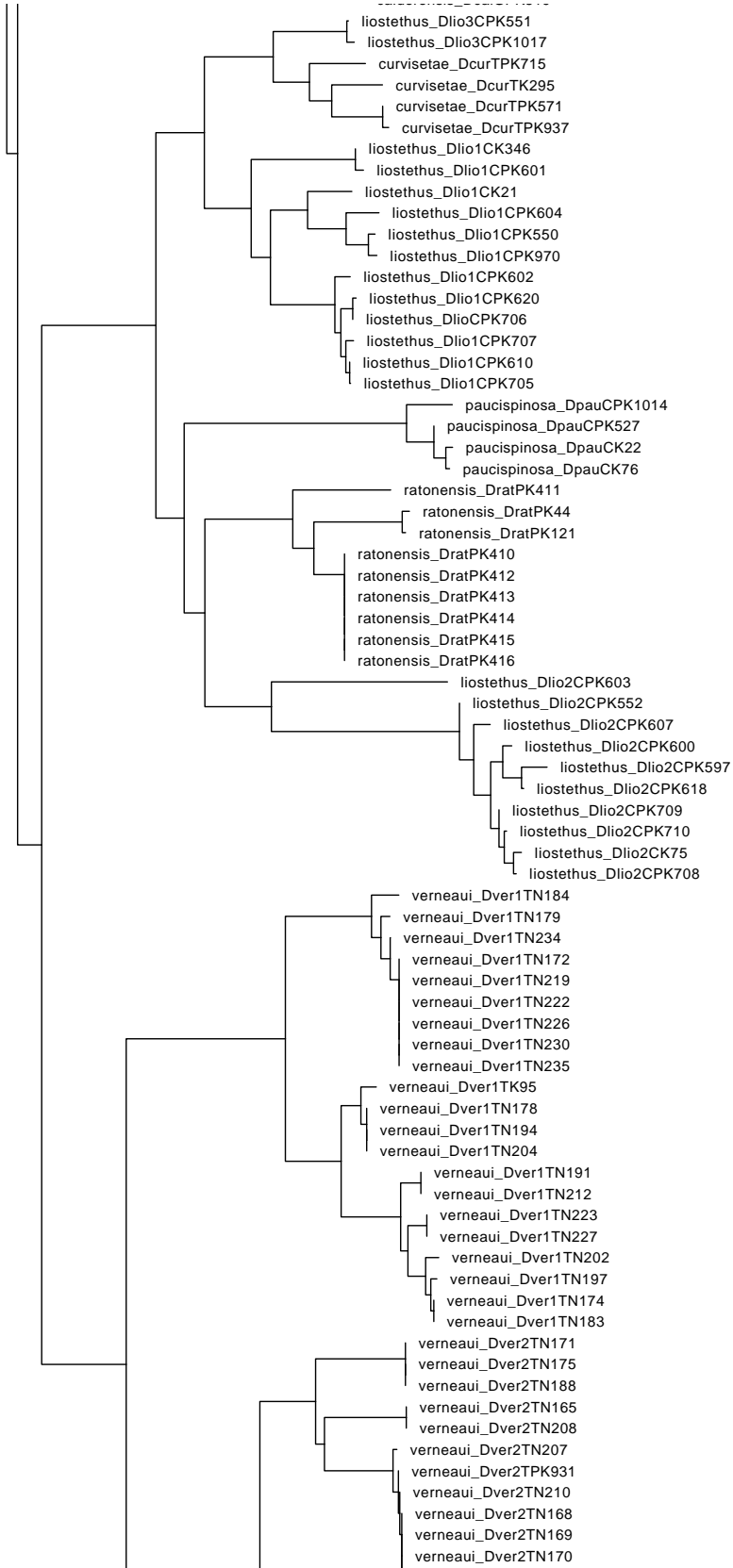


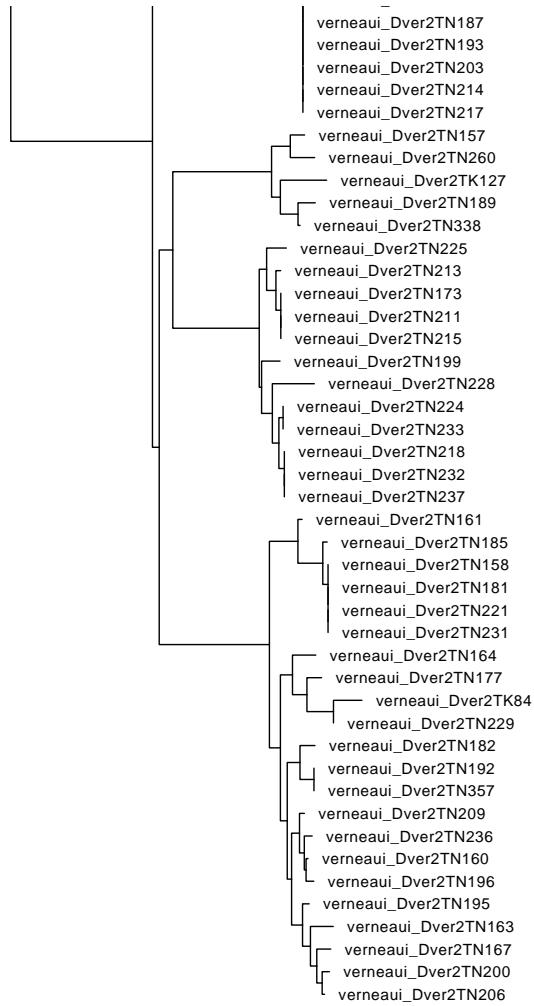












0.02

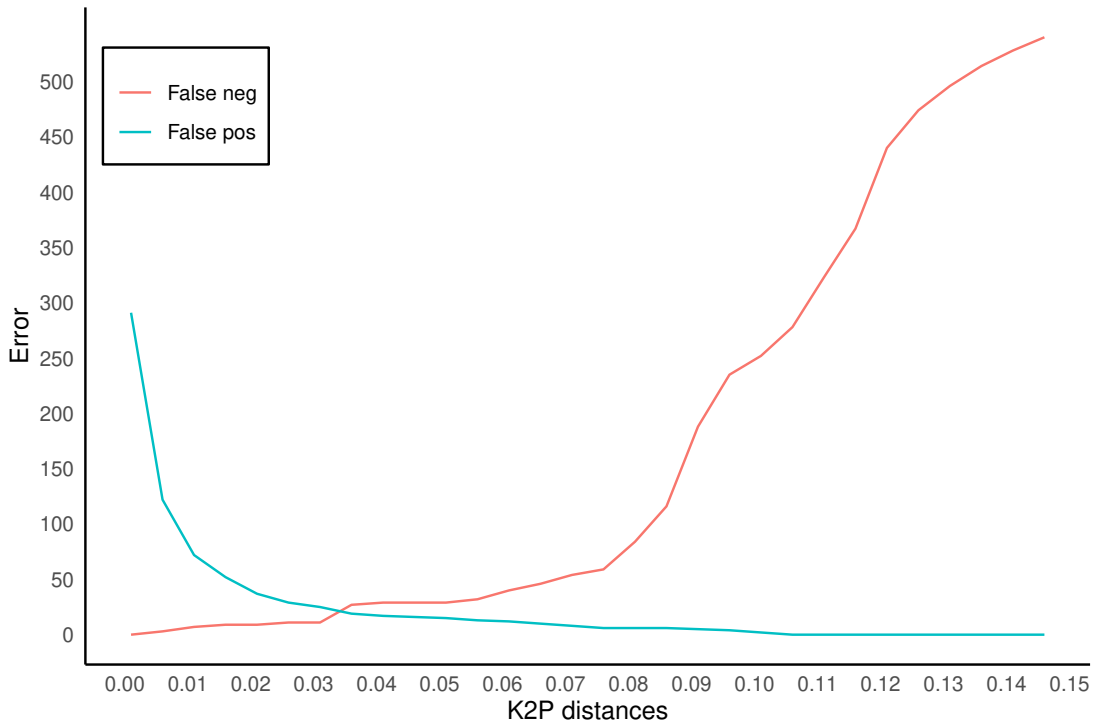


Figure S2 plot of the False positives in blue and false negatives in red inferred by optimising threshold values ranging from 0.001 to 0.15, in intervals of 0.005 increase. The optimum threshold value estimated by function localMinimum in Spider R package was 0.028 K2P distance, with an error of 7%.

Table S1 List of specimens sequenced or retrieved from Genbank in the present study.

Code	DNA code	species	Loc.Latitude	Loc.Longitude	Sample_id	Cris_COI_matrix	co1_NCB1	Haplotypes	Cris ITS_matri	Its_NCB1	Cris_16S_matrix	Cris_ND1_matrix
UB4106_Freezer	K112	alegranzaensis	0	0	DaleAK112	DaleAK112	AF244257.1	DaleAK112	DaleAK112	EU143817.1	DaleAK112	DaleGN75
NMH0000449	N75	alegranzaensis	29.25378	-13.504026	DaleGN75	DaleGN75	EU139612.1	DaleGN75	DaleGN75	EU143817.1	DaleGN75	DaleGN75
UB4090_Freezer	21N	alegranzaensis	28.91952	-13.7637	DaleL21N	DaleL21N	AF244259.1	DaleL21N	DaleL21N	EU143817.1	DaleL21N	DaleL21N
UB4105_Freezer	4105	alegranzaensis	29.211204	-13.484156	DaleL4105	DaleL4105	AF244258.1	DaleL4105	DaleL4105	EU143817.1	DaleL4105	DaleL4105
NMH0000429	N47	alegranzaensis	29.39392	-13.50194	DaleLN47	DaleLN47	EF458132.1	DaleLN47	DaleLN47	EU143814.1	DaleLN47	DaleLN47
NMH0000424	N55	alegranzaensis	28.93287	-13.77366	DaleLN55	DaleLN55	EU139611.1	DaleLN55	DaleLN55	EU143816.1	DaleLN55	DaleLN55
NMH0000462	N79	alegranzaensis	29.05185	-13.66985	DaleLN79	DaleLN79	EU139613.1	DaleLN79	DaleLN79	EU143819.1	DaleLN79	DaleLN79
NMH0000430	N96	alegranzaensis	29.39392	-13.50194	DaleLN96	DaleLN96	KC210092	DaleLN95	DaleLN95	EU143819.1	DaleLN95	DaleLN95
CRBA002681	PK914	alegranzaensis	28.980257	-13.638351	DaleLPK914	DaleLPK914		DaleLPK914	DaleLPK914	EU143819.1	DaleLPK914	DaleLPK914
CRBA002684	PK915	alegranzaensis	28.980257	-13.638351	DaleLPK915	DaleLPK915		DaleLPK915	DaleLPK915	EU143819.1	DaleLPK915	DaleLPK915
NMH0000364	N49	alegranzaensis	29.29886	-13.53533	DaleMN49	DaleMN49	EU139610.1	DaleMN49	DaleMN49	EU143815.1	DaleMN49	DaleMN49
UB3137_132 freez	K150	alegranzaensis	29.24206	-13.51629	DaleRK150	DaleRK150	AF244260.1	DaleRK150	DaleRK150	EU143815.1	DaleRK150	DaleRK150
NMH0000073	N77	alegranzaensis			DaleTN77	DaleTN77	EU139609.1	DaleTN77	DaleTN77	EU143818.1	DaleTN77	DaleTN77
UUL1075	K509	ambulotenta	28.35018	-16.704638	DambTK509	DambTK509	EU068055	DambTK509	DambTK509	EU143818.1	DambTK509	DambTK509
UB2511_102	K71	ambulotenta	28.360891	-16.498084	DambTK71	DambTK71	AF244276	DambTK71	DambTK71	EU143818.1	DambTK71	DambTK71
UB2976	K17	andamanae	28.11145	-15.60197	DandCK17	DandCK17	EU068027	DandCK17	DandCK17	EU143818.1	DandCK17	DandCK17
CRBA000692	K343	andamanae	28.11145	-15.60197	DandCK343	DandCK343	EU068028	DandCK343	DandCK343	EU143818.1	DandCK343	DandCK343
NMH0000608	K510	aneris	30.146105	-15.864976	DaneSK510	DaneSK510	HQ396319	DaneSK510	DaneSK510	HQ396288	DaneSK510	DaneSK510
NMH0000609	K511	aneris	30.146105	-15.864976	DaneSK511	DaneSK511	HQ396320	DaneSK511	DaneSK511	HQ396289	DaneSK511	DaneSK511
NMH0000610	K512	aneris	30.146105	-15.864976	DaneSK512	DaneSK512	HQ396321	DaneSK512	DaneSK512	HQ396290	DaneSK512	DaneSK512
NMH0000611	K513	aneris	30.146105	-15.864976	DaneSK513	DaneSK513	HQ396322	DaneSK513	DaneSK513	HQ396291	DaneSK513	DaneSK513
NMH0000612	K514	aneris	30.146105	-15.864976	DaneSK514	DaneSK514	HQ396323	DaneSK514	DaneSK514	HQ396292	DaneSK514	DaneSK514
NMH0000613	K515	aneris	30.146105	-15.864976	DaneSK515	DaneSK515	HQ396324	DaneSK515	DaneSK515	KC785826	DaneSK515	DaneSK515
rhim000290	X125	aneris			DaneSK125	DaneSK125	EU139634	DaneSK125	DaneSK125	KC785829	DaneSK125	DaneSK125
UB3034_127 freez	K20	arabisenen			DaraCK20	DaraCK20	AF244291	DaraCK20	DaraCK20	EU143818.1	DaraCK20	DaraCK20
UB3051_128 freez	K74	arabisenen	28.03184	-15.67702	DaraCK74	DaraCK74	AF244292	DaraCK74	DaraCK74	EU143818.1	DaraCK74	DaraCK74
CRBA002254	PK950	arabisenen	28.02513	-15.60675	DaraCPK950	DaraCPK950		DaraCPK950	DaraCPK950	KC785824/KC785828	DaraCPK950	DaraCPK950
CRBA002255	PK951	arabisenen	28.02513	-15.60675	DaraCPK951	DaraCPK951		DaraCPK951	DaraCPK951	KC785821	DaraCPK951	DaraCPK951
NMH001954	PK964	arabisenen	27.994244	-15.594384	DaraCPK964	DaraCPK964		DaraCPK964	DaraCPK964	KC785824	DaraCPK964	DaraCPK964
NMH002060	PK966	arabisenen	27.96483	-15.54505	DaraCPK966	DaraCPK966		DaraCPK966	DaraCPK966	KC785824	DaraCPK966	DaraCPK966
NMH003113	PK985	arabisenen	27.952243	-15.527475	DaraCPK985	DaraCPK985		DaraCPK985	DaraCPK985		DaraCPK985	DaraCPK985
NMH003114	PK986	arabisenen	27.952243	-15.527475	DaraCPK986	DaraCPK986		DaraCPK986	DaraCPK986		DaraCPK986	DaraCPK986
UB2980	K77	bandamae	28.11145	-15.60197	Dban1CK77	Dban1CK77	AF244287	Dban1CK77	Dban1CK77	EU143818.1	Dban1CK77	Dban1CK77
NMH001906	PK1015	bandamae	28.032133	-15.7554	Dban1CPK1015	Dban1CPK1015		Dban1CPK1015	Dban1CPK1015	EU143818.1	Dban1CPK1015	Dban1CPK1015
CRBA000588	PK943	bandamae	28.035189	-15.746346	Dban1CPK943	Dban1CPK943		Dban1CPK943	Dban1CPK943	EU143818.1	Dban1CPK943	Dban1CPK943
CRBA000737	PK944	bandamae	28.068779	-15.658864	Dban1CPK944	Dban1CPK944		Dban1CPK944	Dban1CPK944	EU143818.1	Dban1CPK944	Dban1CPK944
CRBA000966	PK945	bandamae	28.11145	-15.60197	Dban1CPK945	Dban1CPK945		Dban1CPK945	Dban1CPK945	EU143818.1	Dban1CPK945	Dban1CPK945
UB3041_128 freez	K23	bandamae	27.93298	-15.48007	Dban2CK23	Dban2CK23	AF244286	Dban2CK23	Dban2CK23	EU143818.1	Dban2CK23	Dban2CK23

CRBA001452	PK514	calderensis	28.151547	-17.162962	DcalGPK514	DcalGPK514						
UB4165(119)_Free	PK515	calderensis	28.151547	-17.162962	DcalGPK515	DcalGPK515						
UB4167(122)_Free	PK516	calderensis	28.151547	-17.162962	DcalGPK516	DcalGPK516						
UB4146(93)_Free	PK518	calderensis	28.19332	-17.29294	DcalGPK518	DcalGPK518						
UB4131(48)_Free	PK519	calderensis	28.149151	-17.220779	DcalGPK519	DcalGPK519						
UB4011_Freezer	K103	6	28.843639	-17.90635	DcalP6	DcalP6	AF244310				DcalP6	
UB4013_Freezer	K103	calderensis	28.843639	-17.90635	DcalPK103	DcalPK103	AF244309/IN689138				DcalPK103	DcalPK103
CRBA002292	PK507	calderensis	28.557572	-17.867541	DcalPK507	DcalPK507						
CRBA002341	PK509	calderensis	28.79636	-17.971169	DcalPK509	DcalPK509						
CRBA002278	PK510	calderensis	28.843639	-17.90635	DcalPK510	DcalPK510	AF244310					
CRBA002340	PK511	calderensis	28.557572	-17.867541	DcalPK511	DcalPK511						
CRBA003064	PK941	calderensis	28.113296	-17.335703	DcalPK941	DcalPK941					DcalPK941	
NMH001446	N369	calderensis	28.113296	-17.335703	DcalXSGN369	DcalXSGN369						
CRBA004138	pk1044	calderensis			DcalXSGPK1044	DcalXSGPK1044						
CRBA004140	pk1046	calderensis			DcalXSGPK1046	DcalXSGPK1046						
CRBA001863	PK567	calderensis	28.09618	-17.20142	DcalXSGPK567	DcalXSGPK567					DcalXSGPK567	
NMH0003237	PK590	calderensis	28.113296	-17.335703	DcalXSGPK590	DcalXSGPK590					DcalXSGPK590	
NMH0003252	PK615	calderensis	28.119283	-17.23729	DcalXSGPK615	DcalXSGPK615					DcalXSGPK615	
CRBA002730	PK954	calderensis	28.11577	-17.33604	DcalXSGPK954	DcalXSGPK954						
UB4821(132)-4	K39	chiensis	28.25057	-16.7763	DchITK39	DchITK39	AF244281				DchITK39	
UB2967	K89	chiensis	28.236393	-16.642253	DchITK89	DchITK89	AF244282				DchITK89	
CRBA003267	PK1047	chiensis	28.360891	-16.498084	DchITPK1047	DchITPK1047						
nhm000286	X116	chiensis	28.31083	-16.37041	DchITX116	DchITX116	EU068030.1				DchITX116	DchITX116
UB????	K102	cribellata	28.531925	-16.279999	DcrrTK102	DcrrTK102					DcrrTK102	DcrrTK102
NMH002110	PK528	cribellata	28.53528	-16.29881	DcrrTPK528	DcrrTPK528						
CRBA001335	PK569	cribellata	28.573489	-16.18638	DcrrTPK569	DcrrTPK569						
NMH001442	PK574	cribellata	28.32455	-16.81944	DcrrTPK574	DcrrTPK574						
NMH001305	PK581	cribellata	28.352711	-16.413852	DcrrTPK581	DcrrTPK581						
NMH000805	PK582	cribellata	28.52907	-16.14816	DcrrTPK582	DcrrTPK582						
CRBA002944	PK930 / PK1185	cribellata	28.53532	-16.2968	DcrrTPK930	DcrrTPK930						
CRBA002951	PK932	cribellata	28.53532	-16.2968	DcrrTPK932	DcrrTPK932						
NMH0003171	PK621	crocata	28.001499	-15.57466	DcroCPK621	DcroCPK621						DcroCPK621
NMH001499	PK619	crocata	28.335996	-16.86576	DcroTPK619	DcroTPK619						
CRBA003026	PK935	crocata	28.35881	-16.58732	DcroTPK935	DcroTPK935						
CRBA000514	K295	curvisetae	28.288321	-16.86186	DcurTK295	DcurTK295	EU068031					DcurTK295
NMH002743	PK571	curvisetae	28.033022	-16.540247	DcurTPK571	DcurTPK571						
NMH0003353	PK715	curvisetae	28.570148	-16.290357	DcurTPK715	DcurTPK715						
CRBA003037	PK937	curvisetae	28.033022	-16.540247	DcurTPK937	DcurTPK937						
UB4130(46)_Free	PK128	enghoffi	28.149151	-17.220779	DengGK128	DengGK128	AF244271.1				DengGK128	DengGK128
UB4163(117)_Free	K129	enghoffi	28.151547	-17.162962	DengGK129	DengGK129	AF244272					
NMH0003253	PK611	enghoffi	28.119283	-17.23729	DengGPK611	DengGPK611						DengGPK611
UB2803	K42	esquiveli	28.35018	-16.704638	Desq1TK42	Desq1TK42	AF244298.1					Desq1TK42
NMH000278	N267	esquiveli	28.35018	-16.704638	Desq1TN267	Desq1TN267						Desq1TN267
CRBA001325	N278	esquiveli	28.360891	-16.498084	Desq2TN278	Desq2TN278						Desq2TN278
NMH000279	N287	esquiveli	28.35018	-16.704638	Desq2TN287	Desq2TN287						Desq2TN287

NMH000280	N298	esquiveli	28.35018	-16.704638	Desq2TN298	Desq2TN298	Desq1TN267				
NMH002746	PK648	esquiveli	28.236393	-16.642253	Desq2TPK648	Desq2TPK648	Desq2TPK648				
CRBA003333	pk1048 / pk1189	esquiveli	28.35018	-16.704638	DesqTPK1048	DesqTPK1048	DesqTPK1048			DesqTPK1048	DesqTPK1048
CRBA003334	pk1049	esquiveli	28.35018	-16.704638	DesqTPK1049	DesqTPK1049	DesqTPK1049				
CRBA003335	pk1050	esquiveli	28.35018	-16.704638	DesqTPK1050	DesqTPK1050	DesqTPK1048				
CRBA003375	pk1053	esquiveli	28.35018	-16.704638	DesqTPK1053	DesqTPK1053	DesqTPK1048				
NMH000717	N156	banot	28.560191	-16.16919	DflaTN156	DflaTN156	DflaTN156			DflaTN156	DflaTN156
CRBA002117	PK252 / PK1191	banot	28.560191	-16.16919	DflaTPK252	DflaTPK252	DflaTPK252				
NMH002945	PK535	banot	28.551966	-16.189225	DflaTPK535	DflaTPK535					
NMH002929	PK568	banot	28.53929	-16.2758	DflaTPK568	DflaTPK568					
CRBA001843	PK1114	guamet	28.1963	-17.28754	DgaiGPK114	DgaiGPK114					
CRBA002056 (NM)	PK1119	guamet	28.1963	-17.28754	DgaiGPK119	DgaiGPK119	DgaiGPK114				
CRBA002058	PK120	guamet	28.1963	-17.28754	DgaiGPK120	DgaiGPK120	DgaiGPK120			DgaiGPK120	DgaiGPK120
CRBA002495	PK164	guamet	28.1963	-17.28754	DgaiGPK164	DgaiGPK164					
NMH002996	pk513	guamet	28.1963	-17.28754	DgaiGPK513	DgaiGPK513					
NMH001884	PK547	guamet	28.1963	-17.28754	DgaiGPK547	DgaiGPK547					
NMH001893	PK548	guamet	28.1963	-17.28754	DgaiGPK548	DgaiGPK548					
CRBA002780	PK921	guamet	28.1963	-17.28754	DgaiGPK921	DgaiGPK921				DgibTK291	DgibTK291
CRBA000580	K291	gibbifera	28.32455	-16.81944	DgibTK291	DgibTK291					
CRBA001082	k488	gibbifera	28.32455	-16.81944	DgibTK488	DgibTK488	EU068033			DgibTK488	DgibTK488
UB2709	K62	gibbifera	28.35018	-16.704638	DgibTK62	DgibTK62	AF244277			DgibTK62	DgibTK62
CRBA002938	PK975	gibbifera	28.32455	-16.81944	DgibTPK975	DgibTPK975				DgibTPK975	DgibTPK975
UB2966	K36	gollumi	28.236393	-16.642253	DgolTK36	DgolTK36	AF244295			DgolTK36	DgolTK36
CRBA000585	PK942	gollumi	28.236393	-16.642253	DgolTPK942	DgolTPK942				DgolTPK942	DgolTPK942
CRBA001094	PK976	gollumi	28.236393	-16.642253	DgolTPK976	DgolTPK976					
ULL1161	X115	gollumi	28.236393	-16.642253	DgolTX115	DgolTX115				DgolTX115	DgolTX115
UB4133 (51), Free	K12	gomerensis	28.108856	-17.241604	Dgom1GK12	Dgom1GK12	AF244317			Dgom1GK12	Dgom1GK12
CRBA001393	LB132	gomerensis	28.147416	-17.291071	Dgom1GLB132	Dgom1GLB132	HO396326.1			Dgom1GLB132	Dgom1GLB132
NMH001447	N370	gomerensis	28.125809	-17.216616	Dgom1GN370	Dgom1GN370	KC785791				
NMH001450	N371	gomerensis	28.106909	-17.233323	Dgom1GN371	Dgom1GN371	KC785792				
NMH001449	N375	gomerensis	28.13665	-17.179063	Dgom1GN375	Dgom1GN375	KC785794				
CRBA001844	PK115	gomerensis	28.1963	-17.28754	Dgom1GPK115	Dgom1GPK115				kk	kk
NMH002928	PK613	gomerensis	28.114684	-17.113168	Dgom1GPK613	Dgom1GPK613					
NMH003255	PK617	gomerensis	28.135646	-17.257454	Dgom1GPK617	Dgom1GPK617					
NMH001445	N373	gomerensis	28.113283	-17.335701	Dgom2GN373	Dgom2GN373	KC785793				
NMH003238	PK591	gomerensis	28.113283	-17.335701	Dgom2GPK591	Dgom2GPK591					
NMH003241	PK592	gomerensis	28.1963	-17.28754	Dgom2GPK592	Dgom2GPK592					
NMH003055	PK612	gomerensis	28.090664	-17.283087	Dgom2GPK612	Dgom2GPK612				contaminant	contaminant
NMH003247	PK616	gomerensis	28.11116	-17.2648	Dgom2GPK616	Dgom2GPK616					
UB4137(70), Free	PK973	gomerensis	28.108856	-17.241604	Dgom2GPK973	Dgom2GPK973				Dgom2GPK616	Dgom2GPK616
CR3199_135	K3	gomerensis	27.740804	-18.05308	DgomHK3	DgomHK3	AF244318			DgomHK3	DgomHK3
UBA001395	LB133	gomerensis	27.737593	-18.022747	DgomHLB133	DgomHLB133	HO396327.1			DgomHLB133	DgomHLB133
NMH001452	N374	gomerensis	27.781744	-17.951391	DgomHN374	DgomHN374	KC785789				
NMH001451	N376	gomerensis	27.712944	-18.022175	DgomHN376	DgomHN376	KC785790				
NMH003372	PK1020	gomerensis	27.823454	-17.996024	DgomHPK1020	DgomHPK1020					

NMH003373	PK1021	gomerensis	27.823454	-17.996024	DgomHPK1021	DgomHPK1020		
NMH003195	PK563	gomerensis	27.740804	-18.05308	DgomHPK563			
NMH003193	PK564	gomerensis	27.781744	-17.951391	DgomHPK564			
NMH003199	PK565	gomerensis	27.712944	-18.022175	DgomHPK565			
NMH003208	PK584	gomerensis	27.732883	-18.140708	DgomHPK566			
CRBA002840	PK924	gomerensis	27.743623	-18.016548	DgomHPK584			
CRBA002841	PK925	gomerensis	27.754861	-18.118218	DgomHPK924	DgomHPK924		
CRBA002894	PK927	gomerensis	27.785991	-18.118218	DgomHPK925	DgomHPK925		
CRBA002895	PK928	gomerensis	27.785991	-17.997508	DgomHPK927			
CRBA002896	PK929	gomerensis	27.785991	-17.997508	DgomHPK928			
NMH002725	PK559/pk1137	garoe	27.692348	-17.972877	DguahPK559/1137	DguahPK559/1137		
CRBA002063	PK595	garoe	27.712944	-18.022175	DguahPK595			
UB3170_134	K93	guayota	28.093144	-16.69889	DguatPK93	DguatPK93	DguatPK93	
CRBA003373	pk1052	macra	28.345548	-16.371103	DguatPK1052			
CRBA002262	PK525	guayota			DguatPK525			
NMH002933	PK577	guayota	28.11665	-16.67335	DguatPK577			
NMH001332	PK583	guayota			DguatPK583			
NMH000918	PK959	guayota	28.093144	-16.69889	DguatPK959			
NMH000919	PK960	guayota	28.093144	-16.69889	DguatPK960	DguatPK960		
NMH001066	PK961	guayota	28.17731	-16.601628	DguatPK961	DguatPK961		
NMH001084	PK962	guayota	28.190338	-16.669163	DguatPK962	DguatPK962		
NMH001440	N361	gaifa	28.113296	-17.335703	DgumGN361			
NMH002927	PK529	gaifa	28.114684	-17.113168	DgumPK529	DgumPK529		
ULL1072	K344	hernandez	28.437553	-16.413396	DherTK344	DherTK344		
NMH001358	N258	hernandez	28.437553	-16.413396	DherTN258	DherTN258		
NMH001460	G309	hirguan	28.125809	-17.216616	DhirGG309	DhirGG309		
NMH001474	PK542	hirguan	28.125809	-17.216616	DhirGPK542	DhirGPK542		
NMH001475	PK543	hirguan	28.125809	-17.216616	DhirGPK543	DhirGPK543		
NMH001453	PK587	hirguan	28.125809	-17.216616	DhirGPK587			
NMH001474	PK994	hirguan	28.125809	-17.216616	DhirGPK994			
UB2600_107	K25	iguanensis	27.938683	-15.708818	DiguACK25	DiguACK25	DiguACK25	
UB4835_freezer	K9	iguanensis	28.56509	-16.165982	DiguATK9	DiguATK9	DiguATK9	
CRBA002243	PK524	iguanensis	28.529535	-16.268309	DiguATPK524			
NMH000637	PK586	iguanensis	28.529535	-16.268309	DiguATPK586			
CRBA002244	PK638 / JL14	iguanensis	28.529535	-16.268309	DiguATPK638	DiguATPK638		
NMH000139	PK936	iguanensis	28.531936	-16.28168	DiguATPK936	DiguATPK936		
CRBA000341	PK1136	iguanensis	28.32455	-16.81944	DiguATPK1136_reversed_	DiguATPK1136		
NMH003063	PK579/pk1138	iguanensis	28.32455	-16.81944	DiguATPK579/1138			
CRBA000967	PK949	iguanensis	28.32455	-16.81944	DiguTPK949	DiguTPK949		
UB4785/(T2)74	K6	insulana	28.550411	-16.203986	DinstK6	DinstK6	DinstK6	
UB3152_133	K86	insulana	28.531925	-16.279999	DinstK86	DinstK86	DinstK86	
NMH003176	PK570	insulana	28.5356	-16.29881	DinstPK570	DinstPK570		
NMH001041	PK575	insulana	28.32455	-16.81944	DinstPK575	DinstPK575		
NMH003041	PK576	insulana	28.32455	-16.81944	DinstPK576	DinstPK576		

CRBA000579	k421	madai	28.32455	-16.81944	DmadTK421	EU068043.1	DmadTK421	DmadTK421	DmadTK421	DmadTK421
NMH0003242	PK593	madai	28.360891	-16.498084	DmadTPK593					
NMH0003304	PK649	madai	28.270218	-16.597251	DmadTPK649					
NMH0003311	PK714	madai	28.299404	-16.541681	DmadTPK714					
NMH0000490	N66	mahan	28.744863	-13.873707	DmahFN66	EU139624	DmahFN66	EU143829	DmahFN66	DmahFN66
NMH0000572	N76	mahan	28.743173	-13.829946	DmahFN76	EU139625	DmahFN76		DmahFN76	DmahFN76
NMH0000451	N58	mahan	29.244485	-13.492957	DmahGN58	EU139621	DmahGN58	EU143827	DmahGN58	DmahGN58
1+8493	K126	mahan	29.194456	-13.427888	DmahLK126	AF244267	DmahLK126		DmahLK126	DmahLK126
NMH0000358	N57	mahan	29.4044184	-13.490834	DmahLN57	EU139620.1	DmahLN57	EU143826.1	DmahLN57	DmahLN57
NMH0000356	N59	mahan	29.1944459	-13.505116	DmahLN59	EU139622	DmahLN59		DmahLN59	DmahLN59
NMH0000447	N65	mahan	28.838823	-13.787028	DmahLN65	EU139623	DmahLN65	EU143828	DmahLN65	DmahLN65
IC2004MFI186NIE	IC2004MFI186NIE	marmorata	28.53407072	-16.53407072	DmarTIC2004		DmarTIC2004		DmarTIC2004	
IC2005MFI186NIE	IC2005MFI186NIE	marmorata	28.53407072	-16.31624704	DmarTIC2005		DmarTIC2005		DmarTIC2005	
NMH0003018	IC3225MFI186AGU	marmorata	28.529535	-16.268309	DmarTIC3225	MT738792				
NMH0003016	IC3698MFI186AGU	marmorata	28.529535	-16.268309	DmarTIC3698	MT738791				
NMH0003019	IC3711MFI186AGU	marmorata	28.529535	-16.268309	DmarTIC3711					
NMH0003017	PK580	marmorata	28.529535	-16.268309	DmarTPK580					
NMH001434	N360	minutissima	28.359658	-16.31624704	DminTN360		DminTN360		DminTN360	DminTN360
NMH0001436	PK963/PK1132	minutissima	28.359658	-16.501015	DminTPK963/1132		DminTPK963/1132		DminTPK963/1132	
UB4795_Frezer	K97	montanetensis	28.43558	-16.3735	DmontTK97		DmontTK97		DmontTK97	DmontTK97
NMH001035	PK541	montanetensis	28.32455	-16.81944	DmonTPK541		DmonTPK541		DmonTPK541	DmonTPK541
UB4107_Frezer	K46	nesiotis	0	0	DnesAK46	AF244262	DnesAK46		DnesAK46	DnesAK46
NMH0000428	N48	nesiotis	29.39392	-13.50194	DnesAN48	EU139616	DnesAN48	EU143821	DnesAN48	DnesAN48
UB4087_Frezer	24	nesiotis	29.211204	-13.484156	DnesL24	AF244266	DnesL24		DnesL24	DnesL24
UB4085_Frezer	4085	nesiotis	29.211204	-13.484156	DnesL4085	AF244264	DnesL4085		DnesL4085	DnesL4085
UB2867	K148	nesiotis	28.91952	-13.7637	DnesLK148	AF244265	DnesLK148		DnesLK148	DnesLK148
NMH0000057	N43	nesiotis	29.130724	-13.516903	DnesLN43	EU139615	DnesLN43	EU143820	DnesLN43	DnesLN43
NMH0000425	N56	nesiotis	28.93287	-13.77366	DnesLN56	EU139617	DnesLN56	EU143823	DnesLN56	DnesLN56
NMH0000398	N78	nesiotis	29.211204	-13.484156	DnesLN78	EU139618	DnesLN78	EU143824	DnesLN78	DnesLN78
NMH0000476	N80	nesiotis	29.05185	-13.66985	DnesLN80	EU139619	DnesLN80	EU143825	DnesLN80	DnesLN80
NMH0000511	N97	nesiotis	29.39392	-13.50194	DnesLN97	KC210115	DnesLN97		DnesLN97	DnesLN97
CRBA002689	PK916	nesiotis	29.130724	-13.516903	DnesPK916	KC210120	DnesPK916		DnesPK916	DnesPK916
UB4093_Frezer	K47	nesiotis	0	0	DnesMK47	AF244263	DnesMK47		DnesMK47	DnesMK47
NMH0000369	N50	nesiotis	29.29886	-13.5353	DnesMN50	EF458133.1	DnesMN50	EU143822.1	DnesMN50	DnesMN50
NMH0000661	N155	tabona	28.56509	-16.165982	DninTN155		DninTN155		DninTN155	DninTN155
NMH001214	pk588	tabona			DninTPK588		DninTPK588		DninTPK588	
NMH001215	PK589	tabona	28.556191	-16.179817	DninTPK589		DninTPK589		DninTPK589	
NMH001486	G58	herii	27.941568	-15.429992	DnspCG58		DnspCG58		DnspCG58	DnspCG58
CRBA002170	PK309	herii	27.988402	-15.478981	DnspCPK309		DnspCPK309		DnspCPK309	
CRBA002172	PK310	herii	27.90405	-15.77354	DnspCPK310		DnspCPK310		DnspCPK310	
NMH0003141	PK598	herii	27.953866	-15.376761	DnspCPK598		DnspCPK598		DnspCPK598	
NMH0003139	PK599	herii	27.910319	-15.530057	DnspCPK599		DnspCPK599		DnspCPK599	
NMH0003291	PK605	herii	27.941568	-15.429992	DnspCPK605		DnspCPK605		DnspCPK605	
NMH0003345	PK711	herii	27.941568	-15.429993	DnspCPK711		DnspCPK711		DnspCPK711	
NMH0003346	PK712	herii	27.941568	-15.429993	DnspCPK712		DnspCPK712		DnspCPK712	
UB3200_136	K163	orahan	27.754861	-18.118218	DoraHK163	AF244313.1	DoraHK163		DoraHK163	DoraHK163

NMHH001127	N204	verneau	28.43558	-16.3735	Dver1TN204	Dver1TN204	Dver1TN178					
NMHH001121	N219	verneau	28.43558	-16.3735	Dver1TN212	Dver1TN212	Dver1TN191					
NMHH001210	N219	verneau	28.556191	-16.179817	Dver1TN219	Dver1TN219	KC785735.1					
NMHH001241	N222	verneau	28.540023	-16.231988	Dver1TN222	Dver1TN222	KC785737					
NMHH001148	N226	verneau	28.316723	-16.59124	Dver1TN223	Dver1TN223						
NMHH000977	N226	verneau	28.540023	-16.231988	Dver1TN226	Dver1TN226						
NMHH001145	N227	verneau	28.316723	-16.59124	Dver1TN227	Dver1TN227	KC785776					Dver1TN227
NMHH000979	N230	verneau	28.540023	-16.231988	Dver1TN230	Dver1TN230						
NMHH001209	N234	verneau	28.556191	-16.179817	Dver1TN234	Dver1TN234	KC785736					
NMHH001240	N235	verneau	28.540023	-16.231988	Dver1TN235	Dver1TN235						
UB3181_135	K127	verneau	28.32455	-16.81944	Dver2TK127	Dver2TK127						Dver2TK127
UB3124_132 free	K84	verneau	28.093144	-16.69889	Dver2TK84	Dver2TK84	AF244321					Dver2TK84
UB3171_134 Free	N157	verneau	28.288195	-16.57339	Dver2TN157	Dver2TN157	KC785779					Dver2TN157
UB4797 (T22)	N158	verneau	28.169368	-16.630688	Dver2TN158	Dver2TN158	KC785768					Dver2TN158
NMHH001076	N160	verneau	28.249217	-16.528748	Dver2TN160	Dver2TN160	KC785763					Dver2TN160
NMHH000990	N161	verneau	28.197701	-16.531151	Dver2TN161	Dver2TN161	KC785767					Dver2TN161
NMHH000881	N163	verneau	28.384498	-16.44741	Dver2TN163	Dver2TN163	KC785751					Dver2TN163
NMHH000829	N164	verneau	28.394697	-16.431984	Dver2TN164	Dver2TN164	KC785749					Dver2TN164
NMHH000820	N165	verneau	28.411118	-16.421127	Dver2TN165	Dver2TN165	KC785746.1					Dver2TN165
NMHH001000	N167	verneau	28.307838	-16.448156	Dver2TN167	Dver2TN167	KC785756					Dver2TN167
NMHH000763	N168	verneau	28.53532	-16.2968	Dver2TN168	Dver2TN168						Dver2TN168
NMHH000079	N169	verneau	28.531925	-16.279999	Dver2TN169	Dver2TN169	KC785824					Dver2TN169
NMHH0000920	N170	verneau	28.531925	-16.279999	Dver2TN170	Dver2TN170	KC785739					Dver2TN170
NMHH000683	N171	verneau	28.5356	-16.29881	Dver2TN171	Dver2TN171	KC785738					Dver2TN171
NMHH000830	N173	verneau	28.394697	-16.431984	Dver2TN173	Dver2TN173						
NMHH000816	N175	verneau	28.5356	-16.29881	Dver2TN175	Dver2TN175						
NMHH000870	N177	verneau	28.384498	-16.44741	Dver2TN177	Dver2TN177	KC785752					
NMHH001070	N181	verneau	28.17731	-16.601628	Dver2TN181	Dver2TN181						
NMHH000880	N182	verneau	28.384498	-16.44741	Dver2TN182	Dver2TN182	KC785753					Dver2TN182
NMHH001071	N185	verneau	28.17731	-16.601628	Dver2TN185	Dver2TN185	KC785769					Dver2TN185
NMHH001114	N186	verneau	28.32455	-16.81944	Dver2TN186	Dver2TN186						Dver2TN186
NMHH001105	N187	verneau	28.248283	-16.529917	Dver2TN187	Dver2TN187						Dver2TN187
NMHH000680	N188	verneau	28.5356	-16.29881	Dver2TN188	Dver2TN188	KC785824					Dver2TN188
NMHH001104	N189	verneau	28.190338	-16.669163	Dver2TN189	Dver2TN189	KC785770					Dver2TN189
NMHH001106	N192	verneau	28.248283	-16.529917	Dver2TN192	Dver2TN192	KC785760					
NMHH000092	N193	verneau	28.531925	-16.279999	Dver2TN193	Dver2TN193						
NMHH001101	N195	verneau	28.384498	-16.44741	Dver2TN195	Dver2TN195	KC785754					
NMHH001073	N196	verneau	28.249217	-16.528748	Dver2TN196	Dver2TN196	KC785762					
NMHH000810	N199	verneau	28.418535	-16.41009	Dver2TN199	Dver2TN199	KC785747					Dver2TN199
NMHH001107	N200	verneau	28.248283	-16.529917	Dver2TN200	Dver2TN200	KC785761					
NMHH000924	N203	verneau	28.531925	-16.279999	Dver2TN203	Dver2TN203						Dver2TN168
NMHH001052	N206	verneau	28.307838	-16.448156	Dver2TN206	Dver2TN206	KC785759					
NMHH000759	N207	verneau	28.53532	-16.2968	Dver2TN207	Dver2TN207	KC785740					
NMHH000821	N208	verneau	28.411118	-16.421127	Dver2TN208	Dver2TN208						Dver2TN165
NMHH001075	N209	verneau	28.249217	-16.528748	Dver2TN209	Dver2TN209	KC785765					

APPENDIX 2.1

Supplementary material for the manuscript:

The Vitruvian spider: segmenting and integrating over different body parts to describe eco-phenotypic variation

Adrià Bellvert, Marcos Roca-Cusachs, Vanina Tonzo, Miquel A. Arnedo & Antigoni Kaliontzopoulou

This supplementary material includes 1 table

Table S1 Pairwise integration test between all pairs of views examined. The lower triangular matrix includes z-scores of the PLS analysis for each combination and the upper part, corresponding p-values.

		P-values								
		Q1	Q2	Q3	C1	C3	L11	L41	L14	L44
Z-scores	Q1		0.001	0.001	0.001	0.005	0.001	0.001	0.001	0.001
	Q2	0.848		0.001	0.001	0.472	0.001	0.037	0.001	0.001
	Q3	0.766	0.749		0.001	0.001	0.001	0.001	0.001	0.001
	C1	0.565	0.657	0.781		0.002	0.001	0.001	0.001	0.001
	C3	0.385	0.224	0.497	0.416		0.014	0.001	0.002	0.001
	L11	0.679	0.652	0.748	0.649	0.317		0.001	0.001	0.001
	L41	0.573	0.348	0.571	0.661	0.473	0.801		0.001	0.001
	L14	0.630	0.608	0.656	0.632	0.381	0.906	0.788		0.001
	L44	0.568	0.455	0.535	0.773	0.428	0.814	0.876	0.836	

APPENDIX 2.2

Supplementary material for the manuscript:

The non-dereliction in evolution: Trophic specialisation drives convergence in the radiation of red devil spiders (Araneae: Dysderidae) in the Canary Islands

Adrià Bellvert, Silvia Adrian-Serrano, Nuria Macías-Hernández, Søren Toft, Antigoni Kaliontzopoulou & Miquel A. Arnedo

This supplementary material includes 7 tables and 7 figures.

Table S1 Summary of the fossil and biogeographic calibrations used in the present study, with information on their implementation.

CLADE	FOSSIL	MIN.AGE	MAX.AGE	ASSIGNABLE TO	PRIOR DISTRIBUTION	UPPER	LOWER	MEAN IN REAL SPACE	SD.	OFFSET	MEDIAN	97.5% HPD	REFERENCE
Mesothelae	<i>Palaeothele montceauensis</i> (Selden)	299	304	Mesothelae stem	Uniform	450	299*						Magalhaes et al. 2020
Mygalomorphae	<i>Rosamygale grauvogeli</i> Selden & Gall	242	247.2	Avicularioidea stem	lognormal			80	0.5	242.0.	313	268-430	Magalhaes et al. 2020
Synspermiata	<i>Eoplectreurys gertschi</i> Selden & Huang	164	175.1	Synspermiata stem	lognormal			70	0.5	165.0.	226	187-329	Magalhaes et al. 2020
Synspermiata	* <i>Montsecarachne amicorum</i> Selden	125	129.4	Synspermiata crown	lognormal			70	0.5	125.0.	187	148-290	Magalhaes et al. 2020
Synspermiata	* <i>Burmarches9na acuminata</i> Wunderlich	98.17	99.41	Oonopidae stem	lognormal			30	0.5	98.17.	125	108-169	Magalhaes et al. 2020
Synspermiata	<i>Priscalecrercera paucispinae</i> Wunderlich	98.17	99.41	Psiloderidae stem	lognormal			30	0.5	98.17.	125	108-169	Magalhaes et al. 2020
Araneoidea	'Linyphiinae' indet.	125	135	Araneoidea stem	lognormal			70	0.5	125.0.	187	148-290	Magalhaes et al. 2020
rt	* <i>Selenops</i> sp. indet.	53	56	Selenopidae stem	lognormal			20	0.75	53.0.	68.1	56.5-119	Magalhaes et al. 2020
Synspermiata	<i>Dasumiana emicans</i> Wunderlich	43	47.8	Harpactelinae crown	lognormal			15	0.75	43.0.	54.3	45.6-92.2	Magalhaes et al. 2020
Synspermiata	<i>Quamtana huberi</i> Penney	53	56	Pholcinae crown	lognormal			20	0.75	53.0.	68.1	56.5-119	Magalhaes et al. 2020
Araneoidea	<i>Mesozygiella dunlapi</i> Penney & Ortuño	115	121	Araneidae stem	lognormal			30	0.5	115.0.	141	125-186	Penney & Ortuño 2006
	Biogeographic event												
<i>Parachtes</i>	Hercinian split			<i>Parachtes</i> crown	normal			29	2.5		29	24.1-33.9	Bidegaray & Arnedo 2011
*EARLIEST EVIDENCE OF LAND ARTHROPODS (ARBITRARY UPPER CONSTRAINT ON ROOT)													

Table S2 Percentage of acceptance of each prey by each *Dysdera* species analysed.

Species	n	Musca	Porcellio	Armadillidium	Pardosa	Carabid
<i>D. alegranzaensis</i>	18	93.75	87.5	43.75	68.75	31.25
<i>D. arabisenen</i>	19	100.00	35.29	29.41	35.29	11.76
<i>D. bandamae</i>	20	95.00	50.00	30.00	60.00	0.00
<i>D. brevisetae</i>	20	95.00	85.00	55.00	30.00	0.00
<i>D. cribellata</i>	20	78.95	94.74	36.84	57.89	0.00
<i>D. gomerensis</i> (La Gomera)	19	47.37	100.00	57.89	47.37	0.00
<i>D. insulana</i>	3	100.00	100.00	66.67	100.00	0.00
<i>D. levipes</i>	6	0.00	100.00	100.00	0.00	0.00
<i>D. macra</i>	19	73.68	94.74	42.11	21.05	10.53
<i>D. nesiotis</i>	20	100.00	90.91	40.91	72.73	9.09
<i>D. ramblae</i>	20	17.65	100.00	23.53	11.76	0.00
<i>D. silva6ca</i> (La Gomera)	20	100.00	90.00	25.00	85.00	5.00
<i>D. 6losensis</i>	7	71.43	85.71	71.43	0.00	0.00
<i>D. verneaui</i>	20	100.00	75.00	15.00	60.00	10.00

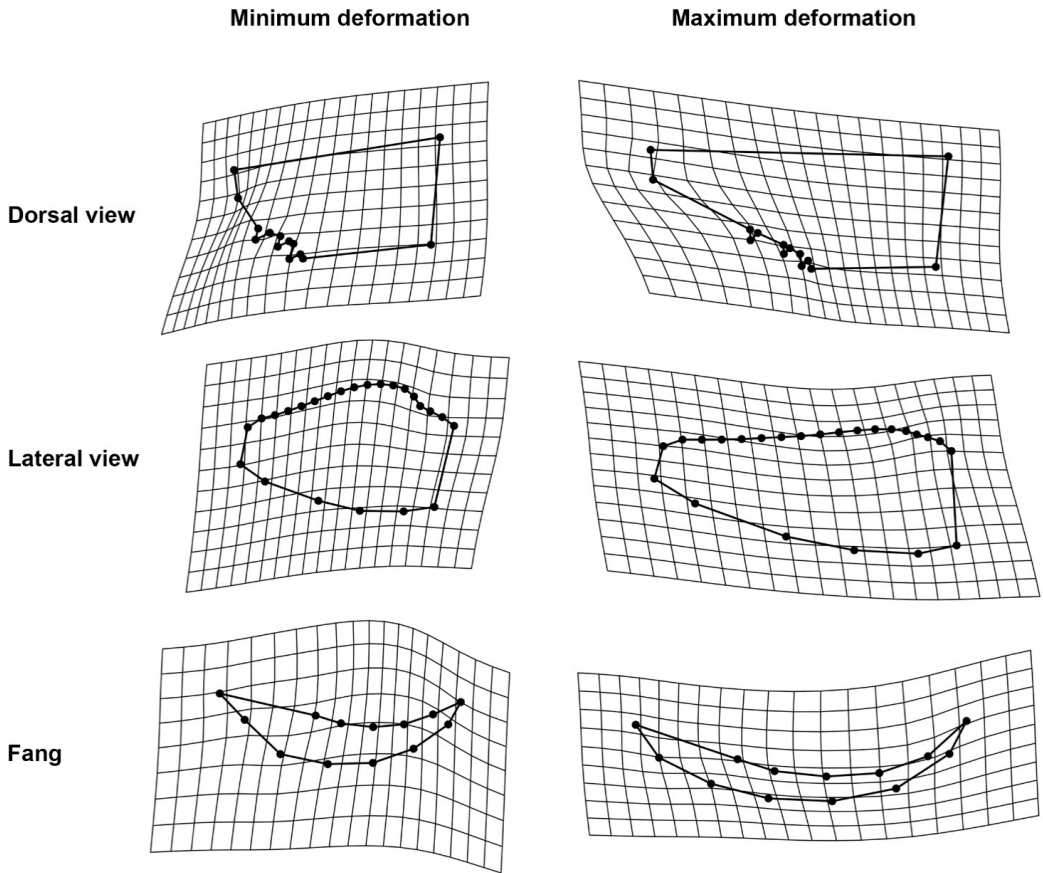


Figure S1 Shape corresponding to the maximum and minimum extremes of PC1 for each cheliceral view, represented using deformation grids. Shape patterns are exaggerated by 1.3x to enhance visualization.

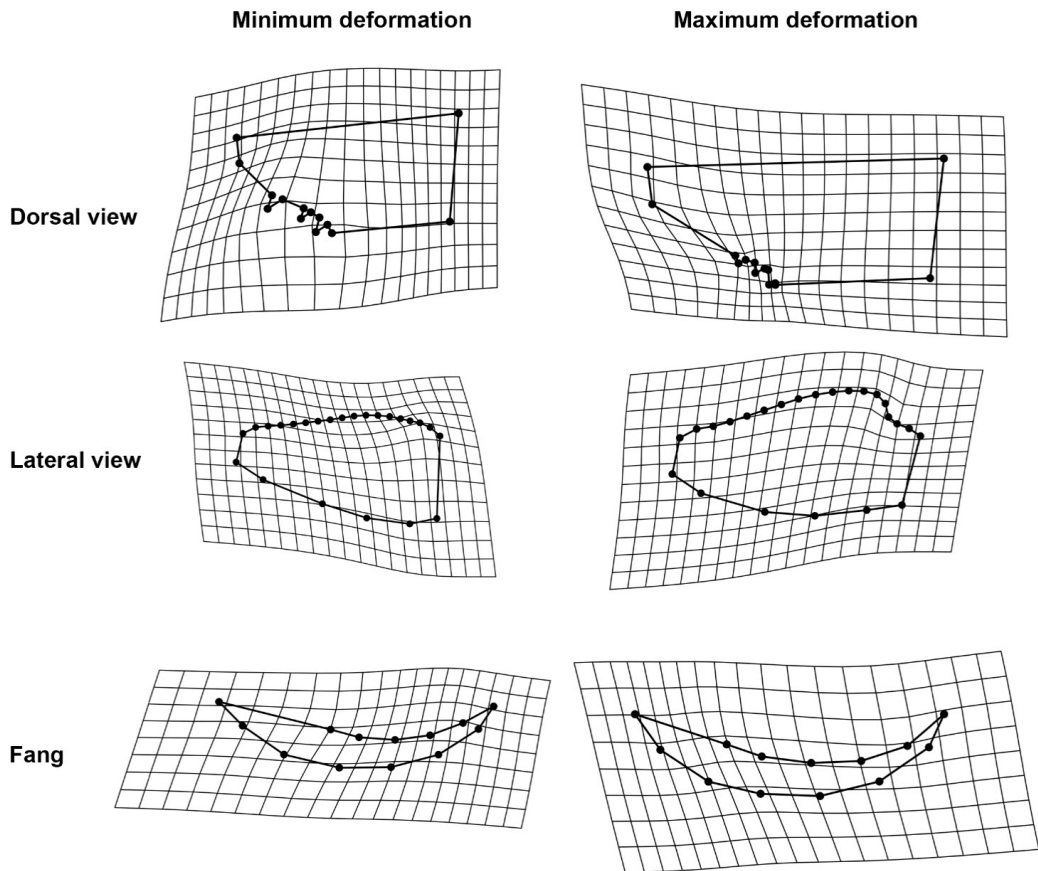


Figure S2 Shape corresponding to the maximum and minimum extremes of PC2 for each cheliceral view, represented using deformation grids. Shape patterns are exaggerated by 1.3x to enhance visualization.

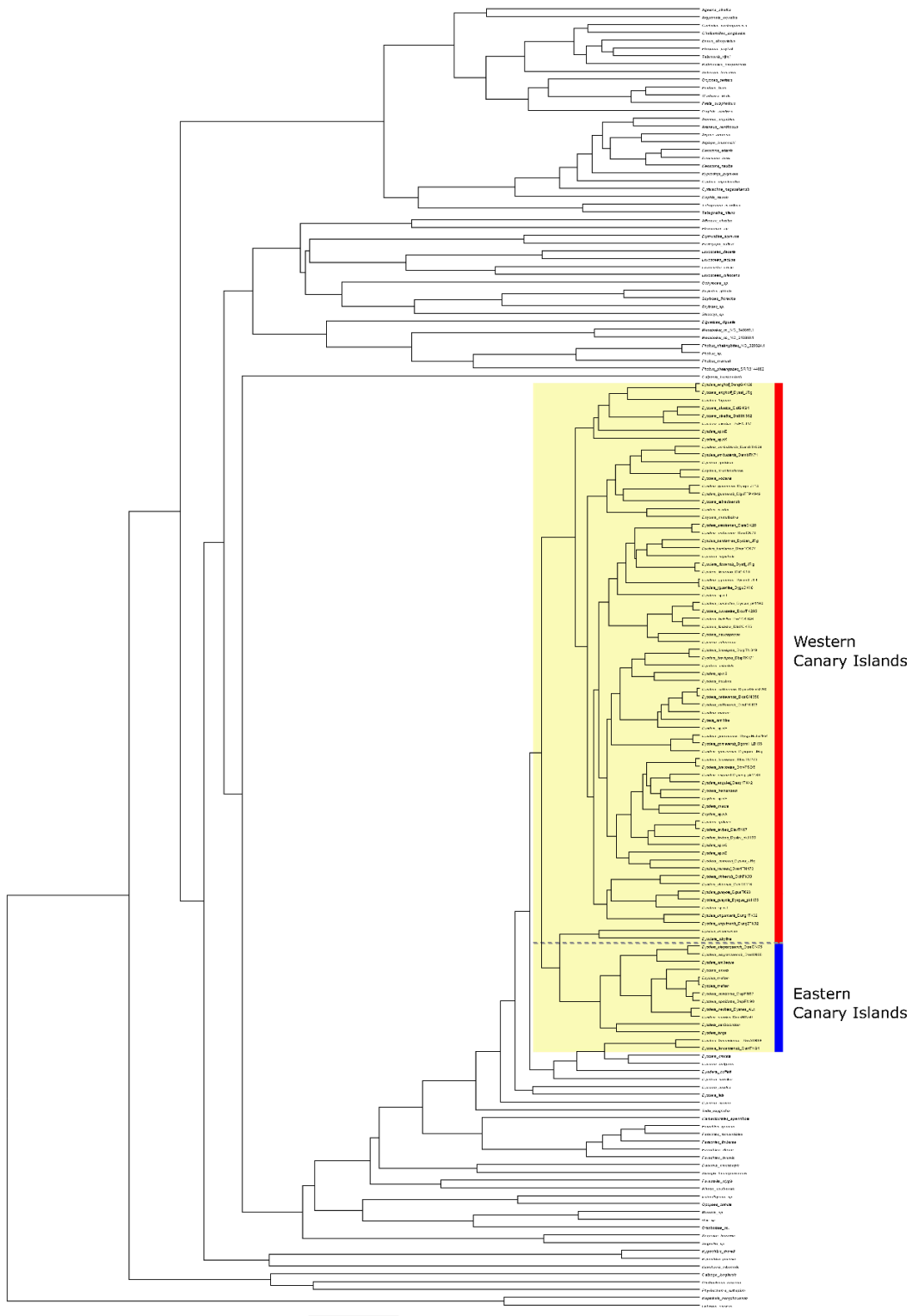


Figure S3 Time-stamped phylogeny including all described *Dysdera* species from the Canary Islands inferred from mitogenome data.

Table S3 PLS eigenvector composition.

Prey	Vector 1	Vector 2	Vector 3	Vector 4	Vector 5
Musca	0.46	-0.75	-0.45	0.14	0.00
Porcellio	0.38	0.14	0.35	0.63	0.56
Armadillidium	0.79	0.37	0.05	-0.48	-0.12
Pardosa	0.02	-0.52	0.80	-0.28	-0.07
carabid	-0.14	-0.09	-0.16	-0.53	0.82

Table S4 Estimated total number of transitions from X to Y (upper matrix) and Y to X (lower matrix) for the constrained ER model.

X	A	B	C	D	E	F	G	H	I
Y									
A		4.02	0.81	1.32	0.30	1.18	3.38	0.76	0.29
B	0.00		0.46	0.00	0.08	0.08	0.47	0.11	0.84
C	0.00	0.35		0.00	0.05	0.05	0.10	0.08	0.06
D	0.16	0.12	0.05		0.74	0.06	0.11	0.09	0.04
E	0.00	0.12	0.03	0.00		0.05	0.09	0.07	0.03
F	0.00	0.12	0.03	0.00	0.05		0.16	0.07	0.03
G	0.00	0.45	0.06	0.00	0.07	0.84		0.10	0.06
H	0.00	0.12	0.03	0.00	0.04	0.05	0.10		0.03
I	0.00	0.16	0.04	0.00	0.04	0.05	0.10	0.08	

Table S5 Estimated total number of transitions from X to Y (upper matrix) and Y to X (lower matrix) for the ER model.

X	A	B	C	D	E	F	G	H	I
Y									
A		10.07	8.55	9.04	8.40	8.52	9.59	8.65	8.36
B	9.42		8.74	8.48	8.29	8.50	9.25	8.32	8.78
C	8.75	8.73		8.41	8.24	8.30	8.48	8.28	8.25
D	8.79	8.70	8.31		8.67	8.30	8.51	8.29	8.25
E	8.74	8.65	8.28	8.43		8.29	8.47	8.24	8.24
F	8.77	8.68	8.28	8.41	8.24		8.52	8.25	8.25
G	9.11	9.20	8.34	8.45	8.26	9.05		8.30	8.26
H	8.75	8.67	8.27	8.41	8.24	8.29	8.49		8.23
I	8.74	8.68	8.28	8.41	8.24	8.29	8.49	8.27	

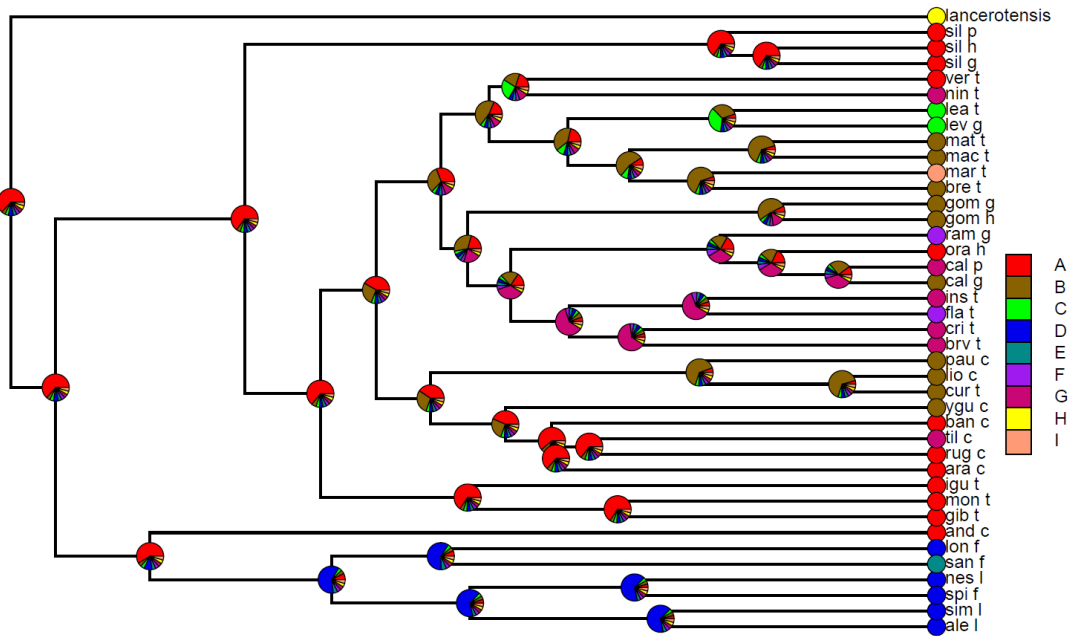


Figure S4 Ancestral state reconstruction with ER model.

Table S6 Estimated total number of transitions from X to Y (upper matrix) and Y to X (lower matrix) for the SYM model.

X	A	B	C	D	E	F	G	H	I
Y									
A		2.96	0.10	0.66	0.06	0.77	4.59	0.66	0.02
B	2.89		0.45	0.05	0.05	1.01	22.50	0.20	1.21
C	0.07	0.05		4.84	1.68	0.93	0.01	2.20	1.97
D	0.22	0.00	4.61		50.55	0.09	0.00	5.71	1.63
E	0.00	0.03	1.66	49.95		0.05	0.00	7.53	1.31
F	0.83	0.73	1.29	0.13	0.06		0.74	0.25	1.12
G	5.11	24.32	0.10	0.02	0.01	2.87		0.01	0.08
H	0.05	0.16	2.23	5.81	7.48	0.17	0.00		1.63
I	0.01	0.25	2.65	1.71	1.33	0.59	0.01	1.75	

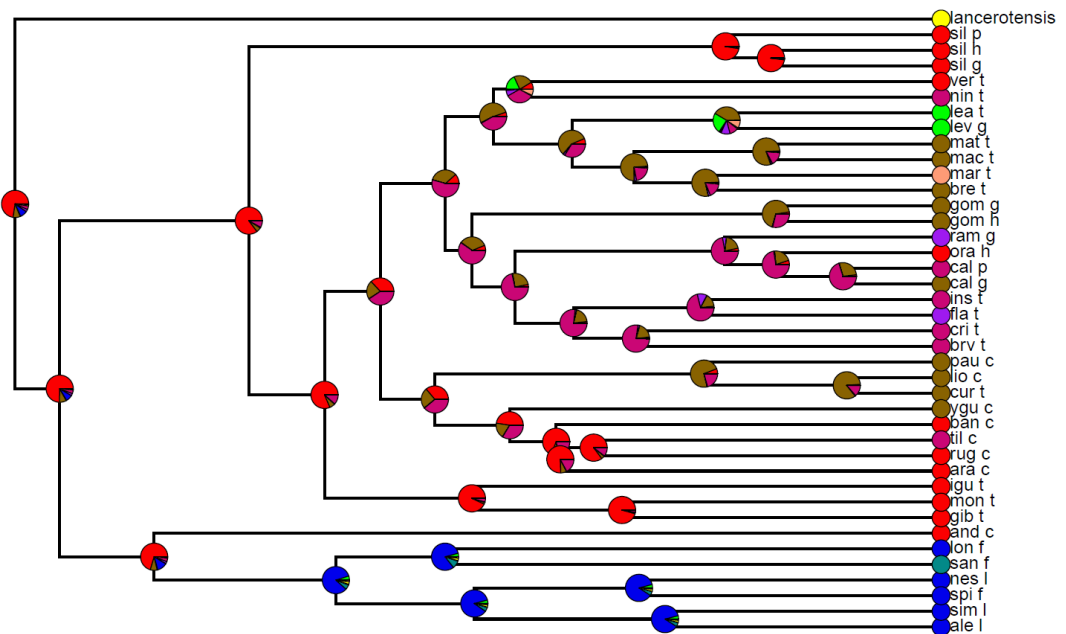


Figure S5 Ancestral state reconstruction with SYM model.

Table S7 Estimated total number of transitions from X to Y (upper matrix) and Y to X (lower matrix) for the ARD model.

X	A	B	C	D	E	F	G	H	I
Y									
A		0.06	0.64	4.61	0.99	0.33	0.60	2.33	0.01
B	0.61		2.33	0.79	0.45	2.51	37.54	0.77	2.56
C	2.72	3.02		1.44	1.45	4.37	3.77	2.08	2.77
D	4.16	1.74	1.46		2.32	1.34	1.32	1.20	0.53
E	1.65	1.30	1.37	1.65		1.15	1.24	1.43	0.76
F	1.83	3.42	4.96	1.22	1.63		4.60	1.97	2.92
G	1.12	30.69	6.21	2.20	1.36	8.55		1.91	3.61
H	2.25	1.88	1.93	1.35	1.47	1.45	1.80		0.95
I	1.38	2.76	2.49	0.66	0.93	2.39	2.48	1.19	

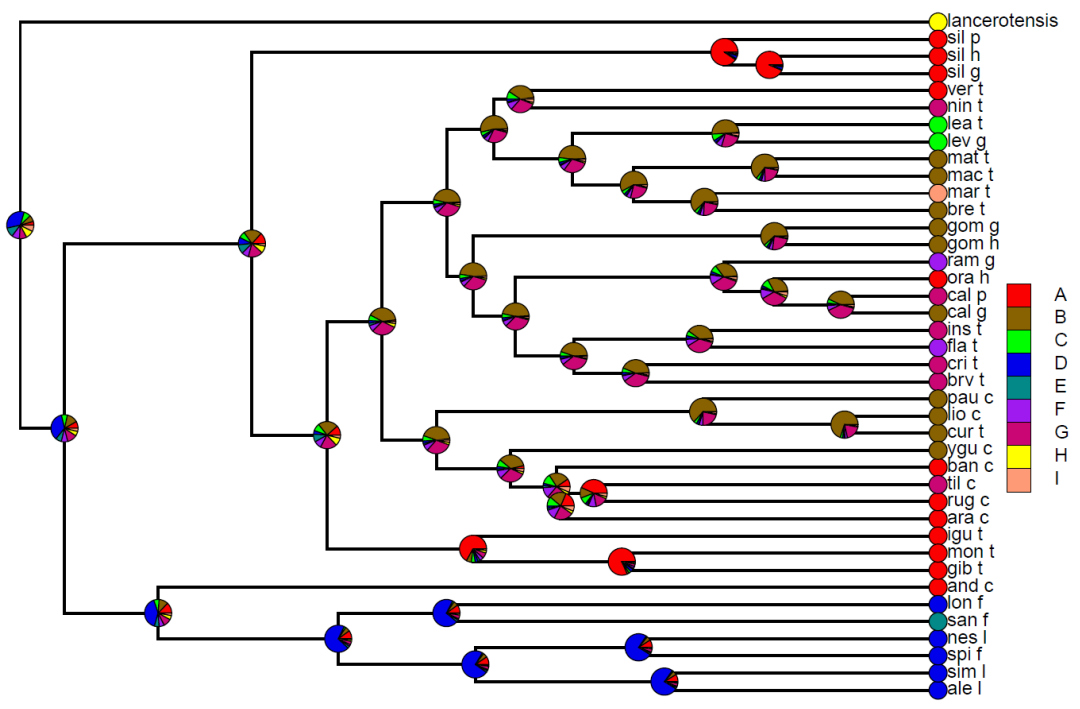


Figure S6 Ancestral state reconstruction with ARD model.

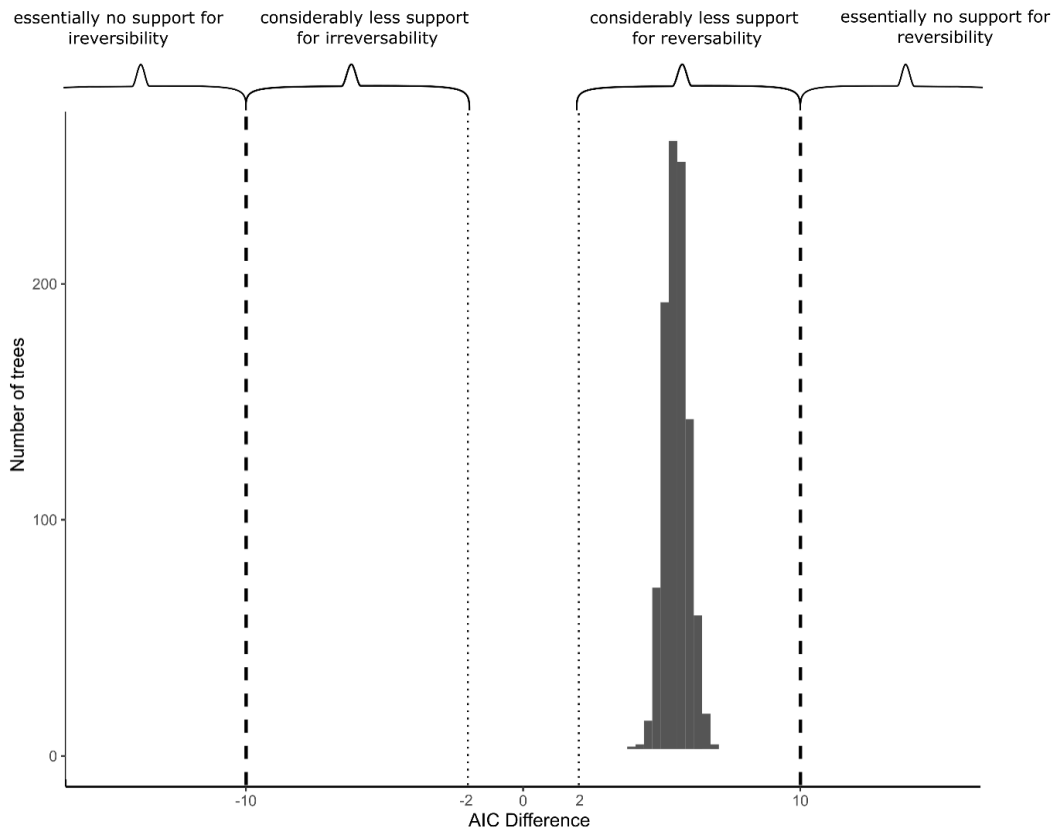


Figure S7 AIC-based tests of irreversibility as performed in Goldberg and Igić (2008). The histogram represents the difference between the AIC of the Mk2 unconstrained and constrained ($q_{SG} = 0$) models. AIC for the constrained model are given in absolute values, indicating better performances of the this model with higher AIC differences. Thresholds for the model preferences are given after Goldberg and Igić (2008) where; lower Δ AIC than 2 (dotted line), means no difference between models; Δ AIC above 10 (dashed line) means no support for the reversible model; values in between show low support for the reversibility model.

Additional references

- Bidegaray-Batista, L., & Arnedo, M. A. (2011). Gone with the plate: The opening of the Western Mediterranean basin drove the diversification of ground-dweller spiders. *BMC Evolutionary Biology*, 11. <https://doi.org/10.1186/1471-2148-11-317>
- Goldberg E.E. & Igić B. 2008. On phylogenetic tests of irreversible evolution. *Evolution* 62 (11): 2727–2741. <https://doi.org/10.1111/j.1558-5646.2008.00505.x>
- Magalhaes, I. L. F., Azevedo, G. H. F., Michalik, P., & Ramírez, M. J. (2020). The fossil record of spiders revisited: implications for calibrating trees and evidence for a major faunal turnover since the Mesozoic. *Biological Reviews*, 95, 184–217.
- Penney, D., & Ortuño, V. M. (2006). Oldest true orb-weaving spider (Araneae: Araneidae). *Biology Letters*, 2, 447–450.

APPENDIX 3.1

Supplementary material for the manuscript:

Diversification tempo and mode in the red devil spiders (Araneae:
Dysderidae) from the Canary Islands

Adrià Bellvert, Jairo Patiño, Laura Pollock, Antigoni Kaliontzopoulou & Miquel A. Arnedo.

This supplementary material includes the discriminant analysis results and 2 tables

Linear discriminant analysis

From the 14 species for which we had morphometric data, but previous studies had no information about the cheliceral group, the LDA analysis assigned 13 to an already preestablished morphotype (posterior probabilities are summarized in Table S1 of supplementary material). The only species that could not be clearly classified to any group was *D. madai*. However, this species is morphologically very similar to other species of group A, as showed by its closeness in the morphospace represented by the first two principal components (Fig 1C). It is true that the differences with this species could be explained by other components, however the first two components explain 60% of the explained variability, and the posterior probabilities of the LDA showed similar values between the cheliceral group A and the unknown group (Table S1). For this reason, and to avoid over-splitting the number of different cheliceral morphotypes present in the Canary Islands, we considered this species to belong to the cheliceral morphotype A.

Table S1. LDA posterior probabilities for each unknown species cheliceral morphology to be adscribed to one of the already known types.

Species	Group A	Group B	Group C	Group D	Group E	Group F	Group G	Group I	Unknown
<i>D. ambulotenta</i>	0.00530	0.14003	0.00093	0.05322	0.41971	0.00058	0.12063	0.00335	0.04007
<i>D. chioensis</i>	0.16418	0.00510	0.00149	0.46749	0.01348	0.14922	0.00001	0.00000	0.19902
<i>D. enghoffi</i>	0.67997	0.00601	0.01530	0.03493	0.00033	0.06281	0.00000	0.00000	0.20065
<i>D. esquivelli</i>	0.09166	0.37993	0.02091	0.03292	0.07623	0.00206	0.05285	0.00124	0.32368
<i>D. gaifa</i>	0.23104	0.00710	0.00264	0.35837	0.01032	0.13678	0.00001	0.00000	0.25373
<i>D. gollumi</i>	0.16034	0.21028	0.61287	0.00000	0.00000	0.00000	0.00442	0.00025	0.01183
<i>D. guayota</i>	0.15824	0.00096	0.00064	0.45649	0.00327	0.27779	0.00000	0.00000	0.10261
<i>D. hernandezi</i>	0.00351	0.39558	0.02222	0.00001	0.00084	0.00000	0.50454	0.04387	0.00669
<i>D. madai</i>	0.38648	0.07878	0.03254	0.03284	0.00557	0.01287	0.00063	0.00001	0.45021
<i>D. mahan</i>	0.17166	0.01128	0.00238	0.42327	0.02309	0.10354	0.00004	0.00000	0.26470
<i>D. minu: sima</i>	0.91765	0.00111	0.02607	0.00161	0.00000	0.02028	0.00000	0.00000	0.03328
<i>D. ratonensis</i>	0.18713	0.35679	0.05989	0.00796	0.01139	0.00130	0.02123	0.00050	0.35137
<i>D. sibyllina</i>	0.44086	0.01547	0.01081	0.10892	0.00361	0.06750	0.00002	0.00000	0.35279
<i>D. unguimanis</i>	0.00107	0.25398	0.00622	0.00001	0.00190	0.00000	0.62130	0.05477	0.00344

Table S2. Binari states cheliceral combinations that has shown significant differences between their diversification rates.

A	B	C	D	E	F	G	I	λ_0	λ_1	p-value
0	1	1	0	0	1	0	0	0.01467329	0.049045711	0.00241025
0	1	0	0	1	1	0	0	0.010343693	0.049264661	0.00040656
0	1	1	0	1	1	0	0	0.010757809	0.046667713	0.00097059
0	1	0	0	0	0	1	0	0.016900501	0.044228815	0.01433236
0	1	1	0	0	0	1	0	0.017557185	0.042202741	0.02465853
0	0	0	0	1	0	1	0	0.012911226	0.056440032	0.00959059
0	1	0	0	1	0	1	0	0.012090296	0.042890574	0.00604434
0	1	1	0	1	0	1	0	0.011975284	0.041307962	0.01647841
0	1	0	0	0	1	1	0	0.018388807	0.042573488	0.01561464
0	1	0	0	1	1	1	0	0.013170213	0.04161216	0.01420913
0	0	1	0	0	0	0	1	0.016663142	0.068813008	0.00121277
0	1	0	0	0	1	0	1	0.013749689	0.05151426	0.00101071
0	0	1	0	0	1	0	1	0.014562464	0.06327448	0.0001861
0	1	1	0	0	1	0	1	0.01490424	0.048240716	0.00312824
0	0	0	0	0	0	1	1	0.014624123	0.054290233	0.00070946
0	1	0	0	0	0	1	1	0.017611685	0.043394353	0.02108051
0	0	1	0	0	0	1	1	0.015393235	0.050277293	0.001908
0	1	1	0	0	0	1	1	0.018166296	0.04154504	0.0322087
0	0	0	0	1	0	1	1	0.013261068	0.053205225	0.00502887
0	1	0	0	1	0	1	1	0.012606966	0.042255608	0.00883915
0	0	1	0	1	0	1	1	0.013490323	0.048113714	0.00500981
0	1	1	0	1	0	1	1	0.012471481	0.040800695	0.03907778
0	1	0	0	0	1	1	1	0.01904088	0.041851796	0.03364306
0	0	1	0	0	1	1	1	0.016528723	0.048041055	0.00492337
0	1	0	0	1	1	1	1	0.013699994	0.041096663	0.03531138

APPENDIX 3.2

Supplementary material for the manuscript:

How the turttables? Species traits modulate ecological release in red devil spiders (Araneae:Dysderidae)?

Adrià Bellvert, Alba Enguídanos, Antigoni Kaliontzopoulou, Jairo Patiño, Laura Pollock & Miquel A. Arnedo.

This supplementary material includes 1 figure and 5 tables.

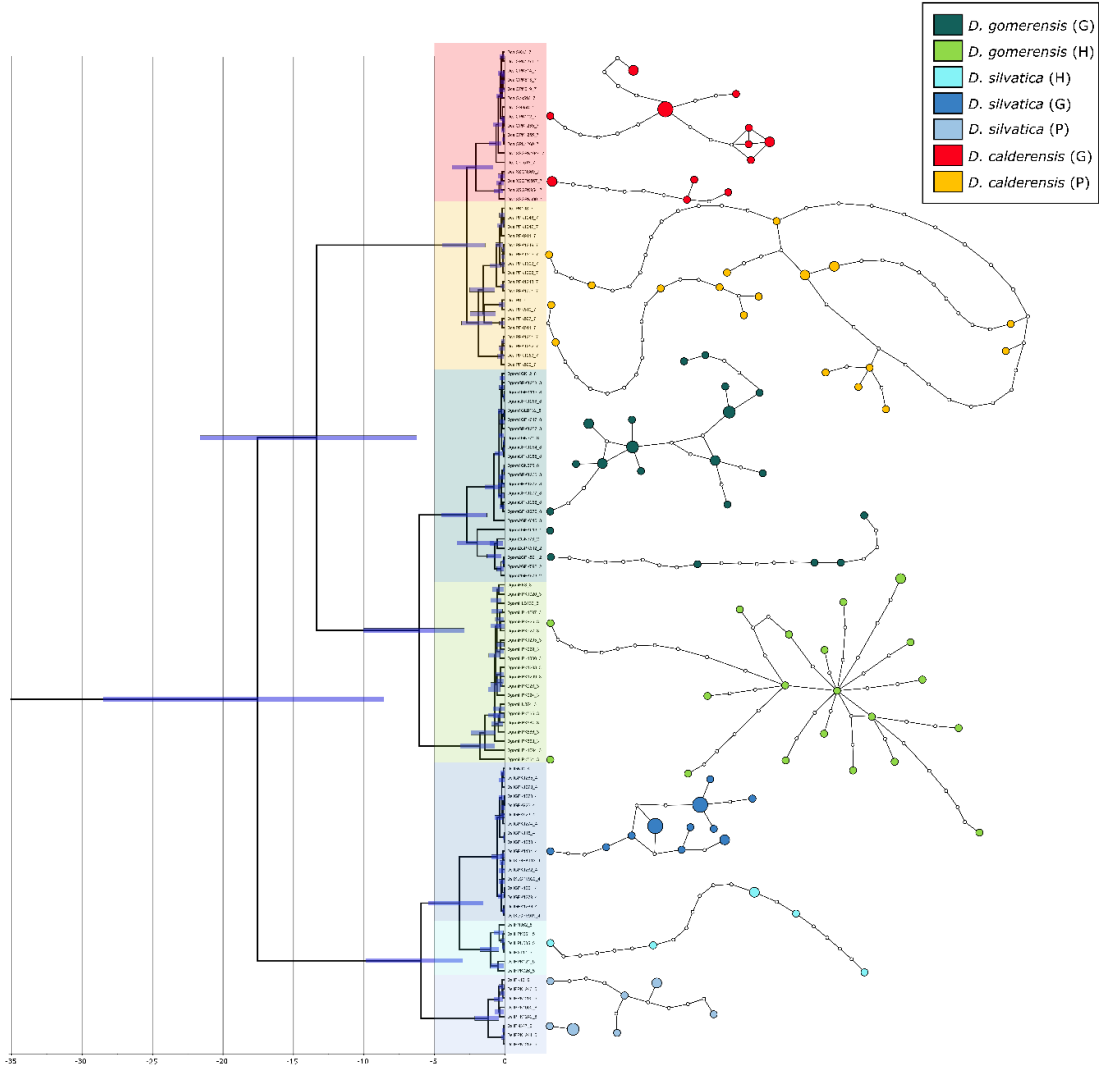


Figure S1. Bayesian multi-coalescent maximum clade credibility DNA barcode gene tree. Terminals coloured according to species and island populations (see box legend). Bars on nodes denote 95% HPD confidence intervals. Associated independent statistical parsimony networks drawn on the right side correspond to haplotype clades.

Table S1. Specimens used for the refraction and extrapolation curves

Genus	SpeciesName	Collection code	Locality Name	Island	Country	Latitude	Longitude
Dysdera	silvatica	CRBA001456	Pto de la Cruz	La Palma	Canary Islands	28.756058	-17.855244
Dysdera	silvatica	CRBA002281	El Castillo	La Palma	Canary Islands	28.79636	-17.971169
Dysdera	silvatica	CRBA002306	Roque Faro	La Palma	Canary Islands	28.798556	-17.879149
Dysdera	silvatica	CRBA002322	Roque Faro	La Palma	Canary Islands	28.798556	-17.879149
Dysdera	silvatica	CRBA002327	Roque Faro	La Palma	Canary Islands	28.798556	-17.879149
Dysdera	silvatica	CRBA002346	Roque de Los Muchachos (PNCT)	La Palma	Canary Islands	28.76088	-17.885206
Dysdera	silvatica	CRBA002347	Barranco las Traves (PNCT)	La Palma	Canary Islands	28.717984	-17.893314
Dysdera	silvatica	CRBA002348	Roque de Los Muchachos (PNCT)	La Palma	Canary Islands	28.76088	-17.885206
Dysdera	silvatica	CRBA002349	Roque de Los Muchachos (PNCT)	La Palma	Canary Islands	28.76088	-17.885206
Dysdera	silvatica	CRBA002350	Roque de Los Muchachos (PNCT)	La Palma	Canary Islands	28.76088	-17.885206
Dysdera	silvatica	CRBA002351	Tenera (Parte alta) (PNCT)	La Palma	Canary Islands	28.719605	-17.899636
Dysdera	silvatica	CRBA002352	Roque de Los Muchachos (PNCT)	La Palma	Canary Islands	28.76088	-17.885206
Dysdera	silvatica	CRBA002353	Roque de Los Muchachos (PNCT)	La Palma	Canary Islands	28.76088	-17.885206
Dysdera	silvatica	CRBA002354	Roque de Los Muchachos (PNCT)	La Palma	Canary Islands	28.76088	-17.885206
Dysdera	silvatica	CRBA002355	Barranco las Traves (PNCT)	La Palma	Canary Islands	28.717984	-17.893314
Dysdera	silvatica	CRBA002358	Roque de Los Muchachos (PNCT)	La Palma	Canary Islands	28.76088	-17.885206
Dysdera	silvatica	CRBA002463	Roque Faro	La Palma	Canary Islands	28.798556	-17.879149
Dysdera	silvatica	CRBA003555	Pinar de Roque Faro	La Palma	Canary Islands	28.798556	-17.879149
Dysdera	silvatica	CRBA003556	Pinar de Roque Faro	La Palma	Canary Islands	28.798556	-17.879149
Dysdera	silvatica	CRBA003557	Pinar de Roque Faro	La Palma	Canary Islands	28.798556	-17.879149
Dysdera	silvatica	CRBA003558	Pinar de Roque Faro	La Palma	Canary Islands	28.798556	-17.879149
Dysdera	silvatica	CRBA003559	Pinar de Roque Faro	La Palma	Canary Islands	28.798556	-17.879149
Dysdera	silvatica	CRBA003560	Pinar de Roque Faro	La Palma	Canary Islands	28.798556	-17.879149
Dysdera	silvatica	CRBA003561	Pinar de Roque Faro	La Palma	Canary Islands	28.798556	-17.879149
Dysdera	silvatica	CRBA003562	Pinar de Roque Faro	La Palma	Canary Islands	28.798556	-17.879149
Dysdera	silvatica	CRBA003579	Pinar de Roque Faro	La Palma	Canary Islands	28.798556	-17.879149
Dysdera	silvatica	CRBA003580	Pinar de Roque Faro	La Palma	Canary Islands	28.798556	-17.879149
Dysdera	silvatica	CRBA003581	Pinar de Roque Faro	La Palma	Canary Islands	28.798556	-17.879149
Dysdera	silvatica	CRBA003582	Pinar de Roque Faro	La Palma	Canary Islands	28.798556	-17.879149
Dysdera	silvatica	CRBA003583	Pinar de Roque Faro	La Palma	Canary Islands	28.798556	-17.879149

<i>Dysdera</i>	<i>silvatica</i>	CRBA003589	El Castillo	La Palma	Canary Islands	28.79636	-17.971169
<i>Dysdera</i>	<i>silvatica</i>	CRBA003591	SE El Castillo (small lava tube)	La Palma	Canary Islands	28.790783	-17.948843
<i>Dysdera</i>	<i>silvatica</i>	CRBA003592	SE El Castillo (small lava tube)	La Palma	Canary Islands	28.790783	-17.948843
<i>Dysdera</i>	<i>silvatica</i>	NMH000226	Juan Adalid	La Palma	Canary Islands	28.843639	-17.90635
<i>Dysdera</i>	<i>silvatica</i>	NMH001395	Pinar de Roque Faro	La Palma	Canary Islands	28.798556	-17.879149
<i>Dysdera</i>	<i>silvatica</i>	NMH001396	Pinar de Roque Faro	La Palma	Canary Islands	28.798556	-17.879149
<i>Dysdera</i>	<i>silvatica</i>	NMH001397	Pinar de Roque Faro	La Palma	Canary Islands	28.798556	-17.879149
<i>Dysdera</i>	<i>silvatica</i>	NMH001398	Pinar de Roque Faro	La Palma	Canary Islands	28.798556	-17.879149
<i>Dysdera</i>	<i>silvatica</i>	NMH001399	Pinar de Roque Faro	La Palma	Canary Islands	28.798556	-17.879149
<i>Dysdera</i>	<i>silvatica</i>	NMH001400	Pinar de Roque Faro	La Palma	Canary Islands	28.798556	-17.879149
<i>Dysdera</i>	<i>silvatica</i>	NMH002925	Cueva de Los Palmeros	La Palma	Canary Islands	28.507538	-17.856808
<i>Dysdera</i>	<i>silvatica</i>	UB2648_109	Roque de Los Muchachos (PNCT)	La Palma	Canary Islands	28.76088	-17.885206
<i>Dysdera</i>	<i>silvatica</i>	UB2759	Juan Adalid	La Palma	Canary Islands	28.843639	-17.90635
<i>Dysdera</i>	<i>silvatica</i>	UB2799_115	Juan Adalid	La Palma	Canary Islands	28.843639	-17.90635
<i>Dysdera</i>	<i>silvatica</i>	UB2815	Juan Adalid	La Palma	Canary Islands	28.843639	-17.90635
<i>Dysdera</i>	<i>silvatica</i>	UB2947	Pista de Machín	La Palma	Canary Islands	28.78971	-17.896884
<i>Dysdera</i>	<i>silvatica</i>	UB2960	Pista de Machín	La Palma	Canary Islands	28.78971	-17.896884
<i>Dysdera</i>	<i>silvatica</i>	UB4177_Freezezer	Pista de Machín	La Palma	Canary Islands	28.78971	-17.896884
<i>Dysdera</i>	<i>silvatica</i>	CRBA001336	Fuente Mencáffite	El Hierro	Canary Islands	27.735497	-18.085804
<i>Dysdera</i>	<i>silvatica</i>	CRBA001341	Hoya del Pino	El Hierro	Canary Islands	27.737154	-18.046305
<i>Dysdera</i>	<i>silvatica</i>	CRBA002059	Pista del Mercader	El Hierro	Canary Islands	27.712944	-18.022175
<i>Dysdera</i>	<i>silvatica</i>	CRBA002060	Cueva de Longueras	El Hierro	Canary Islands	27.74673	-18.026256
<i>Dysdera</i>	<i>silvatica</i>	CRBA002061	Mirador de Bascos	El Hierro	Canary Islands	27.754861	-18.118218
<i>Dysdera</i>	<i>silvatica</i>	CRBA002842	Mirador de Bascos	El Hierro	Canary Islands	27.754861	-18.118218
<i>Dysdera</i>	<i>silvatica</i>	CRBA002843	Mirador de Bascos	El Hierro	Canary Islands	27.754861	-18.118218
<i>Dysdera</i>	<i>silvatica</i>	CRBA002844	Mirador de Bascos	El Hierro	Canary Islands	27.754861	-18.118218
<i>Dysdera</i>	<i>silvatica</i>	CRBA002845	Mirador de Bascos	El Hierro	Canary Islands	27.754861	-18.118218
<i>Dysdera</i>	<i>silvatica</i>	CRBA002858	Mirador de Bascos	El Hierro	Canary Islands	27.754861	-18.118218
<i>Dysdera</i>	<i>silvatica</i>	CRBA002859	Mirador de Bascos	El Hierro	Canary Islands	27.754861	-18.118218
<i>Dysdera</i>	<i>silvatica</i>	CRBA002860	Mirador de Bascos	El Hierro	Canary Islands	27.754861	-18.118218
<i>Dysdera</i>	<i>silvatica</i>	CRBA002861	Mirador de Bascos	El Hierro	Canary Islands	27.754861	-18.118218
<i>Dysdera</i>	<i>silvatica</i>	CRBA002862	Mirador de Bascos	El Hierro	Canary Islands	27.754861	-18.118218
<i>Dysdera</i>	<i>silvatica</i>	CRBA002863	Mirador de Bascos	El Hierro	Canary Islands	27.754861	-18.118218
<i>Dysdera</i>	<i>silvatica</i>	CRBA002864	Mirador de Bascos	El Hierro	Canary Islands	27.754861	-18.118218

<i>Dysdera</i>	<i>silvatica</i>	CRBA002865	Mirador de Bascos	El Hierro	Canary Islands	27.754861	-18.118218
<i>Dysdera</i>	<i>silvatica</i>	CRBA002866	Mirador de Bascos	El Hierro	Canary Islands	27.754861	-18.118218
<i>Dysdera</i>	<i>silvatica</i>	CRBA002867	Mirador de Bascos	El Hierro	Canary Islands	27.754861	-18.118218
<i>Dysdera</i>	<i>silvatica</i>	CRBA002868	Mirador de Bascos	El Hierro	Canary Islands	27.754861	-18.118218
<i>Dysdera</i>	<i>silvatica</i>	CRBA002869	Mirador de Bascos	El Hierro	Canary Islands	27.754861	-18.118218
<i>Dysdera</i>	<i>silvatica</i>	CRBA002870	Mirador de Bascos	El Hierro	Canary Islands	27.754861	-18.118218
<i>Dysdera</i>	<i>silvatica</i>	CRBA002871	Mirador de Bascos	El Hierro	Canary Islands	27.754861	-18.118218
<i>Dysdera</i>	<i>silvatica</i>	CRBA002872	Mirador de Bascos	El Hierro	Canary Islands	27.754861	-18.118218
<i>Dysdera</i>	<i>silvatica</i>	CRBA002873	Mirador de Bascos	El Hierro	Canary Islands	27.754861	-18.118218
<i>Dysdera</i>	<i>silvatica</i>	CRBA002874	Mirador de Bascos	El Hierro	Canary Islands	27.754861	-18.118218
<i>Dysdera</i>	<i>silvatica</i>	CRBA002875	Mirador de Bascos	El Hierro	Canary Islands	27.754861	-18.118218
<i>Dysdera</i>	<i>silvatica</i>	CRBA002876	Mirador de Bascos	El Hierro	Canary Islands	27.754861	-18.118218
<i>Dysdera</i>	<i>silvatica</i>	CRBA002877	Mirador de Bascos	El Hierro	Canary Islands	27.754861	-18.118218
<i>Dysdera</i>	<i>silvatica</i>	CRBA002878	Mirador de Bascos	El Hierro	Canary Islands	27.754861	-18.118218
<i>Dysdera</i>	<i>silvatica</i>	CRBA002879	Mirador de Bascos	El Hierro	Canary Islands	27.754861	-18.118218
<i>Dysdera</i>	<i>silvatica</i>	CRBA002880	Mirador de Bascos	El Hierro	Canary Islands	27.754861	-18.118218
<i>Dysdera</i>	<i>silvatica</i>	CRBA002881	Mirador de Bascos	El Hierro	Canary Islands	27.754861	-18.118218
<i>Dysdera</i>	<i>silvatica</i>	CRBA002882	Mirador de Bascos	El Hierro	Canary Islands	27.754861	-18.118218
<i>Dysdera</i>	<i>silvatica</i>	CRBA002932	Ventejís. Tifón	El Hierro	Canary Islands	27.785991	-17.937508
<i>Dysdera</i>	<i>silvatica</i>	nhm000289	Cueva de Longueras	El Hierro	Canary Islands	27.74673	-18.026256
<i>Dysdera</i>	<i>silvatica</i>	NMH000011	Fuente Mencáñite	El Hierro	Canary Islands	27.735497	-18.085804
<i>Dysdera</i>	<i>silvatica</i>	NMH000030	Hoya del Pino	El Hierro	Canary Islands	27.737154	-18.046305
<i>Dysdera</i>	<i>silvatica</i>	NMH001439	Mirador de Bascos	El Hierro	Canary Islands	27.754861	-18.118218
<i>Dysdera</i>	<i>silvatica</i>	NMH002524	Mirador de Bascos	El Hierro	Canary Islands	27.754861	-18.118218
<i>Dysdera</i>	<i>silvatica</i>	NMH002525	Mirador de Bascos	El Hierro	Canary Islands	27.754861	-18.118218
<i>Dysdera</i>	<i>silvatica</i>	NMH002526	Mirador de Bascos	El Hierro	Canary Islands	27.754861	-18.118218
<i>Dysdera</i>	<i>silvatica</i>	NMH002527	Mirador de Bascos	El Hierro	Canary Islands	27.754861	-18.118218
<i>Dysdera</i>	<i>silvatica</i>	NMH002528	Mirador de Bascos	El Hierro	Canary Islands	27.754861	-18.118218
<i>Dysdera</i>	<i>silvatica</i>	NMH002722	Pista del Mercader	El Hierro	Canary Islands	27.712944	-18.022175
<i>Dysdera</i>	<i>silvatica</i>	NMH002724	Pista del Derrabado	El Hierro	Canary Islands	27.740804	-18.05308
<i>Dysdera</i>	<i>silvatica</i>	NMH003204	Pista del Derrabado	El Hierro	Canary Islands	27.740804	-18.05308
<i>Dysdera</i>	<i>silvatica</i>	NMH003210	Cueva de Jinama	El Hierro	Canary Islands	27.773536	-17.984089
<i>Dysdera</i>	<i>silvatica</i>	NMH003211	Cueva de Jinama	El Hierro	Canary Islands	27.773536	-17.984089
<i>Dysdera</i>	<i>silvatica</i>	NMH003212	Cueva de Longueras	El Hierro	Canary Islands	27.74673	-18.026256

<i>Dysdera</i>	<i>silvatica</i>	NMH003213	Cueva de Longueras	El Hierro	Canary Islands	27.74673	-18.026256
<i>Dysdera</i>	<i>silvatica</i>	NMH003234	Cueva de Longueras	El Hierro	Canary Islands	27.74673	-18.026256
<i>Dysdera</i>	<i>silvatica</i>	U1L3842	Cueva de Longueras	El Hierro	Canary Islands	27.74673	-18.026256
<i>Dysdera</i>	<i>silvatica</i>	U1L3917	Cueva de Longueras	El Hierro	Canary Islands	27.74673	-18.026256
<i>Dysdera</i>	<i>silvatica</i>	U1L4280	Cueva de Longueras	El Hierro	Canary Islands	27.74673	-18.026256
<i>Dysdera</i>	<i>silvatica</i>	CRBA001842	Teselinde. Ermita de Santa Clara	La Gomera	Canary Islands	28.1963	-17.28754
<i>Dysdera</i>	<i>silvatica</i>	CRBA002761	Teselinde. Ermita de Santa Clara	La Gomera	Canary Islands	28.1963	-17.28754
<i>Dysdera</i>	<i>silvatica</i>	CRBA002762	Teselinde. Ermita de Santa Clara	La Gomera	Canary Islands	28.1963	-17.28754
<i>Dysdera</i>	<i>silvatica</i>	CRBA002768	Teselinde. Ermita de Santa Clara	La Gomera	Canary Islands	28.1963	-17.28754
<i>Dysdera</i>	<i>silvatica</i>	2 Pajarito		La Gomera	Canary Islands	28.108856	-17.241604
<i>Dysdera</i>	<i>silvatica</i>	CRBA001092	Barranco de Matasnos, Campamento Viejo, Monte del Cedro	La Gomera	Canary Islands	28.119131	-17.215838
<i>Dysdera</i>	<i>silvatica</i>	CRBA001451	Teselinde. Ermita de Santa Clara	La Gomera	Canary Islands	28.1963	-17.28754
<i>Dysdera</i>	<i>silvatica</i>	CRBA001845	El Cedro, humid laurel forest	La Gomera	Canary Islands	28.125809	-17.216616
<i>Dysdera</i>	<i>silvatica</i>	CRBA001869	Barranco de Pajón	La Gomera	Canary Islands	28.08845	-17.20142
<i>Dysdera</i>	<i>silvatica</i>	CRBA002362	Las Creces	La Gomera	Canary Island	28.138737	-17.287852
<i>Dysdera</i>	<i>silvatica</i>	CRBA002364	Las Tajoras	La Gomera	Canary Island	28.112834	-17.262608
<i>Dysdera</i>	<i>silvatica</i>	CRBA002720	Bosque del Cedro	La Gomera	Canary Islands	28.137044	-17.222569
<i>Dysdera</i>	<i>silvatica</i>	CRBA002721	Bosque del Cedro	La Gomera	Canary Islands	28.137044	-17.222569
<i>Dysdera</i>	<i>silvatica</i>	CRBA002722	Bosque del Cedro	La Gomera	Canary Islands	28.137044	-17.222569
<i>Dysdera</i>	<i>silvatica</i>	CRBA002737	Teselinde. Ermita de Santa Clara	La Gomera	Canary Islands	28.1963	-17.28754
<i>Dysdera</i>	<i>silvatica</i>	CRBA002740	Teselinde. Ermita de Santa Clara	La Gomera	Canary Islands	28.1963	-17.28754
<i>Dysdera</i>	<i>silvatica</i>	CRBA002745	Teselinde. Ermita de Santa Clara	La Gomera	Canary Islands	28.1963	-17.28754
<i>Dysdera</i>	<i>silvatica</i>	CRBA002749	Teselinde. Ermita de Santa Clara	La Gomera	Canary Islands	28.1963	-17.28754
<i>Dysdera</i>	<i>silvatica</i>	CRBA002750	Teselinde. Ermita de Santa Clara	La Gomera	Canary Islands	28.1963	-17.28754
<i>Dysdera</i>	<i>silvatica</i>	CRBA002754	Teselinde. Ermita de Santa Clara	La Gomera	Canary Islands	28.1963	-17.28754
<i>Dysdera</i>	<i>silvatica</i>	CRBA002755	Teselinde. Ermita de Santa Clara	La Gomera	Canary Islands	28.1963	-17.28754
<i>Dysdera</i>	<i>silvatica</i>	CRBA002756	Teselinde. Ermita de Santa Clara	La Gomera	Canary Islands	28.1963	-17.28754
<i>Dysdera</i>	<i>silvatica</i>	CRBA002760	Teselinde. Ermita de Santa Clara	La Gomera	Canary Islands	28.1963	-17.28754
<i>Dysdera</i>	<i>silvatica</i>	CRBA002763	Teselinde. Ermita de Santa Clara	La Gomera	Canary Islands	28.1963	-17.28754
<i>Dysdera</i>	<i>silvatica</i>	CRBA002764	Teselinde. Ermita de Santa Clara	La Gomera	Canary Islands	28.1963	-17.28754
<i>Dysdera</i>	<i>silvatica</i>	CRBA002767	Teselinde. Ermita de Santa Clara	La Gomera	Canary Islands	28.1963	-17.28754
<i>Dysdera</i>	<i>silvatica</i>	CRBA002770	Teselinde. Ermita de Santa Clara	La Gomera	Canary Islands	28.1963	-17.28754
<i>Dysdera</i>	<i>silvatica</i>	CRBA002772	Teselinde. Ermita de Santa Clara	La Gomera	Canary Islands	28.1963	-17.28754
<i>Dysdera</i>	<i>silvatica</i>	CRBA002773	Teselinde. Ermita de Santa Clara	La Gomera	Canary Islands	28.1963	-17.28754

Dysdera	silvatica	CRBA002775	Teselinde. Ermita de Santa Clara	La Gomera	Canary Islands	28.1963	-17.28754
Dysdera	silvatica	CRBA002776	Teselinde. Ermita de Santa Clara	La Gomera	Canary Islands	28.1963	-17.28754
Dysdera	silvatica	CRBA002778	Teselinde. Ermita de Santa Clara	La Gomera	Canary Islands	28.1963	-17.28754
Dysdera	silvatica	CRBA002781	Teselinde. Ermita de Santa Clara	La Gomera	Canary Islands	28.1963	-17.28754
Dysdera	silvatica	CRBA002796	Pajarito	La Gomera	Canary Islands	28.108856	-17.241604
Dysdera	silvatica	CRBA002797	Pajarito	La Gomera	Canary Islands	28.108856	-17.241604
Dysdera	silvatica	CRBA002800	Barranco de Juel, East	La Gomera	Canary Islands	28.14832	-17.15772
Dysdera	silvatica	CRBA002801	Barranco de Juel, East	La Gomera	Canary Islands	28.14832	-17.15772
Dysdera	silvatica	CRBA002802	Barranco de Juel, East	La Gomera	Canary Islands	28.14832	-17.15772
Dysdera	silvatica	CRBA002803	Barranco de Juel, East	La Gomera	Canary Islands	28.14832	-17.15772
Dysdera	silvatica	CRBA002804	Barranco de Juel, East	La Gomera	Canary Islands	28.14832	-17.15772
Dysdera	silvatica	CRBA002809	Barranco de Juel, East	La Gomera	Canary Islands	28.14832	-17.15772
Dysdera	silvatica	CRBA002810	Barranco de Juel, East	La Gomera	Canary Islands	28.14832	-17.15772
Dysdera	silvatica	CRBA002813	Barranco de Juel, East	La Gomera	Canary Islands	28.14832	-17.15772
Dysdera	silvatica	CRBA002816	Barranco de Juel, East	La Gomera	Canary Islands	28.14832	-17.15772
Dysdera	silvatica	CRBA002817	Barranco de Juel, East	La Gomera	Canary Islands	28.14832	-17.15772
Dysdera	silvatica	CRBA002821	Barranco de Juel, East	La Gomera	Canary Islands	28.14832	-17.15772
Dysdera	silvatica	CRBA002822	Barranco de Juel, East	La Gomera	Canary Islands	28.14832	-17.15772
Dysdera	silvatica	CRBA002823	Barranco de Juel, East	La Gomera	Canary Islands	28.14832	-17.15772
Dysdera	silvatica	CRBA002824	Barranco de Juel, East	La Gomera	Canary Islands	28.14832	-17.15772
Dysdera	silvatica	CRBA002825	Barranco de Juel, East	La Gomera	Canary Islands	28.14832	-17.15772
Dysdera	silvatica	CRBA002828	Barranco de Juel, East	La Gomera	Canary Islands	28.14832	-17.15772
Dysdera	silvatica	CRBA002829	Barranco de Juel, East	La Gomera	Canary Islands	28.14832	-17.15772
Dysdera	silvatica	CRBA002830	Barranco de Juel, East	La Gomera	Canary Islands	28.14832	-17.15772
Dysdera	silvatica	CRBA002831	Barranco de Juel, East	La Gomera	Canary Islands	28.14832	-17.15772
Dysdera	silvatica	CRBA002833	Barranco de Juel, East	La Gomera	Canary Islands	28.14832	-17.15772
Dysdera	silvatica	CRBA002834	Barranco de Juel, East	La Gomera	Canary Islands	28.14832	-17.15772
Dysdera	silvatica	CRBA002835	Barranco de Juel, East	La Gomera	Canary Islands	28.14832	-17.15772
Dysdera	silvatica	CRBA003622	Pista Mora Gaspar	La Gomera		28.142375	-17.250954
Dysdera	silvatica	CRBA003631	Teselinde. Ermita de Santa Clara	La Gomera	Canary Islands	28.1963	-17.28754
Dysdera	silvatica	CRBA003634	Teselinde. Ermita de Santa Clara	La Gomera	Canary Islands	28.1963	-17.28754
Dysdera	silvatica	CRBA003635	Teselinde. Ermita de Santa Clara	La Gomera	Canary Islands	28.1963	-17.28754
Dysdera	silvatica	CRBA003643	Teselinde. Ermita de Santa Clara	La Gomera	Canary Islands	28.1963	-17.28754
Dysdera	silvatica	CRBA003649	Teselinde. Ermita de Santa Clara	La Gomera	Canary Islands	28.1963	-17.28754

<i>Dysdera</i>	<i>silvatica</i>	NMH002487	Teselinde. Ermita de Santa Clara	La Gomera	Canary Islands	28.1963	-17.28754
<i>Dysdera</i>	<i>silvatica</i>	NMH002595	Las Creces	La Gomera	Canary Islands	28.138737	-17.287852
<i>Dysdera</i>	<i>silvatica</i>	NMH002596	Las Creces	La Gomera	Canary Islands	28.138737	-17.287852
<i>Dysdera</i>	<i>silvatica</i>	NMH002597	Las Tajoras	La Gomera	Canary Islands	28.112736	-17.262511
<i>Dysdera</i>	<i>silvatica</i>	NMH002598	Las Tajoras	La Gomera	Canary Islands	28.112736	-17.262511
<i>Dysdera</i>	<i>silvatica</i>	NMH002599	Las Tajoras	La Gomera	Canary Islands	28.112736	-17.262511
<i>Dysdera</i>	<i>silvatica</i>	NMH002600	Las Tajoras	La Gomera	Canary Islands	28.112736	-17.262511
<i>Dysdera</i>	<i>silvatica</i>	NMH002601	Las Tajoras	La Gomera	Canary Islands	28.112736	-17.262511
<i>Dysdera</i>	<i>silvatica</i>	NMH002605	Las Tajoras	La Gomera	Canary Islands	28.112736	-17.262511
<i>Dysdera</i>	<i>silvatica</i>	NMH002608	Teselinde. Ermita de Santa Clara	La Gomera	Canary Islands	28.1963	-17.28754
<i>Dysdera</i>	<i>silvatica</i>	NMH002609	Teselinde. Ermita de Santa Clara	La Gomera	Canary Islands	28.1963	-17.28754
<i>Dysdera</i>	<i>silvatica</i>	NMH002610	Teselinde. Ermita de Santa Clara	La Gomera	Canary Islands	28.1963	-17.28754
<i>Dysdera</i>	<i>silvatica</i>	NMH002611	Teselinde. Ermita de Santa Clara	La Gomera	Canary Islands	28.1963	-17.28754
<i>Dysdera</i>	<i>silvatica</i>	NMH002612	Teselinde. Ermita de Santa Clara	La Gomera	Canary Islands	28.1963	-17.28754
<i>Dysdera</i>	<i>silvatica</i>	NMH002613	Teselinde. Ermita de Santa Clara	La Gomera	Canary Islands	28.1963	-17.28754
<i>Dysdera</i>	<i>silvatica</i>	NMH002614	Teselinde. Ermita de Santa Clara	La Gomera	Canary Islands	28.1963	-17.28754
<i>Dysdera</i>	<i>silvatica</i>	NMH002615	Teselinde. Ermita de Santa Clara	La Gomera	Canary Islands	28.1963	-17.28754
<i>Dysdera</i>	<i>silvatica</i>	NMH002616	Teselinde. Ermita de Santa Clara	La Gomera	Canary Islands	28.1963	-17.28754
<i>Dysdera</i>	<i>silvatica</i>	NMH002617	Teselinde. Ermita de Santa Clara	La Gomera	Canary Islands	28.1963	-17.28754
<i>Dysdera</i>	<i>silvatica</i>	NMH002619	Teselinde. Ermita de Santa Clara	La Gomera	Canary Islands	28.1963	-17.28754
<i>Dysdera</i>	<i>silvatica</i>	NMH002630	Teselinde. Ermita de Santa Clara	La Gomera	Canary Islands	28.1963	-17.28754
<i>Dysdera</i>	<i>silvatica</i>	NMH002631	Teselinde. Ermita de Santa Clara	La Gomera	Canary Islands	28.1963	-17.28754
<i>Dysdera</i>	<i>silvatica</i>	NMH003248	Monte del Cedro	La Gomera	Canary Islands	28.119283	-17.23729
<i>Dysdera</i>	<i>silvatica</i>	NMH003249	Monte del Cedro	La Gomera	Canary Islands	28.119283	-17.23729
<i>Dysdera</i>	<i>silvatica</i>	NMH003257	Bosque de Arure	La Gomera	Canary Islands	28.13321	-17.312446
<i>Dysdera</i>	<i>silvatica</i>	UB2666_109	Cerca de Los Acevifios	La Gomera	Canary Islands	28.147358	-17.219868
<i>Dysdera</i>	<i>silvatica</i>	UB2782	Bosque del Cedro	La Gomera	Canary Islands	28.137044	-17.222569
<i>Dysdera</i>	<i>silvatica</i>	UB2826	Barranco de Majona	La Gomera	Canary Islands	28.15183	-17.139235
<i>Dysdera</i>	<i>silvatica</i>	UB2894	Monte de Juan Tomé. La Laja	La Gomera	Canary Islands	28.123022	-17.210137
<i>Dysdera</i>	<i>silvatica</i>	UB2896	Monte de Juan Tomé. La Laja	La Gomera	Canary Islands	28.123022	-17.210137
<i>Dysdera</i>	<i>silvatica</i>	UB2897	Monte de Juan Tomé. La Laja	La Gomera	Canary Islands	28.123022	-17.210137
<i>Dysdera</i>	<i>silvatica</i>	UB2900	Monte del Cedro	La Gomera	Canary Islands	28.119283	-17.23729
<i>Dysdera</i>	<i>silvatica</i>	UB2901	Monte del Cedro	La Gomera	Canary Islands	28.119283	-17.23729
<i>Dysdera</i>	<i>silvatica</i>	UB2902	Monte del Cedro	La Gomera	Canary Islands	28.119283	-17.23729

<i>Dysdera</i>	<i>silvatica</i>	UB2903	Monte del Cedro	La Gomera	Canary Islands	28.119283	-17.23729
<i>Dysdera</i>	<i>silvatica</i>	UB2904	Monte del Cedro	La Gomera	Canary Islands	28.119283	-17.23729
<i>Dysdera</i>	<i>silvatica</i>	UB2905	Barranco Aramaqué. Near Los Acevifios	La Gomera	Canary Islands	28.149151	-17.220779
<i>Dysdera</i>	<i>silvatica</i>	UB2906	Barranco Aramaqué. Near Los Acevifios	La Gomera	Canary Islands	28.149151	-17.220779
<i>Dysdera</i>	<i>silvatica</i>	UB2907	Barranco Aramaqué. Near Los Acevifios	La Gomera	Canary Islands	28.149151	-17.220779
<i>Dysdera</i>	<i>silvatica</i>	UB2912	Pajarito	La Gomera	Canary Islands	28.108856	-17.241604
<i>Dysdera</i>	<i>silvatica</i>	UB2913	Pajarito	La Gomera	Canary Islands	28.108856	-17.241604
<i>Dysdera</i>	<i>silvatica</i>	UB2916	Chorros de Epina	La Gomera	Canary Islands	28.167036	-17.305892
<i>Dysdera</i>	<i>silvatica</i>	UB2917	Chorros de Epina	La Gomera	Canary Islands	28.167036	-17.305892
<i>Dysdera</i>	<i>silvatica</i>	UB2920	Plain Land between Barranco Higuera and Barranco San Juan.	La Gomera	Canary Islands	28.19332	-17.29294
<i>Dysdera</i>	<i>silvatica</i>	UB2923	Plain Land between Barranco Higuera and Barranco San Juan.	La Gomera	Canary Islands	28.19332	-17.29294
<i>Dysdera</i>	<i>silvatica</i>	UB2925	Barranco de Juel	La Gomera	Canary Islands	28.151547	-17.162962
<i>Dysdera</i>	<i>silvatica</i>	UB2927	Barranco de Juel	La Gomera	Canary Islands	28.151547	-17.162962
<i>Dysdera</i>	<i>silvatica</i>	UB2928	Barranco de Juel	La Gomera	Canary Islands	28.151547	-17.162962
<i>Dysdera</i>	<i>silvatica</i>	UB2931	Las Campanas	La Gomera	Canary Islands	28.158055	-17.160623
<i>Dysdera</i>	<i>silvatica</i>	UB2964	Barranco de Majona	La Gomera	Canary Islands	28.15183	-17.139235
<i>Dysdera</i>	<i>silvatica</i>	UB2972	Laguna Grande	La Gomera	Canary Islands	28.126085	-17.233223
<i>Dysdera</i>	<i>silvatica</i>	UB4119 (3) _Freezer	Monte de Juan Tomás. La Laja	La Gomera	Canary Islands	28.123022	-17.210137
<i>Dysdera</i>	<i>silvatica</i>	UB4120 (10) _Freezer	Monte de Juan Tomás. La Laja	La Gomera	Canary Islands	28.123022	-17.210137
<i>Dysdera</i>	<i>silvatica</i>	UB4122(19) _Freezer	Monte de Juan Tomás. La Laja	La Gomera	Canary Islands	28.123022	-17.210137
<i>Dysdera</i>	<i>silvatica</i>	UB4123 (24) _Freezer	Monte del Cedro	La Gomera	Canary Islands	28.119283	-17.23729
<i>Dysdera</i>	<i>silvatica</i>	UB4124 (31) _Freezer	Monte del Cedro	La Gomera	Canary Islands	28.119283	-17.23729
<i>Dysdera</i>	<i>silvatica</i>	UB4125 (32) _Freezer	Monte del Cedro	La Gomera	Canary Islands	28.119283	-17.23729
<i>Dysdera</i>	<i>silvatica</i>	UB4126 (35) _Freezer	Monte del Cedro	La Gomera	Canary Islands	28.119283	-17.23729
<i>Dysdera</i>	<i>silvatica</i>	UB4128 (41) _Freezer	Barranco Aramaqué. Near Los Acevifios	La Gomera	Canary Islands	28.149151	-17.220779
<i>Dysdera</i>	<i>silvatica</i>	UB4129 (44) _Freezer	Barranco Aramaqué. Near Los Acevifios	La Gomera	Canary Islands	28.149151	-17.220779
<i>Dysdera</i>	<i>silvatica</i>	UB4134(62) _Freezer	Pajarito	La Gomera	Canary Islands	28.108856	-17.241604
<i>Dysdera</i>	<i>silvatica</i>	UB4136(69) _Freezer	Pajarito	La Gomera	Canary Islands	28.108856	-17.241604
<i>Dysdera</i>	<i>silvatica</i>	UB4140(77) _Freezer	Chorros de Epina	La Gomera	Canary Islands	28.167036	-17.305892
<i>Dysdera</i>	<i>silvatica</i>	UB4141(80) _Freezer	Chorros de Epina	La Gomera	Canary Islands	28.167036	-17.305892
<i>Dysdera</i>	<i>silvatica</i>	UB4145(87) _Freezer	Plain Land between Barranco Higuera and Barranco San Juan.	La Gomera	Canary Islands	28.19332	-17.29294
<i>Dysdera</i>	<i>silvatica</i>	UB4150(97) _Freezer	Plain Land between Barranco Higuera and Barranco San Juan.	La Gomera	Canary Islands	28.19332	-17.29294
<i>Dysdera</i>	<i>silvatica</i>	UB4152(101) _Freezer	Plain Land between Barranco Higuera and Barranco San Juan.	La Gomera	Canary Islands	28.19332	-17.29294
<i>Dysdera</i>	<i>silvatica</i>	UB4153(102) _Freezer	Plain Land between Barranco Higuera and Barranco San Juan.	La Gomera	Canary Islands	28.19332	-17.29294

<i>Dysdera</i>	<i>silvatica</i>	UB4155(107)_Freezer	Barranco de Juel	La Gomera	Canary Islands	28.151547	-17.162962
<i>Dysdera</i>	<i>silvatica</i>	UB4156 (109)_Freezer	Barranco de Juel	La Gomera	Canary Islands	28.151547	-17.162962
<i>Dysdera</i>	<i>silvatica</i>	UB4157 (111)_Freezer	Barranco de Juel	La Gomera	Canary Islands	28.151547	-17.162962
<i>Dysdera</i>	<i>silvatica</i>	UB4158(112)_Freezer	Barranco de Juel	La Gomera	Canary Islands	28.151547	-17.162962
<i>Dysdera</i>	<i>silvatica</i>	UB4166(120)_Freezer	Barranco de Juel	La Gomera	Canary Islands	28.151547	-17.162962
<i>Dysdera</i>	<i>silvatica</i>	UB4168(124)_Freezer	Barranco de Juel	La Gomera	Canary Islands	28.151547	-17.162962
<i>Dysdera</i>	<i>silvatica</i>	UB4169(125)_Freezer	Barranco de Juel	La Gomera	Canary Islands	28.151547	-17.162962
<i>Dysdera</i>	<i>silvatica</i>	UB4170(126)_Freezer	Las Campanas	La Gomera	Canary Islands	28.158055	-17.160623
<i>Dysdera</i>	<i>silvatica</i>	UB4830 (G1)-4	Barranco de Majona	La Gomera	Canary Islands	28.15183	-17.139235
<i>Dysdera</i>	<i>gomerensis</i>	CRBA001089	Cueva de la Curva	El Hierro	Canary Islands	27.692348	-17.972877
<i>Dysdera</i>	<i>gomerensis</i>	CRBA001395	Casa Forestal de Frontera	El Hierro	Canary Islands	27.737593	-18.022747
<i>Dysdera</i>	<i>gomerensis</i>	CRBA001455	Hoya del Pino	El Hierro	Canary Islands	27.737154	-18.046305
<i>Dysdera</i>	<i>gomerensis</i>	CRBA002062	Pista del Derrabado	El Hierro	Canary Islands	27.740804	-18.05308
<i>Dysdera</i>	<i>gomerensis</i>	CRBA002064	Pista del Mercader	El Hierro	Canary Islands	27.712944	-18.022175
<i>Dysdera</i>	<i>gomerensis</i>	CRBA002065	Pista del Derrabado	El Hierro	Canary Islands	27.740804	-18.05308
<i>Dysdera</i>	<i>gomerensis</i>	CRBA002066	Pista del Mercader	El Hierro	Canary Islands	27.712944	-18.022175
<i>Dysdera</i>	<i>gomerensis</i>	CRBA002839	Hoya del Pino	El Hierro	Canary Islands	27.737154	-18.046305
<i>Dysdera</i>	<i>gomerensis</i>	CRBA002840	Mirador de Bascos	El Hierro	Canary Islands	27.754861	-18.118218
<i>Dysdera</i>	<i>gomerensis</i>	CRBA002841	Mirador de Bascos	El Hierro	Canary Islands	27.754861	-18.118218
<i>Dysdera</i>	<i>gomerensis</i>	CRBA002848	Pista del Mercader	El Hierro	Canary Islands	27.712944	-18.022175
<i>Dysdera</i>	<i>gomerensis</i>	CRBA002849	Mirador de Bascos	El Hierro	Canary Islands	27.754861	-18.118218
<i>Dysdera</i>	<i>gomerensis</i>	CRBA002850	Mirador de Bascos	El Hierro	Canary Islands	27.754861	-18.118218
<i>Dysdera</i>	<i>gomerensis</i>	CRBA002851	Mirador de Bascos	El Hierro	Canary Islands	27.754861	-18.118218
<i>Dysdera</i>	<i>gomerensis</i>	CRBA002852	Mirador de Bascos	El Hierro	Canary Islands	27.754861	-18.118218
<i>Dysdera</i>	<i>gomerensis</i>	CRBA002853	Mirador de Bascos	El Hierro	Canary Islands	27.754861	-18.118218
<i>Dysdera</i>	<i>gomerensis</i>	CRBA002854	Mirador de Bascos	El Hierro	Canary Islands	27.754861	-18.118218
<i>Dysdera</i>	<i>gomerensis</i>	CRBA002855	Mirador de Bascos	El Hierro	Canary Islands	27.754861	-18.118218
<i>Dysdera</i>	<i>gomerensis</i>	CRBA002856	Mirador de Bascos	El Hierro	Canary Islands	27.754861	-18.118218
<i>Dysdera</i>	<i>gomerensis</i>	CRBA002857	Mirador de Bascos	El Hierro	Canary Islands	27.754861	-18.118218
<i>Dysdera</i>	<i>gomerensis</i>	CRBA002883	Pista Garoé	El Hierro	Canary Islands	27.781744	-17.951391
<i>Dysdera</i>	<i>gomerensis</i>	CRBA002884	Pista Garoé	El Hierro	Canary Islands	27.781744	-17.951391
<i>Dysdera</i>	<i>gomerensis</i>	CRBA002885	Pista Garoé	El Hierro	Canary Islands	27.781744	-17.951391
<i>Dysdera</i>	<i>gomerensis</i>	CRBA002886	Pista Garoé	El Hierro	Canary Islands	27.781744	-17.951391
<i>Dysdera</i>	<i>gomerensis</i>	CRBA002887	Pista Garoé	El Hierro	Canary Islands	27.781744	-17.951391

<i>Dysdera</i>	<i>gomerensis</i>	CRBA002924	Ventejis. Tiñor	El Hierro	Canary Islands	27.785991	-17.937508
<i>Dysdera</i>	<i>gomerensis</i>	CRBA002925	Ventejis. Tiñor	El Hierro	Canary Islands	27.785991	-17.937508
<i>Dysdera</i>	<i>gomerensis</i>	CRBA002926	Ventejis. Tiñor	El Hierro	Canary Islands	27.785991	-17.937508
<i>Dysdera</i>	<i>gomerensis</i>	CRBA002927	Ventejis. Tiñor	El Hierro	Canary Islands	27.785991	-17.937508
<i>Dysdera</i>	<i>gomerensis</i>	CRBA002928	Ventejis. Tiñor	El Hierro	Canary Islands	27.785991	-17.937508
<i>Dysdera</i>	<i>gomerensis</i>	CRBA002929	Ventejis. Tiñor	El Hierro	Canary Islands	27.785991	-17.937508
<i>Dysdera</i>	<i>gomerensis</i>	CRBA002930	Ventejis. Tiñor	El Hierro	Canary Islands	27.785991	-17.937508
<i>Dysdera</i>	<i>gomerensis</i>	CRBA002931	Ventejis. Tiñor	El Hierro	Canary Islands	27.785991	-17.937508
<i>Dysdera</i>	<i>gomerensis</i>	NMH000001	Fuente la Llanía	El Hierro	Canary Islands	27.736643	-17.996938
<i>Dysdera</i>	<i>gomerensis</i>	NMH000009	Las Cancelitas	El Hierro	Canary Islands	27.80953	-17.927239
<i>Dysdera</i>	<i>gomerensis</i>	NMH000012	Hoya del Pino	El Hierro	Canary Islands	27.737154	-18.046305
<i>Dysdera</i>	<i>gomerensis</i>	NMH000013	Ventejis. Tiñor	El Hierro	Canary Islands	27.785991	-17.937508
<i>Dysdera</i>	<i>gomerensis</i>	NMH000014	Pico Pedraje. El Mocanal	El Hierro	Canary Islands	27.803692	-17.946575
<i>Dysdera</i>	<i>gomerensis</i>	NMH000027	La Dehesa	El Hierro	Canary Islands	27.738237	-18.136543
<i>Dysdera</i>	<i>gomerensis</i>	NMH000029	Ventejis. Tiñor	El Hierro	Canary Islands	27.785991	-17.937508
<i>Dysdera</i>	<i>gomerensis</i>	NMH000031	Ventejis. Tiñor	El Hierro	Canary Islands	27.785991	-17.937508
<i>Dysdera</i>	<i>gomerensis</i>	NMH000032	Ventejis. Tiñor	El Hierro	Canary Islands	27.785991	-17.937508
<i>Dysdera</i>	<i>gomerensis</i>	NMH000033	Ventejis. Tiñor	El Hierro	Canary Islands	27.785991	-17.937508
<i>Dysdera</i>	<i>gomerensis</i>	NMH000034	Mirador de Bascos	El Hierro	Canary Islands	27.754861	-18.118218
<i>Dysdera</i>	<i>gomerensis</i>	NMH000150	El Brezal	El Hierro	Canary Islands	27.732629	-18.028909
<i>Dysdera</i>	<i>gomerensis</i>	NMH000151	El Brezal	El Hierro	Canary Islands	27.732629	-18.028909
<i>Dysdera</i>	<i>gomerensis</i>	NMH000152	Ventejis. Tiñor	El Hierro	Canary Islands	27.785991	-17.937508
<i>Dysdera</i>	<i>gomerensis</i>	NMH000153	Ventejis. Tiñor	El Hierro	Canary Islands	27.785991	-17.937508
<i>Dysdera</i>	<i>gomerensis</i>	NMH000154	Ventejis. Tiñor	El Hierro	Canary Islands	27.785991	-17.937508
<i>Dysdera</i>	<i>gomerensis</i>	NMH000158	Mirador de Bascos	El Hierro	Canary Islands	27.754861	-18.118218
<i>Dysdera</i>	<i>gomerensis</i>	NMH000159	Mirador de Bascos	El Hierro	Canary Islands	27.754861	-18.118218
<i>Dysdera</i>	<i>gomerensis</i>	NMH000160	Mirador de Bascos	El Hierro	Canary Islands	27.754861	-18.118218
<i>Dysdera</i>	<i>gomerensis</i>	NMH000161	Mirador de Bascos	El Hierro	Canary Islands	27.754861	-18.118218
<i>Dysdera</i>	<i>gomerensis</i>	NMH001451	Pista del Mercader	El Hierro	Canary Islands	27.712944	-18.022175
<i>Dysdera</i>	<i>gomerensis</i>	NMH001452	Pista Garoé	El Hierro	Canary Islands	27.781744	-17.951391
<i>Dysdera</i>	<i>gomerensis</i>	NMH002529	Mirador de Bascos	El Hierro	Canary Islands	27.754861	-18.118218
<i>Dysdera</i>	<i>gomerensis</i>	NMH002530	Mirador de Bascos	El Hierro	Canary Islands	27.754861	-18.118218
<i>Dysdera</i>	<i>gomerensis</i>	NMH002531	Ventejis. Tiñor	El Hierro	Canary Islands	27.785991	-17.937508
<i>Dysdera</i>	<i>gomerensis</i>	NMH002532	Ventejis. Tiñor	El Hierro	Canary Islands	27.785991	-17.937508

Dysdera	gomerensis	NMH003189	Pista Garoé	El Hierro	Canary Islands	27.781744	-17.951391
Dysdera	gomerensis	NMH003190	Pista Garoé	El Hierro	Canary Islands	27.781744	-17.951391
Dysdera	gomerensis	NMH003191	Pista Garoé	El Hierro	Canary Islands	27.781744	-17.951391
Dysdera	gomerensis	NMH003192	Pista Garoé	El Hierro	Canary Islands	27.781744	-17.951391
Dysdera	gomerensis	NMH003193	Pista Garoé	El Hierro	Canary Islands	27.781744	-17.951391
Dysdera	gomerensis	NMH003194	Pista Garoé	El Hierro	Canary Islands	27.781744	-17.951391
Dysdera	gomerensis	NMH003195	Pista del Derrabado	El Hierro	Canary Islands	27.740804	-18.053008
Dysdera	gomerensis	NMH003197	Pista del Mercader	El Hierro	Canary Islands	27.712944	-18.022175
Dysdera	gomerensis	NMH003198	Pista del Mercader	El Hierro	Canary Islands	27.712944	-18.022175
Dysdera	gomerensis	NMH003199	Pista del Mercader	El Hierro	Canary Islands	27.712944	-18.022175
Dysdera	gomerensis	NMH003200	Pista del Mercader	El Hierro	Canary Islands	27.712944	-18.022175
Dysdera	gomerensis	NMH003201	Pista del Mercader	El Hierro	Canary Islands	27.712944	-18.022175
Dysdera	gomerensis	NMH003202	Pista del Derrabado	El Hierro	Canary Islands	27.740804	-18.053008
Dysdera	gomerensis	NMH003203	Pista del Derrabado	El Hierro	Canary Islands	27.740804	-18.053008
Dysdera	gomerensis	NMH003205	Mña. Caldereta	El Hierro	Canary Islands	27.743623	-18.016548
Dysdera	gomerensis	NMH003206	Mña. Caldereta	El Hierro	Canary Islands	27.743623	-18.016548
Dysdera	gomerensis	NMH003207	Mña. Caldereta	El Hierro	Canary Islands	27.743623	-18.016548
Dysdera	gomerensis	NMH003208	Mña. Caldereta	El Hierro	Canary Islands	27.743623	-18.016548
Dysdera	gomerensis	NMH003209	Mña. Caldereta	El Hierro	Canary Islands	27.743623	-18.016548
Dysdera	gomerensis	NMH003230	Cueva Juaclo de las Moleras	El Hierro	Canary Islands	27.732883	-18.140708
Dysdera	gomerensis	NMH003231	Cueva Juaclo de las Moleras	El Hierro	Canary Islands	27.732883	-18.140708
Dysdera	gomerensis	NMH003232	Pista del Mercader	El Hierro	Canary Islands	27.712944	-18.022175
Dysdera	gomerensis	NMH003233	Pista del Mercader	El Hierro	Canary Islands	27.712944	-18.022175
Dysdera	gomerensis	NMH003364	Mirador de Jinama	El Hierro	Canary Islands	27.762755	-17.980418
Dysdera	gomerensis	NMH003365	Cueva del Mocán	El Hierro	Canary Islands	27.717959	-18.00537
Dysdera	gomerensis	NMH003366	Playa Arenas Blancas	El Hierro	Canary Islands	27.76747	-18.122826
Dysdera	gomerensis	NMH003367	Montaña de Fara	El Hierro	Canary Islands	27.795267	-17.950103
Dysdera	gomerensis	NMH003368	Fuente Mencáffite	El Hierro	Canary Islands	27.735497	-18.085804
Dysdera	gomerensis	NMH003369	Charco Manso	El Hierro	Canary Islands	27.843092	-17.918891
Dysdera	gomerensis	NMH003370	Charco Manso	El Hierro	Canary Islands	27.843092	-17.918891
Dysdera	gomerensis	NMH003371	Charco Manso	El Hierro	Canary Islands	27.843092	-17.918891
Dysdera	gomerensis	NMH003372	Roques de Salmor	El Hierro	Canary Islands	27.823454	-17.996024
Dysdera	gomerensis	NMH003373	Roques de Salmor	El Hierro	Canary Islands	27.823454	-17.996024
Dysdera	gomerensis	UB2538_103	El Golfo. MSS (mauri 3)	El Hierro	Canary Islands	27.743924	-18.017786

<i>Dysdera</i>	<i>gomerensis</i>	UB2539_103	El Golfo. MSS (mauri 3)	El Hierro	Canary Islands	27.743924	-18.017786
<i>Dysdera</i>	<i>gomerensis</i>	UB2541_104	Pista del Derrabado	El Hierro	Canary Islands	27.740804	-18.05308
<i>Dysdera</i>	<i>gomerensis</i>	UB2542_104	Sima de las Palomas	El Hierro	Canary Islands	27.73787	-18.0657
<i>Dysdera</i>	<i>gomerensis</i>	UB2543_104	Cueva Juaco de las Moleras	El Hierro	Canary Islands	27.732883	-18.140708
<i>Dysdera</i>	<i>gomerensis</i>	UB2661_109	Punta Arenas Blancas	El Hierro	Canary Islands	27.767373	-18.122125
<i>Dysdera</i>	<i>gomerensis</i>	UB2663_109	El Fayal	El Hierro	Canary Islands	27.733435	-17.99638
<i>Dysdera</i>	<i>gomerensis</i>	UB2742	El Golfo	El Hierro	Canary Islands	27.743924	-18.017786
<i>Dysdera</i>	<i>gomerensis</i>	UB2752	El Golfo	El Hierro	Canary Islands	27.743924	-18.017786
<i>Dysdera</i>	<i>gomerensis</i>	UB2787	Cueva del Hoyo	El Hierro	Canary Islands	27.753511	-18.002527
<i>Dysdera</i>	<i>gomerensis</i>	UB2788	El Golfo	El Hierro	Canary Islands	27.743924	-18.017786
<i>Dysdera</i>	<i>gomerensis</i>	UB2789	El Golfo	El Hierro	Canary Islands	27.743924	-18.017786
<i>Dysdera</i>	<i>gomerensis</i>	UB2790	Sima de las Palomas	El Hierro	Canary Islands	27.73787	-18.0657
<i>Dysdera</i>	<i>gomerensis</i>	UB2793	Sima de las Palomas	El Hierro	Canary Islands	27.73787	-18.0657
<i>Dysdera</i>	<i>gomerensis</i>	UB2795	El Golfo	El Hierro	Canary Islands	27.743924	-18.017786
<i>Dysdera</i>	<i>gomerensis</i>	UB2796	El Golfo	El Hierro	Canary Islands	27.743924	-18.017786
<i>Dysdera</i>	<i>gomerensis</i>	UB2954	Mirador de Las Playas	El Hierro	Canary Islands	27.73197	-17.972127
<i>Dysdera</i>	<i>gomerensis</i>	UB2963	El Sabinar	El Hierro	Canary Islands	27.751746	-18.129598
<i>Dysdera</i>	<i>gomerensis</i>	UB3198_135	Mirador de Bascos	El Hierro	Canary Islands	27.754861	-18.118218
<i>Dysdera</i>	<i>gomerensis</i>	UB3199_135	Pista del Derrabado	El Hierro	Canary Islands	27.740804	-18.05308
<i>Dysdera</i>	<i>gomerensis</i>	UB3201_136	Ventejis. Tiñor	El Hierro	Canary Islands	27.785991	-17.937508
<i>Dysdera</i>	<i>gomerensis</i>	UB3223_137	Cueva de Mauricio	El Hierro	Canary Islands	27.73913	-18.06685
<i>Dysdera</i>	<i>gomerensis</i>	UB3224_137	Cueva de Mauricio	El Hierro	Canary Islands	27.73913	-18.06685
<i>Dysdera</i>	<i>gomerensis</i>	UB4007_Freezer	Mirador de Las Playas (300m hacia La Restinga)	El Hierro	Canary Islands	27.73197	-17.972127
<i>Dysdera</i>	<i>gomerensis</i>	UB4180_Freezer	El Sabinar	El Hierro	Canary Islands	27.751746	-18.129598
<i>Dysdera</i>	<i>gomerensis</i>	UB4779_Freezer	El Sabinar	El Hierro	Canary Islands	27.751746	-18.129598
<i>Dysdera</i>	<i>gomerensis</i>	UB4780_Freezer	El Sabinar	El Hierro	Canary Islands	27.751746	-18.129598
<i>Dysdera</i>	<i>gomerensis</i>	NMH001445	Mña. de Las Pilas, Cno. La Mérica	La Gomera	Canary Islands	28.113283	-17.335701
<i>Dysdera</i>	<i>gomerensis</i>	NMH003055	Las Hueritas	La Gomera	Canary Islands	28.090664	-17.283087
<i>Dysdera</i>	<i>gomerensis</i>	NMH003238	Mña. de Las Pilas, Cno. La Mérica	La Gomera	Canary Islands	28.113283	-17.335701
<i>Dysdera</i>	<i>gomerensis</i>	NMH003241	Teselinde. Ermita de Santa Clara	La Gomera	Canary Islands	28.1963	-17.28754
<i>Dysdera</i>	<i>gomerensis</i>	NMH003247	La Asomadita (Pista forestal Chipude)	La Gomera	Canary Islands	28.1116	-17.2648
<i>Dysdera</i>	<i>gomerensis</i>	UB4137(70)_Freezer	Pajarito	La Gomera	Canary Islands	28.108856	-17.241604
<i>Dysdera</i>	<i>gomerensis</i>	CRBA001393	Cañada de Jorge	La Gomera	Canary Islands	28.147416	-17.291071
<i>Dysdera</i>	<i>gomerensis</i>	CRBA001844	Teselinde. Ermita de Santa Clara	La Gomera	Canary Islands	28.1963	-17.28754

<i>Dysdera</i>	<i>gomerensis</i>	NMH001447	Puntallana	La Gomera	Canary Islands	28.12.5809	-17.216616
<i>Dysdera</i>	<i>gomerensis</i>	NMH001449	Sendero Enchereda	La Gomera	Canary Islands	28.13665	-17.179063
<i>Dysdera</i>	<i>gomerensis</i>	NMH001450	Los Noruegos	La Gomera	Canary Islands	28.106905	-17.233323
<i>Dysdera</i>	<i>gomerensis</i>	NMH002928	Playa de Avalo	La Gomera	Canary Islands	28.114684	-17.113168
<i>Dysdera</i>	<i>gomerensis</i>	NMH003184	Reventón Oscuro. Bosque del Cedro	La Gomera	Canary Islands	28.125809	-17.216616
<i>Dysdera</i>	<i>gomerensis</i>	NMH003255	Mña. La Asomada (Laguna Grande-Juego de Bolas)	La Gomera	Canary Islands	28.135646	-17.257454
<i>Dysdera</i>	<i>gomerensis</i>	UB4133 (51)_Freezer	Pajarito	La Gomera	Canary Islands	28.108856	-17.241604
<i>Dysdera</i>	<i>gomerensis</i>	CRBA001088	Playa Hermigua	La Gomera	Canary Islands	28.17624	-17.175953
<i>Dysdera</i>	<i>gomerensis</i>	CRBA001453	Llanos de Crispin	La Gomera	Canary Islands	28.123806	-17.266567
<i>Dysdera</i>	<i>gomerensis</i>	CRBA001860	Tapagache, old cropland	La Gomera	Canary Islands	28.08413	-17.28902
<i>Dysdera</i>	<i>gomerensis</i>	CRBA001861	Mirador de Alojera	La Gomera	Canary Islands	28.14978	-17.30813
<i>Dysdera</i>	<i>gomerensis</i>	CRBA001862	Barranco de los Castradores	La Gomera	Canary Islands	28.09618	-17.20142
<i>Dysdera</i>	<i>gomerensis</i>	CRBA001864	Barranco de los Castradores	La Gomera	Canary Islands	28.09618	-17.20142
<i>Dysdera</i>	<i>gomerensis</i>	CRBA001866	Las Paredes	La Gomera	Canary Islands	28.09882	-17.24942
<i>Dysdera</i>	<i>gomerensis</i>	CRBA001867	Arure to Las Hayas rd., cropland	La Gomera	Canary Islands	28.129606	-17.300846
<i>Dysdera</i>	<i>gomerensis</i>	CRBA001868	Barranco de Palién	La Gomera	Canary Islands	28.08845	-17.20142
<i>Dysdera</i>	<i>gomerensis</i>	CRBA001870	Ermida del Santo	La Gomera	Canary Islands	28.13102	-17.32273
<i>Dysdera</i>	<i>gomerensis</i>	CRBA002734	Above Arguamul	La Gomera	Canary Islands	28.18905	-17.29991
<i>Dysdera</i>	<i>gomerensis</i>	CRBA002735	Above Arguamul	La Gomera	Canary Islands	28.18905	-17.29991
<i>Dysdera</i>	<i>gomerensis</i>	CRBA002736	Above Arguamul	La Gomera	Canary Islands	28.18905	-17.29991
<i>Dysdera</i>	<i>gomerensis</i>	CRBA002738	Teselinde. Ermita de Santa Clara	La Gomera	Canary Islands	28.1963	-17.28754
<i>Dysdera</i>	<i>gomerensis</i>	CRBA002739	Teselinde. Ermita de Santa Clara	La Gomera	Canary Islands	28.1963	-17.28754
<i>Dysdera</i>	<i>gomerensis</i>	CRBA002746	Teselinde. Ermita de Santa Clara	La Gomera	Canary Islands	28.1963	-17.28754
<i>Dysdera</i>	<i>gomerensis</i>	CRBA002748	Teselinde. Ermita de Santa Clara	La Gomera	Canary Islands	28.1963	-17.28754
<i>Dysdera</i>	<i>gomerensis</i>	CRBA002752	Teselinde. Ermita de Santa Clara	La Gomera	Canary Islands	28.1963	-17.28754
<i>Dysdera</i>	<i>gomerensis</i>	CRBA002753	Teselinde. Ermita de Santa Clara	La Gomera	Canary Islands	28.1963	-17.28754
<i>Dysdera</i>	<i>gomerensis</i>	CRBA002759	Teselinde. Ermita de Santa Clara	La Gomera	Canary Islands	28.1963	-17.28754
<i>Dysdera</i>	<i>gomerensis</i>	CRBA002765	Teselinde. Ermita de Santa Clara	La Gomera	Canary Islands	28.1963	-17.28754
<i>Dysdera</i>	<i>gomerensis</i>	CRBA002766	Teselinde. Ermita de Santa Clara	La Gomera	Canary Islands	28.1963	-17.28754
<i>Dysdera</i>	<i>gomerensis</i>	CRBA002769	Teselinde. Ermita de Santa Clara	La Gomera	Canary Islands	28.1963	-17.28754
<i>Dysdera</i>	<i>gomerensis</i>	CRBA002771	Teselinde. Ermita de Santa Clara	La Gomera	Canary Islands	28.1963	-17.28754
<i>Dysdera</i>	<i>gomerensis</i>	CRBA002774	Teselinde. Ermita de Santa Clara	La Gomera	Canary Islands	28.1963	-17.28754
<i>Dysdera</i>	<i>gomerensis</i>	CRBA002782	Teselinde. Ermita de Santa Clara	La Gomera	Canary Islands	28.1963	-17.28754
<i>Dysdera</i>	<i>gomerensis</i>	CRBA002785	Teselinde. Ermita de Santa Clara	La Gomera	Canary Islands	28.1963	-17.28754

<i>Dysdera</i>	<i>gomerensis</i>	CRBA002786	Teselinde. Ermita de Santa Clara	La Gomera	Canary Islands	28.1963	-17.28754
<i>Dysdera</i>	<i>gomerensis</i>	CRBA002787	Teselinde. Ermita de Santa Clara	La Gomera	Canary Islands	28.1963	-17.28754
<i>Dysdera</i>	<i>gomerensis</i>	CRBA002788	Teselinde. Ermita de Santa Clara	La Gomera	Canary Islands	28.1963	-17.28754
<i>Dysdera</i>	<i>gomerensis</i>	CRBA002789	Teselinde. Ermita de Santa Clara	La Gomera	Canary Islands	28.1963	-17.28754
<i>Dysdera</i>	<i>gomerensis</i>	CRBA002790	Teselinde. Ermita de Santa Clara	La Gomera	Canary Islands	28.1963	-17.28754
<i>Dysdera</i>	<i>gomerensis</i>	CRBA002791	Teselinde. Ermita de Santa Clara	La Gomera	Canary Islands	28.1963	-17.28754
<i>Dysdera</i>	<i>gomerensis</i>	CRBA002792	Teselinde. Ermita de Santa Clara	La Gomera	Canary Islands	28.1963	-17.28754
<i>Dysdera</i>	<i>gomerensis</i>	CRBA002793	Teselinde. Ermita de Santa Clara	La Gomera	Canary Islands	28.1963	-17.28754
<i>Dysdera</i>	<i>gomerensis</i>	CRBA002799	Barranco de Juel, East	La Gomera	Canary Islands	28.14832	-17.15772
<i>Dysdera</i>	<i>gomerensis</i>	CRBA002805	Barranco de Juel, East	La Gomera	Canary Islands	28.14832	-17.15772
<i>Dysdera</i>	<i>gomerensis</i>	CRBA002806	Barranco de Juel, East	La Gomera	Canary Islands	28.14832	-17.15772
<i>Dysdera</i>	<i>gomerensis</i>	CRBA002807	Barranco de Juel, East	La Gomera	Canary Islands	28.14832	-17.15772
<i>Dysdera</i>	<i>gomerensis</i>	CRBA002808	Barranco de Juel, East	La Gomera	Canary Islands	28.14832	-17.15772
<i>Dysdera</i>	<i>gomerensis</i>	CRBA002811	Barranco de Juel, East	La Gomera	Canary Islands	28.14832	-17.15772
<i>Dysdera</i>	<i>gomerensis</i>	CRBA002812	Barranco de Juel, East	La Gomera	Canary Islands	28.14832	-17.15772
<i>Dysdera</i>	<i>gomerensis</i>	CRBA002814	Barranco de Juel, East	La Gomera	Canary Islands	28.14832	-17.15772
<i>Dysdera</i>	<i>gomerensis</i>	CRBA002818	Barranco de Juel, East	La Gomera	Canary Islands	28.14832	-17.15772
<i>Dysdera</i>	<i>gomerensis</i>	CRBA002819	Barranco de Juel, East	La Gomera	Canary Islands	28.14832	-17.15772
<i>Dysdera</i>	<i>gomerensis</i>	CRBA002827	Barranco de Juel, East	La Gomera	Canary Islands	28.14832	-17.15772
<i>Dysdera</i>	<i>gomerensis</i>	CRBA002832	Barranco de Juel, East	La Gomera	Canary Islands	28.14832	-17.15772
<i>Dysdera</i>	<i>gomerensis</i>	CRBA002837	Barranco de Juel, East	La Gomera	Canary Islands	28.14832	-17.15772
<i>Dysdera</i>	<i>gomerensis</i>	CRBA003621	Pista Mora Gaspar	La Gomera		28.142375	-17.250954
<i>Dysdera</i>	<i>gomerensis</i>	CRBA003623	Pista Mora Gaspar	La Gomera		28.142375	-17.250954
<i>Dysdera</i>	<i>gomerensis</i>	CRBA003627	Clra. Cumbre, altura Mora Gaspar	La Gomera	Canary Islands	28.14614	-17.262784
<i>Dysdera</i>	<i>gomerensis</i>	CRBA003636	Teselinde. Ermita de Santa Clara	La Gomera	Canary Islands	28.1963	-17.28754
<i>Dysdera</i>	<i>gomerensis</i>	CRBA003637	Teselinde. Ermita de Santa Clara	La Gomera	Canary Islands	28.1963	-17.28754
<i>Dysdera</i>	<i>gomerensis</i>	CRBA003640	Teselinde. Ermita de Santa Clara	La Gomera	Canary Islands	28.1963	-17.28754
<i>Dysdera</i>	<i>gomerensis</i>	CRBA003644	Teselinde. Ermita de Santa Clara	La Gomera	Canary Islands	28.1963	-17.28754
<i>Dysdera</i>	<i>gomerensis</i>	CRBA003645	Teselinde. Ermita de Santa Clara	La Gomera	Canary Islands	28.1963	-17.28754
<i>Dysdera</i>	<i>gomerensis</i>	CRBA003646	Teselinde. Ermita de Santa Clara	La Gomera	Canary Islands	28.1963	-17.28754
<i>Dysdera</i>	<i>gomerensis</i>	CRBA003662	Teselinde. Ermita de Santa Clara	La Gomera	Canary Islands	28.1963	-17.28754
<i>Dysdera</i>	<i>gomerensis</i>	CRBA003663	Teselinde. Ermita de Santa Clara	La Gomera	Canary Islands	28.1963	-17.28754
<i>Dysdera</i>	<i>gomerensis</i>	CRBA003664	Teselinde. Ermita de Santa Clara	La Gomera	Canary Islands	28.1963	-17.28754
<i>Dysdera</i>	<i>gomerensis</i>	CRBA003665	Teselinde. Ermita de Santa Clara	La Gomera	Canary Islands	28.1963	-17.28754

<i>Dysdera</i>	<i>gomerensis</i>	CRBA003666	Teselinde. Ermita de Santa Clara	La Gomera	Canary Islands	28.1963	-17.28754
<i>Dysdera</i>	<i>gomerensis</i>	CRBA003675	Teselinde. Ermita de Santa Clara	La Gomera	Canary Islands	28.1963	-17.28754
<i>Dysdera</i>	<i>gomerensis</i>	CRBA003695	Teselinde. Ermita de Santa Clara	La Gomera	Canary Islands	28.1963	-17.28754
<i>Dysdera</i>	<i>gomerensis</i>	CRBA003699	Teselinde. Ermita de Santa Clara	La Gomera	Canary Islands	28.1963	-17.28754
<i>Dysdera</i>	<i>gomerensis</i>	CRBA003704	Teselinde. Ermita de Santa Clara	La Gomera	Canary Islands	28.1963	-17.28754
<i>Dysdera</i>	<i>gomerensis</i>	CRBA003707	Teselinde. Ermita de Santa Clara	La Gomera	Canary Islands	28.1963	-17.28754
<i>Dysdera</i>	<i>gomerensis</i>	CRBA003725	Teselinde. Ermita de Santa Clara	La Gomera	Canary Islands	28.1963	-17.28754
<i>Dysdera</i>	<i>gomerensis</i>	CRBA003733	Teselinde. Ermita de Santa Clara	La Gomera	Canary Islands	28.1963	-17.28754
<i>Dysdera</i>	<i>gomerensis</i>	CRBA003734	Teselinde. Ermita de Santa Clara	La Gomera	Canary Islands	28.1963	-17.28754
<i>Dysdera</i>	<i>gomerensis</i>	CRBA003741	Teselinde. Ermita de Santa Clara	La Gomera	Canary Islands	28.1963	-17.28754
<i>Dysdera</i>	<i>gomerensis</i>	CRBA003744	Teselinde. Ermita de Santa Clara	La Gomera	Canary Islands	28.1963	-17.28754
<i>Dysdera</i>	<i>gomerensis</i>	CRBA003759	Teselinde. Ermita de Santa Clara	La Gomera	Canary Islands	28.1963	-17.28754
<i>Dysdera</i>	<i>gomerensis</i>	CRBA003766	Teselinde. Ermita de Santa Clara	La Gomera	Canary Islands	28.1963	-17.28754
<i>Dysdera</i>	<i>gomerensis</i>	CRBA003787	Degollada de Archejo	La Gomera	Canary Islands	28.13344	-17.254938
<i>Dysdera</i>	<i>gomerensis</i>	CRBA003804	Degollada de Archejo	La Gomera	Canary Islands	28.13344	-17.254938
<i>Dysdera</i>	<i>gomerensis</i>	CRBA003810	Degollada de Archejo	La Gomera	Canary Islands	28.13344	-17.254938
<i>Dysdera</i>	<i>gomerensis</i>	CRBA003811	Degollada de Archejo	La Gomera	Canary Islands	28.13344	-17.254938
<i>Dysdera</i>	<i>gomerensis</i>	CRBA003819	Degollada de Archejo	La Gomera	Canary Islands	28.13344	-17.254938
<i>Dysdera</i>	<i>gomerensis</i>	CRBA003836	Barranco de Majona	La Gomera	Canary Islands	28.13438	-17.168397
<i>Dysdera</i>	<i>gomerensis</i>	CRBA003838	Barranco de Juel, East	La Gomera	Canary Islands	28.14832	-17.15772
<i>Dysdera</i>	<i>gomerensis</i>	CRBA003841	Barranco de Juel, East	La Gomera	Canary Islands	28.14832	-17.15772
<i>Dysdera</i>	<i>gomerensis</i>	CRBA003842	Barranco de Juel, East	La Gomera	Canary Islands	28.14832	-17.15772
<i>Dysdera</i>	<i>gomerensis</i>	CRBA003859	Barranco de Juel, East	La Gomera	Canary Islands	28.14832	-17.15772
<i>Dysdera</i>	<i>gomerensis</i>	CRBA003860	Barranco de Juel, East	La Gomera	Canary Islands	28.14832	-17.15772
<i>Dysdera</i>	<i>gomerensis</i>	CRBA003862	Barranco de Juel, East	La Gomera	Canary Islands	28.14832	-17.15772
<i>Dysdera</i>	<i>gomerensis</i>	CRBA003863	Barranco de Juel, East	La Gomera	Canary Islands	28.14832	-17.15772
<i>Dysdera</i>	<i>gomerensis</i>	CRBA003868	Barranco de Juel, East	La Gomera	Canary Islands	28.14832	-17.15772
<i>Dysdera</i>	<i>gomerensis</i>	CRBA003869	Barranco de Juel, East	La Gomera	Canary Islands	28.14832	-17.15772
<i>Dysdera</i>	<i>gomerensis</i>	CRBA003875	Barranco de Juel, East	La Gomera	Canary Islands	28.14832	-17.15772
<i>Dysdera</i>	<i>gomerensis</i>	CRBA003876	Barranco de Juel, East	La Gomera	Canary Islands	28.14832	-17.15772
<i>Dysdera</i>	<i>gomerensis</i>	CRBA003877	Barranco de Juel, East	La Gomera	Canary Islands	28.14832	-17.15772
<i>Dysdera</i>	<i>gomerensis</i>	CRBA003879	Barranco de Juel, East	La Gomera	Canary Islands	28.14832	-17.15772
<i>Dysdera</i>	<i>gomerensis</i>	CRBA003883	Barranco de Juel, East	La Gomera	Canary Islands	28.14832	-17.15772
<i>Dysdera</i>	<i>gomerensis</i>	CRBA003890	Barranco de Juel, East	La Gomera	Canary Islands	28.14832	-17.15772

<i>Dysdera</i>	<i>gomerensis</i>	CRBA003891	Barranco de Juel, East	La Gomera	Canary Islands	28.14832	-17.15772
<i>Dysdera</i>	<i>gomerensis</i>	CRBA003893	Barranco de Juel, East	La Gomera	Canary Islands	28.14832	-17.15772
<i>Dysdera</i>	<i>gomerensis</i>	CRBA003895	Barranco de Juel, East	La Gomera	Canary Islands	28.14832	-17.15772
<i>Dysdera</i>	<i>gomerensis</i>	CRBA003898	Barranco de Juel, East	La Gomera	Canary Islands	28.14832	-17.15772
<i>Dysdera</i>	<i>gomerensis</i>	CRBA003919	Las Hayas	La Gomera	Canary Islands	28.133622	-17.282405
<i>Dysdera</i>	<i>gomerensis</i>	CRBA003920	Las Hayas	La Gomera	Canary Islands	28.133622	-17.282405
<i>Dysdera</i>	<i>gomerensis</i>	CRBA003922	Pajarito	La Gomera	Canary Islands	28.10695	-17.241012
<i>Dysdera</i>	<i>gomerensis</i>	CRBA003923	Pajarito	La Gomera	Canary Islands	28.108856	-17.241604
<i>Dysdera</i>	<i>gomerensis</i>	CRBA003924	Pajarito	La Gomera	Canary Islands	28.108856	-17.241604
<i>Dysdera</i>	<i>gomerensis</i>	CRBA003925	Pajarito	La Gomera	Canary Islands	28.108856	-17.241604
<i>Dysdera</i>	<i>gomerensis</i>	CRBA003926	Pajarito	La Gomera	Canary Islands	28.108856	-17.241604
<i>Dysdera</i>	<i>gomerensis</i>	CRBA003927	Pajarito	La Gomera	Canary Islands	28.108856	-17.241604
<i>Dysdera</i>	<i>gomerensis</i>	NMH000115	Llanos de Crispín	La Gomera	Canary Islands	28.123587	-17.258887
<i>Dysdera</i>	<i>gomerensis</i>	NMH000233	Barranco de Majona	La Gomera	Canary Islands	28.15183	-17.139235
<i>Dysdera</i>	<i>gomerensis</i>	NMH000238	Barranco de Matarnos, Monte del Cedro	La Gomera	Canary Islands	28.12504	-17.242183
<i>Dysdera</i>	<i>gomerensis</i>	NMH001455	Pie del Roque Cano	La Gomera	Canary Islands	28.184542	-17.256932
<i>Dysdera</i>	<i>gomerensis</i>	NMH001456	Túnel de Aguilo (Lado Las Rosas)	La Gomera	Canary Islands	28.192455	-17.198191
<i>Dysdera</i>	<i>gomerensis</i>	NMH001457	El Cepo	La Gomera	Canary Islands	28.191769	-17.216818
<i>Dysdera</i>	<i>gomerensis</i>	NMH001721	Teselinde, Ermita de Santa Clara	La Gomera	Canary Islands	28.1963	-17.28754
<i>Dysdera</i>	<i>gomerensis</i>	NMH001722	Teselinde, Ermita de Santa Clara	La Gomera	Canary Islands	28.1963	-17.28754
<i>Dysdera</i>	<i>gomerensis</i>	NMH001723	Teselinde, Ermita de Santa Clara	La Gomera	Canary Islands	28.1963	-17.28754
<i>Dysdera</i>	<i>gomerensis</i>	NMH001724	Teselinde, Ermita de Santa Clara	La Gomera	Canary Islands	28.1963	-17.28754
<i>Dysdera</i>	<i>gomerensis</i>	NMH001725	Teselinde, Ermita de Santa Clara	La Gomera	Canary Islands	28.1963	-17.28754
<i>Dysdera</i>	<i>gomerensis</i>	NMH001726	Teselinde, Ermita de Santa Clara	La Gomera	Canary Islands	28.1963	-17.28754
<i>Dysdera</i>	<i>gomerensis</i>	NMH001727	Teselinde, Ermita de Santa Clara	La Gomera	Canary Islands	28.1963	-17.28754
<i>Dysdera</i>	<i>gomerensis</i>	NMH001728	Teselinde, Ermita de Santa Clara	La Gomera	Canary Islands	28.1963	-17.28754
<i>Dysdera</i>	<i>gomerensis</i>	NMH001729	Teselinde, Ermita de Santa Clara	La Gomera	Canary Islands	28.1963	-17.28754
<i>Dysdera</i>	<i>gomerensis</i>	NMH001730	Teselinde, Ermita de Santa Clara	La Gomera	Canary Islands	28.1963	-17.28754
<i>Dysdera</i>	<i>gomerensis</i>	NMH001731	Teselinde, Ermita de Santa Clara	La Gomera	Canary Islands	28.1963	-17.28754
<i>Dysdera</i>	<i>gomerensis</i>	NMH001732	Teselinde, Ermita de Santa Clara	La Gomera	Canary Islands	28.1963	-17.28754
<i>Dysdera</i>	<i>gomerensis</i>	NMH001733	Teselinde, Ermita de Santa Clara	La Gomera	Canary Islands	28.1963	-17.28754
<i>Dysdera</i>	<i>gomerensis</i>	NMH001734	Teselinde, Ermita de Santa Clara	La Gomera	Canary Islands	28.1963	-17.28754
<i>Dysdera</i>	<i>gomerensis</i>	NMH001735	Teselinde, Ermita de Santa Clara	La Gomera	Canary Islands	28.1963	-17.28754
<i>Dysdera</i>	<i>gomerensis</i>	NMH001736	Teselinde, Ermita de Santa Clara	La Gomera	Canary Islands	28.1963	-17.28754

<i>Dysdera</i>	<i>gomerensis</i>	NMH002460	Teselinde, Ermita de Santa Clara	La Gomera	Canary Islands	28.1963	-17.28754
<i>Dysdera</i>	<i>gomerensis</i>	NMH002461	Teselinde, Ermita de Santa Clara	La Gomera	Canary Islands	28.1963	-17.28754
<i>Dysdera</i>	<i>gomerensis</i>	NMH002462	Teselinde, Ermita de Santa Clara	La Gomera	Canary Islands	28.1963	-17.28754
<i>Dysdera</i>	<i>gomerensis</i>	NMH002463	Teselinde, Ermita de Santa Clara	La Gomera	Canary Islands	28.1963	-17.28754
<i>Dysdera</i>	<i>gomerensis</i>	NMH002464	Teselinde, Ermita de Santa Clara	La Gomera	Canary Islands	28.1963	-17.28754
<i>Dysdera</i>	<i>gomerensis</i>	NMH002465	Teselinde, Ermita de Santa Clara	La Gomera	Canary Islands	28.1963	-17.28754
<i>Dysdera</i>	<i>gomerensis</i>	NMH002466	Teselinde, Ermita de Santa Clara	La Gomera	Canary Islands	28.1963	-17.28754
<i>Dysdera</i>	<i>gomerensis</i>	NMH002467	Teselinde, Ermita de Santa Clara	La Gomera	Canary Islands	28.1963	-17.28754
<i>Dysdera</i>	<i>gomerensis</i>	NMH002468	Teselinde, Ermita de Santa Clara	La Gomera	Canary Islands	28.1963	-17.28754
<i>Dysdera</i>	<i>gomerensis</i>	NMH002470	Teselinde, Ermita de Santa Clara	La Gomera	Canary Islands	28.1963	-17.28754
<i>Dysdera</i>	<i>gomerensis</i>	NMH002471	Teselinde, Ermita de Santa Clara	La Gomera	Canary Islands	28.1963	-17.28754
<i>Dysdera</i>	<i>gomerensis</i>	NMH002472	Teselinde, Ermita de Santa Clara	La Gomera	Canary Islands	28.1963	-17.28754
<i>Dysdera</i>	<i>gomerensis</i>	NMH002473	Teselinde, Ermita de Santa Clara	La Gomera	Canary Islands	28.1963	-17.28754
<i>Dysdera</i>	<i>gomerensis</i>	NMH002602	Ctra. Juego de Bolas- Laguna Grande	La Gomera	Canary Islands	28.129925	-17.254707
<i>Dysdera</i>	<i>gomerensis</i>	NMH002603	Ctra. Juego de Bolas- Laguna Grande	La Gomera	Canary Islands	28.129925	-17.254707
<i>Dysdera</i>	<i>gomerensis</i>	NMH002604	Ctra. Juego de Bolas- Laguna Grande	La Gomera	Canary Islands	28.129925	-17.254707
<i>Dysdera</i>	<i>gomerensis</i>	NMH002621	Teselinde, Ermita de Santa Clara	La Gomera	Canary Islands	28.1963	-17.28754
<i>Dysdera</i>	<i>gomerensis</i>	NMH002622	Teselinde, Ermita de Santa Clara	La Gomera	Canary Islands	28.1963	-17.28754
<i>Dysdera</i>	<i>gomerensis</i>	NMH002623	Teselinde, Ermita de Santa Clara	La Gomera	Canary Islands	28.1963	-17.28754
<i>Dysdera</i>	<i>gomerensis</i>	NMH002626	Teselinde, Ermita de Santa Clara	La Gomera	Canary Islands	28.1963	-17.28754
<i>Dysdera</i>	<i>gomerensis</i>	NMH002627	Teselinde, Ermita de Santa Clara	La Gomera	Canary Islands	28.1963	-17.28754
<i>Dysdera</i>	<i>gomerensis</i>	NMH002628	Teselinde, Ermita de Santa Clara	La Gomera	Canary Islands	28.1963	-17.28754
<i>Dysdera</i>	<i>gomerensis</i>	NMH002629	Teselinde, Ermita de Santa Clara	La Gomera	Canary Islands	28.1963	-17.28754
<i>Dysdera</i>	<i>gomerensis</i>	NMH002632	Teselinde, Ermita de Santa Clara	La Gomera	Canary Islands	28.1963	-17.28754
<i>Dysdera</i>	<i>gomerensis</i>	NMH002747	Reventón Oscuro. Bosque del Cedro	La Gomera	Canary Islands	28.125809	-17.216616
<i>Dysdera</i>	<i>gomerensis</i>	NMH002931	Ermita de Las Nieves	La Gomera	Canary Islands	28.101134	-17.202401
<i>Dysdera</i>	<i>gomerensis</i>	NMH003239	Mña. de Las Pilas, Cno. La Mérica	La Gomera	Canary Islands	28.113283	-17.335701
<i>Dysdera</i>	<i>gomerensis</i>	NMH003240	Mña. de Las Pilas, Cno. La Mérica	La Gomera	Canary Islands	28.113283	-17.335701
<i>Dysdera</i>	<i>gomerensis</i>	NMH003246	La Asonadita (Pista forestal Chipude)	La Gomera		28.1116	-17.2648
<i>Dysdera</i>	<i>gomerensis</i>	NMH003250	Monte del Cedro	La Gomera	Canary Islands	28.119283	-17.23729
<i>Dysdera</i>	<i>gomerensis</i>	NMH003251	Monte del Cedro	La Gomera	Canary Islands	28.119283	-17.23729
<i>Dysdera</i>	<i>gomerensis</i>	NMH003374	La Campana	La Gomera	Canary Islands	28.158055	-17.160623
<i>Dysdera</i>	<i>gomerensis</i>	UB2593_106	Barranco de Matarnos. Monte del Cedro	La Gomera	Canary Islands	28.12504	-17.242183
<i>Dysdera</i>	<i>gomerensis</i>	UB2595	Barranco de Majona	La Gomera	Canary Islands	28.15183	-17.139235

<i>Dysdera</i>	<i>gomerensis</i>	UB2657_109	Ermita de Las Nieves 1130m	La Gomera	Canary Islands	28.101134	-17.202401
<i>Dysdera</i>	<i>gomerensis</i>	UB2783	Pinar del Infante	La Gomera	Canary Islands	28.130794	-17.282267
<i>Dysdera</i>	<i>gomerensis</i>	UB2784	Pinar del Infante	La Gomera	Canary Islands	28.130794	-17.282267
<i>Dysdera</i>	<i>gomerensis</i>	UB2827_117	Barranco de Majona	La Gomera	Canary Islands	28.151183	-17.139235
<i>Dysdera</i>	<i>gomerensis</i>	UB2828	Barranco de Majona	La Gomera	Canary Islands	28.151183	-17.139235
<i>Dysdera</i>	<i>gomerensis</i>	UB2829	Barranco de Majona	La Gomera	Canary Islands	28.151183	-17.139235
<i>Dysdera</i>	<i>gomerensis</i>	UB2914	Pajarito	La Gomera	Canary Islands	28.108856	-17.241604
<i>Dysdera</i>	<i>gomerensis</i>	UB2919	Plain Land between Barranco Higuera and Barranco San Juan.	La Gomera	Canary Islands	28.19332	-17.29294
<i>Dysdera</i>	<i>gomerensis</i>	UB2924	Barranco de Majona	La Gomera	Canary Islands	28.151183	-17.139235
<i>Dysdera</i>	<i>gomerensis</i>	UB2926	Barranco de Juel	La Gomera	Canary Islands	28.151547	-17.162962
<i>Dysdera</i>	<i>gomerensis</i>	UB2971	Montaña del Dinero	La Gomera	Canary Islands	28.15943312	-17.243576
<i>Dysdera</i>	<i>gomerensis</i>	UB3141_133 (freezer)	Ojila	La Gomera	Canary Islands	28.118032	-17.211105
<i>Dysdera</i>	<i>gomerensis</i>	UB4019_Freezer	Barranco de Majona	La Gomera	Canary Islands	28.151183	-17.139235
<i>Dysdera</i>	<i>gomerensis</i>	UB4020_Freezer	Barranco de Majona	La Gomera	Canary Islands	28.151183	-17.139235
<i>Dysdera</i>	<i>gomerensis</i>	UB4133(70)_Freezer	Pajarito	La Gomera	Canary Islands	28.108856	-17.241604
<i>Dysdera</i>	<i>gomerensis</i>	UB4135(65)_Freezer	Pajarito	La Gomera	Canary Islands	28.108856	-17.241604
<i>Dysdera</i>	<i>gomerensis</i>	UB4143(82)_Freezer	Chorros de Epina	La Gomera	Canary Islands	28.167036	-17.305892
<i>Dysdera</i>	<i>gomerensis</i>	UB4144 (85)_Freezer	Chorros de Epina	La Gomera	Canary Islands	28.167036	-17.305892
<i>Dysdera</i>	<i>gomerensis</i>	UB4148(95)_Freezer	Plain Land between Barranco Higuera and Barranco San Juan.	La Gomera	Canary Islands	28.19332	-17.29294
<i>Dysdera</i>	<i>gomerensis</i>	UB4151 (100)_Freezer	Plain Land between Barranco Higuera and Barranco San Juan.	La Gomera	Canary Islands	28.19332	-17.29294
<i>Dysdera</i>	<i>gomerensis</i>	UB4154(103)_Freezer	Barranco de Majona	La Gomera	Canary Islands	28.151183	-17.139235
<i>Dysdera</i>	<i>gomerensis</i>	UB4159(113)_Freezer	Barranco de Juel	La Gomera	Canary Islands	28.151547	-17.162962
<i>Dysdera</i>	<i>gomerensis</i>	UB4164(118)_Freezer	Barranco de Juel	La Gomera	Canary Islands	28.151547	-17.162962
<i>Dysdera</i>	<i>gomerensis</i>	CRBA003711	Teselinde. Ermita de Santa Clara	La Gomera	Canary Islands	28.1963	-17.28754
<i>Dysdera</i>	<i>calderensis</i>	CRBA002224	Roque Faro	La Palma	Canary Islands	28.798556	-17.879149
<i>Dysdera</i>	<i>calderensis</i>	CRBA002225	Roque Faro	La Palma	Canary Islands	28.798556	-17.879149
<i>Dysdera</i>	<i>calderensis</i>	CRBA002226	Roque Faro	La Palma	Canary Islands	28.798556	-17.879149
<i>Dysdera</i>	<i>calderensis</i>	CRBA002278	Juan Adalid	La Palma	Canary Islands	28.843639	-17.90635
<i>Dysdera</i>	<i>calderensis</i>	CRBA002279	Juan Adalid	La Palma	Canary Islands	28.843639	-17.90635
<i>Dysdera</i>	<i>calderensis</i>	CRBA002280	Juan Adalid	La Palma	Canary Islands	28.843639	-17.90635
<i>Dysdera</i>	<i>calderensis</i>	CRBA002282	El Castillo	La Palma	Canary Islands	28.79636	-17.971169
<i>Dysdera</i>	<i>calderensis</i>	CRBA002283	El Castillo	La Palma	Canary Islands	28.79636	-17.971169
<i>Dysdera</i>	<i>calderensis</i>	CRBA002284	El Castillo	La Palma	Canary Islands	28.79636	-17.971169
<i>Dysdera</i>	<i>calderensis</i>	CRBA002285	El Castillo	La Palma	Canary Islands	28.79636	-17.971169

Dysdera	calderensis	CRBA002286	El Castillo	La Palma	Canary Islands	28.79636	-17.971169
Dysdera	calderensis	CRBA002287	El Castillo	La Palma	Canary Islands	28.79636	-17.971169
Dysdera	calderensis	CRBA002288	El Castillo	La Palma	Canary Islands	28.79636	-17.971169
Dysdera	calderensis	CRBA002289	El Castillo	La Palma	Canary Islands	28.79636	-17.971169
Dysdera	calderensis	CRBA002290	El Castillo	La Palma	Canary Islands	28.79636	-17.971169
Dysdera	calderensis	CRBA002291	El Castillo	La Palma	Canary Islands	28.79636	-17.971169
Dysdera	calderensis	CRBA002292	Mendo	La Palma	Canary Islands	28.55752	-17.867541
Dysdera	calderensis	CRBA002293	Mendo	La Palma	Canary Islands	28.55752	-17.867541
Dysdera	calderensis	CRBA002294	Mendo	La Palma	Canary Islands	28.55752	-17.867541
Dysdera	calderensis	CRBA002295	Mendo	La Palma	Canary Islands	28.55752	-17.867541
Dysdera	calderensis	CRBA002296	Juan Adalid	La Palma	Canary Islands	28.843639	-17.90635
Dysdera	calderensis	CRBA002297	Juan Adalid	La Palma	Canary Islands	28.843639	-17.90635
Dysdera	calderensis	CRBA002298	Juan Adalid	La Palma	Canary Islands	28.843639	-17.90635
Dysdera	calderensis	CRBA002299	Juan Adalid	La Palma	Canary Islands	28.843639	-17.90635
Dysdera	calderensis	CRBA002300	Juan Adalid	La Palma	Canary Islands	28.843639	-17.90635
Dysdera	calderensis	CRBA002301	Juan Adalid	La Palma	Canary Islands	28.843639	-17.90635
Dysdera	calderensis	CRBA002302	Juan Adalid	La Palma	Canary Islands	28.843639	-17.90635
Dysdera	calderensis	CRBA002303	Juan Adalid	La Palma	Canary Islands	28.843639	-17.90635
Dysdera	calderensis	CRBA002304	Juan Adalid	La Palma	Canary Islands	28.843639	-17.90635
Dysdera	calderensis	CRBA002305	Juan Adalid	La Palma	Canary Islands	28.843639	-17.90635
Dysdera	calderensis	CRBA002313	Roque Faro	La Palma	Canary Islands	28.798556	-17.879149
Dysdera	calderensis	CRBA002314	Roque Faro	La Palma	Canary Islands	28.798556	-17.879149
Dysdera	calderensis	CRBA002315	Roque Faro	La Palma	Canary Islands	28.798556	-17.879149
Dysdera	calderensis	CRBA002316	Roque Faro	La Palma	Canary Islands	28.798556	-17.879149
Dysdera	calderensis	CRBA002317	Roque Faro	La Palma	Canary Islands	28.798556	-17.879149
Dysdera	calderensis	CRBA002318	Roque Faro	La Palma	Canary Islands	28.798556	-17.879149
Dysdera	calderensis	CRBA002319	Roque Faro	La Palma	Canary Islands	28.798556	-17.879149
Dysdera	calderensis	CRBA002320	Roque Faro	La Palma	Canary Islands	28.798556	-17.879149
Dysdera	calderensis	CRBA002321	Roque Faro	La Palma	Canary Islands	28.798556	-17.879149
Dysdera	calderensis	CRBA002323	Roque Faro	La Palma	Canary Islands	28.798556	-17.879149
Dysdera	calderensis	CRBA002324	Roque Faro	La Palma	Canary Islands	28.798556	-17.879149
Dysdera	calderensis	CRBA002325	Roque Faro	La Palma	Canary Islands	28.798556	-17.879149
Dysdera	calderensis	CRBA002326	Roque Faro	La Palma	Canary Islands	28.798556	-17.879149
Dysdera	calderensis	CRBA002328	Roque Faro	La Palma	Canary Islands	28.798556	-17.879149

<i>Dysdera calderensis</i>	CRBA002329	Roque Faro	La Palma	Canary Islands	28.798556	-17.879149
<i>Dysdera calderensis</i>	CRBA002330	Roque Faro	La Palma	Canary Islands	28.798556	-17.879149
<i>Dysdera calderensis</i>	CRBA002331	Roque Faro	La Palma	Canary Islands	28.798556	-17.879149
<i>Dysdera calderensis</i>	CRBA002332	Roque Faro	La Palma	Canary Islands	28.798556	-17.879149
<i>Dysdera calderensis</i>	CRBA002333	Roque Faro	La Palma	Canary Islands	28.798556	-17.879149
<i>Dysdera calderensis</i>	CRBA002334	Roque Faro	La Palma	Canary Islands	28.798556	-17.879149
<i>Dysdera calderensis</i>	CRBA002335	Roque Faro	La Palma	Canary Islands	28.798556	-17.879149
<i>Dysdera calderensis</i>	CRBA002336	Roque Faro	La Palma	Canary Islands	28.798556	-17.879149
<i>Dysdera calderensis</i>	CRBA002337	Roque Faro	La Palma	Canary Islands	28.798556	-17.879149
<i>Dysdera calderensis</i>	CRBA002338	Mendo	La Palma	Canary Islands	28.557572	-17.867541
<i>Dysdera calderensis</i>	CRBA002339	Mendo	La Palma	Canary Islands	28.557572	-17.867541
<i>Dysdera calderensis</i>	CRBA002340	Mendo	La Palma	Canary Islands	28.557572	-17.867541
<i>Dysdera calderensis</i>	CRBA002341	El Castillo	La Palma	Canary Islands	28.79636	-17.971169
<i>Dysdera calderensis</i>	CRBA002342	El Castillo	La Palma	Canary Islands	28.79636	-17.971169
<i>Dysdera calderensis</i>	CRBA002343	El Castillo	La Palma	Canary Islands	28.79636	-17.971169
<i>Dysdera calderensis</i>	CRBA002344	El Castillo	La Palma	Canary Islands	28.79636	-17.971169
<i>Dysdera calderensis</i>	CRBA002345	Puerto Santo Domingo de Garafia	La Palma	Canary Islands	28.823215	-17.956515
<i>Dysdera calderensis</i>	CRBA002356	Playa de Taburiente (PNCT)	La Palma	Canary Islands	28.709619	-17.87614
<i>Dysdera calderensis</i>	CRBA002357	Playa de Taburiente (PNCT)	La Palma	Canary Islands	28.709619	-17.87614
<i>Dysdera calderensis</i>	CRBA002359	Playa de Taburiente (PNCT)	La Palma	Canary Islands	28.709619	-17.87614
<i>Dysdera calderensis</i>	CRBA002439	Juan Adalid	La Palma	Canary Islands	28.843639	-17.90635
<i>Dysdera calderensis</i>	CRBA002440	Juan Adalid	La Palma	Canary Islands	28.843639	-17.90635
<i>Dysdera calderensis</i>	CRBA002441	Juan Adalid	La Palma	Canary Islands	28.843639	-17.90635
<i>Dysdera calderensis</i>	CRBA002442	Juan Adalid	La Palma	Canary Islands	28.843639	-17.90635
<i>Dysdera calderensis</i>	CRBA002443	Juan Adalid	La Palma	Canary Islands	28.843639	-17.90635
<i>Dysdera calderensis</i>	CRBA002444	Juan Adalid	La Palma	Canary Islands	28.843639	-17.90635
<i>Dysdera calderensis</i>	CRBA002445	Juan Adalid	La Palma	Canary Islands	28.843639	-17.90635
<i>Dysdera calderensis</i>	CRBA002446	Juan Adalid	La Palma	Canary Islands	28.843639	-17.90635
<i>Dysdera calderensis</i>	CRBA002447	Juan Adalid	La Palma	Canary Islands	28.843639	-17.90635
<i>Dysdera calderensis</i>	CRBA002448	Juan Adalid	La Palma	Canary Islands	28.843639	-17.90635
<i>Dysdera calderensis</i>	CRBA002449	Juan Adalid	La Palma	Canary Islands	28.843639	-17.90635
<i>Dysdera calderensis</i>	CRBA002450	Juan Adalid	La Palma	Canary Islands	28.843639	-17.90635
<i>Dysdera calderensis</i>	CRBA002451	Juan Adalid	La Palma	Canary Islands	28.843639	-17.90635
<i>Dysdera calderensis</i>	CRBA002452	Juan Adalid	La Palma	Canary Islands	28.843639	-17.90635

<i>Dysdera</i>	<i>calderensis</i>	CRBA003587	El Castillo	La Palma	Canary Islands	28.79636	-17.971169
<i>Dysdera</i>	<i>calderensis</i>	CRBA003588	El Castillo	La Palma	Canary Islands	28.79636	-17.971169
<i>Dysdera</i>	<i>calderensis</i>	CRBA003594	Juan Adalid	La Palma	Canary Islands	28.843639	-17.90635
<i>Dysdera</i>	<i>calderensis</i>	CRBA003595	Juan Adalid	La Palma	Canary Islands	28.843639	-17.90635
<i>Dysdera</i>	<i>calderensis</i>	CRBA003599	Juan Adalid	La Palma	Canary Islands	28.843639	-17.90635
<i>Dysdera</i>	<i>calderensis</i>	CRBA003600	Juan Adalid	La Palma	Canary Islands	28.843639	-17.90635
<i>Dysdera</i>	<i>calderensis</i>	CRBA003601	Juan Adalid	La Palma	Canary Islands	28.843639	-17.90635
<i>Dysdera</i>	<i>calderensis</i>	CRBA003602	Juan Adalid	La Palma	Canary Islands	28.843639	-17.90635
<i>Dysdera</i>	<i>calderensis</i>	CRBA003603	Juan Adalid	La Palma	Canary Islands	28.843639	-17.90635
<i>Dysdera</i>	<i>calderensis</i>	CRBA003604	Juan Adalid	La Palma	Canary Islands	28.843639	-17.90635
<i>Dysdera</i>	<i>calderensis</i>	CRBA003605	Juan Adalid	La Palma	Canary Islands	28.843639	-17.90635
<i>Dysdera</i>	<i>calderensis</i>	CRBA003606	Juan Adalid	La Palma	Canary Islands	28.843639	-17.90635
<i>Dysdera</i>	<i>calderensis</i>	CRBA003607	Juan Adalid	La Palma	Canary Islands	28.843639	-17.90635
<i>Dysdera</i>	<i>calderensis</i>	CRBA003608	Juan Adalid	La Palma	Canary Islands	28.843639	-17.90635
<i>Dysdera</i>	<i>calderensis</i>	NMH001390	Espigón Atravesado. Los Tilos	La Palma	Canary Islands	28.782012	-17.816332
<i>Dysdera</i>	<i>calderensis</i>	NMH001391	Espigón Atravesado. Los Tilos	La Palma	Canary Islands	28.782012	-17.816332
<i>Dysdera</i>	<i>calderensis</i>	NMH001392	Espigón Atravesado. Los Tilos	La Palma	Canary Islands	28.782012	-17.816332
<i>Dysdera</i>	<i>calderensis</i>	NMH001393	Espigón Atravesado. Los Tilos	La Palma	Canary Islands	28.782012	-17.816332
<i>Dysdera</i>	<i>calderensis</i>	NMH001394	Espigón Atravesado. Los Tilos	La Palma	Canary Islands	28.782012	-17.816332
<i>Dysdera</i>	<i>calderensis</i>	NMH001401	Pinar de Roque Faro	La Palma	Canary Islands	28.798556	-17.879149
<i>Dysdera</i>	<i>calderensis</i>	NMH001402	Pinar de Roque Faro	La Palma	Canary Islands	28.798556	-17.879149
<i>Dysdera</i>	<i>calderensis</i>	NMH001403	Pinar de Roque Faro	La Palma	Canary Islands	28.798556	-17.879149
<i>Dysdera</i>	<i>calderensis</i>	NMH001404	Pinar de Roque Faro	La Palma	Canary Islands	28.798556	-17.879149
<i>Dysdera</i>	<i>calderensis</i>	NMH001405	Pinar de Roque Faro	La Palma	Canary Islands	28.798556	-17.879149
<i>Dysdera</i>	<i>calderensis</i>	NMH001406	Pinar de Roque Faro	La Palma	Canary Islands	28.798556	-17.879149
<i>Dysdera</i>	<i>calderensis</i>	NMH001407	Pinar de Roque Faro	La Palma	Canary Islands	28.798556	-17.879149
<i>Dysdera</i>	<i>calderensis</i>	NMH001408	Juan Adalid	La Palma	Canary Islands	28.843639	-17.90635
<i>Dysdera</i>	<i>calderensis</i>	NMH001409	Juan Adalid	La Palma	Canary Islands	28.843639	-17.90635
<i>Dysdera</i>	<i>calderensis</i>	NMH001410	Juan Adalid	La Palma	Canary Islands	28.843639	-17.90635
<i>Dysdera</i>	<i>calderensis</i>	NMH001411	Juan Adalid	La Palma	Canary Islands	28.843639	-17.90635
<i>Dysdera</i>	<i>calderensis</i>	NMH001412	Juan Adalid	La Palma	Canary Islands	28.843639	-17.90635
<i>Dysdera</i>	<i>calderensis</i>	NMH001413	Juan Adalid	La Palma	Canary Islands	28.843639	-17.90635
<i>Dysdera</i>	<i>calderensis</i>	NMH001414	Juan Adalid	La Palma	Canary Islands	28.843639	-17.90635
<i>Dysdera</i>	<i>calderensis</i>	UB2544_104	Cueva de los Arreboles	La Palma	Canary Islands	28.493785	-17.82903

<i>Dysdera</i>	<i>calderensis</i>	UB2587_106	Cueva de los Arreboles	La Palma	Canary Islands	28.493785	-17.82903
<i>Dysdera</i>	<i>calderensis</i>	UB2757	Juan Adalid	La Palma	Canary Islands	28.843639	-17.90635
<i>Dysdera</i>	<i>calderensis</i>	UB2758	Juan Adalid	La Palma	Canary Islands	28.843639	-17.90635
<i>Dysdera</i>	<i>calderensis</i>	UB2813	Juan Adalid	La Palma	Canary Islands	28.843639	-17.90635
<i>Dysdera</i>	<i>calderensis</i>	UB2814	Juan Adalid	La Palma	Canary Islands	28.843639	-17.90635
<i>Dysdera</i>	<i>calderensis</i>	UB2944 (4009 freezer)	Pista de Machin	La Palma	Canary Islands	28.78971	-17.896884
<i>Dysdera</i>	<i>calderensis</i>	UB2951	Los Tilos	La Palma	Canary Islands	28.783702	-17.808408
<i>Dysdera</i>	<i>calderensis</i>	UB2953	Juan Adalid	La Palma	Canary Islands	28.843639	-17.90635
<i>Dysdera</i>	<i>calderensis</i>	UB2955	Juan Adalid	La Palma	Canary Islands	28.843639	-17.90635
<i>Dysdera</i>	<i>calderensis</i>	UB2957	Juan Adalid	La Palma	Canary Islands	28.843639	-17.90635
<i>Dysdera</i>	<i>calderensis</i>	UB2959	Pista de Machin	La Palma	Canary Islands	28.78971	-17.896884
<i>Dysdera</i>	<i>calderensis</i>	UB2961 (4010)	Pista de Machin	La Palma	Canary Islands	28.78971	-17.896884
<i>Dysdera</i>	<i>calderensis</i>	UB2962	Pista de Machin	La Palma	Canary Islands	28.78971	-17.896884
<i>Dysdera</i>	<i>calderensis</i>	UB3140_133 (freezer)	Llano Los Caños	La Palma	Canary Islands	28.580523	-17.799465
<i>Dysdera</i>	<i>calderensis</i>	UB3180_135	Cueva de los Arreboles	La Palma	Canary Islands	28.493785	-17.82903
<i>Dysdera</i>	<i>calderensis</i>	UB3202_136	Juan Adalid	La Palma	Canary Islands	28.843639	-17.90635
<i>Dysdera</i>	<i>calderensis</i>	UB3203_136	Juan Adalid	La Palma	Canary Islands	28.843639	-17.90635
<i>Dysdera</i>	<i>calderensis</i>	UB4009_Freezer 4 (2944)	Pista de Machin	La Palma	Canary Islands	28.78971	-17.896884
<i>Dysdera</i>	<i>calderensis</i>	UB4010_(2961)	Pista de Machin	La Palma	Canary Islands	28.78971	-17.896884
<i>Dysdera</i>	<i>calderensis</i>	UB4011_Freezer	Juan Adalid	La Palma	Canary Islands	28.843639	-17.90635
<i>Dysdera</i>	<i>calderensis</i>	UB4012_Freezer	Juan Adalid	La Palma	Canary Islands	28.843639	-17.90635
<i>Dysdera</i>	<i>calderensis</i>	UB4013_Freezer	Juan Adalid	La Palma	Canary Islands	28.843639	-17.90635
<i>Dysdera</i>	<i>calderensis</i>	UB4014_Freezer	Juan Adalid	La Palma	Canary Islands	28.843639	-17.90635
<i>Dysdera</i>	<i>calderensis</i>	UB4016 (4014)_Freezer	Juan Adalid	La Palma	Canary Islands	28.843639	-17.90635
<i>Dysdera</i>	<i>calderensis</i>	UB4017_Freezer	Juan Adalid	La Palma	Canary Islands	28.843639	-17.90635
<i>Dysdera</i>	<i>calderensis</i>	UB4018_Freezer	Juan Adalid	La Palma	Canary Islands	28.843639	-17.90635
<i>Dysdera</i>	<i>calderensis</i>	UB4175_Freezer	Lomo María	La Palma	Canary Islands	28.554734	-17.861913
<i>Dysdera</i>	<i>calderensis</i>	CRBA001863	Barranco de los Castradores	La Gomera	Canary Islands	28.09618	-17.20142
<i>Dysdera</i>	<i>calderensis</i>	CRBA002730	La Mérica	La Gomera	Canary Islands	28.11577	-17.33604
<i>Dysdera</i>	<i>calderensis</i>	NMH001446	Mña. de las Pilas, Cno. La Mérica	La Gomera	Canary Islands	28.113296	-17.335703
<i>Dysdera</i>	<i>calderensis</i>	NMH003236	Mña. de las Pilas, Cno. La Mérica	La Gomera	Canary Islands	28.113296	-17.335703
<i>Dysdera</i>	<i>calderensis</i>	NMH003237	Mña. de las Pilas, Cno. La Mérica	La Gomera	Canary Islands	28.113296	-17.335703
<i>Dysdera</i>	<i>calderensis</i>	NMH003252	Monte del Cedro	La Gomera	Canary Islands	28.119283	-17.23729
<i>Dysdera</i>	<i>calderensis</i>	CRBA001452	Barranco de Juel	La Gomera	Canary Islands	28.151547	-17.162962

<i>Dysdera</i>	<i>calderensis</i>	CRBA001841	Teselinde. Ermita de Santa Clara	La Gomera	Canary Islands	28.1963	-17.28754
<i>Dysdera</i>	<i>calderensis</i>	CRBA002751	Teselinde. Ermita de Santa Clara	La Gomera	Canary Islands	28.1963	-17.28754
<i>Dysdera</i>	<i>calderensis</i>	CRBA002757	Teselinde. Ermita de Santa Clara	La Gomera	Canary Islands	28.1963	-17.28754
<i>Dysdera</i>	<i>calderensis</i>	CRBA003628	Ptra. Cumbre, altura Mora Gaspar	La Gomera	Canary Islands	28.14614	-17.262784
<i>Dysdera</i>	<i>calderensis</i>	CRBA003638	Teselinde. Ermita de Santa Clara	La Gomera	Canary Islands	28.1963	-17.28754
<i>Dysdera</i>	<i>calderensis</i>	CRBA003701	Teselinde. Ermita de Santa Clara	La Gomera	Canary Islands	28.1963	-17.28754
<i>Dysdera</i>	<i>calderensis</i>	CRBA003731	Teselinde. Ermita de Santa Clara	La Gomera	Canary Islands	28.1963	-17.28754
<i>Dysdera</i>	<i>calderensis</i>	CRBA003905	La Miérca	La Gomera	Canary Islands	28.11577	-17.33604
<i>Dysdera</i>	<i>calderensis</i>	CRBA003907	La Miérca	La Gomera	Canary Islands	28.11577	-17.33604
<i>Dysdera</i>	<i>calderensis</i>	NMH001438	Riscos de Alojera	La Gomera	Canary Islands	28.16286	-17.318101
<i>Dysdera</i>	<i>calderensis</i>	NMH001796	Teselinde. Ermita de Santa Clara	La Gomera	Canary Islands	28.1963	-17.28754
<i>Dysdera</i>	<i>calderensis</i>	NMH001797	Teselinde. Ermita de Santa Clara	La Gomera	Canary Islands	28.1963	-17.28754
<i>Dysdera</i>	<i>calderensis</i>	NMH001804	Agua de los Llanos	La Gomera	Canary Islands	28.155715	-17.246339
<i>Dysdera</i>	<i>calderensis</i>	NMH001805	Reventón Oscuro. Bosque del Cedro	La Gomera	Canary Islands	28.125809	-17.216616
<i>Dysdera</i>	<i>calderensis</i>	NMH002255	Teselinde. Ermita de Santa Clara	La Gomera	Canary Islands	28.1963	-17.28754
<i>Dysdera</i>	<i>calderensis</i>	NMH002260	Teselinde. Ermita de Santa Clara	La Gomera	Canary Islands	28.1963	-17.28754
<i>Dysdera</i>	<i>calderensis</i>	NMH002522	Teselinde. Ermita de Santa Clara	La Gomera	Canary Islands	28.1963	-17.28754
<i>Dysdera</i>	<i>calderensis</i>	NMH002523	Teselinde. Ermita de Santa Clara	La Gomera	Canary Islands	28.1963	-17.28754
<i>Dysdera</i>	<i>calderensis</i>	NMH002624	Teselinde. Ermita de Santa Clara	La Gomera	Canary Islands	28.1963	-17.28754
<i>Dysdera</i>	<i>calderensis</i>	NMH003256	Epina	La Gomera		28.09592	-17.18206
<i>Dysdera</i>	<i>calderensis</i>	UB2893	Monte de Juan Tomé. La Laja	La Gomera	Canary Islands	28.123022	-17.210137
<i>Dysdera</i>	<i>calderensis</i>	UB2918	Plain Land between Barranco Higuera and Barranco San Juan.	La Gomera	Canary Islands	28.19332	-17.29294
<i>Dysdera</i>	<i>calderensis</i>	UB2921	Plain Land between Barranco Higuera and Barranco San Juan.	La Gomera	Canary Islands	28.19332	-17.29294
<i>Dysdera</i>	<i>calderensis</i>	UB2922	Plain Land between Barranco Higuera and Barranco San Juan.	La Gomera	Canary Islands	28.19332	-17.29294
<i>Dysdera</i>	<i>calderensis</i>	UB2945	Chorros de Epina	La Gomera	Canary Islands	28.167036	-17.305892
<i>Dysdera</i>	<i>calderensis</i>	UB4118 (2)_Freezer	Monte de Juan Tomé. La Laja	La Gomera	Canary Islands	28.123022	-17.210137
<i>Dysdera</i>	<i>calderensis</i>	UB4131 (48)_Freezer	Barranco Aramaqué. Near Los Acevifios	La Gomera	Canary Islands	28.149151	-17.220779
<i>Dysdera</i>	<i>calderensis</i>	UB4146 (93)_Freezer	Plain Land between Barranco Higuera and Barranco San Juan.	La Gomera	Canary Islands	28.19332	-17.29294
<i>Dysdera</i>	<i>calderensis</i>	UB4160 (114)_Freezer	Barranco de Juel	La Gomera	Canary Islands	28.151547	-17.162962
<i>Dysdera</i>	<i>calderensis</i>	UB4165 (119)_Freezer	Barranco de Juel	La Gomera	Canary Islands	28.151547	-17.162962
<i>Dysdera</i>	<i>calderensis</i>	UB4167 (122)_Freezer	Barranco de Juel	La Gomera	Canary Islands	28.151547	-17.162962

Table S2. Estimates of Evolutionary Divergence over Sequence Pairs between Groups. The number of base differences per site from averaging over all sequence pairs between groups are shown. Standard error estimate(s) are shown above the diagonal. This analysis involved 129 nucleotide sequences. All ambiguous positions were removed for eac.

	D. calderensis				D. gomerensis					D. silvatica			
	calG_8	calG_11	calP_9	calP_10	gomG_1	gomG_2	gomG_3	gomH_4	gomH_13	silG_7	silH_5	silP_6	silP_12
calG_8	0.008	0.008	0.007	0.008	0.014	0.014	0.014	0.014	0.014	0.015	0.014	0.015	0.014
calG_11	0.043	0.009	0.008	0.009	0.013	0.014	0.013	0.014	0.013	0.015	0.014	0.014	0.014
calP_9	0.045	0.055	0.022	0.006	0.013	0.013	0.013	0.013	0.012	0.014	0.014	0.014	0.014
calP_10	0.05	0.061	0.041	0.019	0.012	0.013	0.012	0.013	0.012	0.014	0.013	0.014	0.013
gomG_1	0.14	0.129	0.13	0.131	0.007	0.009	0.008	0.011	0.01	0.014	0.014	0.014	0.014
gomG_2	0.143	0.13	0.139	0.14	0.048	0.041	0.007	0.01	0.011	0.015	0.015	0.015	0.015
gomG_3	0.136	0.129	0.136	0.129	0.048	0.041	0.013	0.011	0.011	0.015	0.015	0.015	0.015
gomH_4	0.146	0.134	0.138	0.141	0.083	0.074	0.087	0.036	0.006	0.015	0.015	0.015	0.015
gomH_13	0.147	0.14	0.142	0.138	0.083	0.085	0.09	0.036	0.022	0.014	0.015	0.015	0.014
silG_7	0.157	0.158	0.149	0.149	0.155	0.166	0.171	0.151	0.153	0.008	0.009	0.011	0.011
silH_5	0.152	0.159	0.148	0.151	0.164	0.165	0.172	0.156	0.161	0.061	0.015	0.011	0.01
silP_6	0.146	0.148	0.15	0.148	0.154	0.162	0.164	0.148	0.152	0.083	0.089	0.001	0.006
silP_12	0.146	0.143	0.143	0.144	0.146	0.161	0.165	0.139	0.146	0.084	0.087	0.025	0.008
	0.06				0.09					0.09			
	G	P			G	H				G	P	H	
	0.04	0.04			0.05	0.036				0.008	0.025	0.015	

Table S3. Isotopic signatures for the specimens used in the trophic analyses.

Collection code	Isobp code	Sex	Collected by	DateCollected (Start)	Locality Name	State/Prov	Latitude	Longitude	Species	d13C	d15N
CFBA002739	ST/A10	♂	Amedo, Bellvert & Oromi	3/17/2017	Tesselde. Ermita de Santa Clara	La Gomera	28.1963	-17.28754	D. gomerensis	4.00991961	-24.74499604
CFBA002740	AB2/B5	♂	Amedo, Bellvert & Oromi	3/17/2017	Tesselde. Ermita de Santa Clara	La Gomera	28.1963	-17.28754	D. silvatica	8.672894816	-23.46632932
CFBA002746	PR/A06	♂	Amedo, Bellvert & Oromi	3/17/2017	Tesselde. Ermita de Santa Clara	La Gomera	28.1963	-17.28754	D. gomerensis	3.39674489	-24.31917368
CFBA002751	ST/A1	♀	Amedo, Bellvert & Oromi	3/17/2017	Tesselde. Ermita de Santa Clara	La Gomera	28.1963	-17.28754	D. calderensis	5.721135469	-25.60994871
CFBA002757	AB2/B2	♂	Amedo, Bellvert & Oromi	3/17/2017	Tesselde. Ermita de Santa Clara	La Gomera	28.1963	-17.28754	D. calderensis	5.334144941	-24.74843568
CFBA002759	PR/A07	♂	Amedo, Bellvert & Oromi	3/17/2017	Tesselde. Ermita de Santa Clara	La Gomera	28.1963	-17.28754	D. gomerensis	3.811743247	-24.60518166
CFBA002763	AB2/A3	♂	Amedo, Bellvert & Oromi	3/17/2017	Tesselde. Ermita de Santa Clara	La Gomera	28.1963	-17.28754	D. silvatica	4.530004371	-24.99372612
CFBA002765	ST/A11	♂	Amedo, Bellvert & Oromi	3/17/2017	Tesselde. Ermita de Santa Clara	La Gomera	28.1963	-17.28754	D. gomerensis	4.436926919	-25.18288448
CFBA002769	ST/A12	♀	Amedo, Bellvert & Oromi	3/17/2017	Tesselde. Ermita de Santa Clara	La Gomera	28.1963	-17.28754	D. gomerensis	4.116140334	-25.43380932
CFBA002770	AB2/A8	♂	Amedo, Bellvert & Oromi	3/17/2017	Tesselde. Ermita de Santa Clara	La Gomera	28.1963	-17.28754	D. silvatica	5.441711796	-25.385366633
CFBA002791	PR/A08	♀	Amedo, Bellvert & Oromi	3/17/2017	Tesselde. Ermita de Santa Clara	La Gomera	28.1963	-17.28754	D. gomerensis	4.202970816	-24.44741925
CFBA002799	PR/A09	♂	Amedo, Bellvert & Oromi	3/18/2017	Barranco de Juel, East	La Gomera	28.14832	-17.15772	D. gomerensis	5.298408008	-25.4866155
CFBA002805	PR/A10	♀	Amedo, Bellvert & Oromi	3/18/2017	Barranco de Juel, East	La Gomera	28.14832	-17.15772	D. gomerensis	4.457516348	-25.11612829
CFBA002814	ST/B1	♀	Amedo, Bellvert & Oromi	3/18/2017	Barranco de Juel, East	La Gomera	28.14832	-17.15772	D. gomerensis	4.381692143	-26.71500202
CFBA002818	PR/A11	♀	Amedo, Bellvert & Oromi	3/18/2017	Barranco de Juel, East	La Gomera	28.14832	-17.15772	D. gomerensis	4.913123137	-25.54361353
CFBA002819	ST/B2	♂	Amedo, Bellvert & Oromi	3/18/2017	Barranco de Juel, East	La Gomera	28.14832	-17.15772	D. gomerensis	4.560142959	-26.3873237
CFBA002840	ST/A9	♂	Fozas	3/22/2017	Mirador de Bascos	El Hierro	27.754861	-18.118218	D. gomerensis	5.133734867	-25.22814935
CFBA002841	ST/G7	♂	Amedo, Bellvert & Fozas	3/22/2017	Mirador de Bascos	El Hierro	27.754861	-18.118218	D. gomerensis	7.402209616	-24.15471425
CFBA002849	ST/A5	♀	Amedo, Bellvert & Fozas	3/22/2017	Mirador de Bascos	El Hierro	27.754861	-18.118218	D. gomerensis	4.622813186	-24.94081581
CFBA002850	ST/A4	♀	Amedo, Bellvert & Fozas	3/22/2017	Mirador de Bascos	El Hierro	27.754861	-18.118218	D. gomerensis	3.205828732	-24.81092531
CFBA002855	ST/A3	♂	Amedo, Bellvert & Fozas	3/22/2017	Mirador de Bascos	El Hierro	27.754861	-18.118218	D. gomerensis	7.456782094	-25.80084839

CRBA002857	ST/A8	♂	Arnedo, Bellvert & Rozas	3/22/2017	Mirador de Bascos	El Hierro	27.754861	-18.118218	D. gomerensis	8.032498416	-25.67981406
CRBA002858	PR/C05	♂	Arnedo, Bellvert & Rozas	3/22/2017	Mirador de Bascos	El Hierro	27.754861	-18.118218	D. silvatica	5.933745058	-25.42467605
CRBA002859	PR/C06	♂	Arnedo, Bellvert & Rozas	3/22/2017	Mirador de Bascos	El Hierro	27.754861	-18.118218	D. silvatica	6.401887387	-25.33605619
CRBA002860	PR/C07	♂	Arnedo, Bellvert & Rozas	3/22/2017	Mirador de Bascos	El Hierro	27.754861	-18.118218	D. silvatica	5.341565018	-25.80231752
CRBA002866	ST/A2	♀	Arnedo, Bellvert & Rozas	3/22/2017	Mirador de Bascos	El Hierro	27.754861	-18.118218	D. silvatica	6.364833054	-25.575580805
CRBA002867	ST/A6	♀	Arnedo, Bellvert & Rozas	3/22/2017	Mirador de Bascos	El Hierro	27.754861	-18.118218	D. silvatica	5.208088373	-25.43971343
CRBA002868	ST/A7	♀	Arnedo, Bellvert & Rozas	3/22/2017	Mirador de Bascos	El Hierro	27.754861	-18.118218	D. silvatica	4.175623939	-26.00257228
CRBA002869	ST/B3	♀	Arnedo, Bellvert & Rozas	3/22/2017	Mirador de Bascos	El Hierro	27.754861	-18.118218	D. silvatica	5.862409031	-24.38681313
CRBA002870	ST/B4	♀	Arnedo, Bellvert & Rozas	3/22/2017	Mirador de Bascos	El Hierro	27.754861	-18.118218	D. silvatica	3.319484906	-25.10317894
CRBA002877	PR/A12	♀	Arnedo, Bellvert & Rozas	3/22/2017	Mirador de Bascos	El Hierro	27.754861	-18.118218	D. silvatica	4.384223082	-24.10644888
CRBA002884	PR/C08	♂	Arnedo, Bellvert & Rozas	3/23/2017	Pista Garoé	El Hierro	27.781744	-17.951391	D. gomerensis	9.195736801	-24.71773122
CRBA002885	PR/C09	♂	Arnedo, Bellvert & Rozas	3/23/2017	Pista Garoé	El Hierro	27.781744	-17.951391	D. gomerensis	8.603556676	-24.81037926
CRBA002886	ST/G4	♀	Arnedo, Bellvert & Rozas	3/23/2017	Pista Garoé	El Hierro	27.781744	-17.951391	D. gomerensis	7.408256895	-25.38248767
CRBA002888	ST/G5	♀	Arnedo, Bellvert & Rozas	3/23/2017	Pista Garoé	El Hierro	27.781744	-17.951391	D. gomerensis	7.304445273	-24.60847843
CRBA003555	AB6/A11	♀	Arnedo & Bellvert	17/3/2019	Pinar de Roque Faro	La Palma	28.798556	-17.879149	D. silvatica	5.829184148	-26.84098172
CRBA003556	AB6/A12	♀	Arnedo & Bellvert	17/3/2019	Pinar de Roque Faro	La Palma	28.798556	-17.879149	D. silvatica	4.67854237	-25.67645814
CRBA003557	AB6/B01	♂	Arnedo & Bellvert	17/3/2019	Pinar de Roque Faro	La Palma	28.798556	-17.879149	D. silvatica	3.880386926	-25.52057703
CRBA003559	AB6/C07	♀	Arnedo & Bellvert	17/3/2019	Pinar de Roque Faro	La Palma	28.798556	-17.879149	D. silvatica	4.440513482	-26.23477741
CRBA003560	AB6/D07	♀	Arnedo & Bellvert	17/3/2019	Pinar de Roque Faro	La Palma	28.798556	-17.879149	D. silvatica	4.671452148	-26.40186566
CRBA003561	AB6/C01	♀	Arnedo & Bellvert	17/3/2019	Pinar de Roque Faro	La Palma	28.798556	-17.879149	D. silvatica	5.412886815	-25.45639069
CRBA003562	AB6/D02	♂	Arnedo & Bellvert	17/3/2019	Pinar de Roque Faro	La Palma	28.798556	-17.879149	D. silvatica	6.257636149	-24.8573182
CRBA003568	AB6/C12	♀	Arnedo & Bellvert	17/3/2019	Pinar de Roque Faro	La Palma	28.798556	-17.879149	D. calderensis	6.11988326	-25.94542947
CRBA003569	AB6/D03	♀	Arnedo & Bellvert	17/3/2019	Pinar de Roque Faro	La Palma	28.798556	-17.879149	D. calderensis	5.436183259	-26.61582012

CRBA003570	AB6/C08	♀	Arnedo & Bellvert	17/3/2019	Pinar de Roque Faro	La Palma	28.798556	-17.879149	D. calderensis	3.363812592	-24.69430627
CRBA003571	AB6/D05	♀	Arnedo & Bellvert	17/3/2019	Pinar de Roque Faro	La Palma	28.798556	-17.879149	D. calderensis	4.56003437	-26.82875576
CRBA003572	AB6/C06	♀	Arnedo & Bellvert	17/3/2019	Pinar de Roque Faro	La Palma	28.798556	-17.879149	D. calderensis	5.109020148	-26.36518775
CRBA003576	AB6/C04	♂	Arnedo & Bellvert	17/3/2019	Pinar de Roque Faro	La Palma	28.798556	-17.879149	D. calderensis	5.131303704	-26.0921411
CRBA003577	AB6/B09	♂	Arnedo & Bellvert	17/3/2019	Pinar de Roque Faro	La Palma	28.798556	-17.879149	D. calderensis	5.543549482	-26.16549692
CRBA003578	AB6/B10	♂	Arnedo & Bellvert	17/3/2019	Pinar de Roque Faro	La Palma	28.798556	-17.879149	D. calderensis	4.645117037	-26.68917594
CRBA003579	AB6/D04	♂	Arnedo & Bellvert	17/3/2019	Pinar de Roque Faro	La Palma	28.798556	-17.879149	D. silvatica	3.872282815	-27.43903539
CRBA003637	AB6/C09	♂	Doménech & Ormí	21/3/2019	Santa Clara	La Gomera	28.1963	-17.28754	D. gomerenis	6.334615704	-25.06006552
CRBA003638	AB1/B7	♀	Arnedo, Bellvert,	21/3/2019	Tesellinde. Ermita de	La Gomera	28.1963	-17.28754	D. calderensis	5.351316979	-25.95162701
CRBA003645	AB6/C10	♀	Doménech & Ormí	21/3/2019	Santa Clara	La Gomera	28.1963	-17.28754	D. gomerenis	5.695482815	-25.30152842
CRBA003646	AB6/D01	♀	Arnedo, Bellvert,	21/3/2019	Tesellinde. Ermita de	La Gomera	28.1963	-17.28754	D. gomerenis	5.438209037	-25.74268214
CRBA003658	AB6/C02	♂	Arnedo, Bellvert,	21/3/2019	Santa Clara	La Gomera	28.1963	-17.28754	D. silvatica	4.180201037	-26.2938696
CRBA003662	AB6/C11	♀	Arnedo, Bellvert,	21/3/2019	Santa Clara	La Gomera	28.1963	-17.28754	D. gomerenis	4.603588593	-24.26333985
CRBA003663	AB6/C05	♀	Arnedo, Bellvert,	21/3/2019	Santa Clara	La Gomera	28.1963	-17.28754	D. gomerenis	4.761599259	-25.28217063
CRBA003664	AB6/C03	♀	Arnedo, Bellvert,	21/3/2019	Santa Clara	La Gomera	28.1963	-17.28754	D. gomerenis	5.360216593	-24.60362933
CRBA003665	AB6/D08	♀	Arnedo, Bellvert,	21/3/2019	Santa Clara	La Gomera	28.1963	-17.28754	D. gomerenis	4.975318815	-25.311069789
CRBA003665	AB6/D09	♂	Arnedo, Bellvert,	21/3/2019	Santa Clara	La Gomera	28.1963	-17.28754	D. gomerenis	5.216386371	-25.36979008
CRBA003700	AB6/D10	♂	Arnedo, Bellvert,	21/3/2019	Santa Clara	La Gomera	28.1963	-17.28754	D. silvatica	4.174123704	-24.76256693
CRBA003701	AB1/B3	♀	Arnedo, Bellvert,	21/3/2019	Santa Clara	La Gomera	28.1963	-17.28754	D. calderensis	4.719141202	-24.739007117
CRBA003704	AB6/D11	♂	Arnedo, Bellvert,	21/3/2019	Santa Clara	La Gomera	28.1963	-17.28754	D. gomerenis	4.171086037	-24.95308829
CRBA003714	AB1/B4	♀	Arnedo, Bellvert,	21/3/2019	Santa Clara	La Gomera	28.1963	-17.28754	D. silvatica	5.406789357	-24.45290483
CRBA003718	AB1/B10	♀	Arnedo, Bellvert,	21/3/2019	Santa Clara	La Gomera	28.1963	-17.28754	D. silvatica	4.941030713	-24.76626826
CRBA003724	AB1/B6	♀	Arnedo, Bellvert,	21/3/2019	Santa Clara	La Gomera	28.1963	-17.28754	D. silvatica	4.6437825	-24.50875178

CRBA003730	AB6E05	♀	Arnedo, Bellvert, Domènech & Oromí	21/3/2019	Tesellinde. Ermita de Santa Clara	La Gomera	28.1963	-17.28754	D. silvatica	3.99484237	-24.61177998
CRBA003731	AB1/A9	♀	Arnedo, Bellvert, Domènech & Oromí	20/3/2019	Tesellinde. Ermita de Santa Clara	La Gomera	28.1963	-17.28754	D. calderensis	6.069317945	-25.18925718
CRBA003736	AB6E06	♀	Arnedo, Bellvert, Domènech & Oromí	21/3/2019	Tesellinde. Ermita de Santa Clara	La Gomera	28.1963	-17.28754	D. silvatica	4.091066815	-25.48797445
CRBA003741	AB6E07	♂	Arnedo, Bellvert, Domènech & Oromí	21/3/2019	Tesellinde. Ermita de Santa Clara	La Gomera	28.1963	-17.28754	D. gomerensis	5.351100593	-24.330568268
CRBA003742	AB6E08	♂	Arnedo, Bellvert, Domènech & Oromí	21/3/2019	Tesellinde. Ermita de Santa Clara	La Gomera	28.1963	-17.28754	D. silvatica	5.425041482	-25.48389913
CRBA003808	AB6F12	♂	Arnedo, Bellvert, Domènech & Oromí	23/3/2019	Las Hayas	La Gomera	28.133622	-17.282405	D. silvatica	5.753696448	-23.995989322
CRBA003809	AB6E11	♂	Arnedo, Bellvert, Domènech & Oromí	23/3/2019	Las Hayas	La Gomera	28.133622	-17.282405	D. silvatica	3.922927259	-26.11557421
CRBA003910	AB6E12	♂	Arnedo, Bellvert, Domènech & Oromí	23/3/2019	Las Hayas	La Gomera	28.133622	-17.282405	D. silvatica	7.070986926	-24.64540139
CRBA003911	AB6F01	♂	Arnedo, Bellvert, Domènech & Oromí	23/3/2019	Las Hayas	La Gomera	28.133622	-17.282405	D. silvatica	6.090662044	-25.72197819
CRBA003912	AB6F02	♂	Arnedo, Bellvert, Domènech & Oromí	23/3/2019	Las Hayas	La Gomera	28.133622	-17.282405	D. silvatica	6.462240421	-24.79817745
CRBA003913	AB6G01	♀	Arnedo, Bellvert, Domènech & Oromí	23/3/2019	Las Hayas	La Gomera	28.133622	-17.282405	D. silvatica	5.86466095	-24.42416078
CRBA003914	AB6F03	♀	Arnedo, Bellvert, Domènech & Oromí	23/3/2019	Las Hayas	La Gomera	28.133622	-17.282405	D. silvatica	6.380798585	-24.44357695
CRBA003915	AB6F04	♀	Arnedo, Bellvert, Domènech & Oromí	23/3/2019	Las Hayas	La Gomera	28.133622	-17.282405	D. silvatica	6.730998479	-23.97350135
CRBA003916	AB6F05	♀	Arnedo, Bellvert, Domènech & Oromí	23/3/2019	Las Hayas	La Gomera	28.133622	-17.282405	D. silvatica	4.53919507	-24.84722882

Table S4. Specimens used for the morphometric analyses.

Collection code	Sex	Date Collected (Start)	Locality Name	State/Prov	Latitude	Longitude	Species Name
NIMH000379	♀	12/9/2004	Meseta de Concheta, La Catedral	Lanzarote	29.399590	-13.526570	<i>D. aleggranzaensis</i>
UB2858	♂	2/22/1995	Mirador del Río	Lanzarote	29.211204	-13.484156	<i>D. aleggranzaensis</i>
UB2859	♂	2/22/1995	Mirador del Río	Lanzarote	29.211204	-13.484156	<i>D. aleggranzaensis</i>
CFBA002682	♀	3/14/2017	Montaña Blanca	Lanzarote	28.980257	-13.638351	<i>D. aleggranzaensis</i>
CFBA002667	♀	3/13/2017	Montaña Tinache	Lanzarote	29.051850	-13.669850	<i>D. aleggranzaensis</i>
CFBA002665	♂	3/13/2017	Montaña Tinache	Lanzarote	29.051850	-13.669850	<i>D. aleggranzaensis</i>
CFBA002670	♂	3/13/2017	Montaña Tinache	Lanzarote	29.051850	-13.669850	<i>D. aleggranzaensis</i>
CFBA002672	♂	3/13/2017	Montaña Tinache	Lanzarote	29.051850	-13.669850	<i>D. aleggranzaensis</i>
CFBA000694	♀	12/27/2000	Bairranco Oscuro	Gran Canaria	28.067250	-15.589010	<i>D. andamanae</i>
CFBA003448	♀	13/8/2019	Brezal del Palmital	Gran Canaria	28.111450	-15.601970	<i>D. andamanae</i>
CFBA000692	♂	4/27/2004	Brezal del Palmital	Gran Canaria	28.111450	-15.601970	<i>D. andamanae</i>
NIMH001954	♂	4/1/2012	Cañadade los Alvarados (Degollada de Becerra)	Gran Canaria	27.994244	-15.594384	<i>D. arabisenren</i>
NIMH002064	♀	4/21/2012	Cuevas Blancas	Gran Canaria	27.964562	-15.546639	<i>D. arabisenren</i>
UB3025_127freezer	♀	2/11/1996	Cumbre de Pajonales	Gran Canaria	27.943295	-15.678000	<i>D. arabisenren</i>
UB3027_127freezer	♀	2/11/1996	Cumbre de Pajonales	Gran Canaria	27.943295	-15.678000	<i>D. arabisenren</i>
UB2993	♀	2/9/1996	El Pinatillo	Gran Canaria			<i>D. arabisenren</i>
UB2995	♀	2/9/1996	El Pinatillo	Gran Canaria			<i>D. arabisenren</i>
UB2996	♀	2/9/1996	El Pinatillo	Gran Canaria			<i>D. arabisenren</i>
UB2997	♀	2/9/1996	El Pinatillo	Gran Canaria			<i>D. arabisenren</i>
UB3030_127freezer	♀	2/12/1996	La Avejeñilla	Gran Canaria			<i>D. arabisenren</i>
UB3034_127freezer	♂	2/12/1996	La Avejeñilla	Gran Canaria			<i>D. arabisenren</i>
CFBA003141	♂	4/16/2018	Llanos de la Pez	Gran Canaria	27.964312	-15.585547	<i>D. arabisenren</i>
CFBA003149	♂	4/16/2018	Llanos de la Pez	Gran Canaria	27.964312	-15.585547	<i>D. arabisenren</i>
CFBA003153	♂	4/16/2018	Llanos de la Pez	Gran Canaria	27.964312	-15.585547	<i>D. arabisenren</i>
NIMH002060	♂	4/21/2012	Presa de Cuevas Blancas	Gran Canaria	27.964830	-15.545050	<i>D. arabisenren</i>
UB3038_127freezer	♀	2/12/1996	Bairranco de Guayadeque	Gran Canaria	27.932980	-15.480070	<i>D. bandamae</i>

UB2980	♂	2/9/1996	Brezal del Palmital	Gran Canaria	28.111450	-15.601970	<i>D. bandamae</i>
UB3020_127 freezer	♀	2/11/1996	Degollada de Las Brujas	Gran Canaria	27.940540	-15.731890	<i>D. bandamae</i>
UB3077_129	♀	2/15/1996	Degollada de Tasartico	Gran Canaria	27.930860	-15.791130	<i>D. bandamae</i>
UB3007_126 freezer	♀	2/10/1996	Inagua	Gran Canaria	27.938683	-15.708818	<i>D. bandamae</i>
UB3010_126 freezer	♀	2/10/1996	Inagua	Gran Canaria	27.938683	-15.708818	<i>D. bandamae</i>
CRBA000738	♀	5/6/2004	Los Berrazales	Gran Canaria	28.068779	-15.658864	<i>D. bandamae</i>
CRBA002173	♂	5/6/2004	Los Berrazales	Gran Canaria	28.068779	-15.658864	<i>D. bandamae</i>
NMH002066	♀	4/21/2012	Pico de las Nieves (zona de acampada)	Gran Canaria	27.968829	-15.569527	<i>D. bandamae</i>
NMH002034	♀	4/21/2012	Presa de Cuevas Blancas	Gran Canaria	27.964830	-15.549050	<i>D. bandamae</i>
NMH002037	♂	4/21/2012	Presa de Cuevas Blancas	Gran Canaria	27.964830	-15.549050	<i>D. bandamae</i>
NMH002038	♂	4/21/2012	Presa de Cuevas Blancas	Gran Canaria	27.964830	-15.549050	<i>D. bandamae</i>
UB2637	♀	12/31/1993	Presa de Las Niñas	Gran Canaria	27.928312	-15.660048	<i>D. bandamae</i>
UB3130_132 freezer	♂		Presa de Las Niñas	Gran Canaria	27.928312	-15.660048	<i>D. bandamae</i>
NMH000651	♀	5/16/2006	Cabezo del Tejo 2	Tenerife	28.565090	-16.165982	<i>D. brevisetae</i>
NMH000648	♂	5/16/2006	Cabezo del Tejo 2	Tenerife	28.565090	-16.165982	<i>D. brevisetae</i>
NMH000649	♂	5/16/2006	Cabezo del Tejo 2	Tenerife	28.565090	-16.165982	<i>D. brevisetae</i>
CRBA001337	♂	4/29/2004	Cruz del Carmen (Sendero restaurante)	Tenerife	28.531925	-16.279999	<i>D. brevisetae</i>
NMH000630	♀	5/29/2006	Monte Aguirre. Anaga	Tenerife	28.529555	-16.268309	<i>D. brevisetae</i>
CRBA002993	♂	3/26/2017	Monte Aguirre. Anaga	Tenerife	28.529555	-16.268309	<i>D. brevisetae</i>
NMH000644	♂	5/29/2006	Monte Aguirre. Anaga	Tenerife	28.529555	-16.268309	<i>D. brevisetae</i>
CRBA002986	♀	3/26/2017	Pista El Batán-Cruz del Carmen	Tenerife	28.535320	-16.296800	<i>D. brevisetae</i>
CRBA002960	♂	3/26/2017	Pista El Batán-Cruz del Carmen	Tenerife	28.535320	-16.296800	<i>D. brevisetae</i>
CRBA002940	♀	3/25/2017	Barranco de los Cochinos. Monte del Agua	Tenerife	28.524550	-16.819440	<i>D. brevispina</i>
CRBA001338	♂	1/15/2004	Cruz del Carmen (Sendero restaurante)	Tenerife	28.531925	-16.279999	<i>D. brevispina</i>
CRBA001078	♀	11/22/2002	El Balladero. Anaga	Tenerife	28.550411	-16.203986	<i>D. brevispina</i>
NMH001269	♀	4/6/2007	Pinar de Ifonche	Tenerife	28.141800	-16.691400	<i>D. brevispina</i>
CRBA001394	♀	6/10/2006	Pista El Moquinal, Anaga	Tenerife	28.537349	-16.309386	<i>D. brevispina</i>
NMH002991	♂	2/10/2015	Pista Las Hiedras-Las Carboneras	Tenerife	28.535600	-16.298810	<i>D. brevispina</i>
NMH002992	♂	2/10/2015	Pista Las Hiedras-Las Carboneras	Tenerife	28.535600	-16.298810	<i>D. brevispina</i>
UB4131	♀	4/28/1995	Barranco Aramaqué. Near Los Aceviños	La Gomera	28.149151	-17.220779	<i>D. calderensis</i>

CRBA001452	♀	8/8/2002	Barranco de Juel	La Gomera	28.151547	-17.162962	<i>D. calderensis</i>
UB2945	♂	4/30/1995	Chorros de Epina	La Gomera	28.167036	-17.305892	<i>D. calderensis</i>
CRBA002283	♀	2/7/2014	El Castillo	La Palma	28.796360	-17.971169	<i>D. calderensis</i>
CRBA002285	♀	2/7/2014	El Castillo	La Palma	28.796360	-17.971169	<i>D. calderensis</i>
CRBA002286	♀	2/7/2014	El Castillo	La Palma	28.796360	-17.971169	<i>D. calderensis</i>
CRBA002284	♂	2/7/2014	El Castillo	La Palma	28.796360	-17.971169	<i>D. calderensis</i>
CRBA002290	♂	2/7/2014	El Castillo	La Palma	28.796360	-17.971169	<i>D. calderensis</i>
CRBA002278	♀	12/21/2013	Juan Adalid	La Palma	28.843639	-17.906350	<i>D. calderensis</i>
CRBA002279	♀	2/7/2014	Juan Adalid	La Palma	28.843639	-17.906350	<i>D. calderensis</i>
CRBA002280	♂	2/7/2014	Juan Adalid	La Palma	28.843639	-17.906350	<i>D. calderensis</i>
CRBA002298	♂	3/13/2014	Juan Adalid	La Palma	28.843639	-17.906350	<i>D. calderensis</i>
CRBA002730	♀	3/17/2017	La Mérica	La Gomera	28.115770	-17.336040	<i>D. calderensis</i>
CRBA002292	♀	2/10/2014	Mendo	La Palma	28.557572	-17.867541	<i>D. calderensis</i>
UB4118	♀	4/28/1995	Monte de Juan Tomé. La Laja	La Gomera	28.123022	-17.210137	<i>D. calderensis</i>
NMH003252	♂	2/2/2008	Monte del Cedro	La Gomera	28.119283	-17.237290	<i>D. calderensis</i>
UB2918	♀	4/30/1995	Barranco San Juan.	La Gomera	28.193320	-17.292940	<i>D. calderensis</i>
UB2921	♀	4/30/1995	Barranco San Juan.	La Gomera	28.193320	-17.292940	<i>D. calderensis</i>
NMH001805	♂	1/4/2010	Reventón Oscuro. Bosque del Cedro	La Gomera	28.123809	-17.216616	<i>D. calderensis</i>
NMH001438	♀	2/21/2008	Riscos de Aljofra	La Gomera	28.162860	-17.318101	<i>D. calderensis</i>
CRBA002757	♂	3/17/2017	Tesellinde. Ermita de Santa Clara	La Gomera	28.196300	-17.287540	<i>D. calderensis</i>
NMH002522	♂	5/14/2013	Tesellinde. Ermita de Santa Clara	La Gomera	28.196300	-17.287540	<i>D. calderensis</i>
NMH001442	♂	9/26/2008	Barranco de los Cochinos. Monte del Agua	Tenerife	28.324550	-16.819440	<i>D. cribellata</i>
UB3151	♀	5/12/1996	Cruz del Carmen (Sendero restaurante)	Tenerife	28.531925	-16.279999	<i>D. cribellata</i>
NMH001305	♂	12/22/2004	Los Barranquillos	Tenerife	28.352711	-16.413852	<i>D. cribellata</i>
UB3162	♂	5/24/1996	Monte de las Mercedes	Tenerife	28.525678	-16.287059	<i>D. cribellata</i>
UB3163	♂	5/24/1996	Monte de las Mercedes	Tenerife	28.525678	-16.287059	<i>D. cribellata</i>
CRBA002963	♀	3/26/2017	Pista El Batán-Cruz del Carmen	Tenerife	28.535320	-16.296800	<i>D. cribellata</i>
CRBA002966	♀	3/26/2017	Pista El Batán-Cruz del Carmen	Tenerife	28.535320	-16.296800	<i>D. cribellata</i>
CRBA002972	♀	3/26/2017	Pista El Batán-Cruz del Carmen	Tenerife	28.535320	-16.296800	<i>D. cribellata</i>
CRBA003000	♂	3/26/2017	Pista Las Hiedras-Las Carboneras	Tenerife	28.535600	-16.298810	<i>D. cribellata</i>

NMH002743	♀	4/6/2014	El Médano (Playa)	Tenerife	28.033022	-16.540247	<i>D. curvisetae</i>
CRBA003247	♂	4/24/2018	El Médano (Playa)	Tenerife	28.033022	-16.540247	<i>D. curvisetae</i>
CRBA003248	♂	4/24/2018	El Médano (Playa)	Tenerife	28.033022	-16.540247	<i>D. curvisetae</i>
CRBA000514	♂	4/13/2003	Playa del Barranco de Natero	Tenerife	28.288321	-16.861860	<i>D. curvisetae</i>
NMH003186	♀	2/5/2009	Campamento Viejo. Monte del Cedro	La Gomera	28.119758	-17.252285	<i>D. enghoffi</i>
NMH003253	♂	2/2/2008	Monte del Cedro	La Gomera	28.119283	-17.237290	<i>D. enghoffi</i>
CRBA001082	♂	12/20/2004	Barranco de los Cochinos. Monte del Agua	Tenerife	28.324550	-16.819440	<i>D. gibbifera</i>
NMH001030	♂	11/30/2006	Barranco de los Cochinos. Monte del Agua	Tenerife	28.324550	-16.819440	<i>D. gibbifera</i>
NMH001466	♂	4/27/2008	Barranco de los Cochinos. Monte del Agua	Tenerife	28.324550	-16.819440	<i>D. gibbifera</i>
UB2779	♂	7/6/1990	Barranco de los Cochinos. Monte del Agua	Tenerife	28.324550	-16.819440	<i>D. gibbifera</i>
UB2926	♂	5/1/1995	Barranco de Juel	La Gomera	28.151547	-17.162962	<i>D. gomerenis</i>
CRBA002805	♀	3/18/2017	Barranco de Juel, East	La Gomera	28.148320	-17.157720	<i>D. gomerenis</i>
CRBA002827	♀	3/18/2017	Barranco de Juel, East	La Gomera	28.148320	-17.157720	<i>D. gomerenis</i>
CRBA002799	♂	3/18/2017	Barranco de Juel, East	La Gomera	28.148320	-17.157720	<i>D. gomerenis</i>
UB2828	♂	12/9/1994	Barranco de Majona	La Gomera	28.151830	-17.139235	<i>D. gomerenis</i>
NMH003247	♂	2/24/2008	La Asomadita (Pista forestal Chipude)	La Gomera	28.111600	-17.264800	<i>D. gomerenis</i>
NMH003055	♀	2/16/2011	Las Hueritas	La Gomera	28.090664	-17.283087	<i>D. gomerenis</i>
NMH001450	♂	5/1/2008	Los Noruegos	La Gomera	28.106905	-17.233323	<i>D. gomerenis</i>
UB3198	♀	2/3/1997	Mirador de Bascos	El Hierro	27.754861	-18.118218	<i>D. gomerenis</i>
CRBA002856	♂	3/22/2017	Mirador de Bascos	El Hierro	27.754861	-18.118218	<i>D. gomerenis</i>
UB4007	♂	10/22/1994	Mirador de Las Playas (300m hacia La Restinga)	El Hierro	27.731970	-17.972127	<i>D. gomerenis</i>
NMH001445	♀	2/4/2008	Mña. de Las Pías, Cno. La Mérica	La Gomera	28.113283	-17.335701	<i>D. gomerenis</i>
NMH003255	♂	2/23/2008	Mña. La Asomadita (Laguna Grande-Juego de Bolas)	La Gomera	28.135646	-17.257454	<i>D. gomerenis</i>
UB2783	♀	1/2/1982	Pinar del Infante	La Gomera	28.130794	-17.282267	<i>D. gomerenis</i>
UB2784	♀	1/2/1982	Pinar del Infante	La Gomera	28.130794	-17.282267	<i>D. gomerenis</i>
UB3199	♀	2/5/1997	Pista del Derrabado	El Hierro	27.740804	-18.053080	<i>D. gomerenis</i>
CRBA002848	♀	3/22/2017	Pista del Mercader	El Hierro	27.712944	-18.022175	<i>D. gomerenis</i>
CRBA002064	♂	1/15/2011	Pista del Mercader	El Hierro	27.712944	-18.022175	<i>D. gomerenis</i>
CRBA002887	♀	3/23/2017	Pista Garoé	El Hierro	27.781744	-17.951391	<i>D. gomerenis</i>
CRBA002883	♂	3/23/2017	Pista Garoé	El Hierro	27.781744	-17.951391	<i>D. gomerenis</i>

NMIH002928	♀	2/17/2011	Playa de Avalo	La Gomera	28.114684	-17.113168	<i>D. gomerensis</i>
NMIH001449	♀	5/2/2008	Sendero Enchereda	La Gomera	28.136650	-17.179063	<i>D. gomerensis</i>
CRBA002791	♀	3/17/2017	Tesellinde. Ermita de Santa Clara	La Gomera	28.196300	-17.287540	<i>D. gomerensis</i>
CRBA002746	♂	3/17/2017	Tesellinde. Ermita de Santa Clara	La Gomera	28.196300	-17.287540	<i>D. gomerensis</i>
CRBA002759	♂	3/17/2017	Tesellinde. Ermita de Santa Clara	La Gomera	28.196300	-17.287540	<i>D. gomerensis</i>
CRBA002928	♀	3/23/2017	Ventelís. Tiñor	El Hierro	27.785991	-17.937508	<i>D. gomerensis</i>
CRBA002897	♂	3/23/2017	Ventelís. Tiñor	El Hierro	27.785991	-17.937508	<i>D. gomerensis</i>
CRBA001087	♀	12/20/2004	Barranco de los Cochinos. Monte del Agua	Tenerife	28.324550	-16.819440	<i>D. iguanensis</i>
NMIH001044	♀	10/27/2005	Barranco de los Cochinos. Monte del Agua	Tenerife	28.324550	-16.819440	<i>D. iguanensis</i>
NMIH001045	♀	10/27/2005	Barranco de los Cochinos. Monte del Agua	Tenerife	28.324550	-16.819440	<i>D. iguanensis</i>
NMIH001046	♀	10/27/2005	Barranco de los Cochinos. Monte del Agua	Tenerife	28.324550	-16.819440	<i>D. iguanensis</i>
NMIH001047	♀	10/27/2005	Barranco de los Cochinos. Monte del Agua	Tenerife	28.324550	-16.819440	<i>D. iguanensis</i>
CRBA000541	♂	8/19/2003	Barranco de los Cochinos. Monte del Agua	Tenerife	28.324550	-16.819440	<i>D. iguanensis</i>
CRBA000693	♂	4/28/2004	Barranco de los Cochinos. Monte del Agua	Tenerife	28.324550	-16.819440	<i>D. iguanensis</i>
NMIH003061	♂	6/24/2009	Barranco de los Cochinos. Monte del Agua	Tenerife	28.324550	-16.819440	<i>D. iguanensis</i>
UB3208	♂	2/22/1997	Barranco de los Cochinos. Monte del Agua	Tenerife	28.324550	-16.819440	<i>D. iguanensis</i>
CRBA001079	♀	11/22/2002	El Pijaral. Anaga	Tenerife	28.551966	-16.189225	<i>D. iguanensis</i>
NMIH000618	♀	5/29/2005	Monte Aguirre. Anaga	Tenerife	28.529555	-16.268309	<i>D. iguanensis</i>
NMIH000637	♀	5/29/2005	Monte Aguirre. Anaga	Tenerife	28.529555	-16.268309	<i>D. iguanensis</i>
NMIH00107	♂	4/29/2004	Monte Aguirre. Anaga	Tenerife	28.529535	-16.268309	<i>D. iguanensis</i>
NMIH000635	♂	5/29/2005	Monte Aguirre. Anaga	Tenerife	28.529535	-16.268309	<i>D. iguanensis</i>
NMIH000636	♂	5/29/2005	Monte Aguirre. Anaga	Tenerife	28.529535	-16.268309	<i>D. iguanensis</i>
NMIH000972	♂	11/6/1984	Monte Aguirre. Anaga	Tenerife	28.529535	-16.268309	<i>D. iguanensis</i>
NMIH000103	♂	5/1/2004	Pista de Jjuana	Tenerife	28.560191	-16.169190	<i>D. iguanensis</i>
NMIH000106	♂	5/1/2004	Pista de Jjuana	Tenerife	28.560191	-16.169190	<i>D. iguanensis</i>
CRBA002937	♀	3/25/2017	Barranco de los Cochinos. Monte del Agua	Tenerife	28.324550	-16.819440	<i>D. insulana</i>
NMIH001041	♀	7/14/2003	Barranco de los Cochinos. Monte del Agua	Tenerife	28.324550	-16.819440	<i>D. insulana</i>
NMIH000098	♂	4/29/2004	Cruz del Carmen (Sendero restaurante)	Tenerife	28.531925	-16.279999	<i>D. insulana</i>
NMIH000099	♂	4/29/2004	Cruz del Carmen (Sendero restaurante)	Tenerife	28.531925	-16.279999	<i>D. insulana</i>
NMIH000100	♂	4/29/2004	Cruz del Carmen (Sendero restaurante)	Tenerife	28.531925	-16.279999	<i>D. insulana</i>

UB2771	♀	1/10/1983	Guamasa	Tenerife	Tenerife				<i>D. insulana</i>
NMH000980	♂	11/26/2003	Hoya de Jjuana, Anaga	Tenerife	Tenerife	28.560191	-16.169199		<i>D. insulana</i>
CRBA002952	♀	3/26/2017	Pista El Batán-Cruz del Carmen	Tenerife	Tenerife	28.535320	-16.296800		<i>D. insulana</i>
NMH002819	♂	11/25/2014	Pista El Batán-Cruz del Carmen	Tenerife	Tenerife	28.535320	-16.296800		<i>D. insulana</i>
NMH003176	♀	4/18/2015	Pista Las Hiedras-Las Carboneras	Tenerife	Tenerife	28.535600	-16.298810		<i>D. insulana</i>
UB2870	♀	2/22/1995	Atalaya de Femés. Los Ajaches	Lanzarote	Lanzarote	28.919520	-13.763700		<i>D. lanceoerensis</i>
UB2869	♂	2/22/1995	Atalaya de Femés. Los Ajaches	Lanzarote	Lanzarote	28.919520	-13.763700		<i>D. lanceoerensis</i>
UB2840	♀	2/17/1995	Barranco del Ciervo. Cumbres de Iandía	Fuerteventura	Fuerteventura	28.093768	-14.363823		<i>D. lanceoerensis</i>
UB2871	♂	2/23/1995	Caldera. Mña. Clara	Montaña Clara	Montaña Clara	29.298865	-13.535305		<i>D. lanceoerensis</i>
UB2872	♂	2/23/1995	Caldera. Mña. Clara	Montaña Clara	Montaña Clara	29.298865	-13.535305		<i>D. lanceoerensis</i>
CRBA000555	♀	11/22/2002	Caleta del Sebo	Lanzarote	Lanzarote	29.232511	-13.505077		<i>D. lanceoerensis</i>
CRBA002655	♂	3/13/2017	Lomo de La Degollada	Lanzarote	Lanzarote	28.929960	-13.768650		<i>D. lanceoerensis</i>
CRBA002662	♂	3/13/2017	Lomo de La Degollada	Lanzarote	Lanzarote	28.929960	-13.768650		<i>D. lanceoerensis</i>
UB2856	♀	2/20/1995	Malpais de Bayuyo	Fuerteventura	Fuerteventura	28.653311	-13.902783		<i>D. lanceoerensis</i>
UB2855	♂	2/20/1995	Malpais de Bayuyo	Fuerteventura	Fuerteventura	28.653311	-13.902783		<i>D. lanceoerensis</i>
NMH000341	♂	12/3/2004	Mña. del Mojón	Lanzarote	Lanzarote	29.242060	-13.516290		<i>D. lanceoerensis</i>
NMH001994	♀	4/12/2012	Montaña Tinache	Lanzarote	Lanzarote	29.051850	-13.669850		<i>D. lanceoerensis</i>
NMH001995	♀	4/12/2012	Montaña Tinache	Lanzarote	Lanzarote	29.051850	-13.669850		<i>D. lanceoerensis</i>
NMH001996	♂	4/12/2012	Montaña Tinache	Lanzarote	Lanzarote	29.051850	-13.669850		<i>D. lanceoerensis</i>
NMH001140	♂	1/18/2007	Pico de la Zarza	Fuerteventura	Fuerteventura	28.097596	-14.362101		<i>D. lanceoerensis</i>
NMH001292	♀	4/1/2007	Pico del Fraile	Fuerteventura	Fuerteventura	28.090043	-14.394320		<i>D. lanceoerensis</i>
NMH001293	♂	4/1/2007	Pico del Fraile	Fuerteventura	Fuerteventura	28.090043	-14.394320		<i>D. lanceoerensis</i>
CRBA000556	♂	11/28/2002	Valle de Fuentedouce. Órzola	Lanzarote	Lanzarote	29.202288	-13.461592		<i>D. lanceoerensis</i>
UB2892	♂	3/1/1995		Alegranza	Alegranza				<i>D. lanceoerensis</i>
CRBA001337	♂	4/29/2004	Cruz del Carmen (Sendero restaurante)	Tenerife	Tenerife	28.531925	-16.279999		<i>D. levisipes</i>
NMH001274	♂	2/16/2007	El Montillo	Tenerife	Tenerife	28.442525	-16.454611		<i>D. levisipes</i>
UB3097	♂	2/18/1996	Palo Blanco	Tenerife	Tenerife	28.357941	-16.586559		<i>D. levisipes</i>
UB3099	♂	2/18/1996	Palo Blanco	Tenerife	Tenerife	28.357941	-16.586559		<i>D. levisipes</i>
NMH001268	♂	4/6/2007	Pinar de Ifonche	Tenerife	Tenerife	28.141800	-16.691400		<i>D. levisipes</i>
NMH003312	♀	7/6/2015	Pinoleris	Tenerife	Tenerife	28.400377	-16.496257		<i>D. levisipes</i>

NMIH002176	♀	4/3/2012	Pista Las Hiedras-Las Carboneras	Tenerife	28.535600	-16.298810	D. Ievipes
NMIH002177	♀	4/3/2012	Pista Las Hiedras-Las Carboneras	Tenerife	28.535600	-16.298810	D. Ievipes
NMIH002178	♀	4/3/2012	Pista Las Hiedras-Las Carboneras	Tenerife	28.535600	-16.298810	D. Ievipes
NMIH003179	♀	4/18/2015	Pista Las Hiedras-Las Carboneras	Tenerife	28.535600	-16.298810	D. Ievipes
NMIH002183	♂	4/3/2012	Pista Las Hiedras-Las Carboneras	Tenerife	28.535600	-16.298810	D. Ievipes
NMIH002344	♂	4/8/2013	Pista Las Hiedras-Las Carboneras	Tenerife	28.535600	-16.298810	D. Ievipes
NMIH002649	♂	5/27/2013	Pista Las Hiedras-Las Carboneras	Tenerife	28.535600	-16.298810	D. Ievipes
NMIH001498	♀	6/6/2009	Teno Alto	Tenerife	28.335996	-16.865760	D. Ievipes
NMIH002711	♀	12/28/2008	Barranco del Draguillo	Gran Canaria	27.941568	-15.429992	D. Ilostetha
NMIH003290	♂	8/16/2007	Barranco del Draguillo	Gran Canaria	27.941568	-15.429992	D. Ilostetha
CRBA000972	♀	5/8/2004	Barranco Tasartico	Gran Canaria	27.930859	-15.791131	D. Ilostetha
NMIH003268	♂	2/18/2007	Barranco Tasartico	Gran Canaria	27.930859	-15.791131	D. Ilostetha
UB3167_134	♂	1/1/1995	Caideros	Gran Canaria	28.075760	-15.649420	D. Ilostetha
UB3091_130	♂	2/15/1996	Degollada de Tasartico	Gran Canaria	27.930860	-15.791130	D. Ilostetha
NMIH003341	♀	8/10/2015	El Sao	Gran Canaria	28.068764	-15.656990	D. Ilostetha
NMIH002721	♀	12/30/2013	El Sao	Gran Canaria	28.068764	-15.656990	D. Ilostetha
NMIH002740	♀	4/1/2013	El Sao	Gran Canaria	28.068764	-15.656990	D. Ilostetha
NMIH002718	♂	4/1/2013	El Sao	Gran Canaria	28.068764	-15.656990	D. Ilostetha
NMIH002720	♂	12/30/2013	El Sao	Gran Canaria	28.068764	-15.656990	D. Ilostetha
NMIH002741	♂	4/1/2013	El Sao	Gran Canaria	28.068764	-15.656990	D. Ilostetha
UB3002_126 freezer	♀	2/10/1996	Inagua	Gran Canaria	27.938683	-15.708818	D. Ilostetha
UB3011_126 freezer	♀	2/10/1996	Inagua	Gran Canaria	27.938683	-15.708818	D. Ilostetha
UB3043_128	♂	2/13/1996	Near Tirajana	Gran Canaria	27.908870	-15.570200	D. Ilostetha
UB2998	♀	2/10/1996	Pico de Viento	Gran Canaria	28.099788	-15.651685	D. Ilostetha
UB3001_126 freezer	♂	2/10/1996	Pico de Viento	Gran Canaria	28.099788	-15.651685	D. Ilostetha
UB3085_130	♂	2/16/1996	Pista de Tirma	Gran Canaria	28.032133	-15.755400	D. Ilostetha
NMIH003269	♂	4/7/2004	Telde	Gran Canaria			D. Ilostetha
UB2837	♀	2/17/1995	Barranco del Ciervo. Cumbres de Jandía	Fuerteventura	28.093768	-14.363823	D. Longa
UB2836	♂	2/17/1995	Barranco del Ciervo. Cumbres de Jandía	Fuerteventura	28.093768	-14.363823	D. Longa
UB2838	♂	2/17/1995	Barranco del Ciervo. Cumbres de Jandía	Fuerteventura	28.093768	-14.363823	D. Longa

NMIH000606	♂	12/31/1974	Cumbre de Jandía	Fuerteventura	28.094636	-14.440265	D. larga
NMIH00168	♀	4/4/2004	Morro del Cavadero	Fuerteventura	28.093768	-14.363823	D. larga
NMIH00169	♀	4/4/2004	Morro del Cavadero	Fuerteventura	28.093768	-14.363823	D. larga
NMIH001283	♀	3/30/2007	Morro del lorao	Fuerteventura	28.117460	-14.334534	D. larga
NMIH001285	♂	4/1/2007	Pico del Fraile	Fuerteventura	28.090043	-14.394320	D. larga
NMIH001286	♂	4/1/2007	Pico del Fraile	Fuerteventura	28.090043	-14.394320	D. larga
NMIH001386	♀	4/4/2008	Barranco de San Andrés	Tenerife	28.519926	-16.189101	D. macra
NMIH001061	♀	1/30/2007	Barranco del Agua	Tenerife	28.307838	-16.448156	D. macra
NMIH001062	♀	1/30/2007	Barranco del Agua	Tenerife	28.307838	-16.448156	D. macra
NMIH000934	♀	5/9/2005	Barranco Samarines	Tenerife	28.345548	-16.371103	D. macra
NMIH000941	♀	5/5/2004	Barranco Samarines	Tenerife	28.345548	-16.371103	D. macra
NMIH000939	♂	5/9/2005	Barranco Samarines	Tenerife	28.345548	-16.371103	D. macra
NMIH000942	♂	3/14/2004	Barranco Samarines	Tenerife	28.345548	-16.371103	D. macra
NMIH001080	♂	1/16/2007	Cumbres de Arico. Pista de Izaña	Tenerife	28.249217	-16.528748	D. macra
UB3215	♂	12/27/1997	Suerque	Tenerife	28.292050	-16.846042	D. macra
NMIH001159	♂	3/27/2007	La Fortaleza (pinar), P.N. del Teide	Tenerife	28.316723	-16.591240	D. macra
NMIH001161	♂	3/27/2007	La Fortaleza (pinar), P.N. del Teide	Tenerife	28.316723	-16.591240	D. macra
NMIH001359	♀	3/1/2006	Las Lajas. Zona recreativa	Tenerife	28.190338	-16.669163	D. macra
NMIH001479	♀	3/31/2009	Los Lomitos. Monte de Las Mesas	Tenerife	28.481365	-16.263627	D. macra
NMIH001480	♀	3/31/2009	Los Lomitos. Monte de Las Mesas	Tenerife	28.481365	-16.263627	D. macra
NMIH001481	♀	3/31/2009	Los Lomitos. Monte de Las Mesas	Tenerife	28.481365	-16.263627	D. macra
NMIH001482	♂	3/31/2009	Los Lomitos. Monte de Las Mesas	Tenerife	28.481365	-16.263627	D. macra
NMIH001483	♂	3/31/2009	Los Lomitos. Monte de Las Mesas	Tenerife	28.481365	-16.263627	D. macra
NMIH000826	♂	12/22/2006	Morada del Viento (Pista Siete Fuentes), Las Lagunetas	Tenerife	28.411180	-16.421127	D. macra
NMIH001333	♂	5/4/2006	Pista a Benijos	Tenerife	28.338981	-16.547893	D. macra
NMIH001069	♀	2/1/2007	Pista a Madre del Agua- Barranco del Río	Tenerife	28.177310	-16.601628	D. macra
NMIH001068	♂	2/1/2007	Pista a Madre del Agua- Barranco del Río	Tenerife	28.177310	-16.601628	D. macra
NMIH001001	♀	1/9/2002	Pista de Los Órganos	Tenerife	28.362888	-16.483766	D. macra
NMIH000991	♀	3/2/2004	Polígono Industrial Arafo-Güímar	Tenerife	28.343305	-16.374289	D. macra
NMIH000992	♀	3/2/2004	Polígono Industrial Arafo-Güímar	Tenerife	28.343305	-16.374289	D. macra

NMIH000906	♀	1/13/2007	Roque del Conde	Tenerife	28.093144	-16.698890	<i>D. macra</i>
NMIH000910	♂	1/13/2007	Roque del Conde	Tenerife	28.093144	-16.698890	<i>D. macra</i>
NMIH001478	♂	3/22/2009	Valle Jiménez	Tenerife	28.498880	-16.273290	<i>D. macra</i>
UB002580	♂	8/4/1985	Aguamansa	Tenerife	28.356576	-16.499748	<i>D. montanetensis</i>
NMIH001018	♀	11/30/2006	Barranco de los Cochinos. Monte del Agua	Tenerife	28.324550	-16.819440	<i>D. montanetensis</i>
NMIH001032	♀	11/30/2006	Barranco de los Cochinos. Monte del Agua	Tenerife	28.324550	-16.819440	<i>D. montanetensis</i>
NMIH001033	♀	11/30/2006	Barranco de los Cochinos. Monte del Agua	Tenerife	28.324550	-16.819440	<i>D. montanetensis</i>
NMIH001035	♂	11/30/2006	Barranco de los Cochinos. Monte del Agua	Tenerife	28.324550	-16.819440	<i>D. montanetensis</i>
UB2867	♂	2/22/1995	Alajaya de Femés. Los Ajaches	Lanzarote	28.919520	-13.763700	<i>D. nesiotis</i>
CRBA002686	♀	3/14/2017	Cabecera Barranco Elvira Sánchez	Lanzarote	29.130724	-13.516903	<i>D. nesiotis</i>
CRBA002690	♀	3/14/2017	Cabecera Barranco Elvira Sánchez	Lanzarote	29.130724	-13.516903	<i>D. nesiotis</i>
CRBA002705	♀	3/14/2017	Cabecera Barranco Elvira Sánchez	Lanzarote	29.130724	-13.516903	<i>D. nesiotis</i>
NMIH002005	♂	4/13/2012	Cabecera Barranco Elvira Sánchez	Lanzarote	29.130724	-13.516903	<i>D. nesiotis</i>
UB2873	♂	2/23/1995	Caldera. Mña. Clara	Montaña Clara	29.298865	-13.535305	<i>D. nesiotis</i>
UB2878	♂	2/23/1995	Caldera. Mña. Clara	Montaña Clara	29.298865	-13.535305	<i>D. nesiotis</i>
UB2861	♂	2/22/1995	Famara Mountains	Lanzarote	29.211204	-13.484156	<i>D. nesiotis</i>
CRBA002656	♀	3/13/2017	Lomo de La Degollada	Lanzarote	28.929960	-13.768650	<i>D. nesiotis</i>
CRBA002676	♀	3/13/2017	Montaña Tinache	Lanzarote	29.051850	-13.669850	<i>D. nesiotis</i>
CRBA001339	♂	11/2/2001	Las Cancellitas	El Hierro	27.809530	-17.927239	<i>D. orahan</i>
CRBA002890	♀	3/23/2017	Ventelís. Tiñor	El Hierro	27.785991	-17.937508	<i>D. orahan</i>
CRBA002891	♀	3/23/2017	Ventelís. Tiñor	El Hierro	27.785991	-17.937508	<i>D. orahan</i>
NMIH002564	♂	4/22/2013	Ventelís. Tiñor	El Hierro	27.785991	-17.937508	<i>D. orahan</i>
NMIH002565	♂	4/22/2013	Ventelís. Tiñor	El Hierro	27.785991	-17.937508	<i>D. orahan</i>
UB3012_126	♂	2/10/1996	Inagua	Gran Canaria	27.938683	-15.708818	<i>D. paucispinosa</i>
CRBA000736	♀	5/6/2004	Los Berrazales	Gran Canaria	28.068779	-15.658864	<i>D. paucispinosa</i>
CRBA002174	♀	5/6/2004	Los Berrazales	Gran Canaria	28.068779	-15.658864	<i>D. paucispinosa</i>
CRBA002826	♂	3/18/2017	Barranco de Juel, East	La Gomera	28.148320	-17.157720	<i>D. ramblae</i>
CRBA002725	♀	3/16/2017	Bosque del Cedro	La Gomera	28.137044	-17.222569	<i>D. ramblae</i>
UB2929	♀	5/1/1995	Las Campanas	La Gomera	28.158055	-17.160623	<i>D. ramblae</i>
UB2930	♀	5/1/1995	Las Campanas	La Gomera	28.158055	-17.160623	<i>D. ramblae</i>

CRBA002838	♂	3/18/2017	Reventón Oscuro, MSS	La Gomera				<i>D. ramblae</i>
CRBA002794	♀	3/17/2017	Tesellinde. Ermita de Santa Clara	La Gomera	28.196300	-17.287540	<i>D. ramblae</i>	
CRBA002795	♀	3/17/2017	Tesellinde. Ermita de Santa Clara	La Gomera	28.196300	-17.287540	<i>D. ramblae</i>	
CRBA002741	♂	3/17/2017	Tesellinde. Ermita de Santa Clara	La Gomera	28.196300	-17.287540	<i>D. ramblae</i>	
CRBA002742	♂	3/17/2017	Tesellinde. Ermita de Santa Clara	La Gomera	28.196300	-17.287540	<i>D. ramblae</i>	
CRBA002779	♂	3/17/2017	Tesellinde. Ermita de Santa Clara	La Gomera	28.196300	-17.287540	<i>D. ramblae</i>	
UB3169_134	♂	8/3/1988	Fontanales	Gran Canaria	28.055530	-15.608730	<i>D. rugichells</i>	
UB3059_128 freezer	♀	2/14/1996	Pinar de Tamadaba	Gran Canaria	28.031840	-15.677020	<i>D. rugichells</i>	
UB3062_129 freezer	♀	2/14/1996	Pinar de Tamadaba	Gran Canaria	28.031840	-15.677020	<i>D. rugichells</i>	
UB3063_129 freezer	♀	2/14/1996	Pinar de Tamadaba	Gran Canaria	28.031840	-15.677020	<i>D. rugichells</i>	
UB3092_130	♀	2/14/1996	Pinar de Tamadaba	Gran Canaria	28.031840	-15.677020	<i>D. rugichells</i>	
UB3048_128 freezer	♂	2/14/1996	Pinar de Tamadaba	Gran Canaria	28.031840	-15.677020	<i>D. rugichells</i>	
UB3055_128 freezer	♂	2/14/1996	Pinar de Tamadaba	Gran Canaria	28.031840	-15.677020	<i>D. rugichells</i>	
NMH000501	♀	2/5/2005	Montaña de la Cruz	Fuerteventura	28.441619	-14.057354	<i>D. sanbarandon</i>	
NMH000502	♀	2/5/2005	Montaña de la Cruz	Fuerteventura	28.441619	-14.057354	<i>D. sanbarandon</i>	
NMH000504	♀	2/5/2005	Montaña de la Cruz	Fuerteventura	28.441619	-14.057354	<i>D. sanbarandon</i>	
NMH000505	♀	2/5/2005	Montaña de la Cruz	Fuerteventura	28.441619	-14.057354	<i>D. sanbarandon</i>	
NMH000500	♂	4/1/2004	Morro Tabaiba. Vallebrón	Fuerteventura	28.592252	-13.943331	<i>D. sanbarandon</i>	
UB2826	♀	12/9/1994	Barranco de Majona	La Gomera	28.151830	-17.139235	<i>D. silvatica</i>	
UB2964	♂	12/26/1994	Barranco de Majona	La Gomera	28.151830	-17.139235	<i>D. silvatica</i>	
CRBA002347	♀	1/10/2000	Barranco las Traves (PNCT)	La Palma	28.717984	-17.893314	<i>D. silvatica</i>	
CRBA002355	♂	6/23/2000	Barranco las Traves (PNCT)	La Palma	28.717984	-17.893314	<i>D. silvatica</i>	
UB4140	♂	4/30/1995	Chorros de Epina	La Gomera	28.167036	-17.305892	<i>D. silvatica</i>	
UB4141	♂	4/30/1995	Chorros de Epina	La Gomera	28.167036	-17.305892	<i>D. silvatica</i>	
CRBA002864	♀	3/22/2017	Mirador de Bascos	El Hierro	27.754861	-18.118218	<i>D. silvatica</i>	
CRBA002873	♀	3/22/2017	Mirador de Bascos	El Hierro	27.754861	-18.118218	<i>D. silvatica</i>	
CRBA002875	♀	3/22/2017	Mirador de Bascos	El Hierro	27.754861	-18.118218	<i>D. silvatica</i>	
CRBA002876	♀	3/22/2017	Mirador de Bascos	El Hierro	27.754861	-18.118218	<i>D. silvatica</i>	
CRBA002879	♀	3/22/2017	Mirador de Bascos	El Hierro	27.754861	-18.118218	<i>D. silvatica</i>	
CRBA002061	♂	7/21/2011	Mirador de Bascos	El Hierro	27.754861	-18.118218	<i>D. silvatica</i>	

CRBA002842	♂	3/22/2017	Mirador de Bascos	El Hierro	27.754861	-18.118218	D. silvatica
CRBA002858	♂	3/22/2017	Mirador de Bascos	El Hierro	27.754861	-18.118218	D. silvatica
CRBA002859	♂	3/22/2017	Mirador de Bascos	El Hierro	27.754861	-18.118218	D. silvatica
CRBA002860	♂	3/22/2017	Mirador de Bascos	El Hierro	27.754861	-18.118218	D. silvatica
UB2903	♀	4/28/1995	Monte del Cedro	La Gomera	28.119283	-17.237290	D. silvatica
UB2923	♀	4/30/1995	Barranco San Juan.	La Gomera	28.193320	-17.292940	D. silvatica
UB4145	♀	4/30/1995	Barranco San Juan.	La Gomera	28.193320	-17.292940	D. silvatica
CRBA002348	♀	5/31/2001	Roque de Los Muchachos (PNCT)	La Palma	28.760880	-17.885206	D. silvatica
CRBA002349	♀	8/24/2000	Roque de Los Muchachos (PNCT)	La Palma	28.760880	-17.885206	D. silvatica
CRBA002353	♂	5/23/2001	Roque de Los Muchachos (PNCT)	La Palma	28.760880	-17.885206	D. silvatica
CRBA002354	♂	6/20/2001	Roque de Los Muchachos (PNCT)	La Palma	28.760880	-17.885206	D. silvatica
CRBA002306	♂	4/4/2014	Roque Faro	La Palma	28.798556	-17.879149	D. silvatica
CRBA002351	♀	4/27/2001	Tenerra (Parte alta) (PNCT)	La Palma	28.719605	-17.899636	D. silvatica
CRBA002691	♀	3/14/2017	Cabecera Barranco Elvira Sánchez	Lanzarote	29.130724	-13.516903	D. simbeque
CRBA002697	♀	3/14/2017	Cabecera Barranco Elvira Sánchez	Lanzarote	29.130724	-13.516903	D. simbeque
CRBA002700	♀	3/14/2017	Cabecera Barranco Elvira Sánchez	Lanzarote	29.130724	-13.516903	D. simbeque
CRBA002704	♀	3/14/2017	Cabecera Barranco Elvira Sánchez	Lanzarote	29.130724	-13.516903	D. simbeque
CRBA002707	♀	3/14/2017	Cabecera Barranco Elvira Sánchez	Lanzarote	29.130724	-13.516903	D. simbeque
CRBA002687	♂	3/14/2017	Cabecera Barranco Elvira Sánchez	Lanzarote	29.130724	-13.516903	D. simbeque
CRBA002692	♂	3/14/2017	Cabecera Barranco Elvira Sánchez	Lanzarote	29.130724	-13.516903	D. simbeque
CRBA002701	♂	3/14/2017	Cabecera Barranco Elvira Sánchez	Lanzarote	29.130724	-13.516903	D. simbeque
CRBA002712	♂	3/14/2017	Cabecera Barranco Elvira Sánchez	Lanzarote	29.130724	-13.516903	D. simbeque
CRBA003012	♀	3/26/2017	Camino el Fraile	Tenerife			D. sp. n. A
NMIH001496	♀	6/6/2009	Cumbre Bolico	Tenerife	28.314186	-16.826940	D. sp. n. A
NMIH001495	♂	6/6/2009	Cumbre Bolico	Tenerife	28.314186	-16.826940	D. sp. n. A
NMIH000860	♀	12/15/2006	El Aderno. Altos de Buenavista	Tenerife	28.358258	-16.864456	D. sp. n. A
NMIH000849	♂	12/15/2006	El Aderno. Altos de Buenavista	Tenerife	28.358258	-16.864456	D. sp. n. A
NMIH000825	♂	12/22/2006	Morada del Viento (Pista Siete Fuentes).	Tenerife	28.411180	-16.421127	D. sp. n. A
NMIH001497	♀	6/6/2009	Teno Alto	Tenerife	28.335996	-16.865760	D. sp. n. A
CRBA003035	♂	3/17/2017	Teno Alto 2	Tenerife			D. sp. n. A

NMIH002943	♀	23/1/2013	Cabezo del Tejo 2	Tenerife	28.565090	-16.165982	D. sp.n. B
NMIH002944	♀	23/1/2013	Cabezo del Tejo 2	Tenerife	28.565090	-16.165982	D. sp.n. B
NMIH002945	♀	11/1/2013	El Pijaral. Anaga	Tenerife	28.551966	-16.189225	D. sp.n. B
NMIH000717	♀	22/5/2006	Pista de Ijuana	Tenerife	28.560191	-16.169190	D. sp.n. B
NMIH003261	♀	5/2/2008	Enchereda (hacia degollada)	La Gomera	28.136650	-17.179063	D. sp.n. C
UB2908	♀	4/29/1995	Pajarito	La Gomera	28.108856	-17.241604	D. sp.n. C
UB2909	♂	4/29/1995	Pajarito	La Gomera	28.108856	-17.241604	D. sp.n. C
NMIH001798	♀	4/8/2011	Teslinde. Ermita de Santa Clara	La Gomera	28.196300	-17.287540	D. sp.n. C
NMIH002301	♂	3/27/2013	Teslinde. Ermita de Santa Clara	La Gomera	28.196300	-17.287540	D. sp.n. C
NMIH000661	♀	5/16/2006	Cabezo del Tejo 2	Tenerife	28.565090	-16.165982	D. sp.n. D
NMIH000702	♂	3/4/2006	Camino La Ensilhada-Chamorra, Anaga	Tenerife	28.556209	-16.179828	D. sp.n. D
NMIH001215	♀	4/13/2007	La Ensilhada (Aparcamiento), Anaga	Tenerife	28.556191	-16.179817	D. sp.n. D
NMIH001214	♂	4/13/2007	La Ensilhada (Aparcamiento), Anaga	Tenerife	28.556191	-16.179817	D. sp.n. D
CRBA002114	♀	1/4/2013	Barranco de Nieto	Tenerife	28.534070	-16.3116255	D. sp.n. F
NMIH002946	♀	12/21/2012	Barranco de Nieto	Tenerife	28.534070	-16.3116255	D. sp.n. F
NMIH002948	♀	1/4/2013	Barranco de Nieto	Tenerife	28.534070	-16.3116255	D. sp.n. F
CRBA002113	♂	1/4/2013	Barranco de Nieto	Tenerife	28.534070	-16.3116255	D. sp.n. F
NMIH002949	♂	1/4/2013	Barranco de Nieto	Tenerife	28.534070	-16.3116255	D. sp.n. F
NMIH002950	♂	1/4/2013	Barranco de Nieto	Tenerife	28.534070	-16.3116255	D. sp.n. F
NMIH003016	♂	2/1/2013	Monte Aguirre. Anaga	Tenerife	28.529535	-16.268309	D. sp.n. F
NMIH003017	♂	2/1/2013	Monte Aguirre. Anaga	Tenerife	28.529535	-16.268309	D. sp.n. F
UB2854	♀	2/20/1995	La Matilla	Fuerteventura	28.561304	-13.954645	D. spinidorsa
NMIH000497	♂	2/5/2005	Montaña de la Cruz	Fuerteventura	28.441619	-14.057354	D. spinidorsa
NMIH000498	♂	2/5/2005	Montaña de la Cruz	Fuerteventura	28.441619	-14.057354	D. spinidorsa
NMIH000499	♂	2/5/2005	Montaña de la Cruz	Fuerteventura	28.441619	-14.057354	D. spinidorsa
UB2843	♀	2/18/1995	Tegú (Carretera Antigua-Betancuría)	Fuerteventura	28.430451	-14.046955	D. spinidorsa
UB2845	♀	2/18/1995	Tegú (Carretera Antigua-Betancuría)	Fuerteventura	28.430451	-14.046955	D. spinidorsa
UB2849	♀	2/18/1995	Tegú (Carretera Antigua-Betancuría)	Fuerteventura	28.430451	-14.046955	D. spinidorsa
UB2851	♀	2/18/1995	Tegú (Carretera Antigua-Betancuría)	Fuerteventura	28.430451	-14.046955	D. spinidorsa
UB2850	♂	2/18/1995	Tegú (Carretera Antigua-Betancuría)	Fuerteventura	28.430451	-14.046955	D. spinidorsa

UB3070_129 freezer	♂	2/14/1996	Barranco Oscuro	Gran Canaria	28.067250	-15.589010	D. filosensis
UB3073_129 freezer	♀	2/15/1996	near Cruz de San Antonio	Gran Canaria	27.916234	-15.691220	D. filosensis
UB3074_129 freezer	♂	2/15/1996	near Cruz de San Antonio	Gran Canaria	27.916234	-15.691220	D. filosensis
UB3000_126 freezer	♀	2/10/1996	Pico de Viento	Gran Canaria	28.099788	-15.651685	D. filosensis
UB2942	♂	4/7/1995	Pico de Viento	Gran Canaria	28.099788	-15.651685	D. filosensis
UB3080_130 freezer	♀	2/16/1996	Pista de Tirma	Gran Canaria	28.032133	-15.755400	D. filosensis
UB3081_130 freezer	♂	2/16/1996	Pista de Tirma	Gran Canaria	28.032133	-15.755400	D. filosensis
UB2638	♂	12/31/1993	Presa de Las Niñas	Gran Canaria	27.928312	-15.666048	D. filosensis
CRBA002933	♀	3/25/2017	Barranco de los Cochinos. Monte del Agua	Tenerife	28.324550	-16.819440	D. verneai
CRBA002934	♀	3/25/2017	Barranco de los Cochinos. Monte del Agua	Tenerife	28.324550	-16.819440	D. verneai
CRBA002935	♀	3/25/2017	Barranco de los Cochinos. Monte del Agua	Tenerife	28.324550	-16.819440	D. verneai
CRBA002939	♀	3/25/2017	Barranco de los Cochinos. Monte del Agua	Tenerife	28.324550	-16.819440	D. verneai
NMH001111	♀	3/1/2006	Barranco de los Cochinos. Monte del Agua	Tenerife	28.324550	-16.819440	D. verneai
NMH001112	♀	3/1/2006	Barranco de los Cochinos. Monte del Agua	Tenerife	28.324550	-16.819440	D. verneai
NMH001113	♂	3/1/2006	Barranco de los Cochinos. Monte del Agua	Tenerife	28.324550	-16.819440	D. verneai
NMH001114	♂	3/1/2006	Barranco de los Cochinos. Monte del Agua	Tenerife	28.324550	-16.819440	D. verneai
UB3181	♂	11/30/1993	Barranco de los Cochinos. Monte del Agua	Tenerife	28.324550	-16.819440	D. verneai
NMH001052	♀	1/30/2007	Barranco del Agua	Tenerife	28.307838	-16.448156	D. verneai
NMH001054	♀	1/30/2007	Barranco del Agua	Tenerife	28.307838	-16.448156	D. verneai
NMH001058	♀	1/30/2007	Barranco del Agua	Tenerife	28.307838	-16.448156	D. verneai
NMH001106	♂	3/9/2006	Caldera de Pedro Gil	Tenerife	28.248283	-16.529917	D. verneai
NMH001107	♂	3/9/2006	Caldera de Pedro Gil	Tenerife	28.248283	-16.529917	D. verneai
NMH001240	♀	4/20/2007	Camino a Ichires. Anaga	Tenerife	28.540023	-16.231988	D. verneai
NMH001108	♀	3/4/2006	Camino La Enhillada-Chamorga. Anaga	Tenerife	28.556209	-16.179828	D. verneai
NMH000920	♀	1/13/2007	Cruz del Carmen (Sendero restaurante)	Tenerife	28.531925	-16.279999	D. verneai
NMH000791	♂	5/24/2006	Cruz del Carmen (Sendero restaurante)	Tenerife	28.531925	-16.279999	D. verneai
NMH001078	♂	1/16/2007	Cumbres de Añico. Pista de Izaña	Tenerife	28.249217	-16.528748	D. verneai
NMH000838	♀	12/15/2006	El Aderno. Altos de Buenavista	Tenerife	28.358258	-16.864456	D. verneai
NMH000839	♀	12/15/2006	El Aderno. Altos de Buenavista	Tenerife	28.358258	-16.864456	D. verneai
NMH000841	♂	12/15/2006	El Aderno. Altos de Buenavista	Tenerife	28.358258	-16.864456	D. verneai

NMIH000842	♂	12/15/2006	El Adermo. Altos de Buenavista	Tenerife	28.358258	-16.864456	<i>D. verneai</i>
NMIH001209	♂	4/13/2007	La Ensilada (Aparcamiento). Anaga	Tenerife	28.556191	-16.179817	<i>D. verneai</i>
NMIH001210	♂	4/13/2007	La Ensilada (Aparcamiento). Anaga	Tenerife	28.556191	-16.179817	<i>D. verneai</i>
NMIH001148	♀	3/27/2007	La Fortaleza (pinar). P.N. del Teide	Tenerife	28.316723	-16.591240	<i>D. verneai</i>
NMIH001146	♂	3/27/2007	La Fortaleza (pinar). P.N. del Teide	Tenerife	28.316723	-16.591240	<i>D. verneai</i>
NMIH000809	♂	5/1/2006	Las Lagunetas	Tenerife	28.418535	-16.410090	<i>D. verneai</i>
NMIH000820	♀	12/22/2006	Morada del Viento (Pista Siete Fuentes).	Tenerife	28.411180	-16.421127	<i>D. verneai</i>
NMIH001070	♀	2/1/2007	Pista a Madre del Agua - Barranco del Río	Tenerife	28.177310	-16.601628	<i>D. verneai</i>
NMIH000830	♀	12/22/2006	Torre del Galtero	Tenerife	28.394697	-16.431984	<i>D. verneai</i>
NMIH003124	♀	8/27/2003	Barranco del Andén	Gran Canaria	28.025130	-15.606750	<i>D. yguanirae</i>
NMIH002705	♂	1/3/2009	Barranco Oscuro	Gran Canaria	28.067250	-15.589010	<i>D. yguanirae</i>
NMIH003278	♀	1/2/2007	Brezal del Palmital	Gran Canaria	28.111450	-15.601970	<i>D. yguanirae</i>

Table S5. Localities for each species used in the SDM analyses.

Locality Name	District	State/Prov	Autonomous Community	Country	Latitude	Longitude	Genus	SpeciesName
Casa Forestal de Frontera	Frontera	El Hierro	Canary Islands	Spain	27.737593	-18.022747	Dysdera	gomerensis_H
Charco Manso	Valverde	El Hierro	Canary Islands	Spain	27.843092	-17.918891	Dysdera	gomerensis_H
Cueva de la Curva		El Hierro	Canary Islands	Spain	27.692348	-17.972877	Dysdera	gomerensis_H
Cuevade Mauricio		El Hierro	Canary Islands	Spain	27.73913	-18.06685	Dysdera	gomerensis_H
Cueva del Hoyo		El Hierro	Canary Islands	Spain	27.753511	-18.002527	Dysdera	gomerensis_H
Cuevadel Mocán	Frontera	El Hierro	Canary Islands	Spain	27.717959	-18.00537	Dysdera	gomerensis_H
Cueva Juado de las Moleras		El Hierro	Canary Islands	Spain	27.732883	-18.140708	Dysdera	gomerensis_H
El Brezal	Frontera	El Hierro	Canary Islands	Spain	27.732629	-18.028909	Dysdera	gomerensis_H
El Fayal	Frontera	El Hierro	Canary Islands	Spain	27.739435	-17.99638	Dysdera	gomerensis_H
El Golfo	Frontera	El Hierro	Canary Islands	Spain	27.743924	-18.017786	Dysdera	gomerensis_H
El Golfo, MSS (mauri 3)		El Hierro	Canary Islands	Spain	27.743924	-18.017786	Dysdera	gomerensis_H
El Sabinar	Frontera	El Hierro	Canary Islands	Spain	27.751746	-18.129598	Dysdera	gomerensis_H
Fuente la Llanía		El Hierro	Canary Islands	Spain	27.73643	-17.996938	Dysdera	gomerensis_H
Fuente Mencáñite	El Golfo	El Hierro	Canary Islands	Spain	27.736497	-18.085804	Dysdera	gomerensis_H
Hoya del Pino	Frontera	El Hierro	Canary Islands	Spain	27.737154	-18.046305	Dysdera	gomerensis_H
La Dehesa	Frontera	El Hierro	Canary Islands	Spain	27.738237	-18.136543	Dysdera	gomerensis_H
Las Cancelitas	Confimar Pedro	El Hierro	Canary Islands	Spain	27.80953	-17.927239	Dysdera	gomerensis_H
Mirador de Bascos	Frontera	El Hierro	Canary Islands	Spain	27.754861	-18.118218	Dysdera	gomerensis_H
Mirador de Jinama	Valverde	El Hierro	Canary Islands	Spain	27.762755	-17.980418	Dysdera	gomerensis_H
Mirador de Las Playas	Frontera	El Hierro	Canary Islands	Spain	27.73197	-17.972127	Dysdera	gomerensis_H
Mirador de Las Playas (300m hacia La Restinga)	Frontera	El Hierro	Canary Islands	Spain	27.73197	-17.972127	Dysdera	gomerensis_H
Miña Caldereta	Frontera	El Hierro	Canary Islands	Spain	27.743623	-18.016548	Dysdera	gomerensis_H
Montaña de Fara	Valverde	El Hierro	Canary Islands	Spain	27.795267	-17.950103	Dysdera	gomerensis_H
Pico Pedraje. El Mocanal	Valverde	El Hierro	Canary Islands	Spain	27.803692	-17.946575	Dysdera	gomerensis_H
Pista Binto	Frontera	El Hierro	Canary Islands	Spain	27.729061	-18.084246	Dysdera	gomerensis_H
Pista del Derrabado	Frontera	El Hierro	Canary Islands	Spain	27.740804	-18.05308	Dysdera	gomerensis_H
Pista del Mercader	El Pinar	El Hierro	Canary Islands	Spain	27.712944	-18.022175	Dysdera	gomerensis_H
Pista Garoé		El Hierro	Canary Islands	Spain	27.781744	-17.951391	Dysdera	gomerensis_H

Playa Arenas Blancas	Frontera	El Hierro	Canary Islands	Spain	27.76747	-18.1122826	Dysdera	gomerensis_H
Punta Arenas Blancas	Frontera	El Hierro	Canary Islands	Spain	27.767373	-18.11212125	Dysdera	gomerensis_H
Roques de Salmor	Valverde	El Hierro	Canary Islands	Spain	27.822454	-17.996024	Dysdera	gomerensis_H
Sima de las Palomas	Frontera	El Hierro	Canary Islands	Spain	27.73787	-18.0657	Dysdera	gomerensis_H
Ventejis. Tiñor	Valverde	El Hierro	Canary Islands	Spain	27.785991	-17.937508	Dysdera	gomerensis_H
Cueva de Jinama	Frontera	El Hierro	Canary Islands	Spain	27.773536	-17.984089	Dysdera	silvatica_H
Cueva de Longueras	Frontera	El Hierro	Canary Islands	Spain	27.74673	-18.026256	Dysdera	silvatica_H
Fuente Mencáffite	El Golfo	El Hierro	Canary Islands	Spain	27.735497	-18.085804	Dysdera	silvatica_H
Hoya del Pino	Frontera	El Hierro	Canary Islands	Spain	27.737154	-18.046305	Dysdera	silvatica_H
Mirador de Bassos	Frontera	El Hierro	Canary Islands	Spain	27.754851	-18.118218	Dysdera	silvatica_H
Pista del Derrabado	Frontera	El Hierro	Canary Islands	Spain	27.740804	-18.05308	Dysdera	silvatica_H
Pista del Mercader	El Pinar	El Hierro	Canary Islands	Spain	27.712944	-18.022175	Dysdera	silvatica_H
Ventejis. Tiñor	Valverde	El Hierro	Canary Islands	Spain	27.785991	-17.937508	Dysdera	silvatica_H
Agua de los Llanos	Aguilo	La Gomera	Canary Islands	Spain	28.155715	-17.246339	Dysdera	calderensis_G
Barranco Aramaqué. Near Los Aceviños		La Gomera	Canary Islands	Spain	28.149151	-17.220779	Dysdera	calderensis_G
Barranco de Juel	Hermigua	La Gomera	Canary Islands	Spain	28.151547	-17.162962	Dysdera	calderensis_G
Barranco de los Castradores		La Gomera	Canary Islands	Spain	28.09618	-17.20142	Dysdera	calderensis_G
Chorros de Epina		La Gomera	Canary Islands	Spain	28.167036	-17.305892	Dysdera	calderensis_G
Ctra. Cumbre, altura Mora Gaspar		La Gomera	Canary Islands	Spain	28.14614	-17.262784		calderensis_G
Epina		La Gomera	Canary Islands	Spain	28.09592	-17.18206	Dysdera	calderensis_G
La Mérica	Valle Gran Rey	La Gomera	Canary Islands	Spain	28.11577	-17.33604	Dysdera	calderensis_G
Mña. de Las Pilas, Cno. La Mérica	Valle Gran Rey	La Gomera	Canary Islands	Spain	28.113296	-17.335703	Dysdera	calderensis_G
Monte de Juan Tomé. La Laja	San Sebastián	La Gomera	Canary Islands	Spain	28.123022	-17.210137	Dysdera	calderensis_G
Monte del Cedro		La Gomera	Canary Islands	Spain	28.119283	-17.23729	Dysdera	calderensis_G
Plain Land between Barranco Higuera and Barranco San Juan.		La Gomera	Canary Islands	Spain	28.19332	-17.29294	Dysdera	calderensis_G
Reventón Oscuro. Bosque del Cedro	Hermigua	La Gomera	Canary Islands	Spain	28.125809	-17.216616	Dysdera	calderensis_G
Riscos de Alojera	Vallehermoso	La Gomera	Canary Islands	Spain	28.16286	-17.318101	Dysdera	calderensis_G
Teselinde. Ermita de Santa Clara	Vallehermoso	La Gomera	Canary Islands	Spain	28.1963	-17.28754	Dysdera	calderensis_G
Above Arguamul	Vallehermoso	La Gomera	Canary Islands	Spain	28.18905	-17.29991	Dysdera	gomerensis_G
Arure to Las Hayas rd.; cropland	Valle Gran Rey	La Gomera	Canary Islands	Spain	28.129606	-17.300846	Dysdera	gomerensis_G
Barranco de Juel	Hermigua	La Gomera	Canary Islands	Spain	28.151547	-17.162962	Dysdera	gomerensis_G
Barranco de Juel, East	Hermigua	La Gomera	Canary Islands	Spain	28.14832	-17.15772	Dysdera	gomerensis_G

Barranco de los Castradores		La Gomera	Canary Islands	Spain	28.09618	-17.20142	Dysdera	gomerensis_G
Barranco de Majona	Hermigua	La Gomera	Canary Islands	Spain	28.13438	-17.168397	Dysdera	gomerensis_G
Barranco de Majona	San Sebastián	La Gomera	Canary Islands	Spain	28.15183	-17.139235	Dysdera	gomerensis_G
Barranco de Matamos: Monte del Cedro	Hermigua	La Gomera	Canary Islands	Spain	28.12504	-17.242183	Dysdera	gomerensis_G
Barranco de Pajón		La Gomera	Canary Islands	Spain	28.08845	-17.20142	Dysdera	gomerensis_G
Cañada de Jorge		La Gomera	Canary Islands	Spain	28.147416	-17.291071	Dysdera	gomerensis_G
Chorros de Epina		La Gomera	Canary Islands	Spain	28.167036	-17.305892	Dysdera	gomerensis_G
Ctra. Cumbre, altura Mora Gaspar		La Gomera	Canary Islands	Spain	28.14614	-17.262784	Dysdera	gomerensis_G
Ctra. Juego de Bolas: Laguna Grande	Agulo	La Gomera	Canary Islands	Spain	28.129925	-17.254707	Dysdera	gomerensis_G
Degollada de Archejo	Hermigua	La Gomera	Canary Islands	Spain	28.13344	-17.254938	Dysdera	gomerensis_G
El Cepo	Agulo	La Gomera	Canary Islands	Spain	28.191769	-17.216818	Dysdera	gomerensis_G
Ermita de Las Nieves		La Gomera	Canary Islands	Spain	28.101134	-17.202401	Dysdera	gomerensis_G
Ermita de Las Nieves 1130m		La Gomera	Canary Islands	Spain	28.101134	-17.202401	Dysdera	gomerensis_G
Ermita del Santo		La Gomera	Canary Islands	Spain	28.13102	-17.32273	Dysdera	gomerensis_G
La Asomadita (Pista forestal Chipude)	Vallehermoso	La Gomera	Canary Islands	Spain	28.11116	-17.2648	Dysdera	gomerensis_G
La Asomadita (Pista forestal Chipude)	Vallehermoso	La Gomera	Canary Islands	Spain	28.11116	-17.2648	Dysdera	gomerensis_G
La Campana	Hermigua	La Gomera	Canary Islands	Spain	28.158055	-17.160623	Dysdera	gomerensis_G
Las Hayas	Valle Gran Rey	La Gomera	Canary Islands	Spain	28.133622	-17.282405	Dysdera	gomerensis_G
Las Hueritas	Vallehermoso	La Gomera	Canary Islands	Spain	28.090664	-17.283087	Dysdera	gomerensis_G
Las Paredes	P.N. Garajonay	La Gomera	Canary Islands	Spain	28.09882	-17.24942	Dysdera	gomerensis_G
Llanos de Crispín		La Gomera	Canary Islands	Spain	28.123806	-17.266567	Dysdera	gomerensis_G
Llanos de Crispín	Vallehermoso	La Gomera	Canary Islands	Spain	28.123587	-17.258887	Dysdera	gomerensis_G
Los Noruegos		La Gomera	Canary Islands	Spain	28.106905	-17.233323	Dysdera	gomerensis_G
Mirador de Alojera		La Gomera	Canary Islands	Spain	28.14978	-17.30813	Dysdera	gomerensis_G
Mña. de Las Pilas, Cno. La Mérica	Valle Gran Rey	La Gomera	Canary Islands	Spain	28.113283	-17.335701	Dysdera	gomerensis_G
Mña. La Asomada (Laguna Grande-Juego de Bolas)	Vallehermoso	La Gomera	Canary Islands	Spain	28.135646	-17.257454	Dysdera	gomerensis_G
Montaña del Dinero		La Gomera	Canary Islands	Spain	28.15943312	-17.243576	Dysdera	gomerensis_G
Monte del Cedro		La Gomera	Canary Islands	Spain	28.119283	-17.23729	Dysdera	gomerensis_G
Ojila		La Gomera	Canary Islands	Spain	28.118032	-17.21105	Dysdera	gomerensis_G
Pajarito	Hermigua	La Gomera	Canary Islands	Spain	28.108856	-17.241604	Dysdera	gomerensis_G
Pajarito	San Sebastian	La Gomera	Canary Islands	Spain	28.10695	-17.241012	Dysdera	gomerensis_G
Pajarito	San Sebastian	La Gomera	Canary Islands	Spain	28.108856	-17.241604	Dysdera	gomerensis_G

Pic del Roque Cano	Vallehermoso	La Gomera	Canary Islands	Spain	28.184542	-17.256932	Dysdera	gomerensis_G
Pinar del Infante	Vallehermoso	La Gomera	Canary Islands	Spain	28.130794	-17.282267	Dysdera	gomerensis_G
Pista Mora Gaspar	Vallehermoso	La Gomera	Canary Islands	Spain	28.142375	-17.250954	Dysdera	gomerensis_G
Plain Land between Barranco Higueru and Barranco San Juan.		La Gomera	Canary Islands	Spain	28.19332	-17.29294	Dysdera	gomerensis_G
Playa de Avalo	San Sebastián	La Gomera	Canary Islands	Spain	28.114684	-17.113168	Dysdera	gomerensis_G
Playa Hermigua	Hermigua	La Gomera	Canary Islands	Spain	28.17624	-17.175953	Dysdera	gomerensis_G
Puntallana	San Sebastián	La Gomera	Canary Islands	Spain	28.125809	-17.216616	Dysdera	gomerensis_G
Reventón Oscuro. Bosque del Cedro	Hermigua	La Gomera	Canary Islands	Spain	28.125809	-17.216616	Dysdera	gomerensis_G
Sendero Enchereda	San Sebastián	La Gomera	Canary Islands	Spain	28.13665	-17.179063	Dysdera	gomerensis_G
Tapagache, old cropland		La Gomera	Canary Islands	Spain	28.08413	-17.28902	Dysdera	gomerensis_G
Teselinde. Ermita de Santa Clara	Vallehermoso	La Gomera	Canary Islands	Spain	28.1963	-17.28754	Dysdera	gomerensis_G
Túnel de Agulo (Lado Las Rosas)	Agulo	La Gomera	Canary Islands	Spain	28.192455	-17.198191	Dysdera	gomerensis_G
Vallehermoso	Vallehermoso	La Gomera	Canary Islands	Spain	28.1963	-17.28754	Dysdera	gomerensis_G
Barranco Aramaqué. Near Los Aceviños		La Gomera	Canary Islands	Spain	28.149151	-17.220779	Dysdera	silvatica_G
Barranco de Juel	Hermigua	La Gomera	Canary Islands	Spain	28.151547	-17.162962	Dysdera	silvatica_G
Barranco de Juel, East	Hermigua	La Gomera	Canary Islands	Spain	28.14832	-17.15772	Dysdera	silvatica_G
Barranco de Majona	San Sebastián	La Gomera	Canary Islands	Spain	28.15183	-17.139235	Dysdera	silvatica_G
Barranco de Matasnos, Campamento Viejo, Monte del Cedro		La Gomera	Canary Islands	Spain	28.119131	-17.215838	Dysdera	silvatica_G
Barranco de Pajén		La Gomera	Canary Islands	Spain	28.08845	-17.20142	Dysdera	silvatica_G
Bosque de Anure	Valle Gran Rey	La Gomera	Canary Islands	Spain	28.13321	-17.312446	Dysdera	silvatica_G
Bosque del Cedro	Hermigua	La Gomera	Canary Islands	Spain	28.137044	-17.222569	Dysdera	silvatica_G
Bosque del Cedro		La Gomera	Canary Islands	Spain	28.137044	-17.222569	Dysdera	silvatica_G
Cerca de Los Aceviños	Bosque del Cedro	La Gomera	Canary Islands	Spain	28.147358	-17.219868	Dysdera	silvatica_G
Chorros de Epina		La Gomera	Canary Islands	Spain	28.167036	-17.305892	Dysdera	silvatica_G
Ctra. Juego de Bolas- Laguna Grande	Agulo	La Gomera	Canary Islands	Spain	28.129932	-17.254706	Dysdera	silvatica_G
Degollada de Archejo	Hermigua	La Gomera	Canary Islands	Spain	28.13344	-17.254938	Dysdera	silvatica_G
El Cedro, humid laurel forest		La Gomera	Canary Islands	Spain	28.125809	-17.216616	Dysdera	silvatica_G
La Zarrita	Hermigua	La Gomera	Canary Islands	Spain	28.111342	-17.218806	Dysdera	silvatica_G
Laguna Grande		La Gomera	Canary Islands	Spain	28.126085	-17.233223	Dysdera	silvatica_G
Las Campanas	Hermigua	La Gomera	Canary Islands	Spain	28.158055	-17.160623	Dysdera	silvatica_G
Las Creces	P.N. Garajonay	La Gomera	Canary Islands	Spain	28.138737	-17.287852	Dysdera	silvatica_G
Las Creces	P.N. Garajonay	La Gomera	Canary Islands	Spain	28.138737	-17.287852	Dysdera	silvatica_G

Las Hayas	Valle Gran Rey	La Gomera	Canary Islands	Spain	28.133622	-17.282405	Dysdera	silvatica_G
Las Tajoras	P. N. Garajonay	La Gomera	Canary Islands	Spain	28.112834	-17.262608	Dysdera	silvatica_G
Las Tajoras	P. N. Garajonay	La Gomera	Canary Islands	Spain	28.112736	-17.262511	Dysdera	silvatica_G
Los Noruegos		La Gomera	Canary Islands	Spain	28.106905	-17.233323	Dysdera	silvatica_G
Monte de Juan Tomé. La Laja	San Sebastián	La Gomera	Canary Islands	Spain	28.123022	-17.210137	Dysdera	silvatica_G
Monte del Cedro		La Gomera	Canary Islands	Spain	28.119283	-17.237279	Dysdera	silvatica_G
Pajarito	Hermigua	La Gomera	Canary Islands	Spain	28.108856	-17.241604	Dysdera	silvatica_G
Pista Mora Gaspar	Vallehermoso	La Gomera	Canary Islands	Spain	28.142375	-17.250954	Dysdera	silvatica_G
Plain Land between Barranco Higuera and Barranco San Juan.		La Gomera	Canary Islands	Spain	28.19332	-17.29294	Dysdera	silvatica_G
Teselinde. Ermita de Santa Clara	Vallehermoso	La Gomera	Canary Islands	Spain	28.1963	-17.28754	Dysdera	silvatica_G
Cueva de los Arreboles		La Palma	Canary Islands	Spain	28.493785	-17.82903	Dysdera	calderensis_P
El Castillo	Garafia	La Palma	Canary Islands	Spain	28.79636	-17.971169	Dysdera	calderensis_P
Espigón Atravesado. Los Tilos	San Andrés y Sauces	La Palma	Canary Islands	Spain	28.782012	-17.816332	Dysdera	calderensis_P
Juan Adalid	Garafia	La Palma	Canary Islands	Spain	28.843639	-17.90635	Dysdera	calderensis_P
Llano Los Caños	Mazo	La Palma	Canary Islands	Spain	28.580523	-17.799465	Dysdera	calderensis_P
Lomo María	El Paso	La Palma	Canary Islands	Spain	28.554734	-17.861913	Dysdera	calderensis_P
Los Tilos	San Andrés y Sauces	La Palma	Canary Islands	Spain	28.783702	-17.808408	Dysdera	calderensis_P
Mendo	El Paso	La Palma	Canary Islands	Spain	28.557572	-17.867541	Dysdera	calderensis_P
Pinar de Roque Faro	Garafia	La Palma	Canary Islands	Spain	28.798556	-17.879149	Dysdera	calderensis_P
Pista de Machín	Garafia	La Palma	Canary Islands	Spain	28.78971	-17.896884	Dysdera	calderensis_P
Playa de Taburiente (PNCT)	El Paso	La Palma	Canary Islands	Spain	28.709619	-17.87614	Dysdera	calderensis_P
Puerto Santo Domingo de Garafia	Garafia	La Palma	Canary Islands	Spain	28.823215	-17.956515	Dysdera	calderensis_P
Roque Faro	Garafia	La Palma	Canary Islands	Spain	28.798556	-17.879149	Dysdera	calderensis_P
Barranco las Traves (PNCT)	El Paso	La Palma	Canary Islands	Spain	28.717984	-17.893314	Dysdera	silvatica_P
Cueva de Los Palmeros	Fuencaliente	La Palma	Canary Islands	Spain	28.507538	-17.856808	Dysdera	silvatica_P
El Castillo	Garafia	La Palma	Canary Islands	Spain	28.79636	-17.971169	Dysdera	silvatica_P
Juan Adalid	Garafia	La Palma	Canary Islands	Spain	28.843639	-17.90635	Dysdera	silvatica_P
Pico de la Cruz	El Paso	La Palma	Canary Islands	Spain	28.756058	-17.855244	Dysdera	silvatica_P
Pinar de Roque Faro	Garafia	La Palma	Canary Islands	Spain	28.798556	-17.879149	Dysdera	silvatica_P
Pista de Machín	Garafia	La Palma	Canary Islands	Spain	28.78971	-17.896884	Dysdera	silvatica_P
Roque de Los Muchachos (PNCT)	Garafia	La Palma	Canary Islands	Spain	28.76088	-17.885206	Dysdera	silvatica_P
Roque Faro	Garafia	La Palma	Canary Islands	Spain	28.798556	-17.879149	Dysdera	silvatica_P

SE El Castillo (small lava tube)	Garafia	La Palma	Canary Islands	Spain		28.790783	-17.948843	Dysdera	silvatica_P
Tenerra (Parte alta) (PNCT)	El Paso	La Palma	Canary Islands	Spain		28.719605	-17.895636	Dysdera	silvatica_P

Understanding the origins of, and identifying the processes that shape, biodiversity are among the major goals of biology ever since Darwin published "On the Origin of Species". Similarly, the ability to predict organismal response to natural selection lies at the very core of evolutionary biology. One well known process that has helped to shed light on the link between evolution and ecology is that of adaptive radiation, which has been defined as the evolution of ecophenotypically distinct species from a single common ancestor that has occurred in a short period of time. Typically, adaptive radiations are characterized by a fast synchronous diversification of lineages and phenotypes after the colonization of a new environment, which slows down as ecological niches are filled. The study of adaptive radiations has greatly contributed to understanding the mechanisms that drive speciation and promote ecophenotypic diversification, along with many other related ecological and evolutionary processes.



Natural selection plays a key role in deterministic evolution, as clearly illustrated by the multiple cases of repeated evolution of ecomorphological characters observed in adaptive radiations. Unlike most spiders, *Dugesiella* species display a high variability of cheliceral morphologies, which has been suggested to reflect different levels of specialisation to feed on isopods. In this study, we integrate geometric morphometrics and experimental trials with a fully resolved phylogeny of the highly diverse endemic species from the Canary Islands to 1) quantitatively define the different cheliceral morphotypes present in the archipelago, 2) test their association with trophic specialisation, as reported for continental species, 3) reconstruct the evolution of these ecomorphs throughout the diversification of the group, 4) test the hypothesis of convergent evolution of the different morphotypes, and 5) examine whether specialisation constitutes a case of evolutionarily irreversibility in this group.